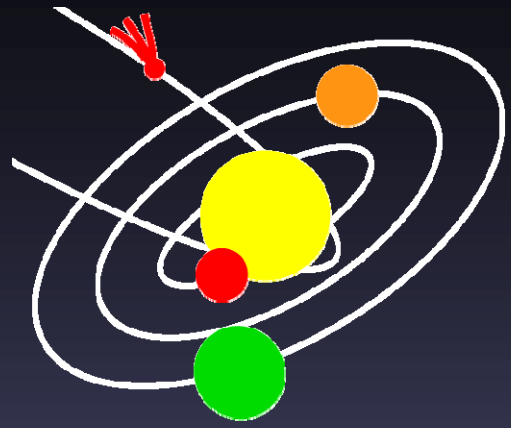

Introduction to Solar Physics

Sami K. Solanki

IMPRS lectures

~~**Jan. 2005**~~ **Nov. 2008**

Structure of lectures I

- Introduction and overview
- Core and interior: energy generation and standard solar model
- Solar oscillations and helioseismology
- Solar rotation
- Solar radiation and spectrum
  - Solar spectrum
  - Radiative transfer
  - Formation of absorption and emission lines
- Convection: The convection zone and granulation etc.

Structure of lectures II

- The solar atmosphere: structure
  - Photosphere
  - Chromosphere
  - Transition Region
  - Corona
  - Solar wind and heliosphere
- The magnetic field
  - Zeeman effect and Unno-Rachkovsky equations
  - Magnetic elements and sunspots
  - Chromospheric and coronal magnetic field
  - The solar cycle
  - Coronal heating

Structure of lectures III

- Solar cycle and solar dynamo
- Atmospheric heating
- Explosive and eruptive phenomena
  - Flares
  - CMEs
  - Explosive events
- Sun-Earth connection
  - CMEs and space weather
  - Longer term variability and climate
- Solar-stellar connection (not this time)
  - Activity-rotation relationship
  - Sunspots vs. starspots

The Sun: a brief overview

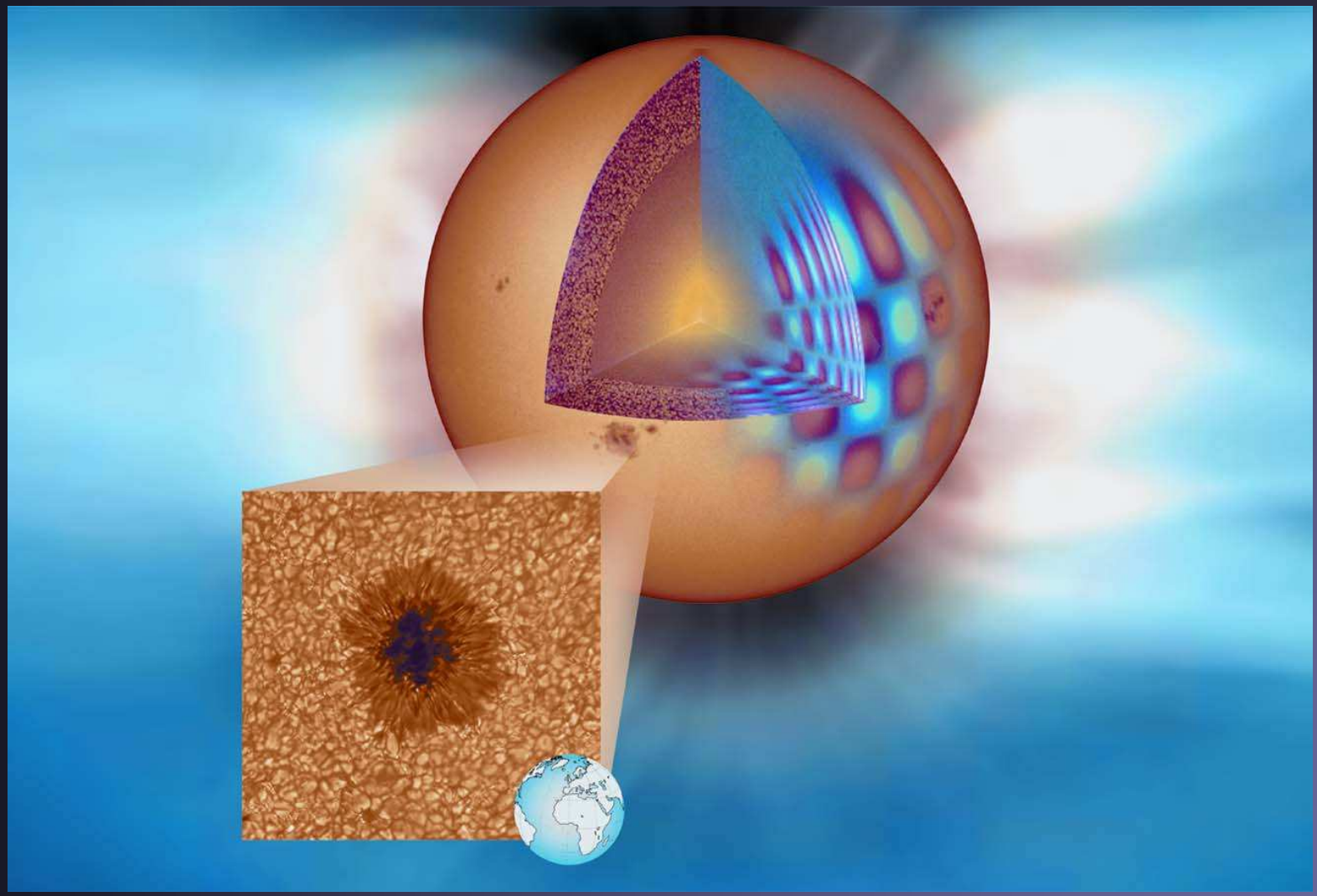

The Sun, our star

- The Sun is a normal star: middle aged (4.5 Gyr) main sequence star of spectral type G2
- The Sun is a special star: it is the only star on which we can resolve the spatial scales on which fundamental processes take place.
- The Sun is a special star: it provides almost all the energy to the Earth
- The Sun is a special star: it provides us with a unique laboratory in which to learn about various branches of physics.

The Sun: a few numbers

- Mass = 1.99 10^{30} kg (= 1 $M_{\odot}$)
- Average density = 1.4 g/cm^3
- Core density = 1.5×10^2 g/cm^3
- Luminosity = 3.84 10^{26} W (= 1 $L_{\odot}$)
- Effective temperature = 5777 K (G2 V)
- Core temperature = 15 10^6 K
- Surface gravitational acceleration g = 274 m/s^2
- Age = 4.55 10^9 years (from meteorite isotopes)
- Radius = 6.96 10^5 km
- Distance = 1 AU = 1.496 (+/-0.025) 10^8 km (≈8 light minutes)
- 1 arc sec = 722±12 km on solar surface (elliptical Earth orbit)
- Rotation period = 27 days at equator (synodic, i.e. as seen from Earth; Carrington rotation)

The Sun's Structure

Solar interior:

- Everything below the Sun's (optical) surface
- Divided into hydrogen-burning core, radiative and convective zones

Solar atmosphere:

- Directly observable part of the Sun.
- Divided into photosphere, chromosphere, corona, heliosphere

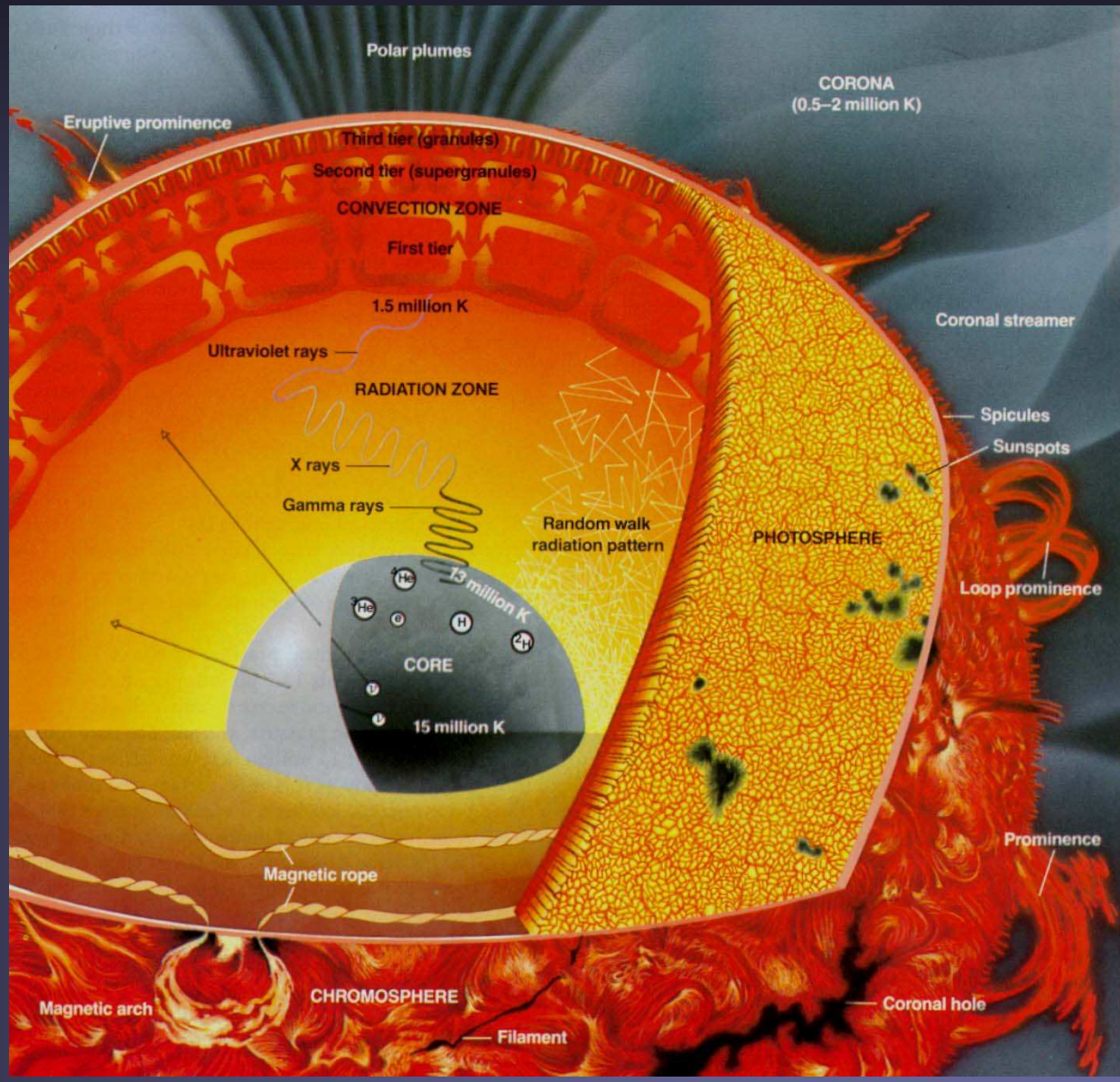

The solar surface

- Solar material exhibits no phase transition (e.g. from solid or liquid to gaseous as on Earth) ➔ define solar surface through its radiation.
- Photons in solar interior make a random walk, since they are repeatedly absorbed & reemitted. Mean free path increases rapidly with radial distance from the solar core (density and opacity decrease).
- Solar surface: where average vertical mean free path becomes so large that photons escape from Sun. Surface corresponds to optical depth $\tau = 1$. Its height depends on λ.
- Often $\tau = 1$ at λ=5000 Å is used as standard for the solar surface.

Wide range of physical parameters

- Between core and corona Sun presents a wide variety of physical phenomena and processes.
- E.g. Gas density varies by ≈ 30 orders of magnitude, temp. T by 4 orders, relevant time scales from 10^{-10} sec to 10 Gyr

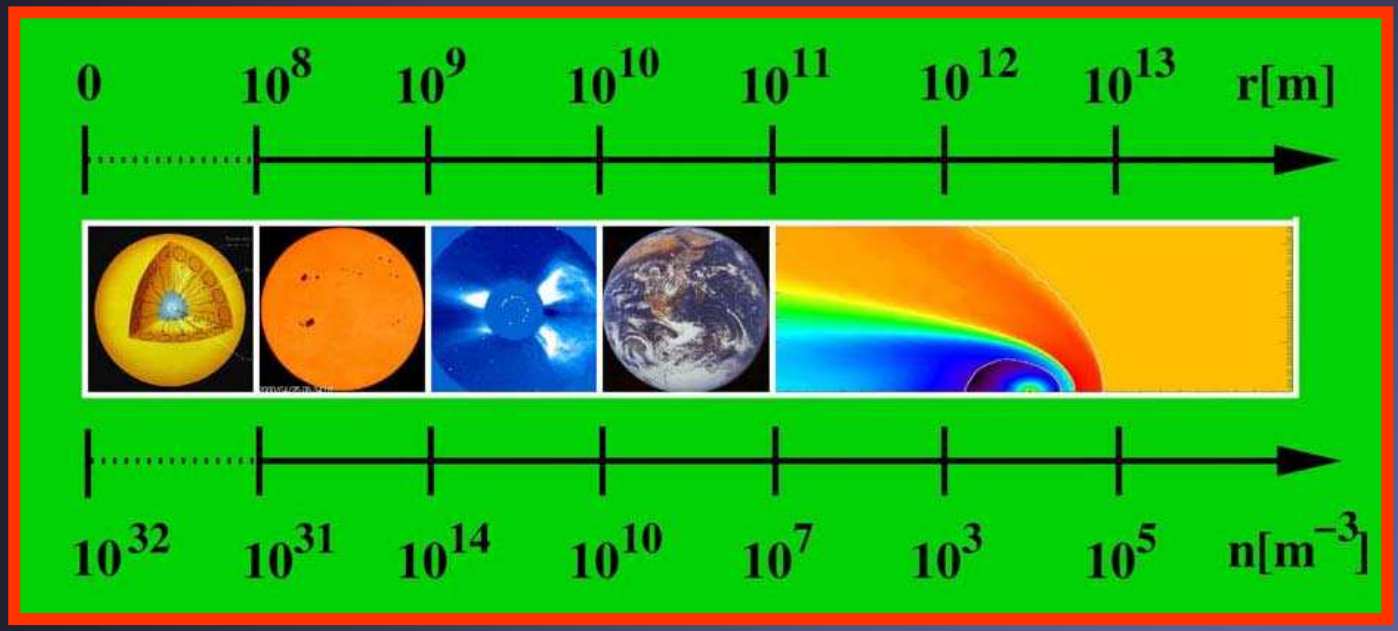

➔ Different observational and theoretical techniques needed to study different parts of Sun, e.g. helioseismology & nuclear physics for interior, polarimetry & MHD for magnetism, etc.

Solar physics in relation to other branches of physics

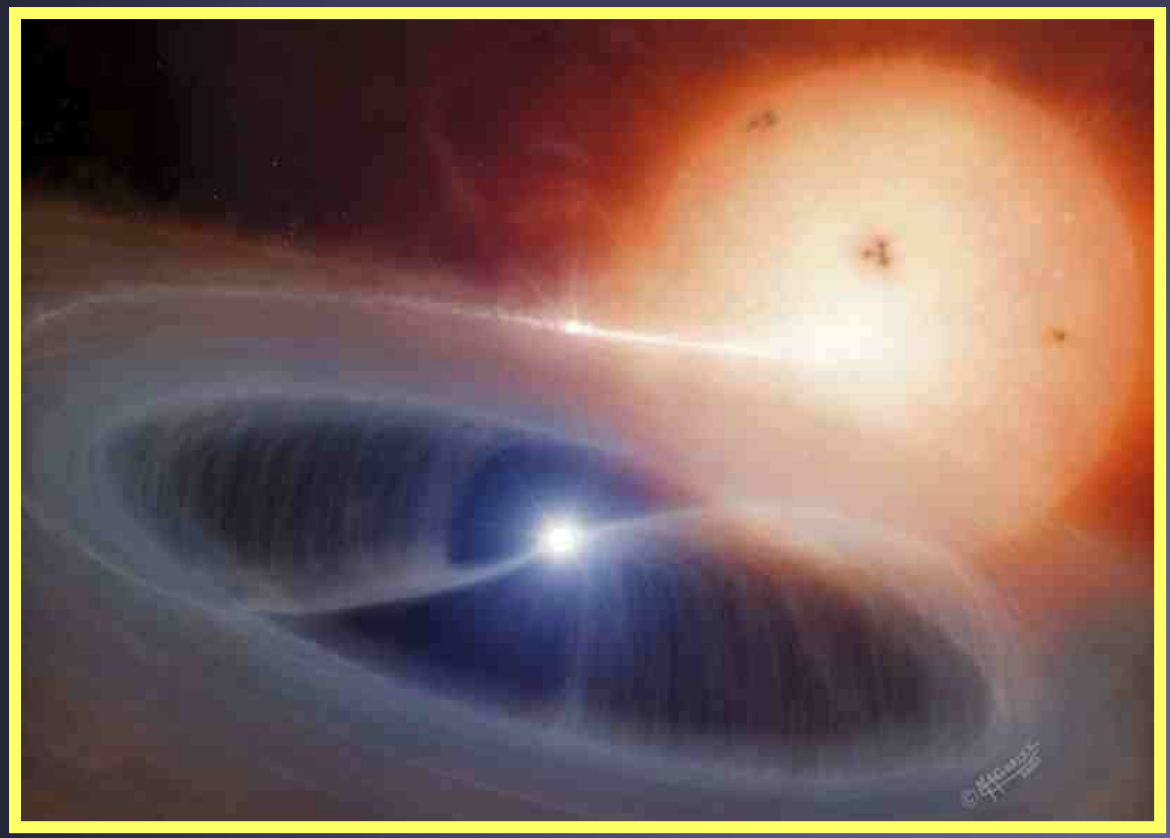

Solar Physics in Relation to Other Fields

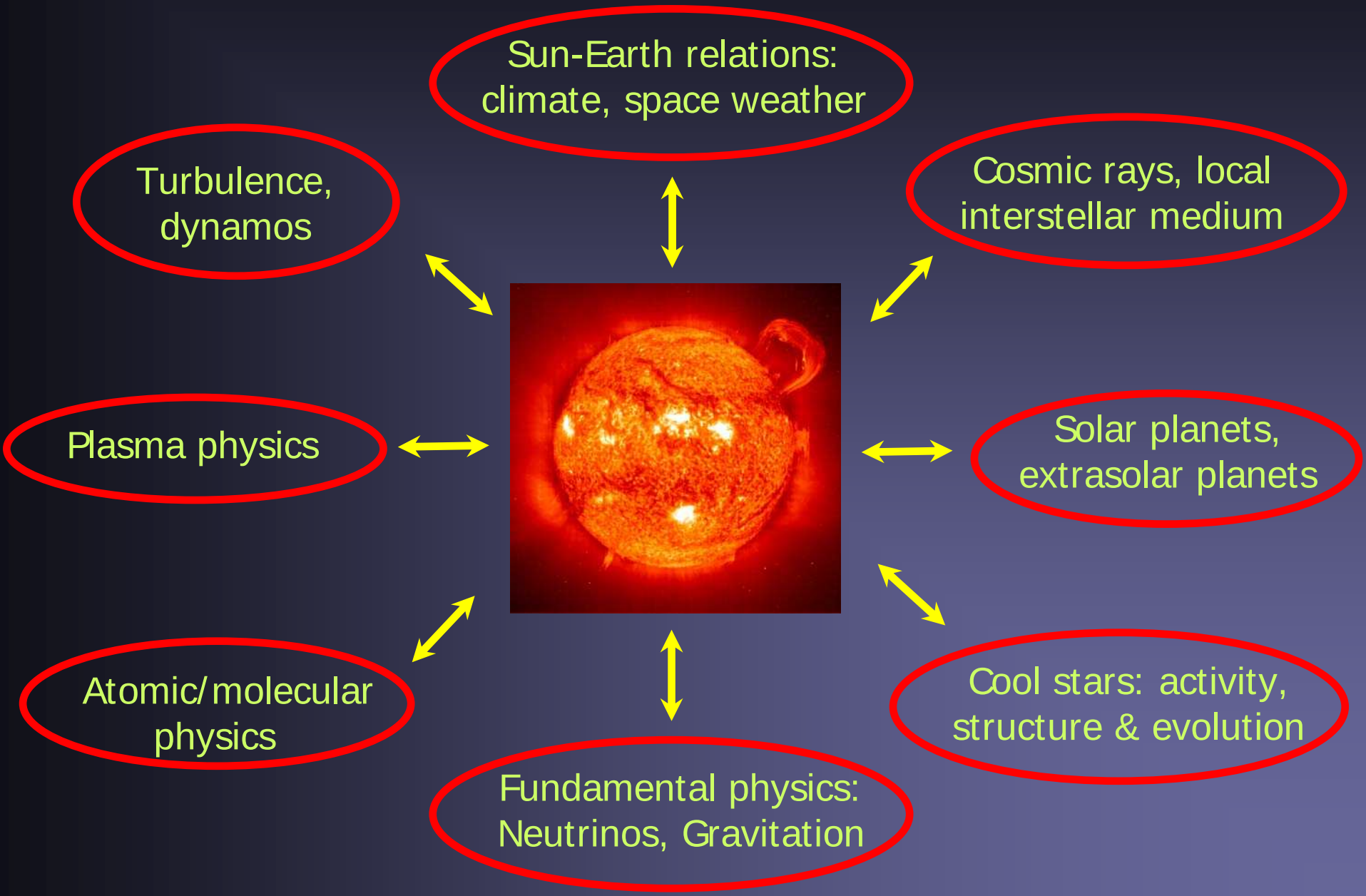

The Sun as a plasma physics lab.

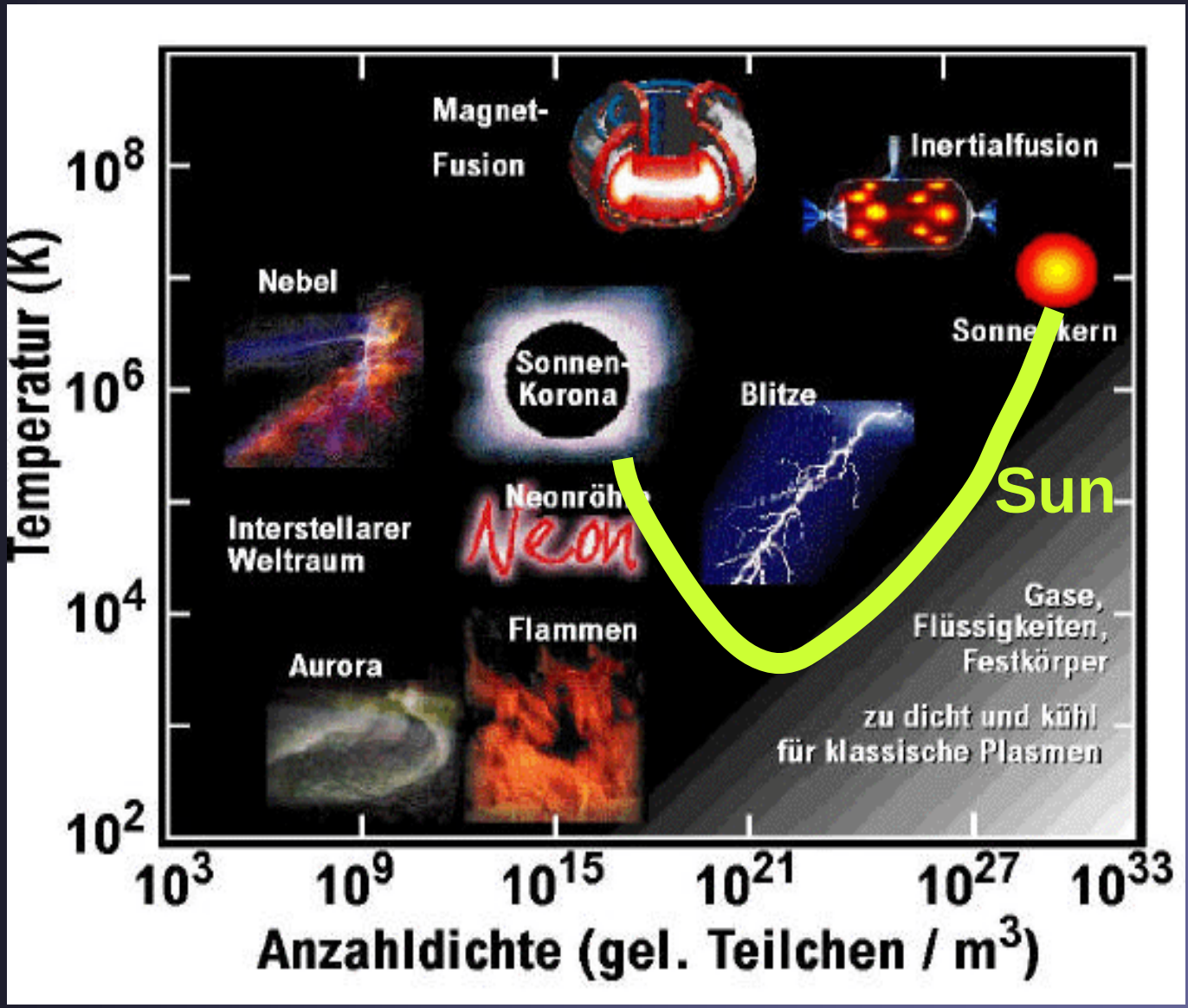

Solar Tests of Gravitation Physics

- Curved light path in solar gravitational field → Test of General Relativity
- Red shift of solar spectral lines → Test of EEP
- Oblate shape of Sun → Quadrupol moment of solar gravitational field: Test of Brans-Dicke theory
- Comparison of solar evolution models with observations → Limits on evolution of fundamental constants
- Polarization of solar spectral lines: Tests gravitational birefringence → Tests of equivalence principle & alternative theories of gravity

Which stars have magnetic fields or show magnetic activity?

- Best studied star: Sun
- F, G, K & M stars (outer convection zones) show magnetic activity & have <B> fields of G-kG.
- Early type stars: Ap, Bp, (kG-100kG), Be (100G)
- White dwarfs have B ≈ kG-10^9 G, no activity
- Not on diagram: pulsars

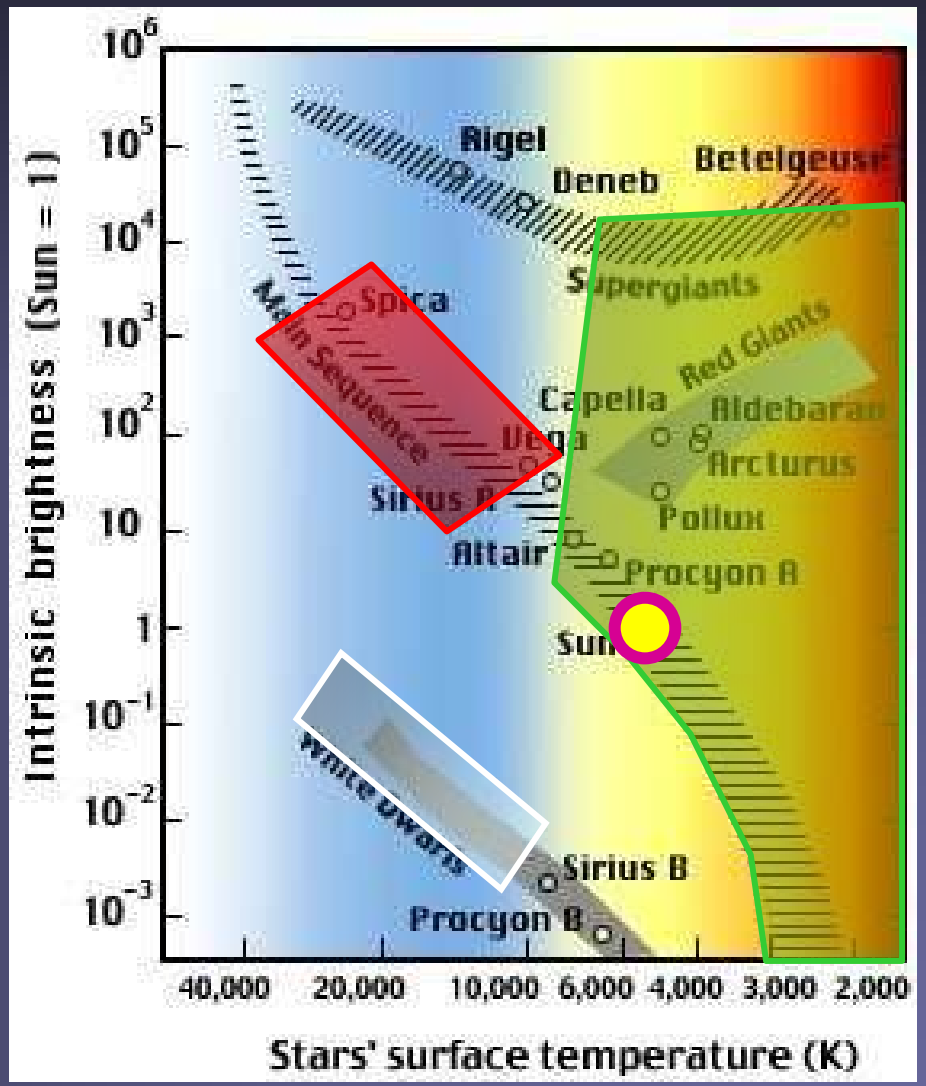

The Sun compared with an active star

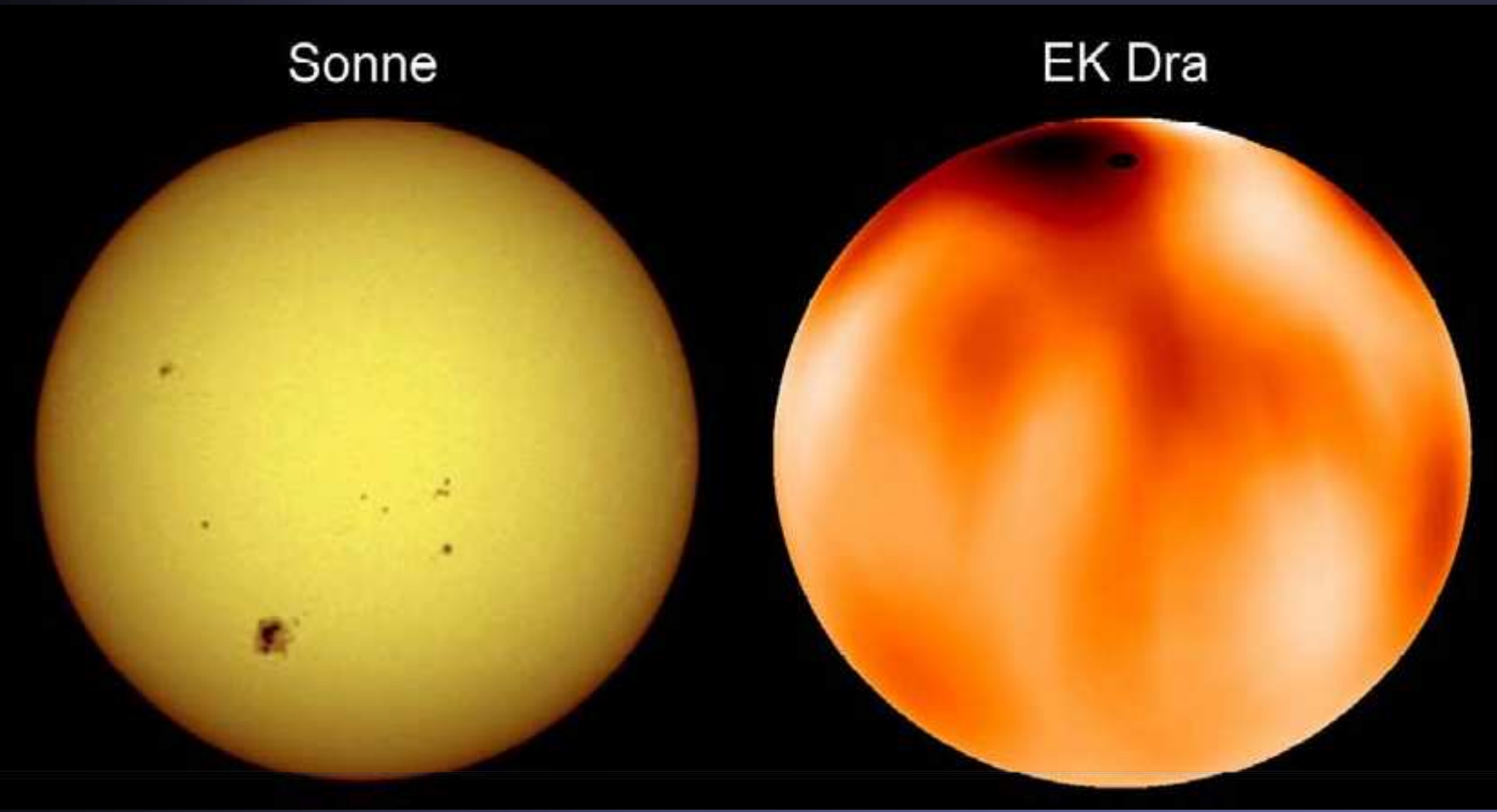

Sun, Earth and planets

- Solar output affects the magnetospheres and atmospheres of planets
- Solar energy is responsible for providing a habitable environment on Earth
- Solar evolution and liquid water on Mars...

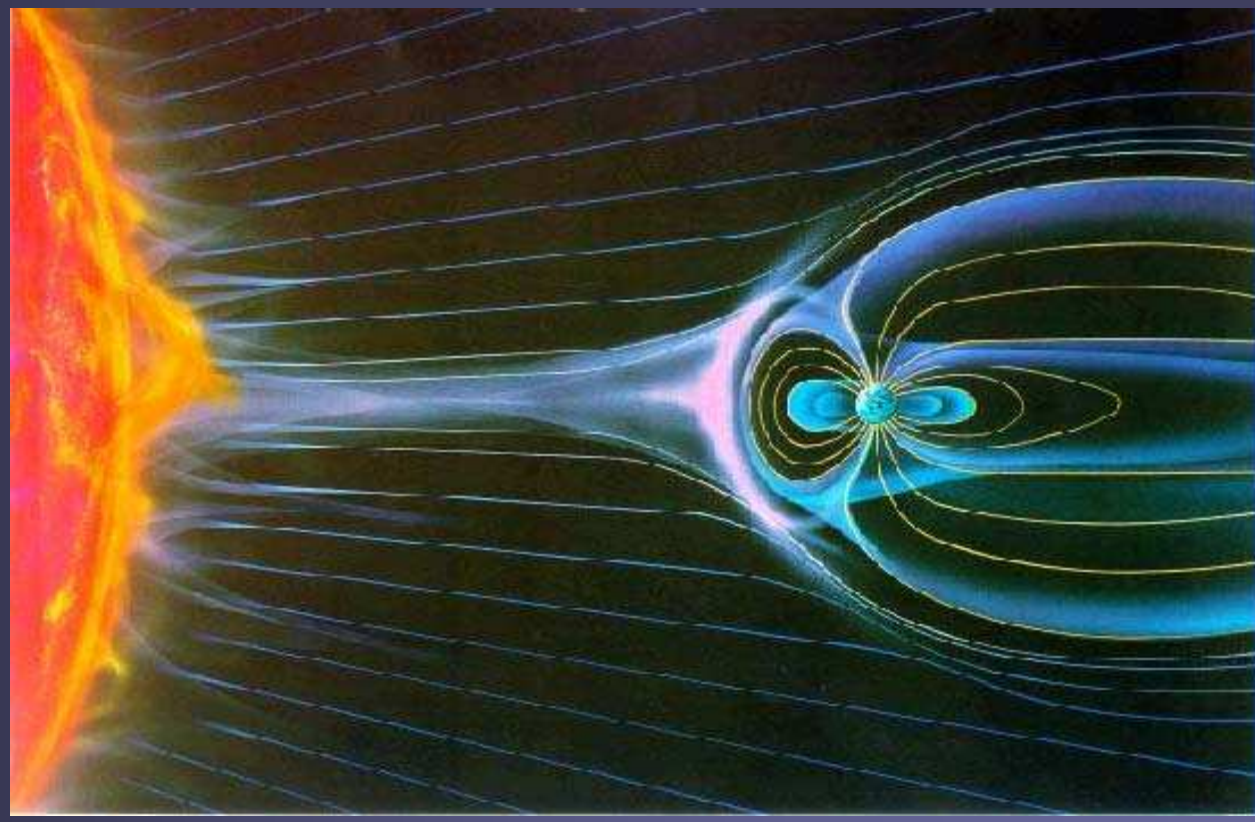

The solar interior

The Sun's core

- In the Sun's core, mass is turned into energy.
- Nuclear reactions burn $7x10^{11}$ kg/s of hydrogen into helium.
- In core, particle density and temperature are high → individual protons ram into each other at sufficient speed to overcome the Coulomb barrier, forming He nuclii (α) and releasing energy

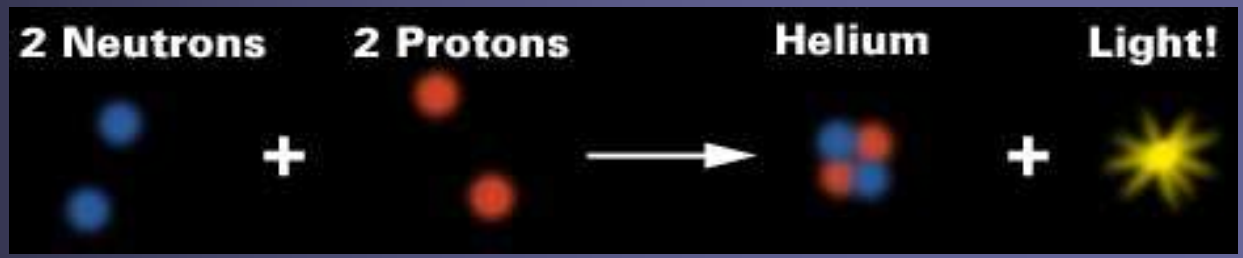

Nuclear reactions in cores of stars

- Sun gains practically all its energy from the reaction $4p \rightarrow \alpha + 2e^{+} + 2\nu = {}^{4}He + 2e^{+} + 2\nu$
- Two basic routes
  - p-p chain: yields about 99% of energy in Sun
  - CNO cycle : 1% of energy released in present day Sun (but dominant form of energy release in hotter stars)
- Both chains yield a total energy Q of 26.7 MeV per He nucleus, mainly in the form of γ-radiation Q_{γ} (which is absorbed and heats the gas) and neutrinos Q_{ν} (which escapes from the Sun).
- 0.7% of each protons mass is converted into energy

Nuclear reactions of pp-chain

- p=proton
- d=deuterium
- α=Helium
- γ=radiation
- ν=neutrino
- 2nd reaction replaces step 3 of 1st reaction
- 3rd reaction replaces steps 2+3 of 2nd reaction
- Branching ratios:
  - 1st vs. 2nd + 3rd 87 : 13
  - 2nd vs. 3rd → 13 : 0.015

Table 2.1. Nuclear reactions of the pp chains. Energy values according to Bahcall and Ulrich (1988) and Caughlan and Fowler (1988)

	Reaction	Q'[MeV]	Q_ν[MeV]	Rate symbol
ppI	$p(p,e^+\nu)d$	1.177 (x2)	0.265	λ_{pp}
	$d(p,\gamma)^3He$	5.494 (x2)		λ_{pd}
	$^3He(^3He,2p)\alpha$	12.860		λ_{33}
ppII	$^3He(\alpha,\gamma)^7Be$	1.586		λ_{34}
	$^7Be(e^-,\nu\gamma)^7Li$	0.049	0.815	λ_{e7}
	$^7Li(p,\alpha)\alpha$	17.346		λ'_{17}
ppIII	$^7Be(p,\gamma)^8B$	0.137		λ_{17}
	$^8B(,e^+\nu)^8Be^*$	8.367	6.711	λ_8
	$^8Be^*(,\alpha)\alpha$	2.995		λ'_8

Nuclear reactions of CNO-cycle

- C, N and O act only as catalysts: Basically the same things happens as with proton chain.

Table 2.2. Nuclear reactions of the CNO cycle. Energy values according to Bahcall and Ulrich (1988) and Caughlan and Fowler (1988)

Reaction	Q'[MeV]	Q_ν[MeV]	Rate symbol
$^{12}C(p,\gamma)^{13}N$	1.944		λ_{p12}
$^{13}N(,e^+\nu)^{13}C$	1.513	0.707	λ_{13}
$^{13}C(p,\gamma)^{14}N$	7.551		λ_{p13}
$^{14}N(p,\gamma)^{15}O$	7.297		λ_{p14}
$^{15}O(,e^+\nu)^{15}N$	1.757	0.997	λ_{15}
$^{15}N(p,\alpha)^{12}C$	4.966		λ_{p15}

Temperature dependence of pp-chain and CNO cycle

- p-p chain in cool main-sequence stars
- CNO cycle in hot main-sequence stars
- Triple alpha process in red giants: 3He → C
- T dependence of p-p chain:: $\eta(T/10^6)^4$, where η depends on many other parameters.

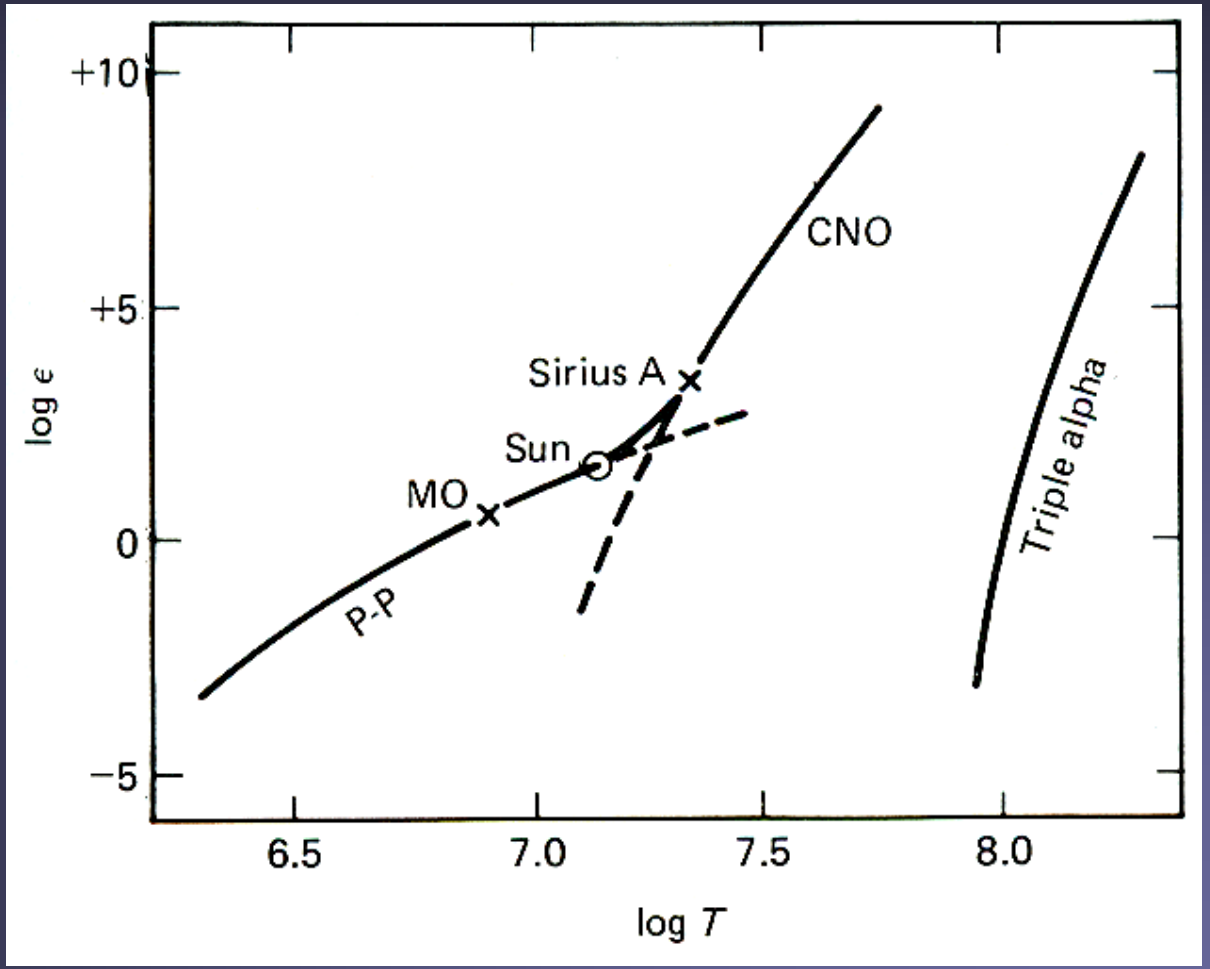

Solar neutrinos

- Neutrinos, ν, are produced at various stages of the pp-chain.
- Neutrinos are also produced by the reaction: p(p e^- , ν)d , so-called pep reaction. Being a 3-body reaction it is too rare to contribute to the energy, but does contribute to number of ν.

	Reaction	Q'[MeV]	Q_ν[MeV]
ppI	$p(p,e^+\nu)d$	1.177	0.265
	$d(p,\gamma)^3He$	5.494	
	$^3He(^3He,2p)\alpha$	12.860	
ppII	$^3He(\alpha,\gamma)^7Be$	1.586	
	$^7Be(e^-,\nu\gamma)^7Li$	0.049	0.815
	$^7Li(p,\alpha)\alpha$	17.346	
ppIII	$^7Be(p,\gamma)^8B$	0.137	
	$^8B(,e^+\nu)^8Be^*$	8.367	6.711
	$^8Be^*(,\alpha)\alpha$	2.995	

Solar neutrino spectrum

- Continua: number/(cm^2 s MeV)
- Lines: number/(cm^2 s)
- Bars at top & shading: sensitivity of different materials to ν

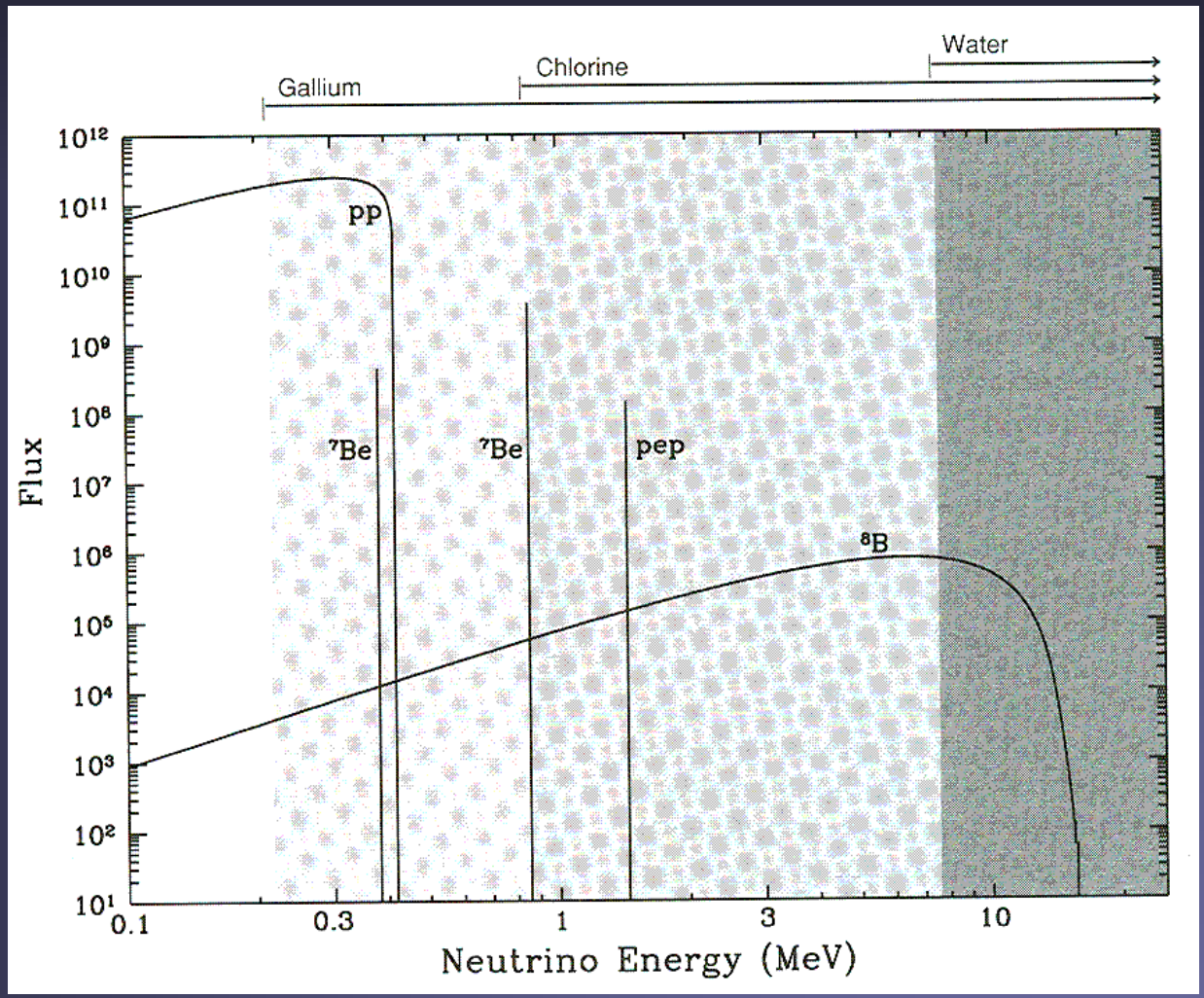

Solar neutrinos II

- Since 1968 the Homestake ^{37}Cl experiment has given a value of 2.1 ± 0.3 snu (1snu =1 ν / 10^{36} target atoms)
- Standard solar models predict: 7±2 snu

→Solar Neutrino Problem!

- In 1980s & 90s water based Kamiokande and larger Superkamiokande detectors found that approximately half the rare, high energy ^{8}B ν were missing.
- ^{71}Ga experiments (GALLEX at Gran Sasso and SAGE in Russia) showed that the neutrino flux was too low, even including the p(p,e^+ ν)d neutrinos.

Results of neutrino experiments

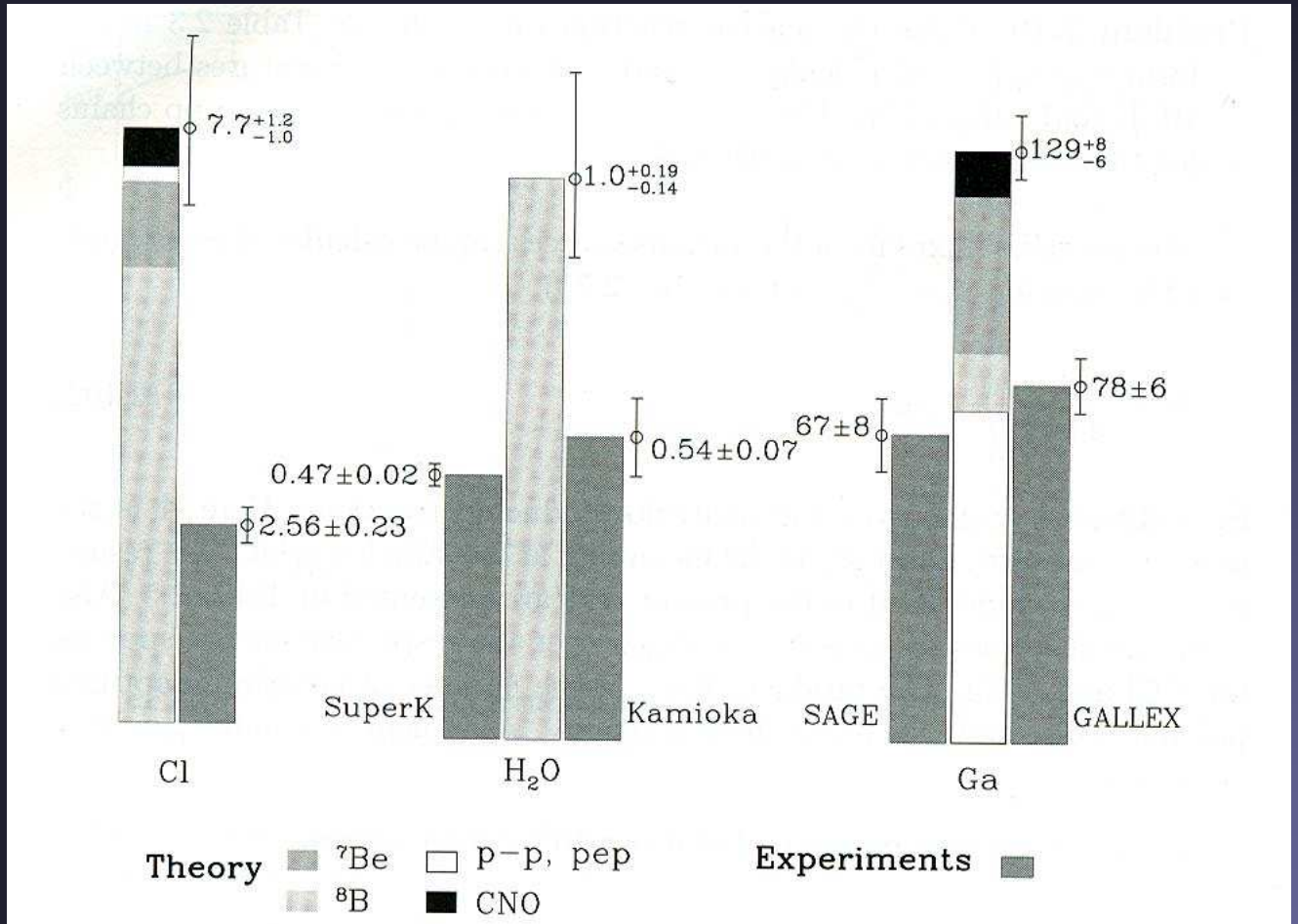

Fig. 2.13. Solar neutrinos: Prediction from the standard solar model BP98 of J. N. Bahcall and M. H. Pinsonneault (*high columns*) and experimental results (*lower columns*), for the ^{37}Cl (*left*), water (*middle*), and ^{71}Ga detectors (*right*). The *shading* indicates the contributions to the theoretical prediction from the diverse nuclear reactions in the Sun, as indicated at the bottom

Solar neutrinos III

- Sensitivity of H_2O, ^{71}Ga and ^{37}Cl to ν increases ~ exponentially with increasing ν energy.

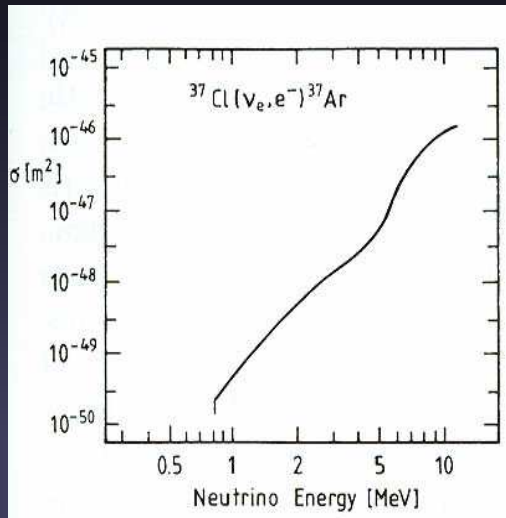

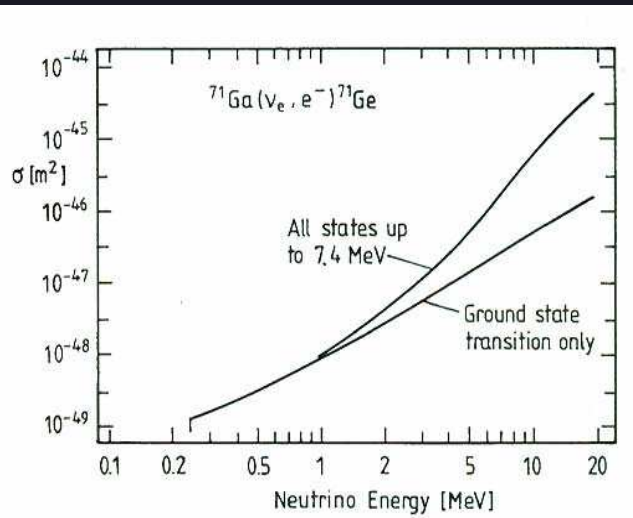

➔ Homestake ^{37}Cl detector and (Super-) Kamiokande see mainly high-energy ν from rare β^+-decay of ^8B.

- Branching ratios between the various chains: central for predicting exact ν-flux detectable by ^{37}Cl & H_2O
- Branching ratios depend very sensitively on T(r=0), while total ν-flux depends only linearly on luminosity.
- Even ^{71}Ga experiments are sensitve largely to high energy ν.

Resolution of neutrino problem

- SNO (Sudbury Neutrino Observatory) in Sudbury, Canada uses D_2O and can detect not just the electron neutrino, but also μ and τ neutrinos

➔ The neutrinos aren't missing, e^- neutrinos produced in the Sun just convert into μ and τ neutrinos

➔ The problem lies with the neutrino physics.

- The neutrino has a small rest mass (10^{-8} m_e), which allows it to oscillate between the three flavours: e^- neutrino, μ neutrino and τ neutrino (proposed 1969 by russian theorists: Bruno Pontecorvo and Vladimir Gribov, … but nobody believed them)
- Confirmation by measuring anti-neutrinos from power plant (with Superkamiokande).

Resolution of neutrino problem II

- Lesson learnt: neutrinos have a multiple personality problem (J. Bahcall)
- Other lesson learnt: the “dirty” and difficult solar model turned out to be correct, the clean and beautiful standard theory of particle physics turned out to be wrong, or at least incomplete (J. Bahcall)
- 2002: Raymond Davis got Nobel prize for uncovering the neutrino problem

Hawkin's theory of progress

Progress does not consist in replacing a theory that is wrong by one that is right. It consists in replacing a theory that is wrong by one that is more subtly wrong.

Standard solar model

- Ingredients: Conservation laws and material dependent equations
  - Mass conservation
  - Hydrostatic equilibrium (= momentum conservation in a steady state)
  - Energy conservation
  - Energy transport
  - Equation of state
  - Expression for entropy
  - Nuclear reaction networks and reaction rates → energy production
  - Opacity
- Assumptions: standard abundances, no mixing in core or in radiative zone, hydrostatic equilibrium, i.e. model passes through a stage of equilibria (the only time dependence is introduced by reduction of H and build up of He in core).

Equations describing solar interior

- Equations are given in spherical geometry
- They can be derived by considering a thin shell centred on the solar core

Mass m conservation :

$$\frac{\partial r}{\partial m} = \frac{1}{4\pi\rho r^2}$$

$r =$ radial distance, $\rho =$ gas density

Hydrostatic equilibrium :

$$\frac{\partial P}{\partial m} = -\frac{Gm}{4\pi r^4}$$

$P =$ pressure

$G =$ Gravitational constant

Energy balance :

$$\frac{\partial L}{\partial m} = \varepsilon - T\frac{\partial S}{\partial T}$$

$\varepsilon =$ energy generation per unit mass

$T =$ temperature

$S =$ entropy

Equations describing solar interior II

- Also: equations describing
  - nuclear reaction networks
  - radiative transport of energy
  - convective energy transport
  - conductive energy transport
  - opacity
  - ionisation equilibria (for opacity)
  - diffusion “constants”
  - etc. etc.

Equation of state:

$$\rho = \rho(P,T)$$

or (for an ideal gas):

$$P_G = \frac{\rho \Re T}{\mu}$$

P_G = gas pressure

$\Re$ = gas constant

μ = mean molecular weight

Energy transport:

$$F = F_{\mathrm{R}} + F_{\mathrm{C}} + F_{\mathrm{cond}} = \frac{L}{4\pi r^2}$$

F = total energy flux

F_{R} = radiative flux

F_{C} = convective flux

F_{cond} = conductive flux

L = luminosity

Internal structure of the Sun

- Internal models shown for ZAMS Sun (subscript z) and for present day Sun (radius reaching out to 1.0, subscript ⊙)

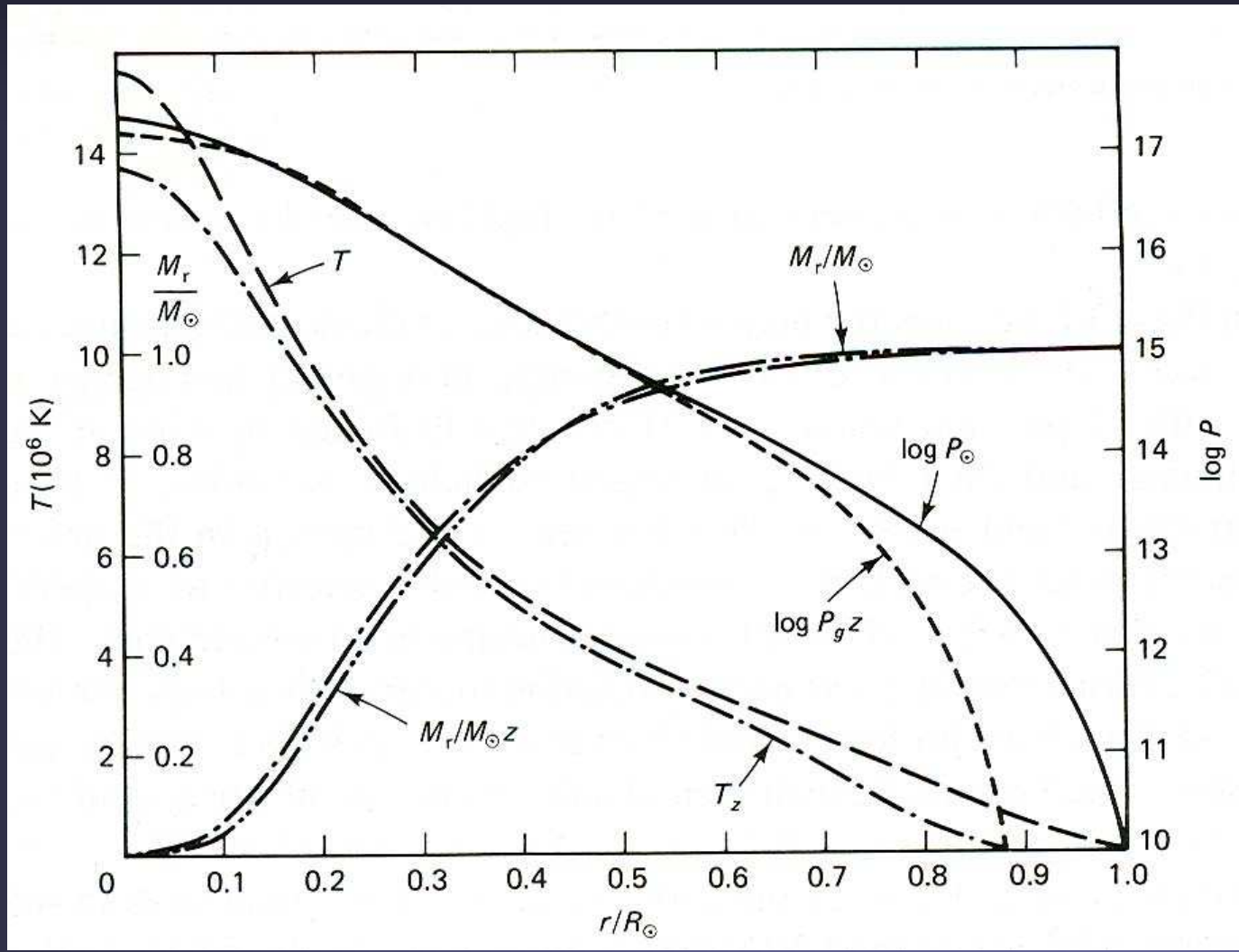

Elemental abundances

- **Photospheric values**
- Logarithmic (to base 10) abundances of the 32 lightest elements on a scale on which H has an abundance of 12
- Heavier elements all have low abundances
- In general solar photospheric abundances are very similar to those of meteorites. Exception: Li, which is depleted by a factor of 100.
- All elements except H, He and Li were produced within earlier generations of stars & released at their death

Element	Photosphere	Meteorites
1 H	12.00	–
2 He	10.93 ± 0.004	–
3 Li	1.10 ± 0.10	3.31 ± 0.04
4 Be	1.40 ± 0.09	1.42 ± 0.04
5 B	2.55 ± 0.30	2.79 ± 0.05
6 C	8.52 ± 0.06	–
7 N	7.92 ± 0.06	–
8 O	8.83 ± 0.06	–
9 F	4.56 ± 0.3	4.48 ± 0.06
10 Ne	8.08 ± 0.06	–
11 Na	6.33 ± 0.03	6.32 ± 0.02
12 Mg	7.58 ± 0.05	7.58 ± 0.01
13 Al	6.47 ± 0.07	6.49 ± 0.01
14 Si	7.55 ± 0.05	7.56 ± 0.01
15 P	5.45 ± 0.04	5.56 ± 0.06
16 S	7.33 ± 0.11	7.20 ± 0.06
17 Cl	5.5 ± 0.3	5.28 ± 0.06
18 Ar	6.40 ± 0.06	–
19 K	5.12 ± 0.13	5.13 ± 0.02
20 Ca	6.36 ± 0.02	6.35 ± 0.01
21 Sc	3.17 ± 0.10	3.10 ± 0.01
22 Ti	5.02 ± 0.06	4.94 ± 0.02
23 V	4.00 ± 0.02	4.02 ± 0.02
24 Cr	5.67 ± 0.03	5.69 ± 0.01
25 Mn	5.39 ± 0.03	5.53 ± 0.01
26 Fe	7.50 ± 0.05	7.50 ± 0.01
27 Co	4.92 ± 0.04	4.91 ± 0.01
28 Ni	6.25 ± 0.04	6.25 ± 0.01
29 Cu	4.21 ± 0.04	4.29 ± 0.04
30 Zn	4.60 ± 0.08	4.67 ± 0.04
31 Ga	2.88 ± 0.10	3.13 ± 0.02
32 Ge	3.41 ± 0.14	3.63 ± 0.04

Solar evolution

- Path of the Sun in the HR diagram, starting in PMS stage ‘P’ and ending at
  - Red giant stage
  - White dwarf stage
- Note the complex patch during the red giant phase due to various phases of Helium burning and core contraction and expansion, etc.
- η ~ mass loss rate

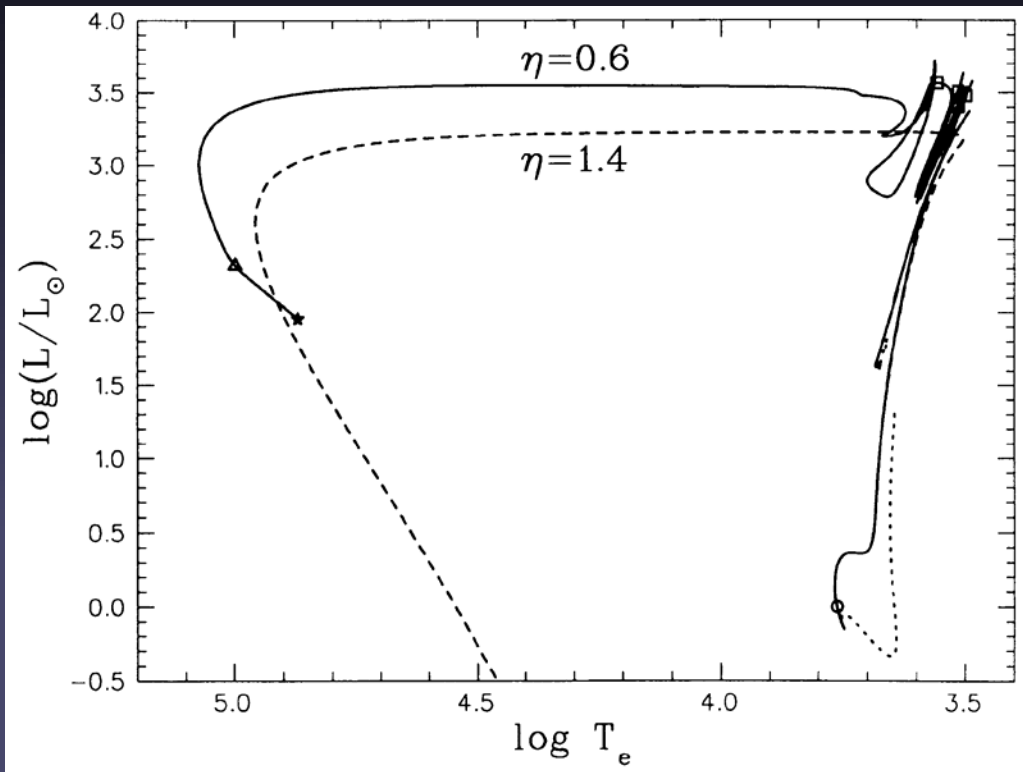

FIG. 5.—The Sun's evolution in the HR diagram, from the pre–main-sequence state to the pre–white dwarf stage. For our preferred mass-loss case (*solid curve*: $\eta = 0.6$), the triangle indicates the beginning of the final helium shell flash, and the star its peak, where computations were terminated. The dashed curve shows our extreme mass-loss case ($\eta = 1.4$), which leaves the RGB to become a helium white dwarf.

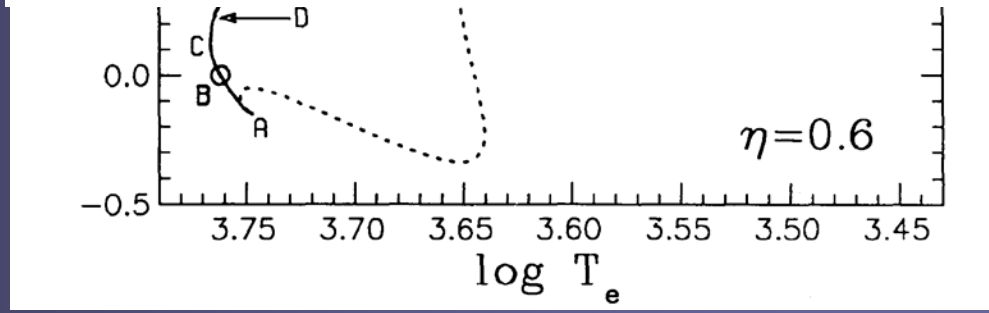

Evolution of Sun's past luminosity

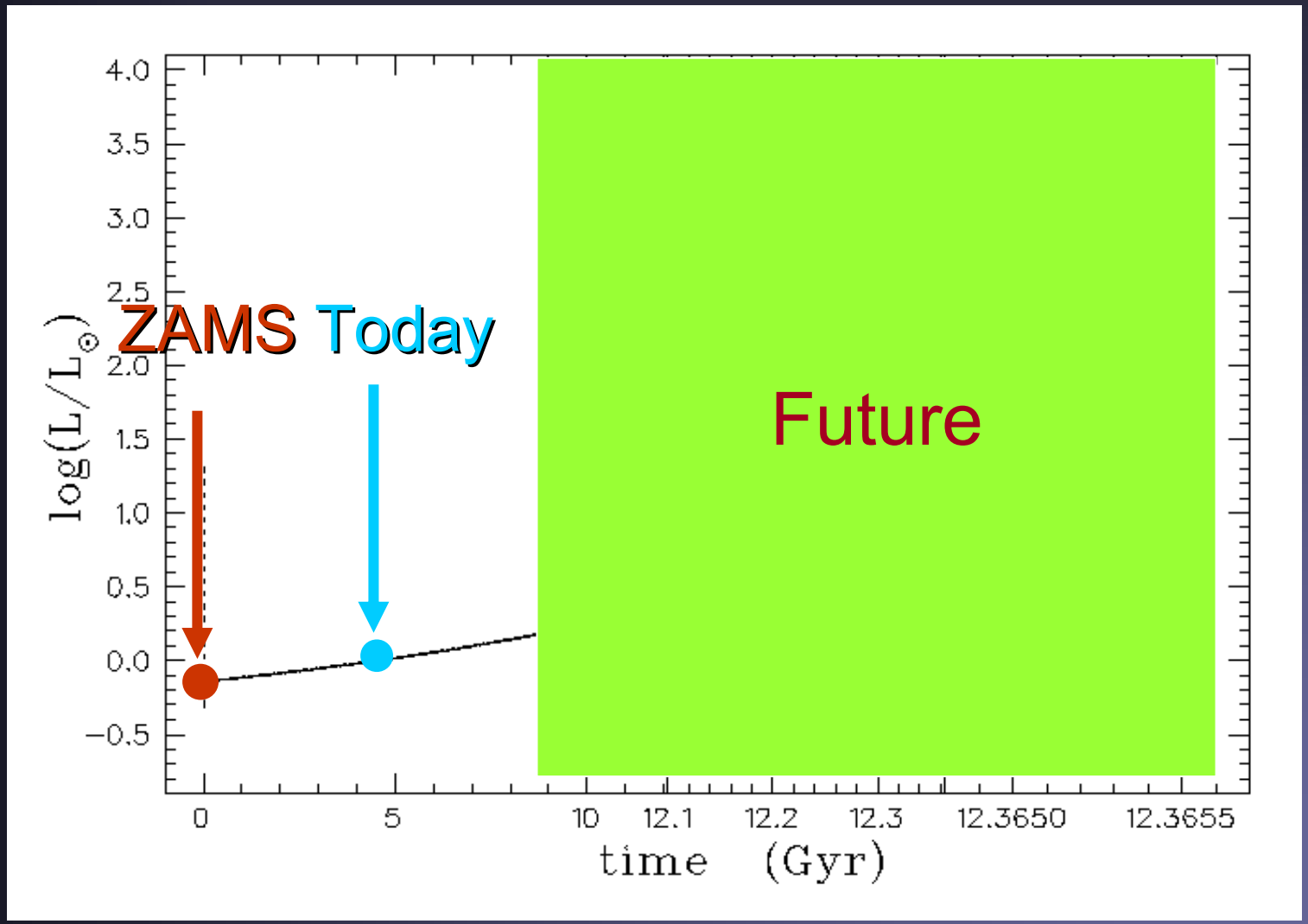

Faint young Sun paradox

- According to the standard solar model the Sun was approximately 30% less bright at birth than it is today
- Too faint to keep the Earth free of ice!
- Problem: Life started at the Earth's surface at least 3.5Million years ago
- Obviously the Earth was not covered with ice at that time
- So what is the solution?

- This and next 4 slides kindly provided by Piet Martens

A Faint Young Sun Leaves the Earth Frozen Solid

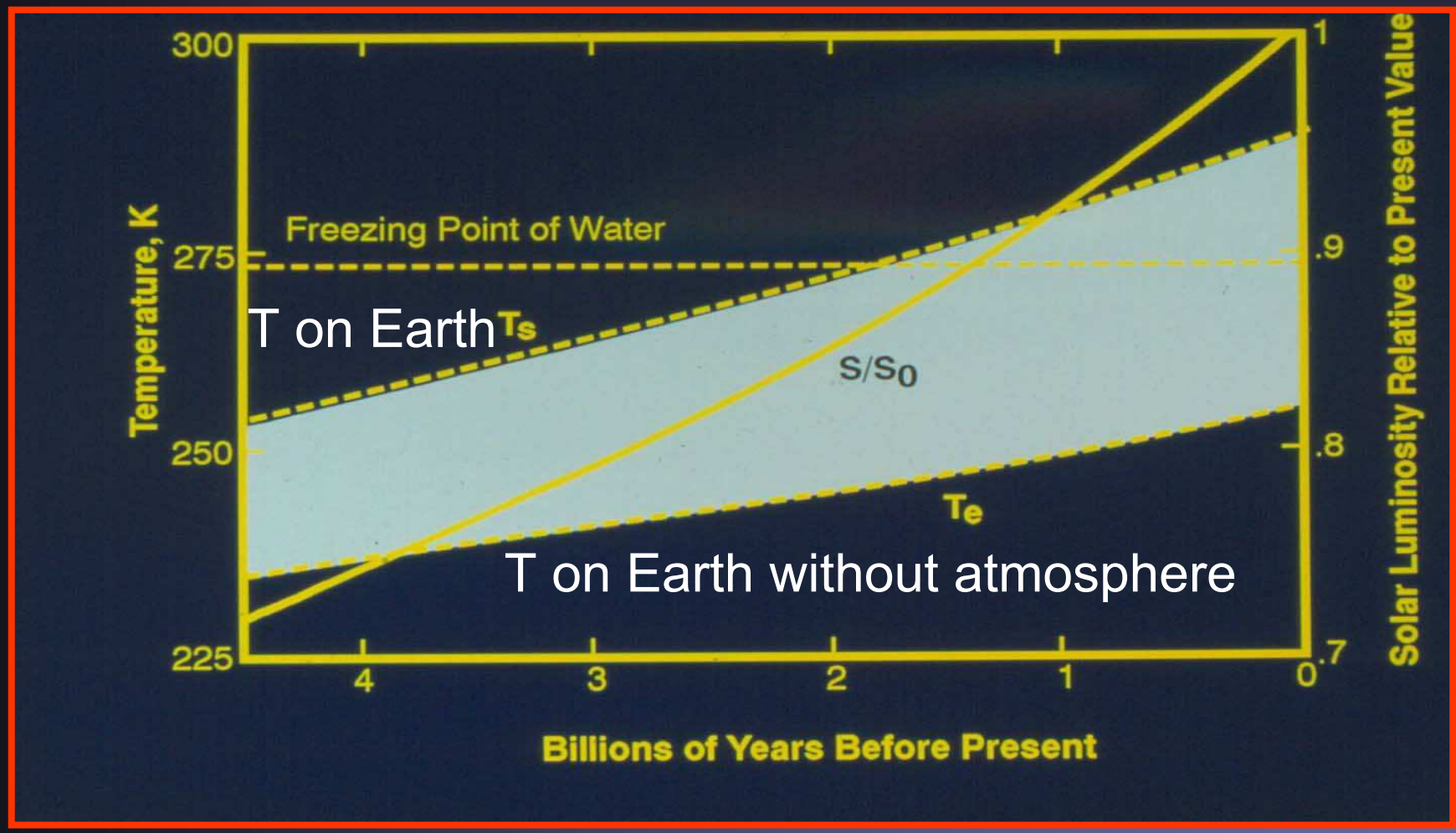

Kasting et al, Scientific American, 1988

Where to look for a solution?

- Astrophysical Solutions: Young Sun was not faint
- Eartly Earth Atmosphere: Much more greenhouse gases
- Geology: Much more geothermal energy
- Biology: Life developed on a cold planet
- Fundamental Physics: e.g., gravitational constant has varied

Was the young Sun really faint?

- Solar luminosity is a strong function of solar mass: $L_\odot \sim M_\odot^4$
- Planetary orbital distance varies inversely with solar mass: $a \sim M_\odot^{-1}$
- Solar flux varies inversely with orbital distance: $S \sim a^{-2}$
- Flux to the planets therefore goes as: $S \sim M_\odot^6$
- Even small increase in mass of young sun would have been enough to keep Earth (and Mars!) warm

Estimated mass loss rate vs. stellar age

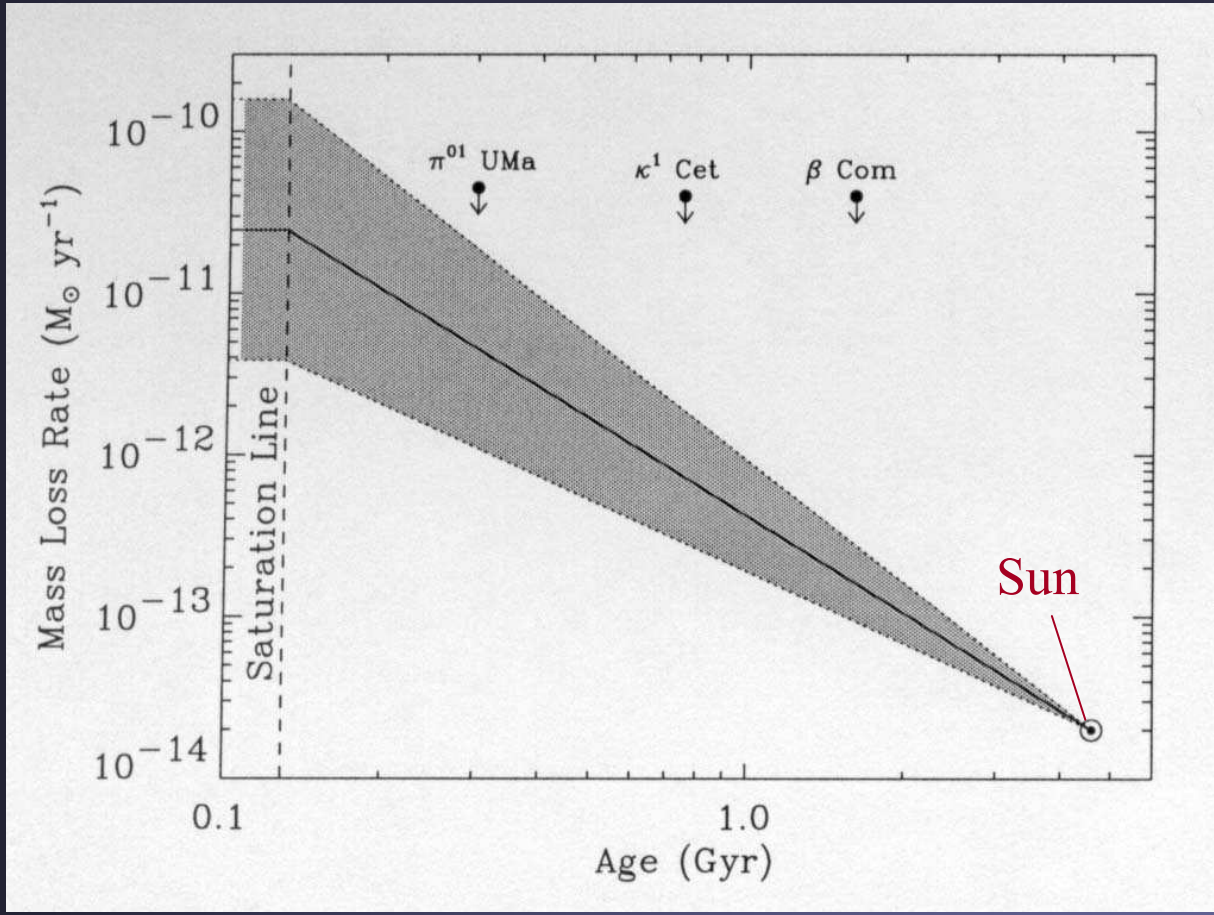

Wood et al. (2002)

Integrated mass loss vs. time

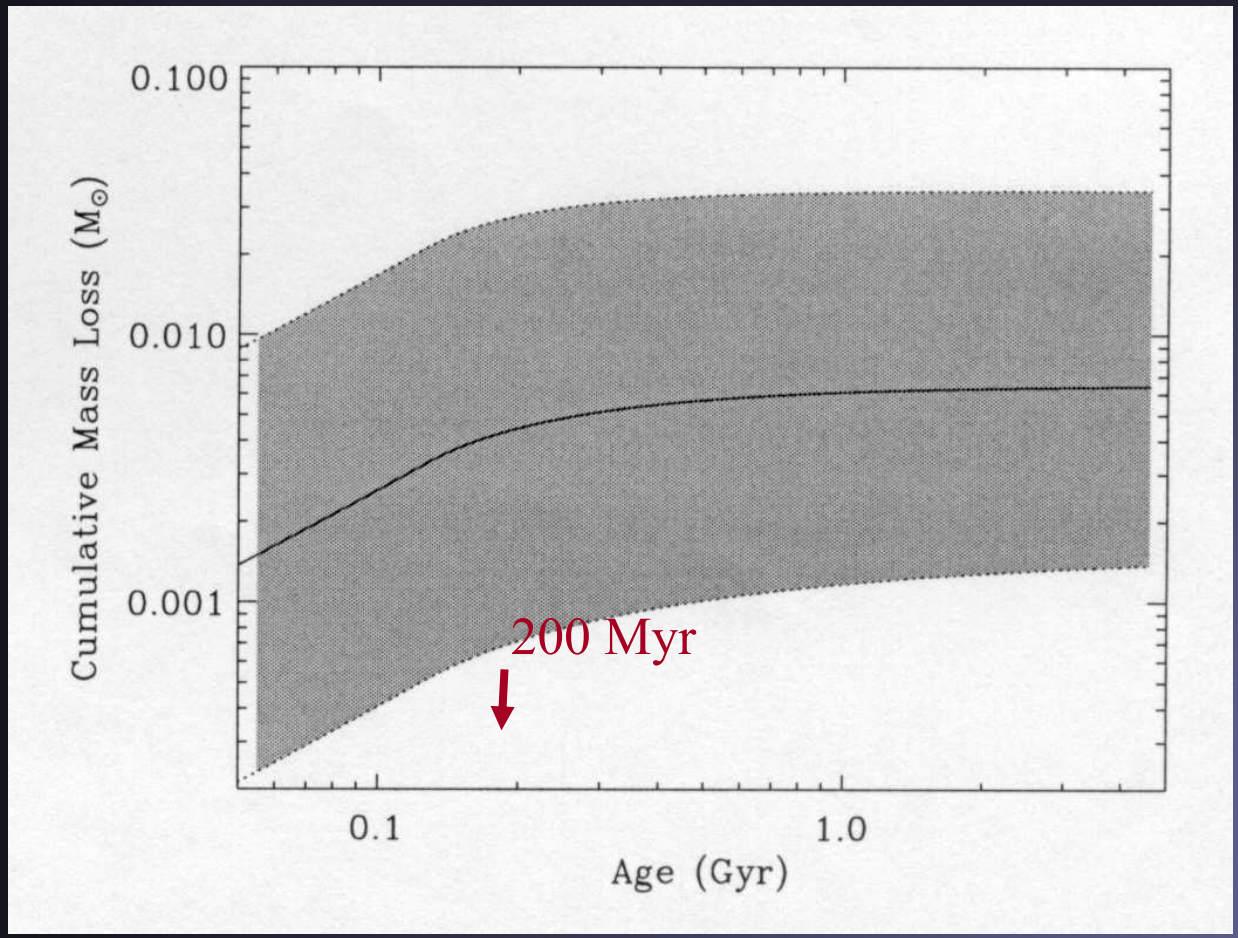

% Changes

Mass loss	ΔS
0.6	3.6
1.0	6.2
2.0	13
3.0	19

Wood et al. (2002)

⇒ The Sun was probably back on the standard solar evolution curve by ~4.4 Ga (*i.e.*, 4.4 Gyr ago)

Where we stand regarding the faint young Sun paradox

- Young Sun was probably less luminous, yet its UV, EUV and X-ray emission was an order of magnitude larger (could that have changed the Earth's atmospheric chemistry & thus the climate?)
- Young Earth was probably warmer than today, and single-cell organisms were present from very early on
- No silver bullet has devised yet to reconcile these results

… and the future?

- Sun will continue to grow **brighter...** and **bigger**, first gradually, then rapidly.
- It will get 4000 times brighter than today!
- Will the Sun eventually cook the Earth, even evaporate it? When will it become too hot for life?

Evolution of solar luminosity

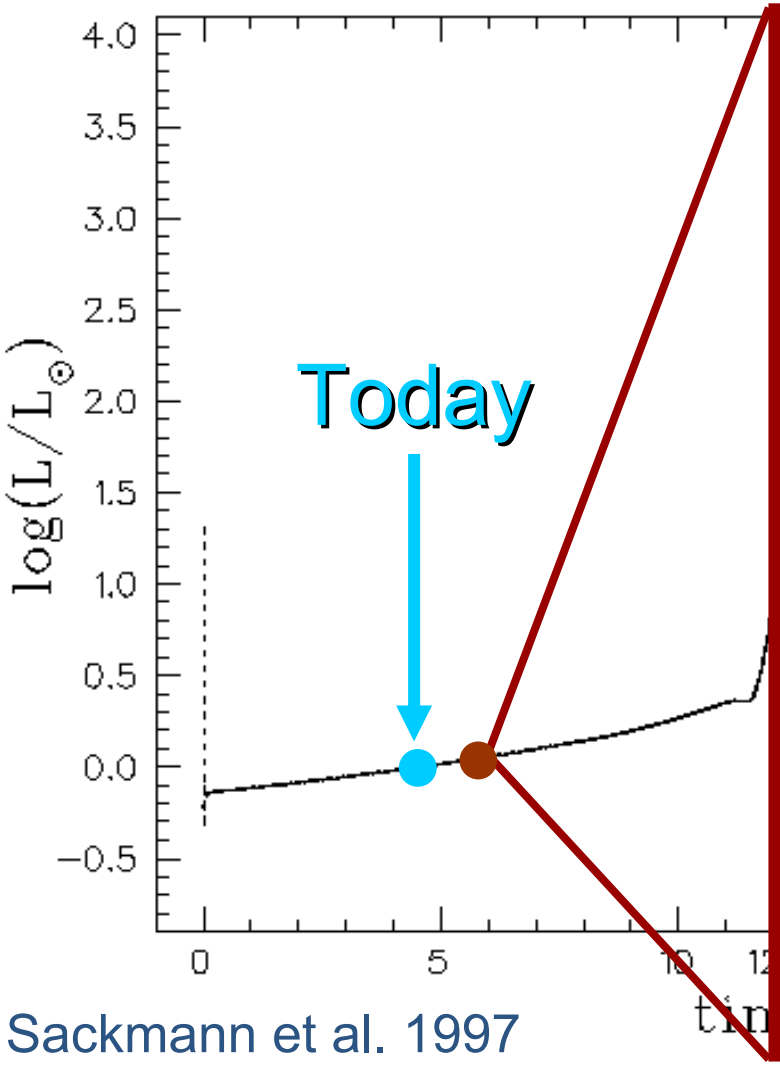

Sackmann et al. 1997

… and the future?

- Sun will continue to grow **brighter...** and **bigger**, first gradually, then rapidly.
- It will get 4000 times brighter than today!
- Will the Sun eventually cook the Earth, even evaporate it? When will it become too hot for life?
- It will eventually be so bloated that it will extend up to today's orbit of Earth!
- Will the Sun eventually swallow the Earth?

Will the Sun swallow the Earth?

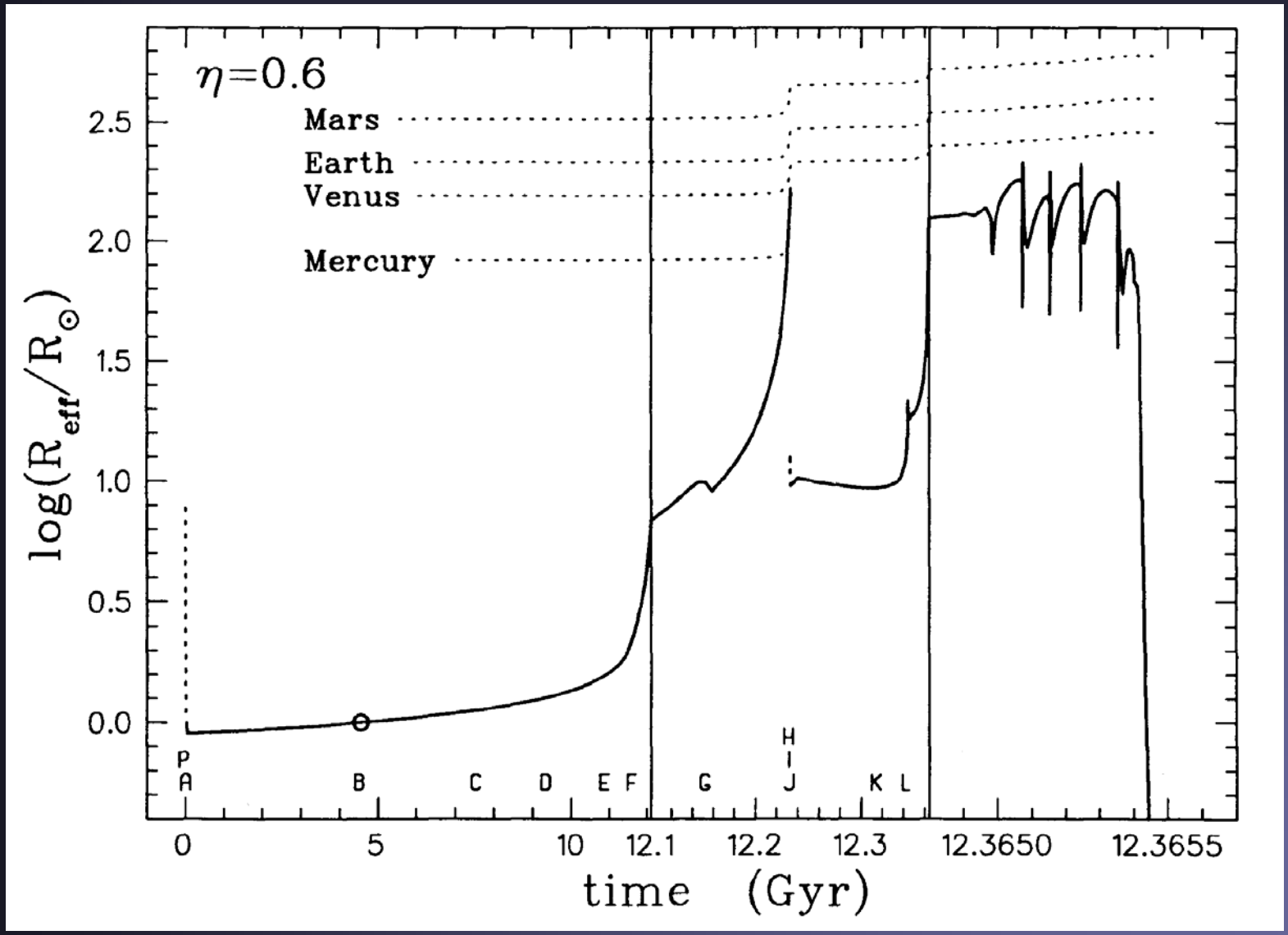

Will the Earth really get away unharmed?

Oscillations and helioseismology

5-minute oscillations

- Entire Sun vibrates from a complex pattern of acoustic waves (called p-modes), with a period of around 5 minutes
- The oscillations are best seen as Doppler shifts of spectral lines, but are also visible as intensity variations.
- Spatio-temporal properties of oscillations best revealed by 3-D Fourier transforms (2-D space + 1-D time)

Hear the Sun sing!

Sound waves speeded up 42,000 times

Doppler shift

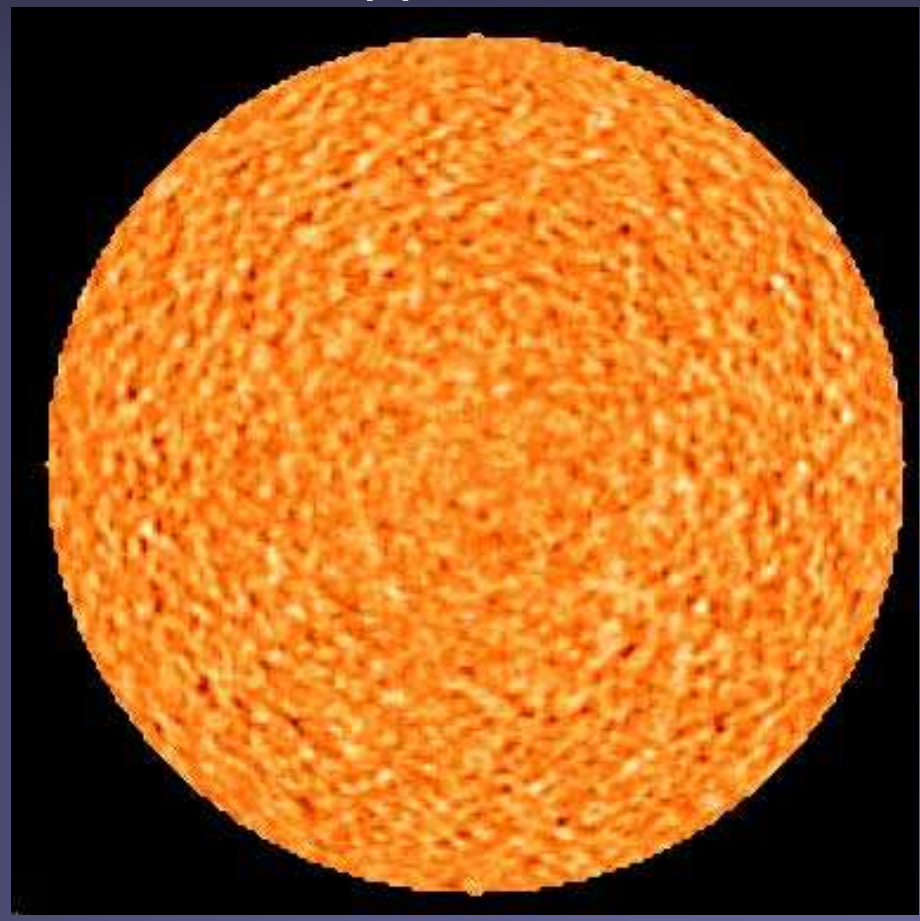

Solar Eigenmodes

- p-modes show a distinctive dispersion relation (k-ω diagram: $k \sim \omega^2$)
- Important: there is power only in certain ridges, i.e. for a given k^2 ($= k_x^2 + k_y^2$), only certain frequencies contain power.
- This discrete spectrum suggests the oscillations are trapped, i.e. eigenmodes of the Sun.

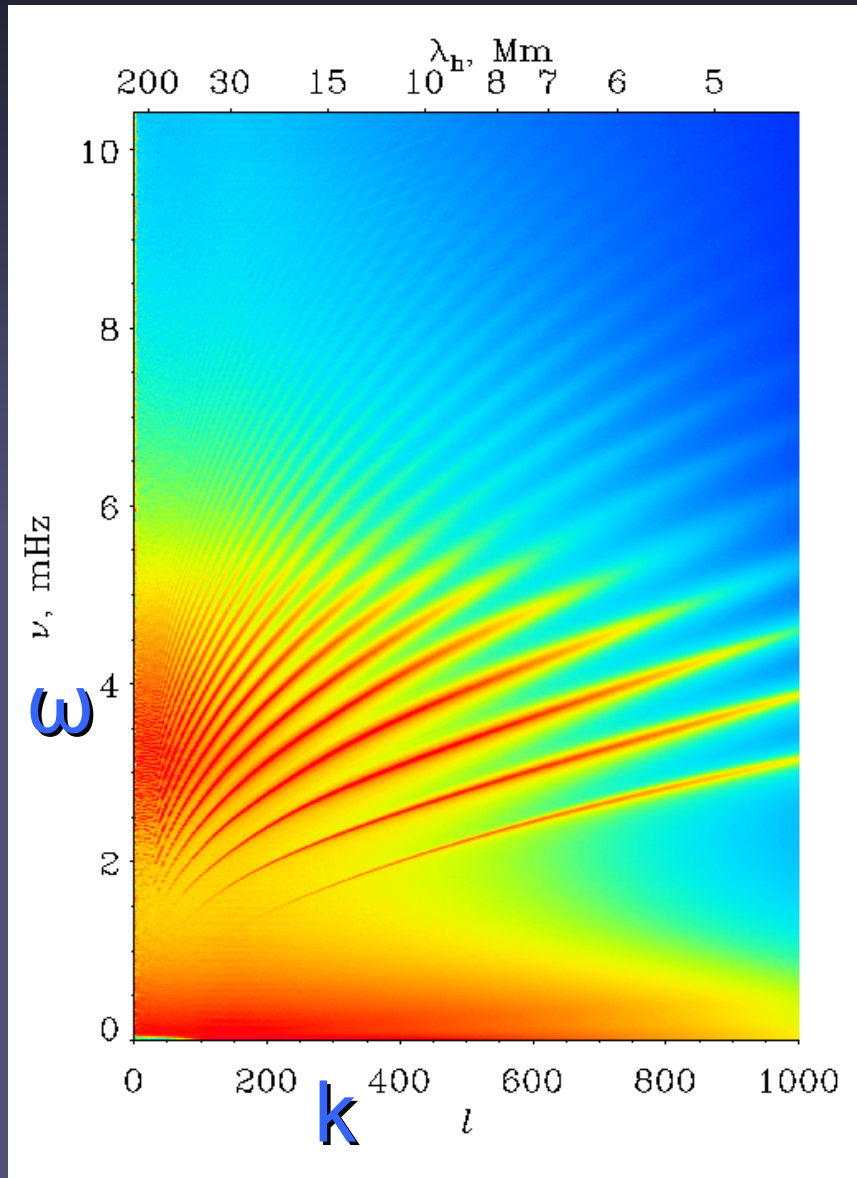

Global oscillations

- Sun's acoustic waves bounce (are reflected) at the solar surface, causing it to oscillate up and down.
- Modes differ in the depth to which they penetrate: they turn around due to refraction: because sound speed ($C_S \sim T^{1/2}$) increases with depth
- p-modes are influenced by conditions inside the Sun. E.g. they carry info on sound speed ~ $T^{1/2}$
- By observing these oscillations on the surface we can learn about the structure of the solar interior

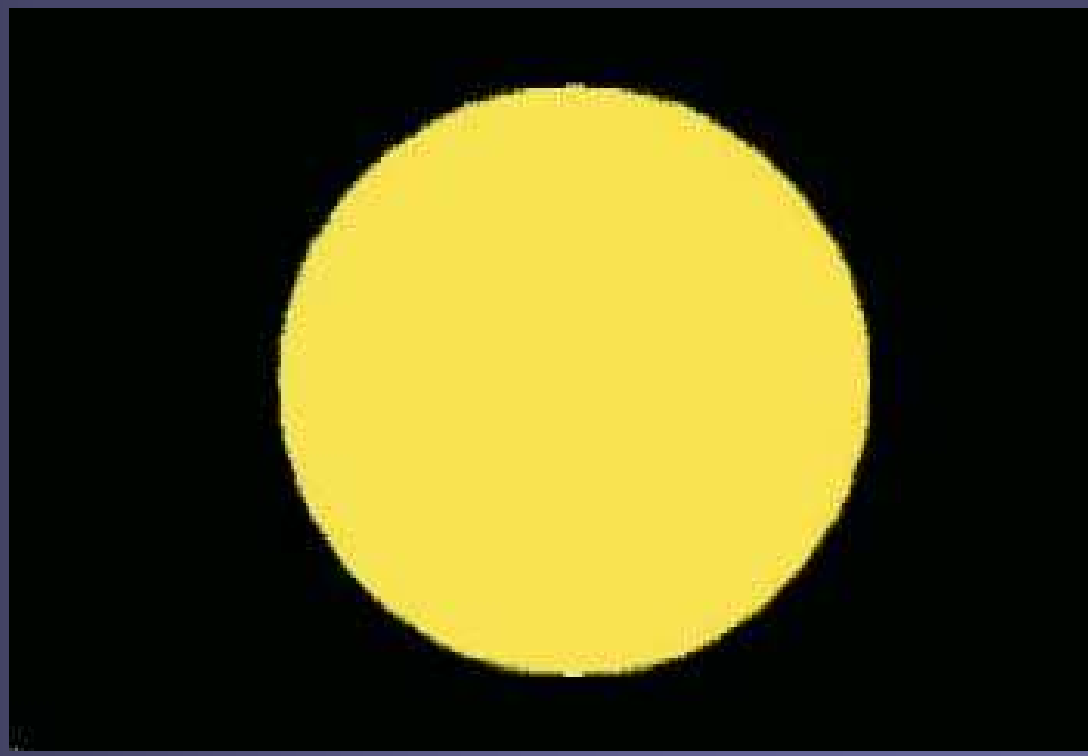

Description of solar eigenmodes

- Eigen-oscillations of a sphere are described by spherical harmonics
- Each oscillation mode is identified by a set of three parameters:
  - n = number or radial nodes
  - l = number of nodes on the solar surface
  - m = number of nodes passing through the poles (next slide)

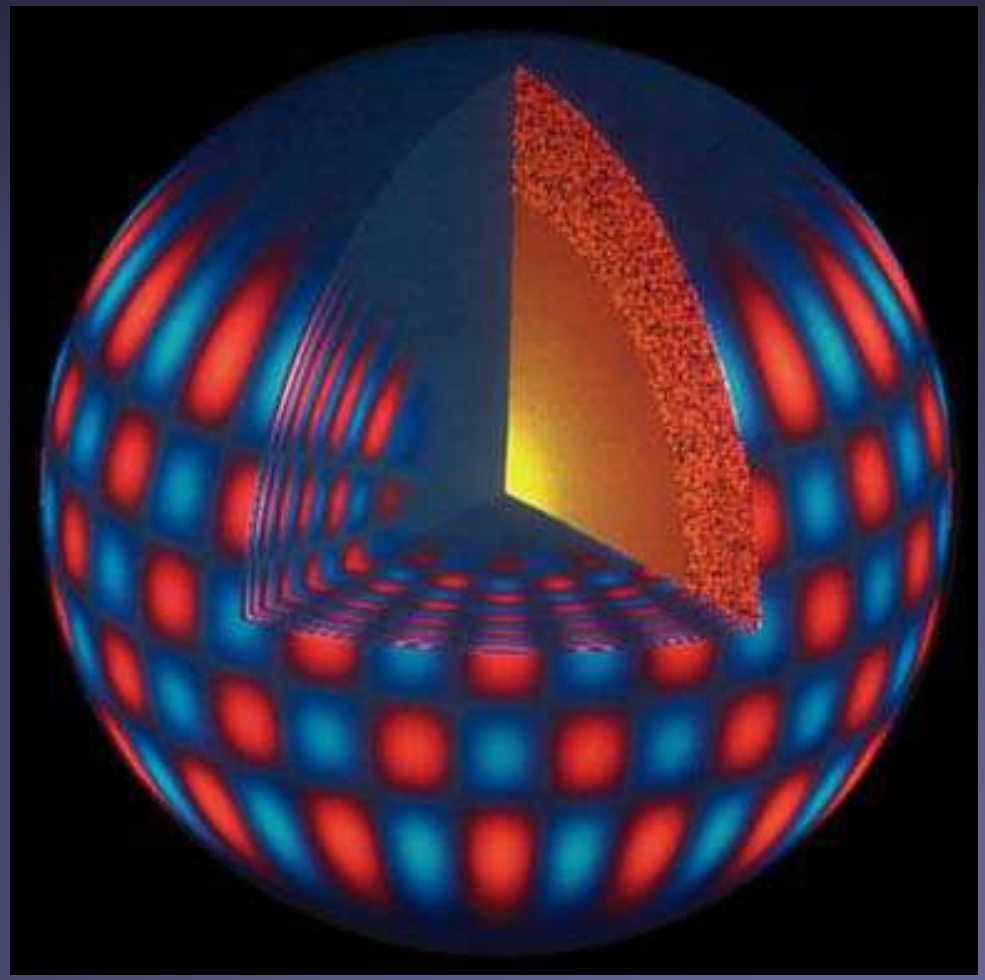

Illustration of spherical harmonics

- l = total number of nodes (in images: $l = 6$) = degree
- m = number of nodes connecting the “poles”

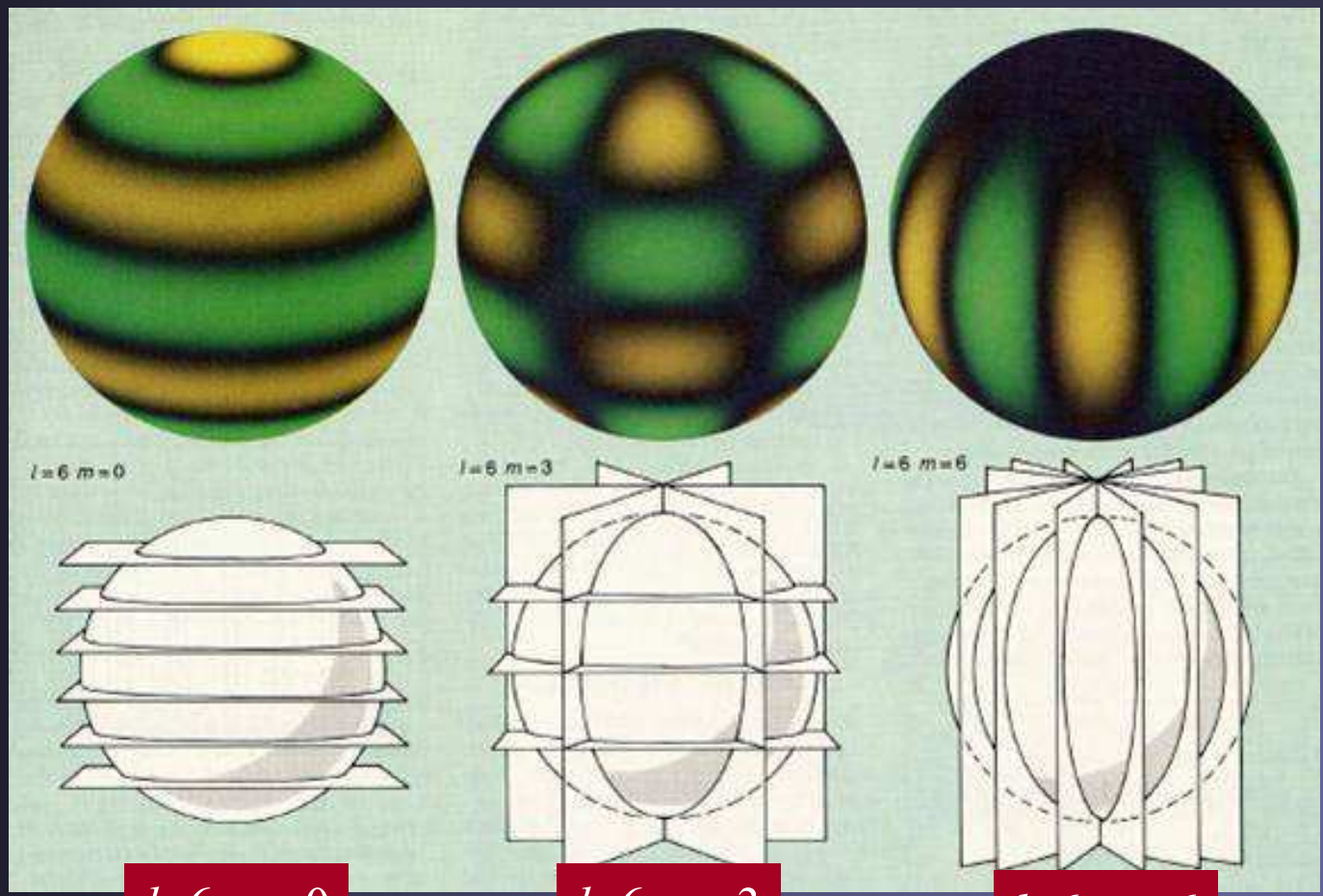

l=6, m=0 l=6, m=3 l=6, m=6

Spherical harmonics

- Let $v(\theta,\varphi,t)$ be the velocity, e.g. as measured at the solar surface over time t. Then:

$$v(\theta,\varphi,t) = \sum_{l=0}^{\infty} \sum_{m=-l}^{l} a_{lm}(t)\, Y_l^m(\theta,\varphi)$$

- The temporal dependence lies in a_{lm}, the spatial dependence in the spherical harmonic Y_l^m.

$$Y_l^m(\theta,\varphi) = P_l^{|m|}(\theta)\exp(im\varphi)$$

$$P_l^{|m|}(\theta) = \text{associated Legendre Polynomial}$$

- Due to the normalization of the spherical harmonic, the Fourier power is given by $F(a)F(a)^*$
- Here $F(a)$ is the Fourier transform of the amplitude $a_{lm,}$ and $F(a)^*$ is its complex conjugate

More examples and a problem with identifying spherical harmonics

- General problem: Since we see only half of the Sun, the decomposition of the sum of all 10^7 oscillations into spherical harmonics isn't unique.
- This results in an uncertainty in the deduced l and m

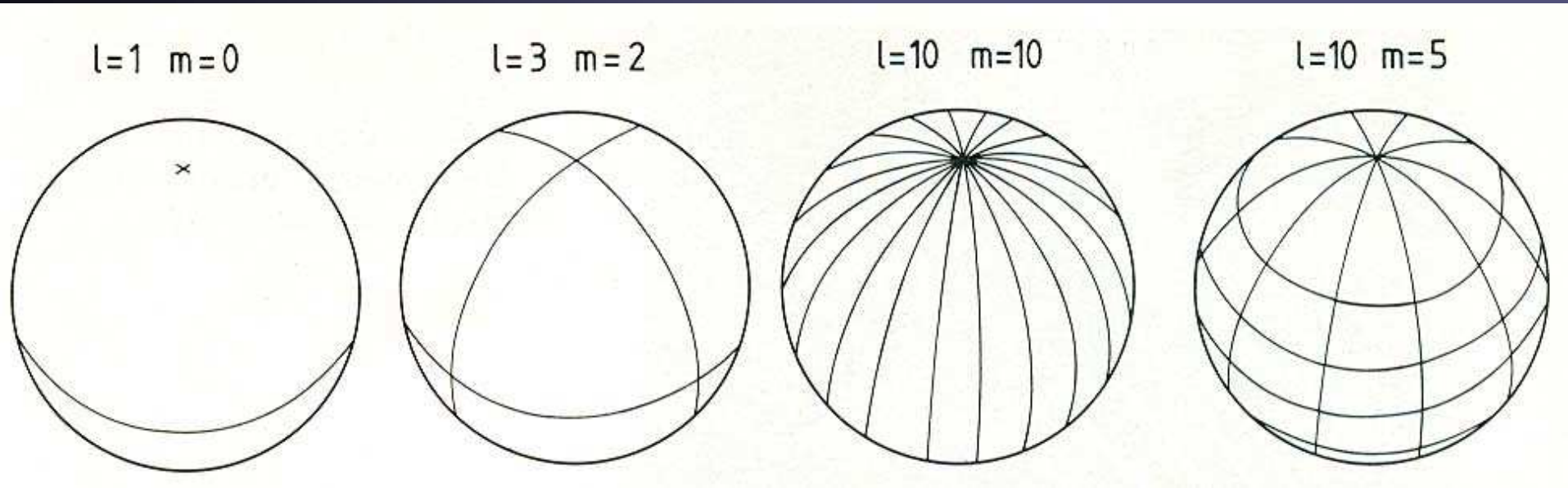

Interpretation of k-ω or ν-l diagram

- At a fixed l, different frequencies show significant power. Each of these power ridges belongs to a different order n (n = number of radial nodes), with n increasing from bottom to top.
- Typical are small values of n, but intermediate to large degree l (100-1000; with some spatial resolution dependence)

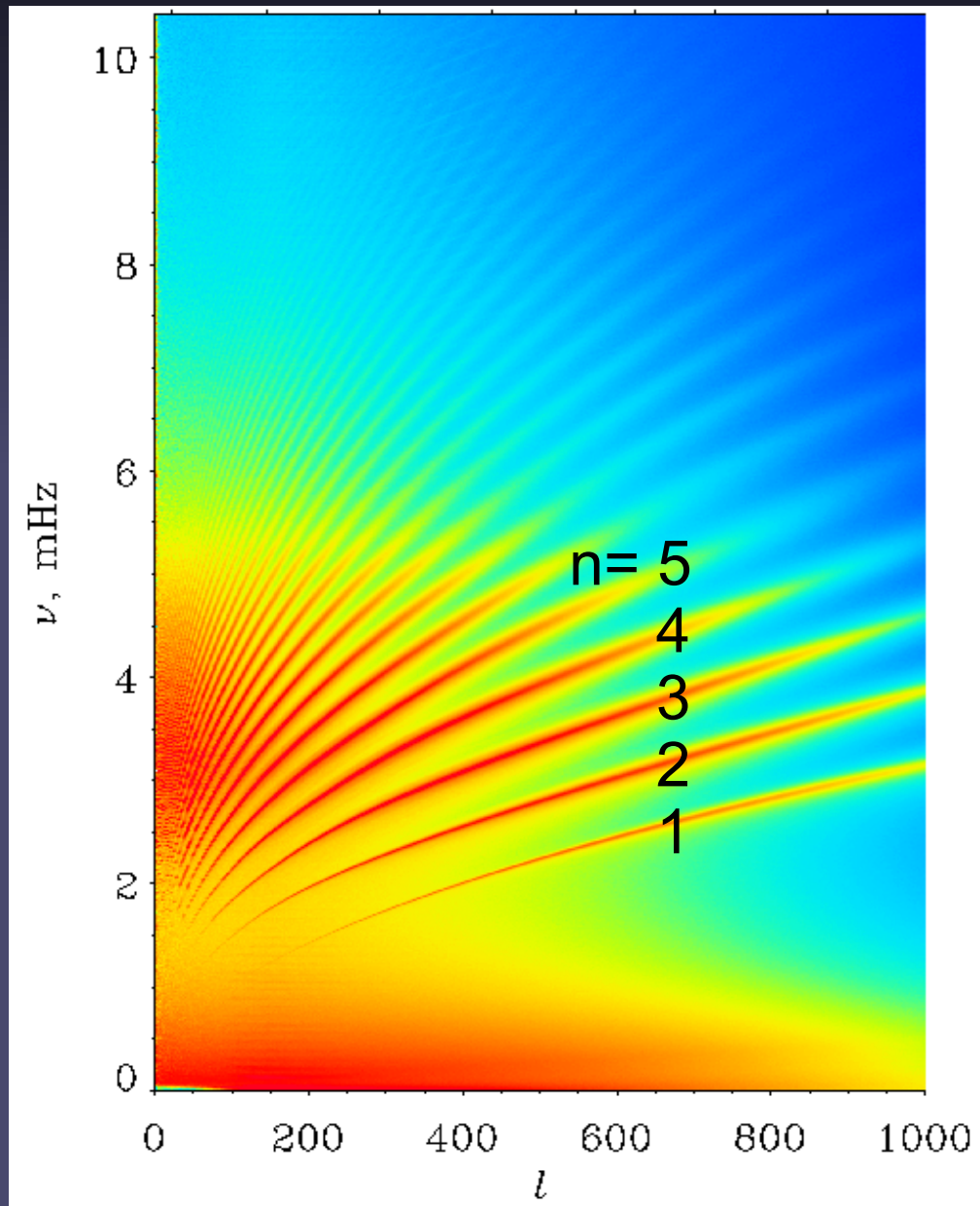

A few observational remarks

- 10^7 modes are present on the surface of the Sun at any given time (all interfering linearly with each other).
- Typical amplitude of a single mode: < 20 cm/s
- Total velocity of all 10^7 modes: a few 100 m/s
- Accuracy of current instruments: better than 1 cm/s
- Frequency resolution ~ length of time series (Heisenberg's uncertainty principle) ~ lowest detectable frequency

→ Longer time series are better (even longer than maximum mode lifetime of a few weeks - months).

- Gaps in time series produce side lobes (i.e. spurious peaks in the power spectrum) → best are uninterrupted obs.
- Highest detectable frequency ~ cadence of obs.

Accuracy of frequency measurements

- Plotted are identified frequencies and error bars (yellow). They correspond to 1000σ for blue freq., 100σ for red freq. below 5 mHz and 1σ for higher freq.)
- Best achievable freq. resolution: a few parts in 10^5; limit set by mode lifetime ~100 d

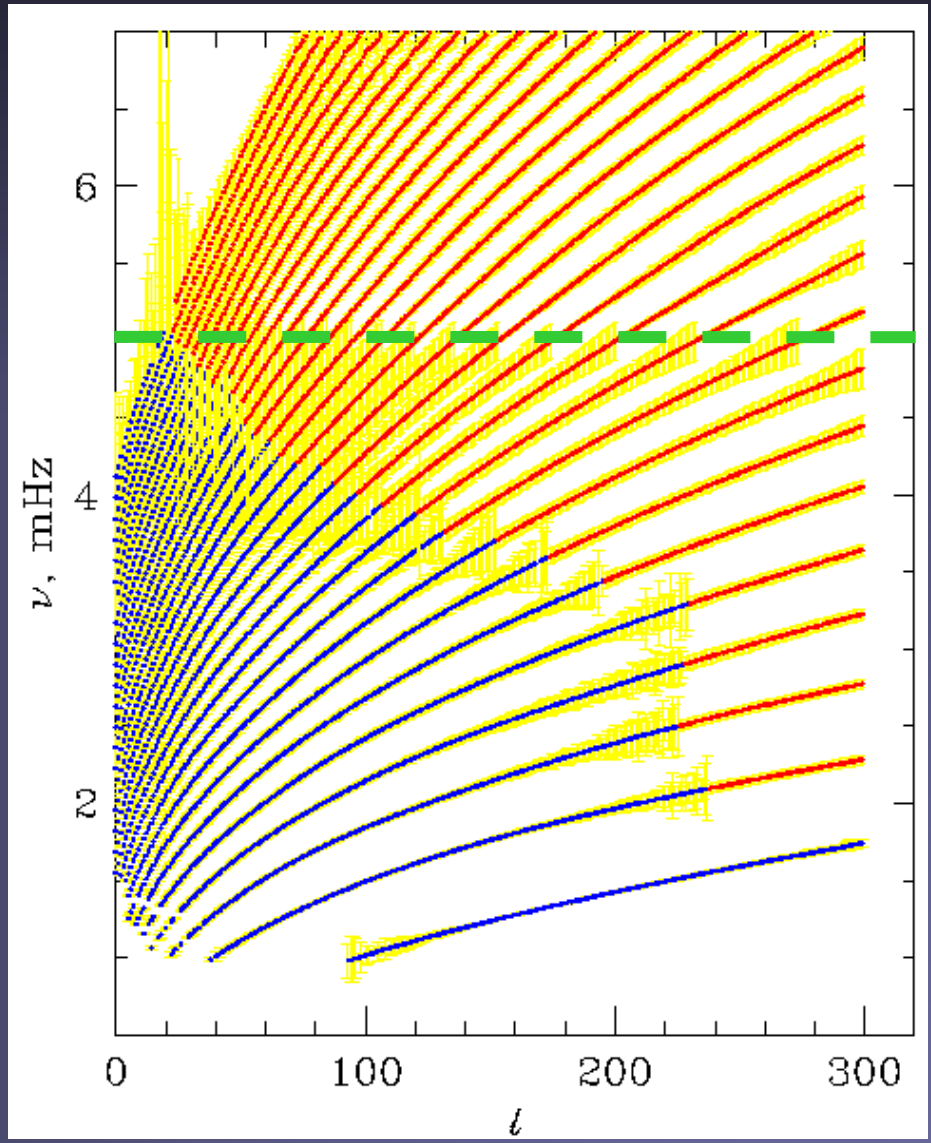

Frequency vs. amplitude

- Frequencies are the important parameter, more so than amplitudes of modes or of power peaks.
- Frequencies are more constant & are measured with greater accuracy.
- Amplitudes depend on the excitation, while the frequencies do not. They carry the main information on the structure of the solar interior.
- p-modes are excited by turbulence, which excites all frequencies. At eigenfrequencies of the Sun the modes reach large amplitudes (eigenmodes), at other frequencies they decay quickly.

The measured low-l eigenmode signal

- Sun seen as a star: Due to cancellation effects, only modes with l=0,1,2 are visible ➔ simpler power spectrum.
- Low l modes are important for 2 reasons:
  - They reach particularly deep into the Sun (see cartoon on earlier slide).
  - These are the only modes measurable on other Sun-like stars.
- These modes are sometimes called “global” modes.

Best current low-l power spectrum

Given l has different peaks: different n values (n=15...25 typical)

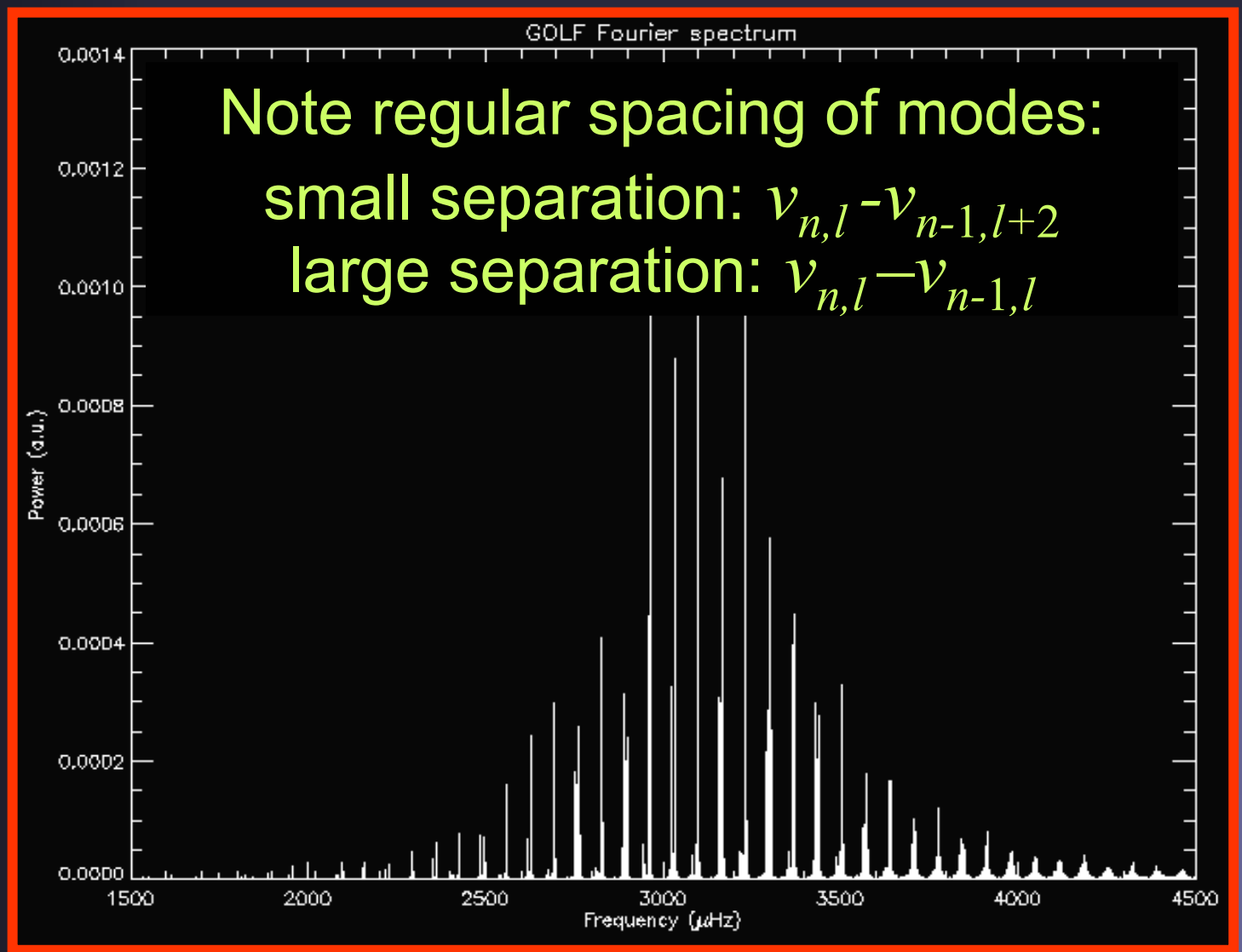

Mode structure of low-l spectrum

- GOLF/SOHO observations showing a blowup of the power spectrum with an $l = 0$ and an $l = 2$ mode.
- The noise is due to random re-excitation of the oscillation mode by turbulence

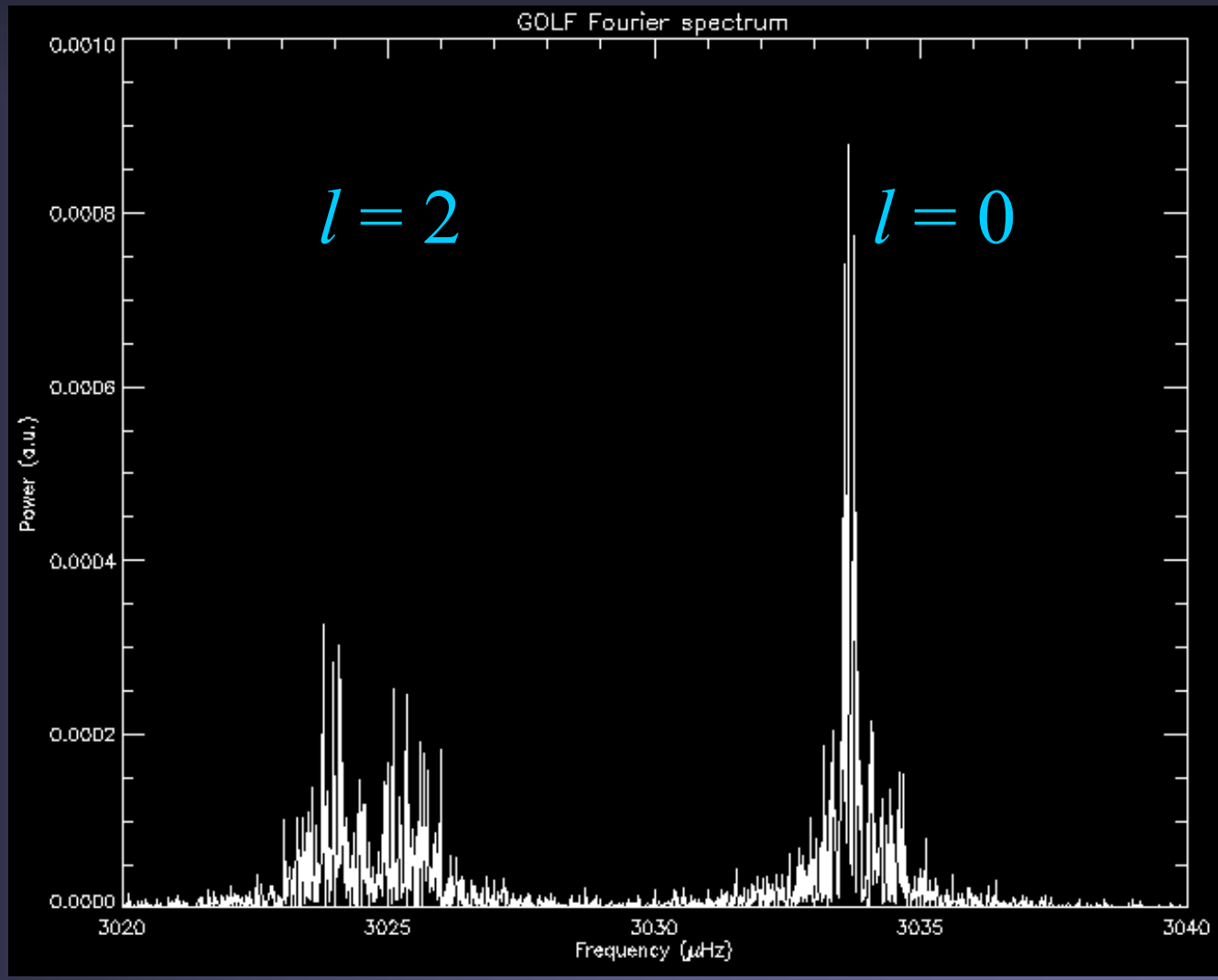

Types of oscillations

- Solar eigenmodes can be of 2 types:
  - p-modes, where restoring force is pressure, i.e. normal sound waves
  - g-modes, where the restoring force is gravity (also called buoyancy modes)
- So far only p-modes have been detected on the Sun with certainty.
- They are excited by the turbulence associated with the convection, mainly the granulation near the solar surface (since there the convection is most vigorous).
- Being p-modes, they travel with the sound speed C_S. They dwell longest where C_S is lowest. Since $C_S \sim T^{1/2}$, this is at the solar surface.

p-modes vs. g-modes

- p-modes propagate throughout the solar interior, but are evanescent (later slide) in the solar atmosphere
- g-modes propagate in the radiative interior and in the atmosphere, but are evanescent in the convection zone (their amplitude drops exponentially there, so that very small amplitudes are expected at the surface). Convection means buoyancy instability (density blobs keep rising or falling); gravity-based oscillations require stability (density blobs oscillate)
- g-modes are expected to be most sensitive to the very core of the Sun, while p-modes are most sensitive to the surface
- Current upper limit on solar interior g-modes lies below 1 cm/s.

Solar oscillations: simple treatment

- Equations describing radial structure of adiabatic oscillations, neglecting any perturbations to the gravitational potential, are:

$$\frac{1}{r^2}\frac{d}{dr}(r^2\xi_r) - \frac{\xi_r}{c^2} + \frac{1}{\rho_0}\left(\frac{1}{c^2} - \frac{l(l+1)}{r^2\omega^2}\right)P_1 = 0$$

$$\frac{1}{\rho_0}\frac{dP_1}{dr} + \frac{g}{\rho_0 c^2}P_1 - \left(\omega^2 - N^2\right)\xi_r = 0$$

$$\text{where } N^2 = g\left(\frac{1}{\Gamma P_0}\frac{dP}{dr} - \frac{1}{\rho_0}\frac{d\rho_0}{dr}\right) = \text{Brunt - Vaisala frequency}$$

- Here ξ_r is radial displacement and P_1 is pressure perturbs. Quantities with subscript 0 refer to the unperturbed Sun. Γ is the adiabatic exponent: $\Gamma = \left(\frac{d\ln P}{d\ln \rho}\right)$

Solar oscillations: simplified treatment II

- Analytical solutions of these equations for an isothermal atmosphere are readily obtained:

$$\xi_r(r) \sim \rho_0^{-1/2} \exp(ik_r r)$$

$$P_1(r) \sim \rho_0^{1/2} \exp(ik_r r)$$

- These oscillations are trapped in the body of the Sun. Since the time scale on which the atmosphere reacts to disturbances is low, waves which are travelling in the solar interior are evanescent in the atmosphere → They are present only for discrete frequencies (similar to the bound states in atomic physics).

Regimes of oscillation

- In regimes of acoustic and gravity waves $k_r^2 > 0$, while in regime of evanescent waves $k_r^2 < 0$ (exponential damping). The solid lines show $k_r^2 = 0$.
- Evanescent waves occur when the period is so long that the whole (exponentially stratified) medium has time to adapt to the perturbation, achieving a new equilibrium. Therefore the wave does not propagate, but rather the medium as a whole oscillates.

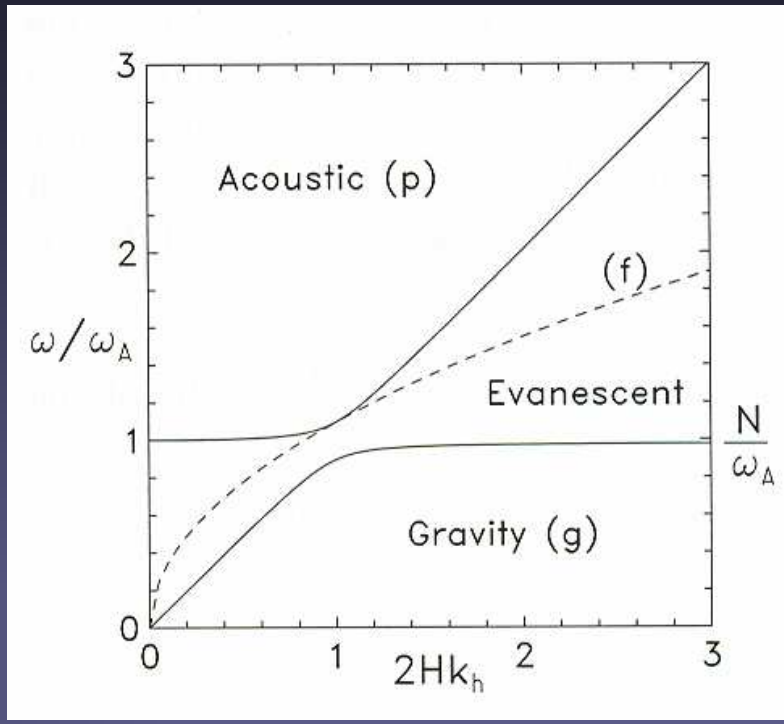

Cutoff frequency for acoustic waves in a stratified medium:

$$\omega_C = C_S/2H$$

Deducing internal structure from solar oscillations

- Global helioseismology: Gives mainly the radial dependence of solar properties, although latitudinal dependence can also be deduced.
  - Radial structure of sound speed
  - Structure of differential rotation (torsional velocities)
- Local helioseismology: Allows in principle 3-D imaging of solar interior. E.g. time-distance helioseismology does not measure frequencies, but rather the time that a wave requires to travel a certain distance (relatively new)

Global helioseismology

- Use frequencies of many modes.
- Basically two techniques for deducing information on the Sun's internal structure
  - Forward modelling: make a model of the Sun's internal structure (e.g. standard model discussed earlier), compute the frequencies of the eigenoscillations of the model and compare with observations
  - Inverse technique: Deduce the sound speed and rotation by inverting the oscillations (i.e. without any prior comparison with models)
- Note that forward modelling is required in order to first identify the modes. Only after that can inversions be carried out.

Testing the standard solar model: results of forward modelling

- Relative difference between C_S^2 obtained from inversions and from standard solar model plotted vs. radial distance from Sun centre.
- Typical difference: 0.002 ➔ good!
- Typical error bars from inversion: 0.0002 ➔ poor!
- Problem areas:
  - solar core
  - bottom of CZ
  - solar surface

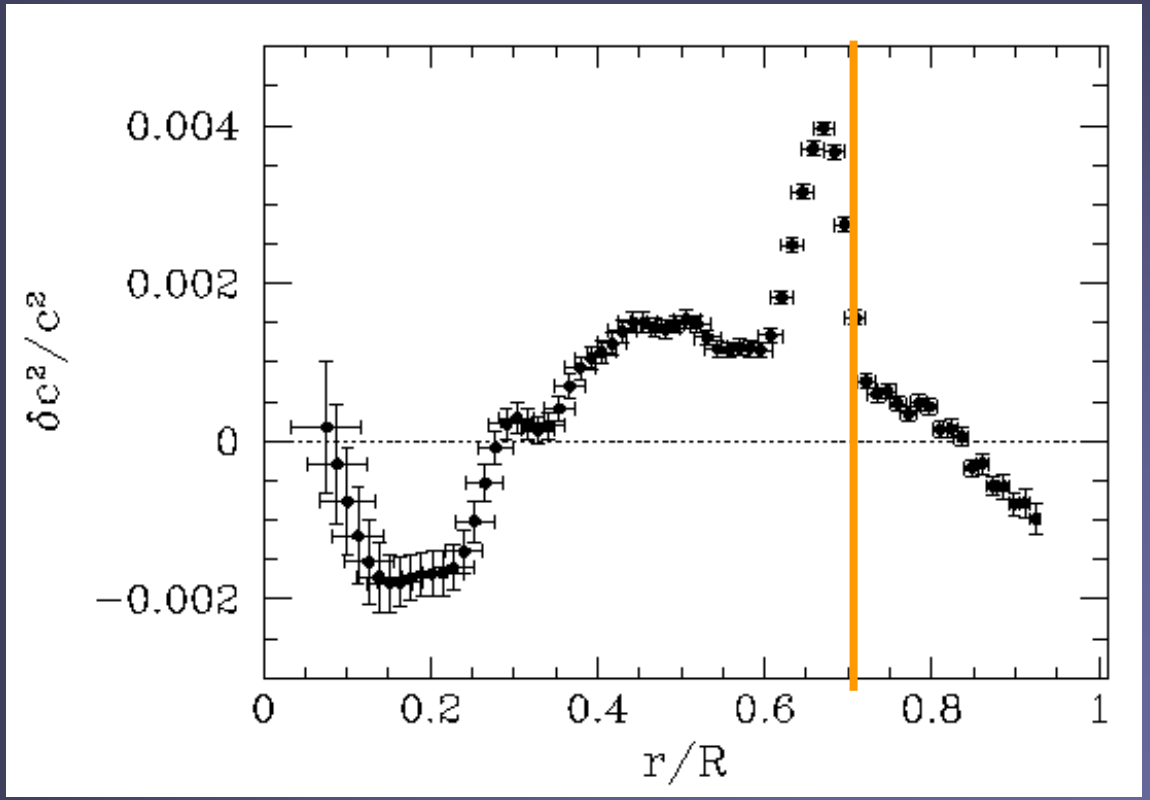

Variation of the solar rotation velocity with period of 1.3 years

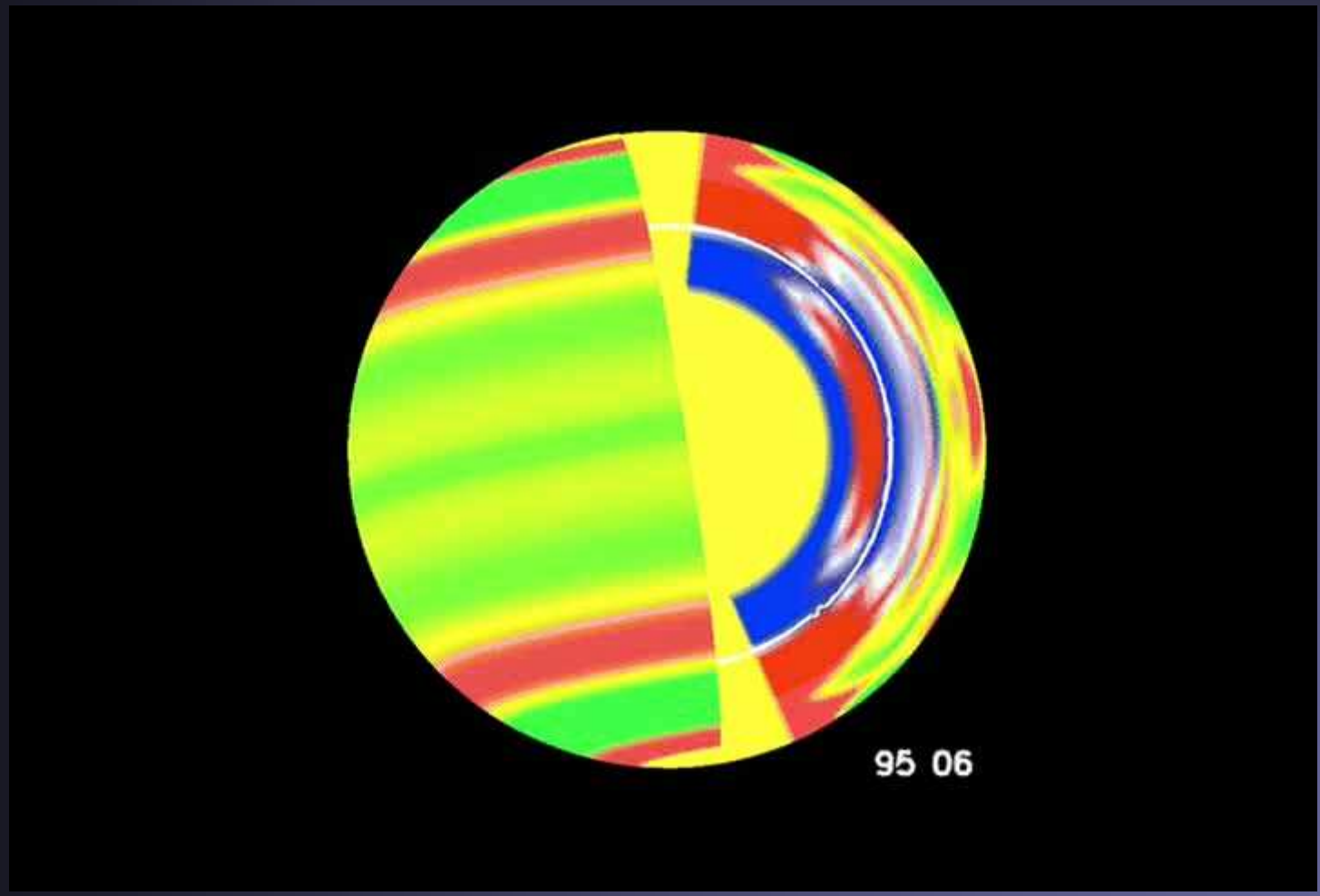

Local excitation of waves by a flare

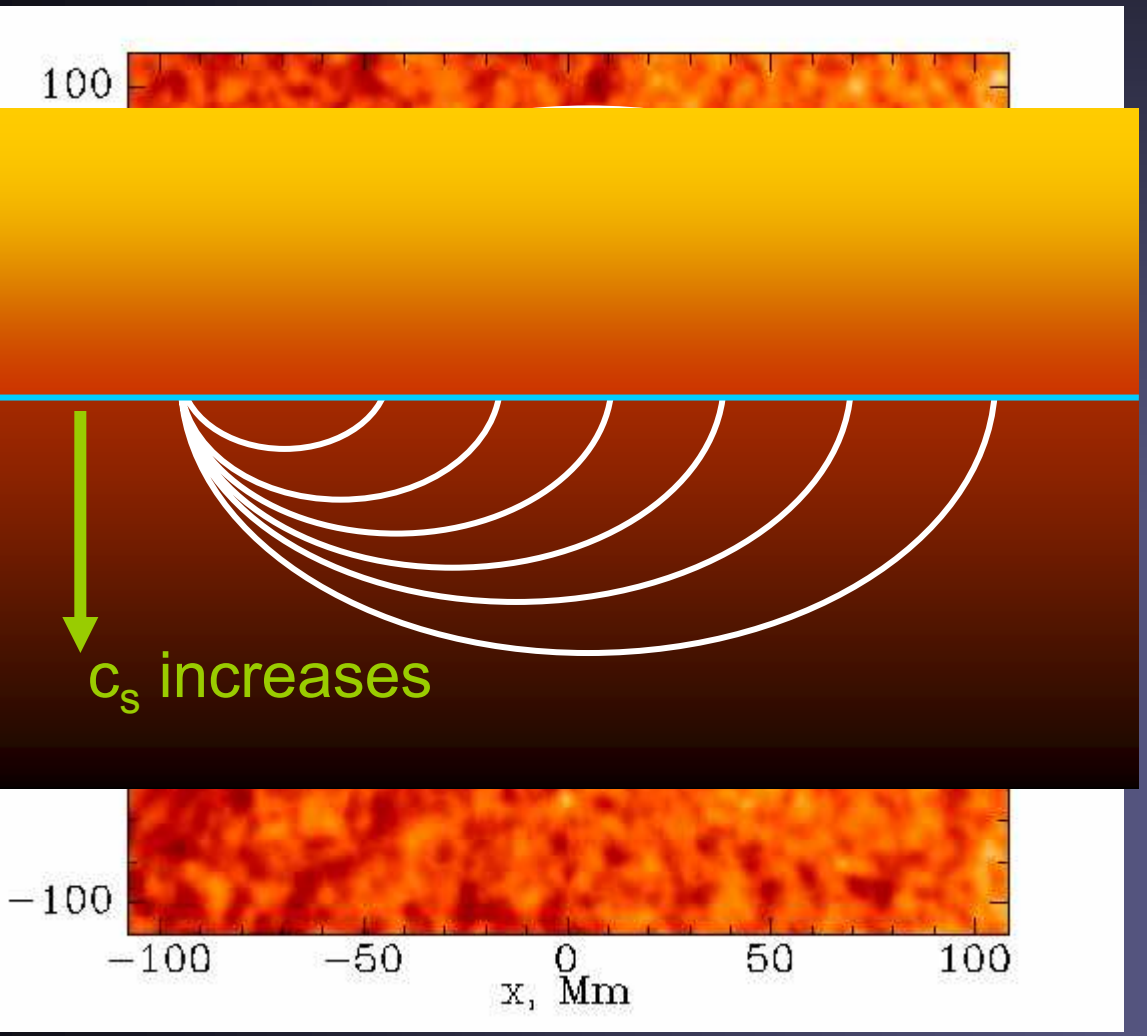

- Clear example of wave being triggered.
- The wave is not travelling at the surface, but rather reaching the surface further out at later times. Note how it travels ever faster. Why?

Local helioseismology

- Does not build upon measuring frequencies of eigenmodes, but rather measures travel times of waves through the solar interior, between two “bounces” at the solar surface (for particular technique of time-distance helioseismology).

- The travel time between source and first bounce depends on the structure of C_S below the surface. By considering waves following different paths inhomogeneous distributions of C_S can be determined.

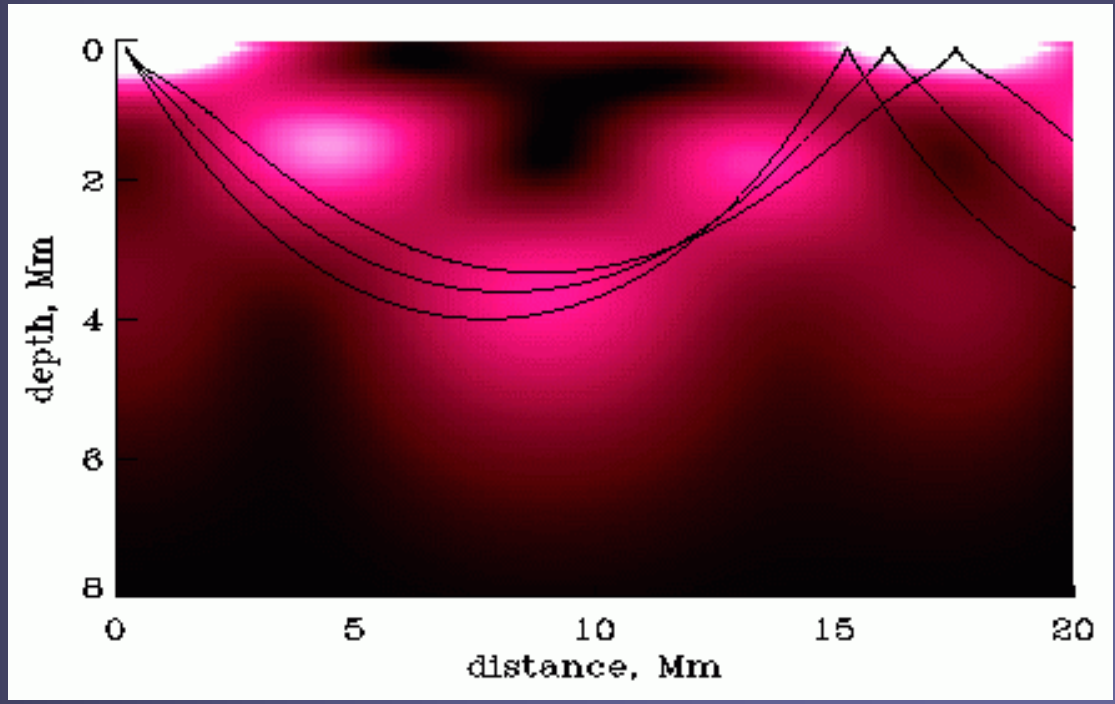

Local helioseismology II

- Distinguish temperature and velocity structures
  - a wave will propagate faster along a flow than against it.
  - By considering waves passing in both directions it is possible to distinguish between T and velocity.
- At right: 1st images of convection zone of a star

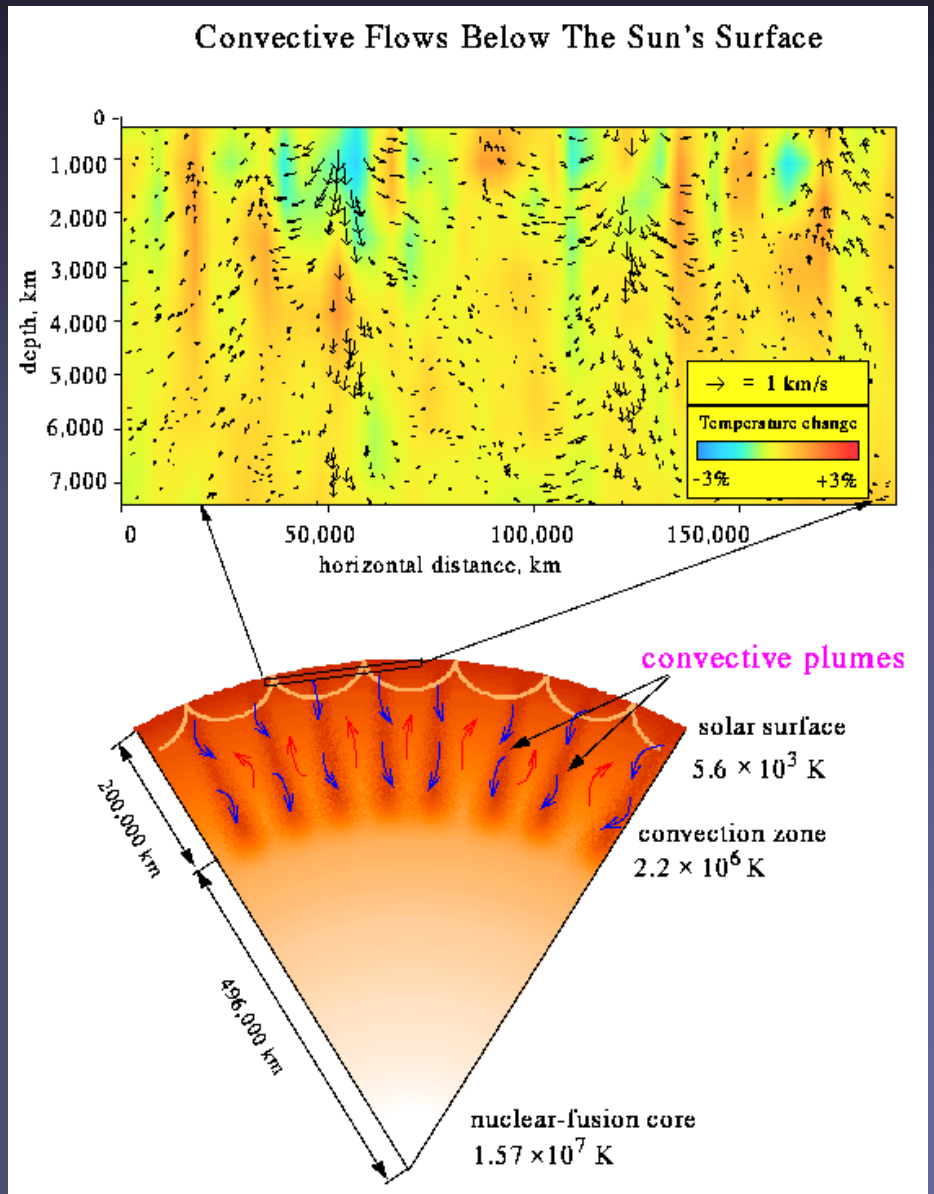

Time-Distance Helioseismology of a sunspot

- Subsurface structure of sunspots
- Sunspots are good targets, due to the large temperature contrast AND large B
- Early work neglected influence of magnetic field on waves!

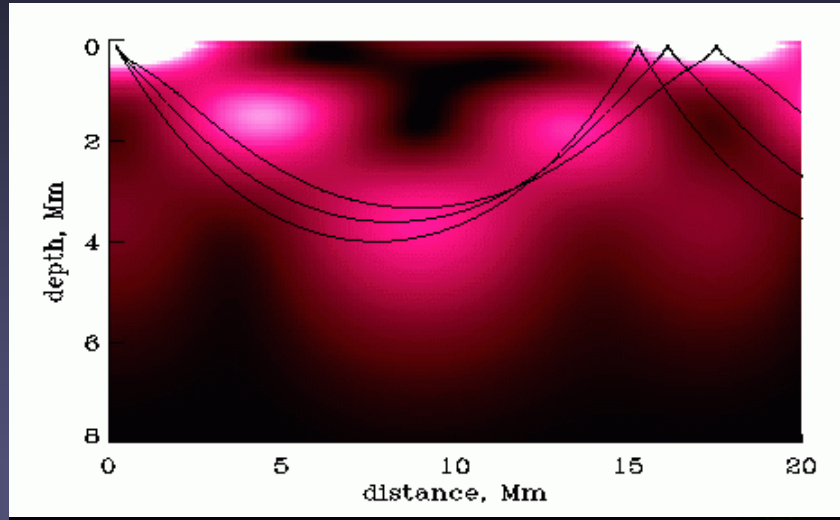

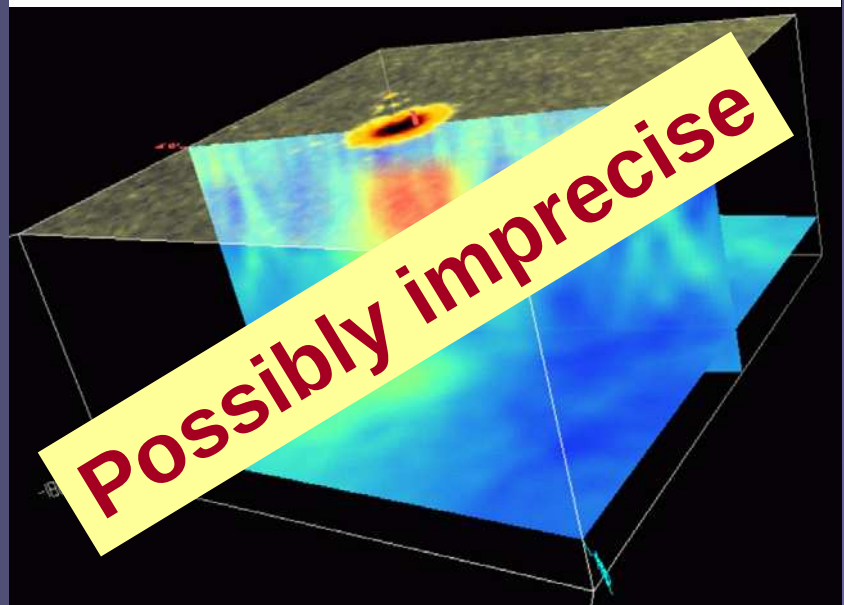

Wave-sunspot interaction: Comparison of simulations with observations

Top: observations (SOHO/MDI cross-covariance function)

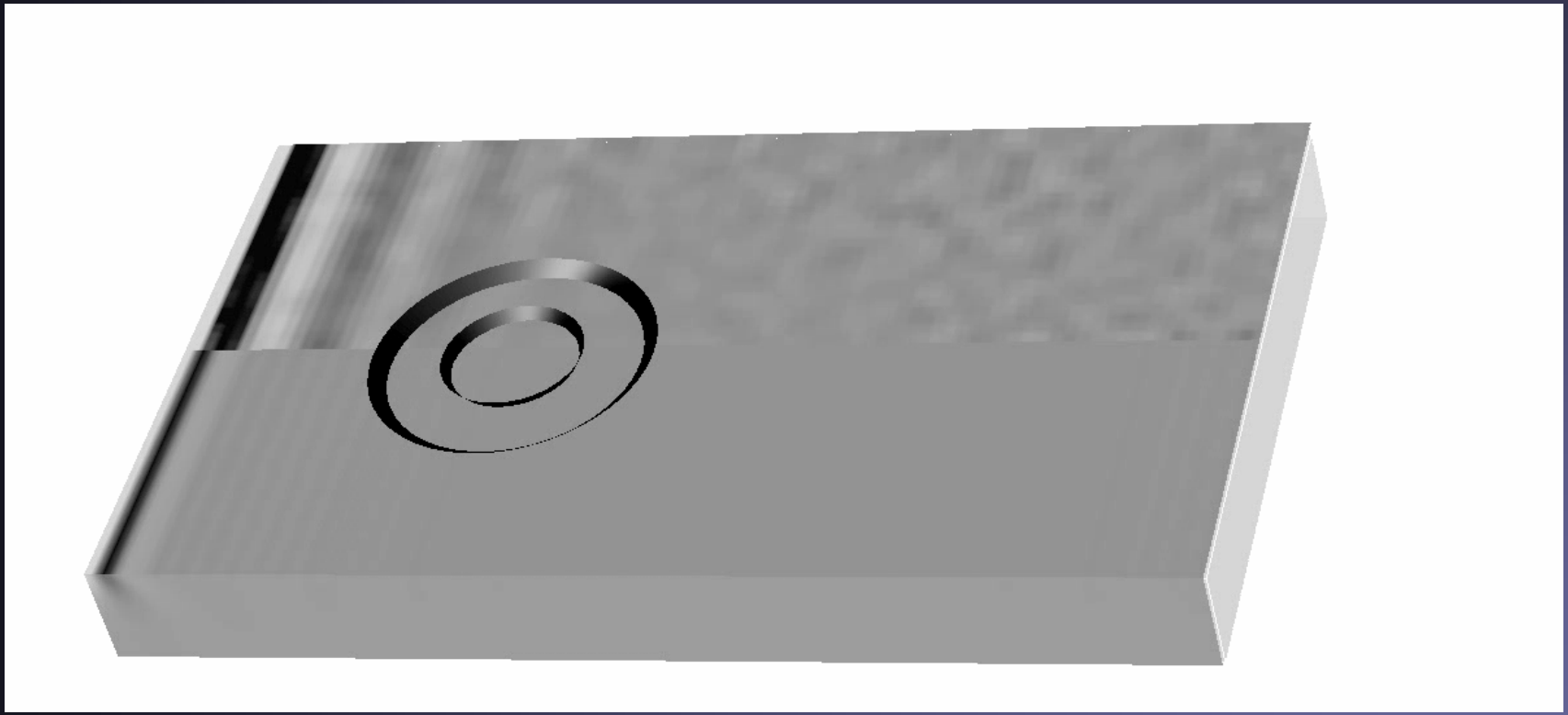

Bottom: SLiM numerical solution for Bz=3kG

Cameron, Gizon & Duvall (2007)

Subsurface Structure of Sunspots

1 Mm depth, longuest arrow corresponds to 400 m/s

Dark shades: surface magnetic field

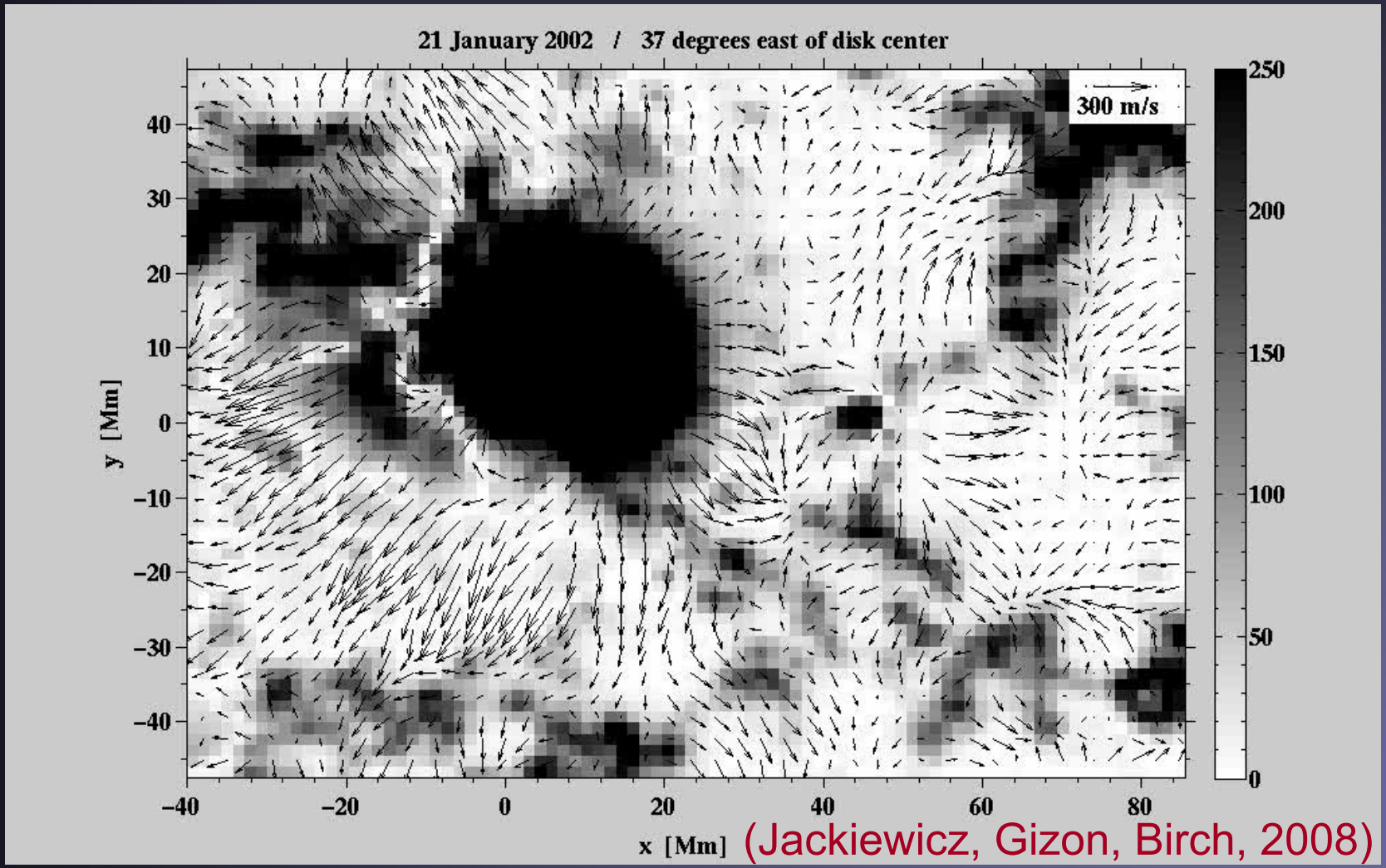

(Jackiewicz, Gizon, Birch, 2008)

Seeing right through the Sun

- A technique called two-skip far-side seismic holography gives images of the far side of the Sun
- Waves from back reach front, after skipping at the surface on the way
- Acoustic waves speed up in active regions (hotter subsurface layers)
- Sound waves delayed by ≈12 sec in a total travel time of 6 hours

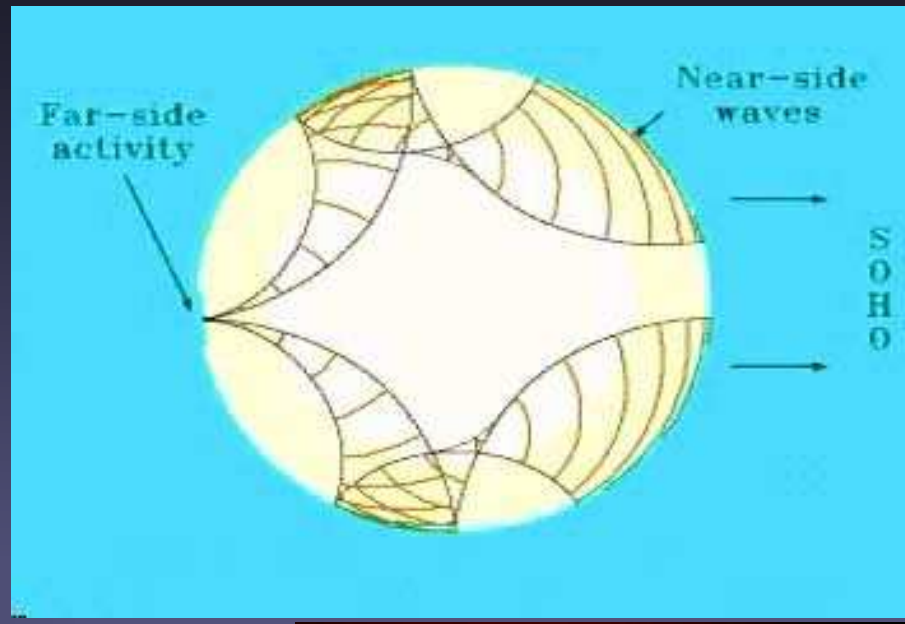

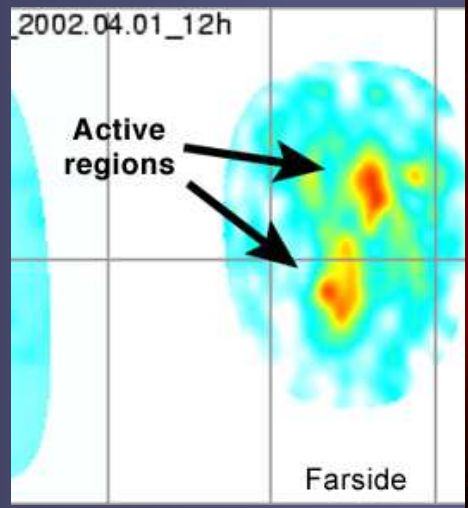

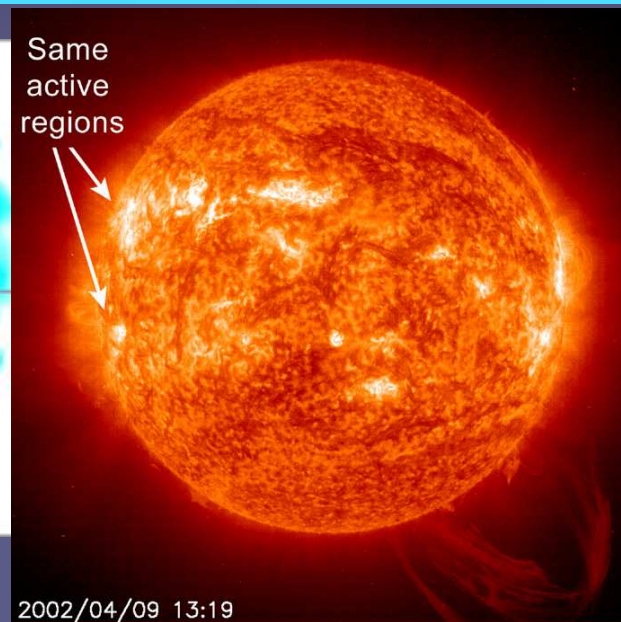

Seeing right through the Sun II

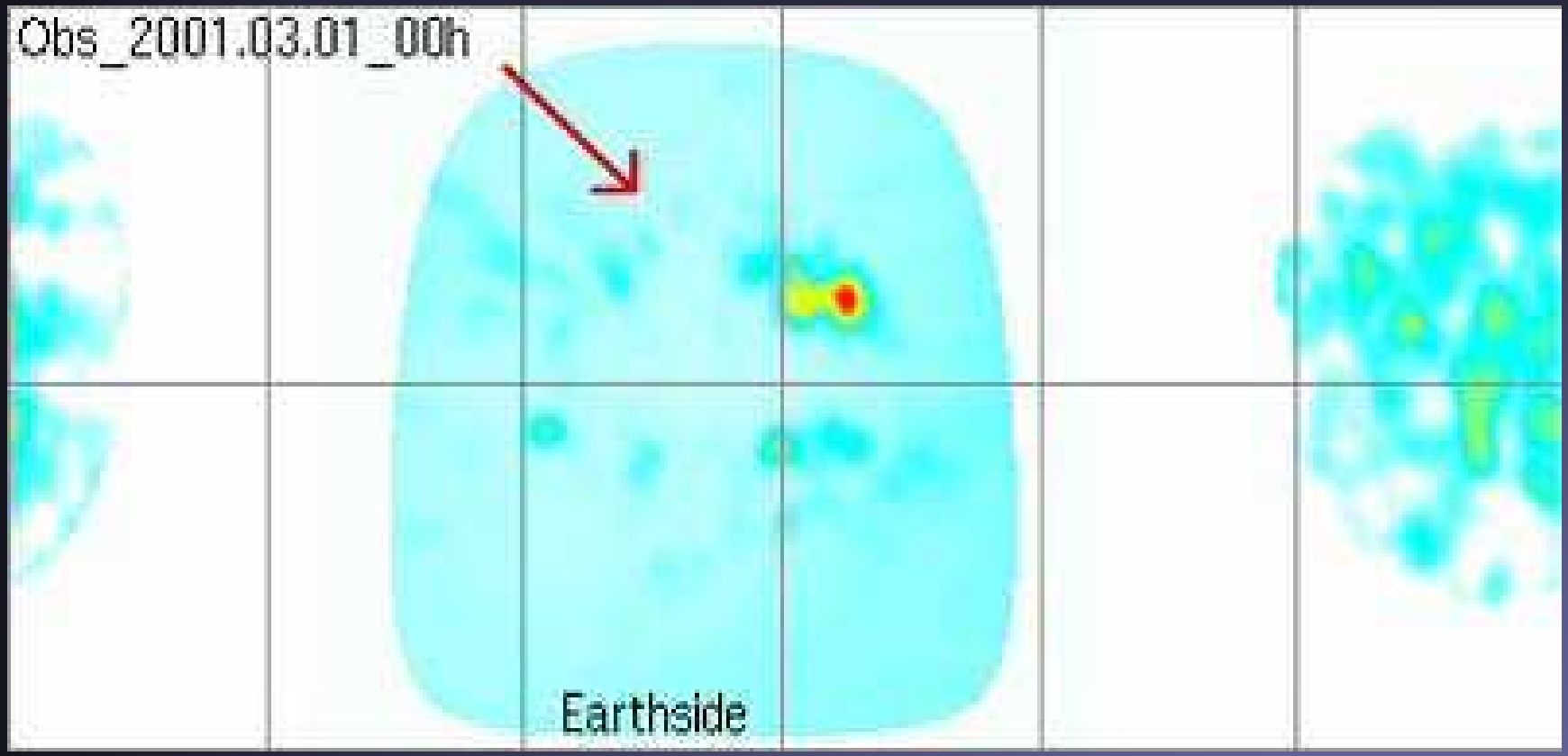

Real-time far side images:
http://soi.stanford.edu/data/farside/index.html

Helioseismology instruments

- Needed:
  - uninterrupted, long time series of observations
  - Either high velocity sensitivity, or high intensity sensitivity (and extremely good stability)
  - Low noise
  - Spatial resolution better than 1” (for local helioseismology)
- Instruments are either:
  - Ground based global networks (GONG+, BiSON)
  - Space based instruments in special full-Sun orbits (advantage of lower noise relative to ground-based networks; MDI, GOLF, VIRGO on SOHO, HMI on SDO)
  - Usually filter instruments with high spectral or intensity fidelity

Asteroseismology

First reliable detection of oscillations on the near solar analogue, α Centauri, and other Sun-like stars. Note the shift in the p-mode frequency range to lower values for α Centauri, which is older than the Sun (note also factor 10^3 difference in ν scale)

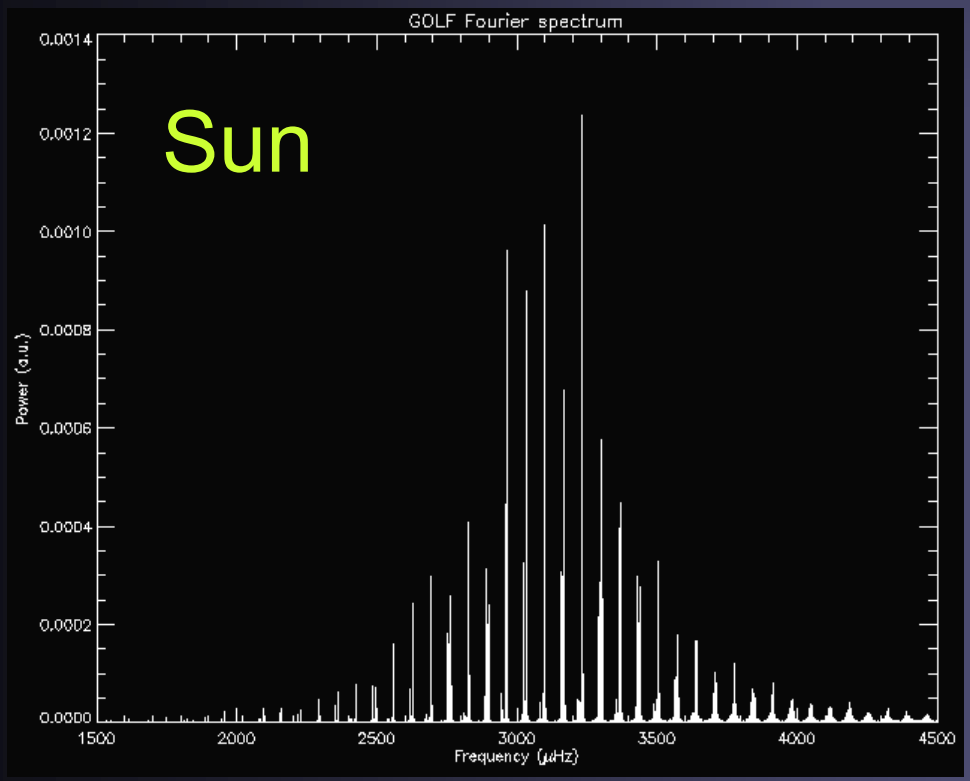

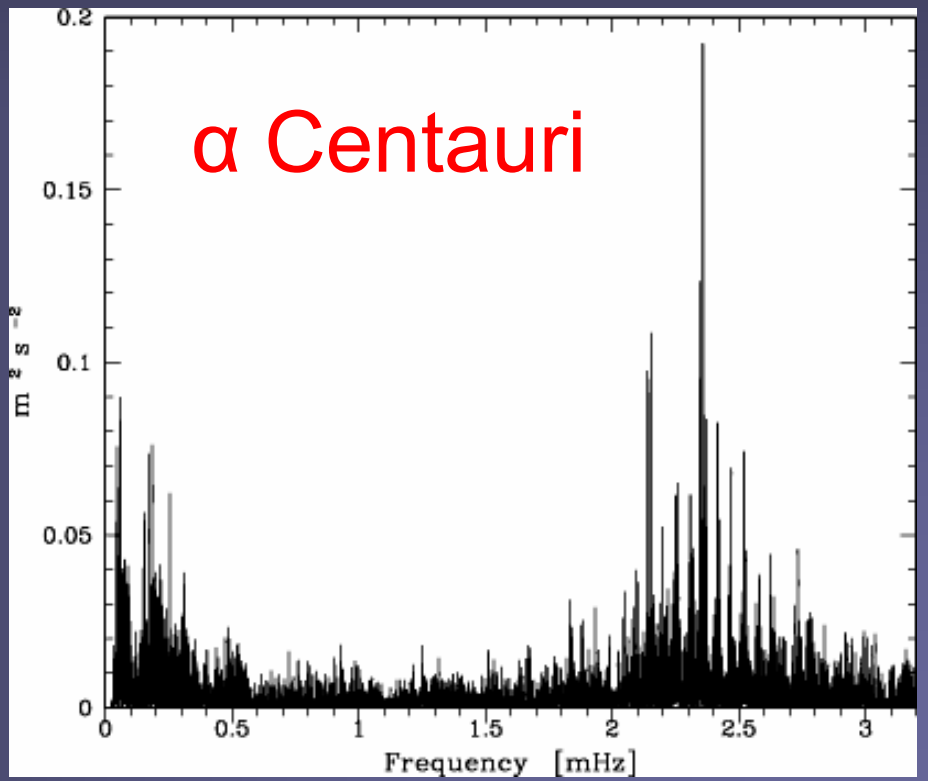

Solar rotation

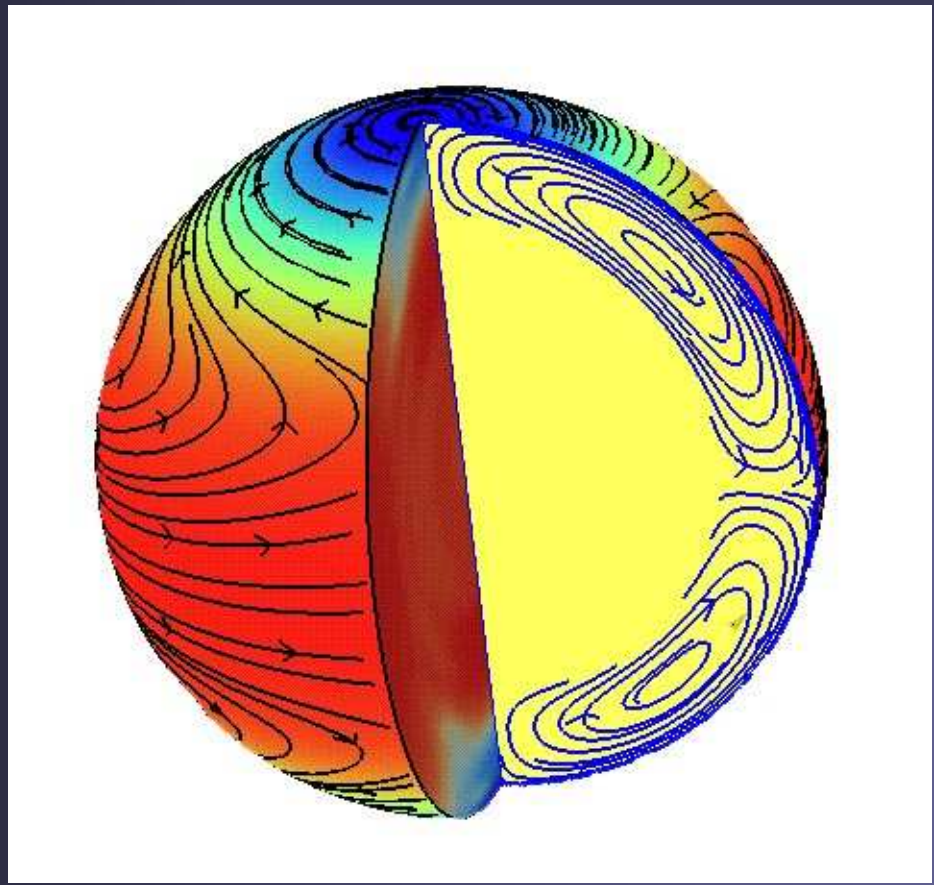

Solar rotation

- The Sun rotates differentially, both in latitude (equator faster than poles) and in depth (strong shear at bottom of convection zone).
- Standard value of solar rotation: Carrington rotation period: 27.2753 days (the time taken for the solar coordinate system to complete one rotation as seen from Earth).
- Sun's rotation axis is inclined by 7.1^{o} relative to the Earth's orbital axis (i.e. the Sun's equator is inclined by 7.1^{o} relative to the ecliptic).

Sidereal and synodic rotation

- Synodic rotation period = rotation period as seen from Earth. I.e. the period of time it takes for a feature on the Sun to return to the same position as seen from Earth.
  - the Standard synodic rotation period is the Carrington period of 27.2753 days
- Sidereal rotation period = rotation period relative to the stars
  - The sidereal rotation period corresponding to the Carrington period is: 25.38 days
- Difference between the two is due to the rotation of the Earth around the Sun.

Discovery of solar rotation

- Galileo Galilei and Christoph Scheiner noticed already that sunspots move across the solar disk in accordance with the rotation of a round body

→ Sun is a rotating sphere

- Movie based on Galileo Galilei's historical data

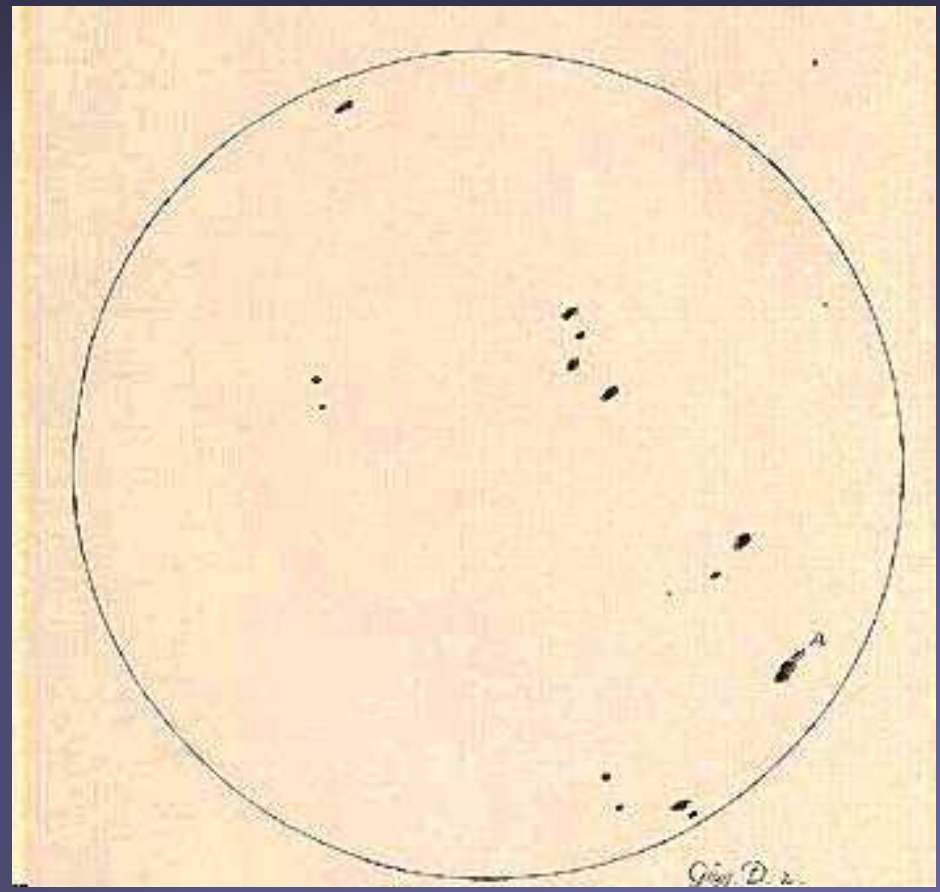

Surface differential rotation

- Poles rotate more slowly than equator.
- Surface differential rotation from measurements of:
  - Tracers: sunspots or magnetic field elements (these indicate the rotation rate of magnetic field)
  - Coronal holes (not plotted) rotate rigidly
  - Doppler shifts of the gas

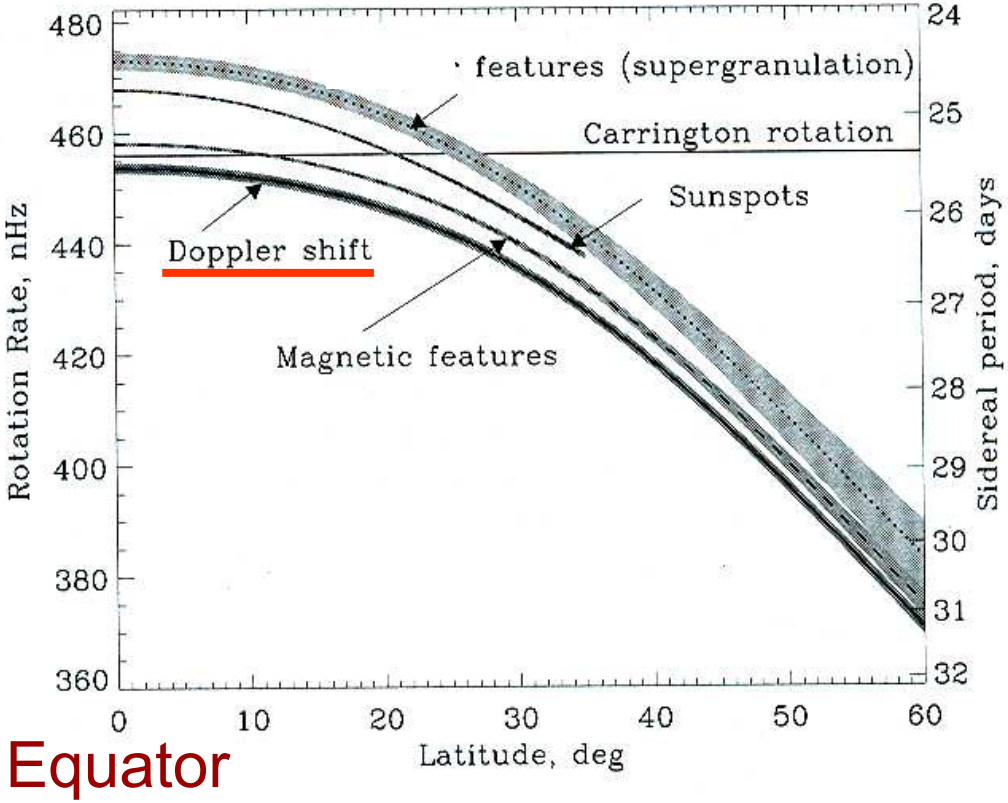

Figure 1. Rotation rate, $\Omega/2\pi$, and period of various tracers on the Sun's surface: recurrent (old) sunspots (dashed curve), magnetic features (dot–dash), and Doppler features (dots). The rotation rate and period determined spectroscopically through the Doppler shift are shown by the full curve. The shaded areas show the 1σ error estimates.

Surface differential rotation

- Description:

$$\Omega = A + B \sin^2\psi + C \sin^4\psi$$

where ψ is the latitude, $A = \Omega$ at the equator and $A+B+C = \Omega$ at the poles.

- Different tracers give different A, B, C values. E.g. spots rotate faster than the surface gas.

Internal differential rotation

- Method: Helioseismic inversions
  - In a non-rotating star the individual modes of oscillation, described by "quantum numbers" n,l,m are degenerate in that their frequency depends only on n and l, but not on m.
  - Similar to Zeeman effect. Note that m distinguishes between the surface distribution of oscillation nodes. For a spherically symmetric star (no rotation) all these modes must have same frequency.
  - In a rotating Sun the degeneracy is removed and modes with different m have slightly different frequency.
  - Since modes with different l sample the solar latitudes in different ways, it is possible to determine not just vertical, but also latitudinal differential rotation by helioseismology.

Mode structure: Rotational splitting

- GOLF/SOHO observations showing a blowup of the power spectrum with an $l=0$ and an $l=2$ mode.
- The noise is re-excitation noise
- The extra width of the $l=2$ mode is due to solar rotation splitting

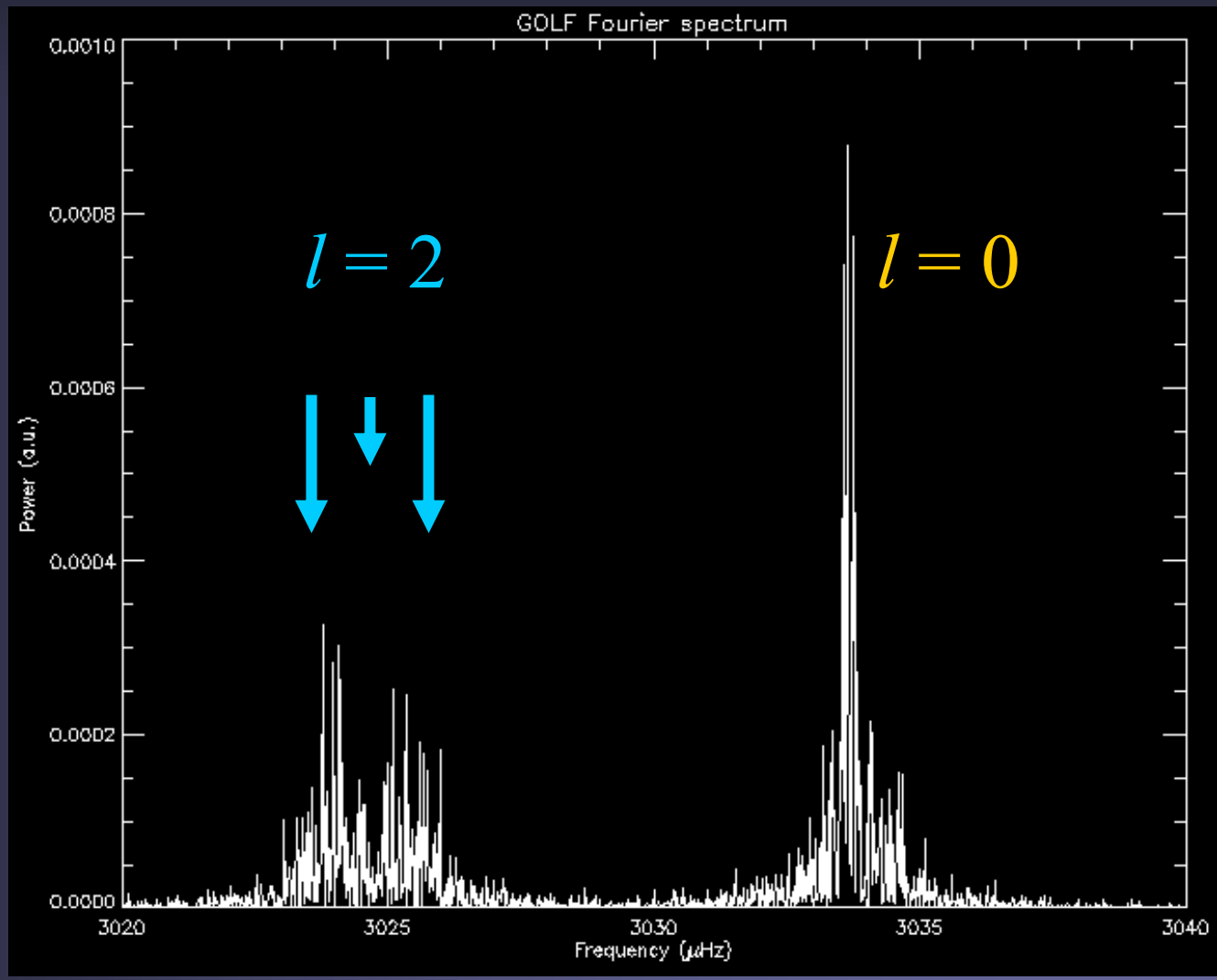

Internal differential rotation II

- Structure of internal rotation deduced from MDI data
- Note: differential rotation in CZ, solid rotation below

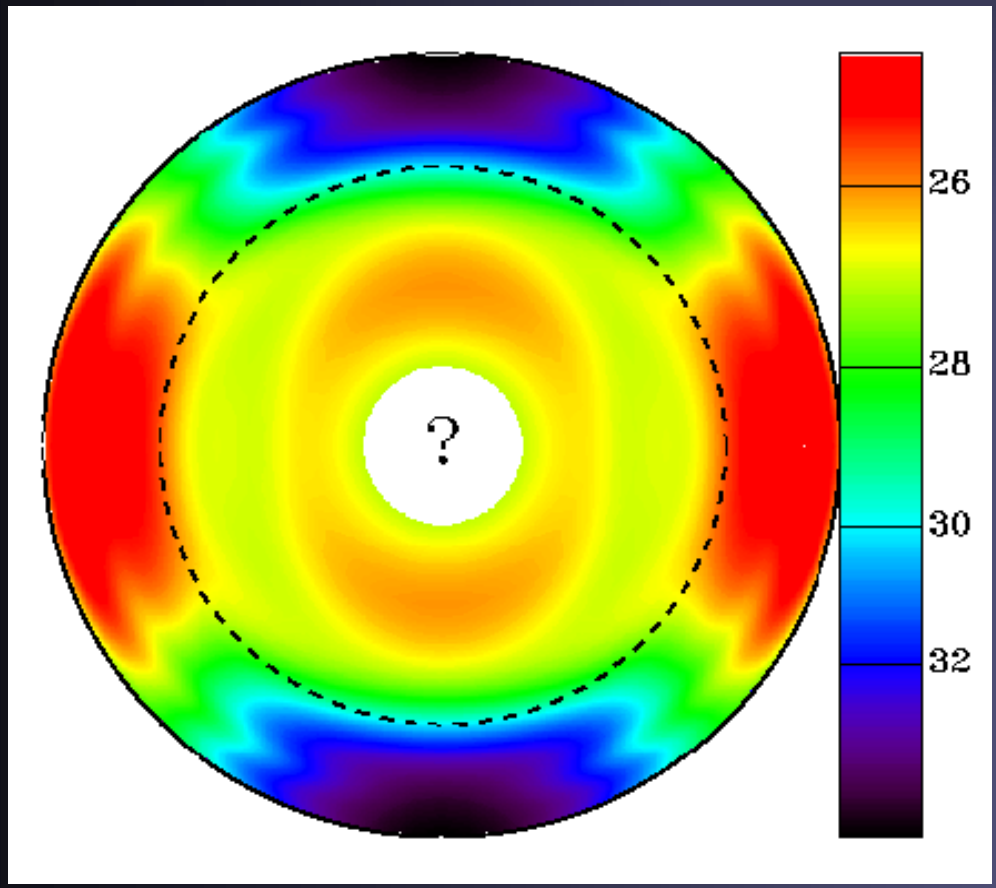

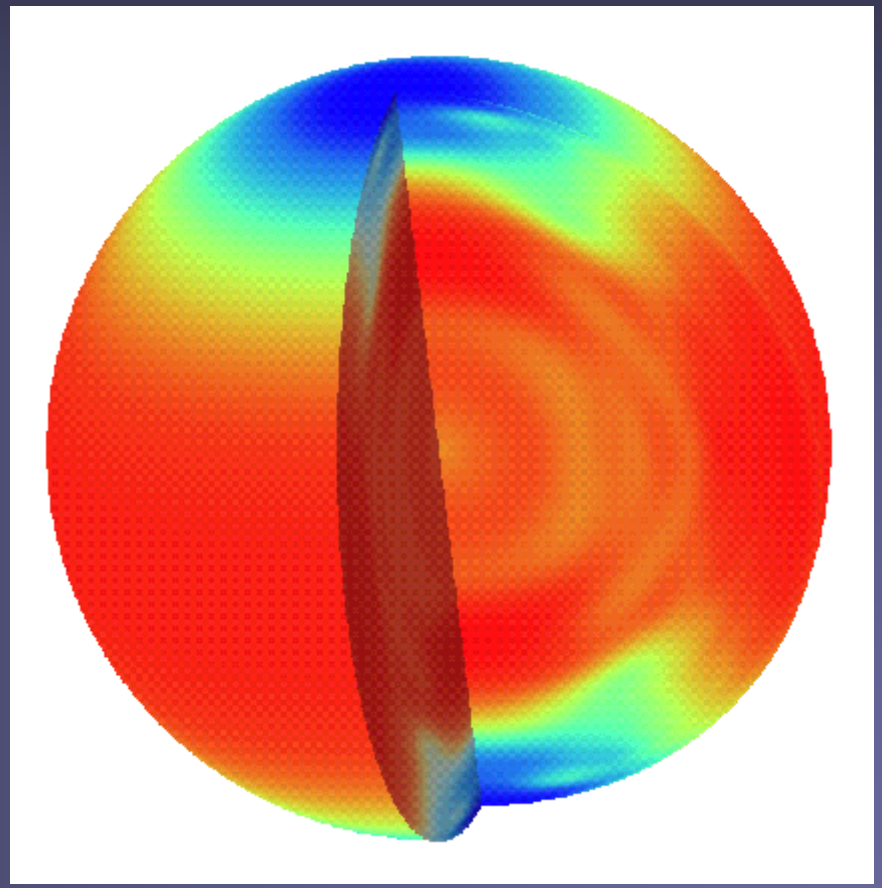

Internal differential rotation III : tachocline

Large radial gradients in rotation rate at bottom of CZ (tachocline), but also just below solar surface (enigmatic). Note the slight missmatch of helioseismic and Doppler measurements

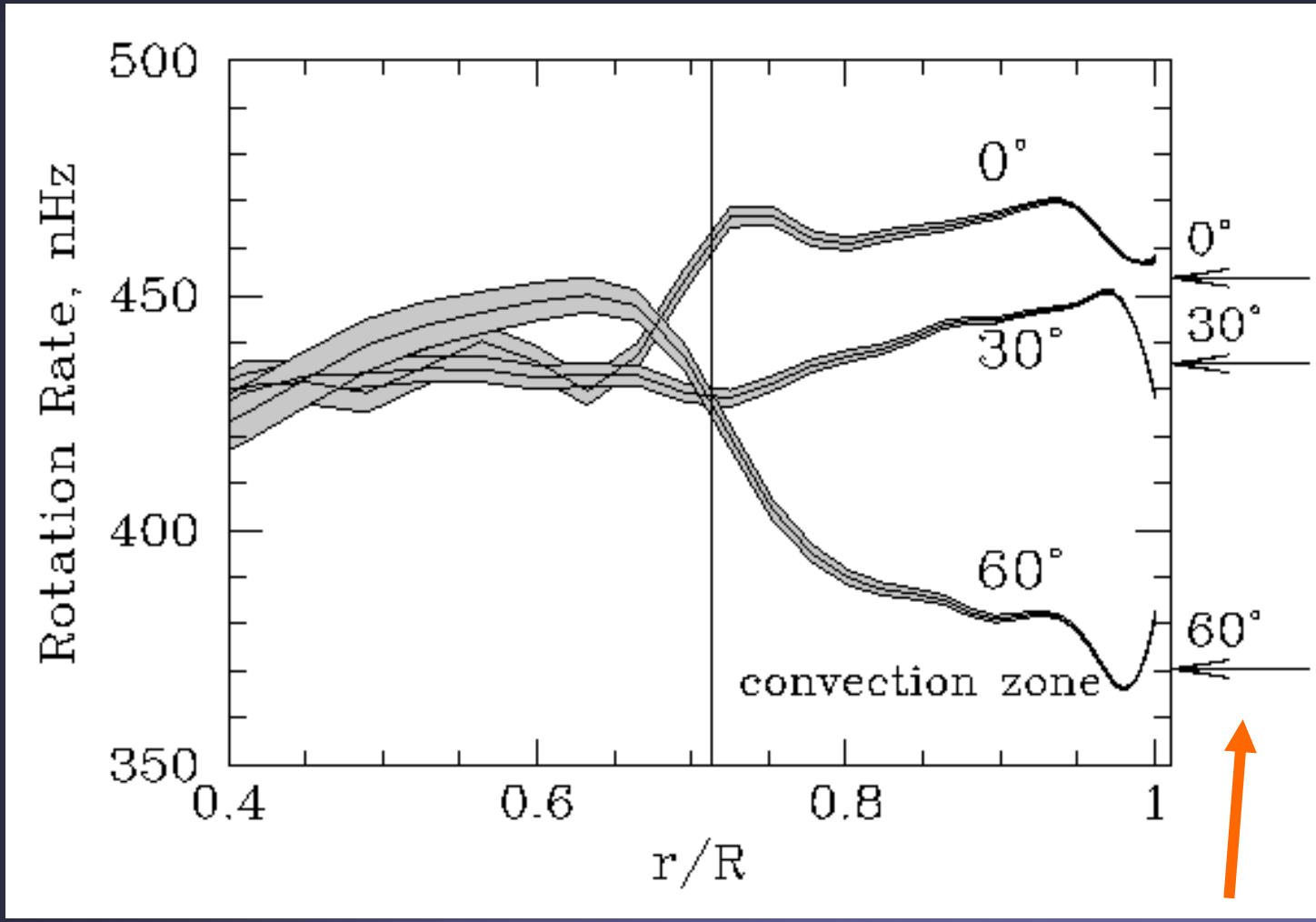

What about rotation of solar core?

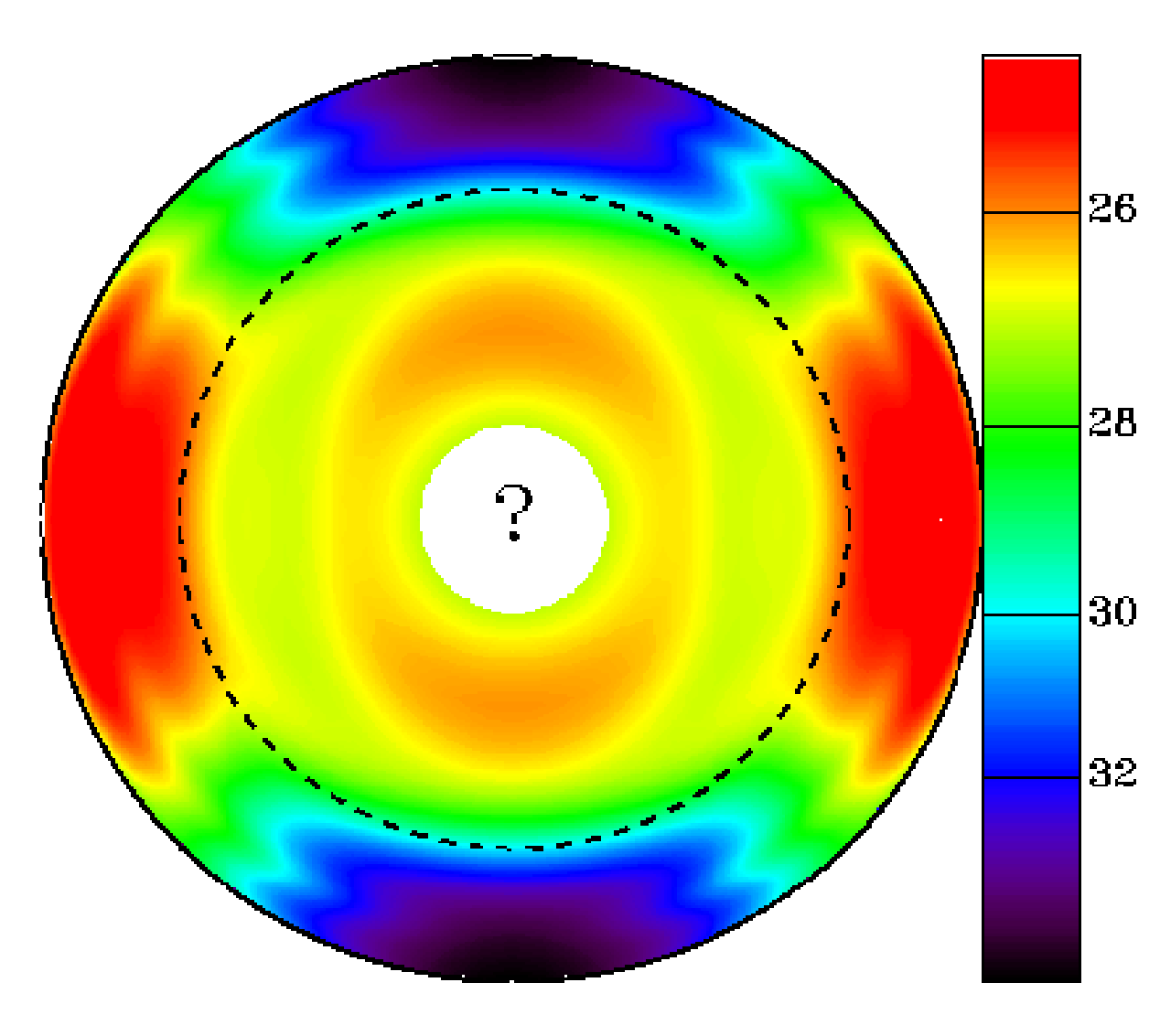

What about rotation of solar core?

- Rotation rate of solar core is hard to determine, since p-modes do not penetrate to the Sun's centre.
- Different values in the literature for the core's rotation rate: $\Omega(r=0) = \Omega(r=R_\odot)$ ... $2\,\Omega(r=R_\odot)$
- One way to set limits on $\Omega(r=0)$: quadrupole moment of Sun.
- Solar rotation leads to oblateness, i.e. diameter is larger at equator than between the poles.
- If core rotates more rapidly than surface, then oblateness will be larger than expected due to surface rotation rate.

Solar oblateness

- Oblateness = $\Delta R/R_\odot$
- Direct measurements: $\Delta R/R_\odot \approx 10^{-5}$
  - Very tricky, since oblateness 10^{-5} corresponds to ΔR = 14 km (best spatial resolution achievable: 100 km).
  - Systematic errors due to concentration of magnetic activity to low latitudes → affects measurements of solar diameter, since shape of limb is distorted.
  - Initial measurements due to Dicke & Goldenberg (1967) gave $\Delta R/R_\odot \approx 5 \times 10^{-5}$ → required change of general relativity to explain motion of Mercury's perihelion (but was consistent with Brans-Dicke gravitation theory)
- Helioseismic measurements give for the acoustic radius of the Sun (which is not the same as the optical radius, but similar): $\Delta R/R_\odot \approx 10^{-5}$

Evolution of solar rotation

- Young stars are seen to rotate up to 100 times faster than the Sun.
- Did the Sun also rotate faster when it was young?
- Skumanich law: $\Omega \sim t^{-1/2}$, where t is the age of the star (deduced from observing stars in clusters of different ages). I.e. old cool stars also rotate slowly.

➔Sun also rotated faster as a young star.

- Question: where did all the angular momentum go?

Evolution of solar rotation II

- Question: where did all the angular momentum go?
- Answer part 1: Solar wind! The solar wind carries away angular momentum with it. Torque j, i.e. rate of change of angular momentum, exerted by solar wind (without magnetic field):

$$j = \Omega R_{\odot} dm/dt$$

- Here dm/dt is the solar mass-loss rate (mass carried away by solar wind)
- Problem: j is 2-3 orders of magnitude too small to cause a significant braking of solar rotation…

Evolution of solar rotation III

- Answer part 2: Magnetic field!
- Below Alfven radius R_A, i.e. point where wind speed becomes > Alfven speed, wind is channeled by the field. Up to that radius, the wind rotates rigidly with the solar surface (forced to do so by rigid field lines), i.e. wind carries angular momentum away only beyond R_A. It is as if the Sun had the radius R_A. Proper expression for Torque:

$$j = \Omega R_A dm/dt$$

- R_A typically is 10-20 times larger than $R_\odot$ for today's Sun.

Evolution of rotation IV

- $j = \Omega R_A dm/dt \sim \Omega$

→ The faster the star rotates, the quicker it spins down.

- Additional corrections:
  - dm/dt depends on Ω (more rapidly rotating star, more magnetic field, hotter the corona, larger the dm/dt)
  - R_A depends on Ω (although not in a straightforward manner: more rapidly rotating star, more magnetic field, but also larger the density and velocity of wind).
- In general $j = k\Omega^{\alpha}$, where α typically > 1, although there are signs that for very large Ω, the α value becomes very small (saturation).

Solar rotation velocity evolution

Spinup as the star contracts towards the main sequence

Spindown due to magnetic braking (wind loss)

Current Rotation rate independent of starting value

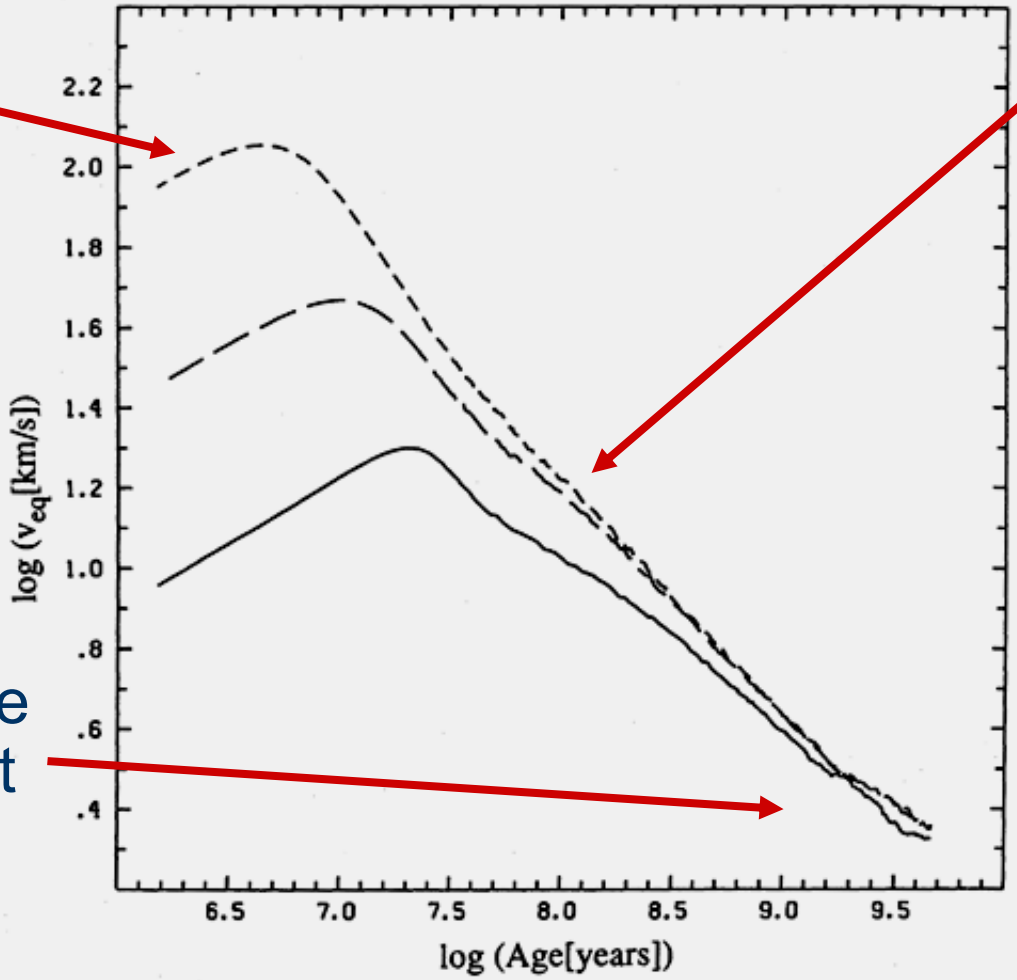

Pinsonnault et al.

FIG. 3.—Surface rotation velocity as a function of time for three models differing only in initial angular momentum. The solid line is the reference solar model (case A in Table 2) with $J_0 = 5 \times 10^{49}$ g cm^2 s^{-1}. The long-dashed line is a model with $J_0 = 1.63 \times 10^{50}$ g cm^2 s^{-1} (case B). The short-dashed line is a model with $J_0 = 5 \times 10^{50}$ g cm^2 s^{-1} (case C). An order of magnitude in J_0 produces only a small variation in the surface rotation velocity on the main sequence ($\log t > 8$).

Complexity

- Solar physics is a complex field, requiring a lot of teamwork.

➔ Finagle's rule:

Teamwork is essential. It allows you to blame someone else when things go wrong.

Solar radiation and spectrum

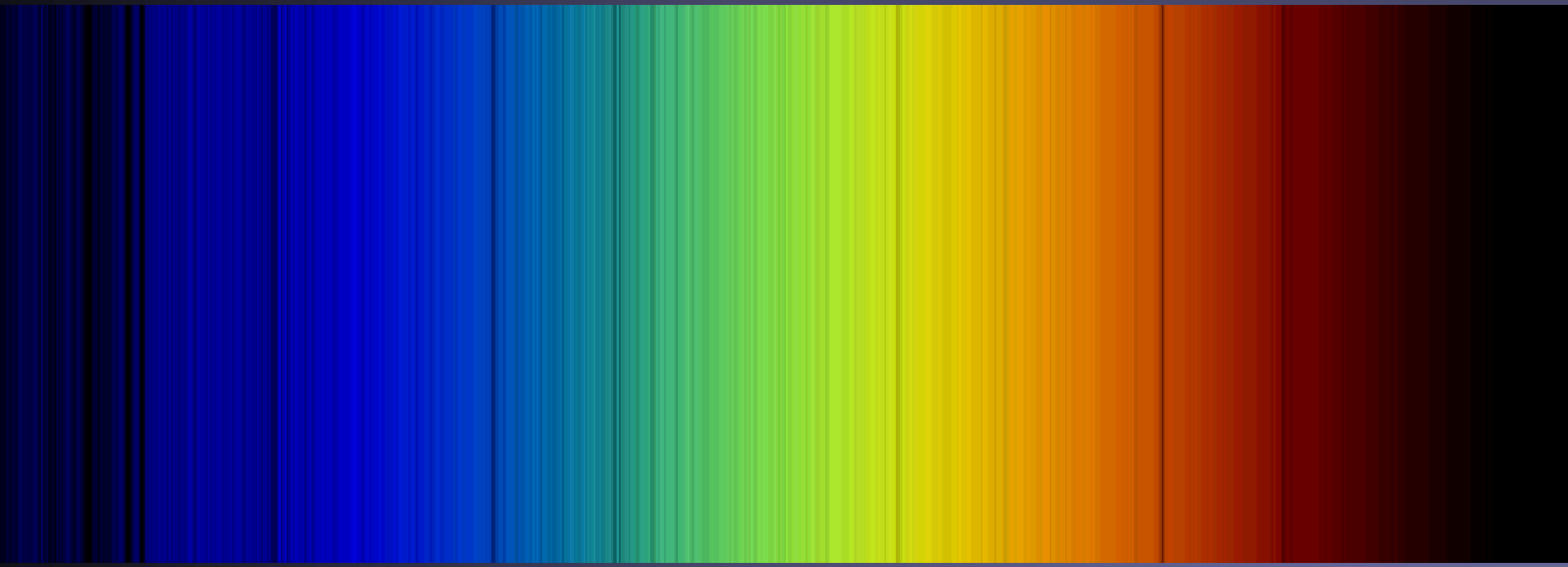

The Sun in white light: Limb darkening

- In the visible, Sun's limb is darker than solar disc centre (➔ limb darkening)
- Since intensity ~ Planck function, $B_\nu(T)$, T is lower near limb.
- Due to grazing incidence we see higher near limb: T decreases outward

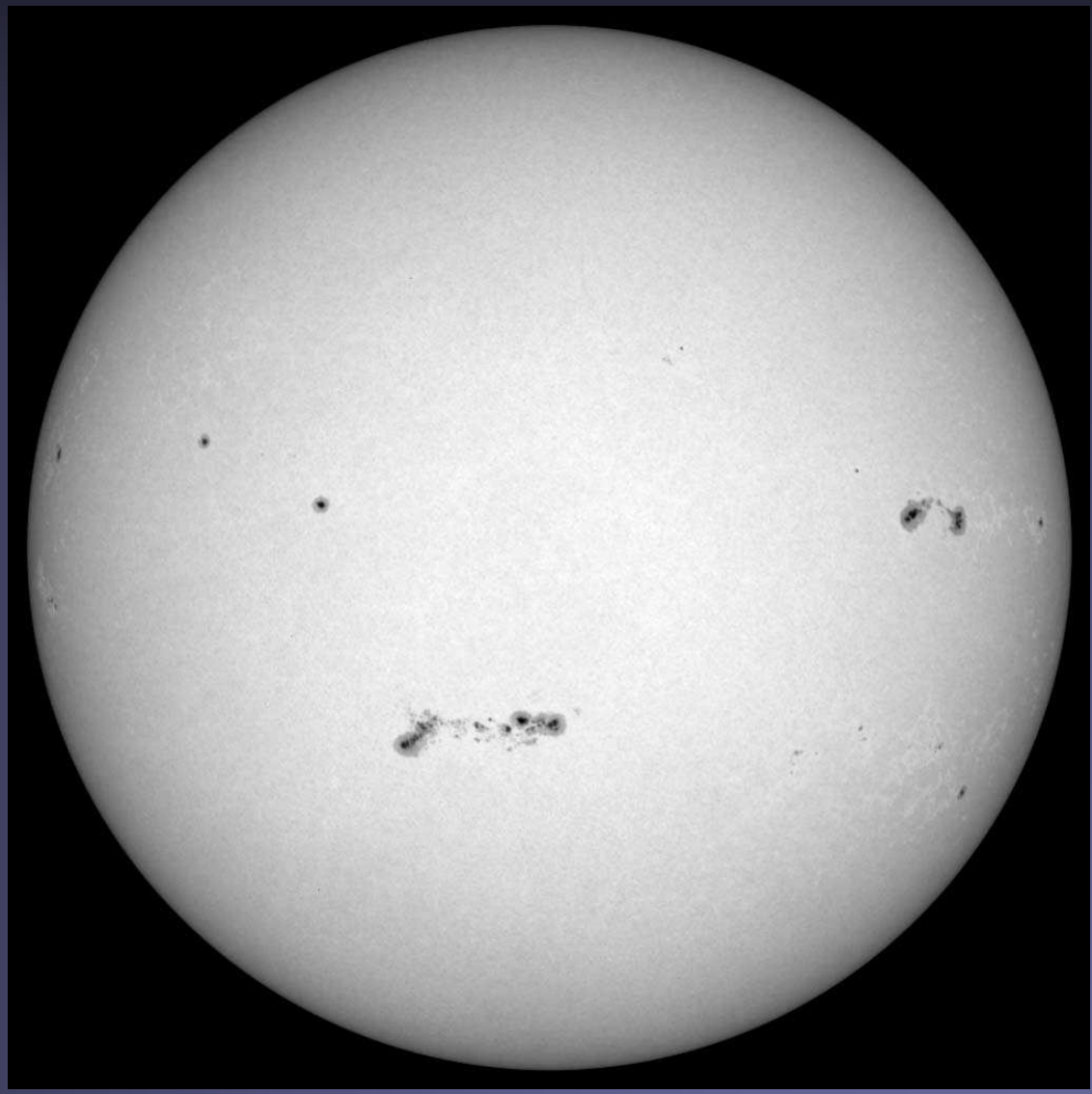

Limb darkening vs. λ

- short λ: large limb darkening;
- long λ: small limb darkening
- departure from straight line: limb darkening is more complex than $I(\theta) \sim \cos(\theta)$

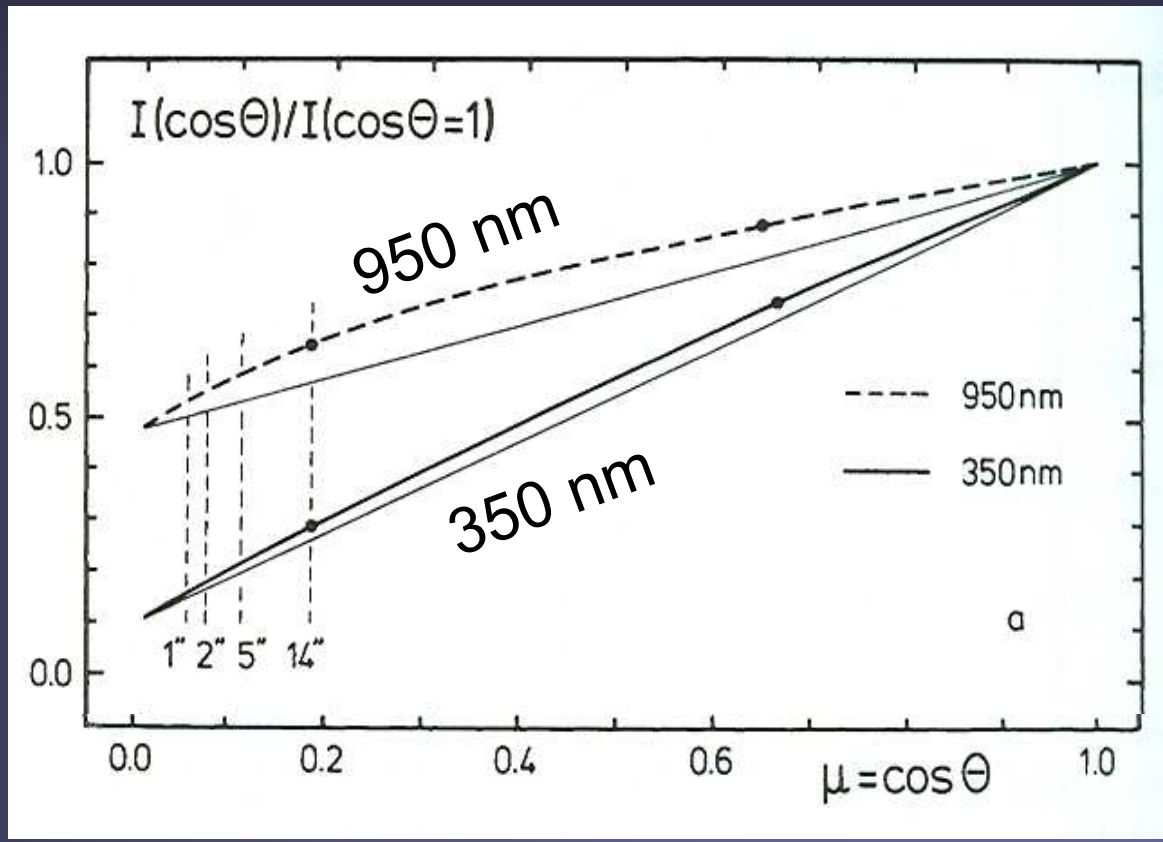

The Sun in the EUV: Limb brightening

- In the EUV, Sun's limb is brighter than disc centre (➔ limb brightening)
- Solar atmosphere is optically thin at EUV wavelengths ➔ intensity ~ thickness of layer contributing to it. Near the limb this layer appears thicker (optically thin radiation comes from roughly the same height everywhere).

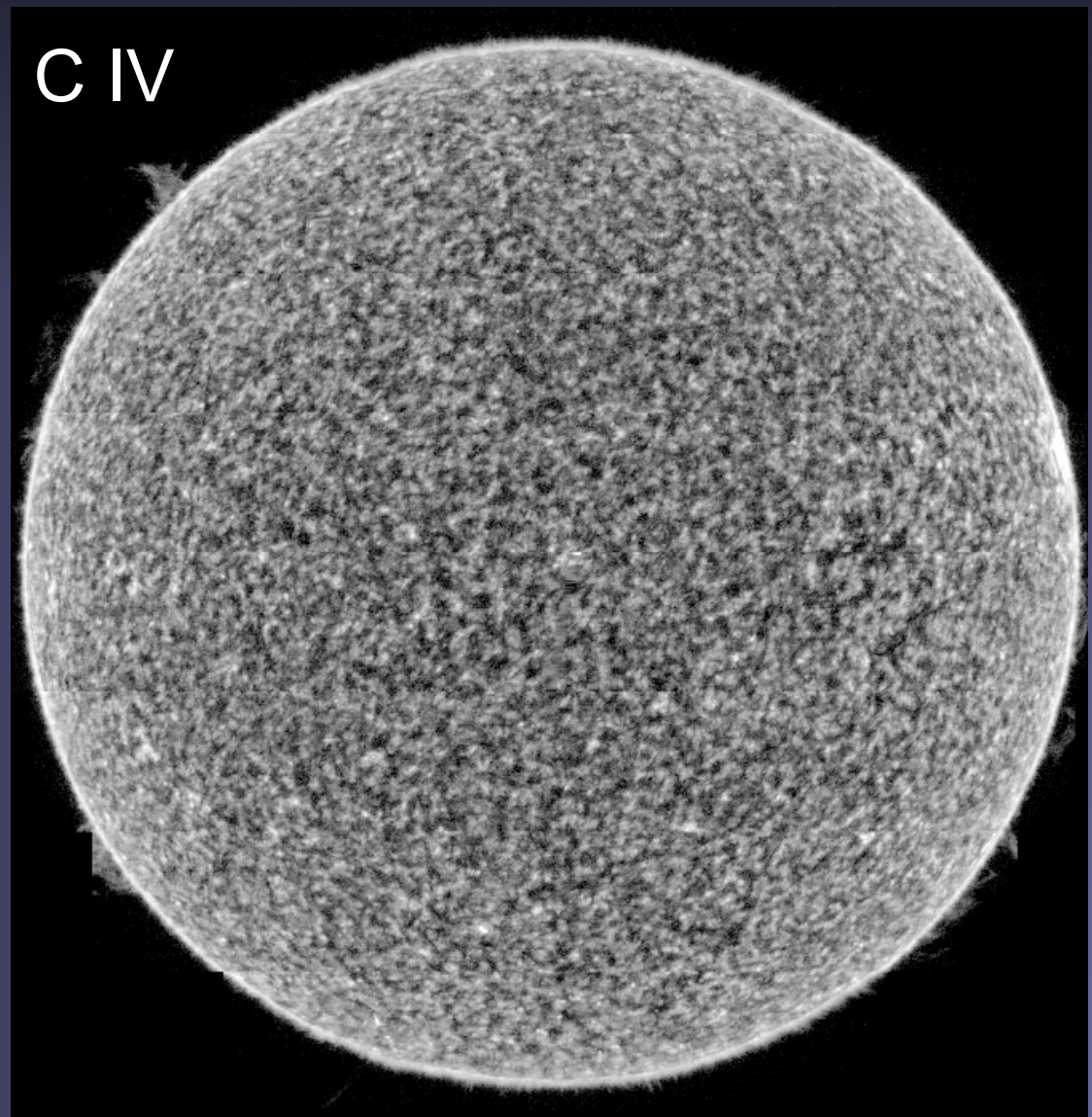

The Sun in the EUV: Limb brightening

- Limb brightening in optically thin lines does NOT imply that temperature increases outwards (although by chance it does in these layers....)

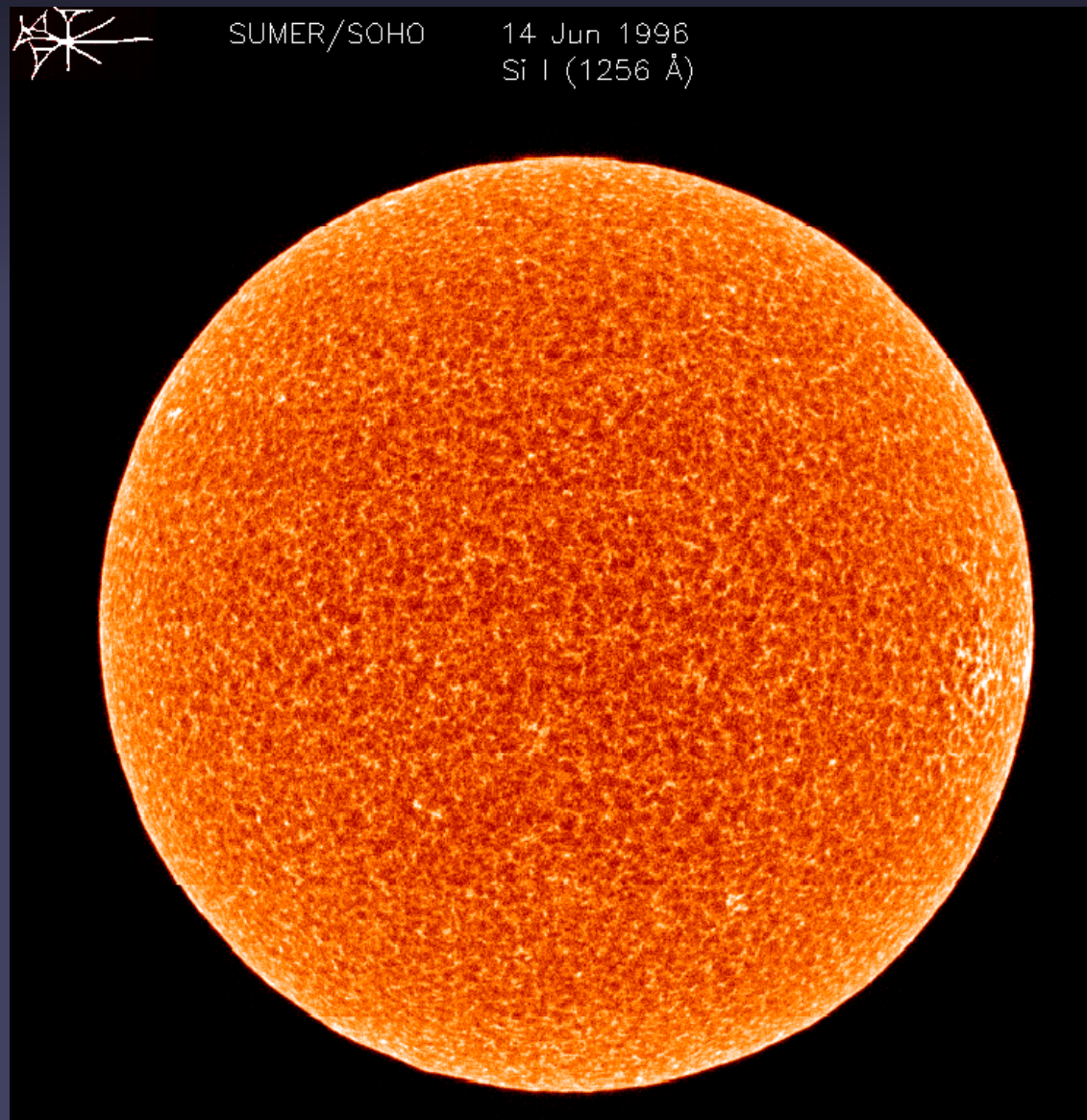

Solar irradiance spectrum

Irradiance = solar flux at 1AU

Spectrum is similar to, but not equal to Planck function ➔ Radiation comes from layers with diff. temperatures.

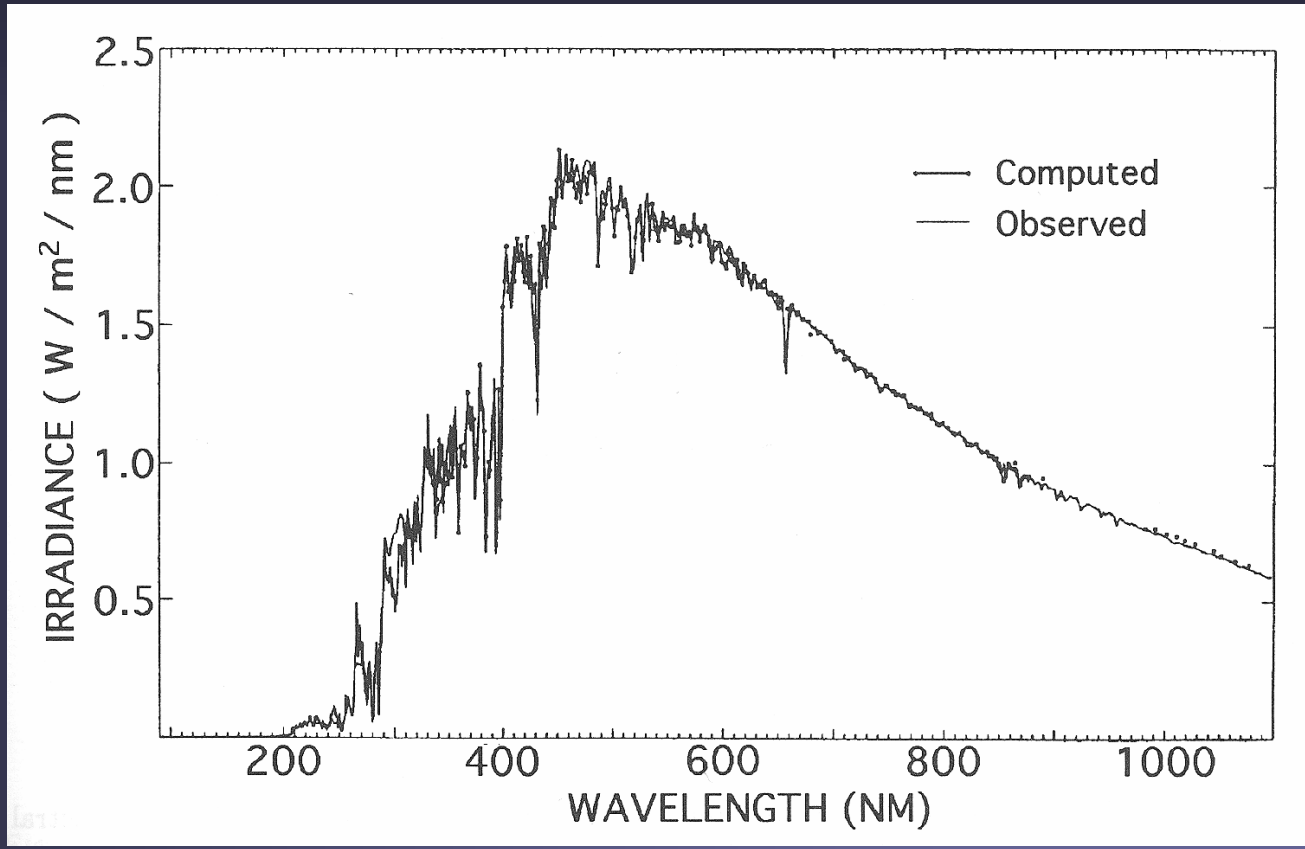

Often used temperature measure for stars: Effective temp: σT^4_{eff} = Area under flux curve

Spectrum above and under the Earth's atmosphere

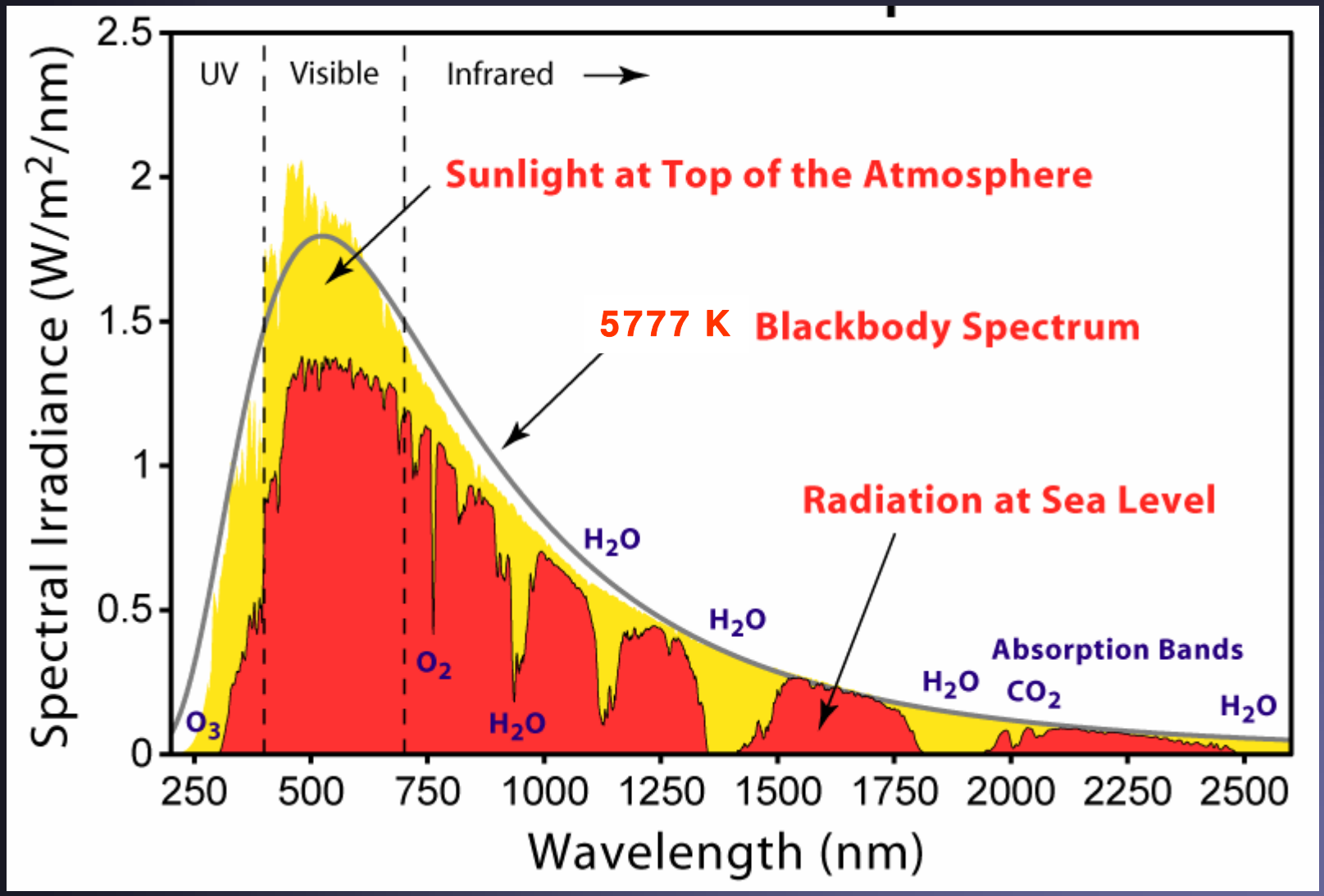

Planck's function

- Amplitude and area increases approximately exponentially with temperature ➔ from e.g. λ-integrated intensity we get effective temperature
- Wavelength of maximum changes linearly with temperature (Wien's law)

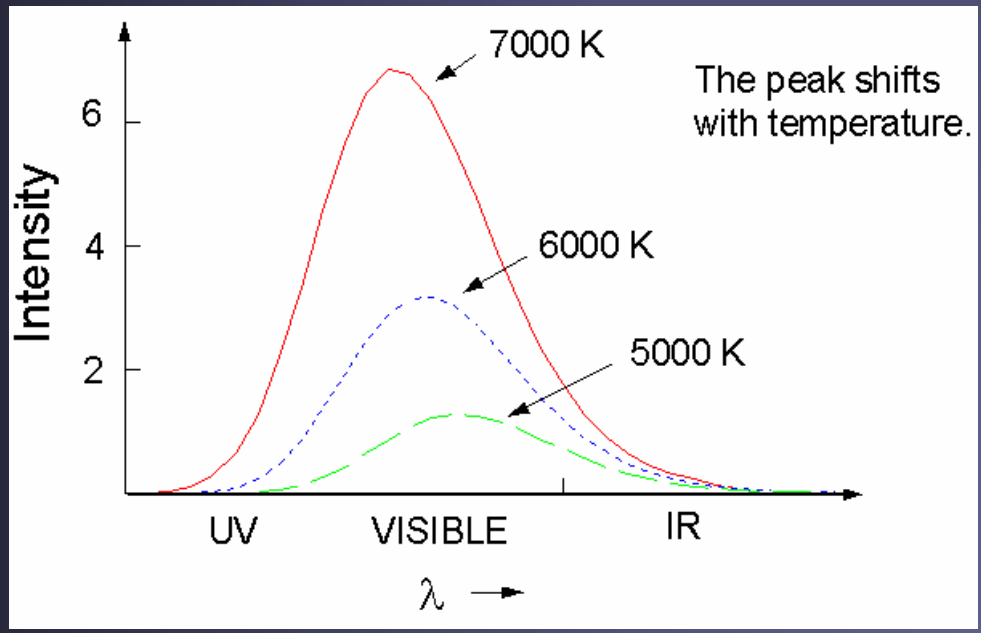

The solar spectrum: continua with absorption and emission lines

- Solar spectrum changes in character at different λ
- X-rays: Emission lines of highly ionized species
- EUV: Emission lines of neutral to multiply ionized species plus recombination continua
- UV: stronger recombination continua and absorption lines
- Visible: H^- b-f continuum with absorption lines
- FIR: H^- f-f continuum, increasingly cleaner (i.e. less lines, except molecular bands)
- Radio: thermal and, at longer λ, increasingly non-thermal continua

Visible

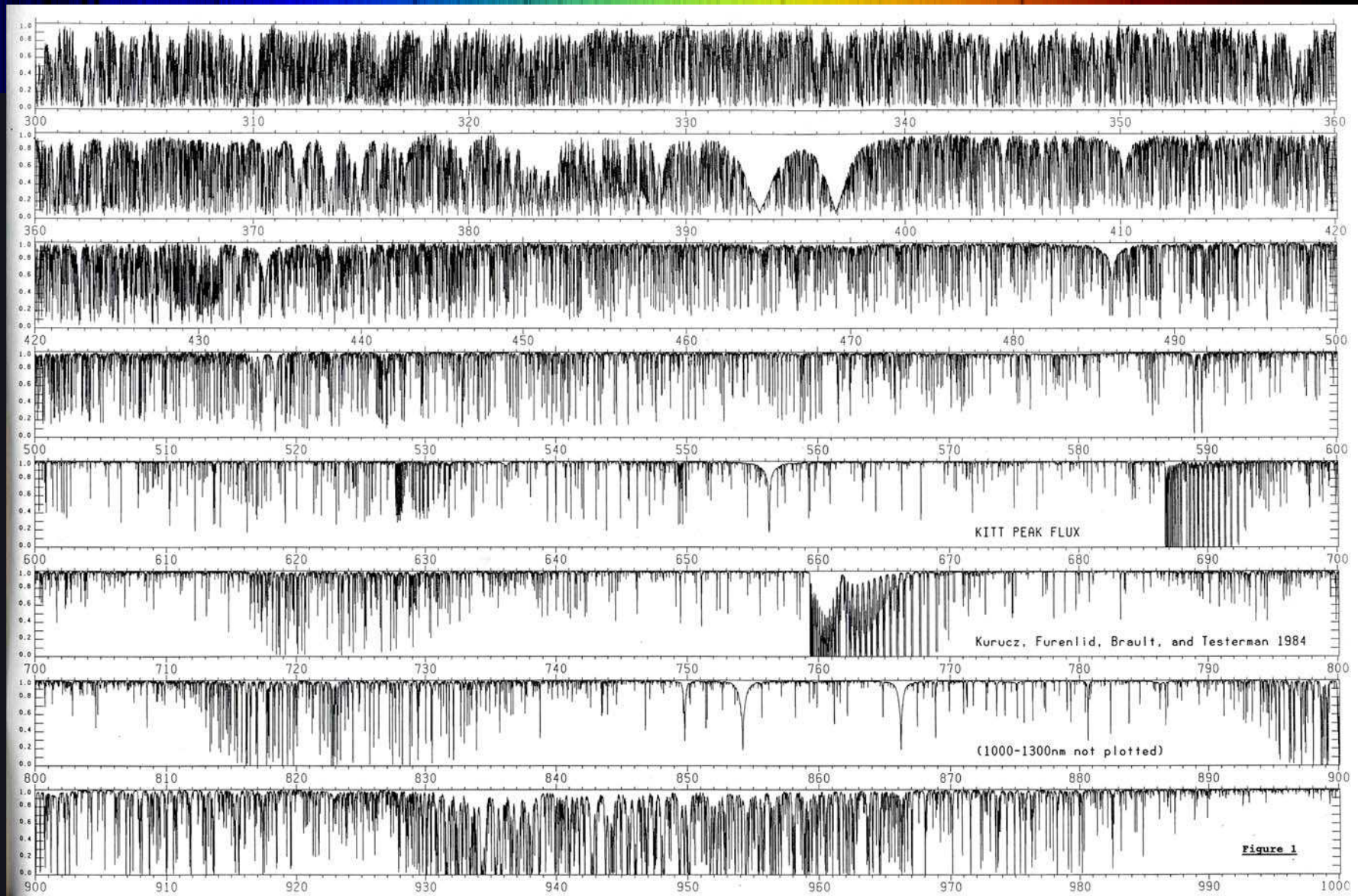
KITT PEAK FLUX
Kurucz, Furenlid, Brault, and Testerman 1984
(1000-1300nm not plotted)
Figure 1

EUV spectrum

The solar spectrum from 670 Å to 1620 Å measured by SUMER (logarithmic scale)

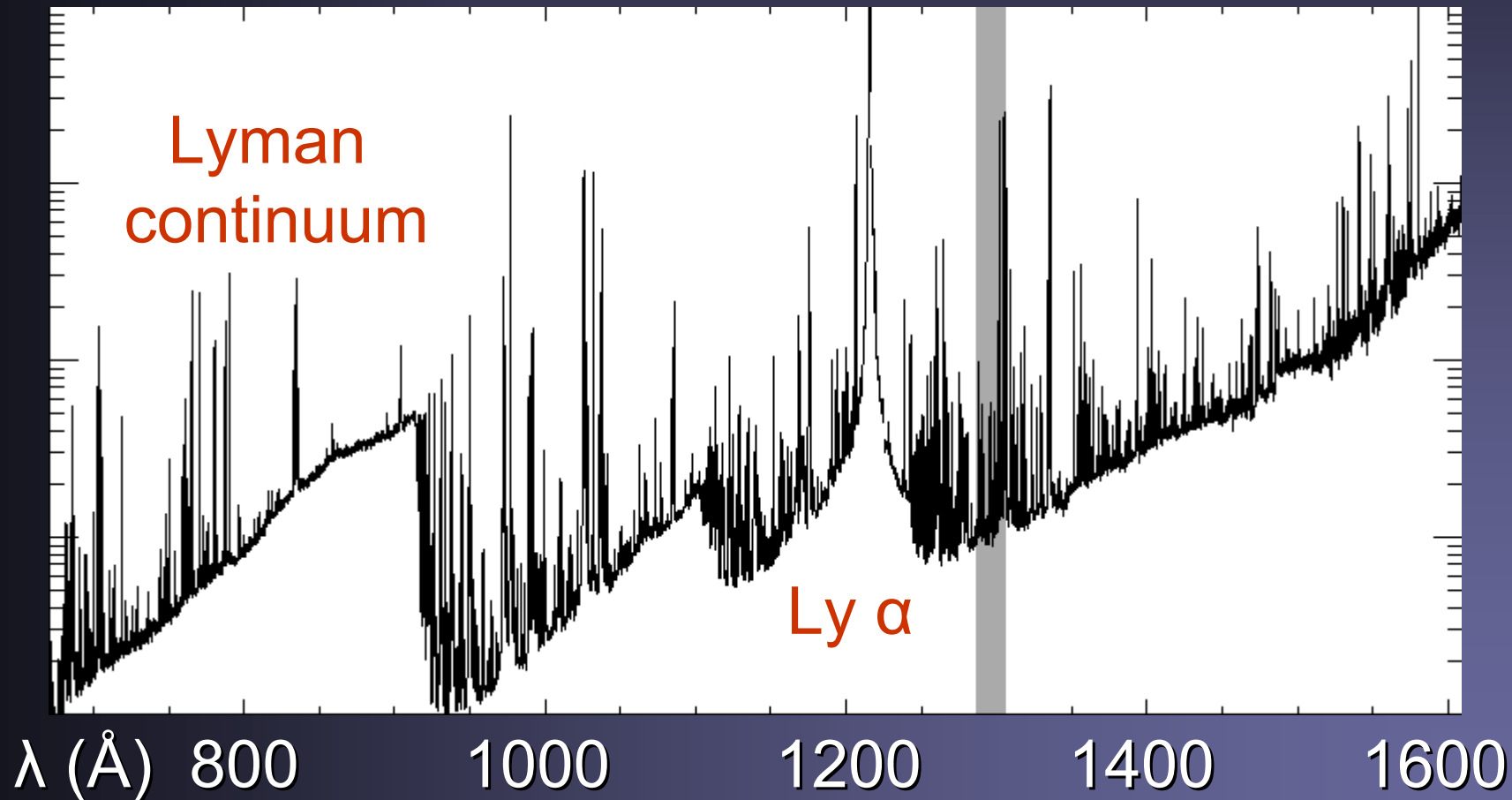

Detail of EUV spectrum by SUMER

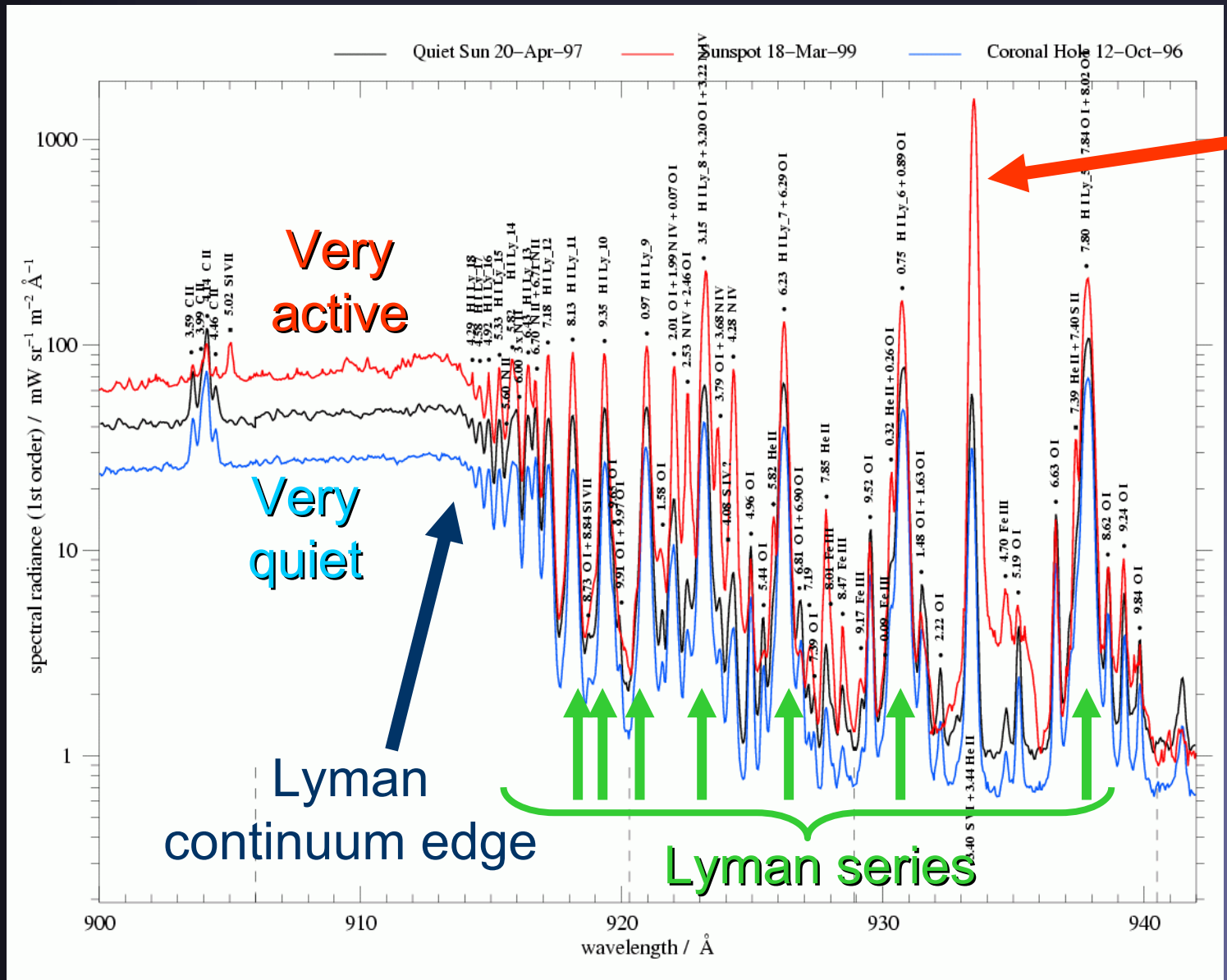

Activity sensitive line: S VI

Radiative transfer: optical depth

- Axis z points in the direction of light propagation
- Optical depth: $\Delta\tau_\nu = -\kappa_\nu \Delta z$,

where κ_ν is the absorption coefficient [cm^{-1}] and ν is the frequency of the radiation. Light only knows about the τ_ν scale and is unaware of z

→ Integration over z: $\tau_\nu = -\int \kappa_\nu(z) dz$

(note that the scales are floating, no constant of integration is fixed)

Optical depth and solar surface

- Radiation at frequency ν escaping from the Sun is emitted mainly at heights around $\tau_\nu \approx 1$.
- At wavelengths at which κ_ν is larger, the radiation comes from higher layers in the atmosphere.
- In solar atmosphere κ_ν is small in visible and near IR, but large in UV and FIR ➔ We see deepest in visible and NIR, but sample higher layers at shorter and longer wavelengths.

Height of τ = 1, brightness temperature and opacity vs. λ

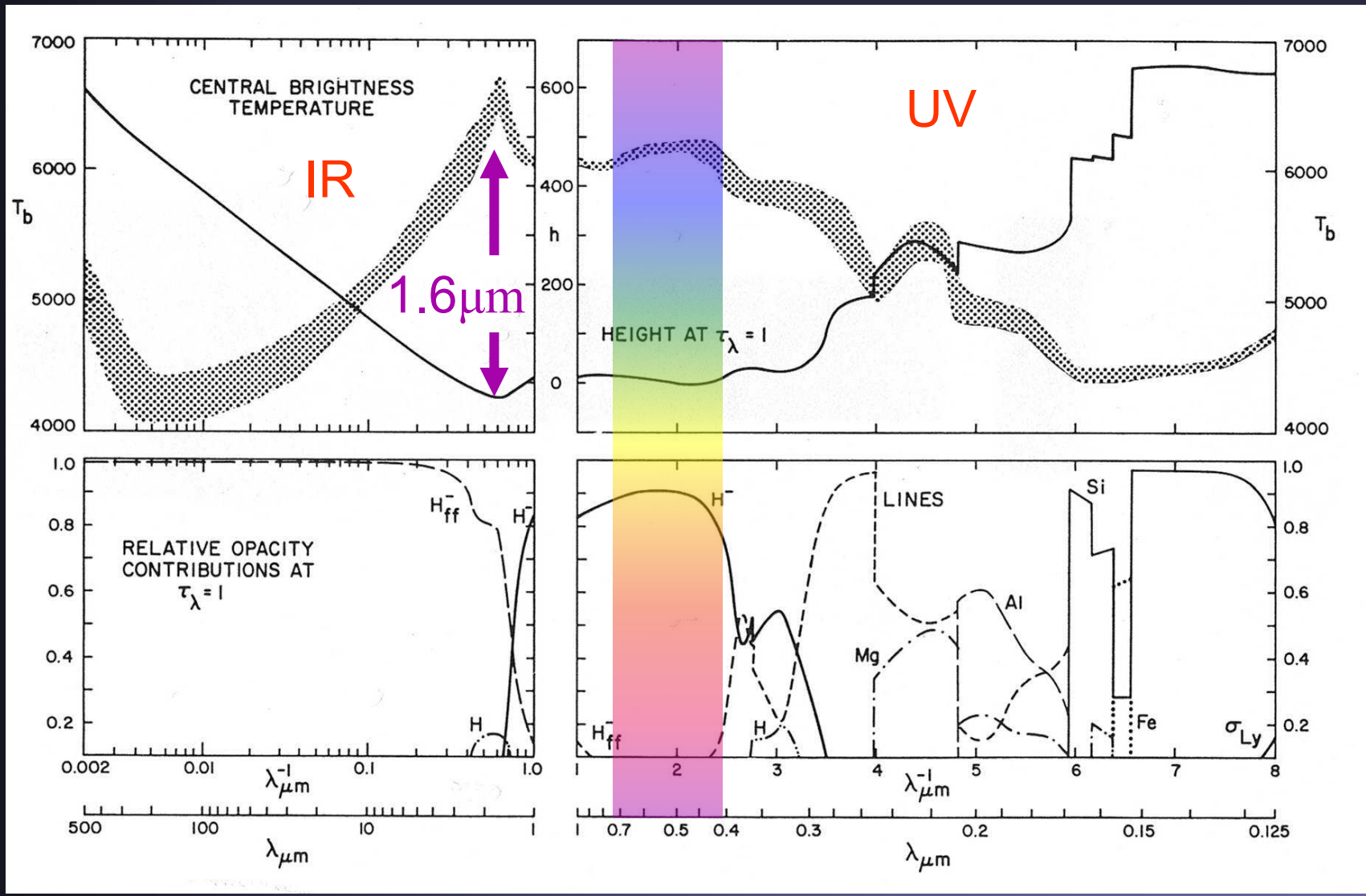

Radiative Transfer Equation

- Equation of radiative transfer:

$$\mu \, \mathrm{d}I_\nu / \mathrm{d}\tau_\nu = I_\nu - S_\nu$$

where I_ν is the intensity (i.e. the measured quantity) and S_ν is the source function. $\mu = \cos\theta$, where $\theta =$ angle of line-of-sight to surface normal.

- S_ν = emissivity ε_ν divided by absorption coefficient κ_ν
- The physics is hidden in ε_ν and κ_ν , i.e. in τ_ν and S_ν .
- These quantities depend on temperature, pressure, elemental abundances and frequency (or wavelength)

Formal solution of RT equation

- For $S_\nu = 0$ the solution of the RTE in a slab with (optical) boundaries $\tau_{\nu 2}$ and $\tau_{\nu 1}$ is ($\tau_{\nu 2} > \tau_{\nu 1}$):

$$I_\nu(\tau_{\nu 1}) = I_\nu(\tau_{\nu 2}) \exp(-\tau_{\nu 2} + \tau_{\nu 1})$$

- For general case formal solution reads (formal soln. assumes that we already know S_ν)

$$I_\nu(\tau_{\nu 1}) = I_\nu(\tau_{\nu 2}) \exp(-\tau_{\nu 2} + \tau_{\nu 1}) + \int S_\nu \exp(-\tau_\nu)\, d\tau_\nu$$

- 1st term describes radiation that enters through lower boundary (only absorption, no emission in slab), 2nd term describes radiation emitted in slab.
- In a stellar atmosphere $\tau_{\nu 2} = \infty$, so that only the 2nd term survives (lower boundary is unimportant).

When is an emission line formed, when an absorption line?

- Continua are formed deeper in a stellar atmosphere than spectral lines at the same wavelengths:

  $\kappa_L + \kappa_C > \kappa_C$

- A line is in absorption if S_ν decreases with height, i.e. if the absorption at greater heights dominates over emission ($S_L < S_C$)

- A line is in emission if S_ν increases with height, i.e. if the emission at greater heights dominates over absorption ($S_L > S_C$)

Statistical equilibrium

- In general both S_ν and κ_ν require a computation of the full statistical equilibrium for the atomic species being considered.
- This implies computing how much each atomic/ionic/molecular level is populated, i.e. solving rate equations describing transitions to and from each considered level.
- Requires detailed knowledge of atomic, ionic, molecular structure and transitions.

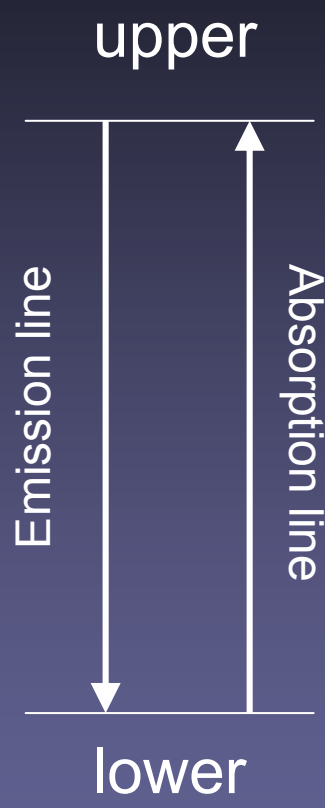

The assumption of LTE

- In solar interior and photosphere (i.e. where density is large and collisions are common) we can assume Local Thermodynamic Equilibrium (LTE)
- Thermodynamic equilibrium (TE): a single temp. everywhere = blackbody ➔ Emerging radiation follows Planck function $B_\nu(T)$.
- LTE: Each layer of the solar atmosphere has its own temperature ➔ Replace S_ν by $B_\nu(\tau, T)$ in the RTE and its solution.
  - ➔Problem of knowing S_ν is reduced to knowing $T(\tau)$ in the atmosphere.
  - ➔equilibrium reduces to Saha-Boltzmann equilibrium ➔ 0nly T and n_e need to be known.

Saha and Boltzmann equations

Excitation (Bolzmann) and ionization (SAHA) in LTE

$$\frac{n_{low}}{n_{up}} = \frac{g_{low}}{g_{up}} e^{-(E_{low}-E_{up})/kT}$$

Boltzmann

n = number density of particles in a particular energy state
g= statitical weight of level: $g=2J+1$, J= angular momentum
E= Energy of levels involved in the transition

$$\frac{n_{\mathrm{up}}}{n_{\mathrm{low}}} = \frac{2}{n_{\mathrm{e}}} \left(\frac{2\pi m_{\mathrm{e}} kT}{h^3} \right)^{3/2} \frac{g_{\mathrm{up}}}{g_{\mathrm{low}}} e^{-(E_{\mathrm{up}}-E_{\mathrm{low}})/kT}$$

Saha

n_e = electon density
Basically: n_{up}/n_{lower} = function (T, n_e)

Analytical radiative transfer: the Milne-Eddington atmosphere

- A simple analytical solution for a spectral line exists for a Milne-Eddington atmosphere (i.e. $\eta_0 = (\kappa_L / \kappa_C)$ independent of τ_C and S_L depending only linearly on τ_L).

  $I(\mu)/I_C(\mu) = \beta\,\mu / (1+\eta_0)$,

  $I(\mu)/I_C(\mu)$ = continuum-normalized emergent intensity, where $\eta_0 = (\kappa_L / \kappa_C)$ and β is derivative of Planck function with respect to τ_v .

- The term $(1+\eta_0)$ takes care of line saturation.

- As absorbtion due to line, η_0, increases, $I(\mu)$ initially decreases, but for large η_0 saturates around 0.

Illustration of line saturation

- 4 spectral lines computed in Milne-Eddington atmospheres
- As η_0 increases the line initially becomes deeper, then wider, finally showing prominent line wings

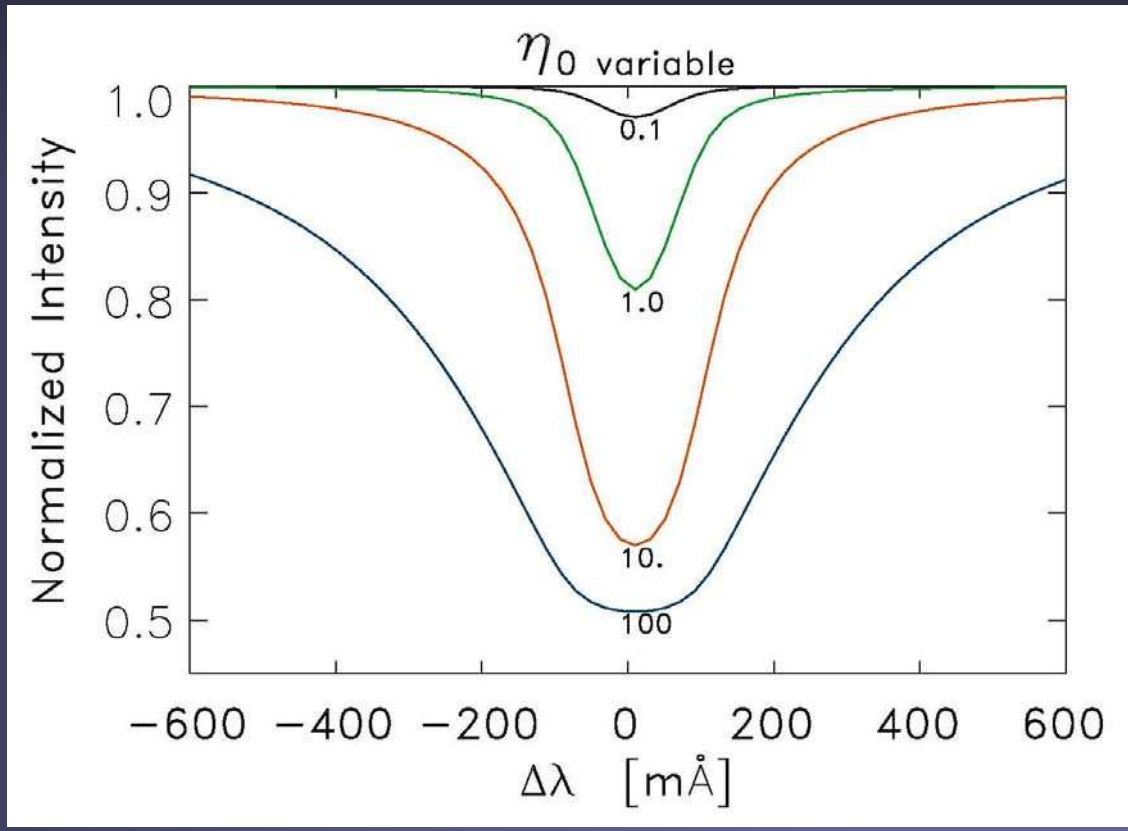

Figure kindly provide by J.M. Borrero

Diagnostic power of spectral lines

- Different parameters describing line strength and line shape contain information on different parameters of the solar/stellar atmosphere:
  - Doppler shift of line: (net) flows in the LOS direction.
  - Line width: temperature and turbulent velocity
  - Equivalent width: elemental abundance, temperature (via ionisation and excitation balance)
  - Line depth: temperature and temperature gradient
  - Line asymmetry: velocity gradients, v, T inhomogenieties
  - Wings of strong lines: gas pressure
  - Polarisation and splitting: magnetic field

Heights of formation: on which layers do lines give information ?

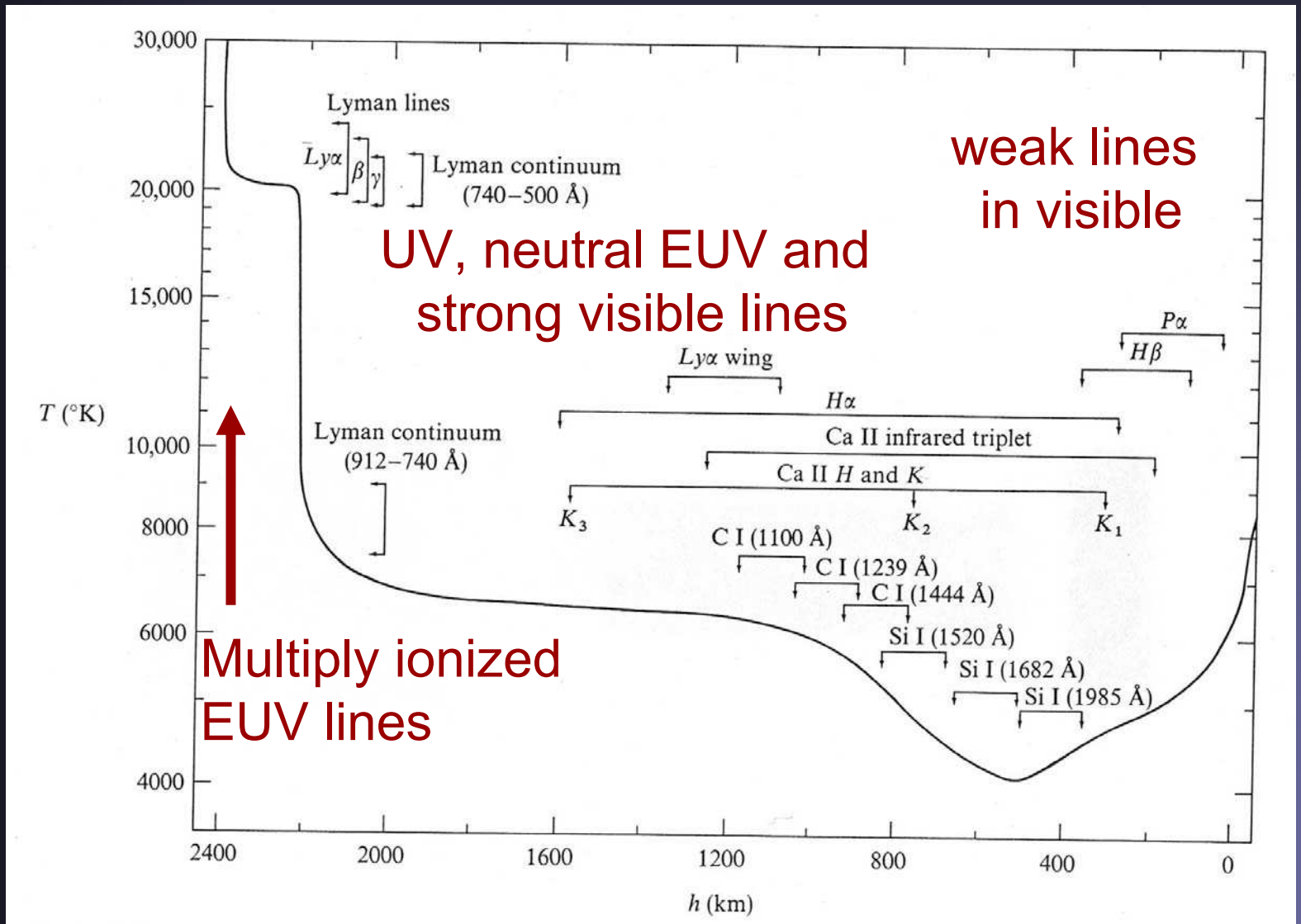

Solar convection

Hydrostatic equilibrium

- Sun is (nearly) hydrostatically stratified (this is the case even in the convection zone). I.e. gas satisfies:

$$dP/dz = -g\rho = -gP/\mu RT$$

(P pressure, g grav. accel., ρ density, μ mean molec. weight, R gas constant)

- Solution for constant temperature:

$$P = P_0 \exp(-z/H)$$

- Here H is the pressure scale height. $H \sim T^{1/2}$ and varies between 100 km in photosphere (solar surface) and 10^4 km at base of convection zone.

The convection zone

- Through the outermost 30% of solar interior, energy is transported by convection instead of by radiation
- In this layer the gas is convectively unstable.
- I.e. the process changes from a random walk of the photons through the radiative zone (due to high density, the mean free path in the core is well below a millimeter) to convective energy transport
- The unstable region ends just below the solar surface. I.e. the visible signs of convection are actually due to overshooting (see following slides)
- $t_{\text{radiative}} \sim 10^6$ years >> $t_{\text{convective}} \sim$ days-weeks

Scales of solar convection

- Observations: 4 main scales
  - **granulation**
  - mesogranulation
  - **supergranulation**
  - giant cells
- **Colour:**
  - **well observed**
  - less strong evidence
- Theory: larger scales at greater depths. Most details still unclear

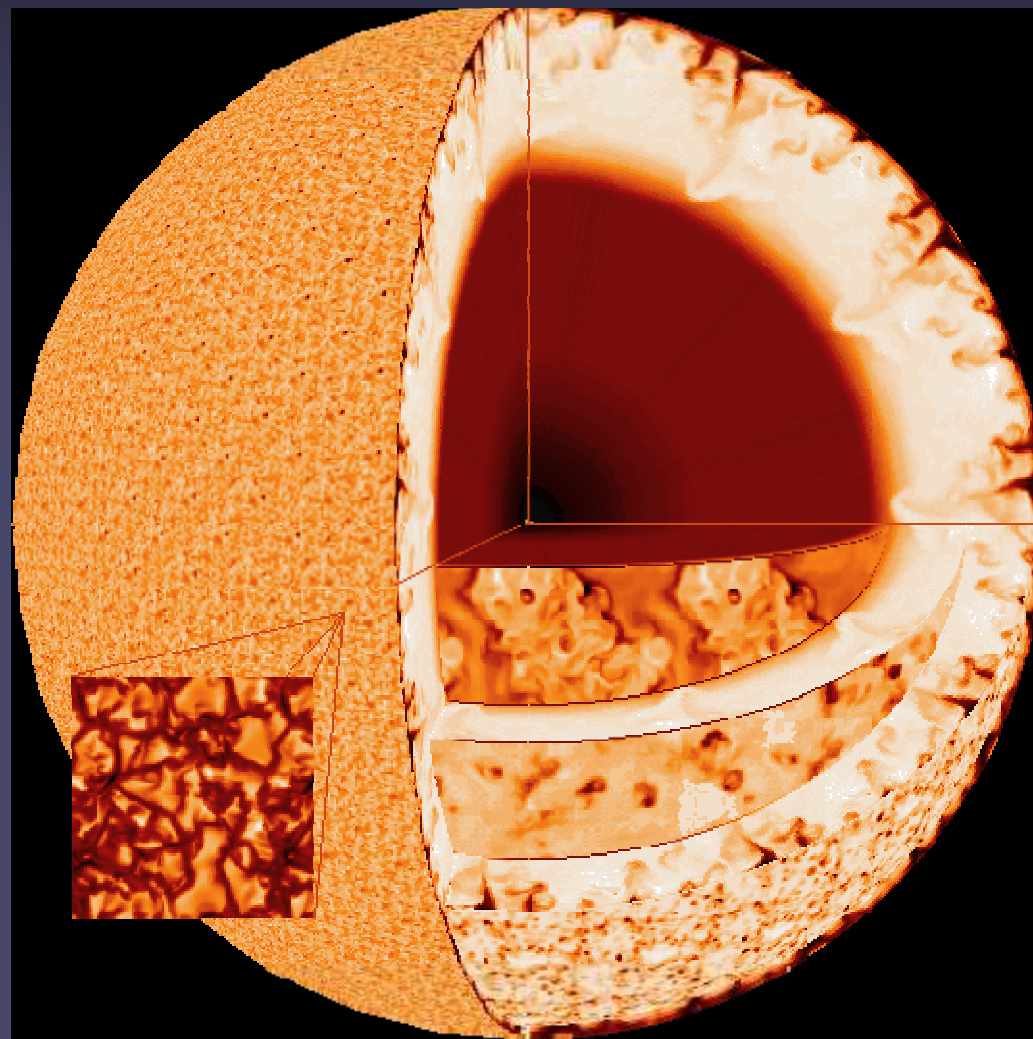

Surface manifestation of convection: granulation

- Typical size: 2 Mm
- Lifetime: 6-8 min
- Velocities: 1 km/s (but peak velocities > 10 km/s, i.e. supersonic)
- Brightness contrast: 15% in visible(yellow) continuum (under ideal conditions)
- All quantities show a continuous distribution of values
- At any one time 10^6 granules on sun.

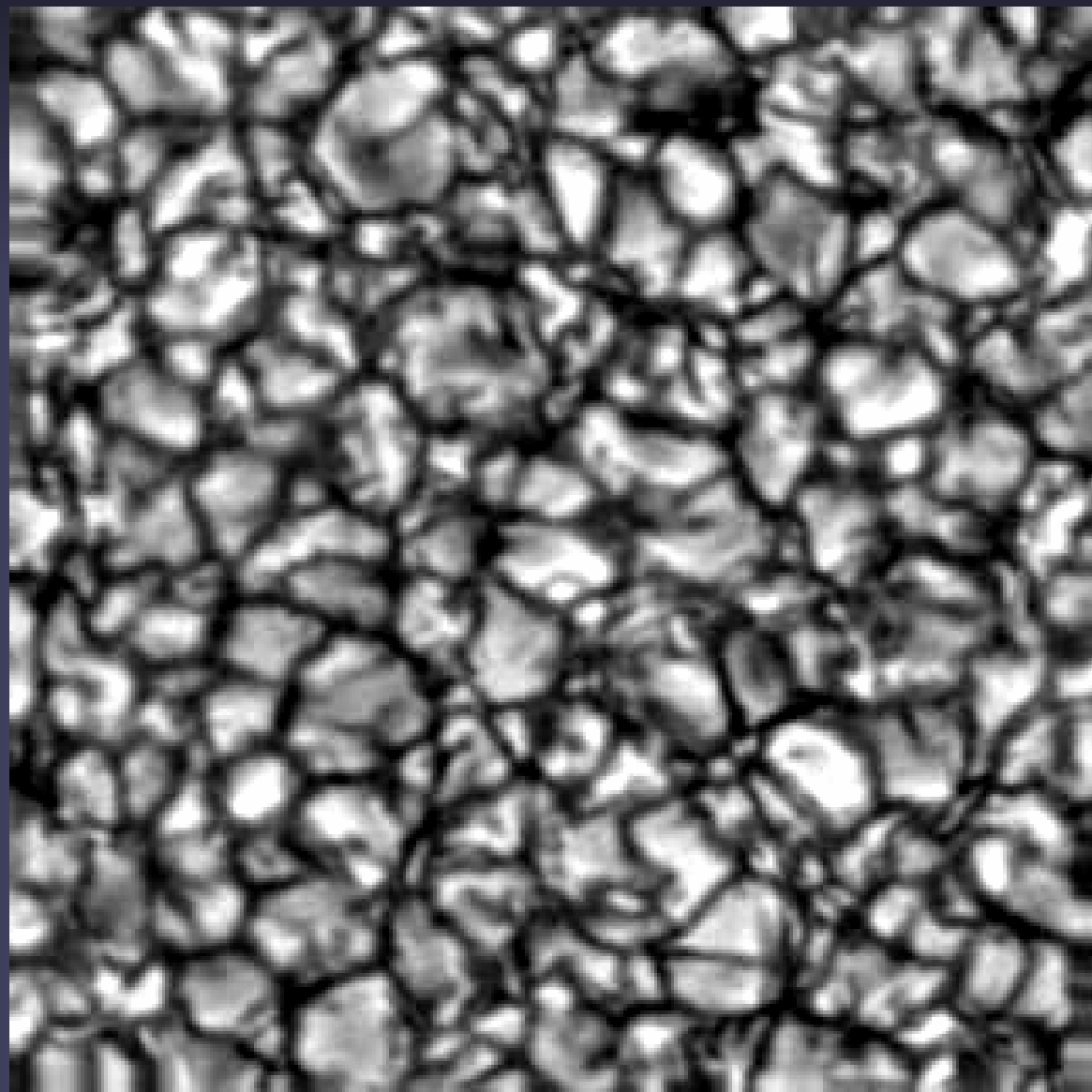

Surface mainfesttion of convection: Supergranulation

- 1 hour average of MDI Dopplergrams (averages out oscillations).
- Dark-bright: flows towards/away from observer.
- No supergranules visible at disk centre: velocity is mainly horizontal
- Size: 20-30 Mm, lifetime: days, horiz. speed: 400 m/s, no contrast in visible

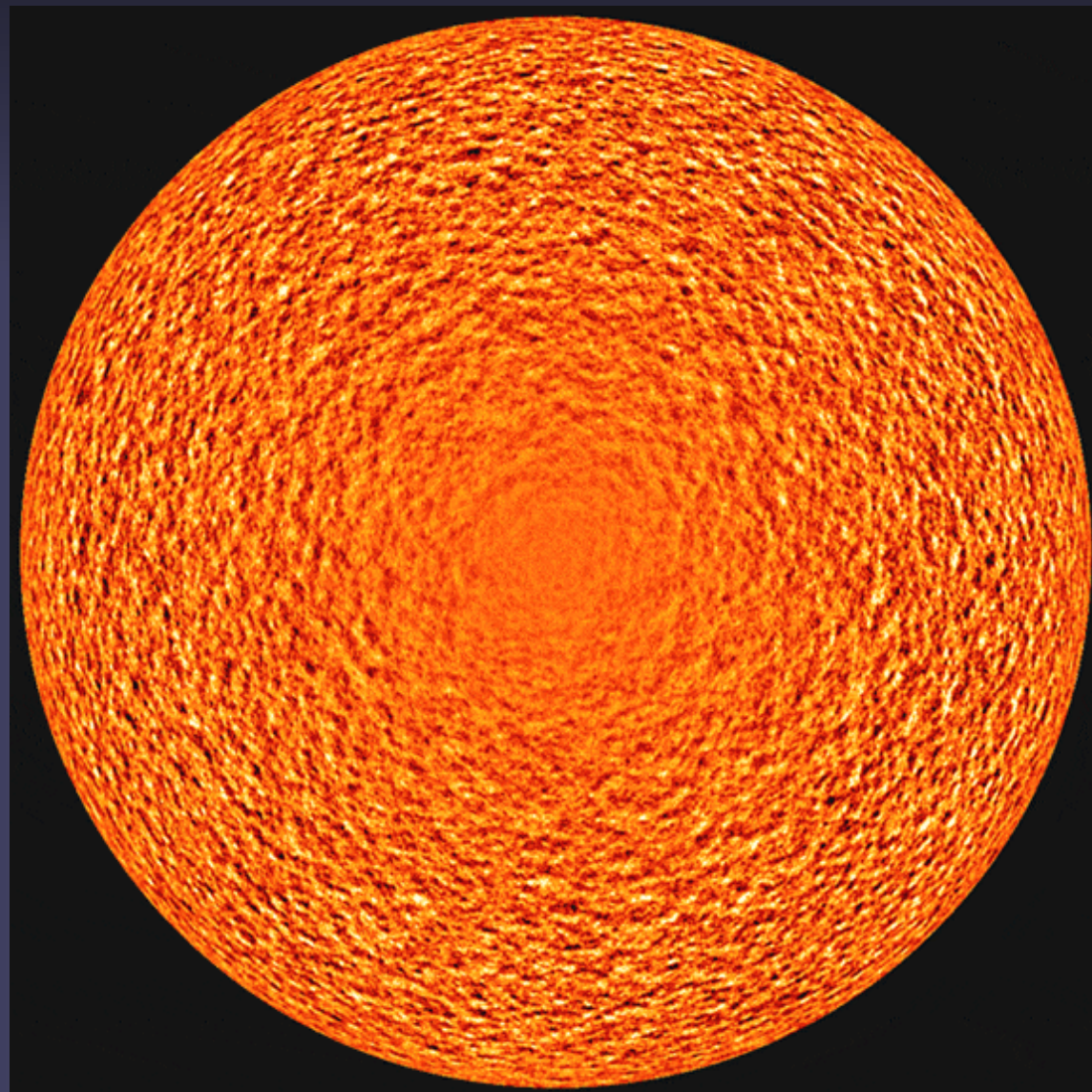

Observing convection

- Observing granulation
  - Continuum images and movies at high spatial resolution: gives sizes, lifetimes and evolution (splitting and dissolving granules), contrasts
  - Spectral lines. Line bisectors, line widths and convective blue shifts: contrasts, area factors, stratification
- Observing supergranulation
  - Images and movies in cores of chromospheric spectral lines, or magnetograms: observe the magnetic field at the edges of the supergranules instead of the supergranules directly
  - Helioseismic techniques

Line bisectors

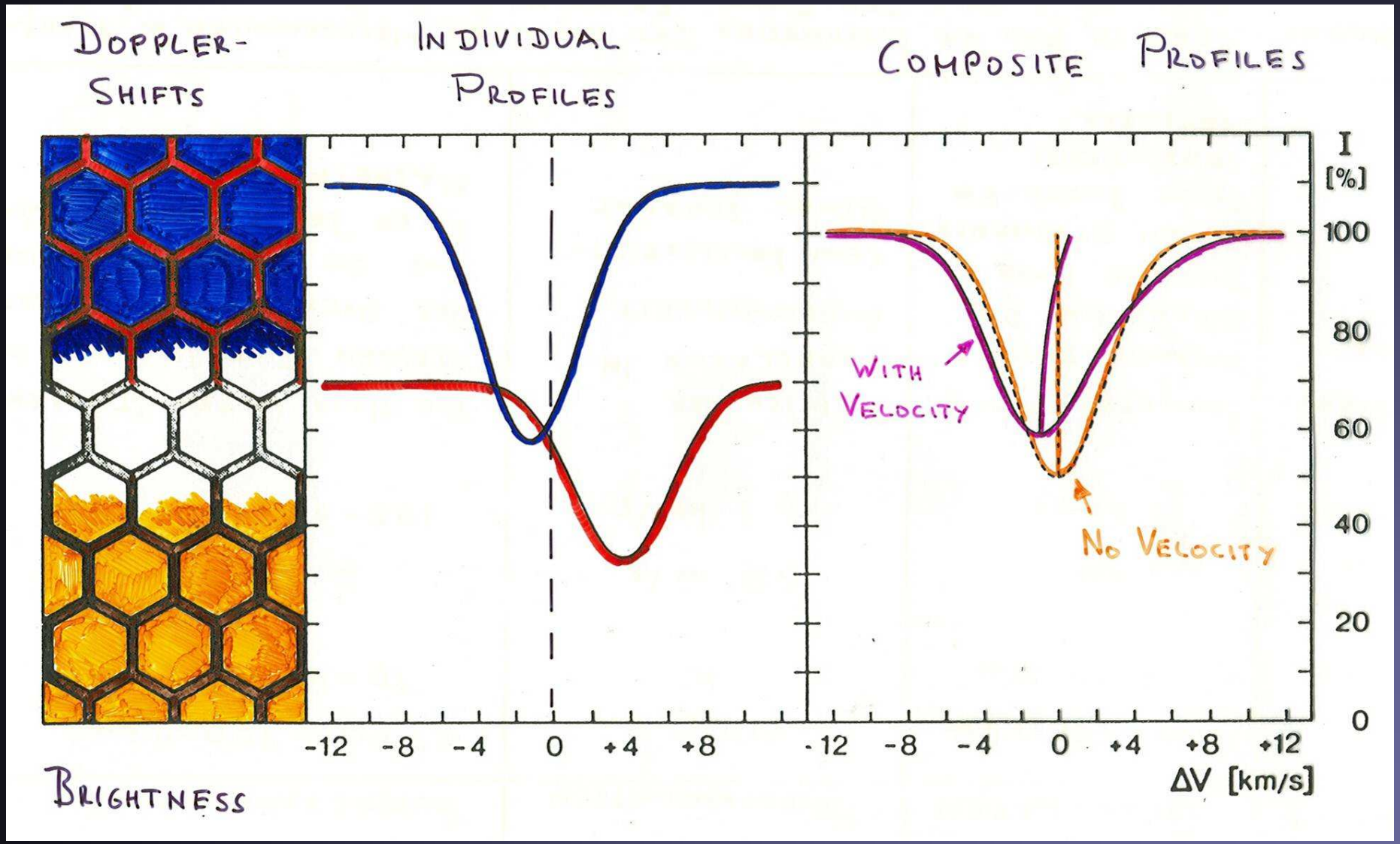

Observed line bisectors: “C” shape

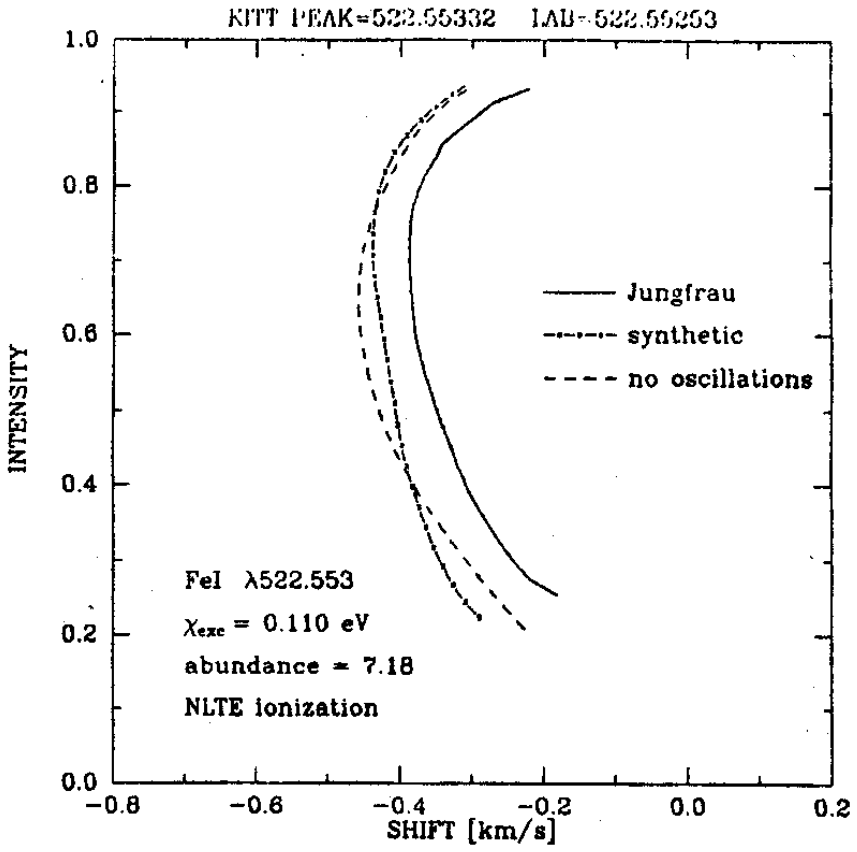

C.

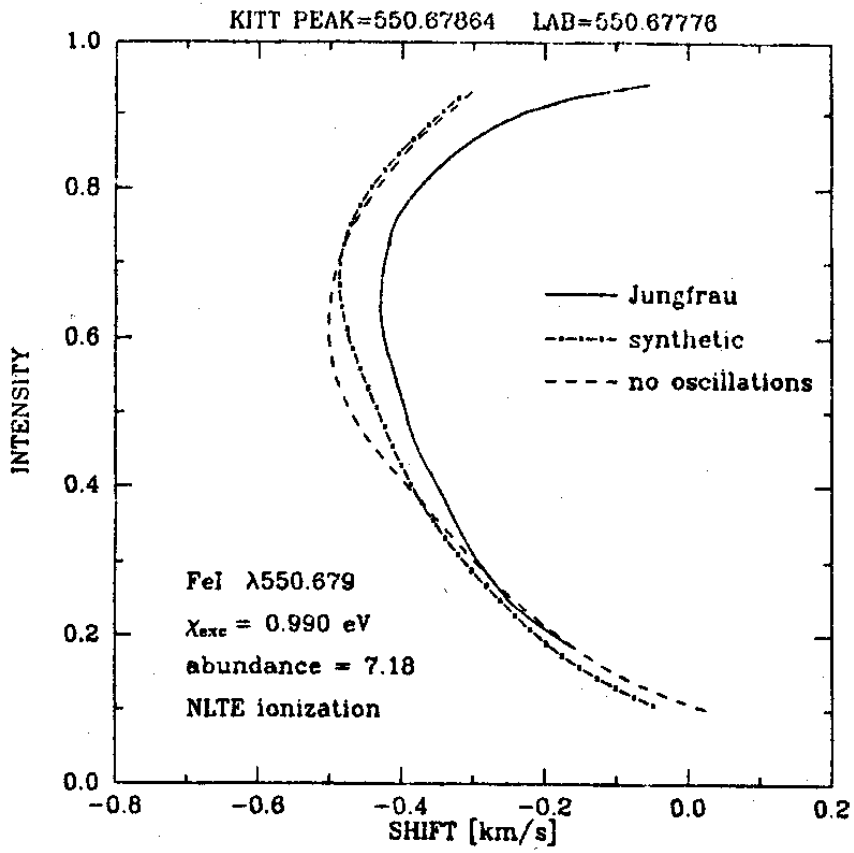

Supergranules seen by SUMER

- Si I 1256 Å full disk scan by SUMER in 1996
- Bright network indicates location of magnetic network
- Darker cells: supergranules

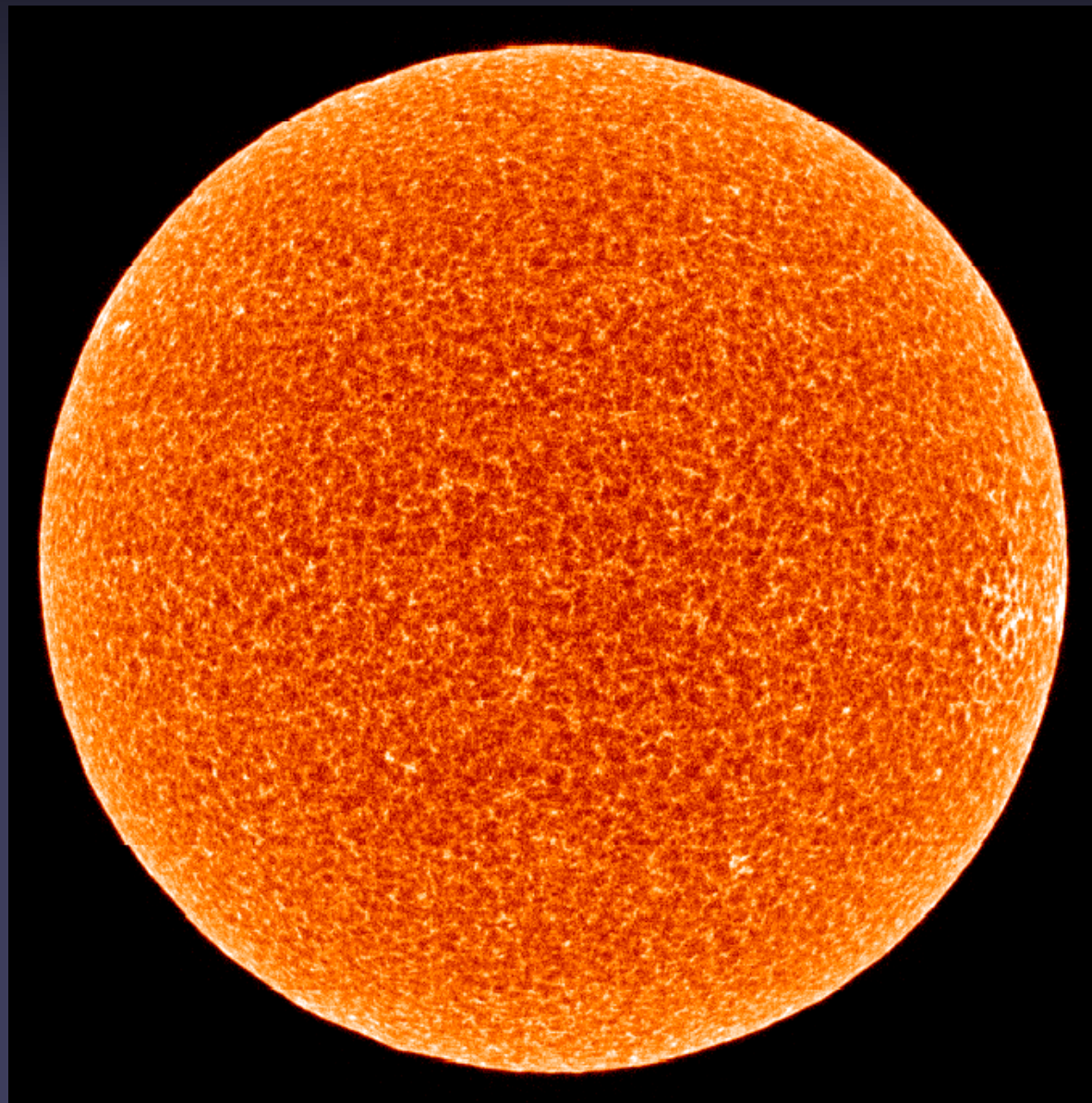

Supergranules & magnetic field

- Why are super-granules seen in chromospheric and transition region lines?
- Supergranules are related to the magnetic network.
- Network magnetic fields are located at edges of supergranules. They appear bright in UV.

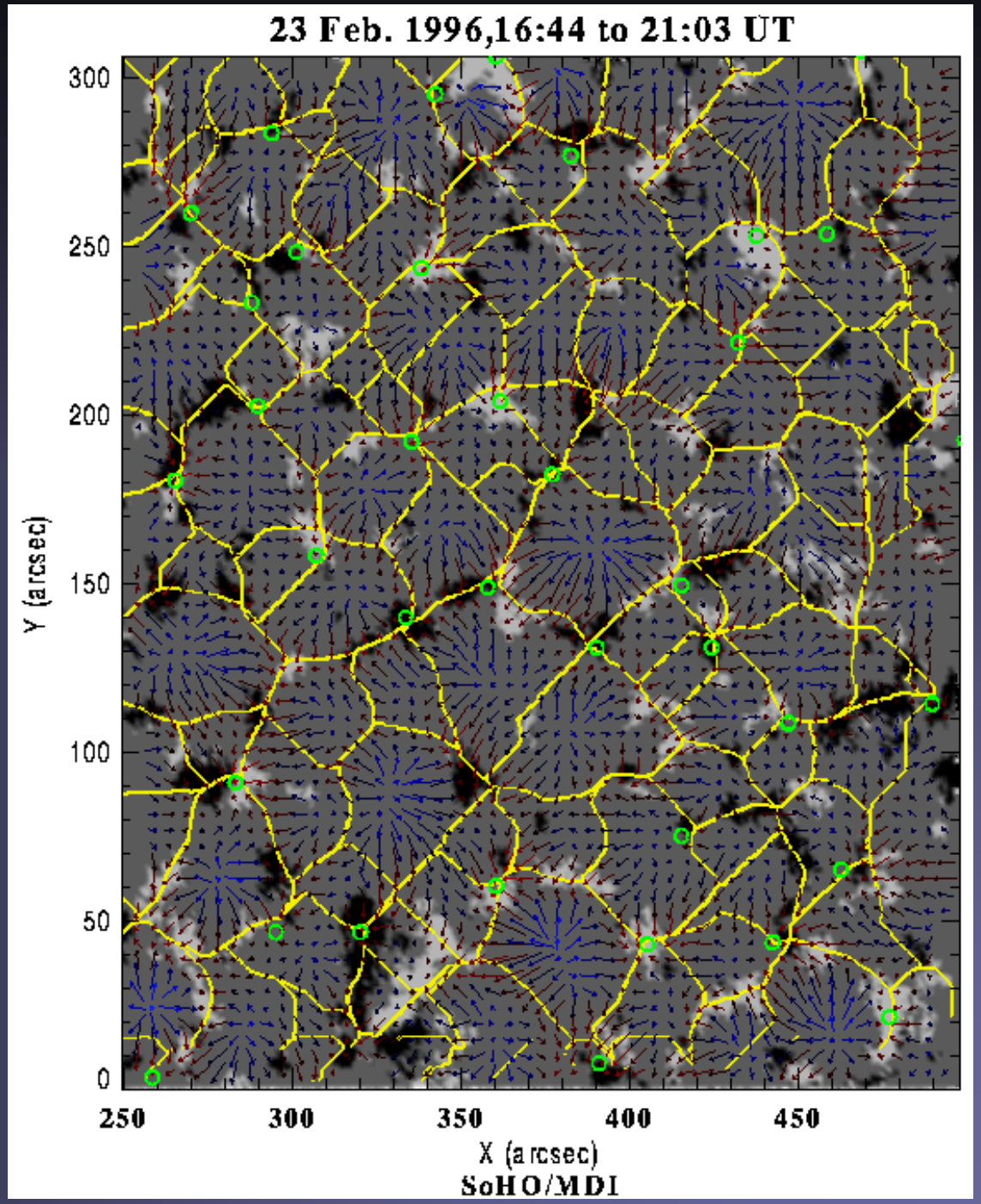

Onset of convection

Schwarzschild's instability criterion

Consider a rising bubble of gas:

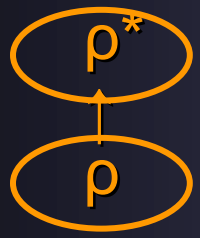

ρ^*	$\rho_0-\Delta\rho$	$z-\Delta z$
ρ	ρ_0 ($=\rho$)	z
bubble	surroundings	depth

Condition for convective instability: $\rho^* < \rho_0-\Delta\rho$

For small Δz, bubble will not have time to exhange heat with surroundings: adiabatic behaviour. Convectively unstable if:

$$[d\rho/dz - (d\rho/dz)_{adiab}]\,\Delta z < 0$$

$d\rho/dz$: stellar density gradient if in radiative equilibrium

$(d\rho/dz)_{adiab}$: adiabatic gradient

Illustration of convectively stable and unstable situations

Convectively stable

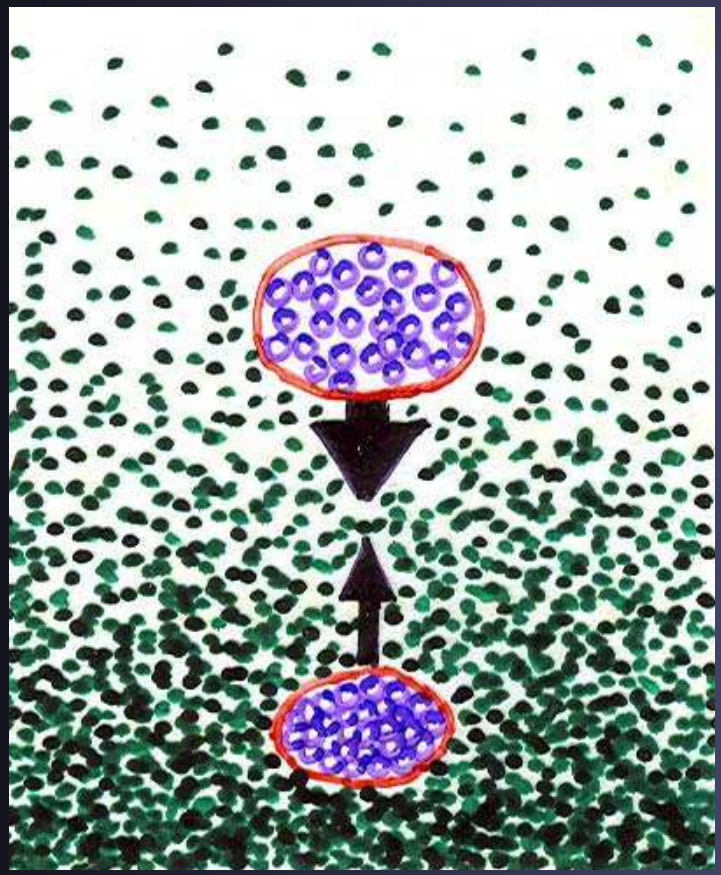

Convectively unstable

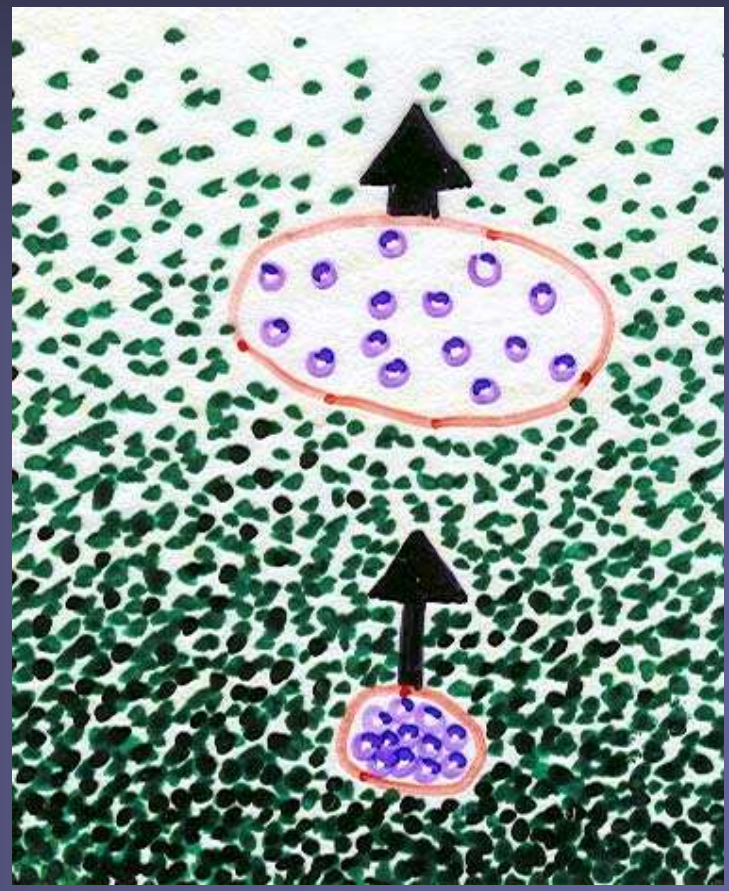

Onset of convection II

Rewriting in terms of temperature and pressure:

$\nabla_{ad} = (d \log T / d \log P)_{ad}$

$\nabla_{rad} = (d \log T / d \log P)_{rad}$ = gradient in an atmosphere with radiative energy transport

Schwarzschild's convective instability criterion:

$$\nabla_{ad} < \nabla_{rad}$$

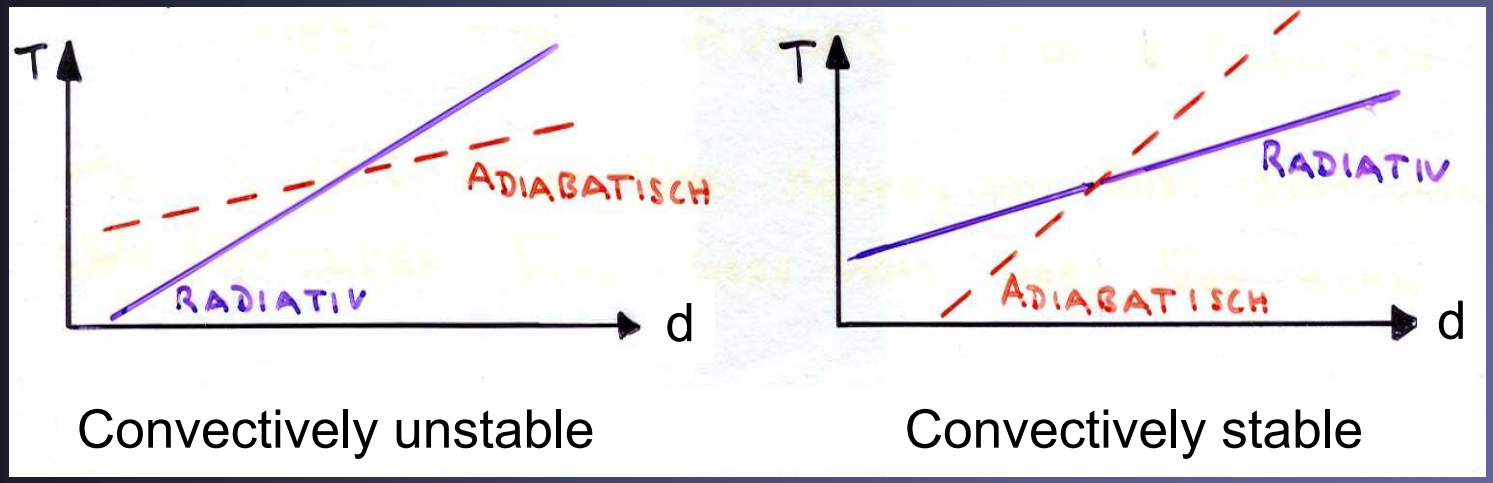

Why an outer convection zone?

- Why does radiative grad exceed adiabatic gradient?
- Mainly: radiative gradient becomes very large due to ionization of H and He below the solar surface.
- Expression for radiative gradient (for Eddington approximation):

$$\nabla_{rad} = (3F_r / 16\sigma g)(\kappa_{gr} P_g / T^4)$$

  - F_r = radiative flux (≈ constant)
  - σ = Stefan-Boltzmann constant
  - g = gravitational acceleration (≈ constant)
  - κ_{gr} = absorption coefficient per gram. At surface H and He are neutral. They become ionized with depth as T grows ➔ κ_{gr} increases rapidly, leading to large radiative gradient.

Ionisation of H and He

- Ionisation balance is described by Saha's equation: degree of ionisation depends on T and n_e
- H ionisation happens just below solar surface
- $He \rightarrow He^+ + e^-$ happens 7000 km below surface
- $He^+ \rightarrow He^{++} + e^-$ happens 30'000 km below surface
- Since H is most abundant, it provides most electrons (largest opacity) and drives convection most strongly
- At still greater depth, ionization of other elements also provides a minor contribution.

Radiative, adiabatic & actual gradients

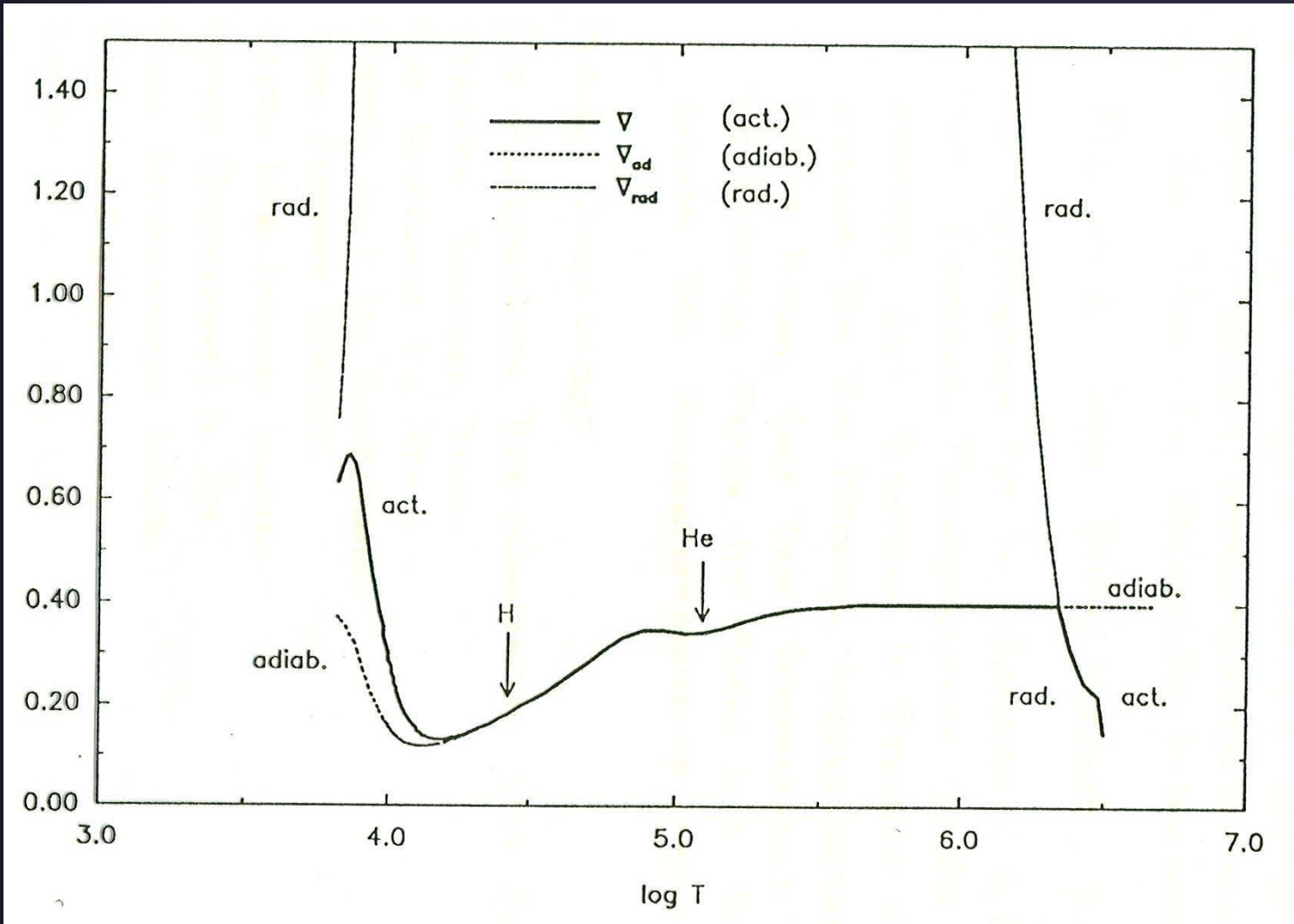

The mixing length

- As a gas packet rises, diffusion of particles and thermal exchange with surroundings causes it to lose its identity and to stop moving on.
- Length travelled up to that point: mixing length l (from L. Prandtl)
- Often used parameterization of l: $l = \alpha H_p$
  - H_p = pressure scale height
  - α = mixing length parameter, typically 1-2 (determined empirically)

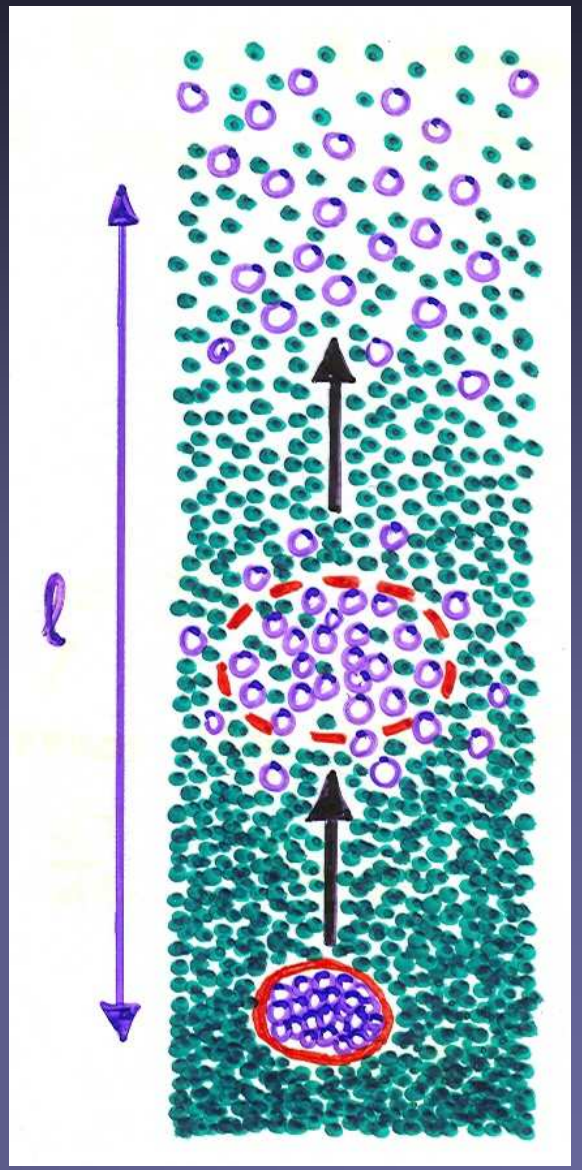

Convective overshoot

- Due to their inertia, the packets of gas reaching the boundary of the CZ pass into the convectively stable layers, where they are braked & finally stopped.

➔overshooting convection

- Typical width of overshoot layer: order of H_p
- This happens at both the bottom and top boundaries of the CZ and is important:
  - top boundary: Granulation is overshooting material. $H_p \approx$ 100 km in photosphere
  - bottom boundary: the overshoot layer allows B-field to be stored → seat of the dynamo?

Convection simulations

- 3-D hydrodynamic simulations reproduce a number of observations and provide new insights into solar convection.
- These codes solve for mass conservation, momentum conservation (force balance, Navier-Stokes equation), and energy conservation including as many terms as feasible.
- Problem: Simulations can only cover 2-3 orders of magnitude in length scale (due to limitations in computing power), while the physical processes on the Sun act over at least 6 orders of magnitude.
- Also, simulations can only cover a part of the size scale of solar convection, either granulation, supergranulation, or larger scales, but not all.

Convection simulations II

- Simulations do not achieve the solar Reynolds number ($R_e = \mathrm{v}l/\nu$) of 10^{10} , where v = typical velocity, l = typical length scale, ν = kinematic viscosity (R_e ~ ratio of viscous to advection time scales).
- For comparison with observations it is important that the simulations describe the surface layers well, i.e. code needs to consider:
  - radiative transport of energy. Only few simulation codes do this properly.
  - partial ionization of many elements
  - as low a viscosity as numerically possible
- The role of radiation is primarily to transport energy. At the solar surface the energy transported by radiation becomes comparable to that by convection.

Simulations of solar granulation

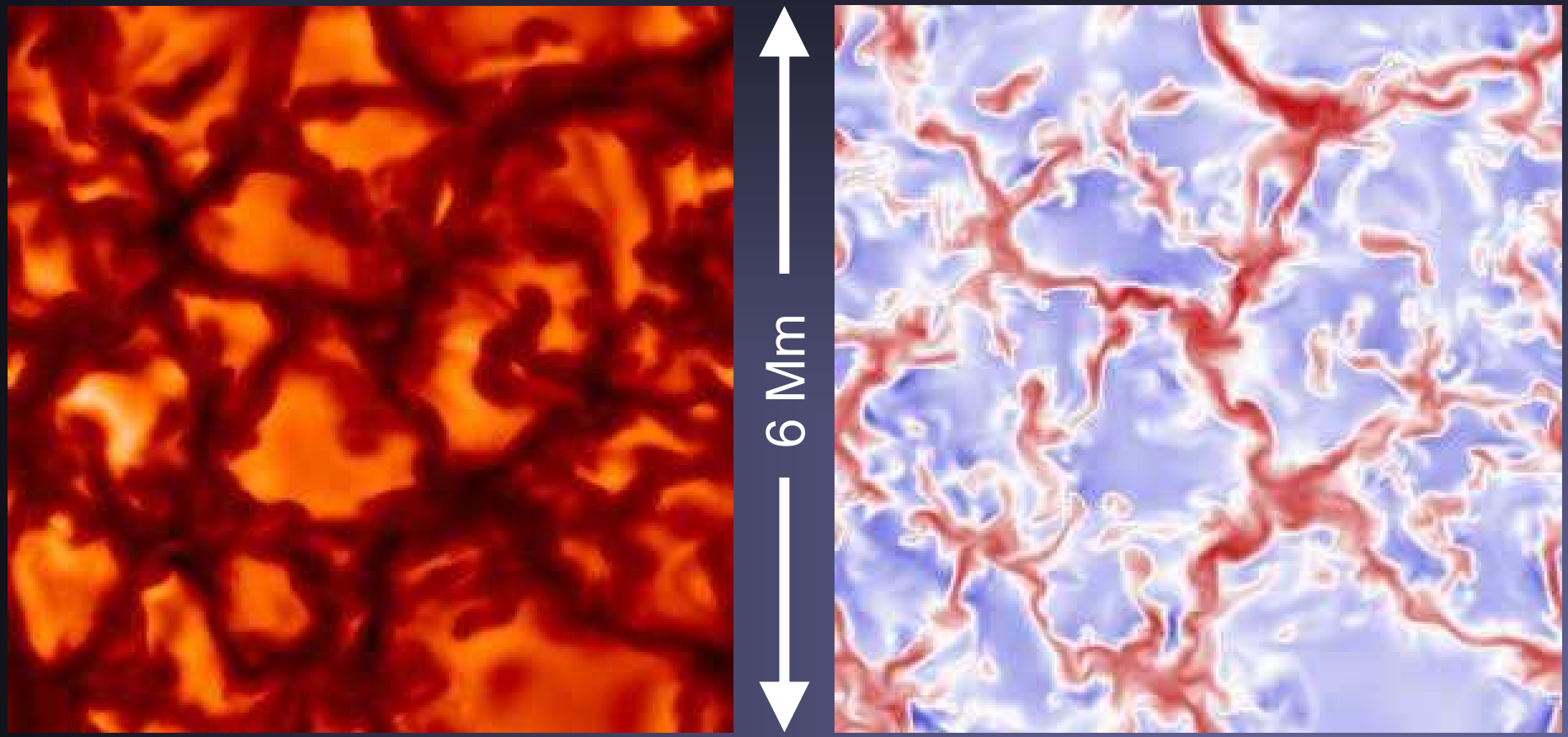

Solution of Navier-Stokes equation etc. describing fluid dynamics in a box (6000 km x 6000 km x 1400 km) containing the solar surface. Realistic looking granulation is formed.

Testing the simulations

Comparison between observed and computed bisectors for selected spectral lines (2 computed bisectors shown: one each with and without oscillations in the atmosphere)

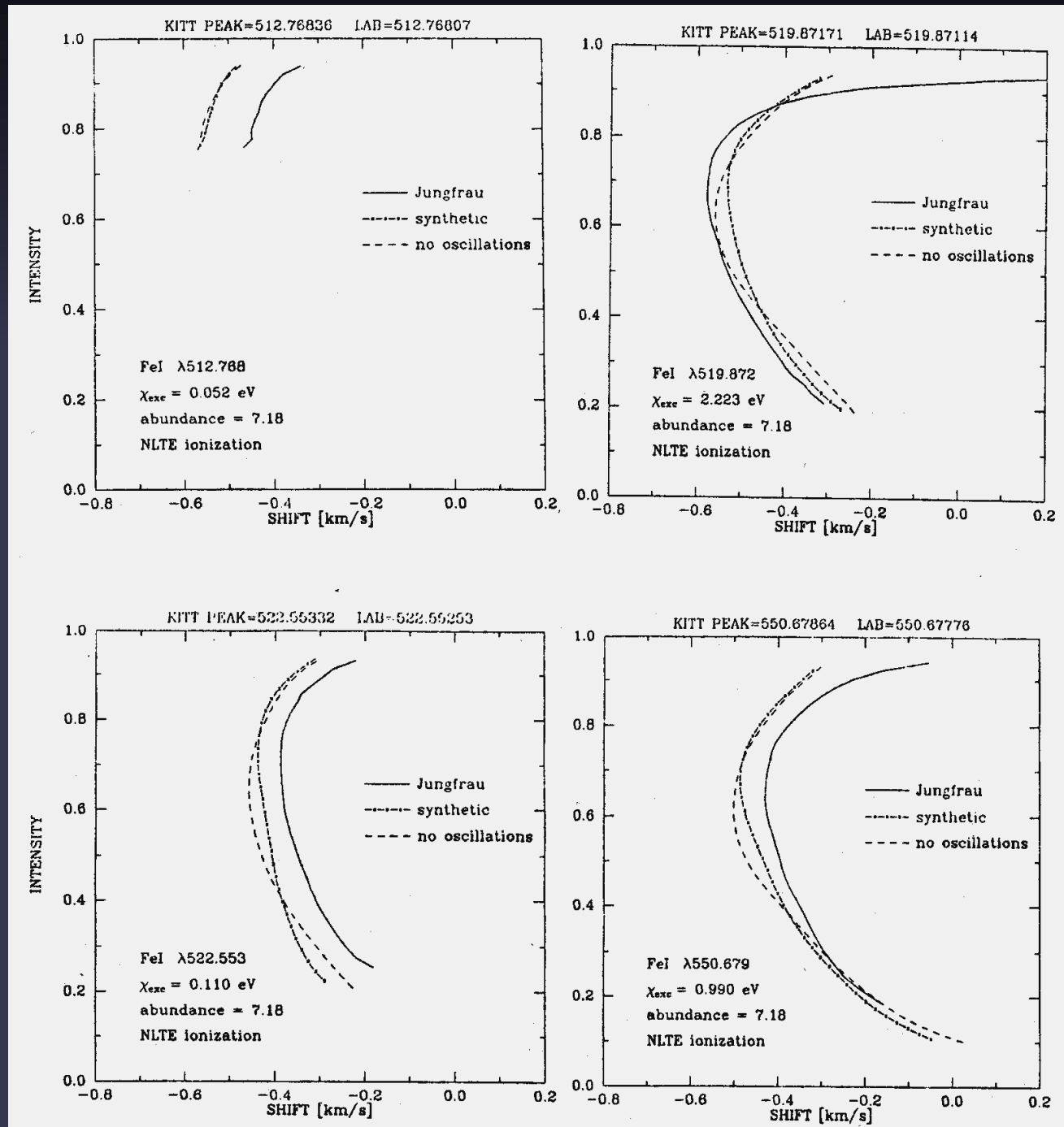

Granule structure

Upflows are broad & slow, downflows are narrow and fast. Why?

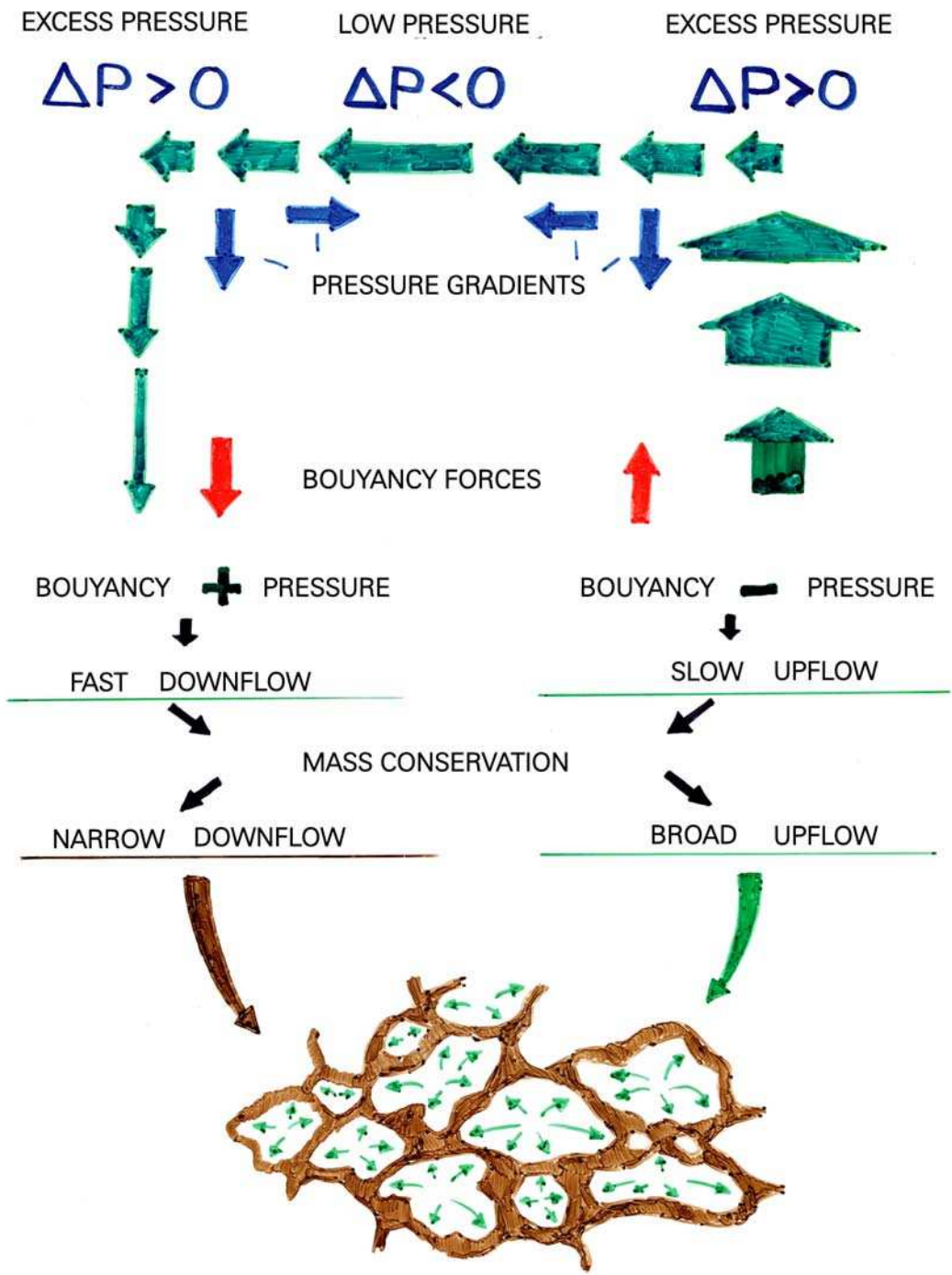

Granule evolution

- Granules die in two ways:
  - dissolve: grow fainter and smaller until they disappear (small granules)
  - split: break into two smaller granules (large granules)
- Granules are born in two ways:
  - as fragments of a large splitting granule
  - appearing as small structures and growing
- Initially most granules grow in size, some keep growing until they become unstable (see next slide) and split, others stop growing and start shrinking until they disappear (all within 5-10 min).

Relation between granules and supergranules

- Downflows of granules continue to bottom of simulations, but the intergranular lanes break up into isolated narrow downflow plumes.
- I.e. topology of flow reverses with depth:
  - At surface: isolated upflows, connected downflows
  - At depth: connected upflows, isolated downflows
- Idea put forward by Spruit et al. 1990: At increasingly greater depth the narrow downflows from different granules merge, forming a larger and less fine-meshed network that outlines the supergranules

Increasing size of convective cells with depth

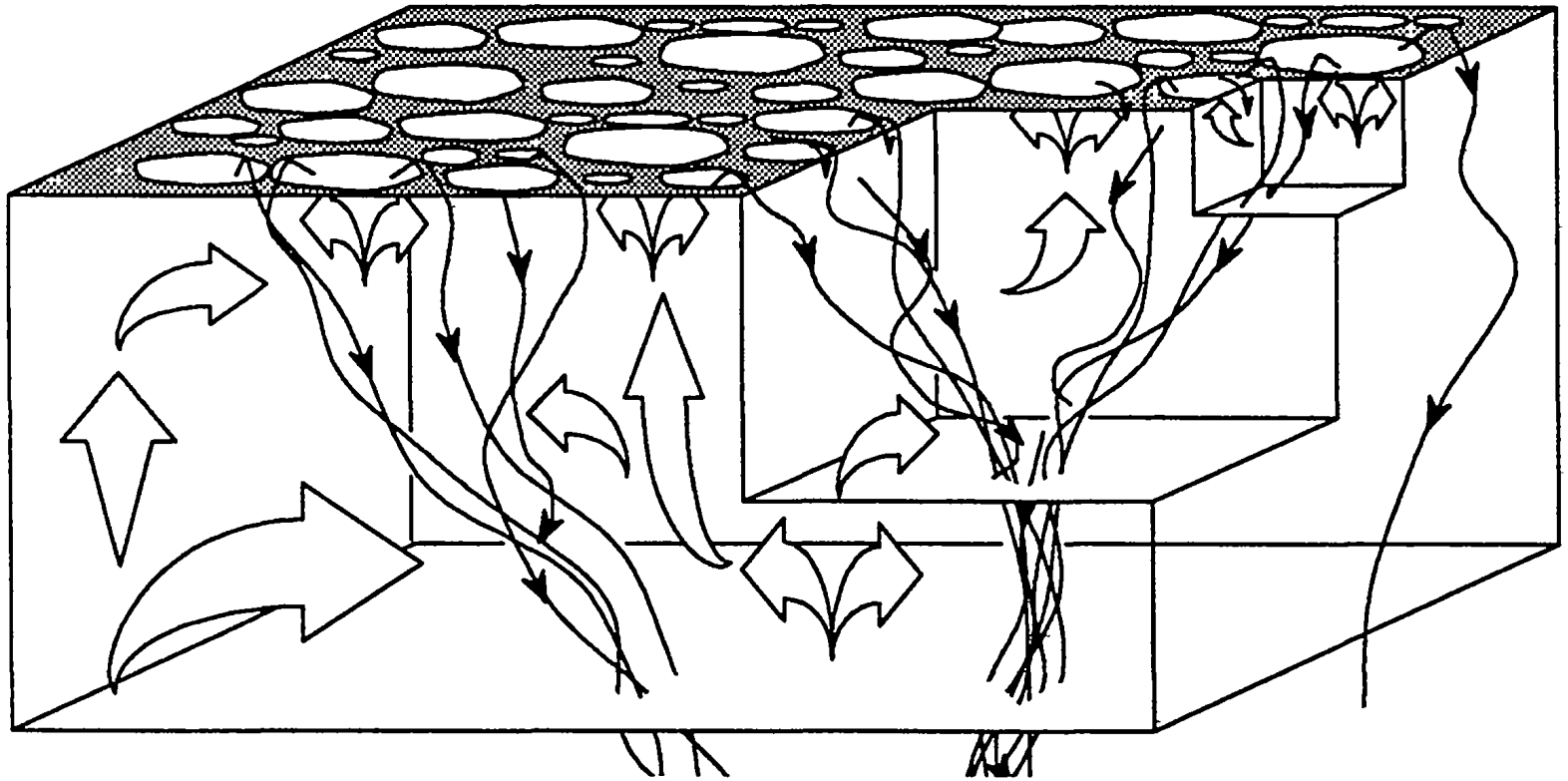

Figure 7 Flow lines showing the merging of the downdrafts on successively larger scales (schematic). The boxes cut out illustrate how the same process occurs on (in this illustration) three different scales.

Convection on other stars

- F, G, K & M stars (& cool WDs) posses outer convection zones
- Observations are difficult since surfaces cannot be resolved.

→ Use line bisectors

- A,F stars show inverse bisectors: granulation has different geometry.
- Hot stars have an inner convection zone

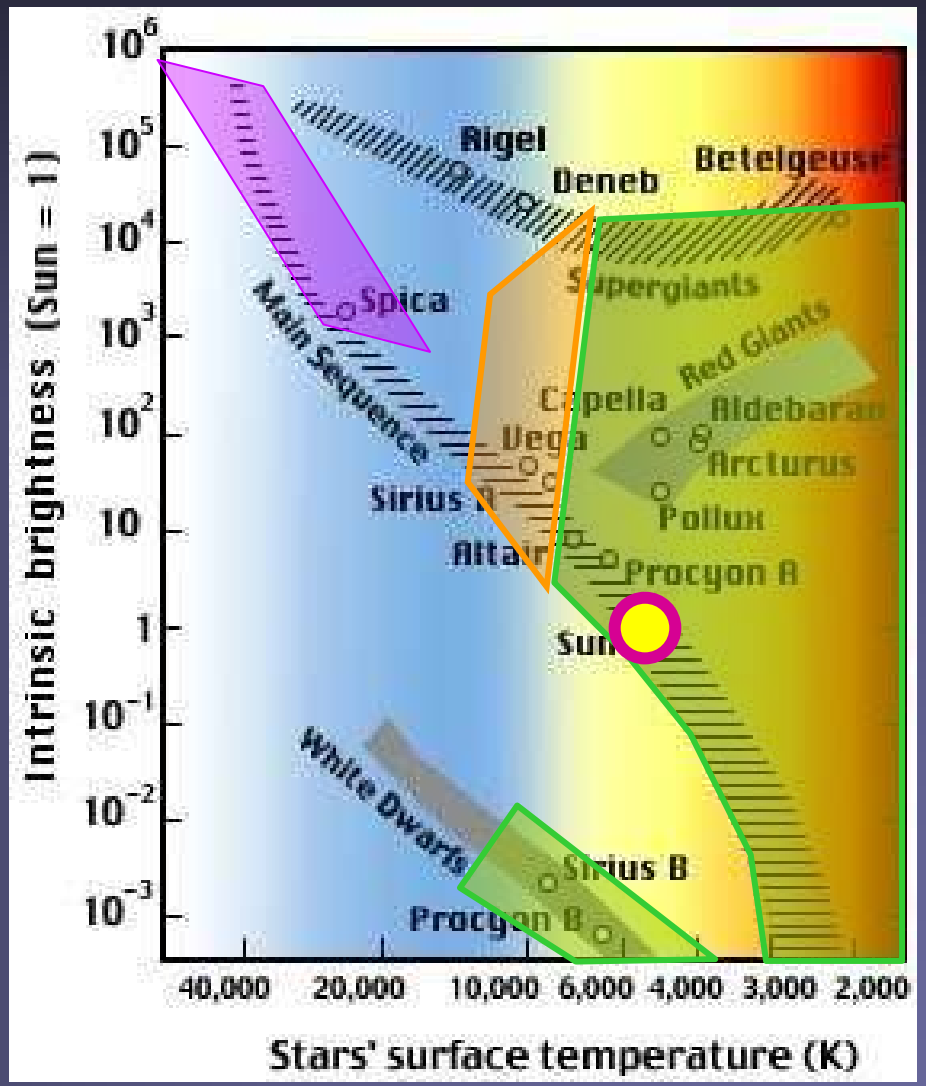

The solar atmosphere

The Sun's atmosphere

- Solar atmosphere generally described by multiple layers. From bottom to top: photosphere, chromosphere, transition region, corona
- In its simplest form it is modelled as a single component plane-parallel atmosphere.
- Density drops exponentially: $\rho(z) = \rho_0 \exp(-z/H_\rho)$ (for isothermal atmosphere). T=6000K ➔ $H_\rho \approx 100\mathrm{km}$
- Mass of the solar atmosphere ≈ mass of the Indian ocean (≈ mass of the photosphere)
- Mass of the chromosphere ≈ mass of the Earth's atmosphere

1-D stratification

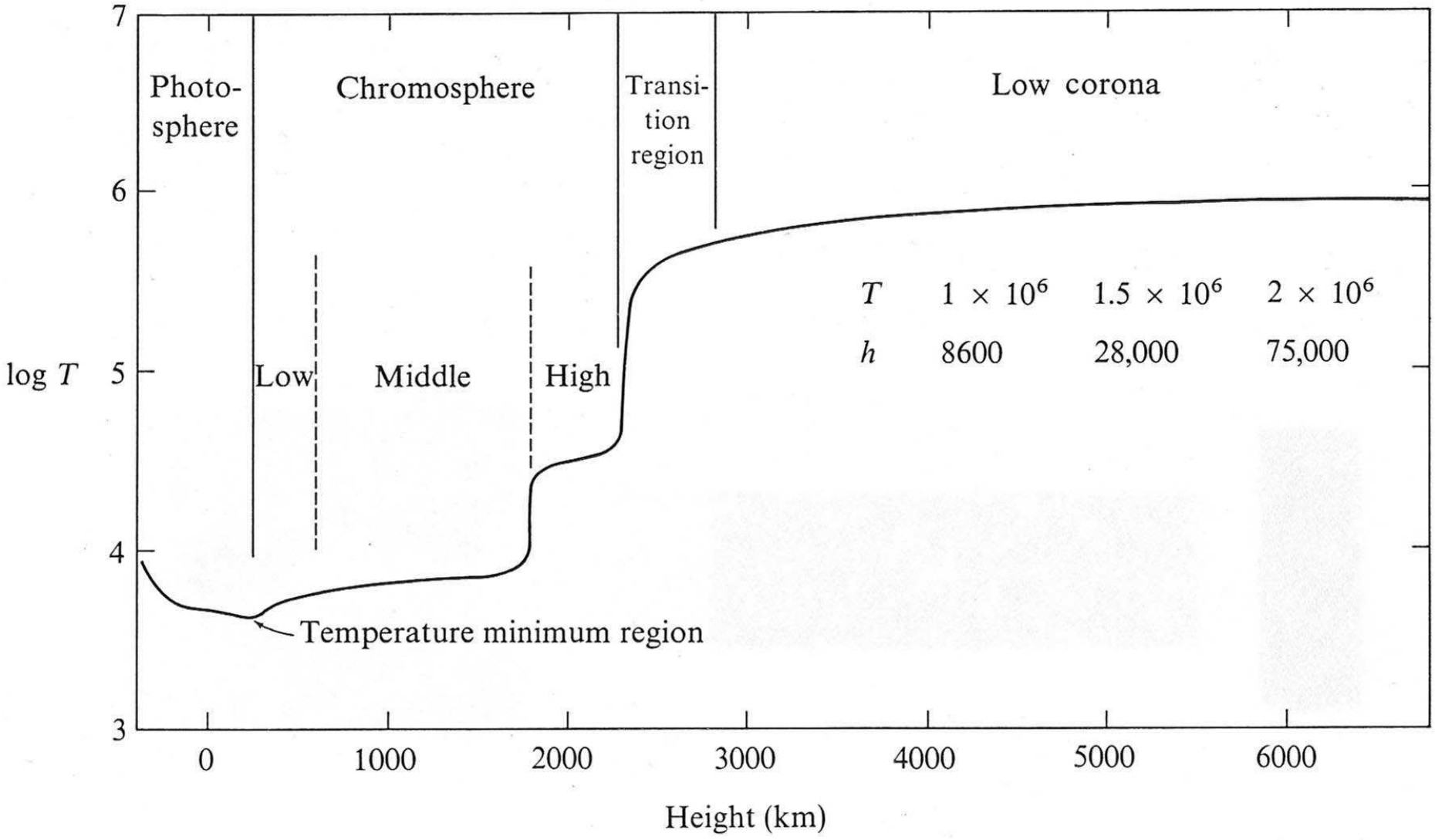

How good is the 1-D approximation?

- 1-D models reproduce extremely well large parts of the spectrum obtained with low spatial resolution (see spectral synthesis slide)
- However, any high resolution image of the Sun shows that its atmosphere has a complex structure (as seen at almost any wavelength)
- Therefore: 1-D models may well describe averaged quantities relatively well, although they probably do not describe any particular part of the real Sun.

Photosphere

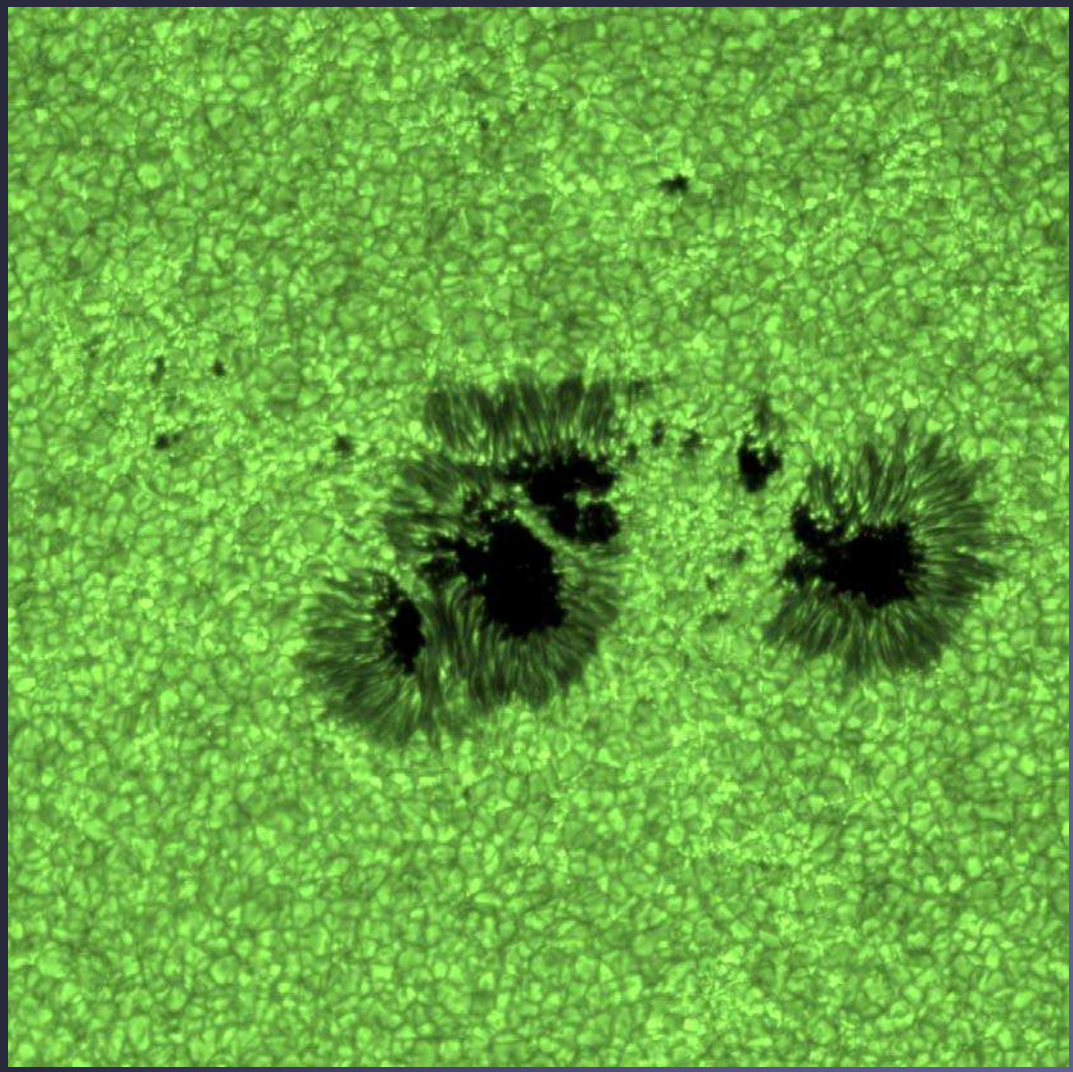

Lower chromosphere

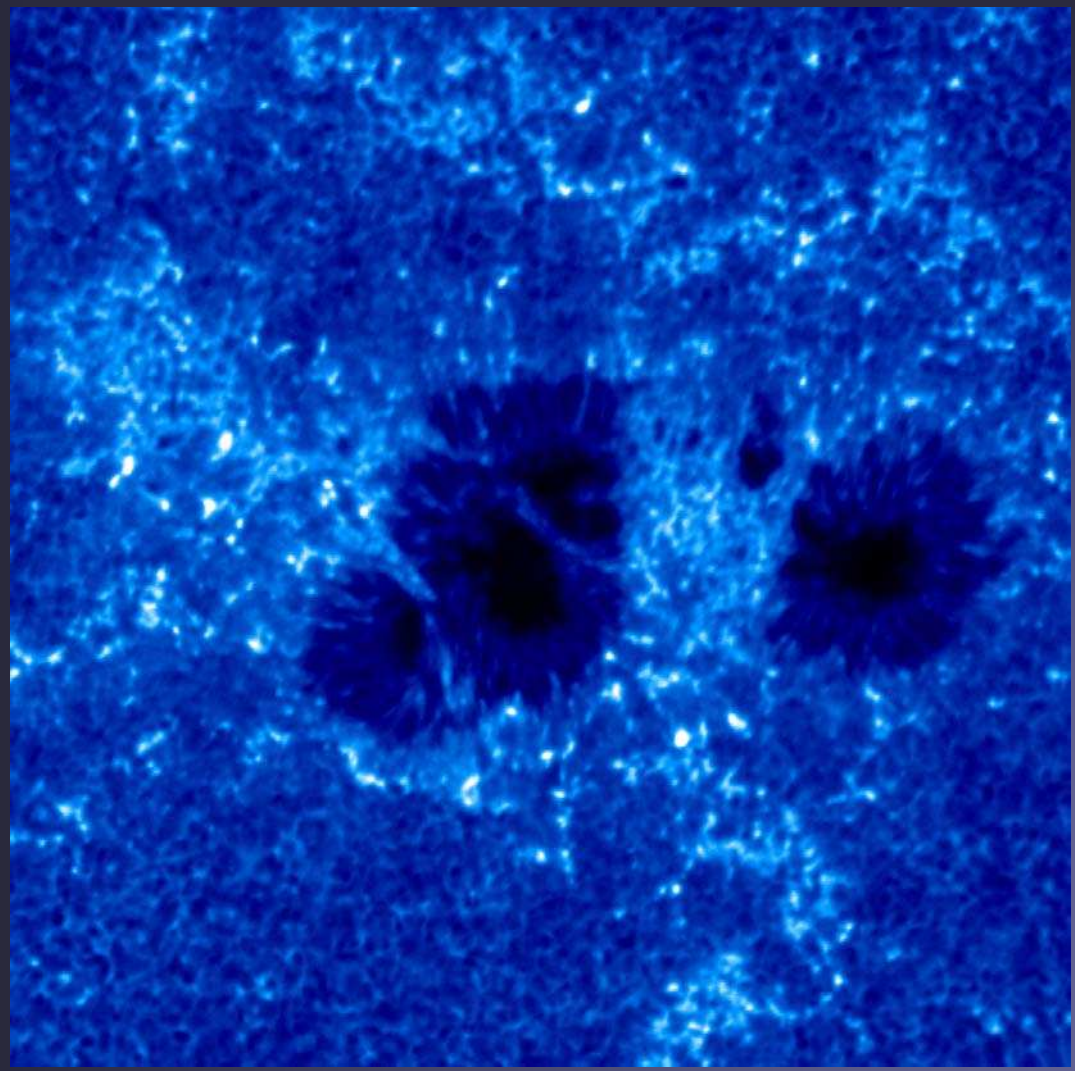

Upper chromosphere

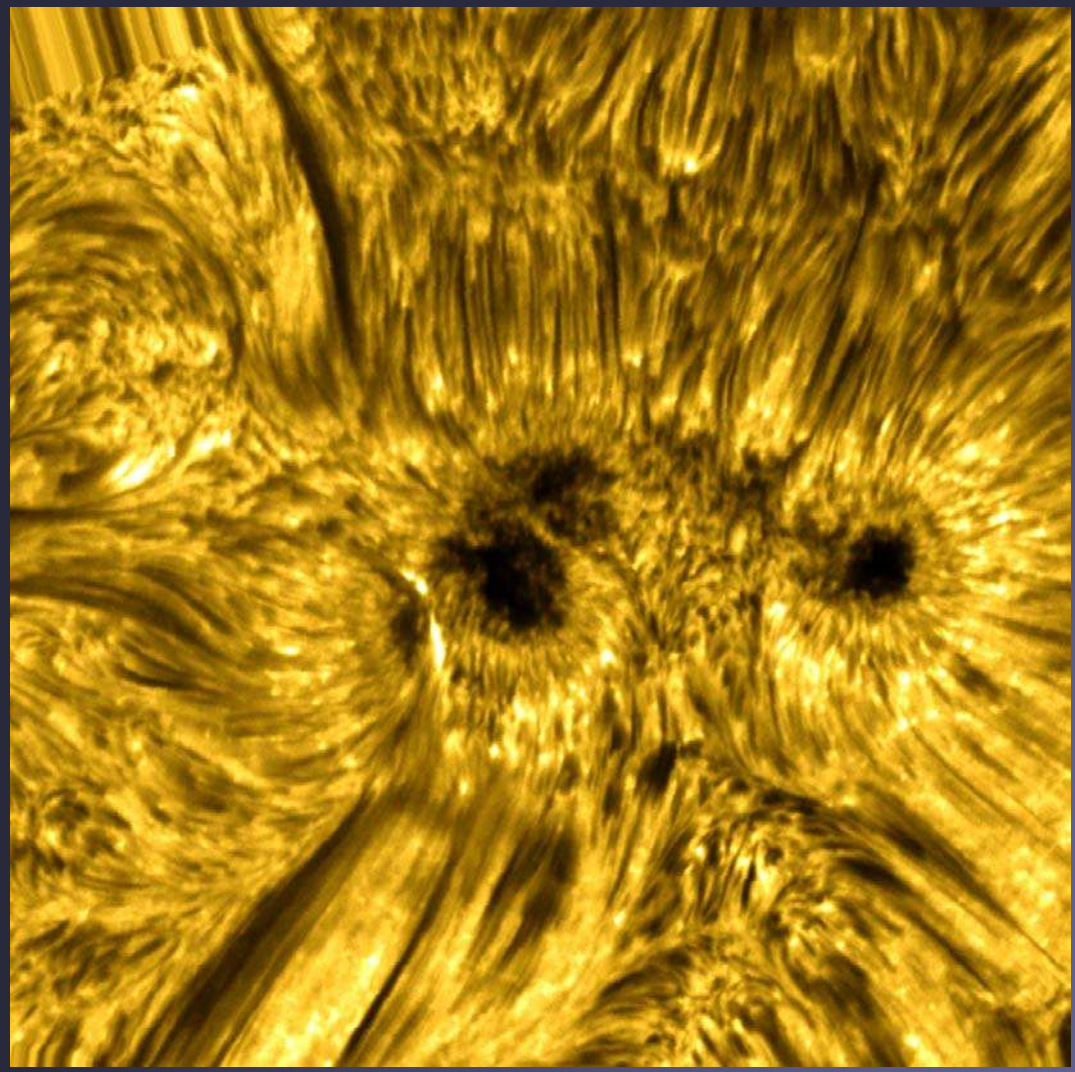

Corona

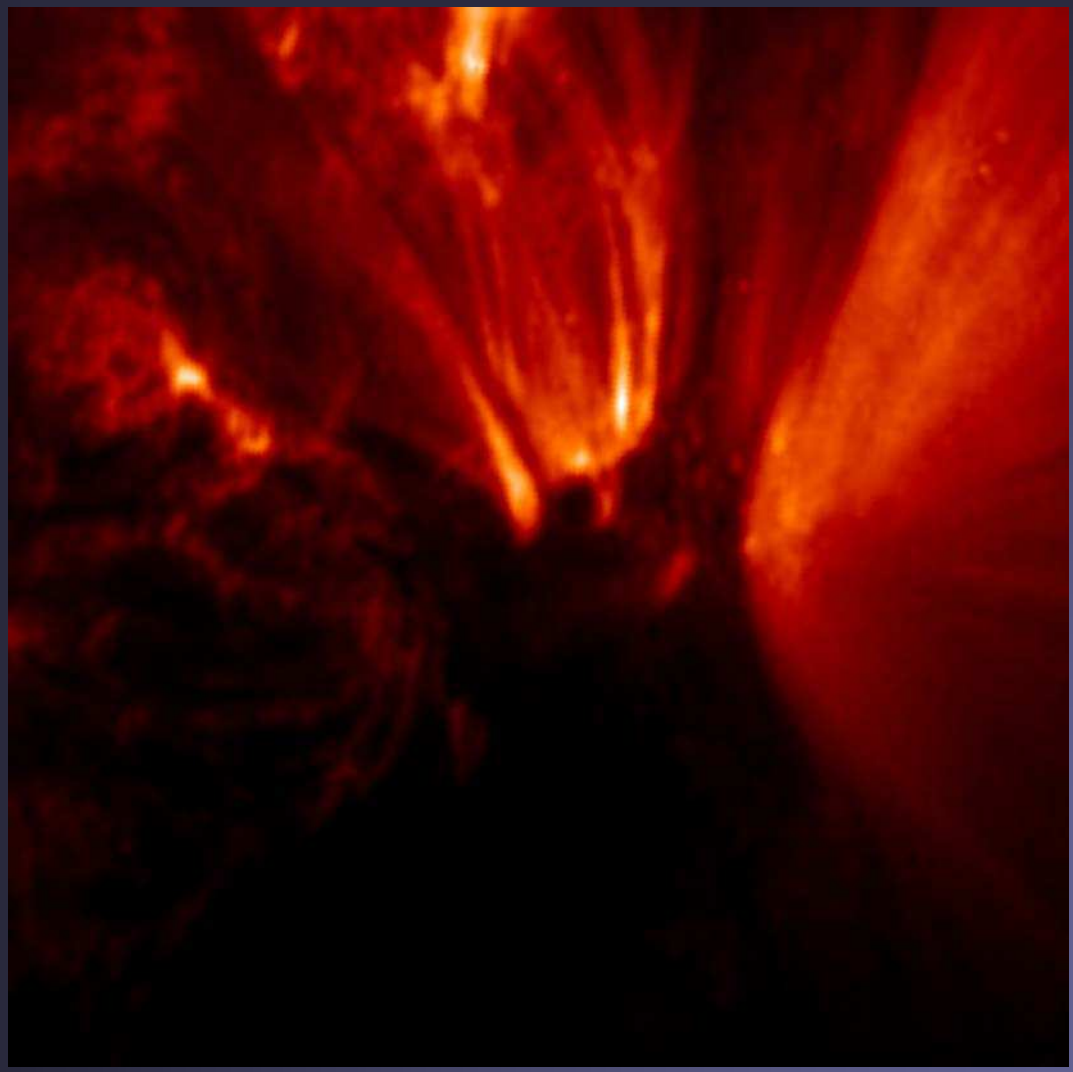

Photosphere

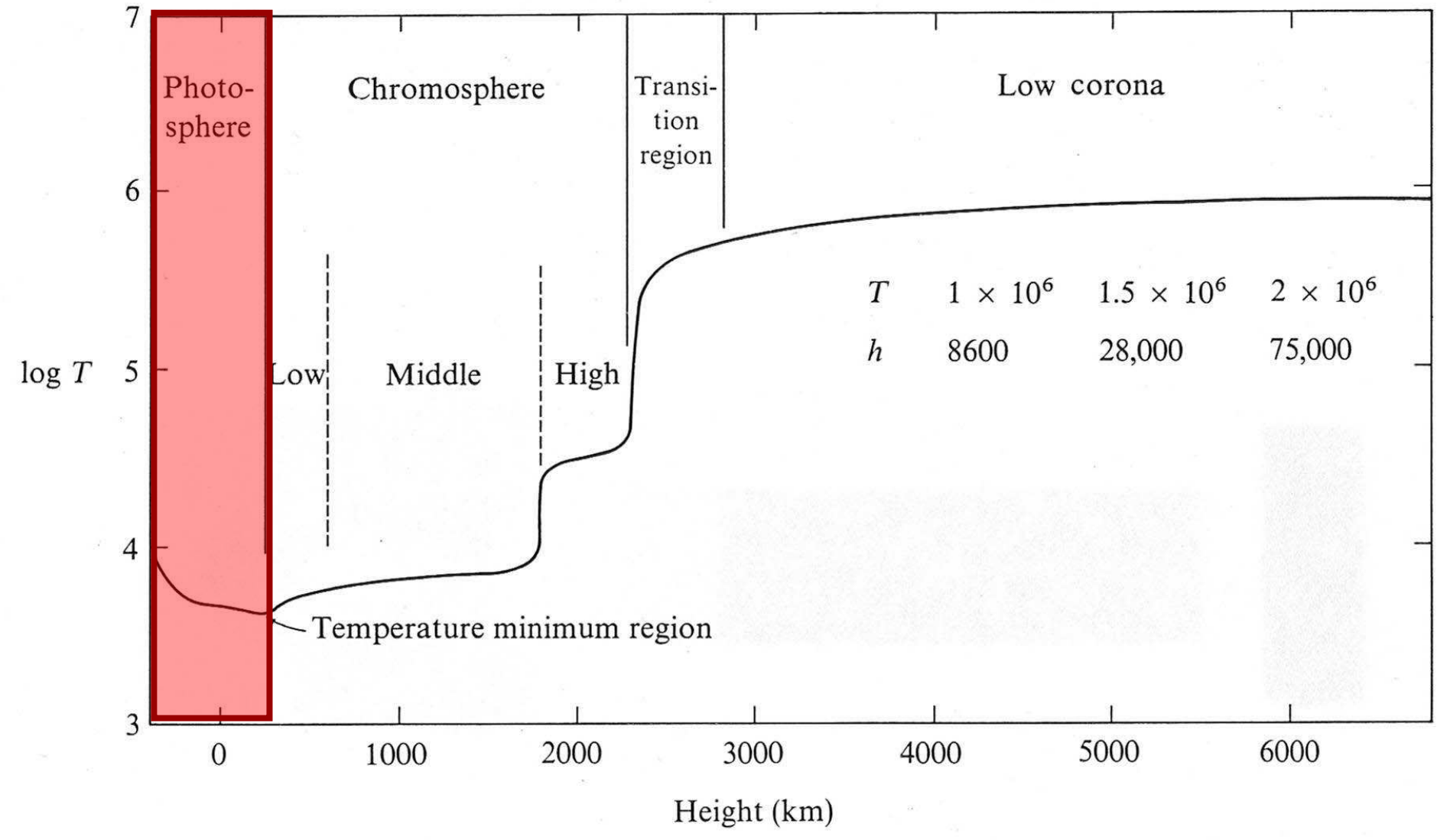

The photosphere

- Photosphere extends between solar surface and temperature minimum (400-600 km)
- It is the source of most of the solar radiation. The visible, UV (λ> 1600Å) and IR (< 100μm) radiation comes from the photosphere.
- 4000 K < T(photosphere) < 6000 K
- T decreases outwards ➔ $B_\nu(T)$ decreases outward ➔ photosphere produces an absorption spectrum
- LTE is a good approximation
- Energy transport by radiation (and convection)
- Main structures: Granules, sunspots and faculae

The Sun in White Light

(limb darkening removed)

MDI on SOHO

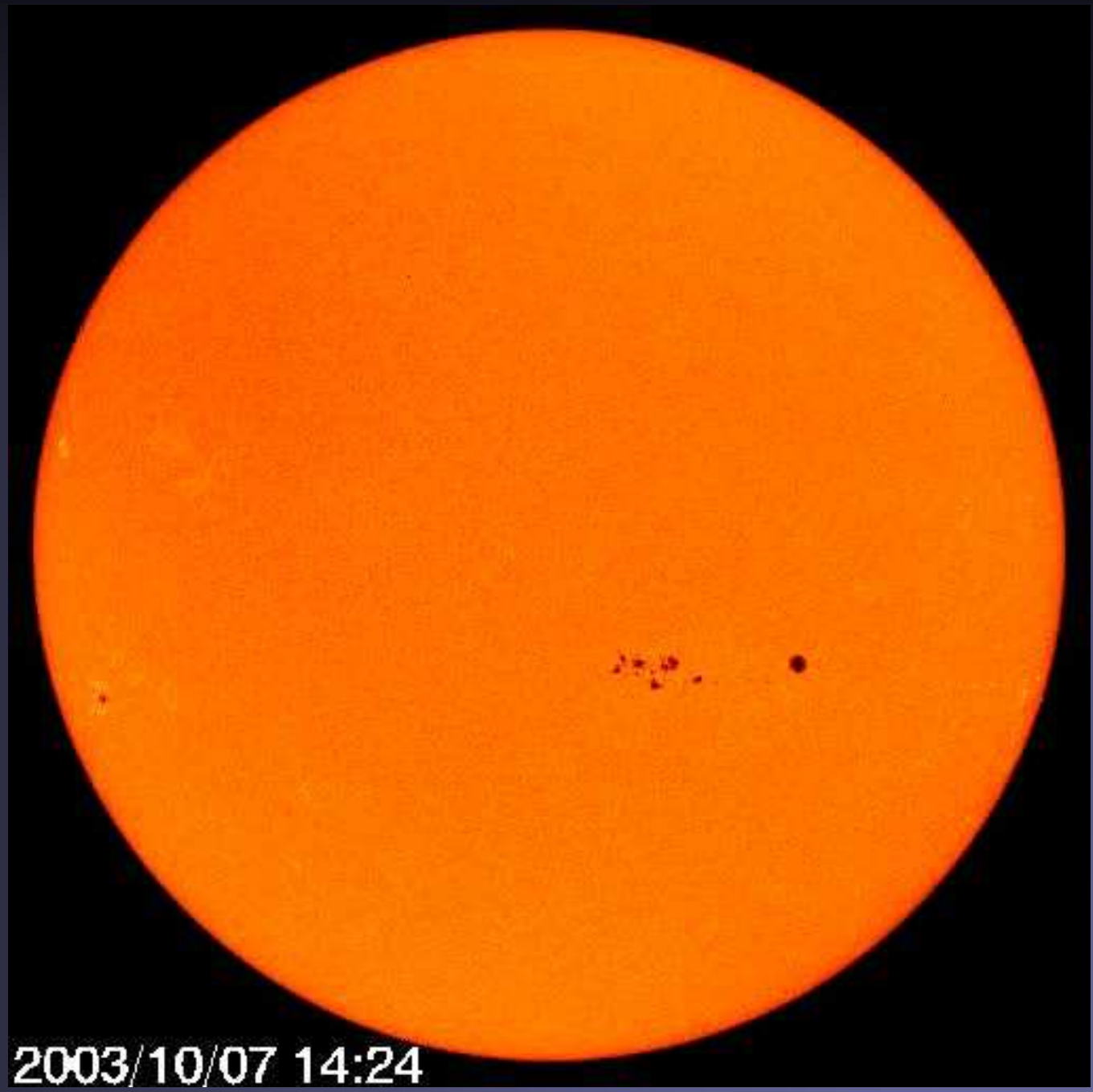

The photosphere: a boring place?

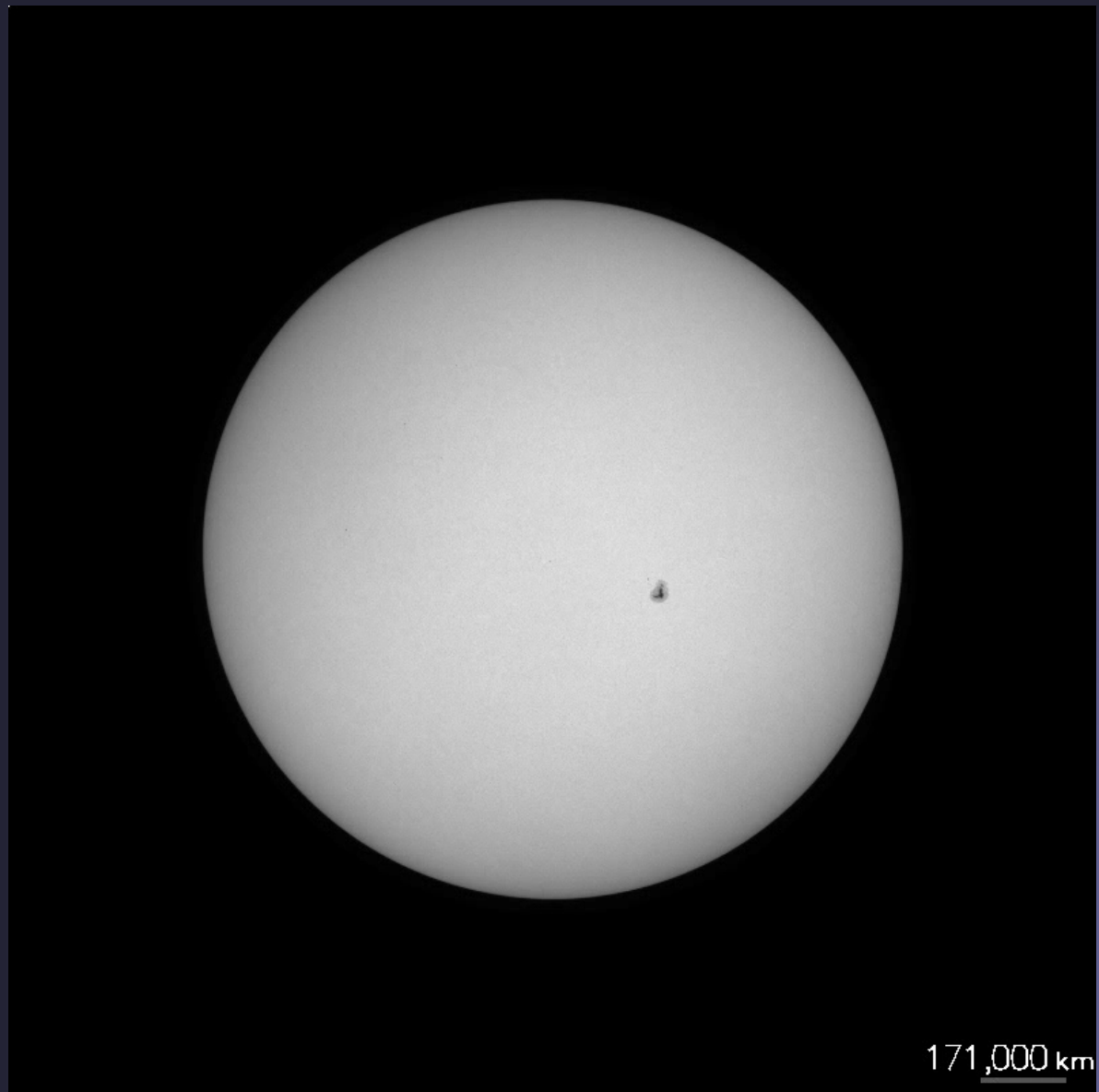

Photospheric structure: Granulation

- Physics of convection and the properties of granulation and supergranulation have been discussed earlier, so that we can skip them here.

Photospheric structure: Sunspots

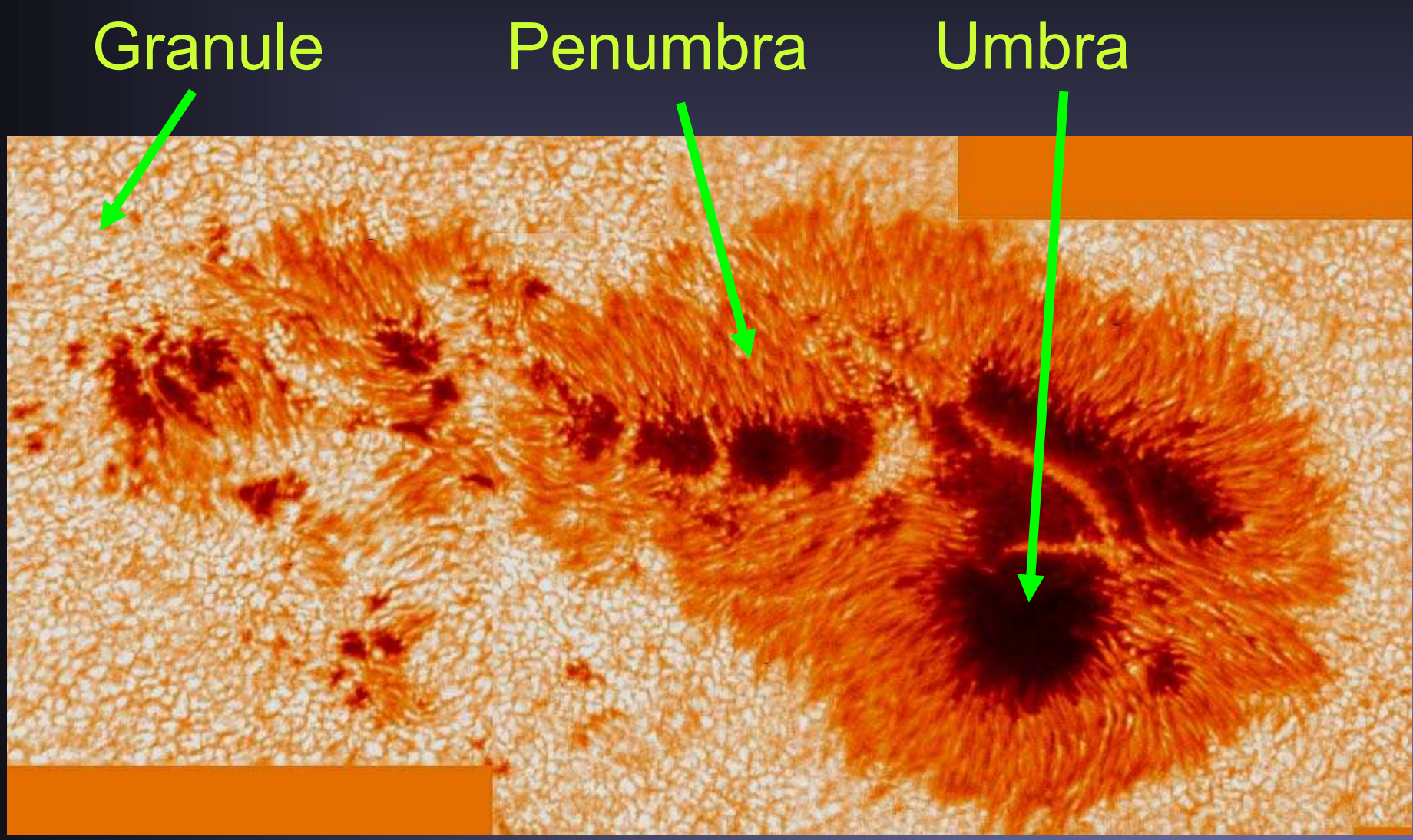

H. Schleicher, KIS/VTT, Obs. del Teide, Tenerife

Chromosphere

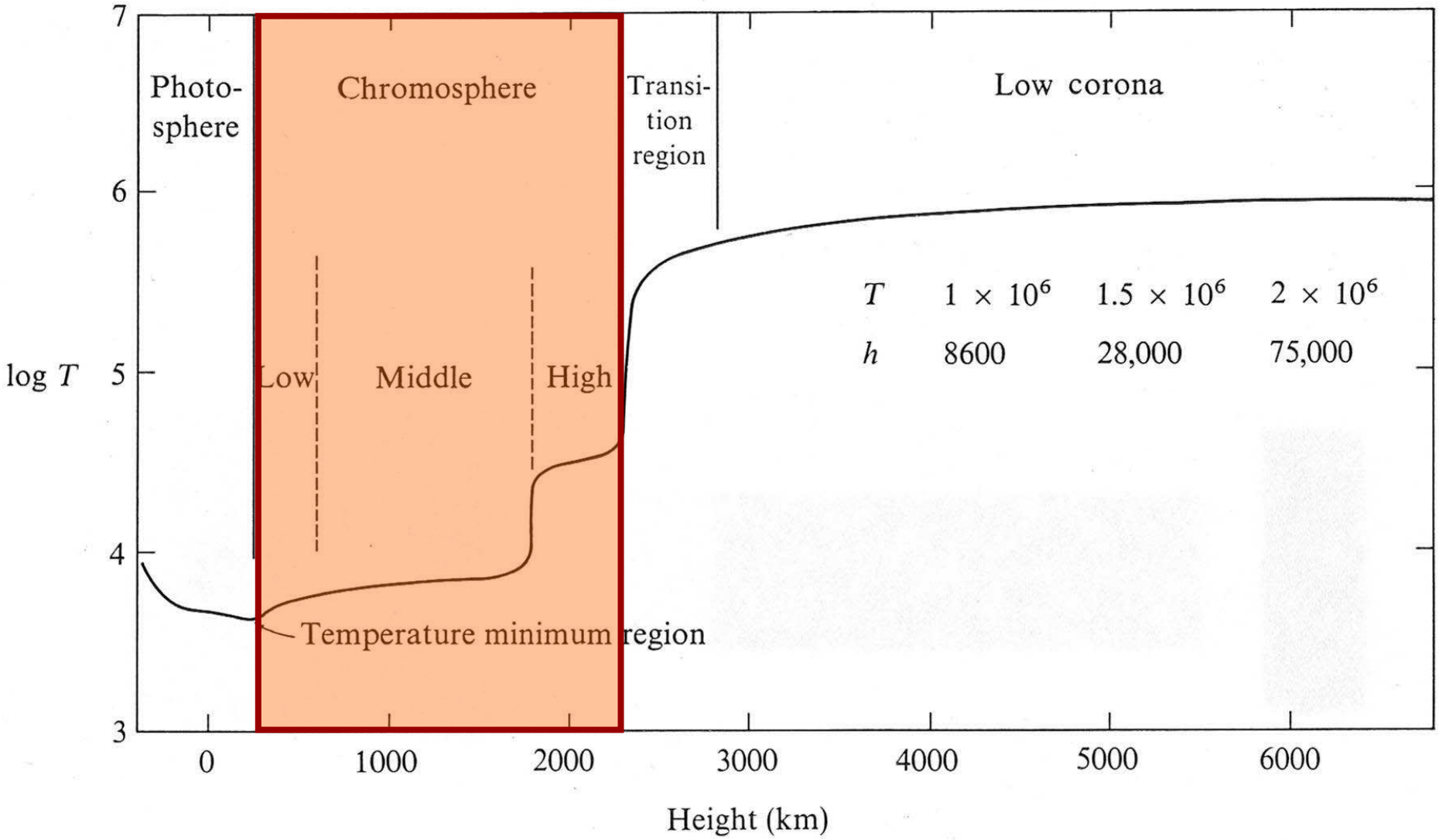

Chromosphere

- Layer just above photosphere, at which temperature appears to increase outwards (classically forming a temperature plateau at around 7000 K)
- Strong evidence for a spatially and temporally inhomogeneous chromosphere (gas at T<4000K is present beside gas with T>8000 K)
- Assumption of LTE breaks down
- Assumption of plane parallel atmosphere very likely breaks down (i.e. radiative transfer in 3-D needed)
- Energy transport mainly by radiation and waves

Discovery of Chromosphere

- Flash spectrum seen seconds before and after totality

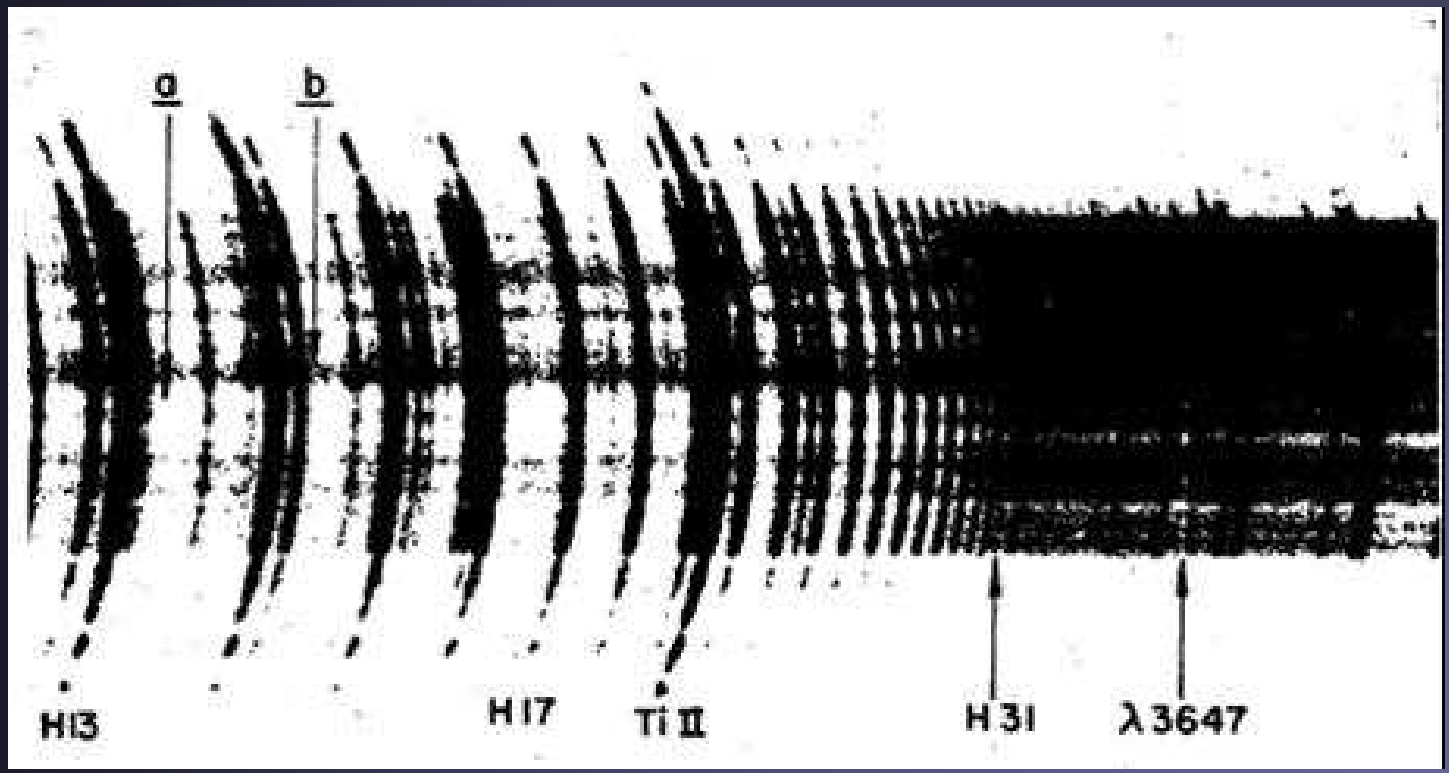

Chromospheric structure

Spots plages

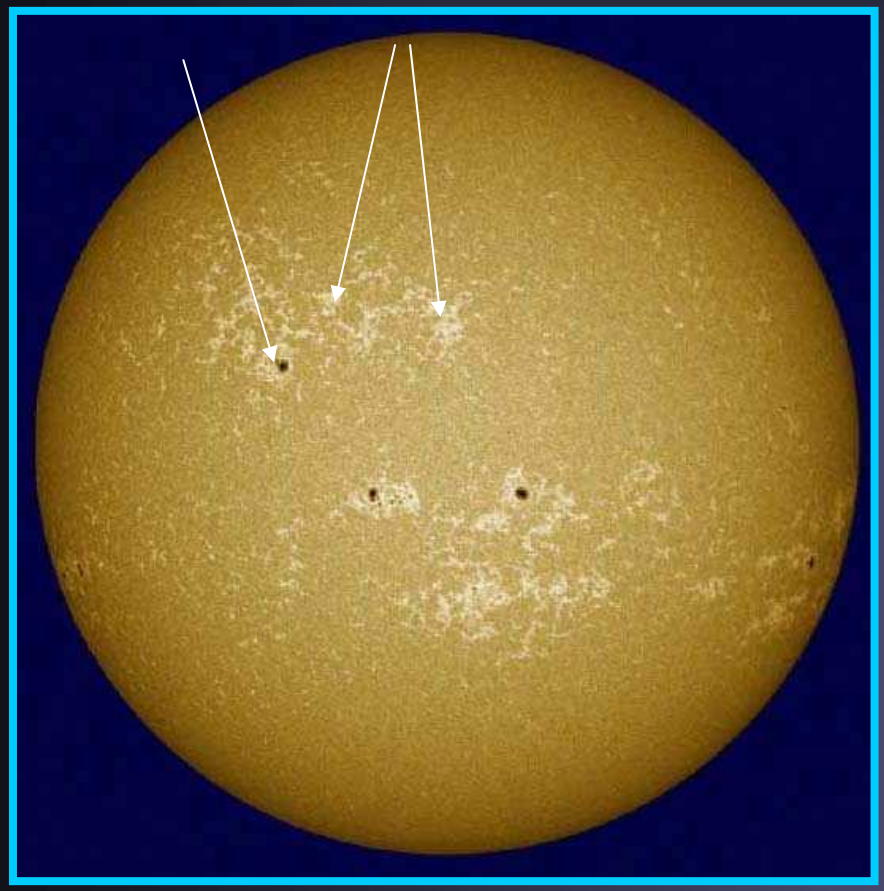

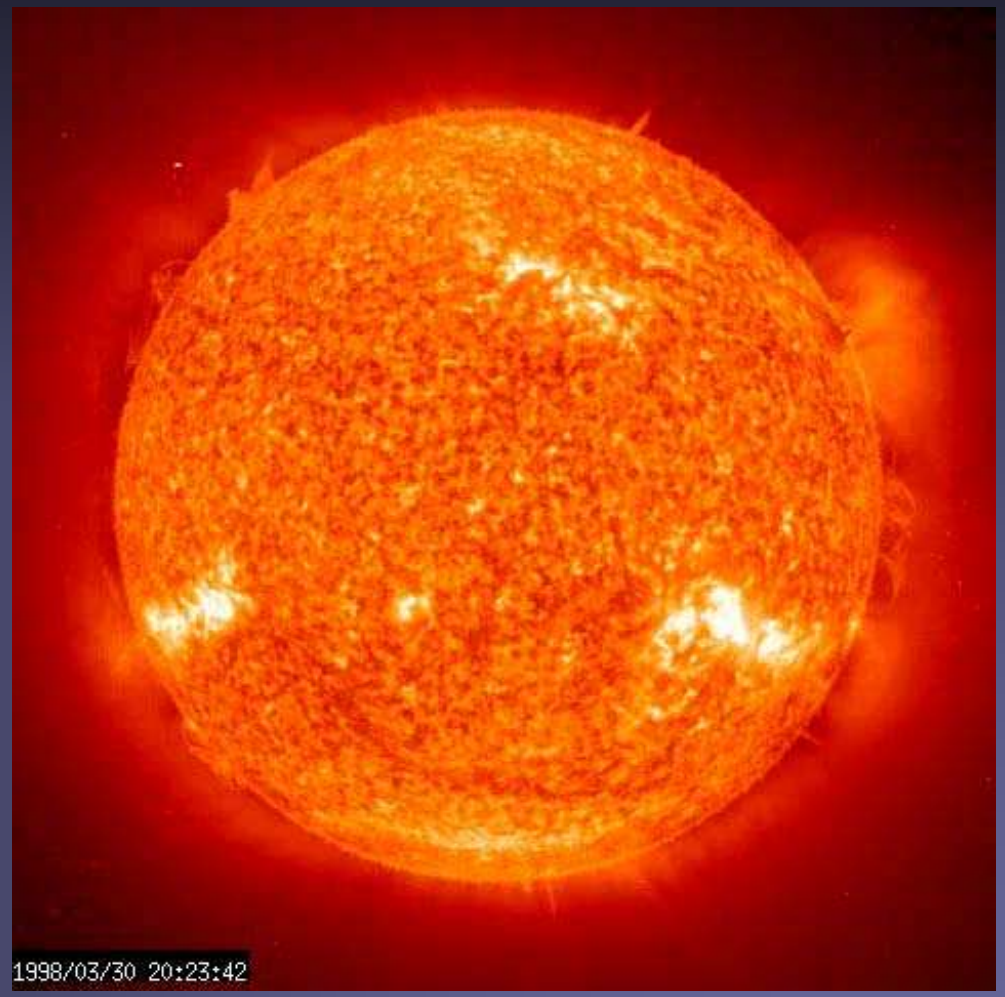

7000 K gas Ca II K

5 10^4 K gas (EIT He 304 Å)

Chromospheric structure III CHANGE!!!

- The chromosphere exhibits a very wide variety of structures. E.g.,
  - Sunspots and Plages
  - Network and internetwork (grains)
  - Spicules
  - Prominences and filaments
  - Flares and eruptions

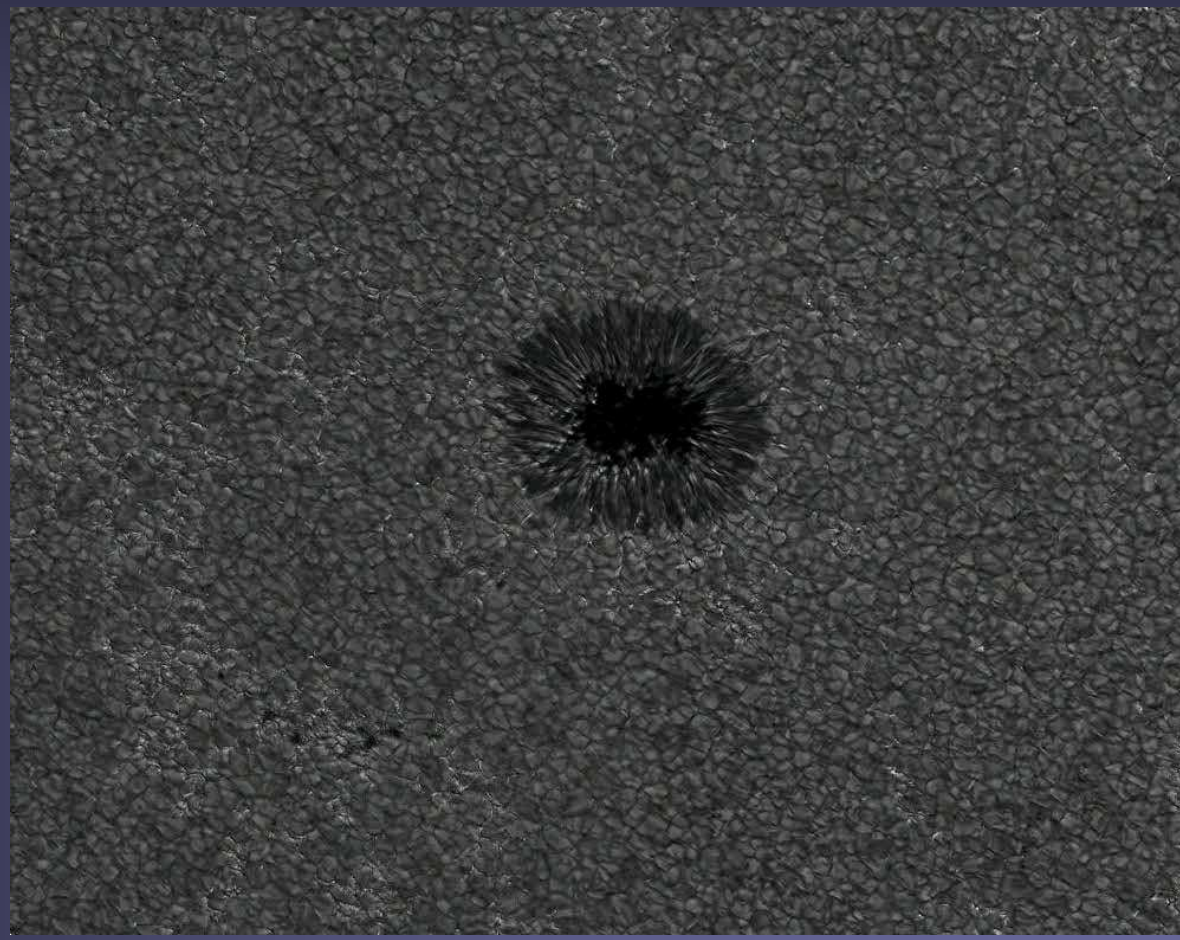

Chromospheric structure

- The chromosphere exhibits a very wide variety of structures. E.g.,
  - Sunspots and Plages
  - Network and internetwork
  - Spicules
  - Prominences and filaments
  - Flares and eruptions

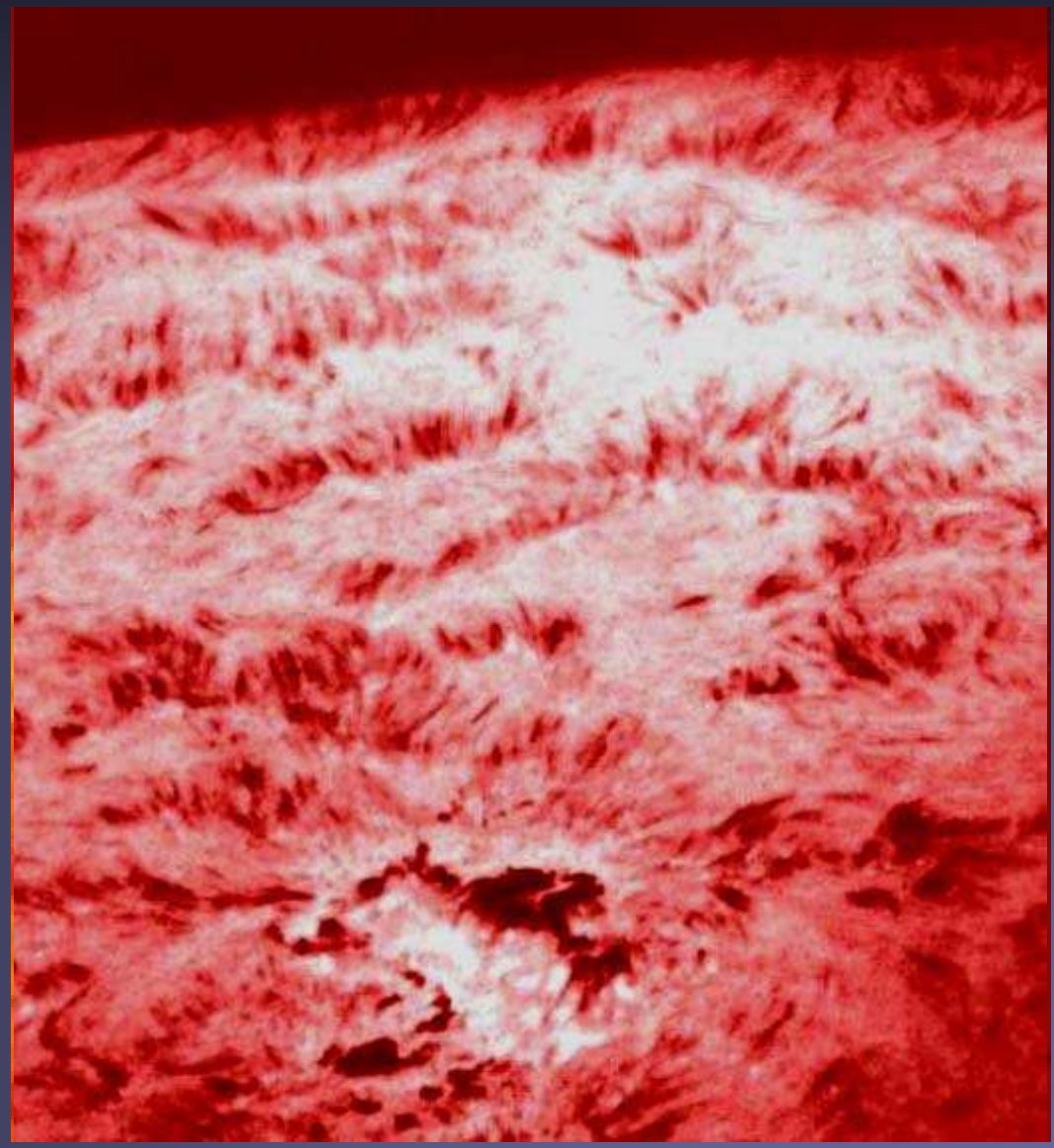

Chromospheric structure

- The chromosphere exhibits a very wide variety of structures. E.g.,
  - Sunspots and Plages
  - Network and internetwork
  - Spicules
  - Prominences and filaments
  - Flares and eruptions

Chromospheric structure

- Spicules
- Prominences and filaments

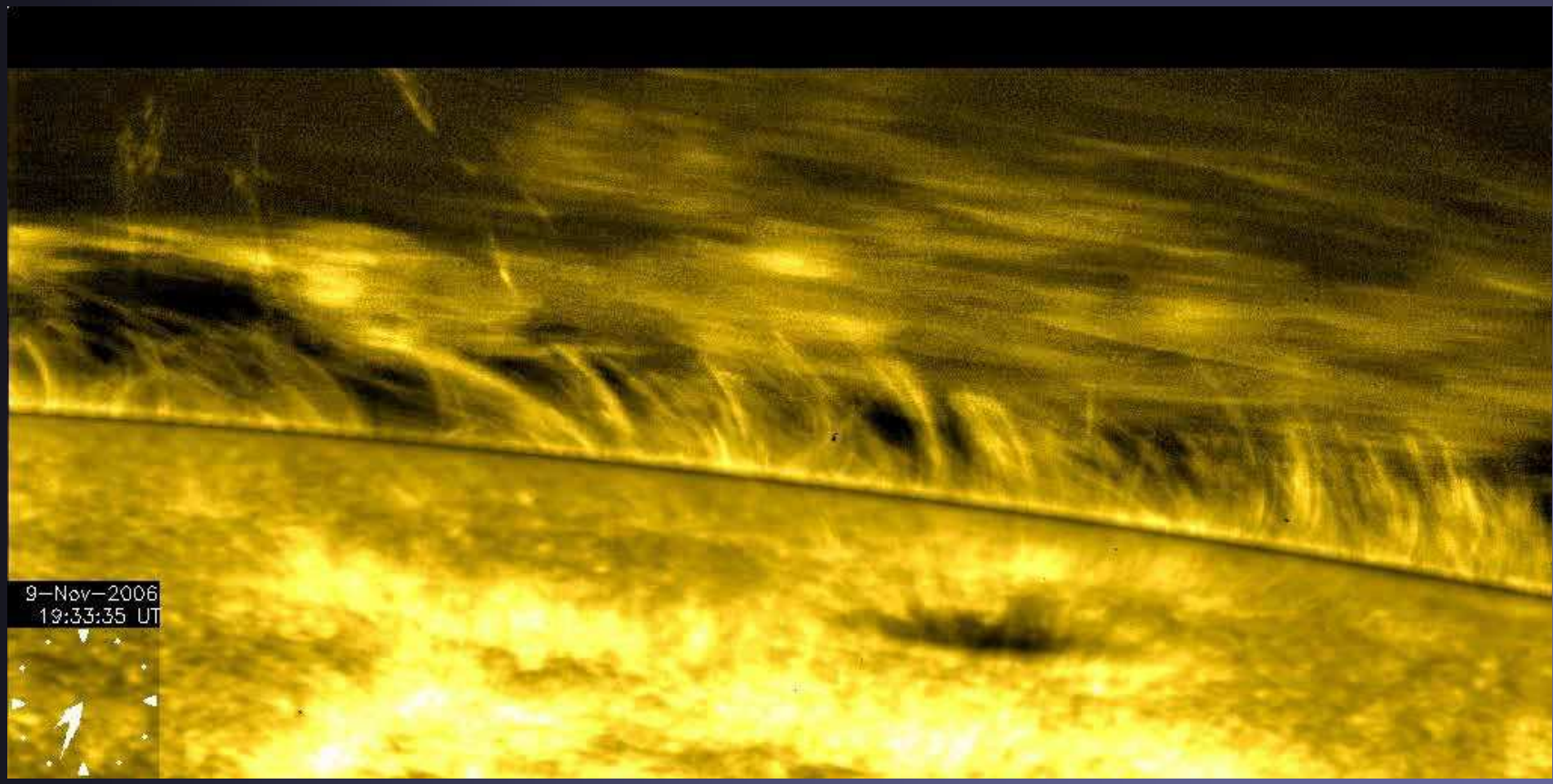

Chromospheric dynamics

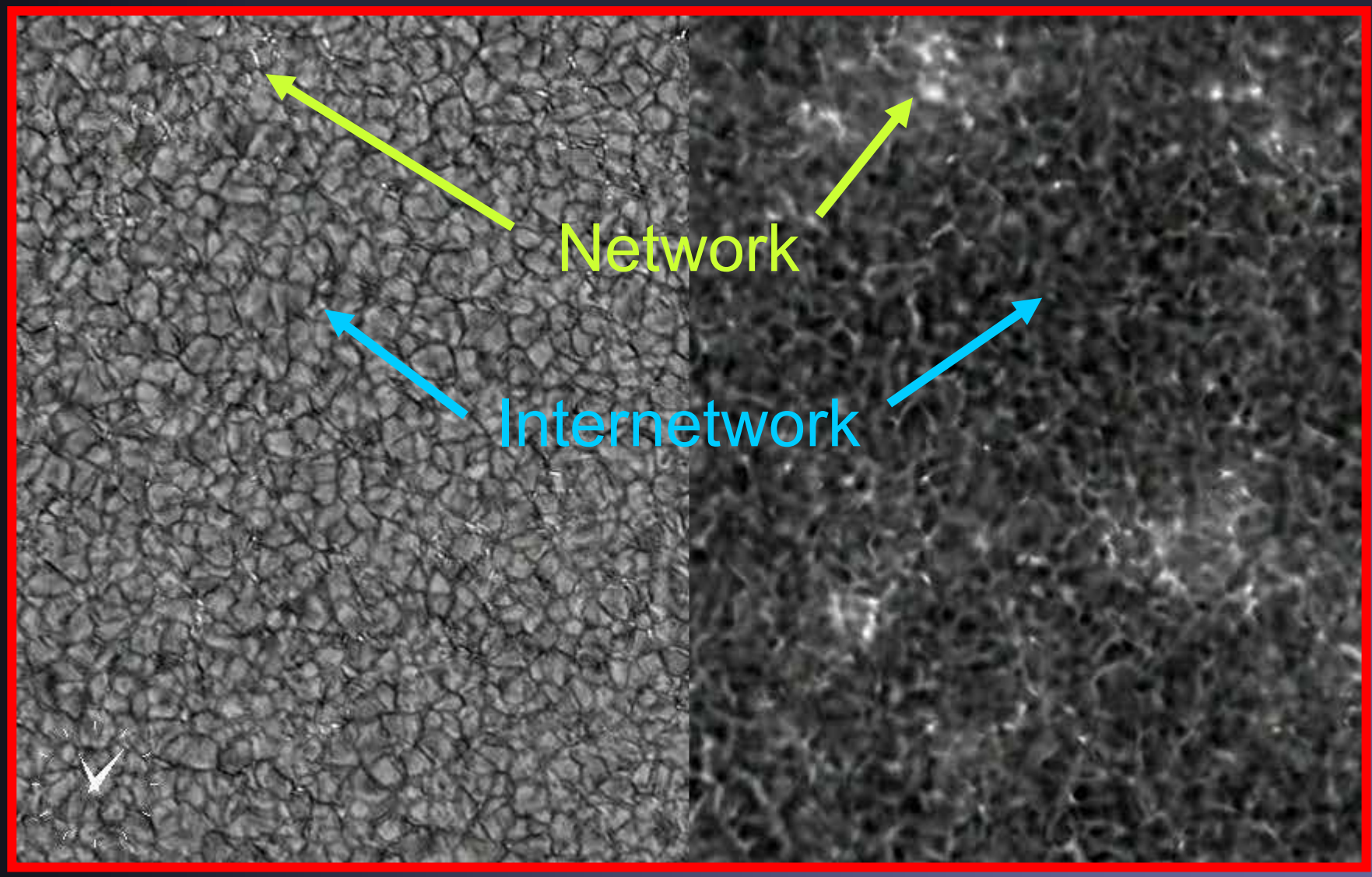

Chromospheric dynamics

- Oscillations, seen in cores of strong lines
- Power peaks: oscillations, not turbulence
- Power at 3 min in Inter-network
- Power at 5-7 min in Network

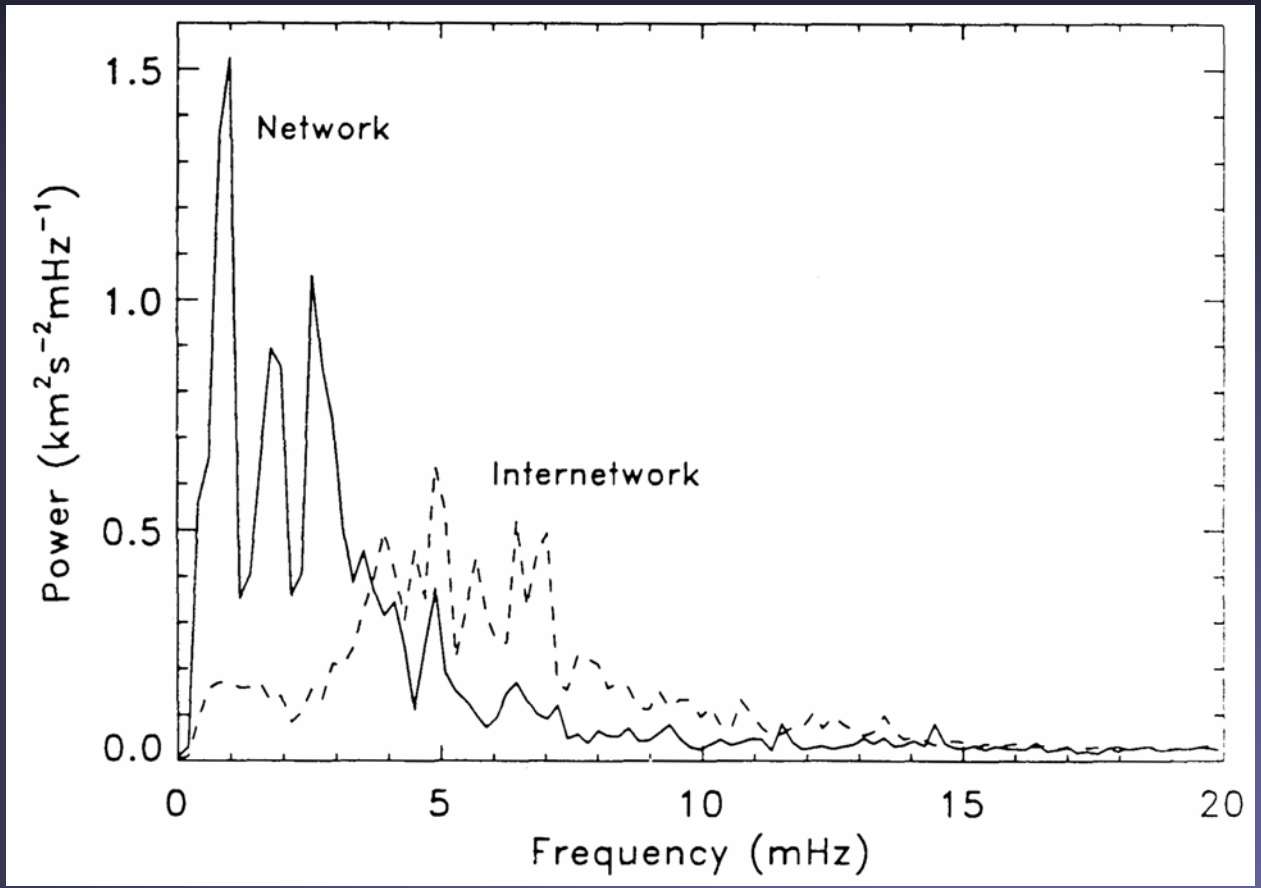

Lites et al. 2002

1 year of EIT: upper chromosphere

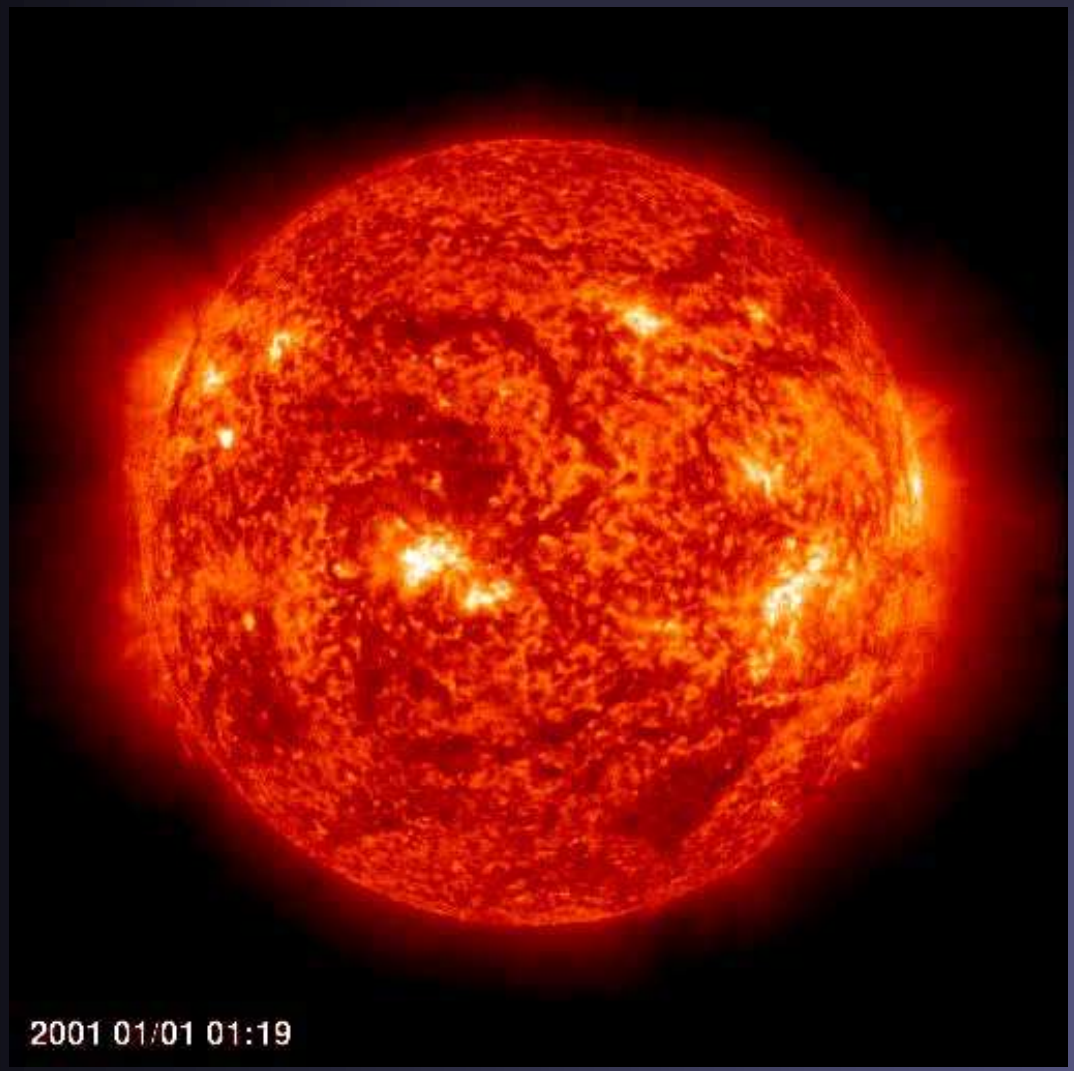

- He II 304 Å with EIT/SOHO
- samples gas at ≈50 kK (with contribution also from corona: coronal holes are visible)

Models: the classical chromosphere

- Classical picture: plane parallel, multi-component atmospheres
- Chromosphere is composed of a gentle rise in temperature between $T_{\min}$ and transition region.

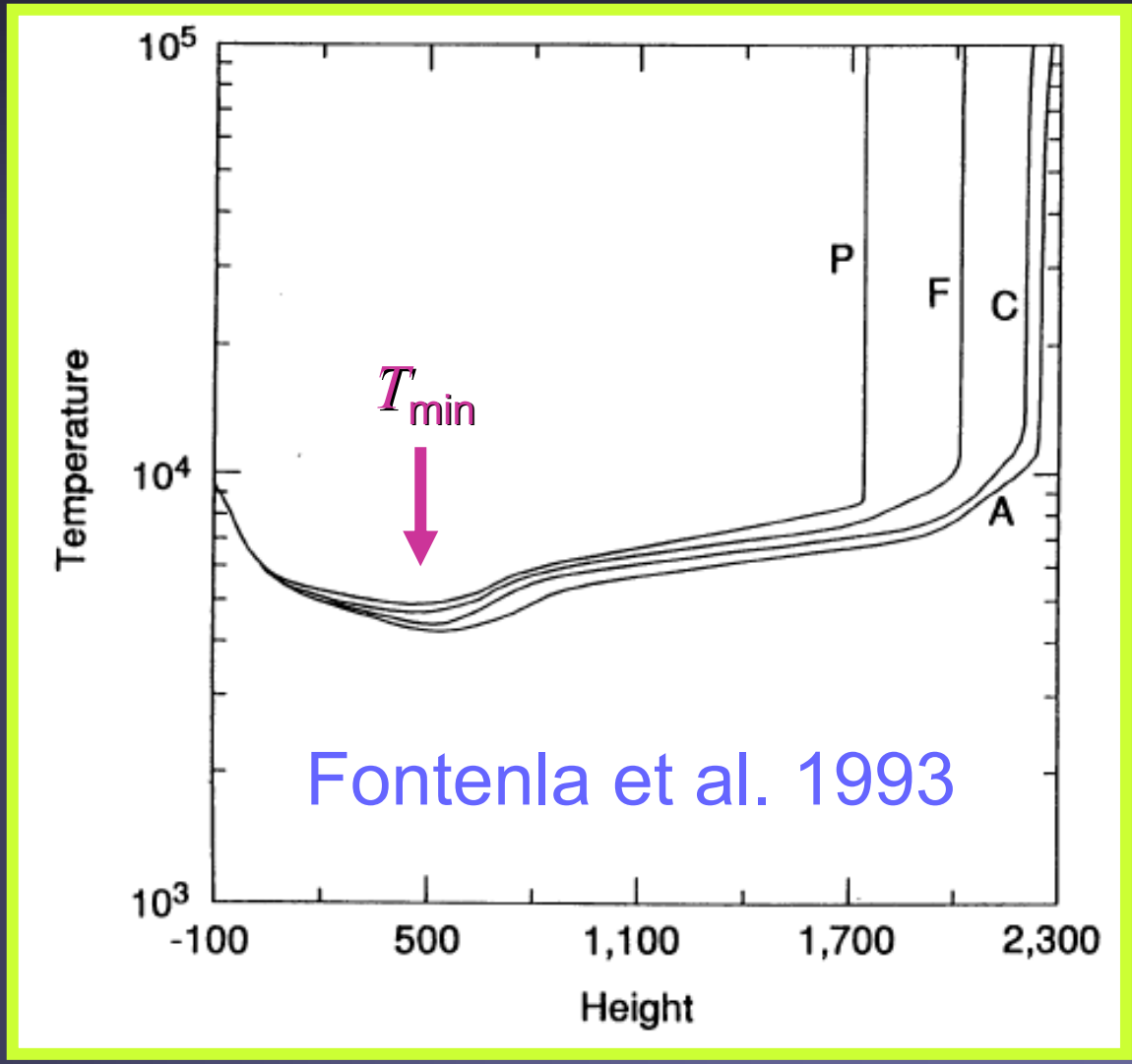

Need to heat the chromosphere

- Radiative equilibrium, RE: only form of energy transport is radiation & atmosphere is in thermal equilibrium.
- VAL-C: empirical model
- Dashed curves: temp. stratifications for increasing amount of heating (from bottom to top).

➔Mechanical heating needed to reproduce obs.

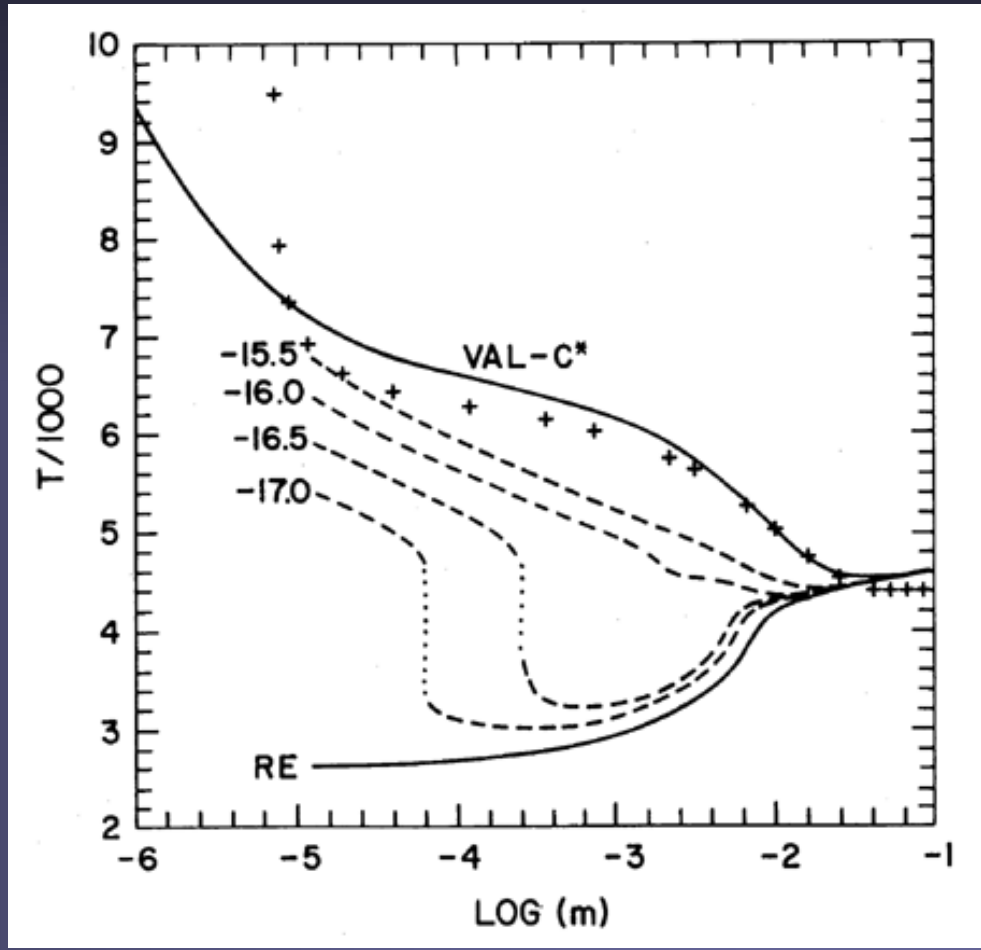

Anderson & Athay 1993

Dynamic models

- Start with piston in convection zone, consistent with obs. of photospheric oscillations
- Waves with periods of ≤3min propagate into chromosphere
- Energy conservation ($\rho v^2/2 = \text{const.}$) & strong ρ decrease → wave amplitudes increase with height: waves steepen and shock

→ Temp. at chromospheric heights varies between 3000 K and 10000 K

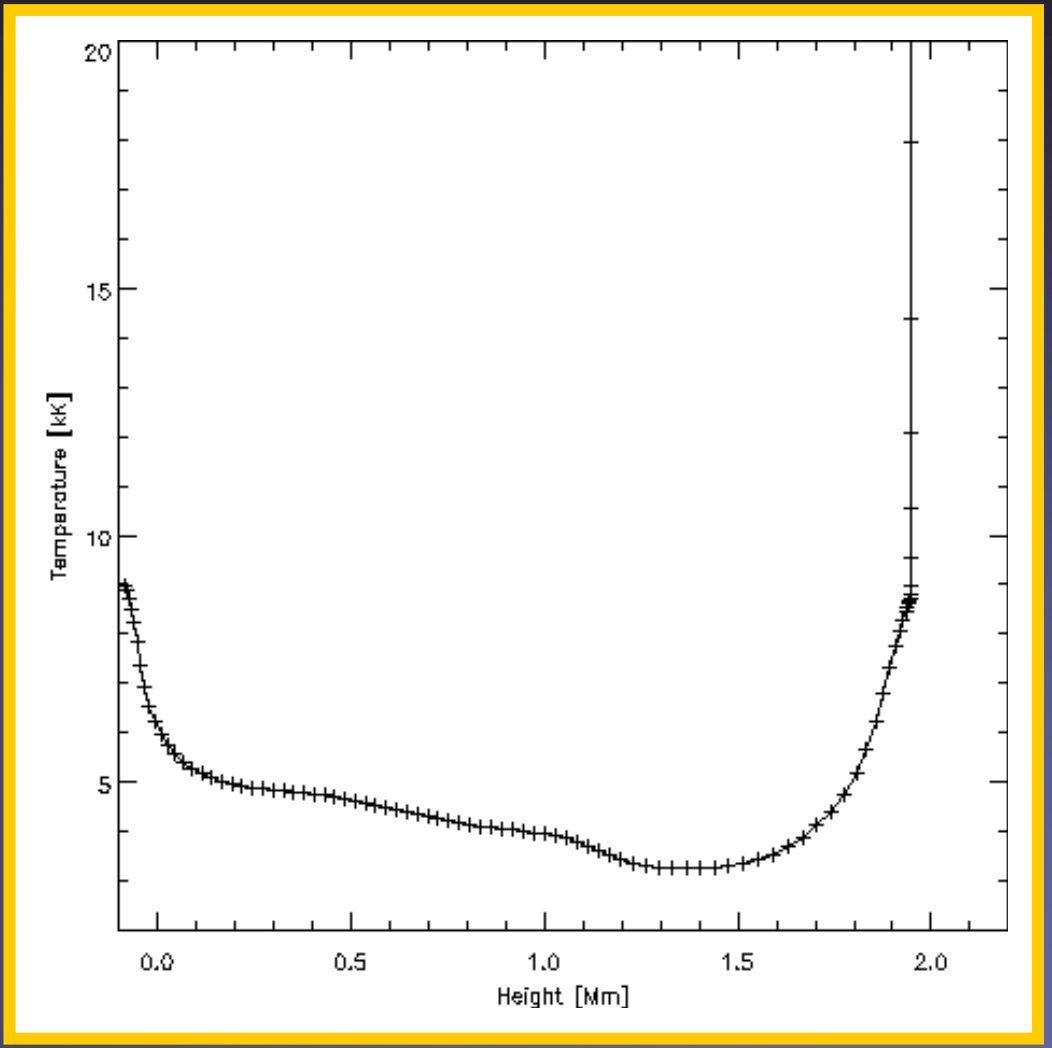

Carlsson & Stein

Transition Region

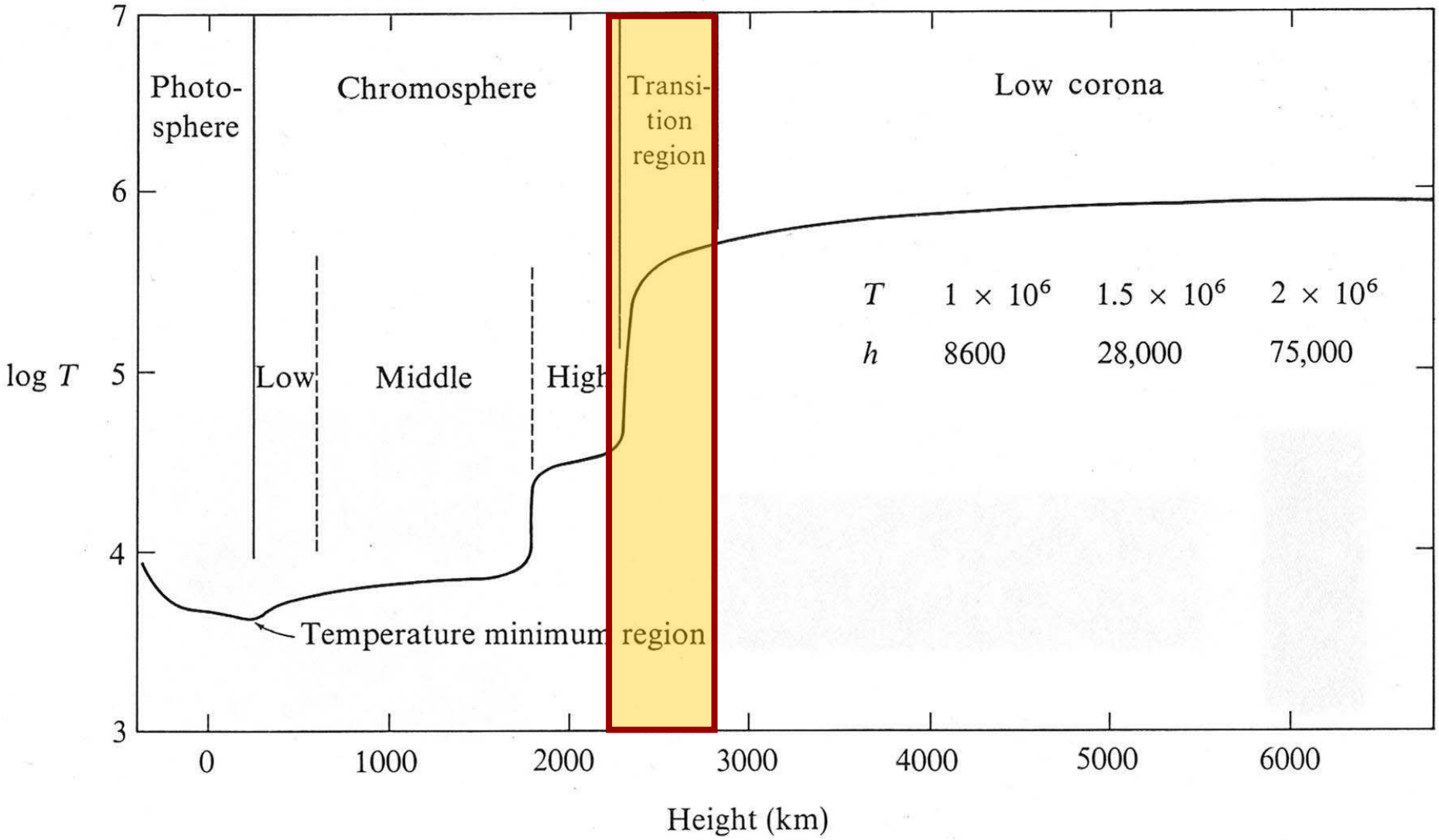

Transition Region

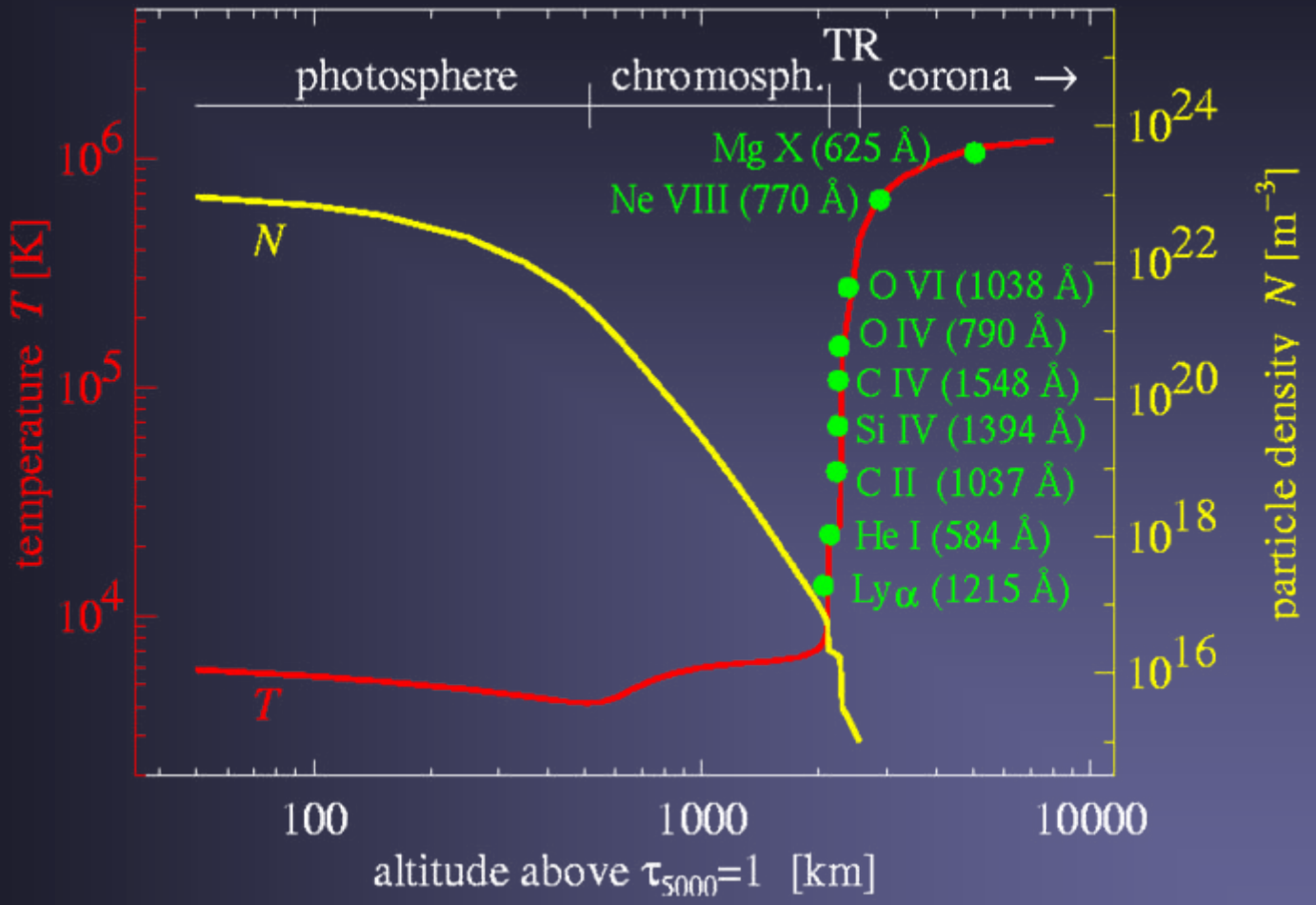

Semi-empirical 1D-models of solar atmosphere: steep increase of T in transition region (TR): < 100 km thick

Transition region properties

- Temperature increases from 5 10^4 K to 1 MK
- Density drops ➔ P_g remains almost constant
- Divided into
  - lower transition region: T< 5 10^5 K. Shows networt structure, similar to Chromosphere
  - upper transition region: T> 5 10^5 K. Shows loop structures, similar to Corona
- Populated by 3 types of structures: footpoints of coronal loops, footpoints of open field lines, cool transition region loops.
- Heating thought to be mainly by heat conduction from corona (for those parts magneticly connected to corona).

TR spatial structure

- Lower transition region ($T<5\ 10^5$ K) shows structure very similar to chromosphere, with network, plage etc.
- C IV (10^5 K) imaged by SUMER
- In upper transition region structures are more similar to corona

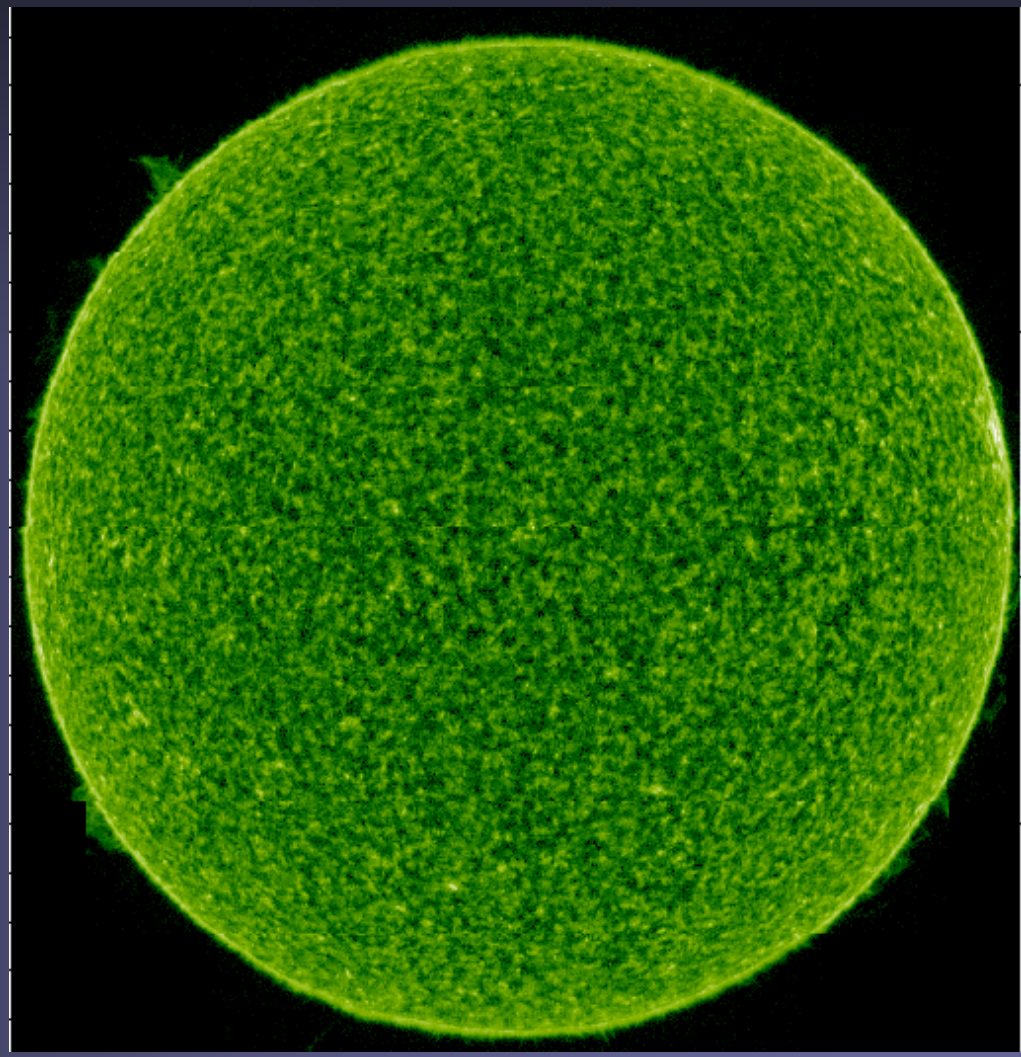

TR dynamic phenomena: blinkers

- Brightness variability in Quiet-sun transition region is larger than in any other layer of solar atmosphere
- Typical brightening: blinkers
- Occur everywhere, all the time. Last for minutes to hours. How much of the brightening is due to overlapping blinkers?
- 1 time step ≈ 1 minute

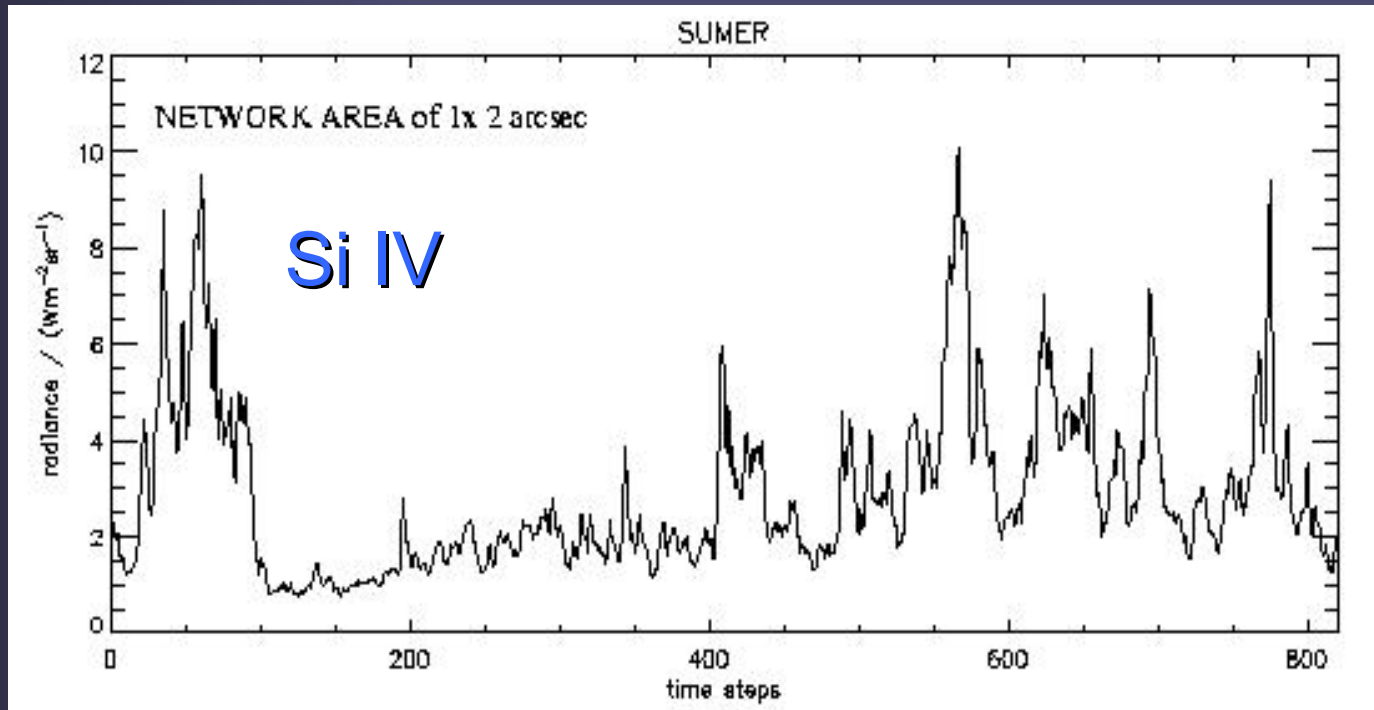

Explosive events

- Broadenings of TR spectral lines at 1-3 10^5 K
- Typical “normal” line width is 20 km/s; in explosive event: up to 400 km/s. Cover only a few 1000 km and last only a few minutes
- Typically a few 1000 present on Sun at any given time

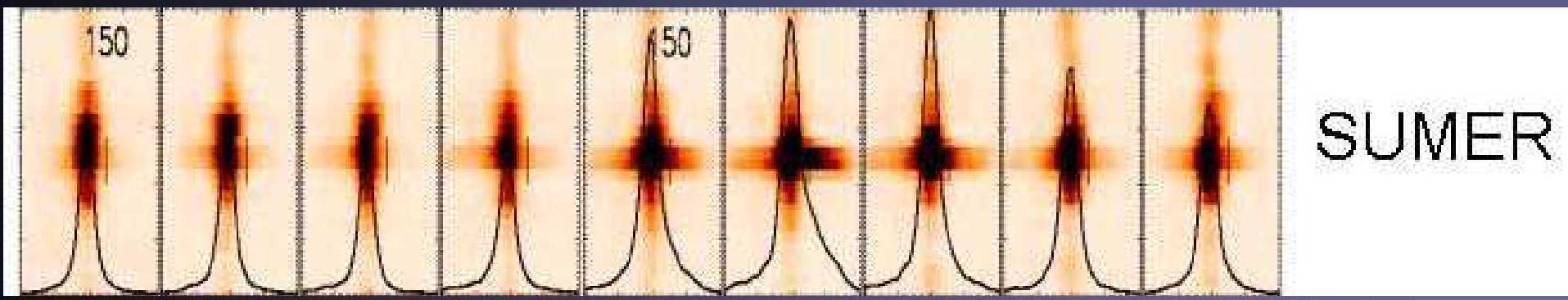

Corona

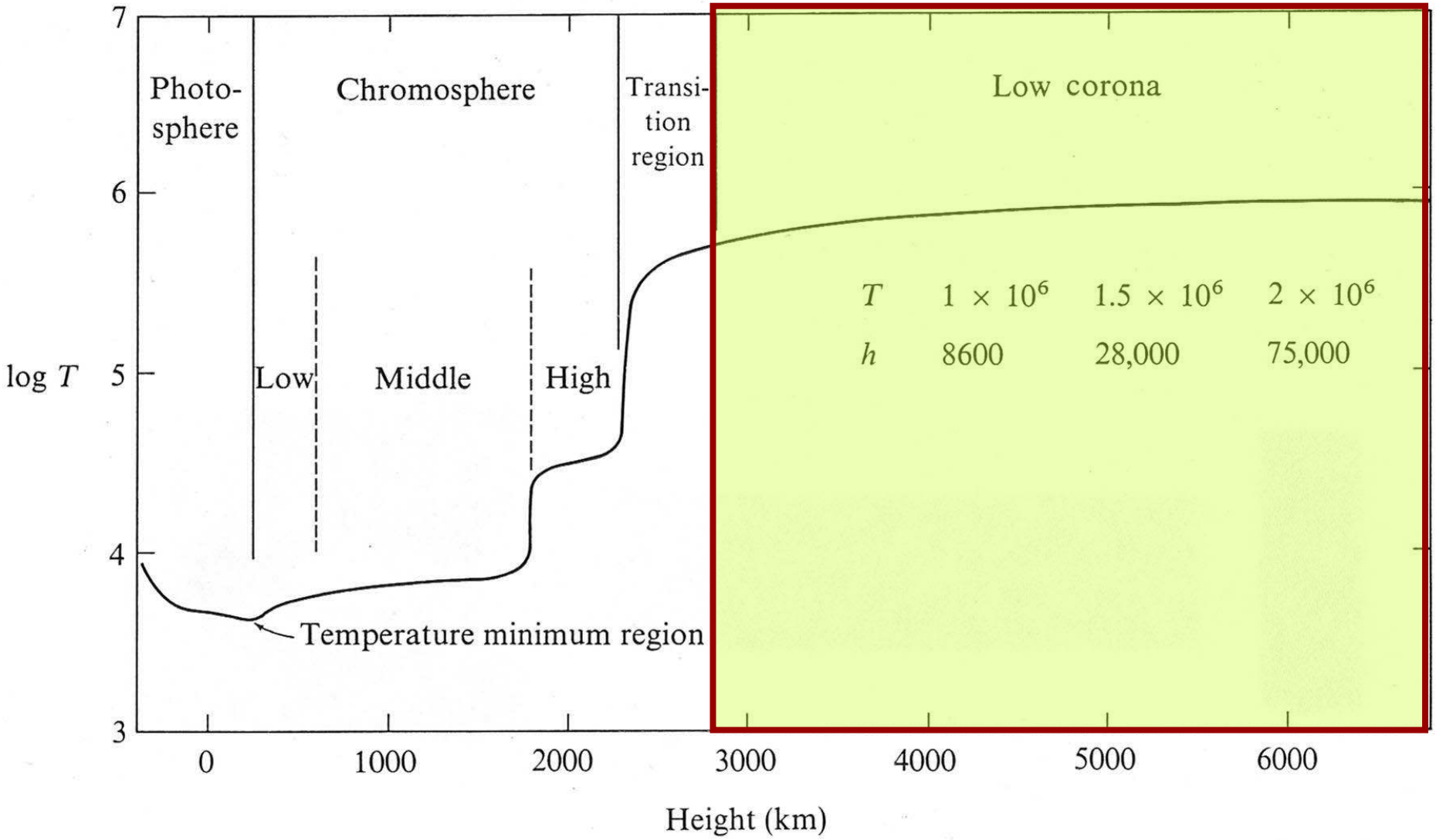
Photo-
sphere
Chromosphere
Transi-
tion
region
Low corona
Low
Middle
High
Temperature minimum region
log T
7
6
5
4
3
T 1 × 10^6 1.5 × 10^6 2 × 10^6
h 8600 28,000 75,000
0
1000
2000
3000
4000
5000
6000
Height (km)

The Solar Corona

While the surface is about 6,000 K, the temperature in the corona reaches about 2 million K.

What causes this rapid increase in temperature is still one of the big mysteries in solar physics.

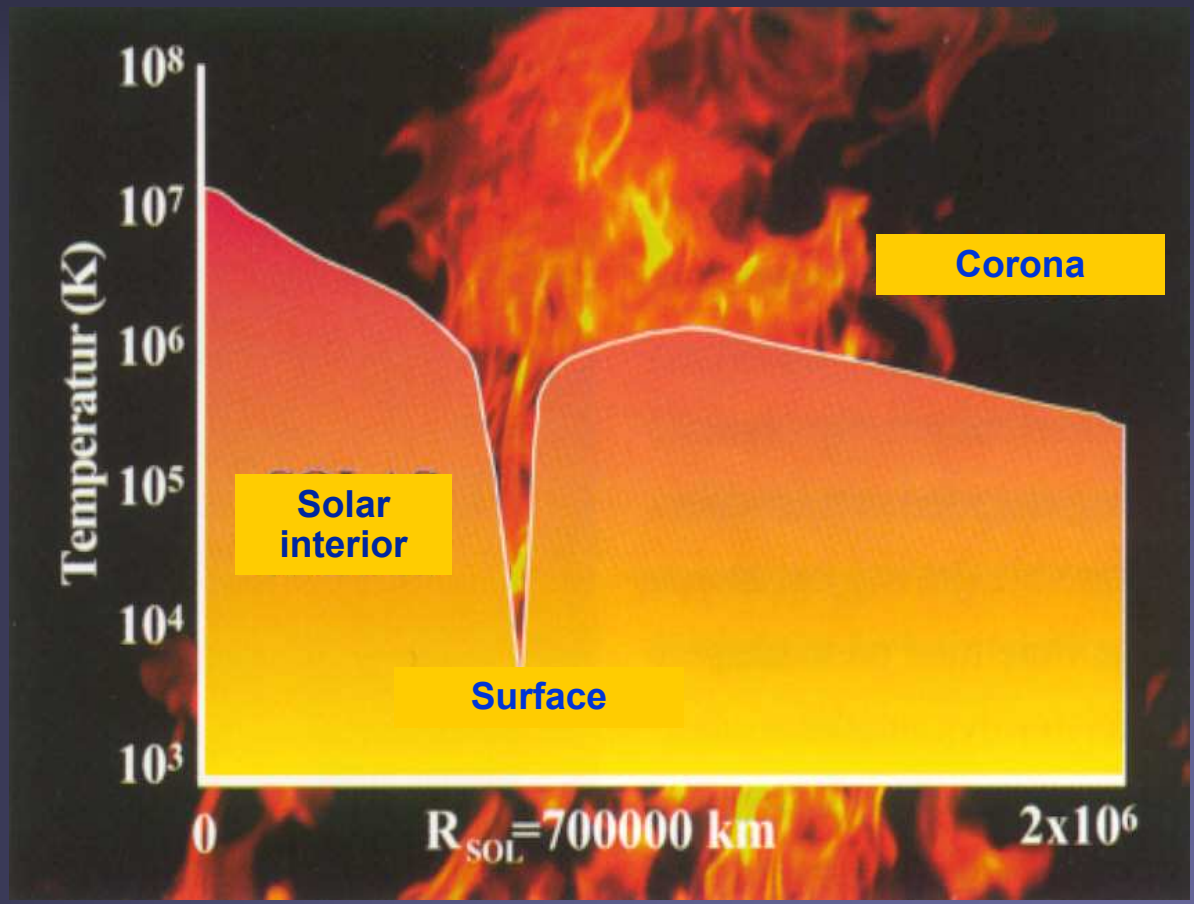

The Hot and Dynamic Corona

Corona during an Eclipse

EUV Corona: Plasma at >1 Mio K (EIT 195 Å)

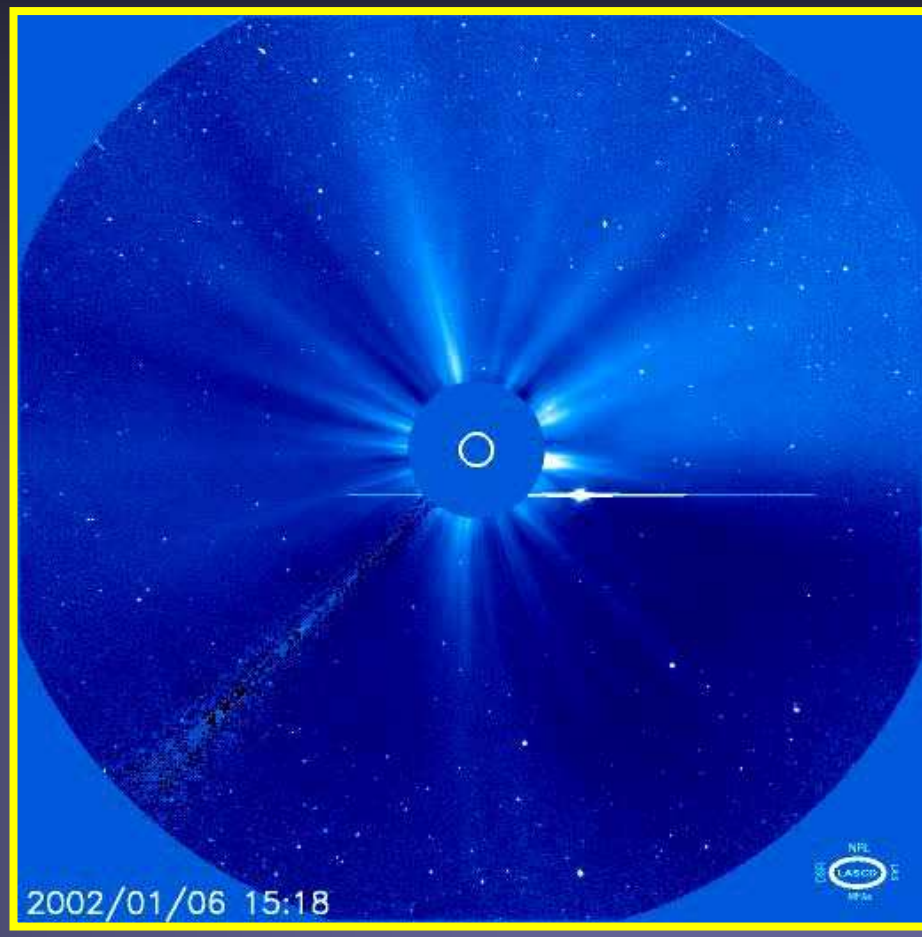

Artificial eclipse (LASCO C3 / SOHO, MPS)

Eclipse corona

- K corona: Inner portion of sun's corona, having a continuous spectrum caused by electron scattering (Thomson scattering)
- F corona: Outer portion of solar corona, consisting of sunlight scattered from interplanetary dust between sun and earth. Also known as Fraunhofer corona: shows Fraunhofer lines.
- L corona: Emission line corona (forbidden lines). Negligible contribution to coronal brightness

Coronal brightness

- Total visible flux from corona
  - Activity maximum: $1.5\ 10^{-6}\ F_{\odot} = 0.66$ full Moon
  - Activity minimum: $0.6\ 10^{-6}\ F_{\odot} = 0.26$ full Moon
- Visibility: during an eclipse corona typically extends for 4 solar radii until its brightness drops below sky brightness levels
- Intensity vs. distance R from limb (I_0=disk centre intensity)

$$\frac{I}{I_o} = 10^{-6}\left(\frac{0.0532}{R/R_o^{2.5}} + \frac{1.425}{R/R_o^{7}} + \frac{2.565}{R/R_o^{17}}\right)$$

Dominates: far intermediate close

Coronal temperature

- Different temperatures & densities co-exist in the corona
- Range of temps: <1 MK (Coronal hole) to 10 MK (act. region)
- Range of e^- densities (inner corona):
  - Loop: 10^{10}
  - coronal hole: 10^7

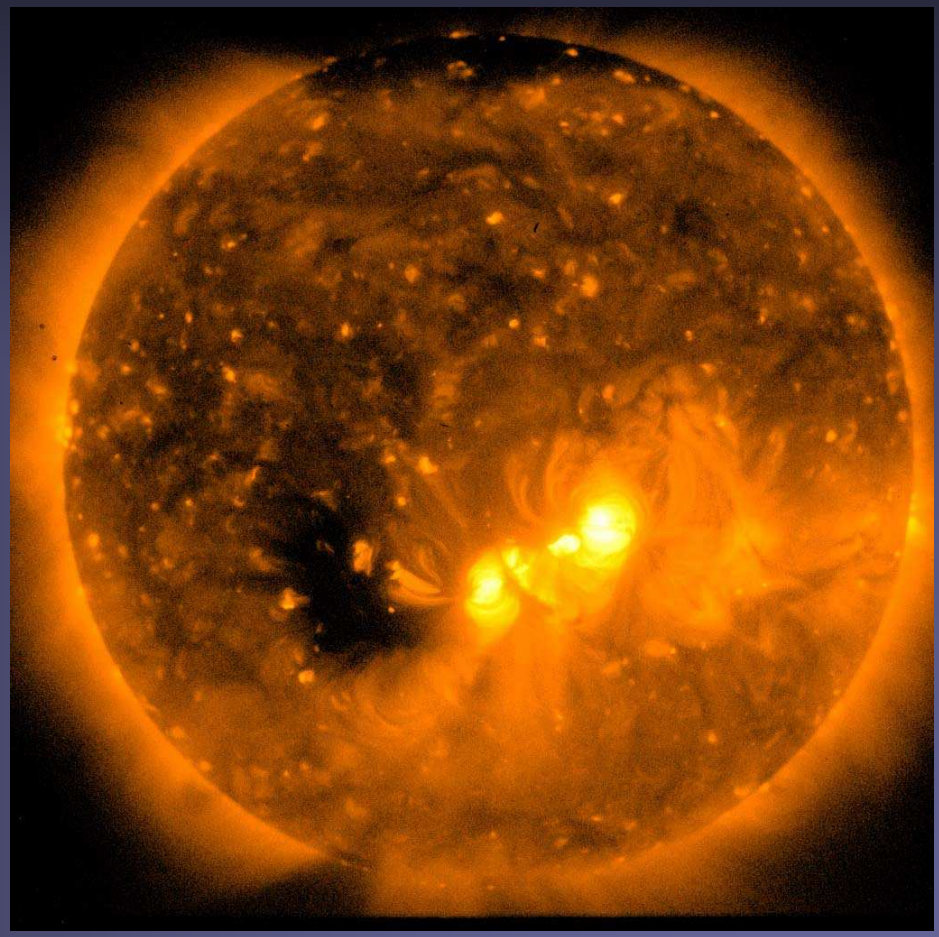

Hinode XRT: 2-5MK gas

Coronal spectrum

- Coronal spectrum: spectrum of the radiation produced in the corona. In contrast to K & F corona, which is radiation coming from the photosphere & only scattered in the corona.
- It is dominated by emission lines of highly ionized species (e.g. Fe IX – Fe XX) with no continuum contribution

- **GET FIGURE !!!!!!!!!!!!!!!!!!!!!! X-RAY SPECTRUM**

Coronal structures

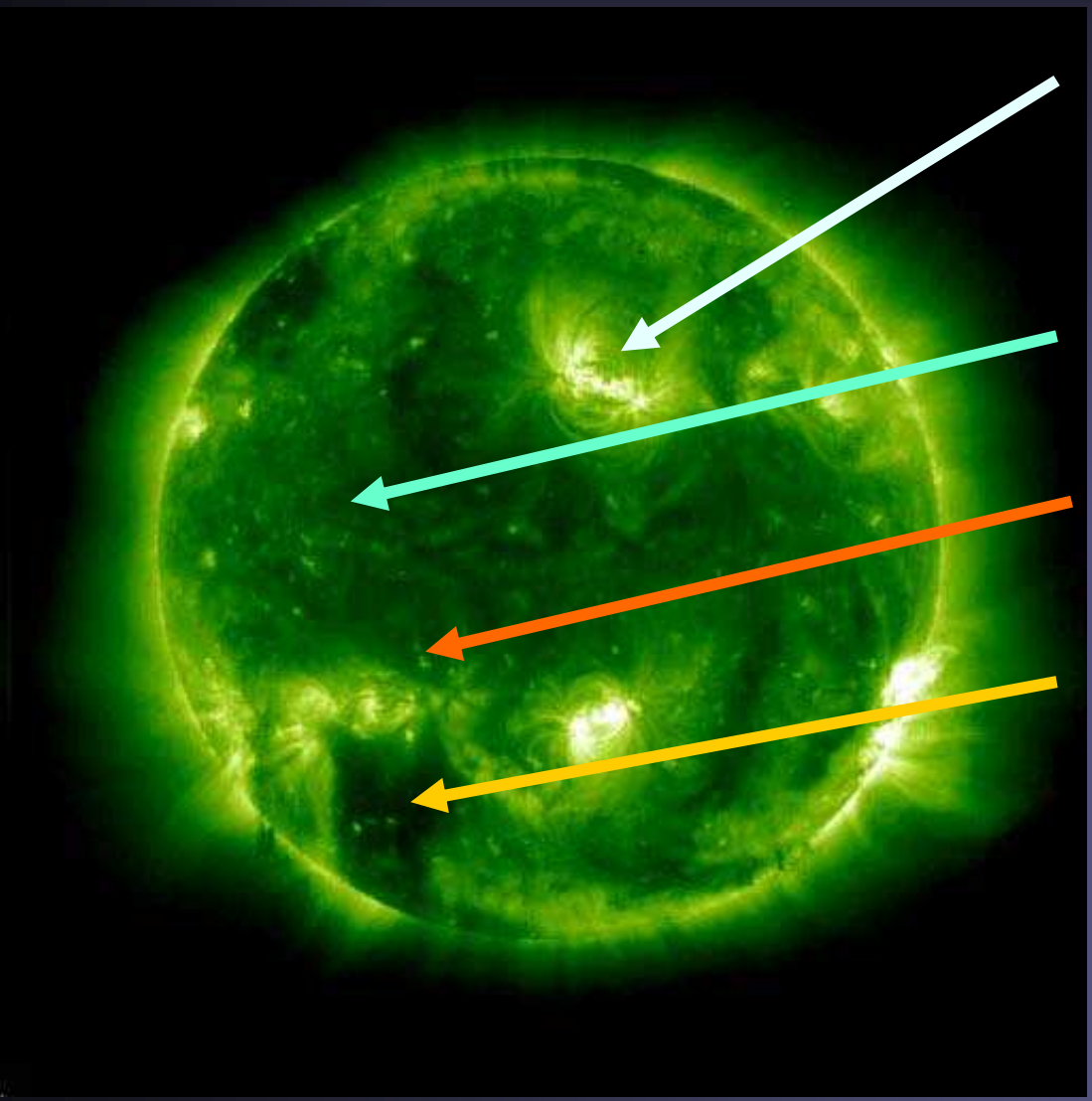

- Active regions (loops)
- Quiet Sun
- X-ray bright points
- Coronal holes
- Arcades

Fe XII 195 Å
(1.500.000 K)
17 May - 8 June 1998

Coronal structure: active region loops

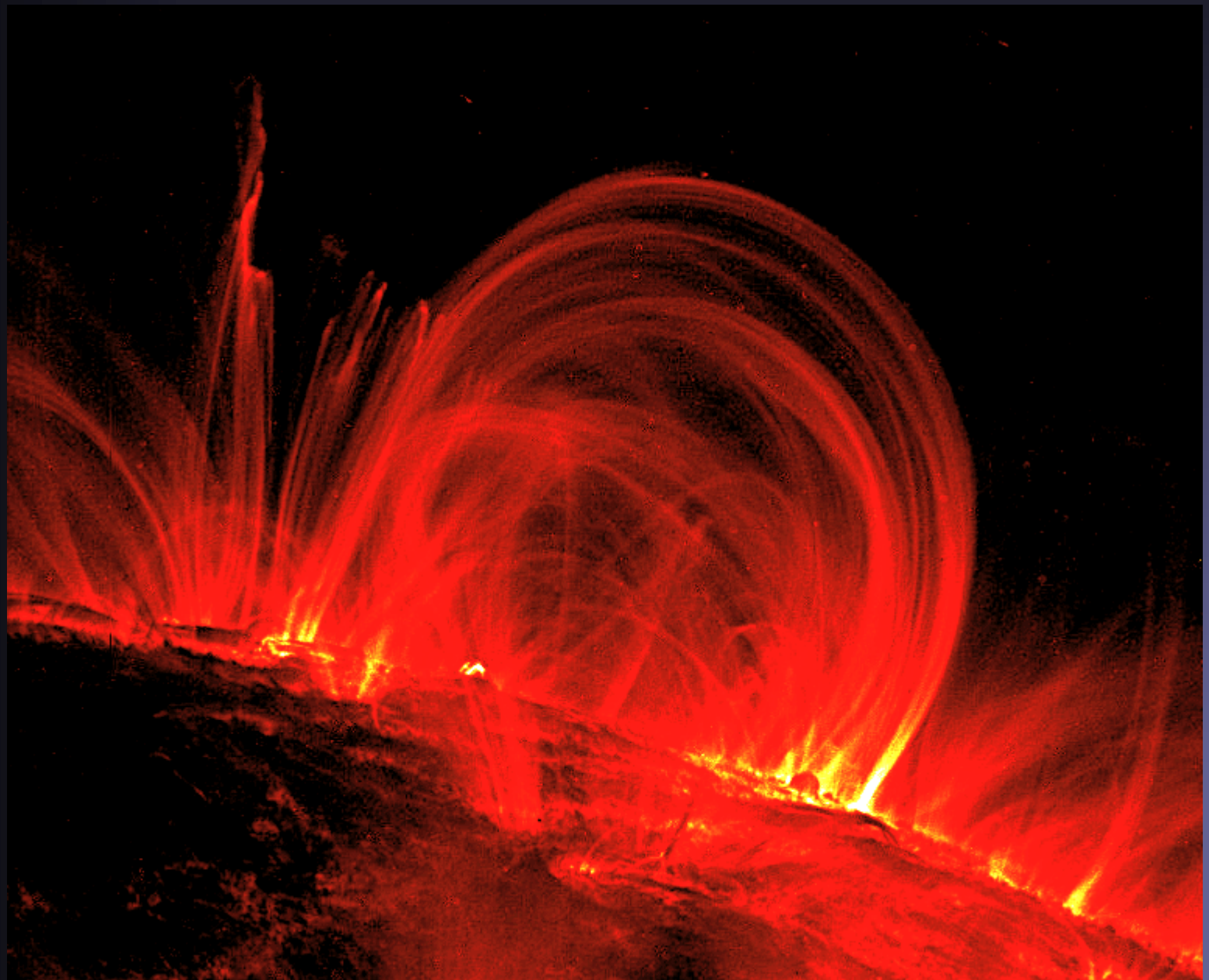

TRACE, 1999

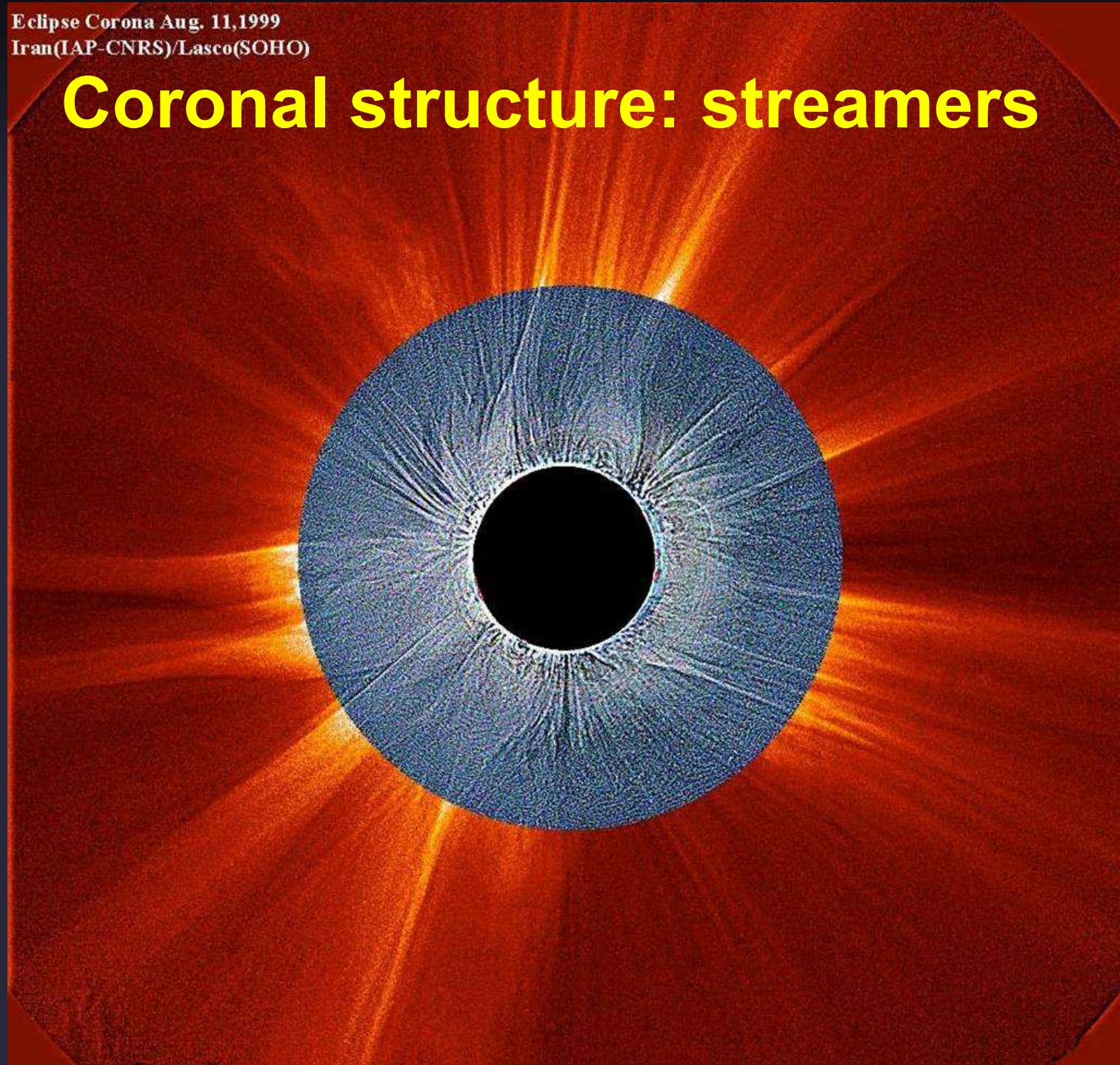

Coronal structure: streamers

Coronal structures: coronal holes

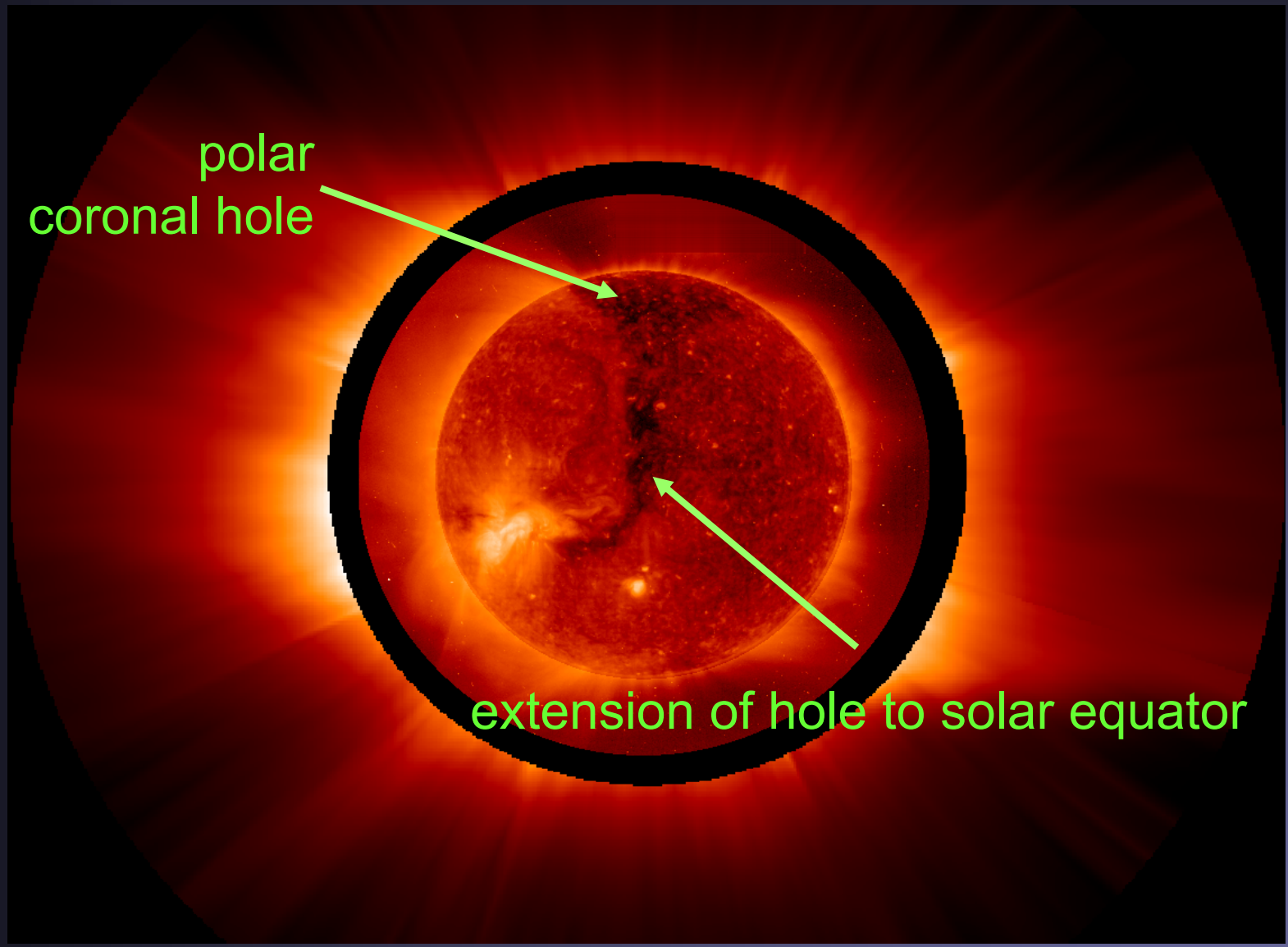

Coronal structures: coronal jets

XRT observations
Model (Moreno Insertis et al.

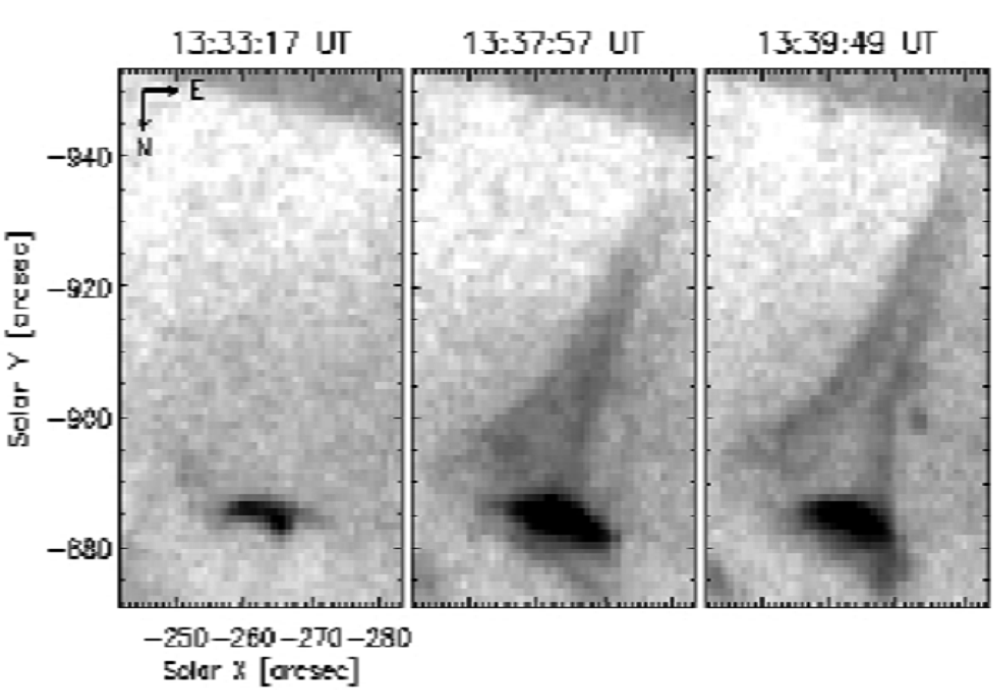

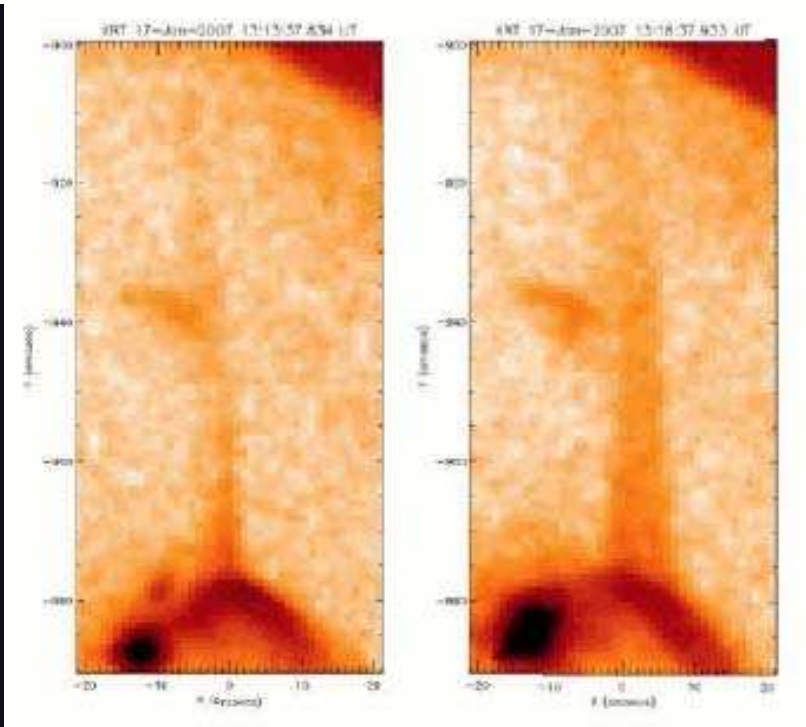

Velocity map

(t=22 min)

The solar wind

A constant stream of particles flowing from the Sun's corona, witha temperature of about a million degrees and with a velocity of ≈450 km/s. Solar wind reaches to well beyond Pluto's orbit, with the heliopause located roughly at 100-120 AU

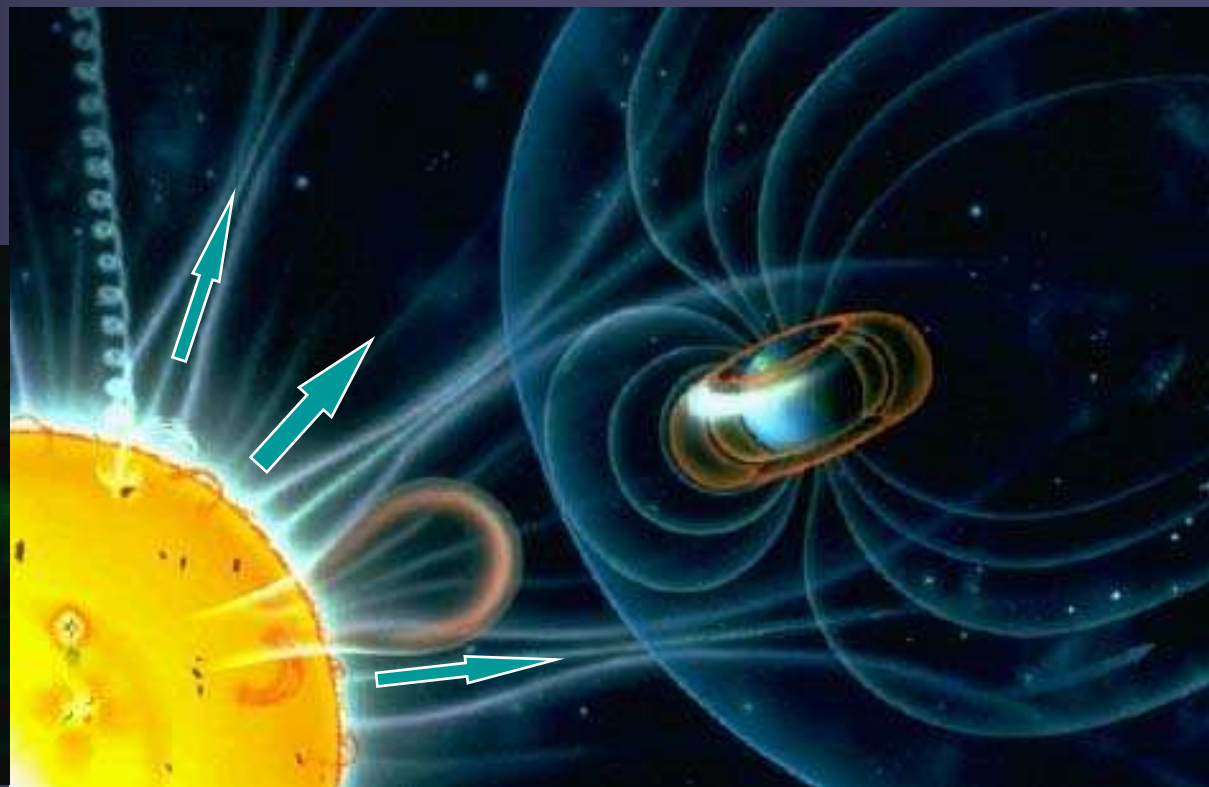

Discovery of the solar wind

- Ludwig Biermann at MPI für Physik und Astrophysik noticed that the tails of comets always pointed away from the Sun. Solar radiation pressure was insufficient to explain this.

➔Postulated a solar wind

- Independently, Parker (1958) realized that a hot corona must expand if it was to be in equilibrium with the interstellar medium. Only a supersonic solar wind was compatible with theory and observations.

➔Supersonic solar wind

Comets and the solar wind

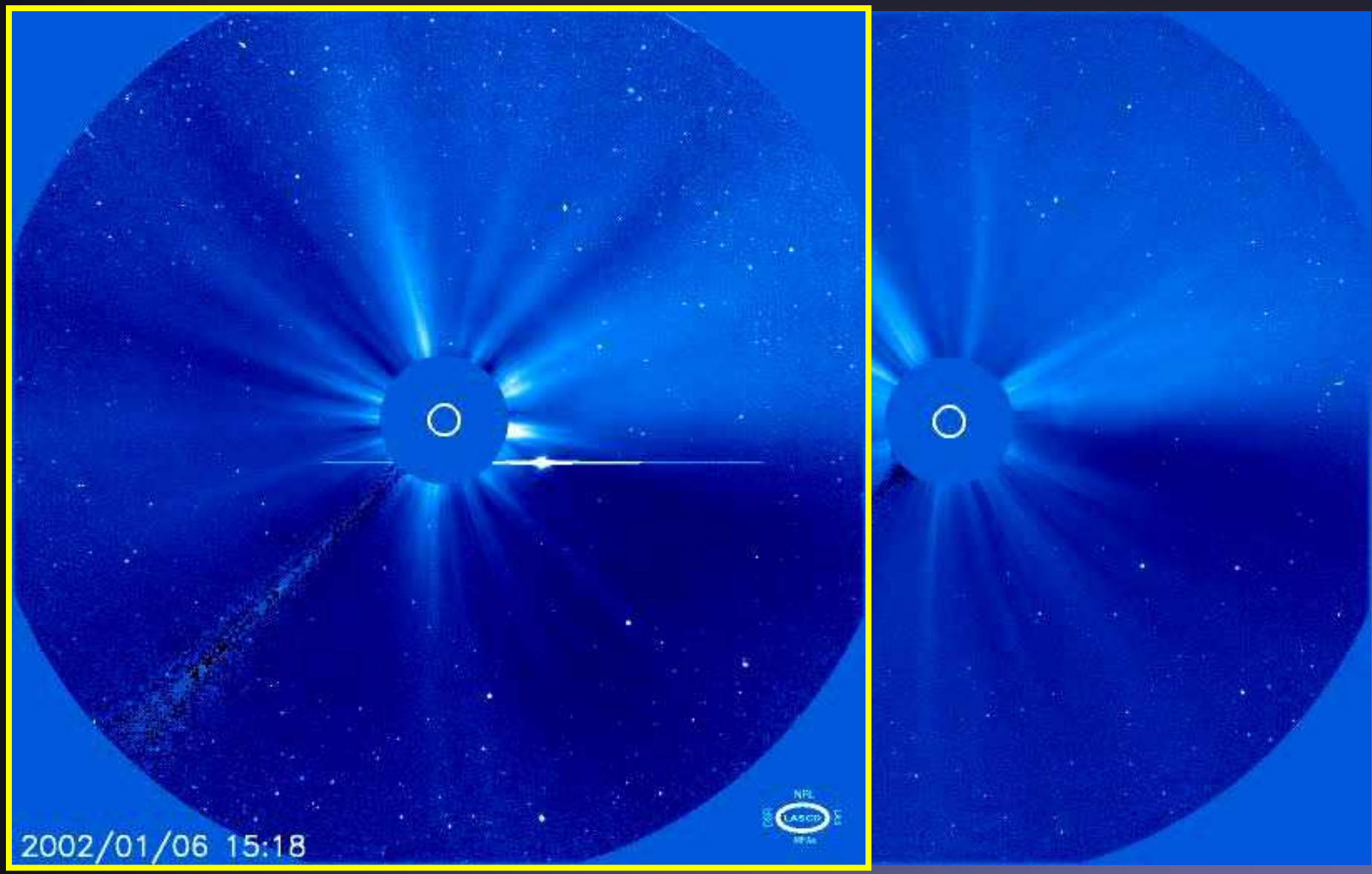

Solar wind characteristics at 1AU

Fast solar wind

- speed > 400 km/s
- $n_p \approx 3$ cm^{-3}
- homogeneous
- B≈ 5 nT = 0.00005G
- 95% H, 4% He
- Alfvenic fluctuations
- Origin: coronal holes

Slow solar wind

- < 400 km/s
- ≈ 8 cm^{-3}
- high variability
- B < 5 nT
- 94% H, 5% He
- Density fluctuations
- Origin: in connection with coronal streamers

Transient solar wind

- speed from < 300 km/s up to >2000 km/s
- Variable B, with B up to 100 nT (0.001G)
- Often very low density
- Sometimes up to 30% He
- Often associated with interplanetary shock waves
- Origin: CMEs

3-D structure of the Solar Wind: Variation over the Solar Cycle

1st Orbit: 3/1992 - 11/1997
declining / minimum phase

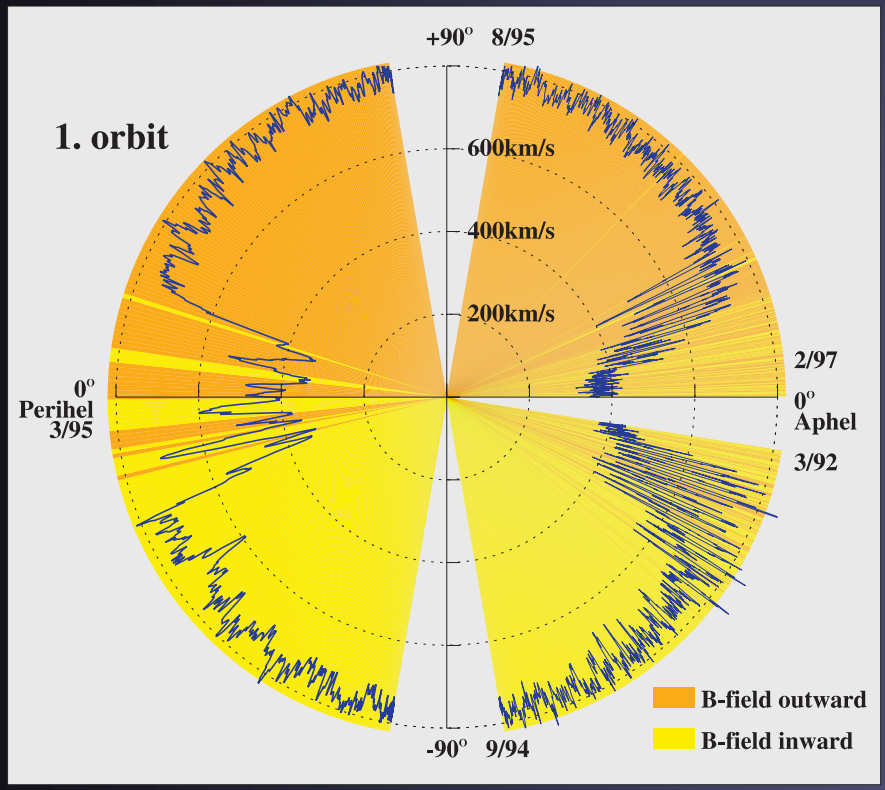

2nd Orbit: 12/1997 - 2/2002
rising / maximum phase

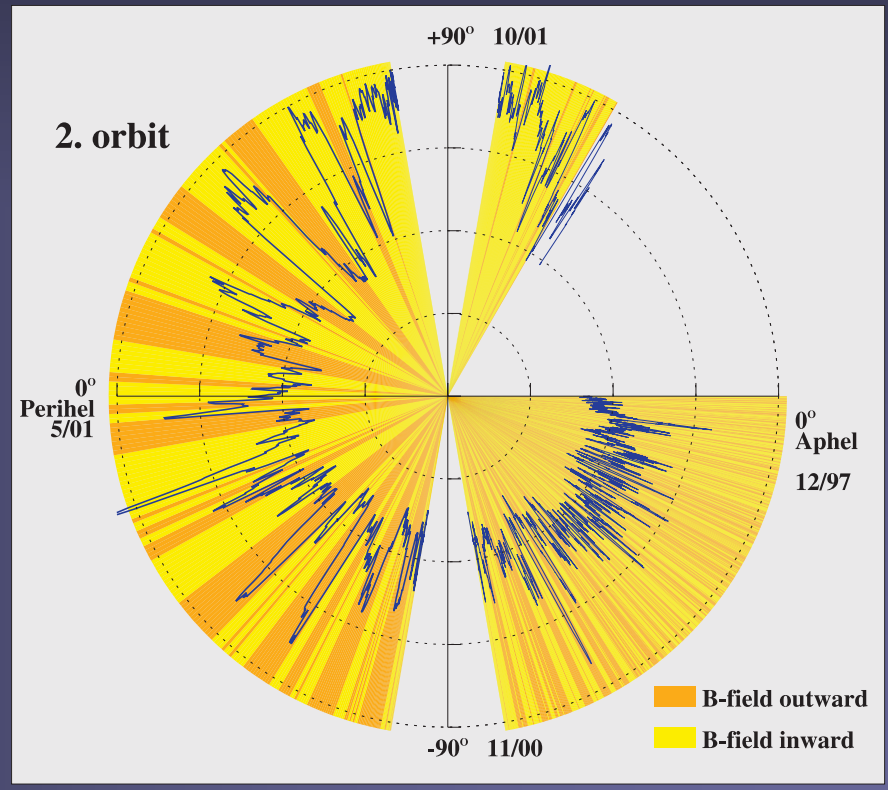

Ulysses SWICS data

Woch et al. GRL

Coronal Shape & Solar Wind: Ulysses Data & 3D-Heliosphere

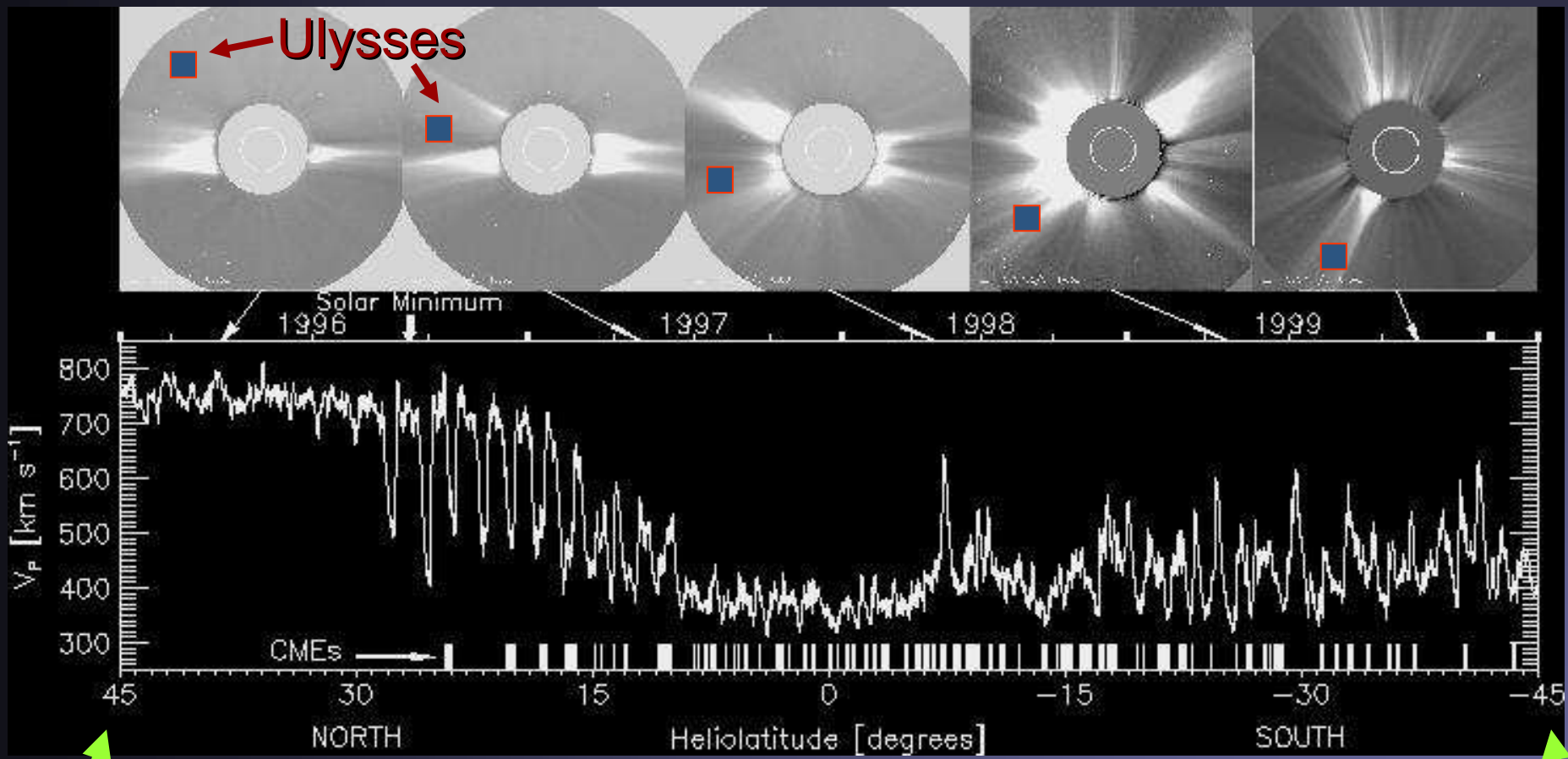

Activity minimum

Activity maximum

Parker's theory of the solar wind

- Basic idea: dynamic equilibrium between hot corona and interstellar medium. Mass and momentum balance equations:

$$\frac{d}{dr}(\rho r^2 v) = 0$$

$$v\frac{dv}{dr} = -\frac{1}{\rho}\frac{dP}{dr}\frac{GM}{r^2}$$

➔ Parker's Eq. for solar wind speed (isothermal atmosphere)

$$\frac{1}{v}\frac{dv}{dr}(v^2 - c_S{}^2) = \frac{2c_S{}^2}{r} - \frac{GM}{r^2}$$

Parker's solar wind solutions

- Parker found 4 families of solar wind solutions
- 2 not supported by Obs. (supersonic at solar surface)
- 2 do not give sufficient pressure against the interstellar medium.
- Correct solution must be thick line in Fig.

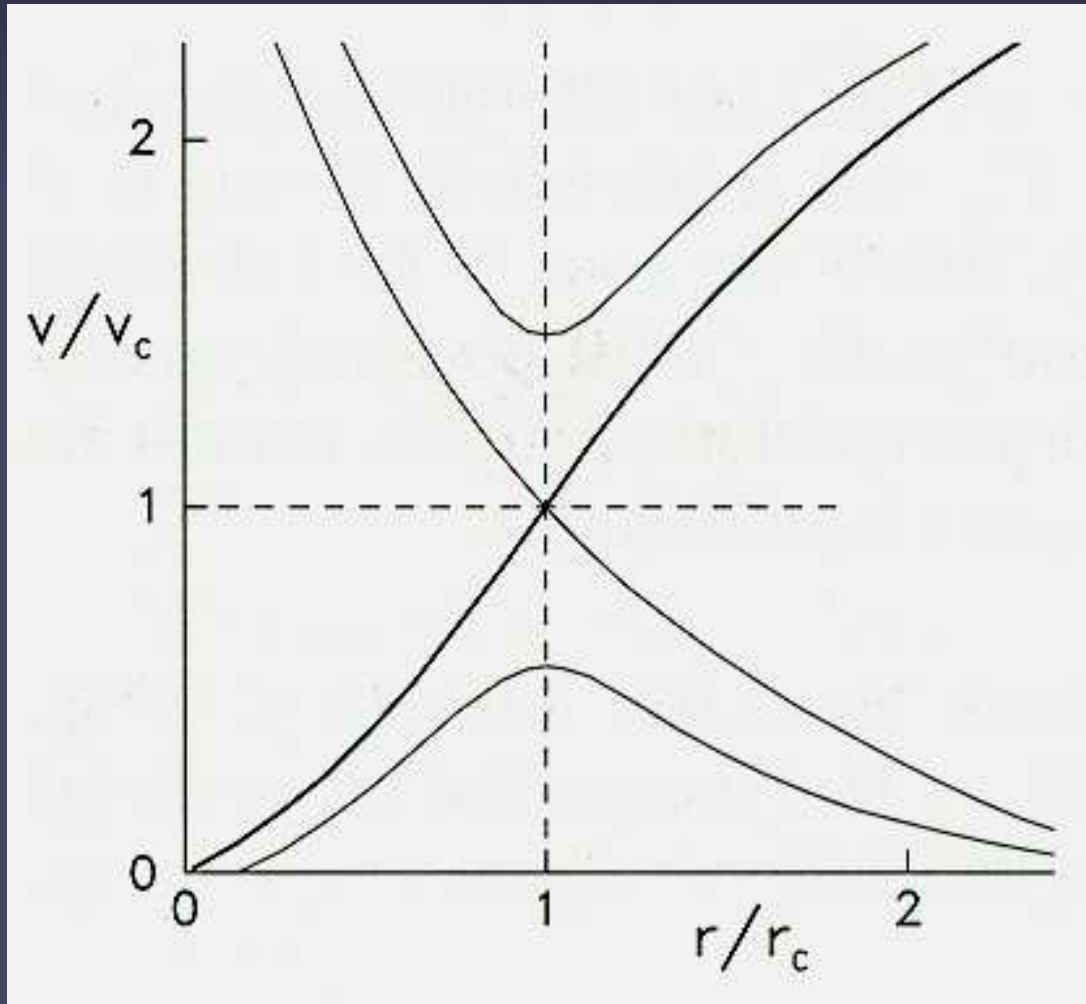

Solar wind speed

Speed of solar wind predicted by Parker's model for different coronal (simple, isothermal case; no magnetic field)

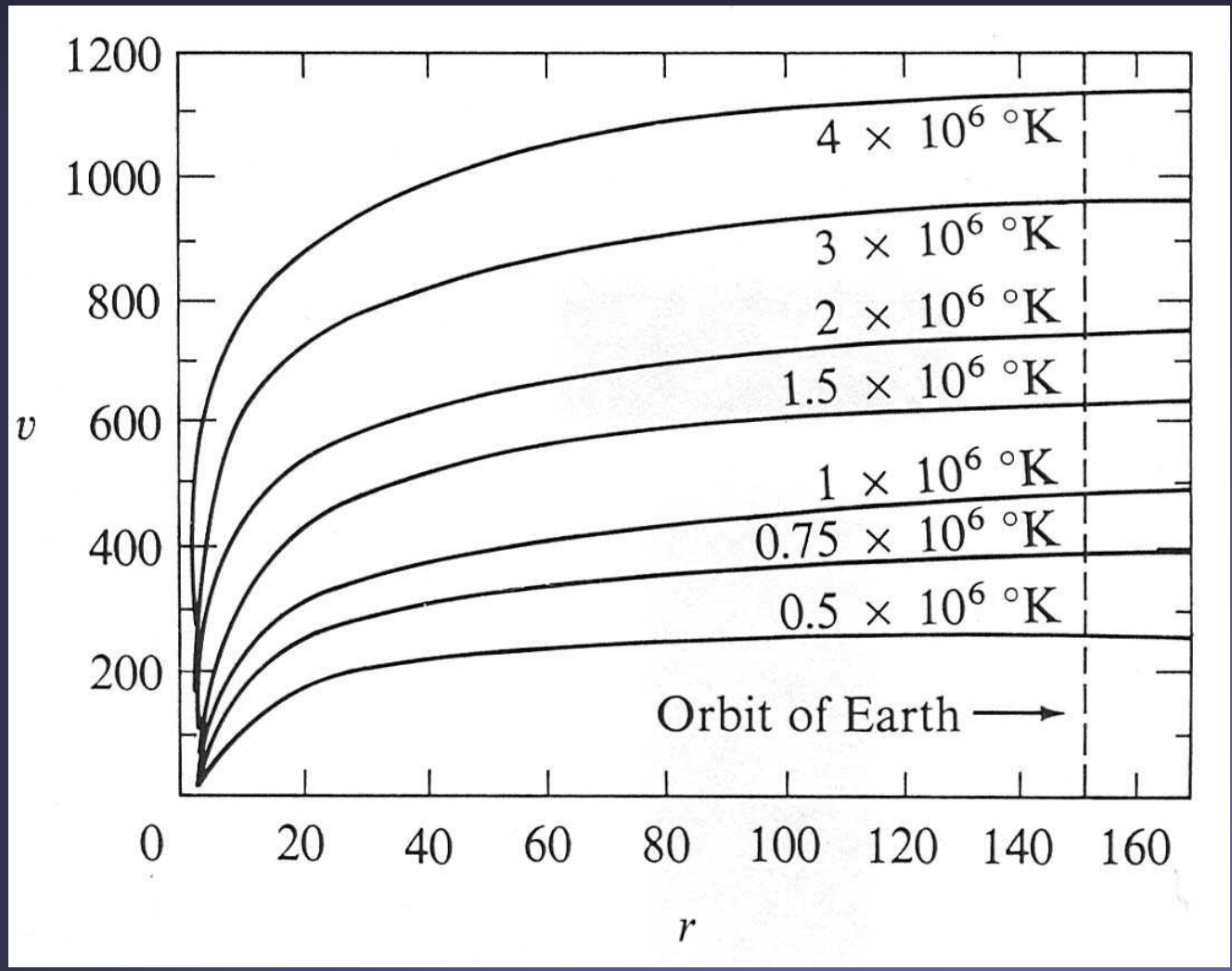

Sources of solar wind: fast wind

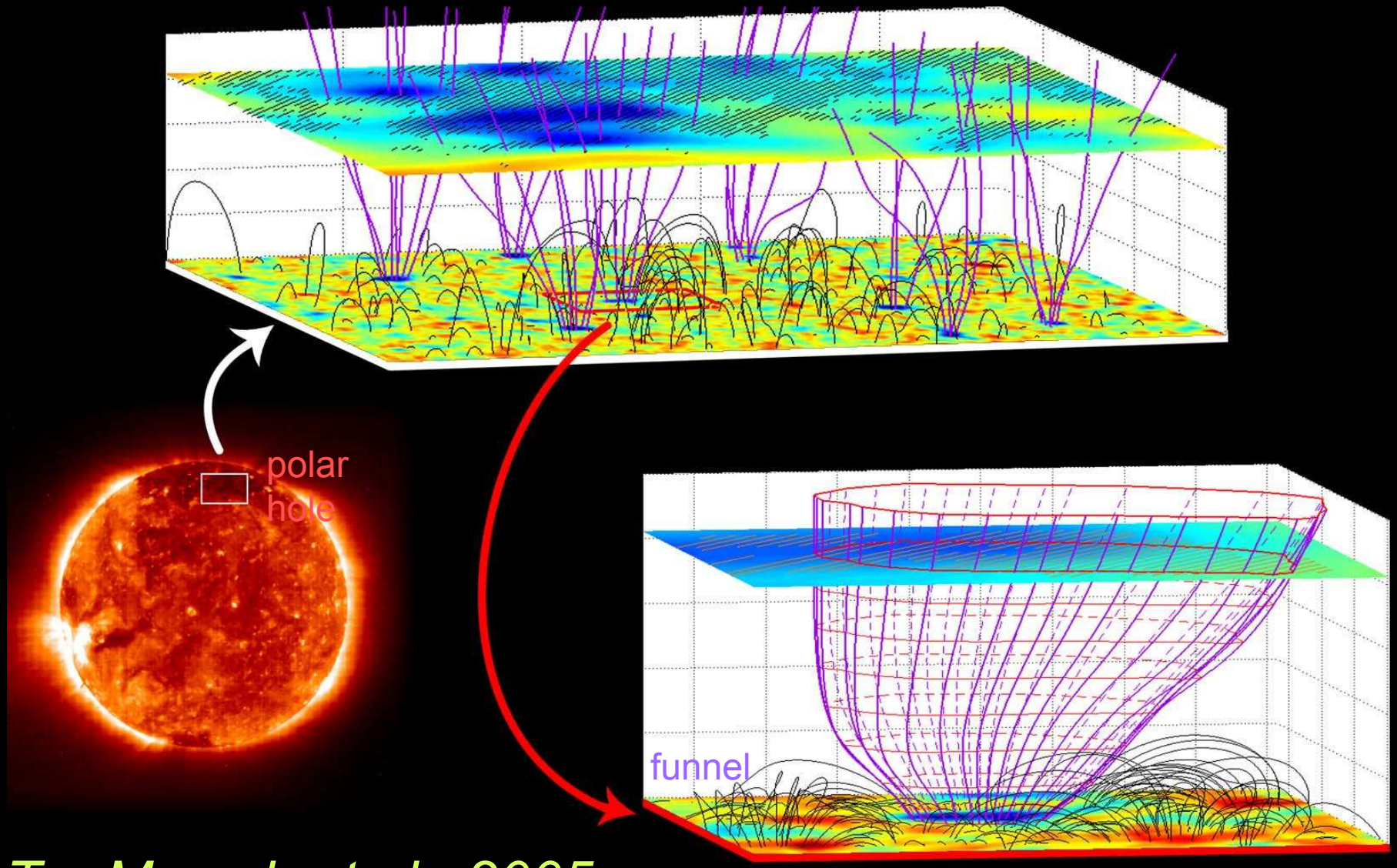

Tu, Marsch et al., 2005

The Heliosphere

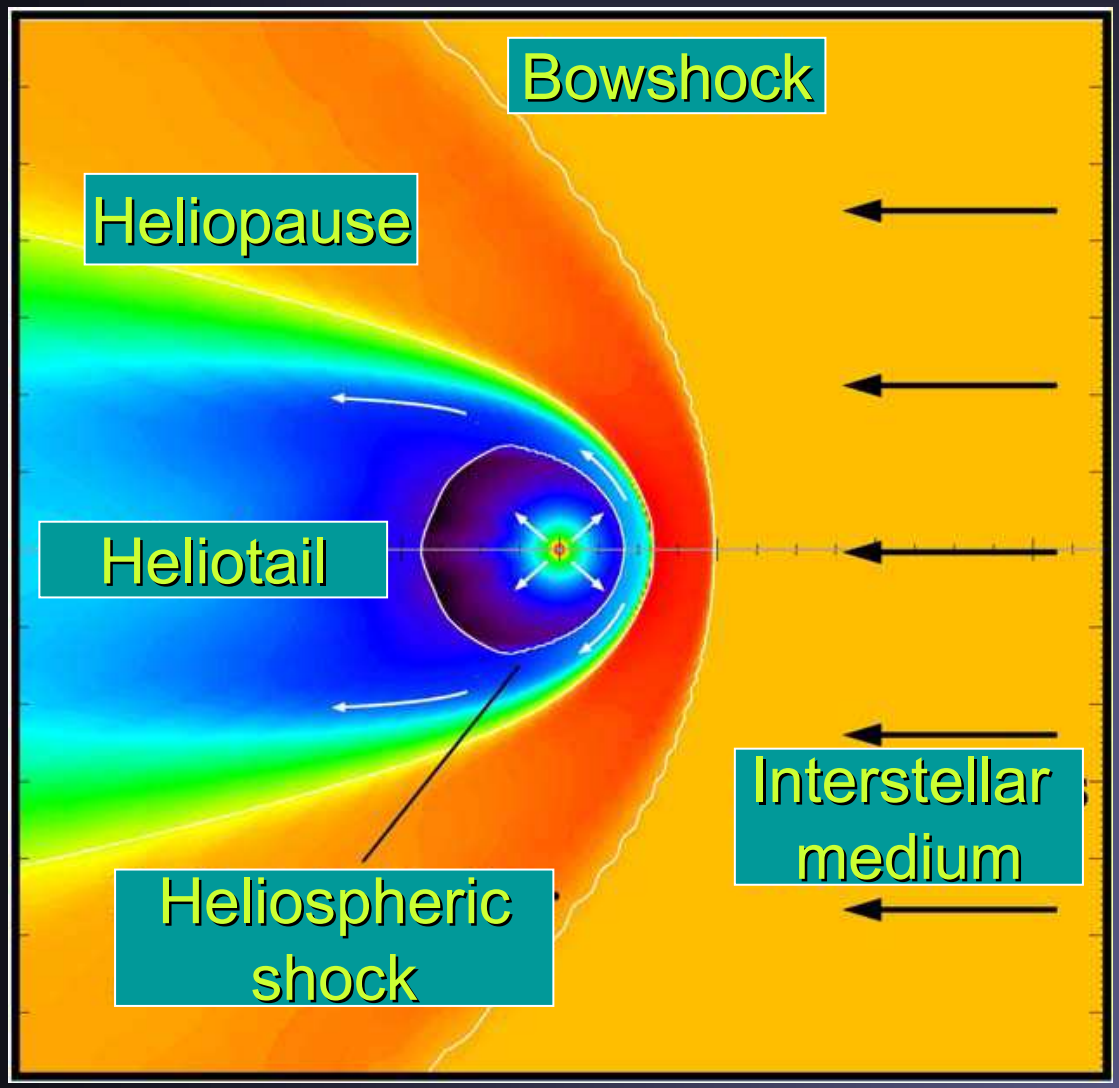

- Heliosphere = region of space in which the solar wind and solar magnetic field dominate over the interstellar medium and the galactic magnetic field.
- Bowshock: where the interstellar medium is slowed relative to the Sun.
- Heliospheric shock: where the solar wind is decelerated relative to Sun
- Heliopause: boundary of the heliosphere

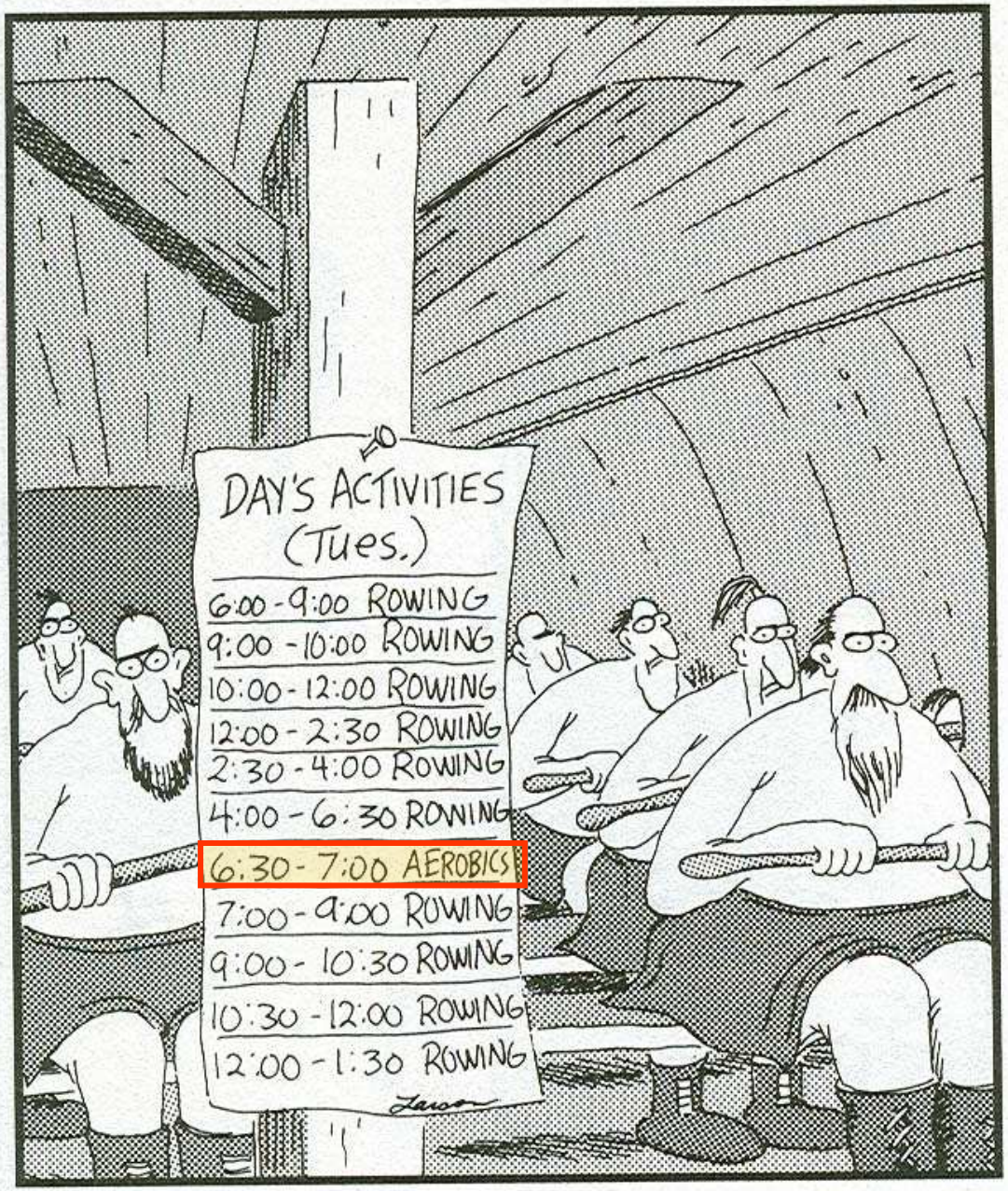

Slave-ship daily schedules

Magnetic Field

The source of the Sun's activity is the magnetic field

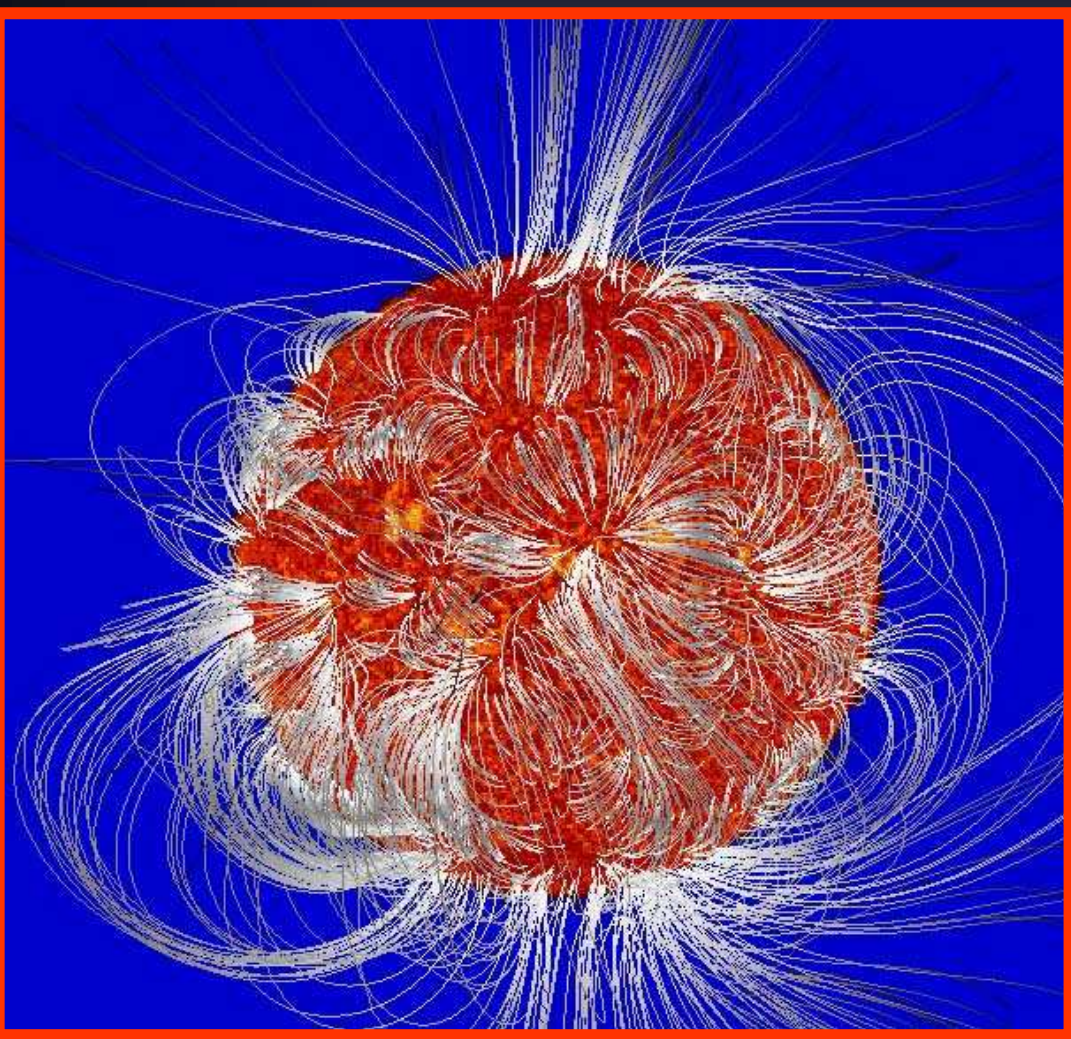

In order to understand the dynamics and activity of the Sun we need measurements and theory of its magnetic field

Thomas Wiegelmann

Correlation of field with brightness

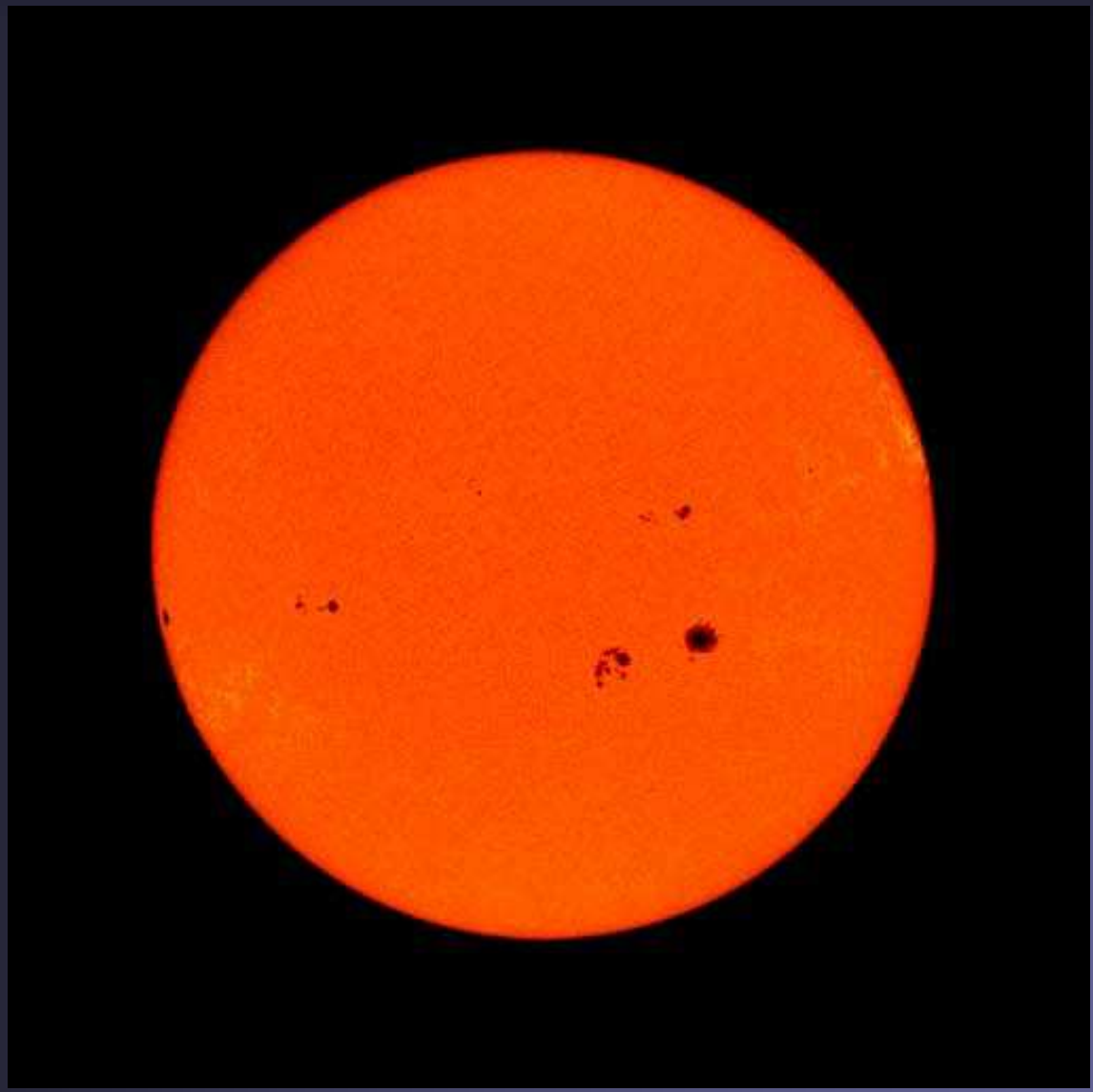

Open and closed magnetic flux

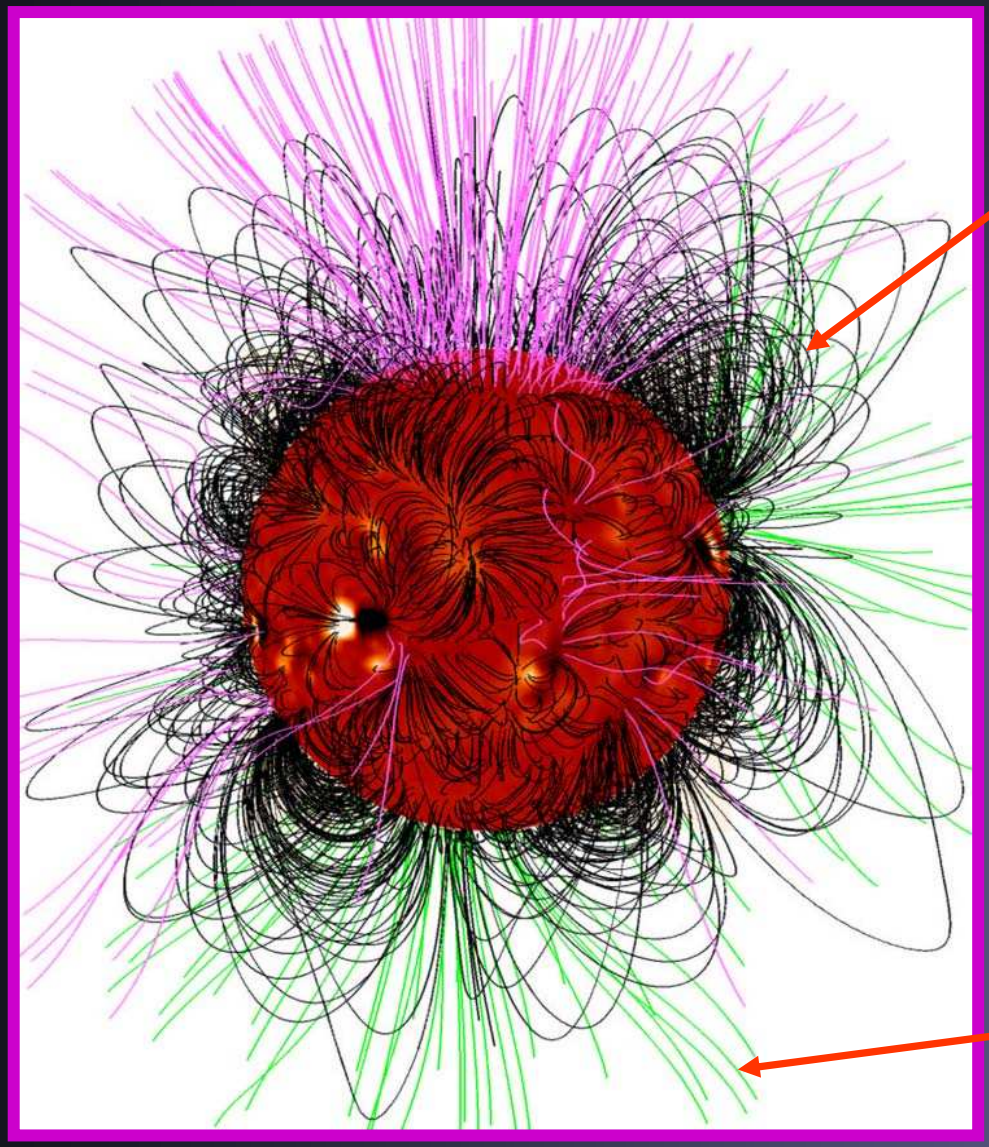

Closed flux: slow solar wind

Most of the solar flux returns to the solar surface within a few $R_\odot$ (closed flux)

A small part of the total flux through the solar surface connects as open flux to interplanetary space

Open flux: fast solar wind

Measured Magnetic Field at Sun's Surface

Month long sequence of magnetograms (approx. one solar rotation)

MDI/SOHO
May 1998

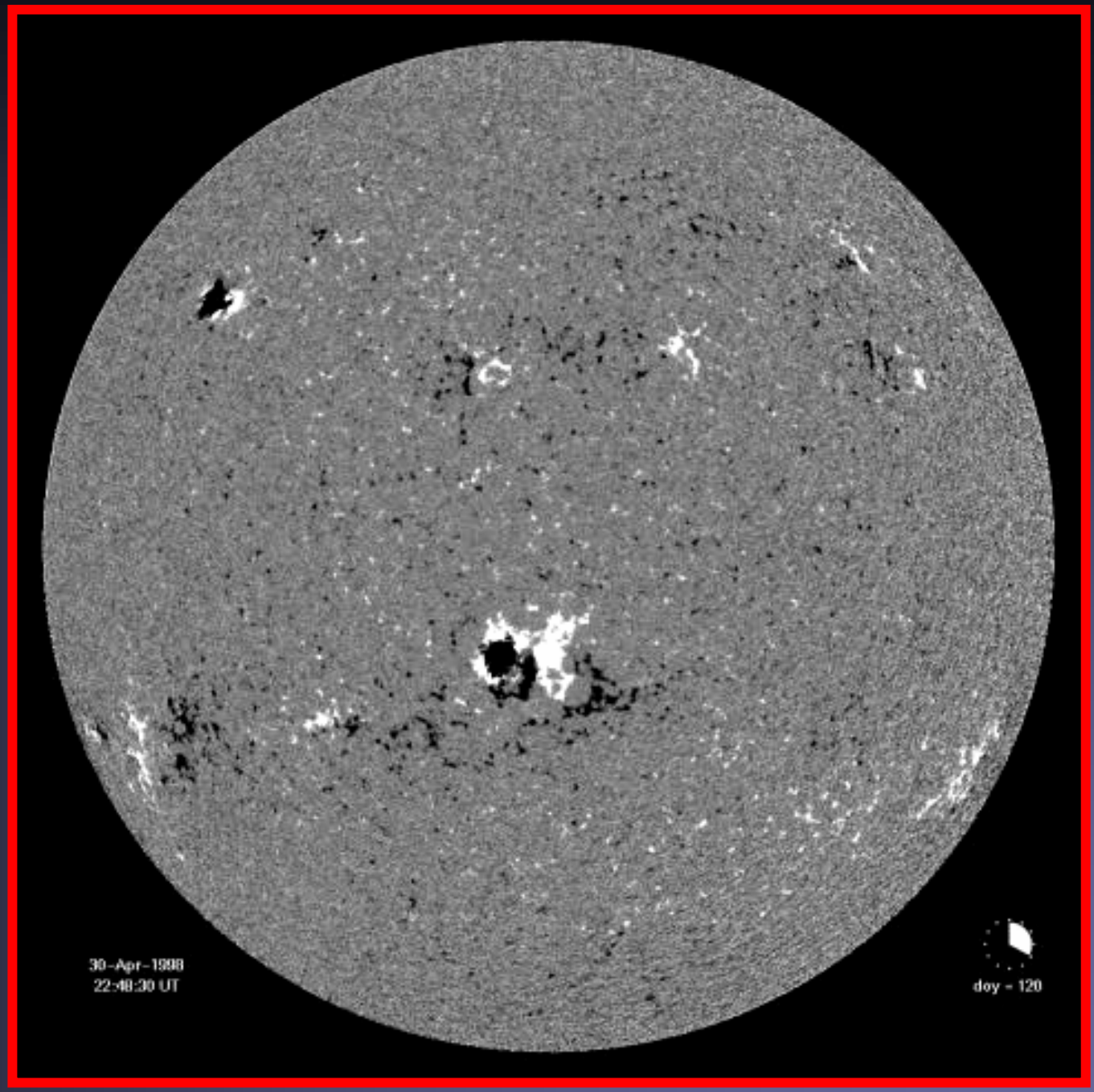

Methods of magnetic field measurement

- Direct methods:
  - Zeeman effect → polarized radiation
  - Hanle effect → polarized radiation
  - Gyroresonance → radio spectra
- Indirect methods: Proxies
  - Bright or dark features in photosphere (sunspots, G-band bright points)
  - Ca II H and K plage
  - Fibrils seen in chromospheric lines, e.g. Hα
  - Coronal loops seen in EUV or X-radiation

Example of proxies: Continuum vs. G-band

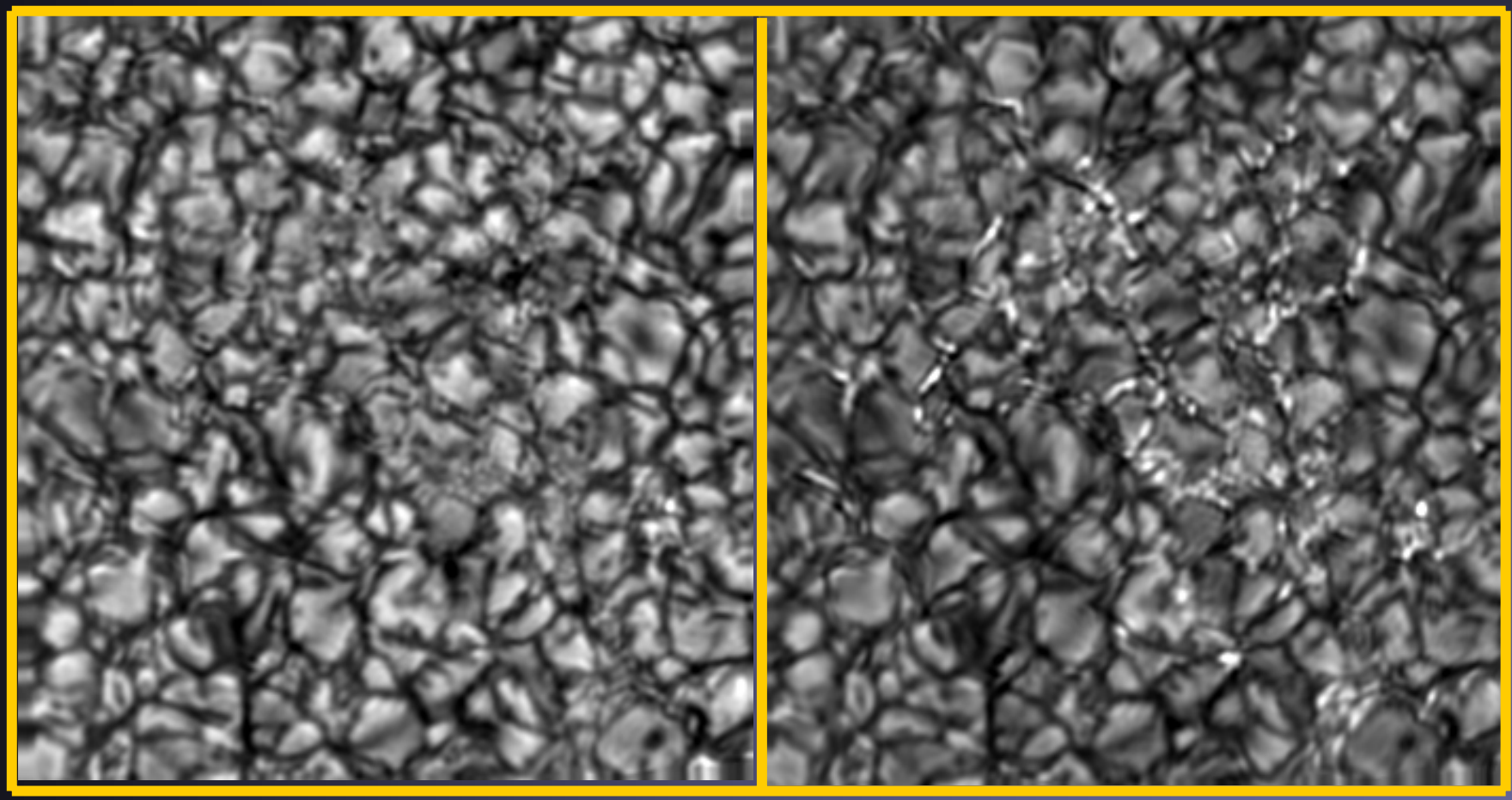

Continuum

G-band

Ca II K as a magnetic field proxy

- Ca II H and K lines, the strongest lines in the visible solar spectrum, become brighter with non-spot magnetic flux.
- $I_{core}/I_{wing} \sim \langle B \rangle^{0.6}$
- Magnetic regions (except sunspots) appear bright in Ca II H+K ➔ Ca plage and network regions

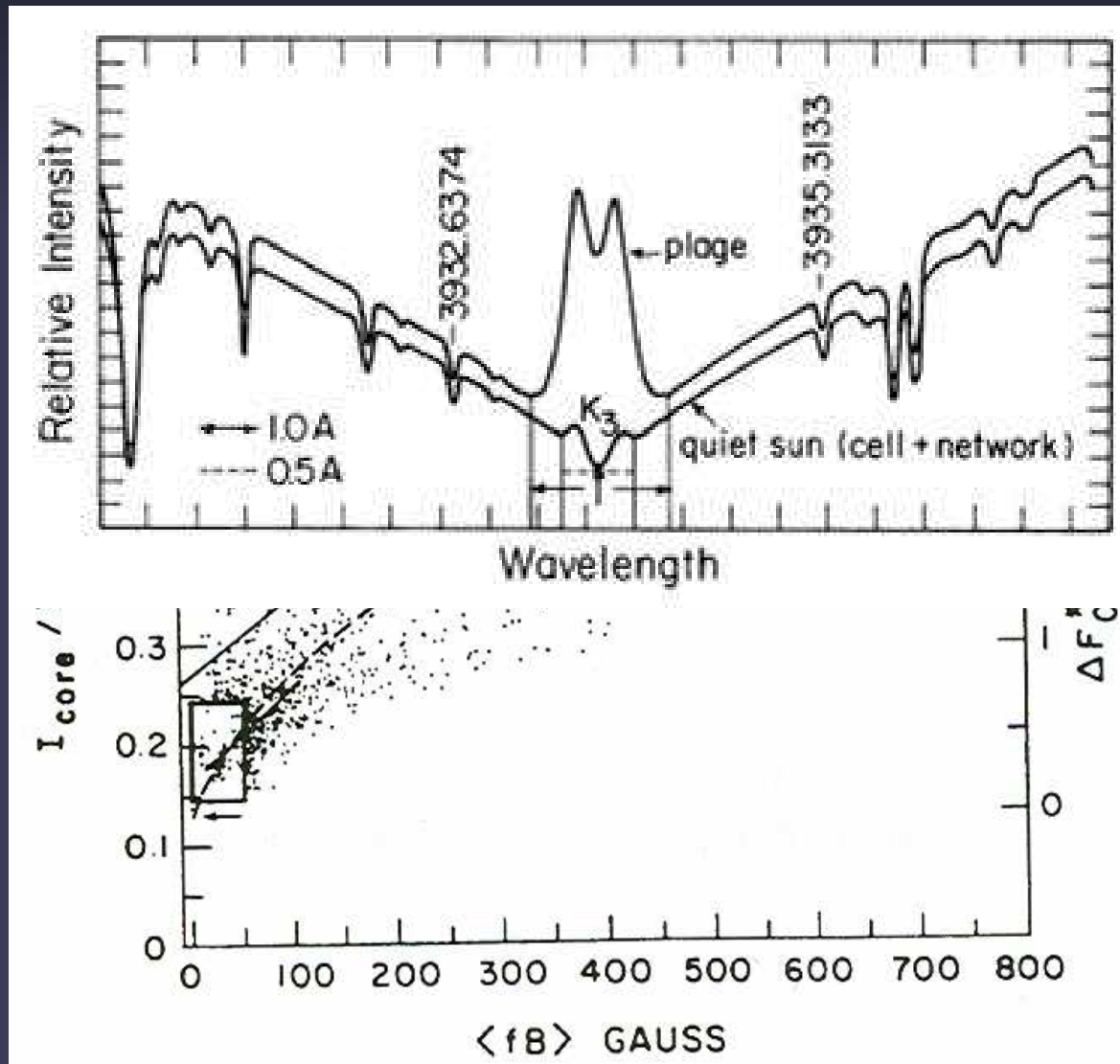

Hα and the chromospheric field

- Hα image of quiet Sun shows many loop-like structures. Do they (roughly) follow the field lines?
- Do they imply a relatively horizontal chromospheric field?

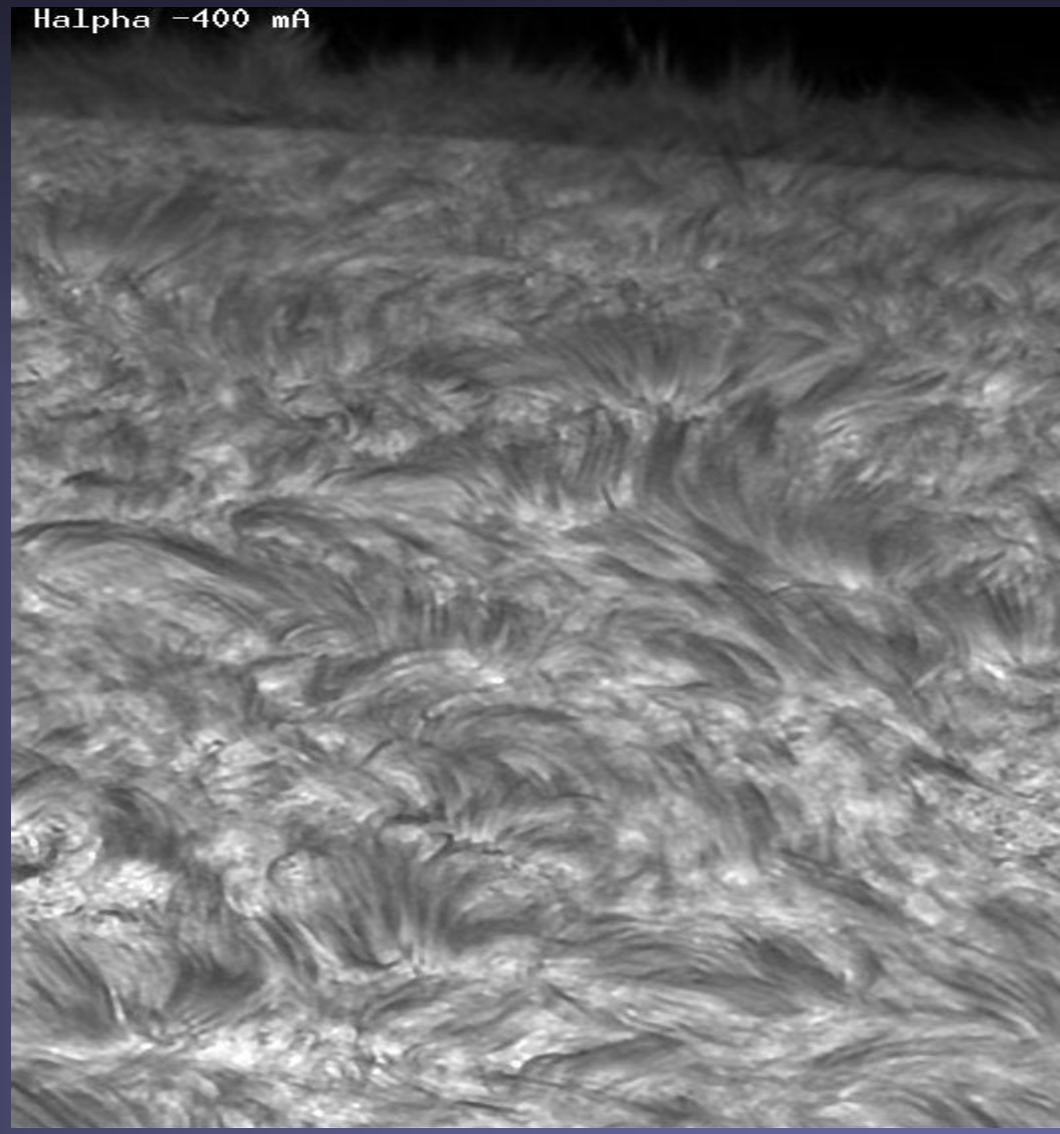

Zeeman diagnostics

- Direct detection of magnetic field by obs. of magnetically induced splitting and polarisation of spectral lines
- Ob Sun: Zeeman effect changes not just spectral shape of a spectral line (often subtle and difficult to measure), but also introduces a unique polarisation signature

➔Measurement of polarization is central to measuring solar magnetic fields.

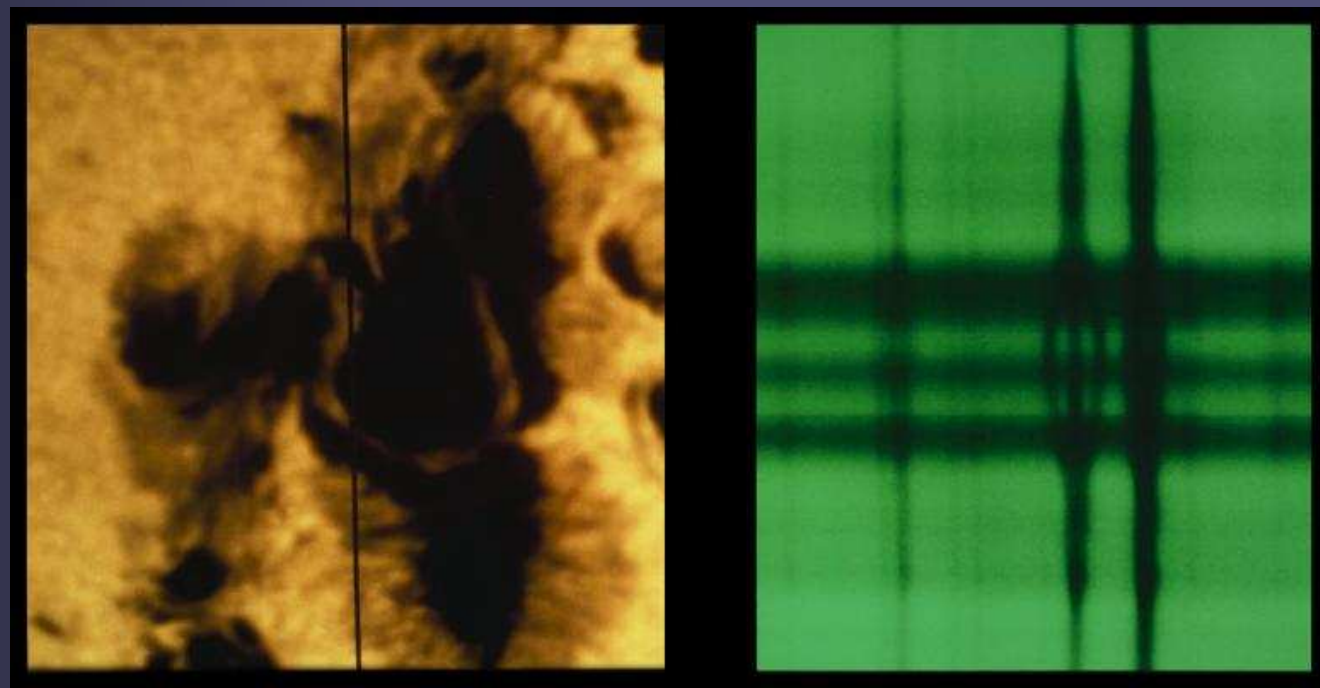

Polarized radiation

- Polarized radiation is described by the 4 Stokes parameters: *I*, *Q*, *U* and *V*

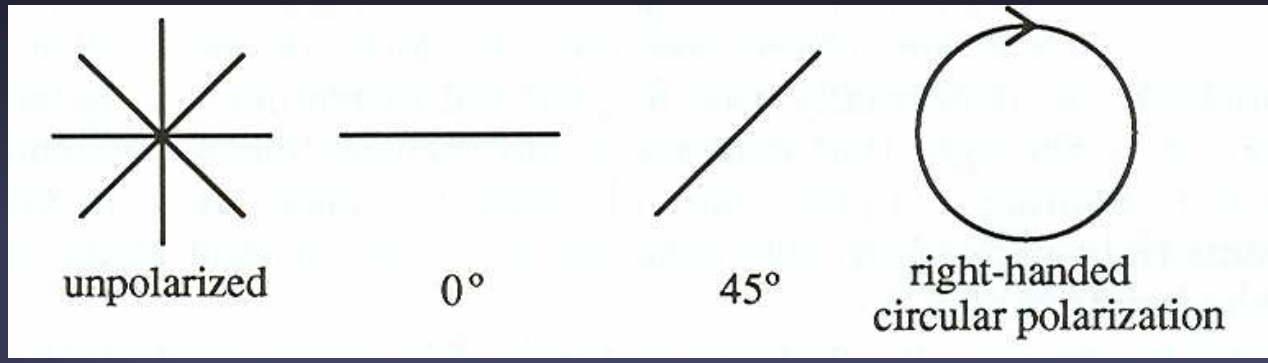

- I = total intensity = $I_{\rm lin}(0^{\rm o}) + I_{\rm lin}(90^{\rm o}) = I_{\rm lin}(45^{\rm o}) + I_{\rm lin}(135^{\rm o}) = I_{circ}({\rm right}) + I_{\rm circ}({\rm left})$
- $Q = I_{\rm lin}(0^{\rm o}) - I_{\rm lin}(90^{\rm o})$
- $U = I_{\rm lin}(45^{\rm o}) - I_{\rm lin}(135^{\rm o})$
- $V = I_{\rm circ}({\rm right}) - I_{\rm circ}({\rm left})$
- Note: Stokes parameters are sums and differences of intensities, i.e. they are directly measurable

Zeeman splitting of atomic levels

- In a B-field a level with total angular moment J splits into $2J+1$ sub-levels with different M.
- $E_{J,M} = E_J + \mu_0 g M_J B$
- Transitions are allowed between levels with
  $\Delta J = 0, \pm 1$ &
  $\Delta M = 0\ (\pi), \pm 1\ (\sigma_b, \sigma_r)$
- Splitting is determined by Lande factor g :

  $g(J,L,S) = 1+(J(J+1)+ S(S+1)-L(L+1))/2J(J+1)$

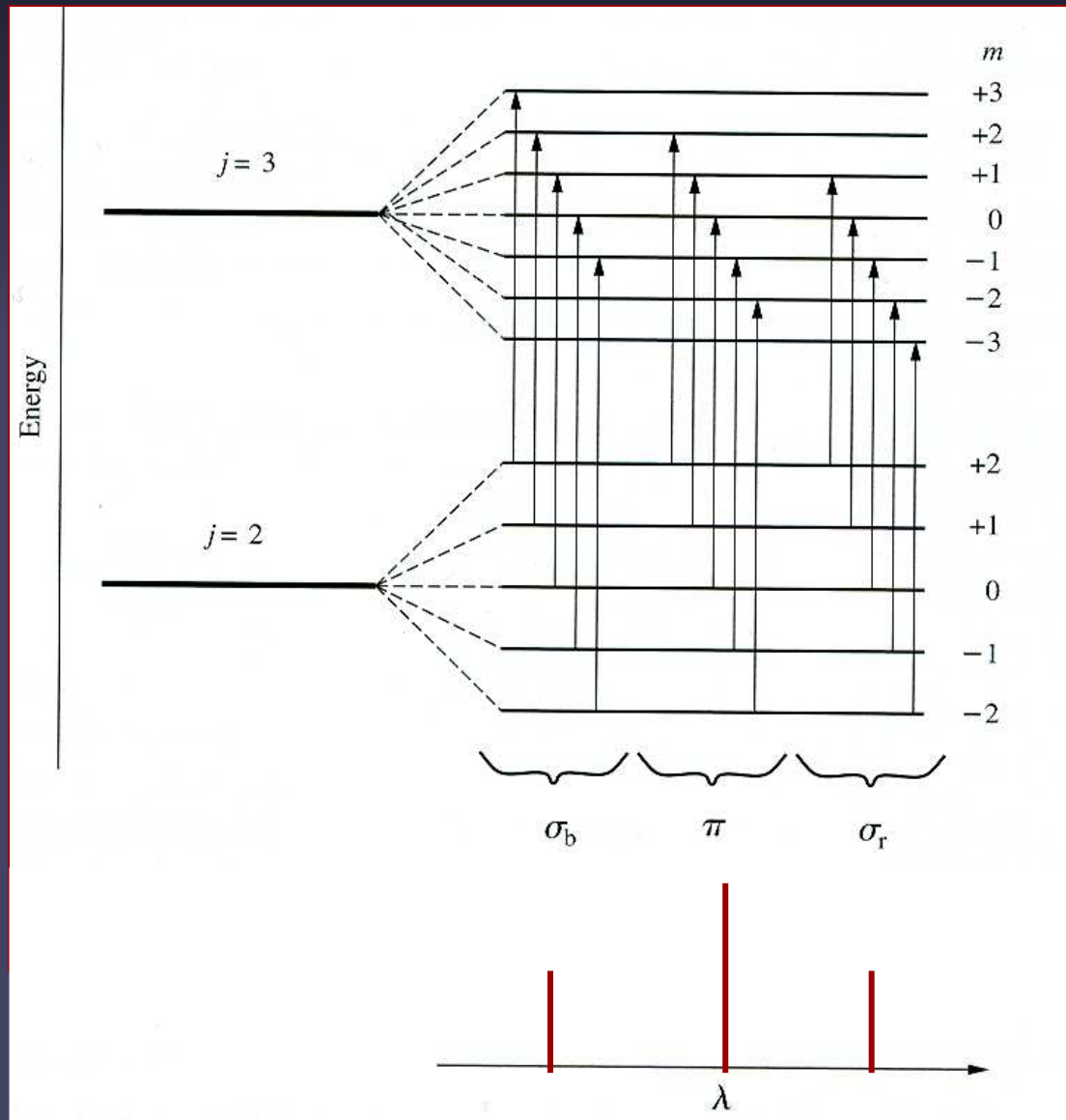

Splitting patterns of lines

- Depending on g of the upper and lower levels, the spectral line shows different splitting patterns
- Positive: π components: $\Delta M=0$
- Negative: σ components: $\Delta M=\pm 1$
- Top left: normal Zeeman effect (rare)
- Rest: anomalous Zeeman effect (usual)

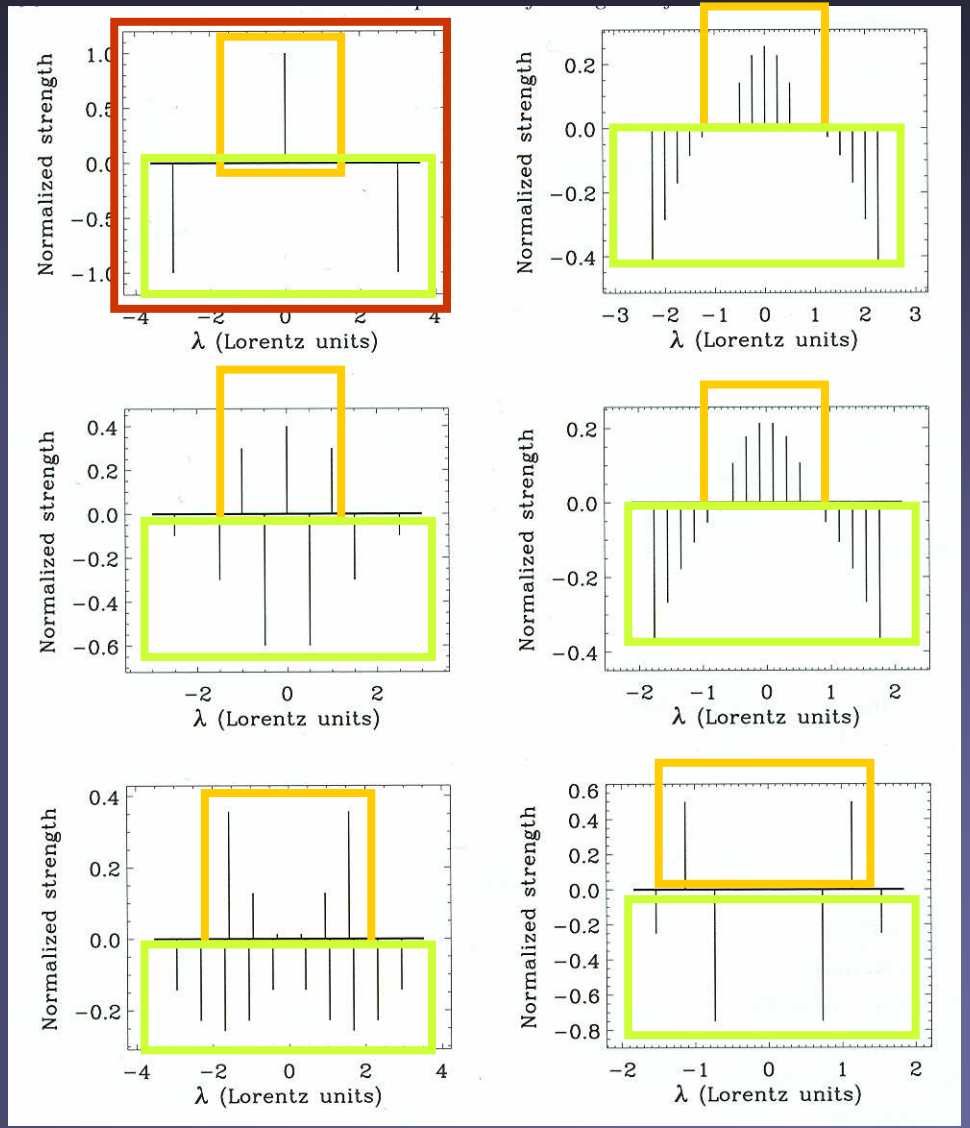

Polarization and Zeeman effect

Longitudinal Zeeman Effect

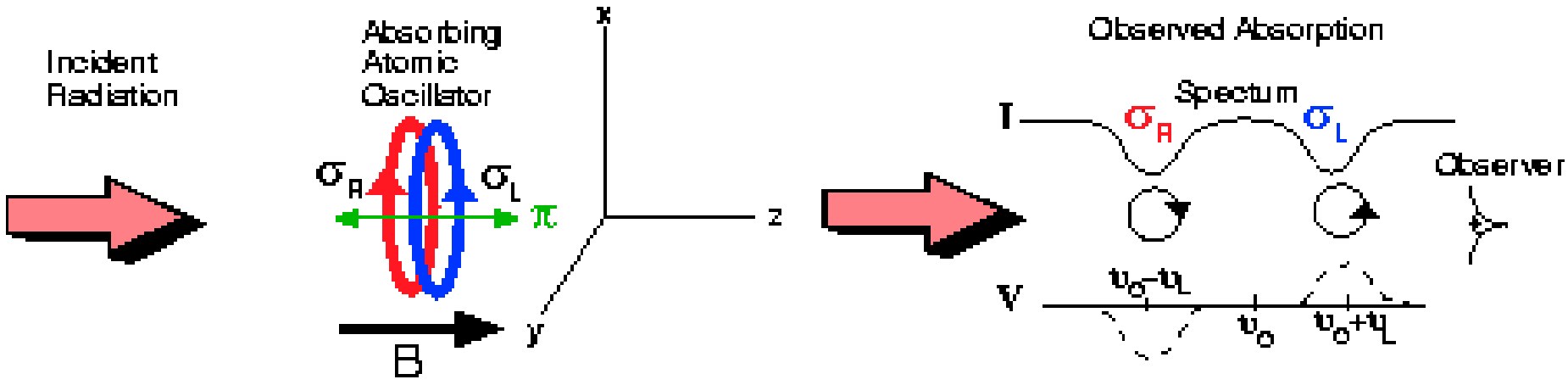

Transverse Zeeman Effect

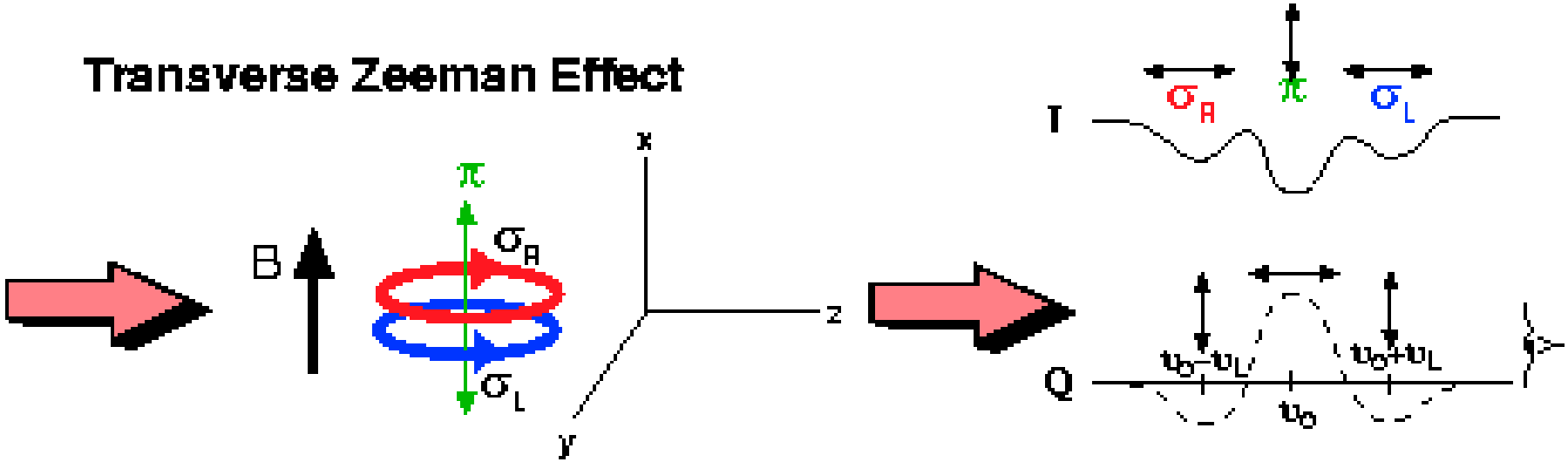

Effect of changing field strength

Formula for Zeeman splitting (for B in G, λ in Å):

$$\Delta\lambda_H = 4.67\ 10^{-13}\ g_{eff} B \lambda^2 \quad [Å]$$

g_{eff}=effective Landé factor of line

For large B: $\Delta\lambda_H = \Delta\lambda$ between σ-component peaks

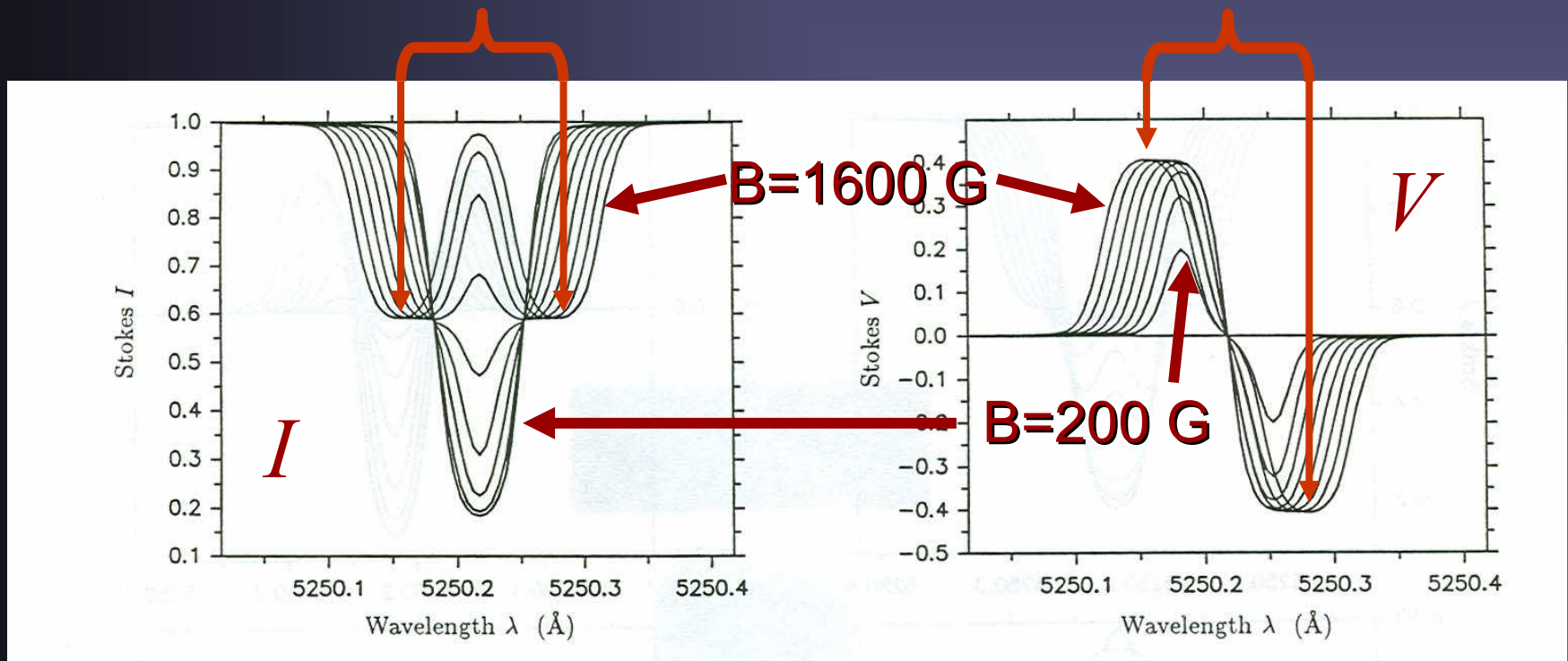

Dependence on B, γ, and φ

- $I \sim \kappa_\sigma(1+\cos^2\gamma)/4 + \kappa_\pi \sin^2\gamma/2$
- $Q \sim B^2 \sin^2\gamma \cos 2\varphi$
- $U \sim B^2 \sin^2\gamma \sin 2\varphi$
- $V \sim B \cos\gamma$

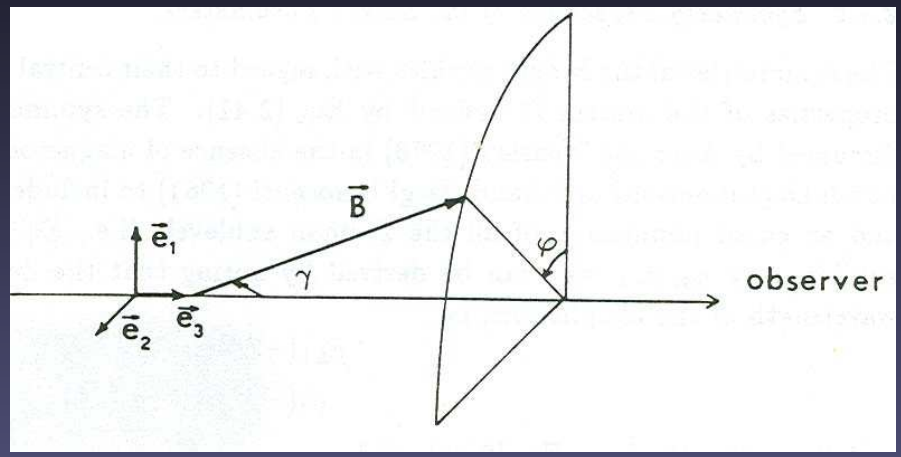

- V: longitudinal component of B
- Q, U: transverse component of B
- Above formulae for Q,U,V refer to relatively weak fields (e.g. B and B^2 dependence of field)
- Zeeman splitting etc. is hidden in κ_σ and κ_π. For Q, U, V these dependences have not been given for simplicity.

Juanma Borrero

Dependence on B, γ, and φ

- $I \sim \kappa_\sigma(1+\cos^2\gamma)/4 + \kappa_\pi \sin^2\gamma/2$
- $Q \sim B^2 \sin^2\gamma \cos 2\varphi$
- $U \sim B^2 \sin^2\gamma \sin 2\varphi$
- $V \sim B \cos\gamma$

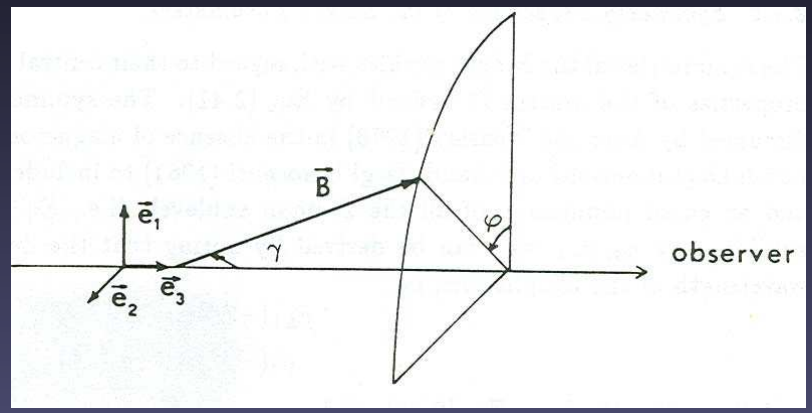

- Q, U: transverse component of B
- V: longitudinal component of B

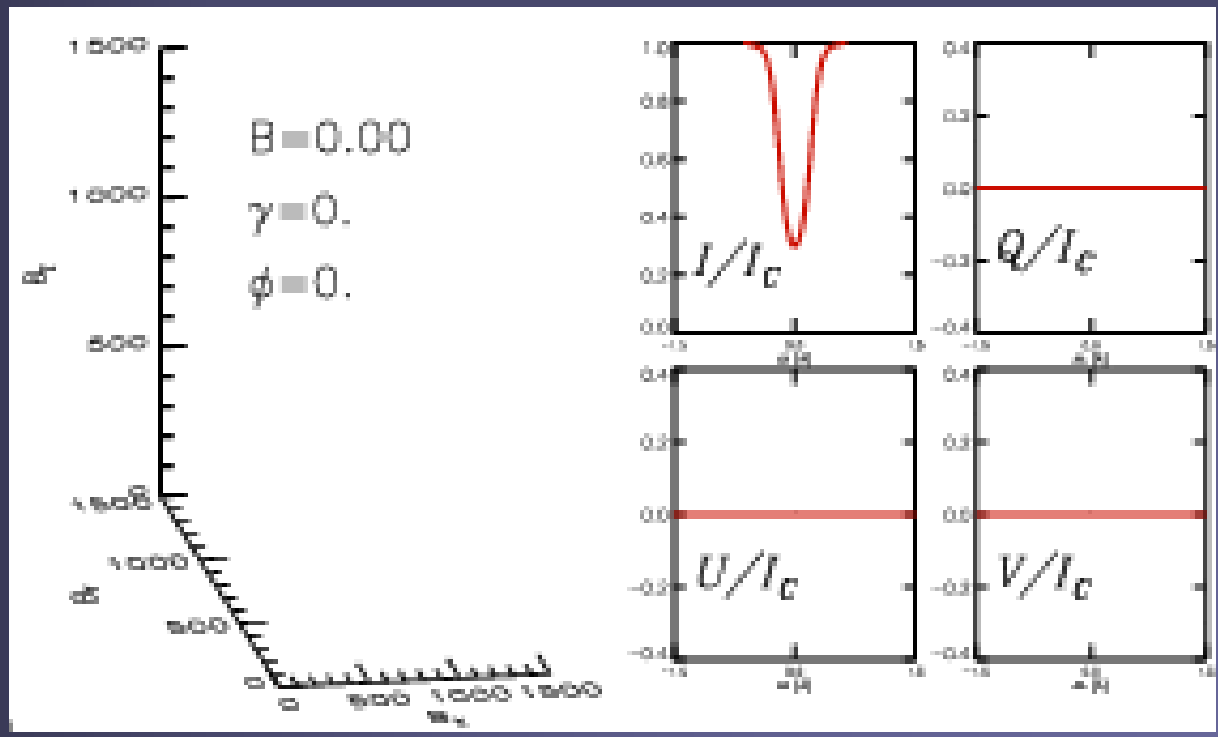

Juanma Borrero

Zeeman polarimetry

- Most widely used remote sensing technique of astrophysical (and certainly solar) magnetic fields
- Effective measurement of field strength if Zeeman splitting is comparable to Doppler width or more: $B > 200$ G … 1000 G (depending on spectral line) ➔ works best in photosphere and chromosphere
- Splitting scales with λ ➔ works best in IR
- Sensitive to cancellation of opposite magnetic polarities ➔ needs high spatial resolution (but usually small-scale magnetic structure is not resolved)

Zeeman splitting ~ λ^2

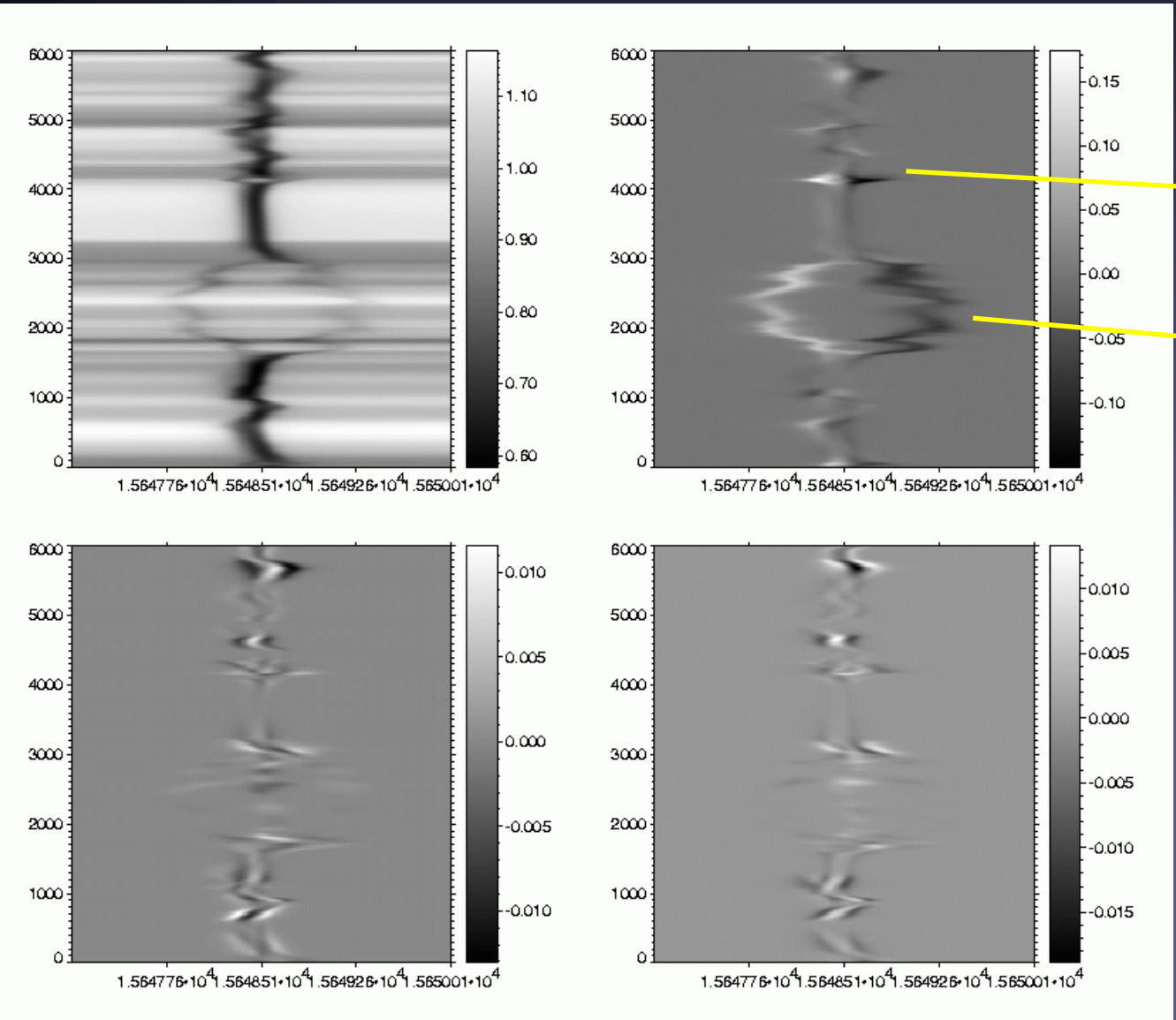

Fe I 15642.8nm

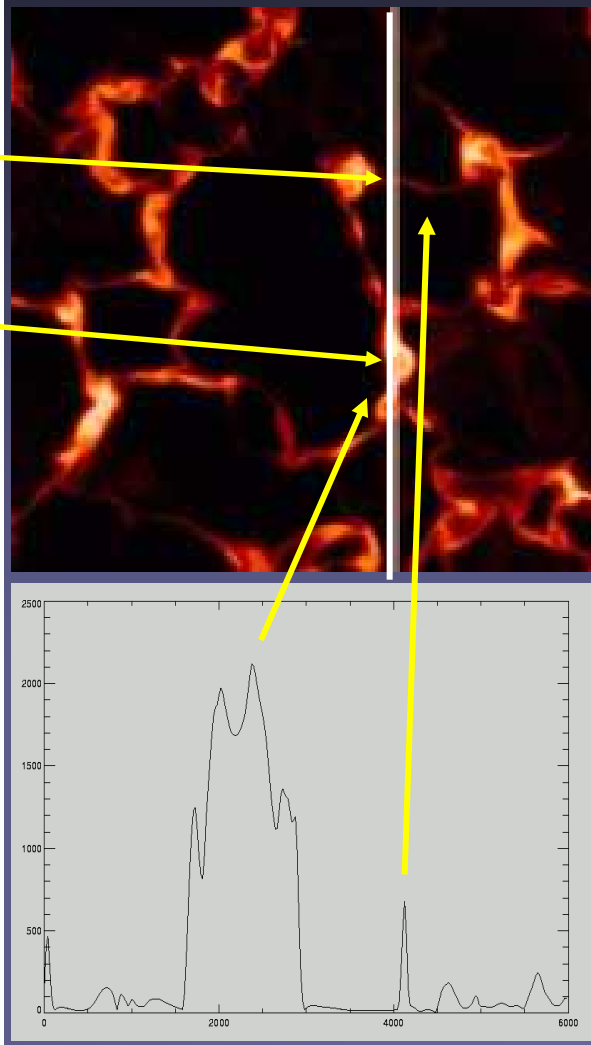

Cancellation of magnetic polarity

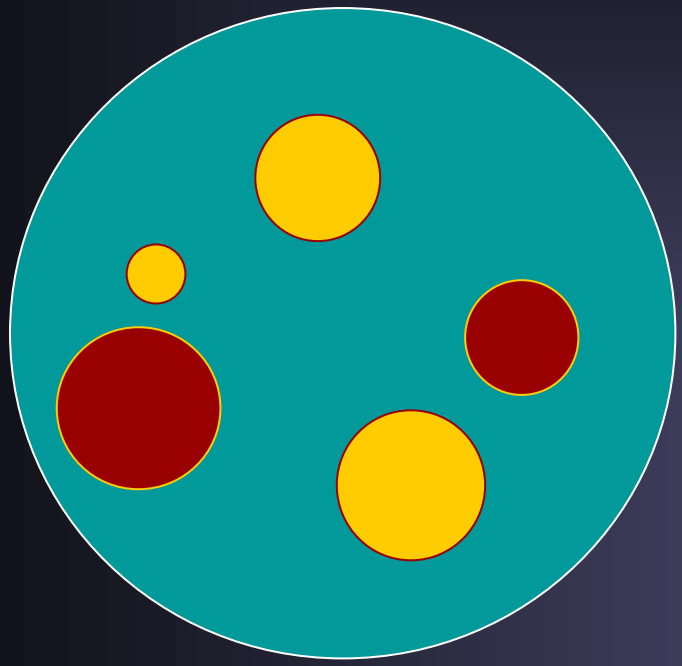

Spatial resolution element

= positive polarity magnetic field

= negative polarity magnetic field

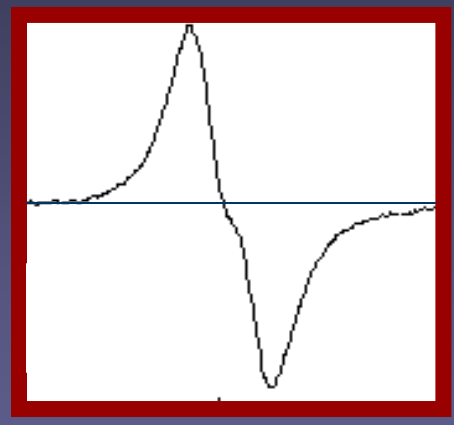

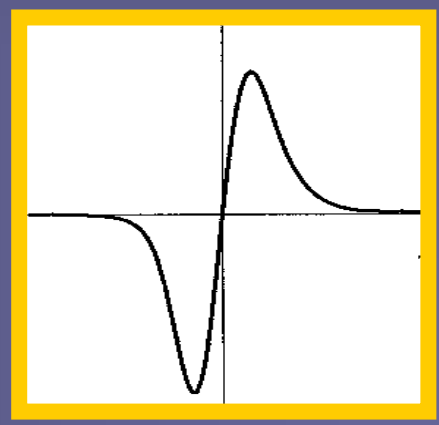

Stokes V signal cancellation

negative polarity

positive polarity

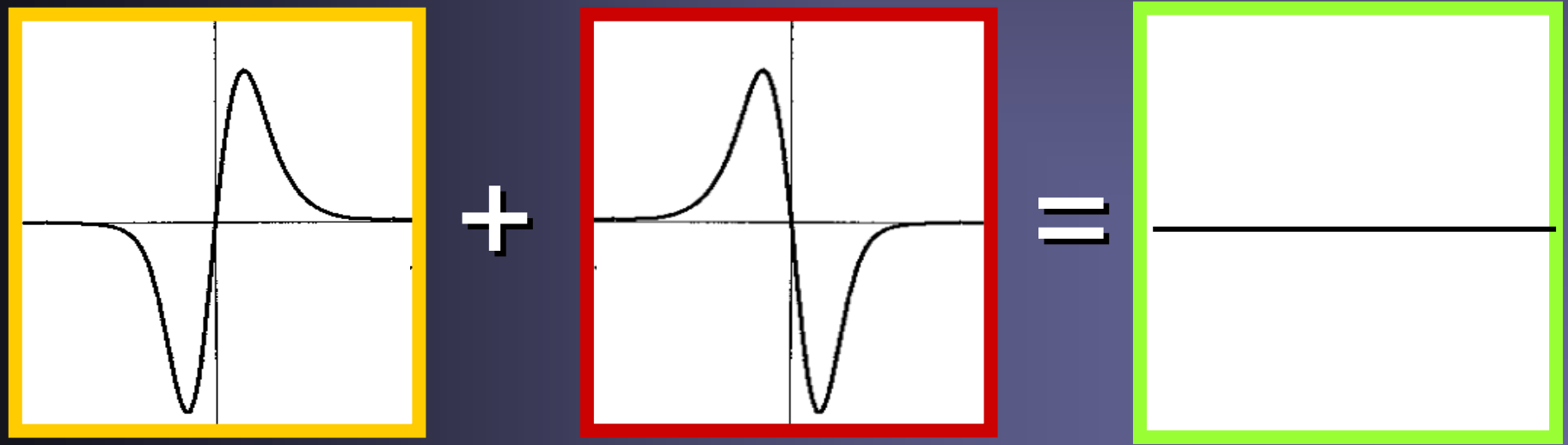

Magnetograms

- Magnetograph: Instrument to make maps of (net circular) polarization in wing of Zeeman sensitive line.
- Right: Example of magnetogram obtained by MDI
- Conversion of polarization into magnetic field requires a careful calibration.

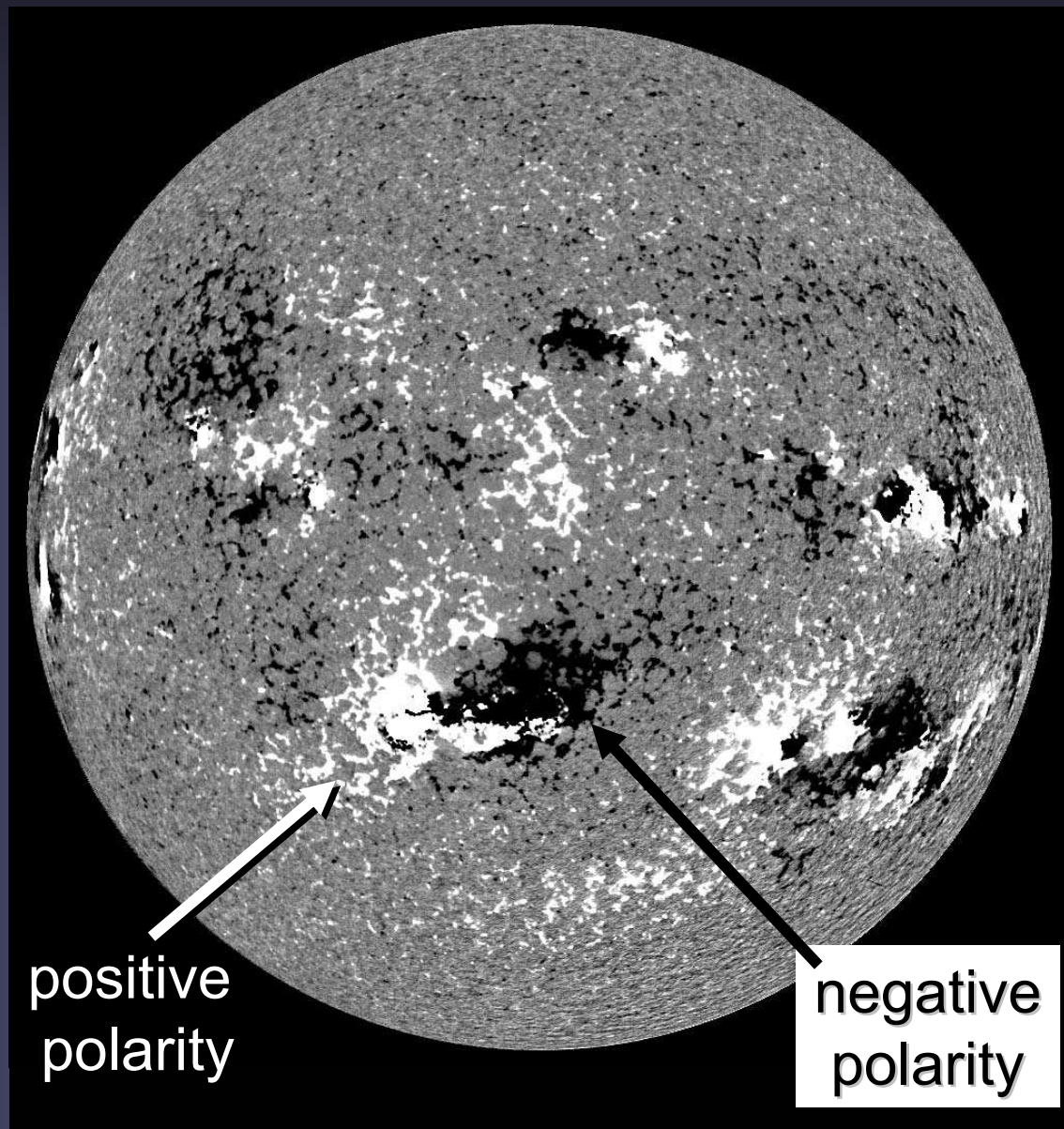

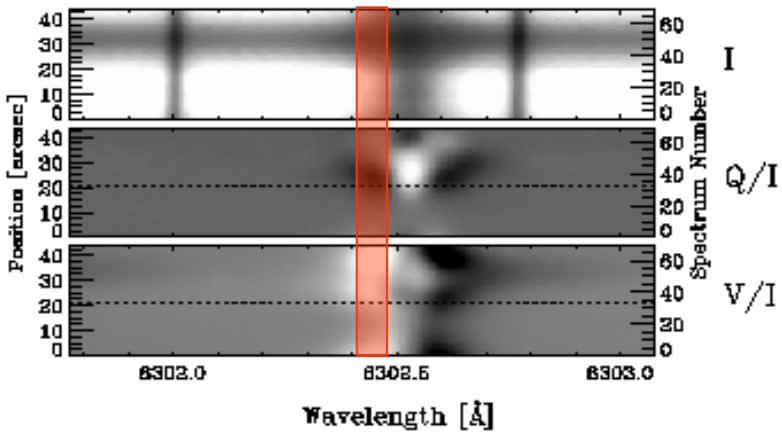

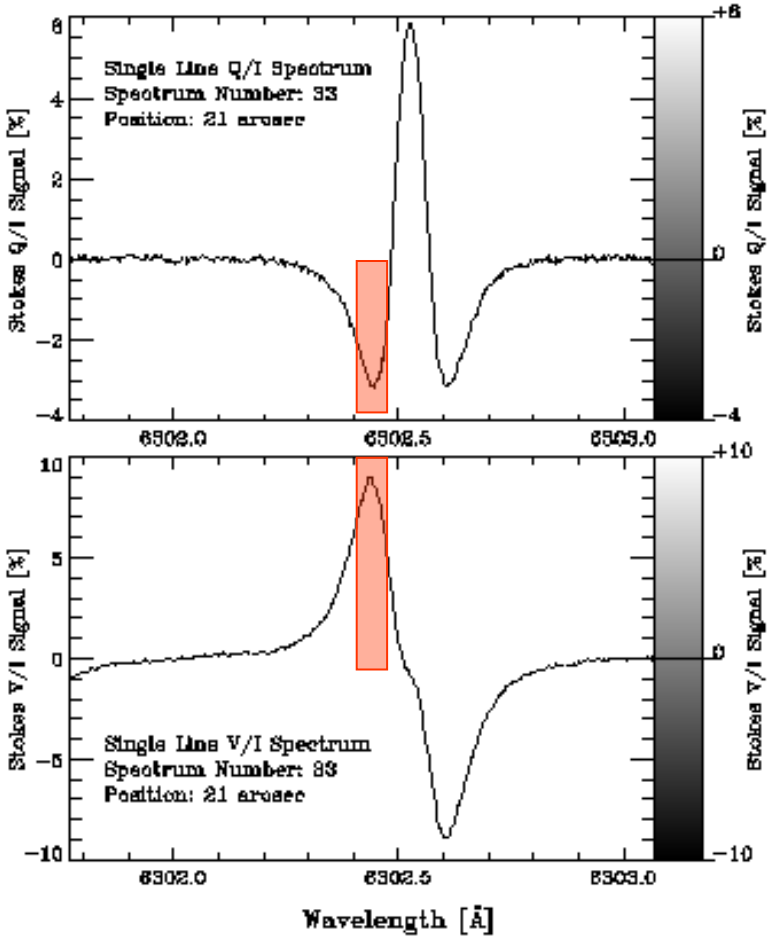

What does a magnetogram show?

- Plotted at left:
  - Top: Stokes I, Q and V along a spectrograph slit
  - Middle: Sample Stokes Q profile
  - Bottom: Sample Stokes V profile
  - Red bars: example of a spectral range used to make a magnetogram. Generally only Stokes V is used (simplest to measure), gives longitudinal component of B.

Synoptic charts

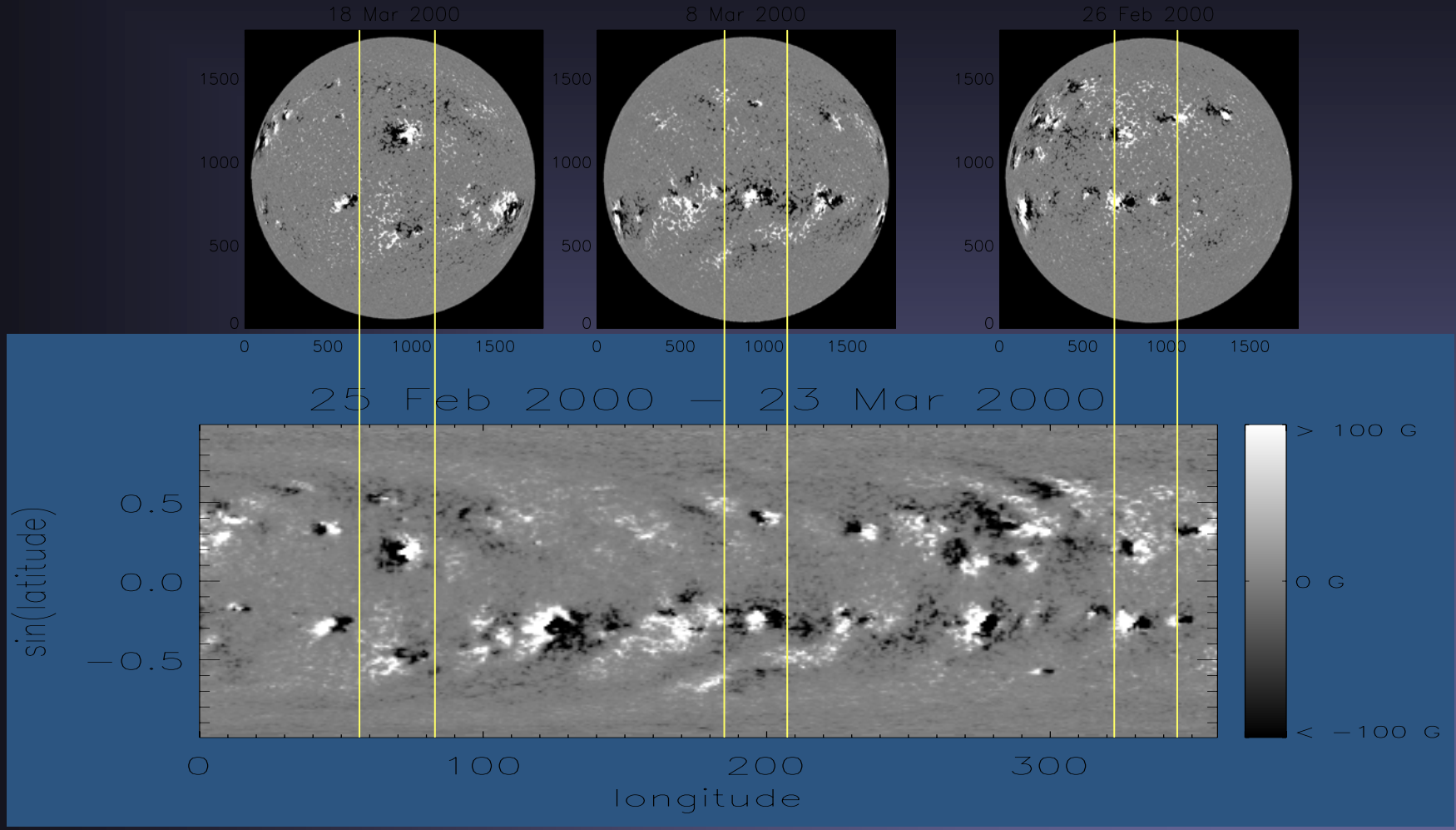

Synoptic maps approximate the radial magnetic flux observed near the central meridian over a period of 27.27 days (= 1 Carrington rotation)

Polarized radiative transfer

- If light is polarized than a separ. RTE is required for each of 4 Stokes parameters: Written as differential equation for Stokes vector $\mathbf{I}_\nu = (I_\nu, Q_\nu, U_\nu, V_\nu)$
- In plane parallel atmosphere for a spectral line (Unno-Rachkowsky equations):

$$\mu \, d\mathbf{I}_\nu / d\tau_c = \mathbf{\Omega}_\nu \mathbf{I}_\nu - \mathbf{S}_\nu$$

- $\mathbf{\Omega}_\nu$ = absorption matrix (basically ratio of line to continuum absorption coefficient), $\mathbf{S}_\nu$ = source function vector, τ_c = continuum optical depth.

Polarized radiative transfer II

The absorption matrix

$$\Omega_\nu = \begin{pmatrix} 1+\eta_I & \eta_Q & \eta_U & \eta_V \\ \eta_Q & 1+\eta_I & -\rho_V & \rho_U \\ \eta_U & \rho_V & 1+\eta_I & \rho_Q \\ \eta_V & -\rho_U & -\rho_Q & 1+\eta_I \end{pmatrix}$$

$\eta_I, \eta_Q, \eta_U, \eta_V$ are the line-to-continuum absorption ratios for each of the Stokes parameters, respectively ($\eta_I = \kappa_{IL}/\kappa_C$)

ρ_Q, ρ_U, ρ_V are magneto-optical coefficients for *Q*, *U* and *V*

Polarized radiative transfer III

- The Zeeman effect only enters through $\boldsymbol{\Omega}_\nu$
- $\boldsymbol{\Omega}_\nu$ contains
  - absorption due to Zeeman-split line $(\eta_I, \eta_Q, \eta_U, \eta_V)$. I.e. influence of B on absorption coefficient κ of medium
  - magnetooptical effects, (ρ_Q, ρ_U, ρ_V) . I.e. influence of B on refractive index n of medium
- Example magnetooptical effect: Faraday rotation, i.e. rotation of plane of polarization when light passes through B.
- $\boldsymbol{\Omega}_\nu = \boldsymbol{\Omega}_\nu(\gamma, \varphi, B)$, i.e. $\boldsymbol{\Omega}_\nu$ depends on the full magnetic vector (in addition to the usual quantities that the absorption coefficient depends on)

LTE

- In LTE the Unno-Rachkowsky equations simplify since

  $\mathbf{S}_\nu = (B_\nu, 0, 0, 0)$

  Here B_ν = Planck function

- Also, $\mathbf{\Omega}_\nu$ is simplified. The $\eta_I, \eta_Q, \eta_U, \eta_V$ and ρ_Q, ρ_U, ρ_V values only require application of Saha-Boltzmann equations (similar situation as for LTE in case of normal radiative transfer). Each of these quantities is, of course, frequency dependent.

Solution of Unno Eqs.: Unno solution

- General solution best done numerically (even formal solution is non-trivial: needs exponent of matrix $\mathbf{\Omega}_\nu$)
- Simple analytical solutions exist for a Milne-Eddington atmosphere (i.e. for $\mathbf{\Omega}_\nu$ independent of τ_ν and $\mathbf{S}_\nu$ depending only linearly on τ_ν). Particularly simple if we neglect magneto-optical effects
- $I(\mu) = \beta\, \mu\, (1+\eta_I)/\Delta$
- $P(\mu) = \beta\, \mu\, \eta_P/\Delta$, where $P = Q, U,$ or V
- $\Delta = (1+\eta_I)^2 - \eta_Q^2 - \eta_U^2 - \eta_V^2$

  takes care of line saturation
- β is derivative of Planck function with respect to τ_ν .

MHD = Magnetohydrodynamics

- Here only a very few basics. See also special courses on MHD within the IMPRS curriculum
- MHD is an extension of hydrodynamics to a partly ionized gas (plasma) including the influence of a magnetic field. It is also a particular simplification of the particle-based (statistical mechanics) description of plasmas.
- The MHD equations are obtained by combining Maxwell's equations with equations of fluid mechanis (hydrodynamics).
- MHD is a good approximation in most of the Sun

MHD equations I

- Relevant Maxwell's equations, Ohm's law:

$$c\nabla\times\mathbf{B}=4\pi\mathbf{j},\qquad c\nabla\times\mathbf{E}=-\frac{\partial\mathbf{B}}{\partial t},\qquad \nabla\mathbf{B}=0$$

$$\mathbf{j}=\sigma(\mathbf{E}+\frac{1}{c}\mathbf{v}\times\mathbf{B}),\qquad \sigma=\text{electrical conductivity}$$

- Mass conservation:

$$\frac{\partial\rho}{\partial t}+\nabla\cdot(\rho\mathbf{v})=0$$

- j=current density, $\mathbf{E}$=electric field, $\mathbf{B}$=magnetic field, c=speed of light, $\mathbf{v}$=velocity, ρ= mass density

MHD equations II

- Force balance = equation of motion = momentum conservation

$$\rho \frac{\partial \mathbf{v}}{\partial t} + \rho(\mathbf{v}\nabla)\mathbf{v} = -\nabla P + \frac{1}{c}\mathbf{j}\times\mathbf{B} - \rho g + \rho \upsilon \Delta \mathbf{v}$$

- Equation of state (e.g. ideal gas law)

$$P = f(\rho, T)$$

- Energy equation (which takes on different forms in different parts of the Sun)

Terms of force balance equation

$\rho \frac{\partial \mathbf{v}}{\partial t} + \rho(\mathbf{v}\nabla)\mathbf{v}$	total derivative of impulse-dens
∇p	pressure gradient
$\frac{1}{c}\mathbf{j}\times\mathbf{B}$	magnetic forces
ρg	gravity
$\rho \upsilon \Delta \mathbf{v}$	viscous friction

Some simplifications

- Ideal MHD: no viscosity: $\rho\upsilon\Delta\mathbf{v} = 0$
- Stationary state: $\partial/\partial t = 0$
- Magnetohydrostatics: $\mathbf{v} = 0$
- No magnetic tension: $\frac{1}{4\pi}(\mathbf{B}\cdot\nabla)\mathbf{B} = 0$
- Force-free field: $\mathbf{j}\times\mathbf{B} = (\nabla\times\mathbf{B})\times\mathbf{B} = \mathbf{0}$
- Potential field: $\nabla\times\mathbf{B} = \mathbf{0}$
- Force-free field: valid when magnetic terms in force balance equation dominate over all the others.
- Potential field:valid when additionally there are no currents

MHD: plasma β

- Plasma β describes the ratio of thermal to magnetic energy density:

$$\beta = \frac{8\pi P}{B^2}$$

- $\beta < 1$ ➔ Magnetic field dominates and dictates the dynamics of the gas
- $\beta > 1$ ➔ Thermal energy, i.e. gas dominates & forces the field to follow
- β changes with $r/R_\odot$
  - $\beta > 1$ in convection zone, solar wind
  - $\beta < 1$ in atmosphere, particularly in corona $\beta << 1$

Plasma β vs. height in solar atmosphere

Field dominates ← → Gas dominates

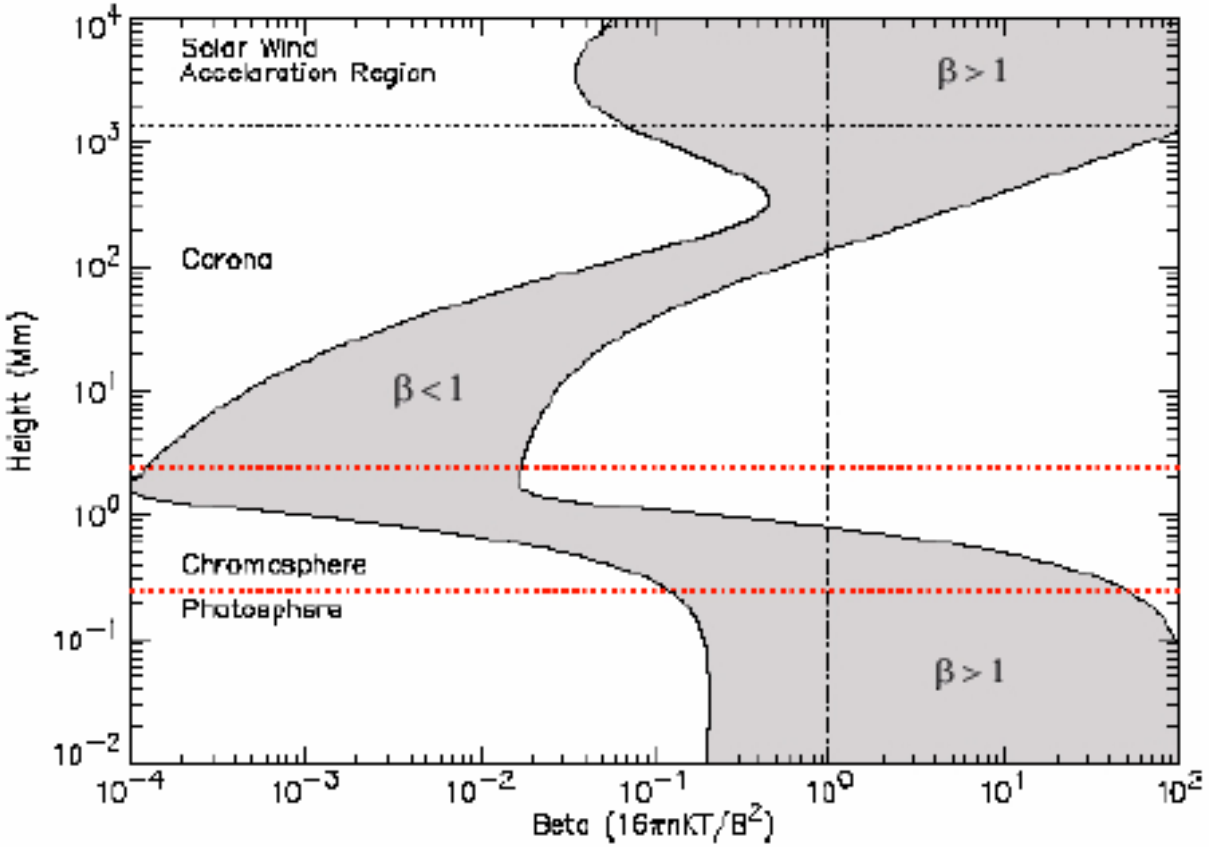

Figure 1. Ratio of gas pressure to magnetic pressure (β) as a function of height[1].

(Gary 2000)

Supergranules and magnetic field

- Magnetogram: black and white (oppos. polarities)
- Horizontal velocity: arrows
- Divergence: blue arrows > 0; red arrows: < 0
- Supergranule boundaries: yellow
- Magnetic field is concentrated at edges of supergranules

➔ B swept out by flow of supergranules

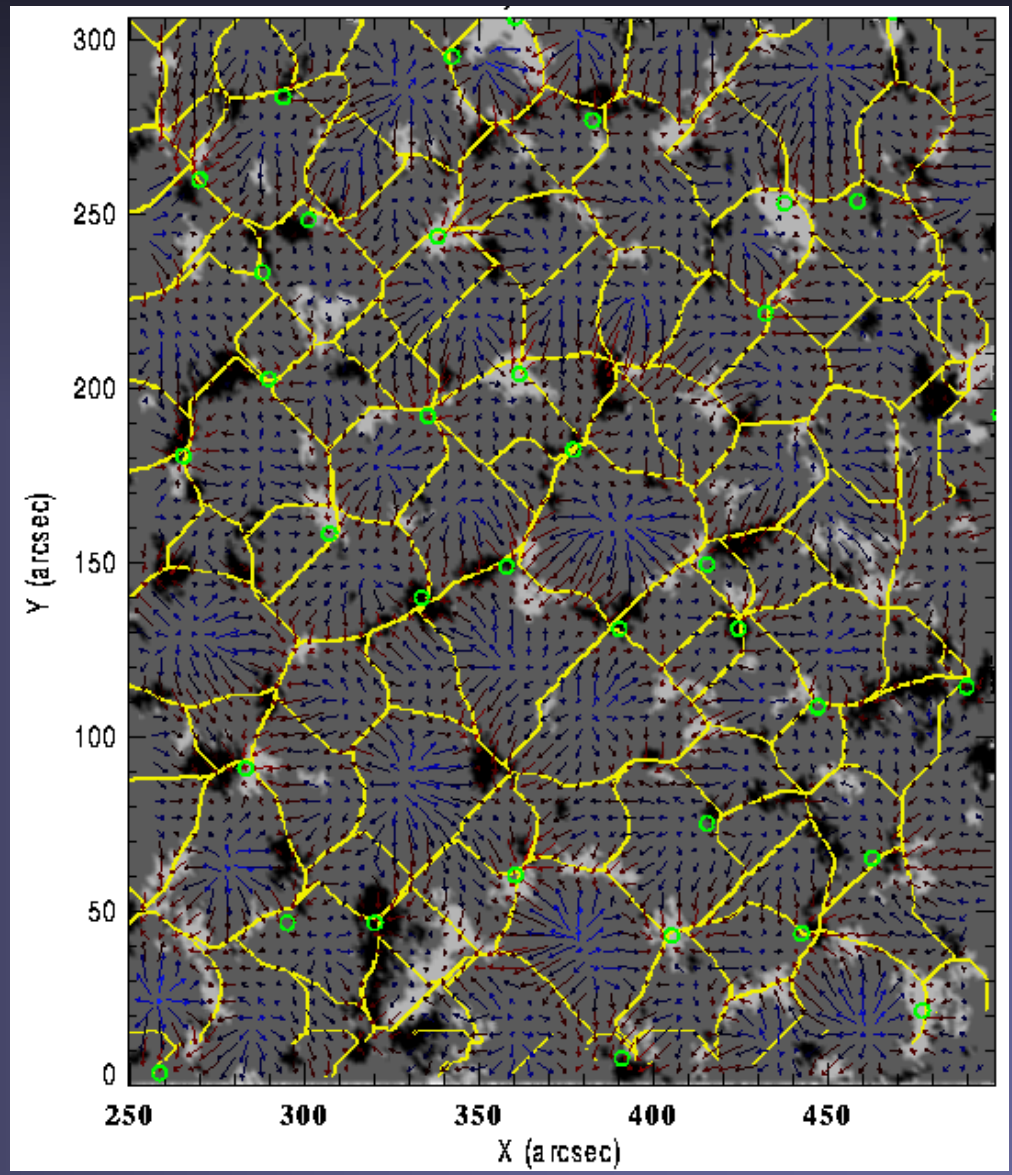

Frozen-in magnetic fields

- Magnetic field is swept to supergranule boundaries ➔ magnetic field is “frozen” into the plasma
- This happens if there are a sufficient number of ionised particles, or equivalently, if the electric conductivity is very high, since charged particles cannot cross field lines (gyration)
- Valid even in photosphere of sunspots (only 10^{-4} of all particles are ionized), due to common collisions

➔ If plasma moves perpendicularly to B-field,

- $\beta > 1$: it drags the field with it
- $\beta < 1$: it is stopped by the field

- Flows parallel to the field are unaffected.

Magnetic flux tubes

- In convection zone and in photosphere most of magnetic energy is in concentrated magnetic flux tubesbundles of magnetic field (bounded by topologically simple surface)
- The flux tube has a current sheet at its boundary
- Consider a thin flux tube ($R<H_P$) that is homogeneous inside (no variation of B and P across cross-section)

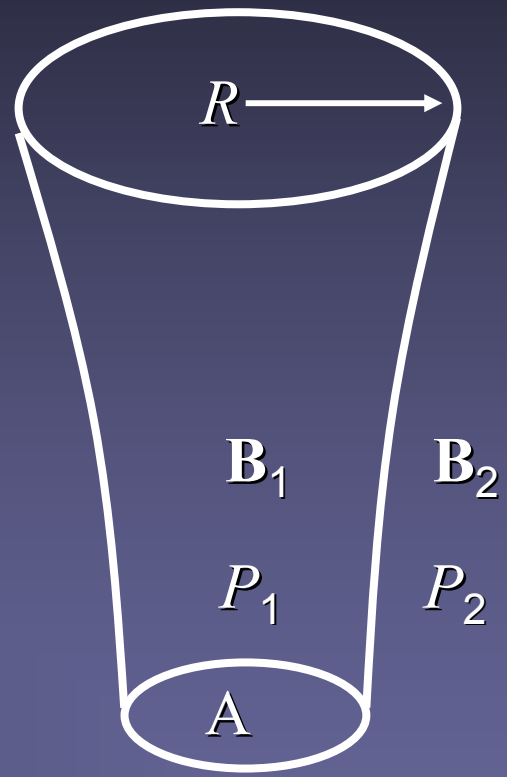

Rump of a flux tube

Simplified force balance: pressure balance

- Consider a static, vertical, thin magnetic flux tube, FT (typical in lower solar atmosphere):
  - Interior of FT 1: field $\mathbf{B}_i$, pressure p_i, density ρ_i
  - Exterior of FT: field $\mathbf{B}_e$, pressure p_e, density ρ_e

→ Vertical force balance is independent in the individual components.

  - For a vertical field (for each comp):

$$\nabla p - \rho g = 0$$

- Horizontal force balance between the components is then reduced to pressure balance.

Pressure balance

- pressure balance between thin flux tube interior i and exterior e

$$\frac{B_i^2}{8\pi} + P_i = P_e + \frac{B_e^2}{8\pi}$$

- If, e.g. $B_\mathrm{e} = 0$, then $P_\mathrm{i} < P_\mathrm{e}$ and it follows:

➔Magnetic features are evacuated compared to surroundings.

- If $B_\mathrm{r} = 0$ and $T_i = T_e$, then also $\rho_\mathrm{i} < \rho_\mathrm{e}$, so that the magnetic features are buoyant compared to the surrounding gas.
- In convection zone this buoyancy means that rising magnetic flux tubes keep rising (unless stopped by another force, e.g. magnetic curvature force) ➔ field cannot be stably stored in convection zone

Emergence of a magnetic flux tube

Magnetic field is believed to be generated mainly in the Tachocline near bottom of convection zone.
Due to its buoyancy (see next section) a magnetic field will rise towards the solar surface. At the solar surface it will produce a bipolar active region.

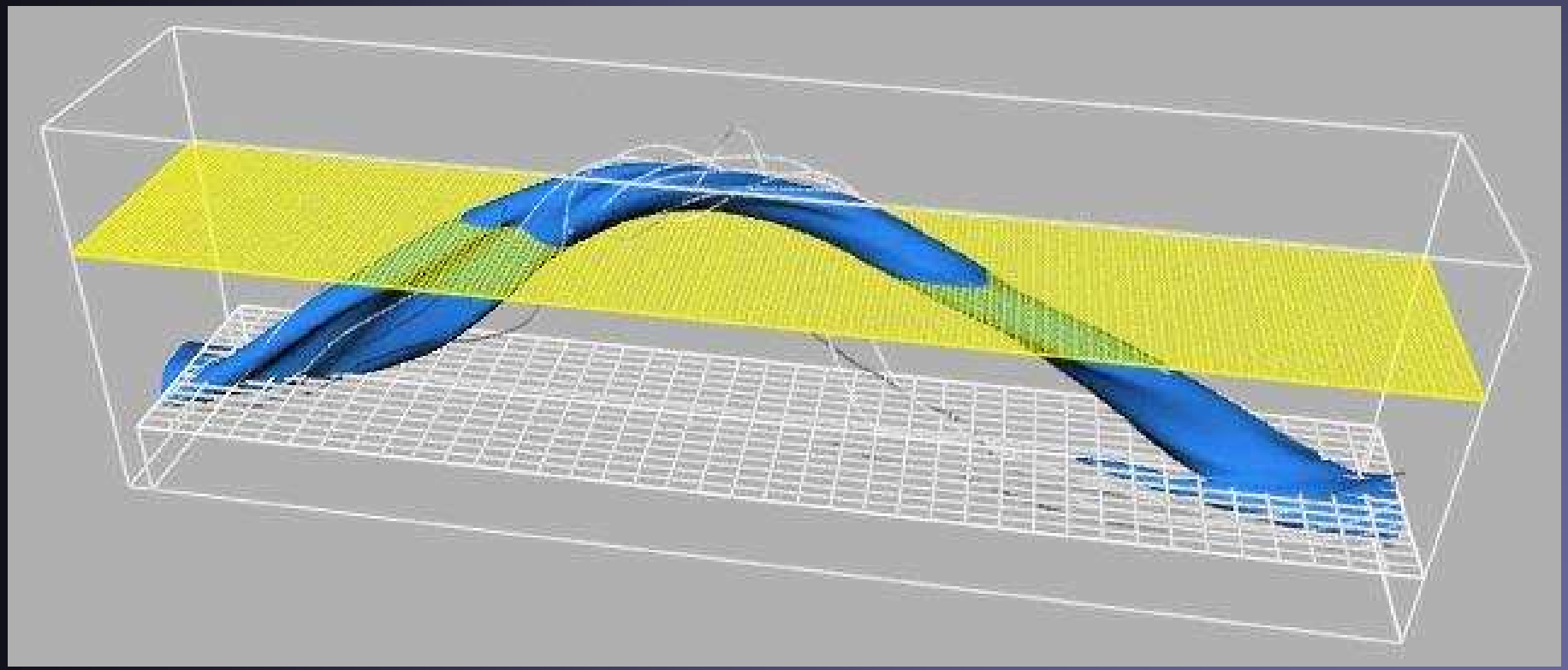

Photosphere: magnetoconvection

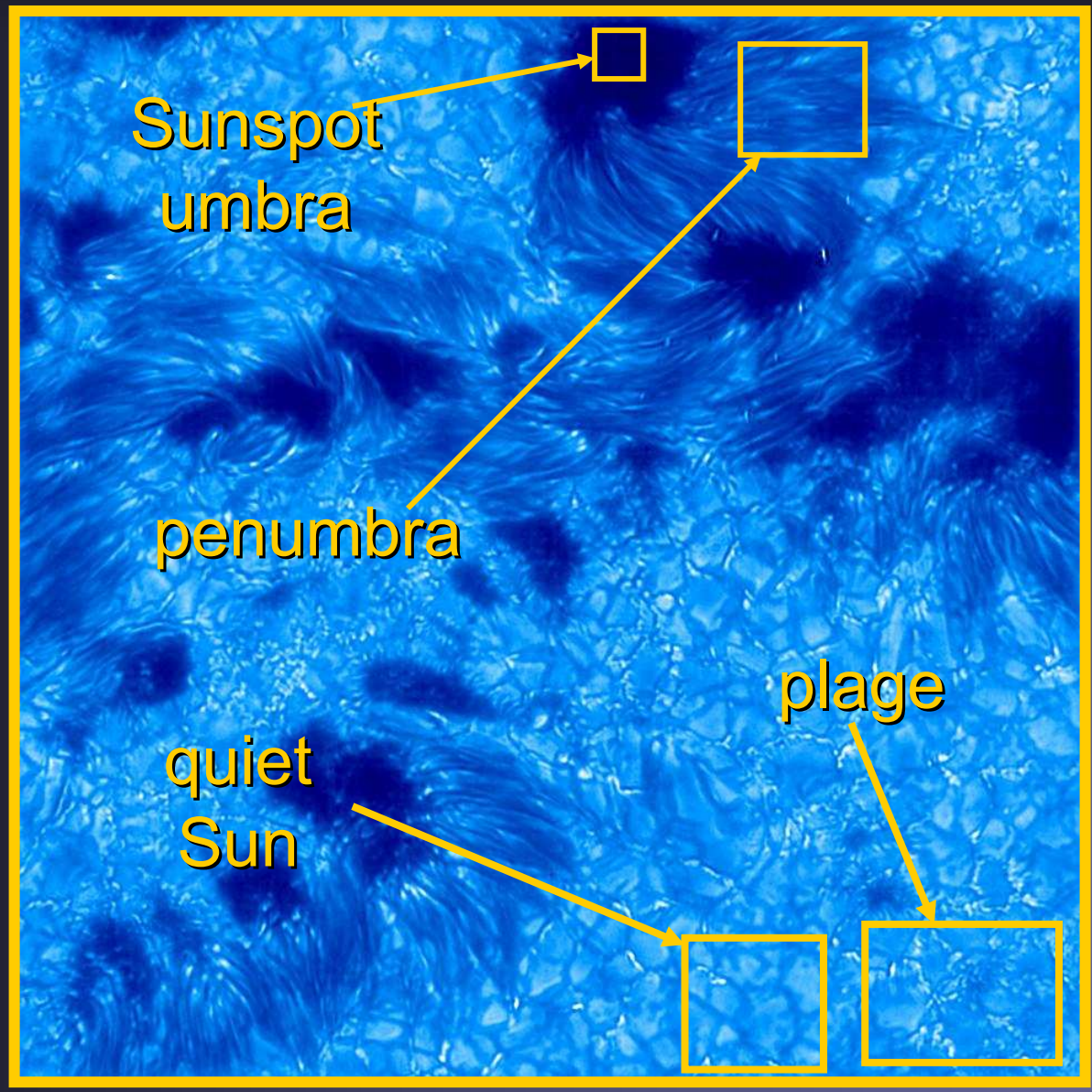

Sunspots

Umbra

Penumbra

Granule

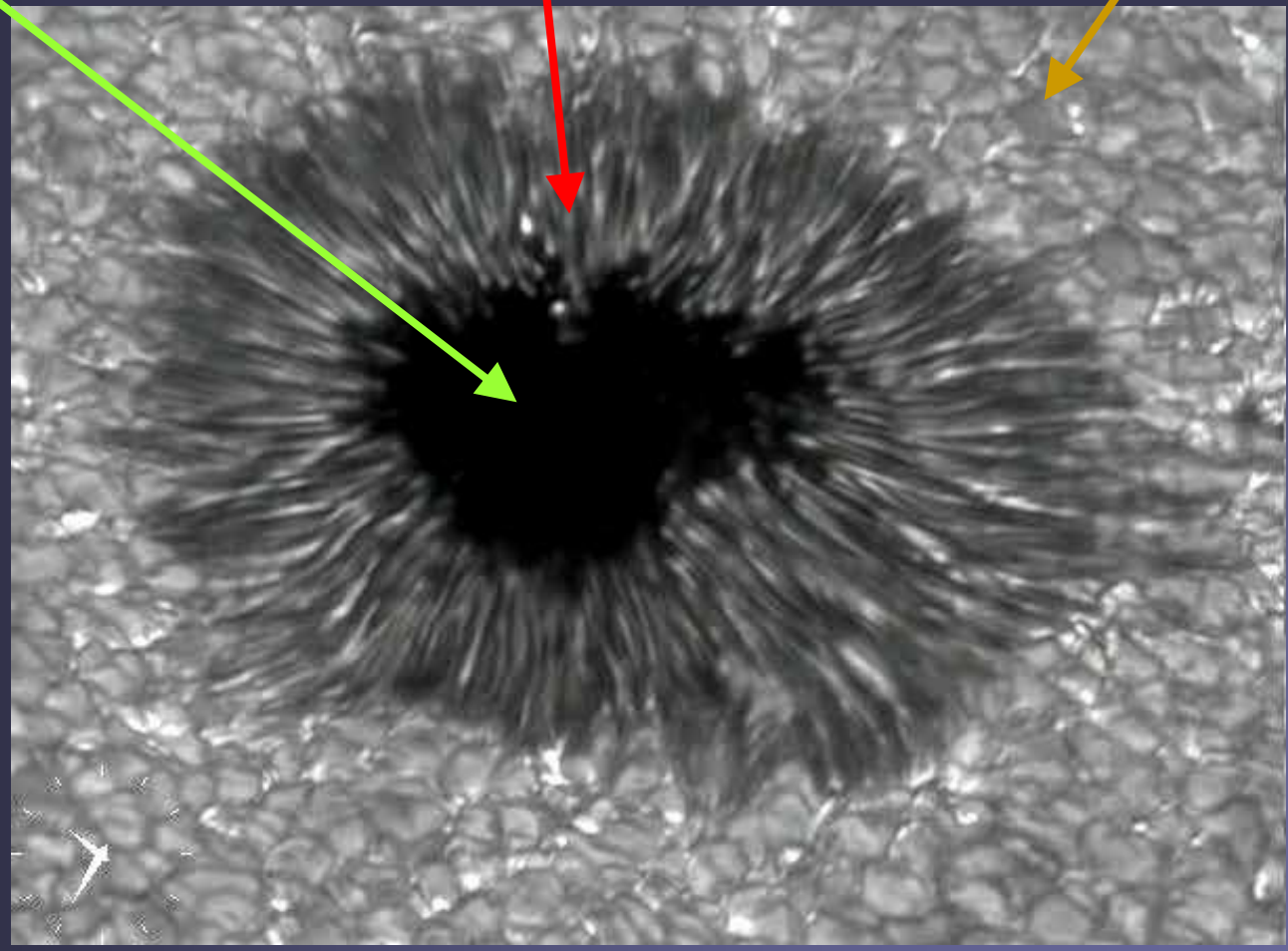

$T_{\text{eff}} \approx 4500$ K

$T_{\text{eff}} \approx 5500$ K

$T_{\text{eff}} \approx 5800$ K

Sunspots, some properties

- Field strength: Peak values 2000-3500 G
- Brightness: umbra: 20% of quiet Sun, penumbra: 75%
- Sizes: Log-normal size distribution. Overlap with pores (log-normal = Gaussian on a logarithmic scale)
- Lifetimes: T between hours & months: Gnevyshev-Waldmeier rule: $A_{\max} \sim T$, where $A_{\max}$ = max spot area.

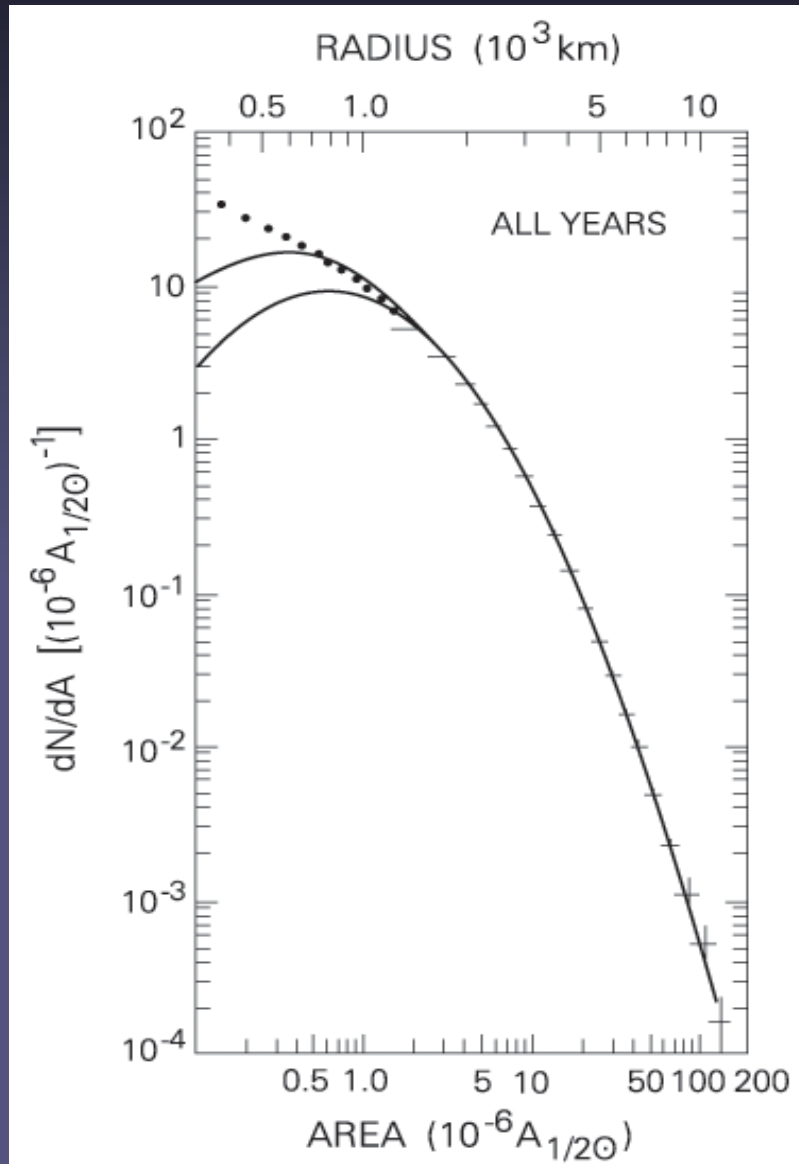

Lognormal distributions

- Normal distribution = Gaussian distribution
- Log-normal distribution = Gaussian distribution if plotted on the logarithm of the x-axis (params: σ, μ)

$$f(x) = \frac{1}{x\sigma\sqrt{2\pi}} \exp\left(-\frac{1}{2\sigma^2}\left(\log(x) - \mu^2\right)\right)$$

- Lognormal distributions are found in many natural and man-made systems, particularly when values cannot be negative, means, μ, are low and variances, σ, large.
- E.g. lengths of latent periods of infectious diseases, file sizes on disks, concentration of chemicals in honey samples, sunspot areas, solar UV radiances, ...
- Gaussians are due to additive processes, while lognormals are often produced by multiplicative processes, which are additive on a log-scale.

The Wilson effect

- Near the solar limb the umbra and centre-side penumbra disappear

➔We see 400-800 km deeper into sunspots than in photosphere

- Correct interpretation by Wilson (18th century).

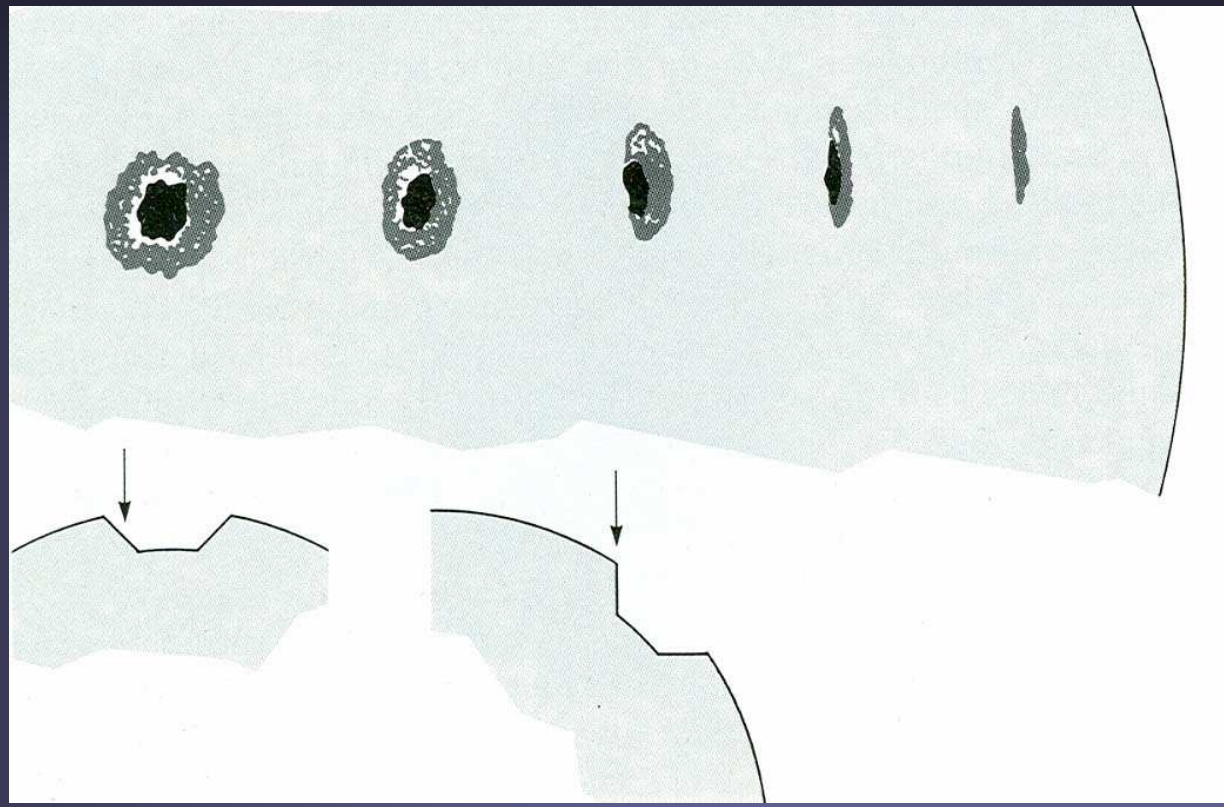

Other interpretation by e.g. W. Herschell: photosphere is a layer of hot clouds through which we see deeper, cool layers: the true, populated surface of the Sun.

Why are sunspots dark?

- Basically the strong nearlly vertical magnetic field, not allowing motions across the field lines, quenches convection inside the spot.
- Since convection is the main source of energy transport just below the surface, less energy reaches the surface through the spot ➔ dark

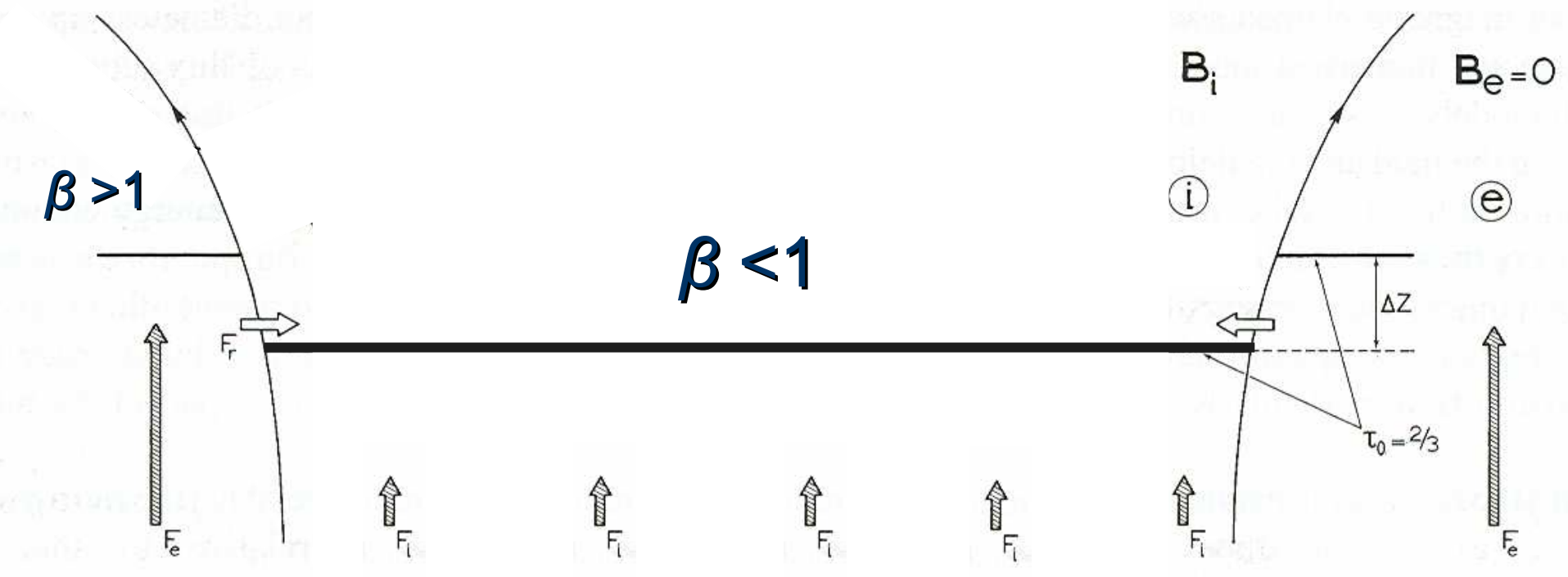

Why are sunspots dark? II

- Where does the energy blocked by sunspots go?
- Spruit (1982) showed: both heat capacity and thermal conductivity of convection zone (CZ) gas is very large

→ High thermal conductivity: blocked heat is redistributed throughout CZ (no or only very weak bright rings around sunspots)

High heat capacity: the additional heat does not lead to a measurable increase in temperature

- In addition: time scale for thermal relaxation of the CZ is long, 10^5 years: excess energy is released almost imperceptibly.

Solar irradiance during passage of a sunspot group

- The Sun as a whole darkens when spots move across its disc
- I.e. the blocked heat does not reappear somewhere else
- I.e. no strong bright rings around spots

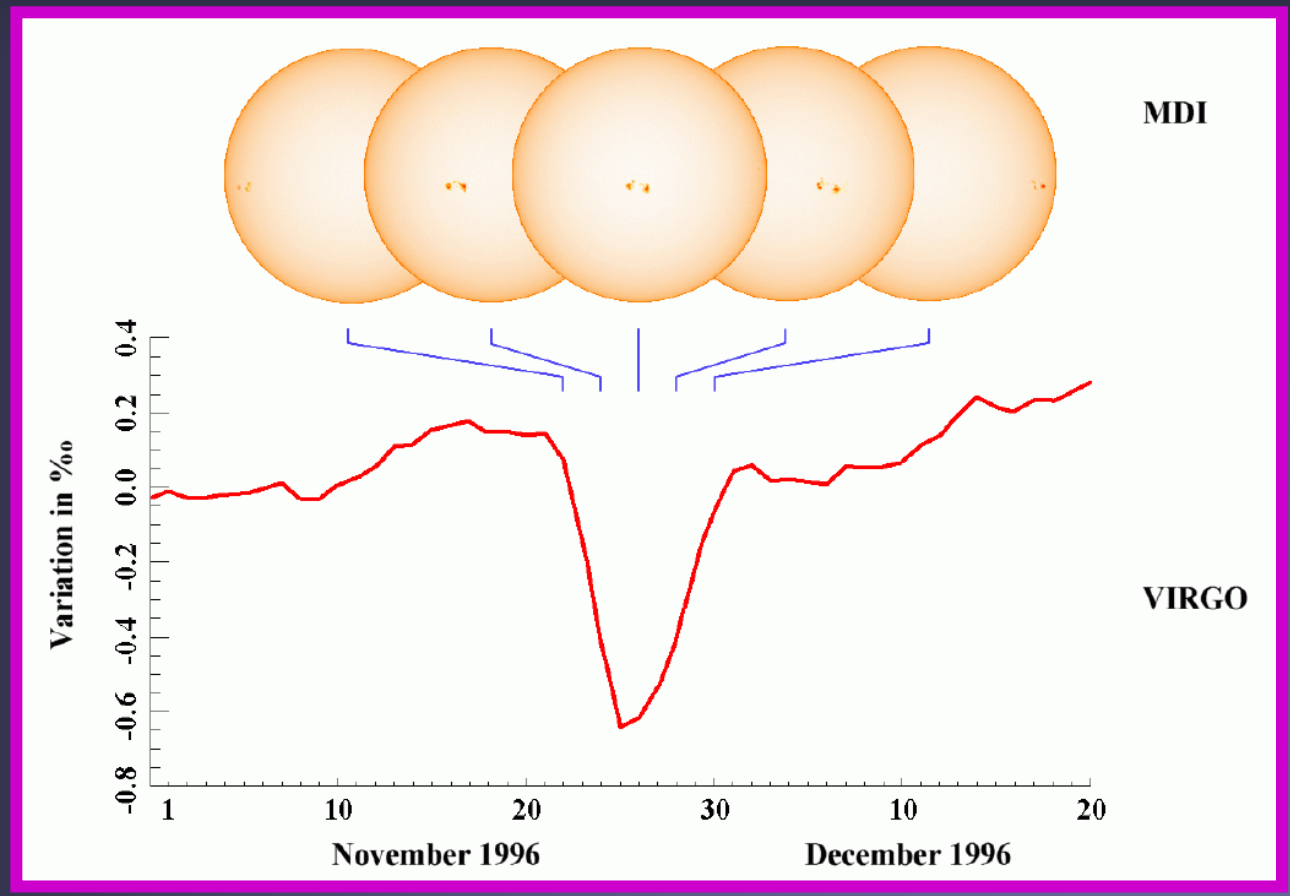

Magnetic structure of sunspots

- Peak field strength ≈ 2000 – 3500 G (usually in darkest, central part of umbra)
- B drops steadily towards boundary, $B(R_{\text{spot}}) \approx 1000$ G
- At centre, field is vertical. It becomes almost horizontal near R_{spot} .
- Regular spots have a field structure similar to a buried dipole

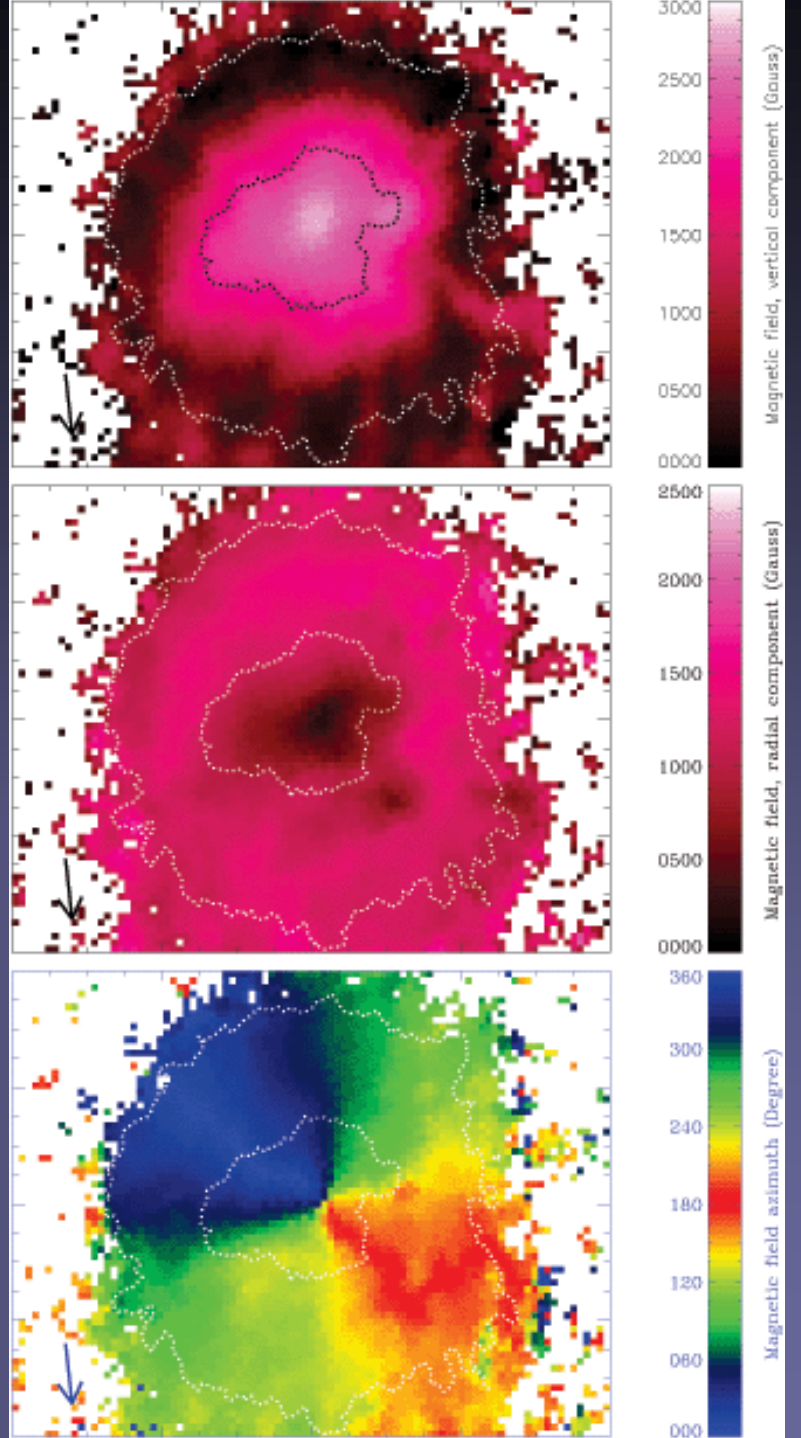

Magnetic structure of sunspots II

Azimuthal averages of the various magnetic field components in a sample of regular (near-circular) medium-sized sunspots.

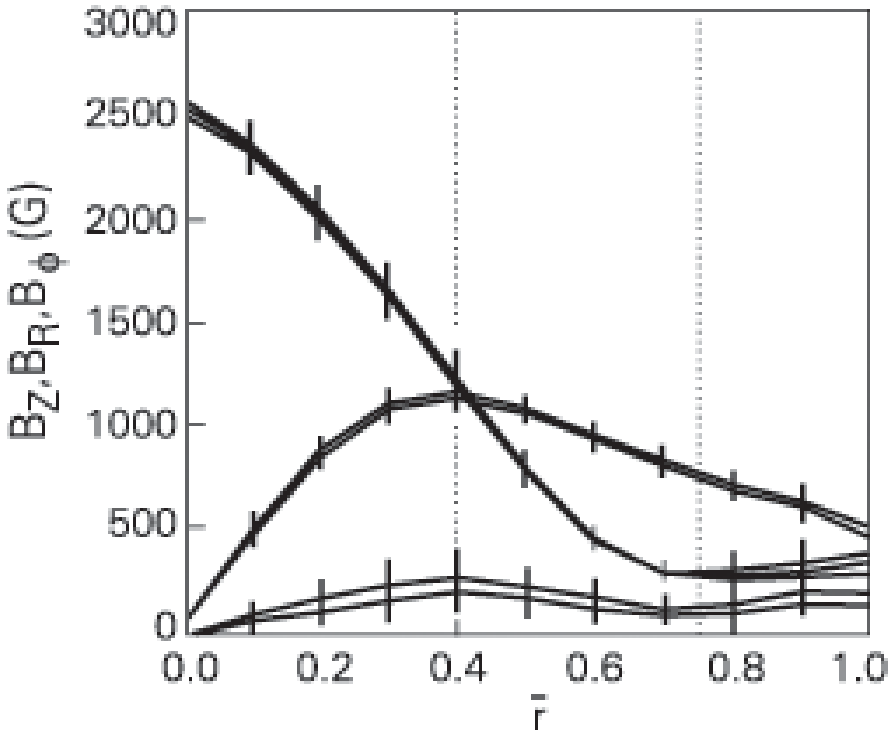

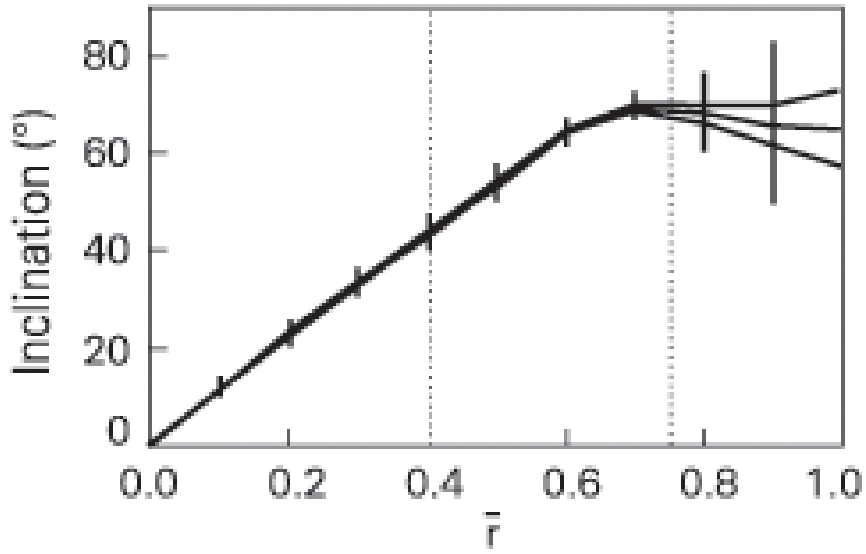

Evershed effect

- Observation: Penumbra seen at $\mu<1$ shows
  - on limb side: Doppler red shift
  - on disc side: Doppler blue shift
- Interpretation: horizontal OUTflow of material from inner penumbra to outer

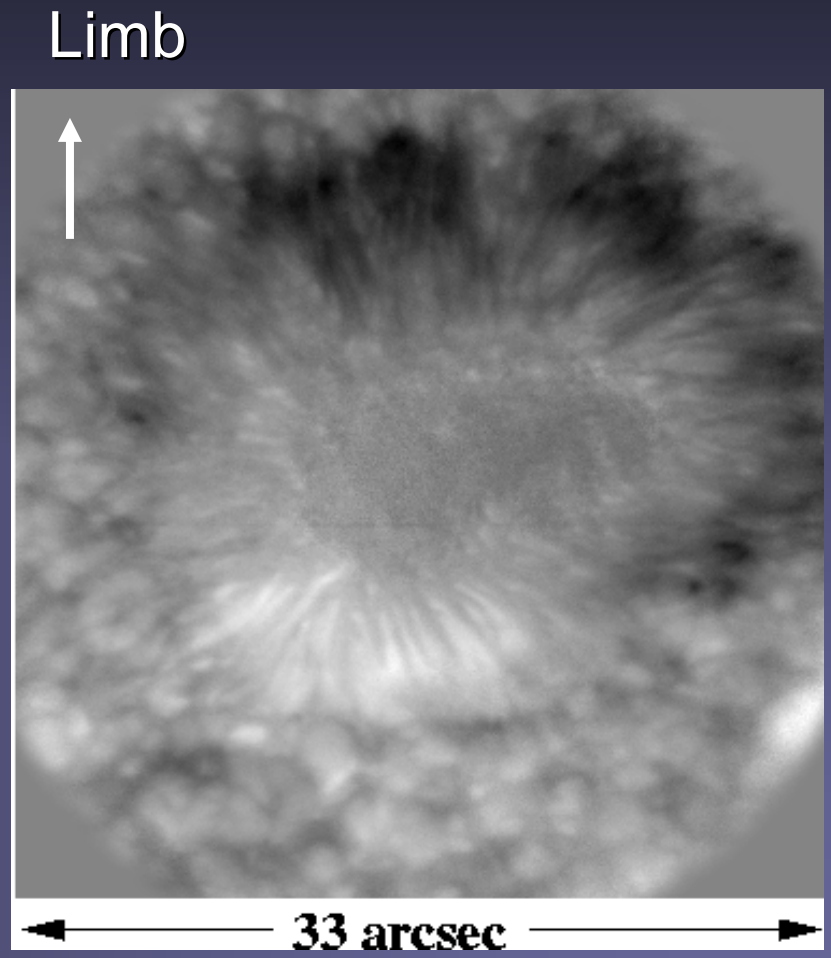

dark: redshift, light: blueshift

Evershed effect

In photospheric layers penumbra shows nearly horizontal outward flows of 1-2 km/s on average (peak flows: supersonic)
Umbra remains at rest. In chromosphere: inward directed flow

Brightness

Doppler shift

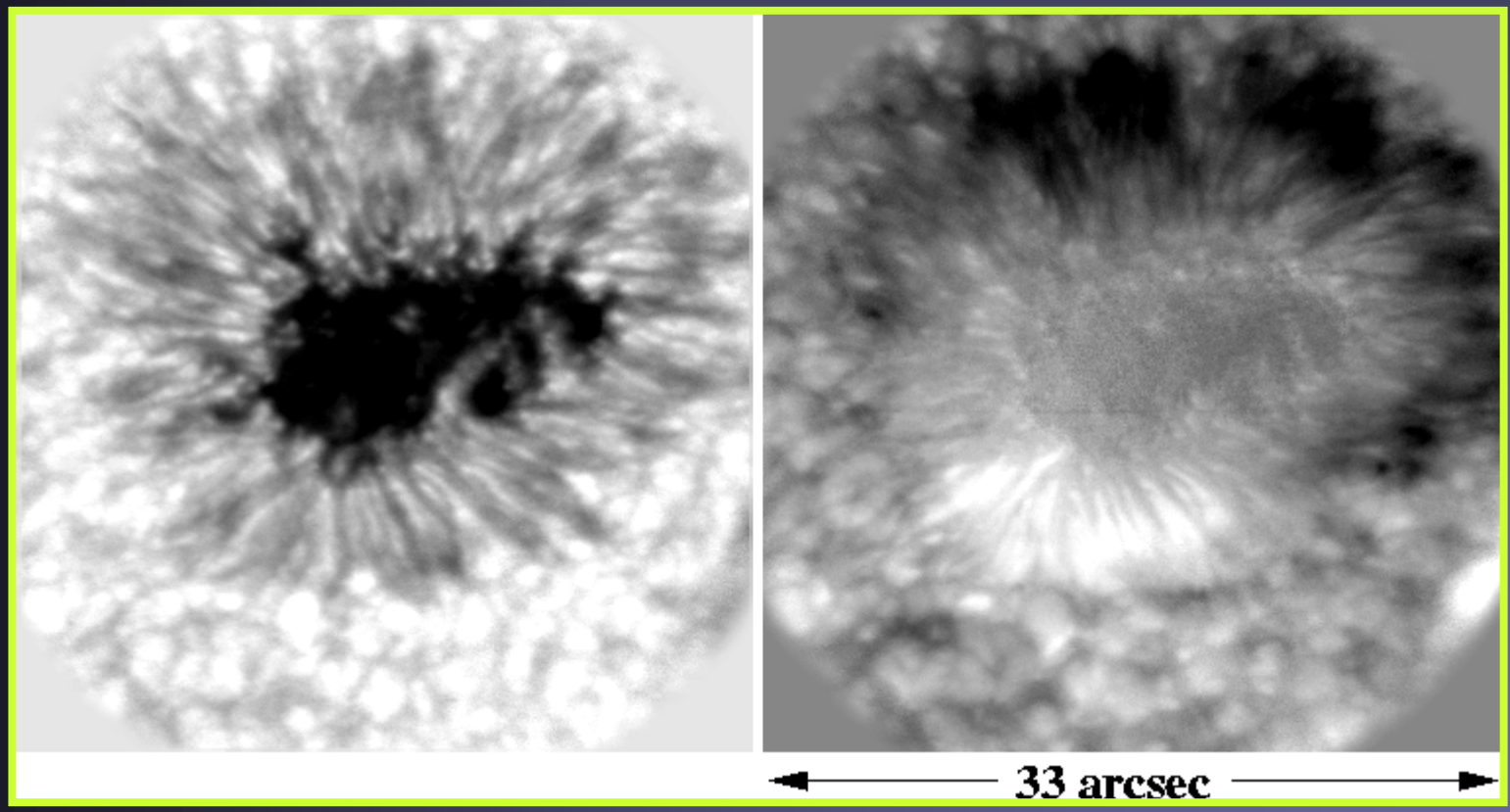

Evershed effect: illustration

- Almost horizontal outflow of matter seen in the penumbra of a sunspot.
- Thought to be driven by either
  - siphon flow
  - convection

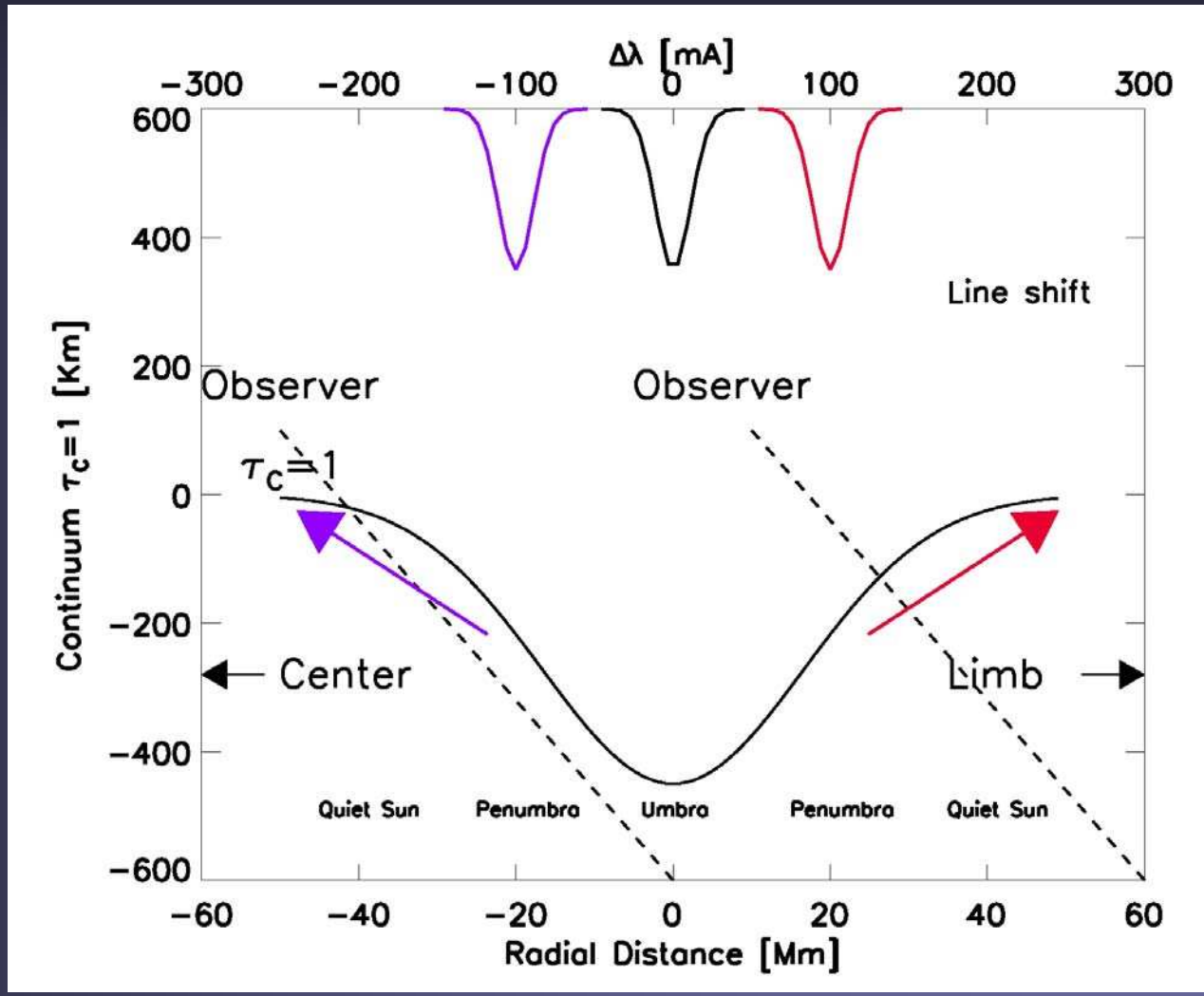

Siphon flow model of Eversheed effect

- Proposed by Meyer & Schmidt (1968).
- If there is an imbalance in the field strength of the two footpoints of a loop, then gas will flow from the footpoint with lower B to that with higher B.
- Supersonic flows are possible.

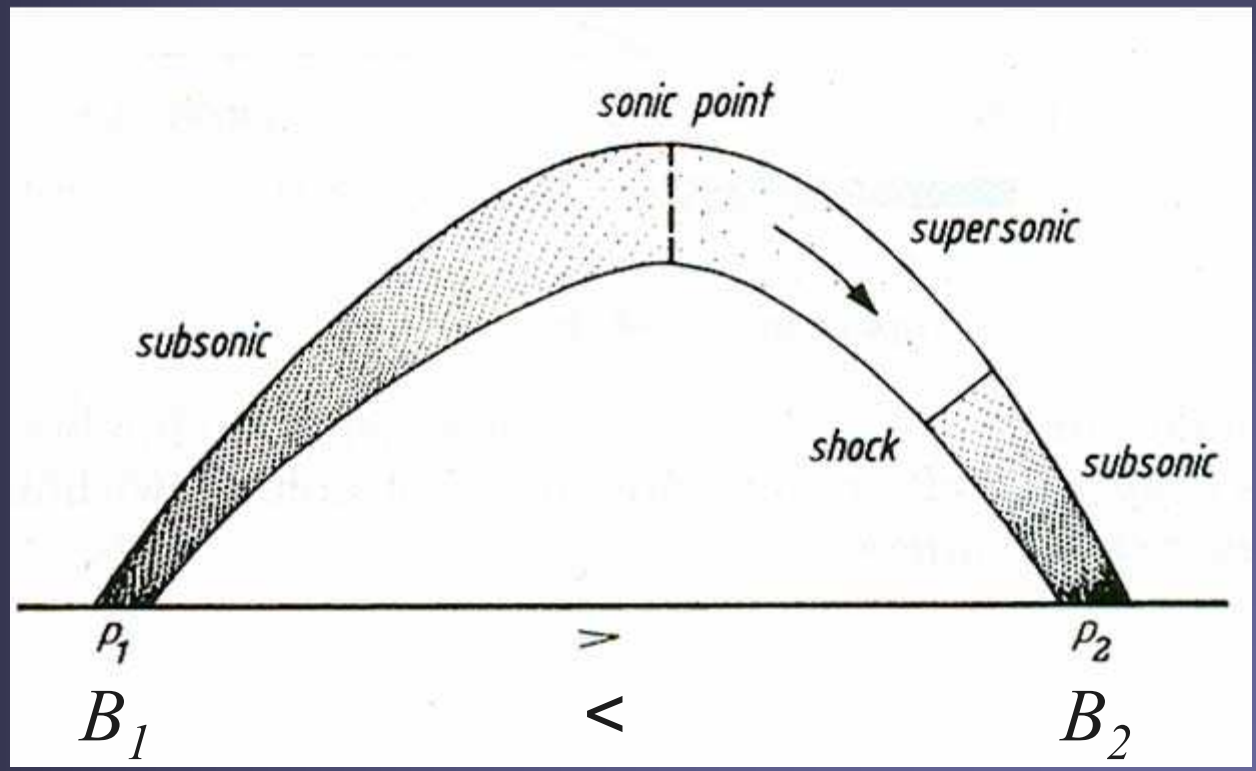

Sunspot fine structure

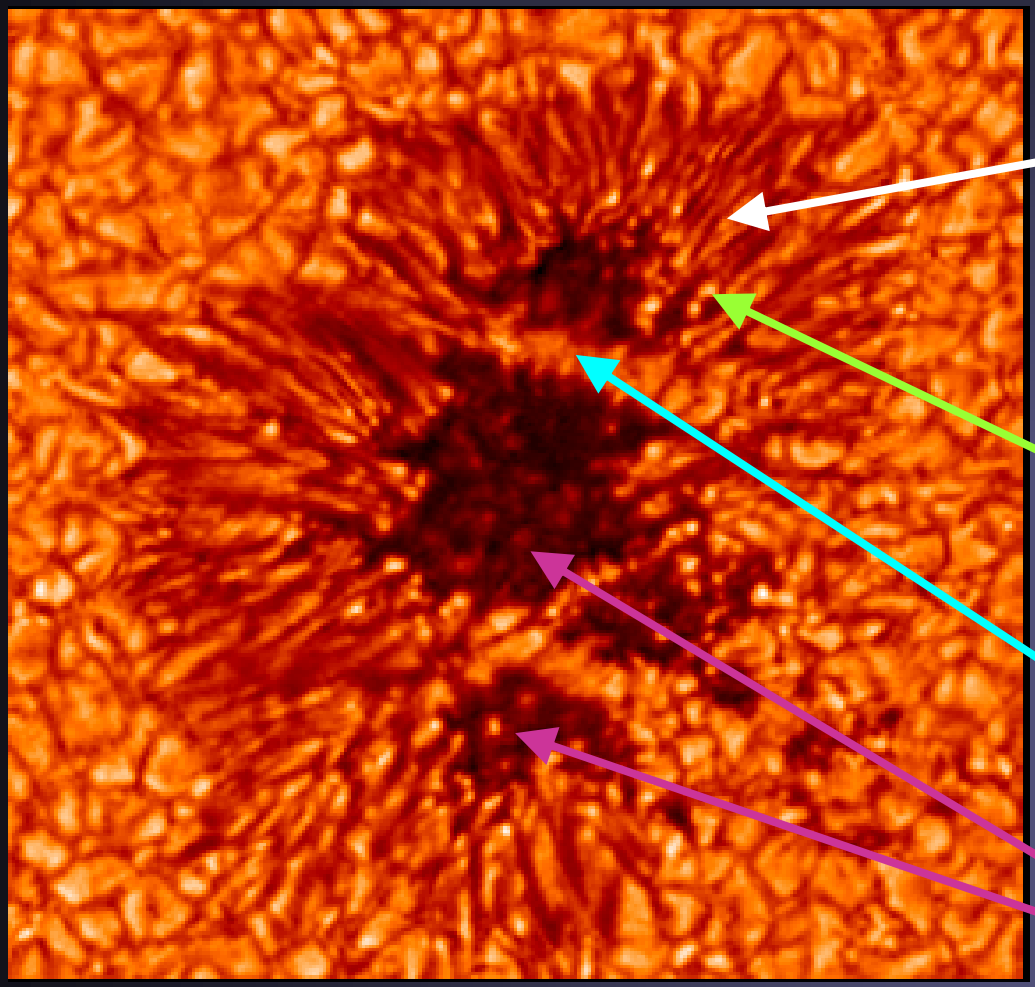

Highest resolution

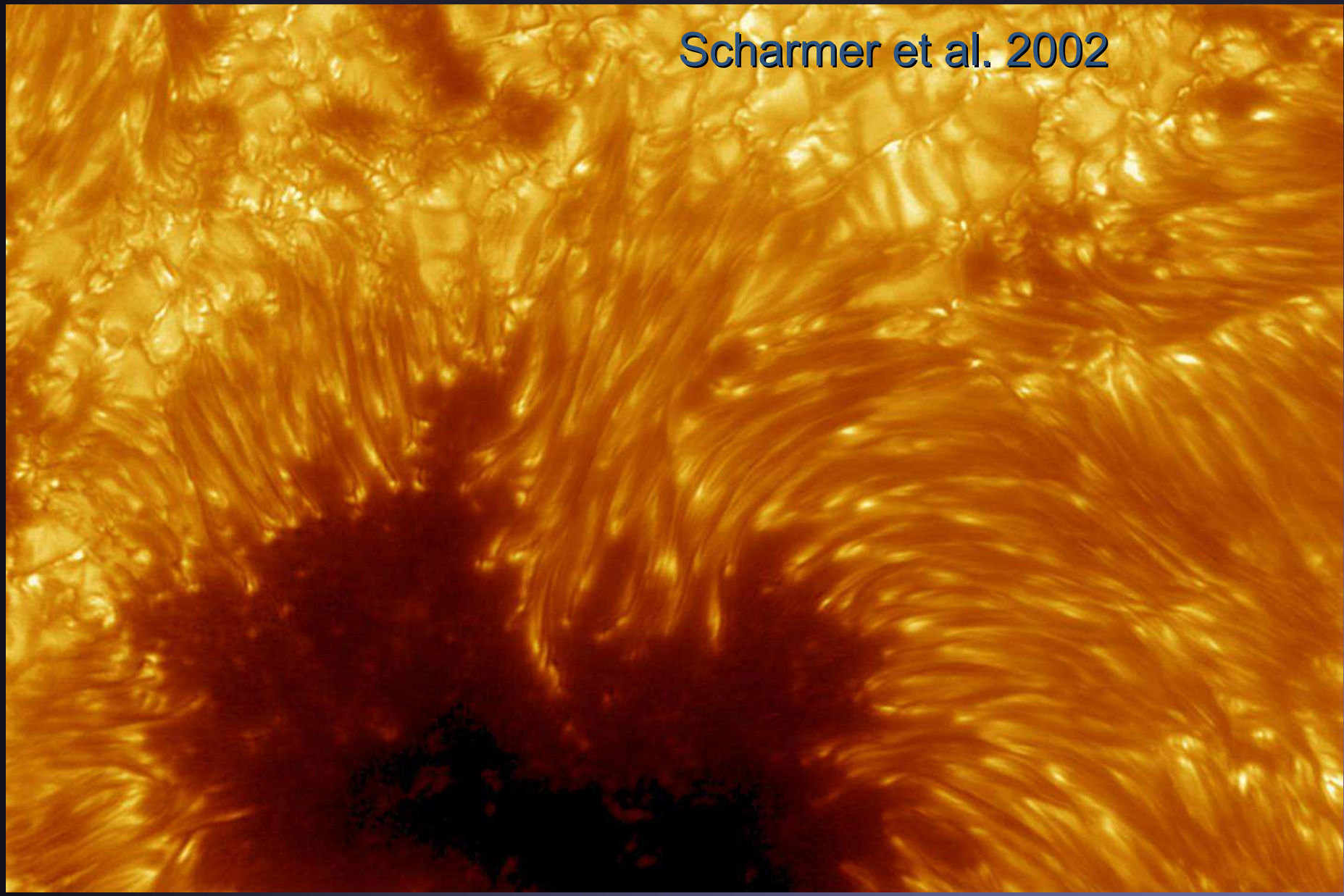

Umbral dots seen in TiO

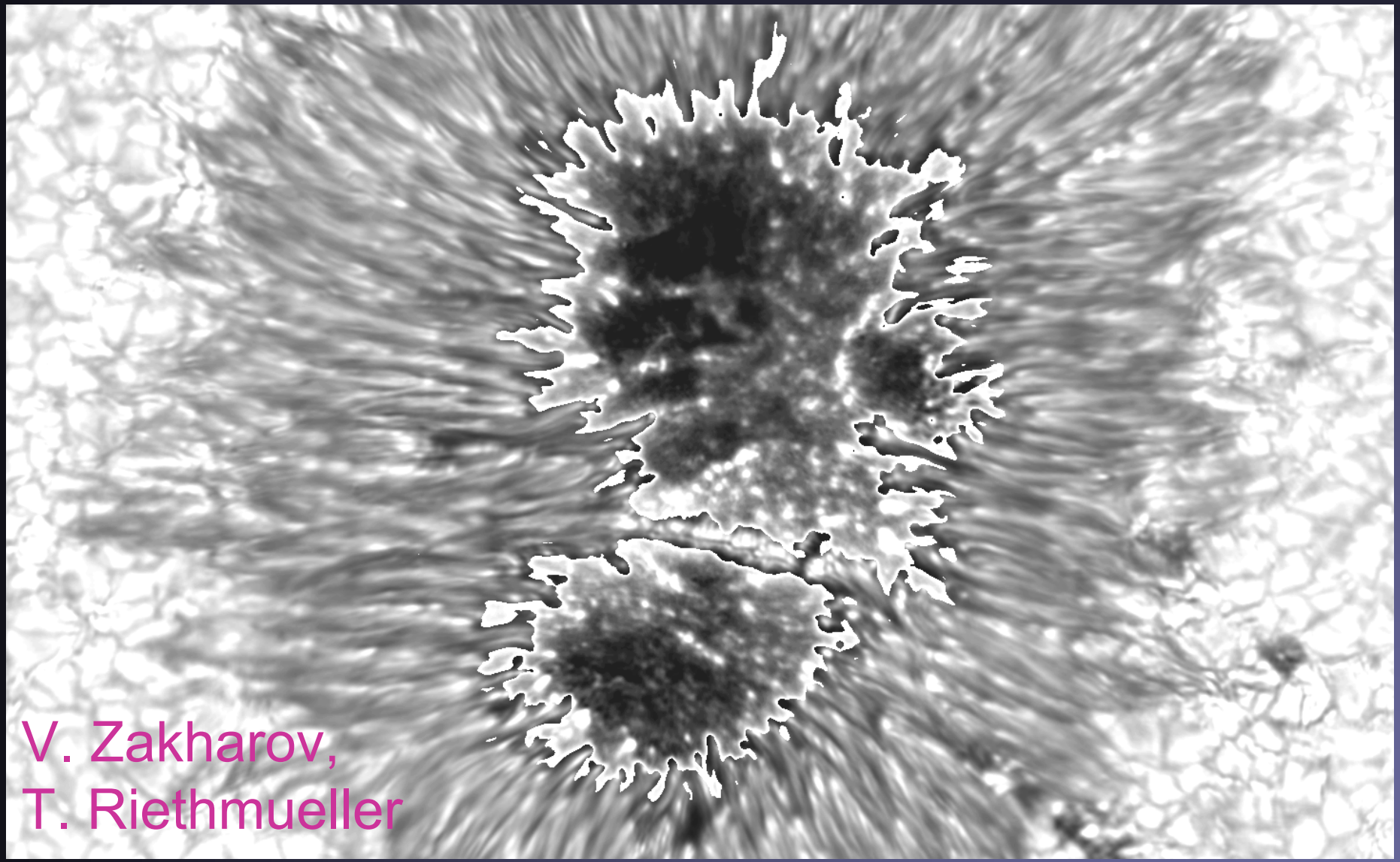

Magnetic structure of sunspots

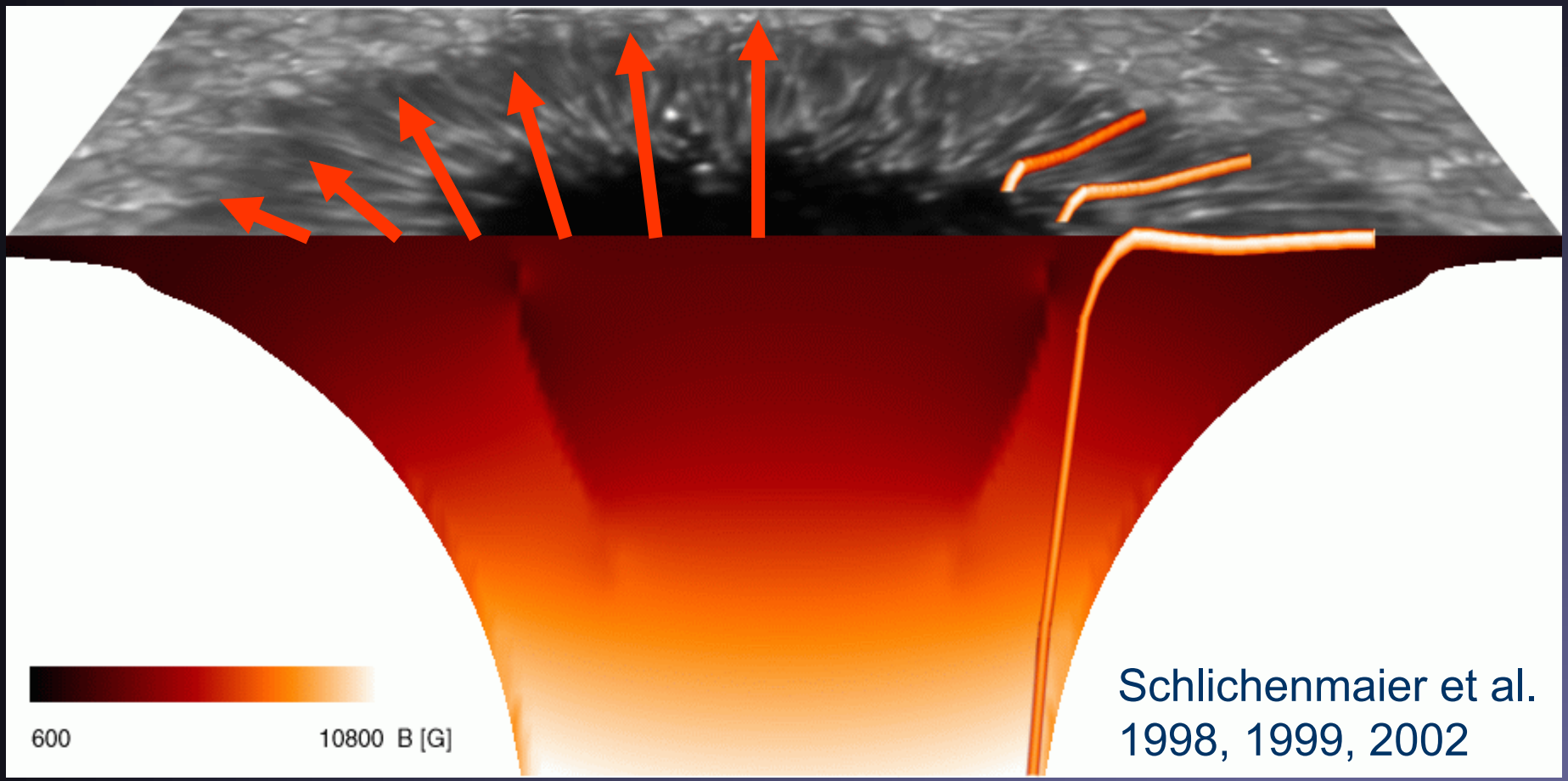

- Regular on large scales (≈ dipole, B_{max} ≈ 2500 G, for simple spots)
- Extremely complex on small scales (penumbra, subsurface)

Magnetic structure of sunspots

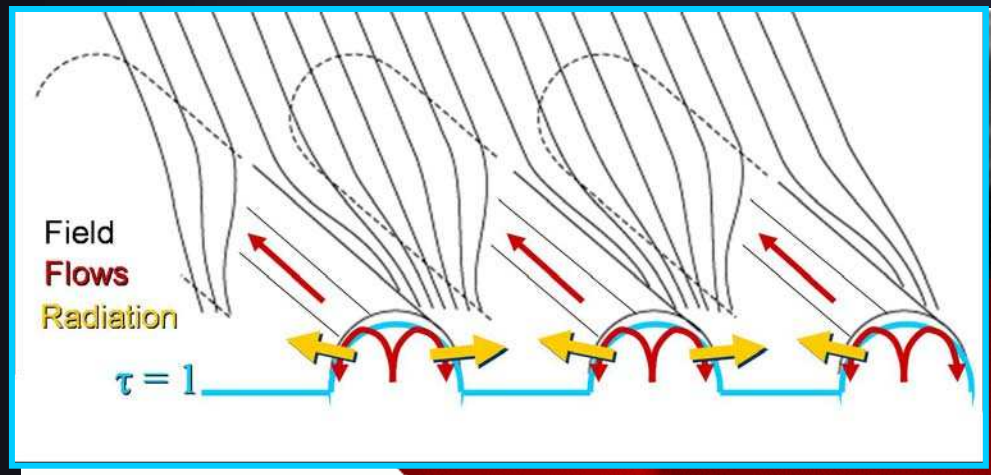

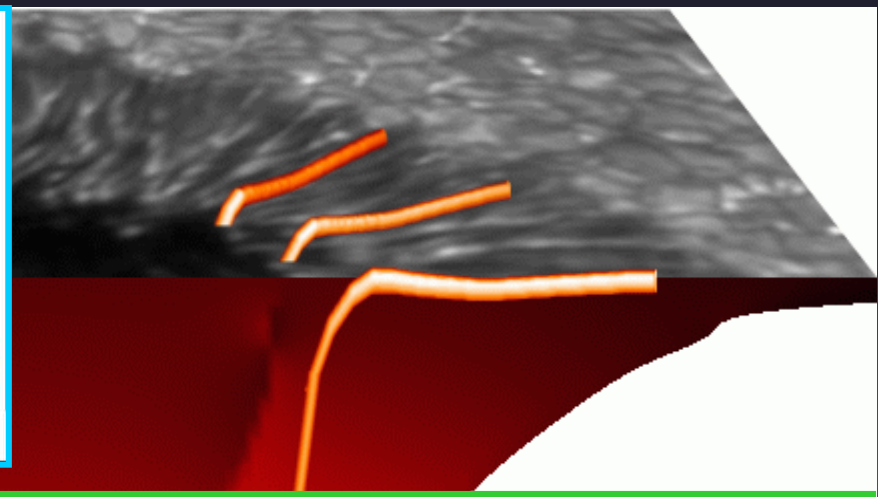

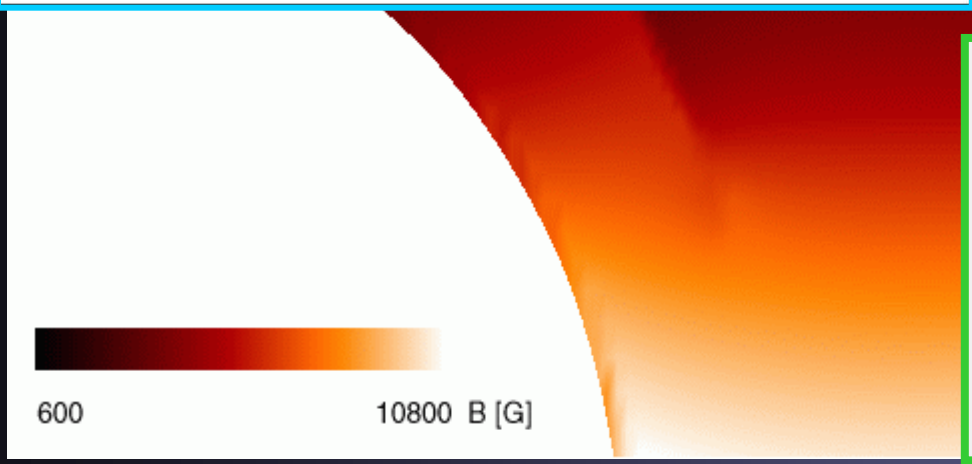

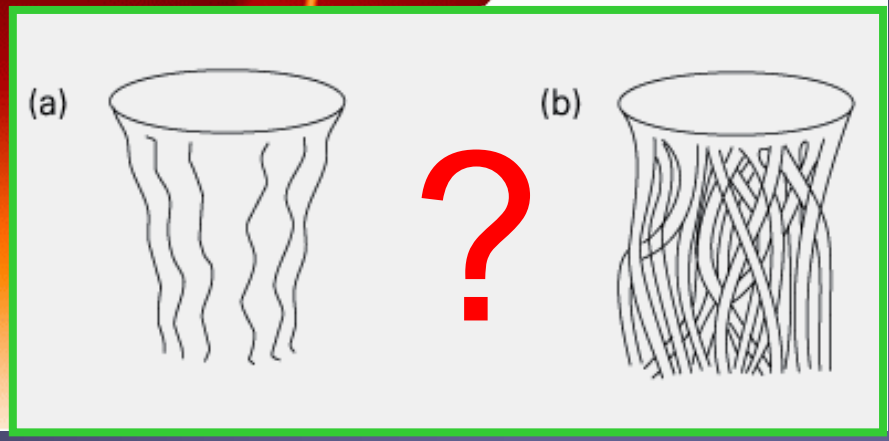

Sunspots span too many spatial and temporal scales to be successfully simulated from first principles.

Current view of fine-structure of penumbra

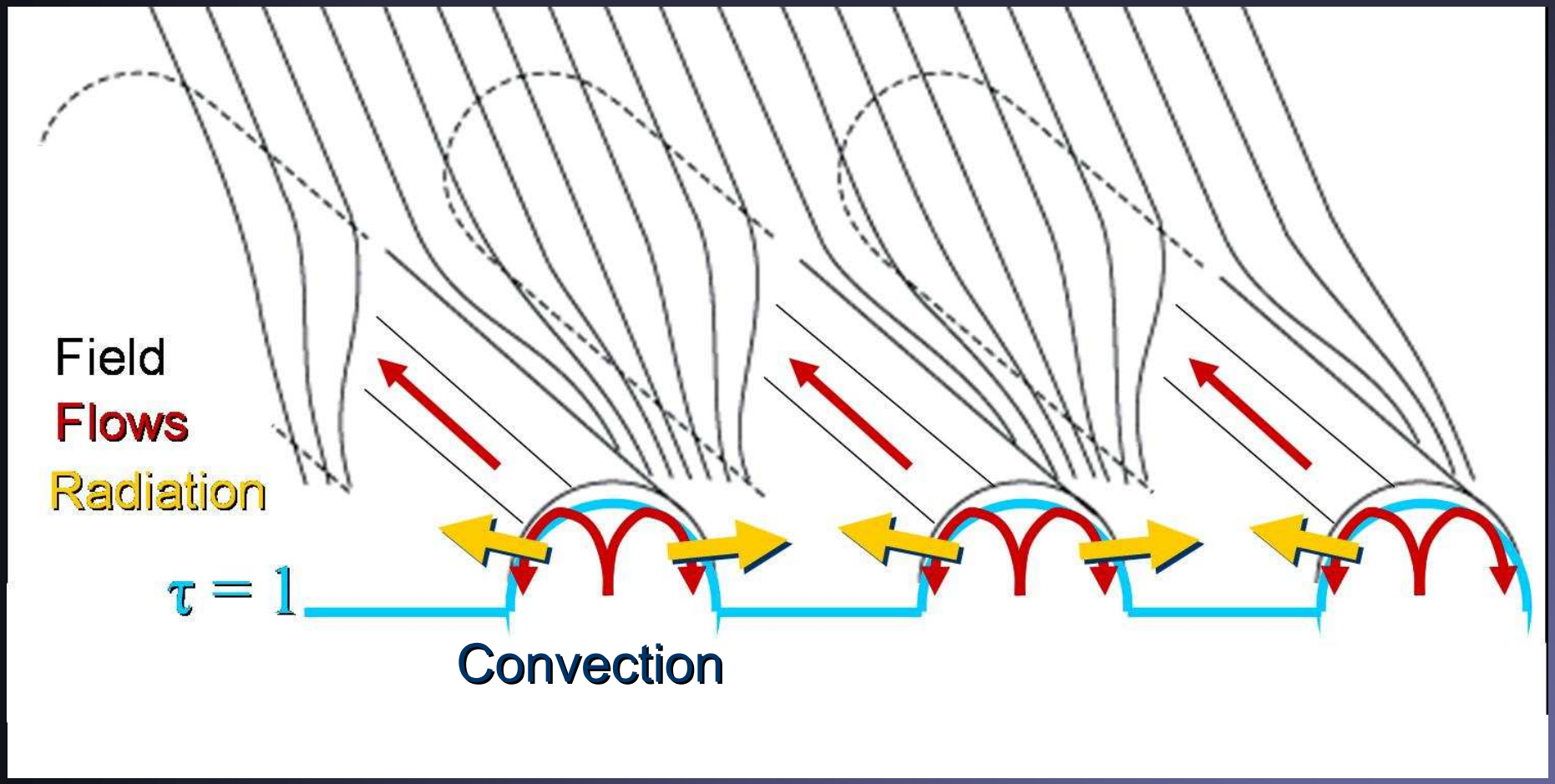

Zakharov et al. 2008, Rempel et al. 2008

Sunspot Wilson depression

Map of Wilson depression (from T & B measurements and assumption that sunspot magnetic field is close to potential)

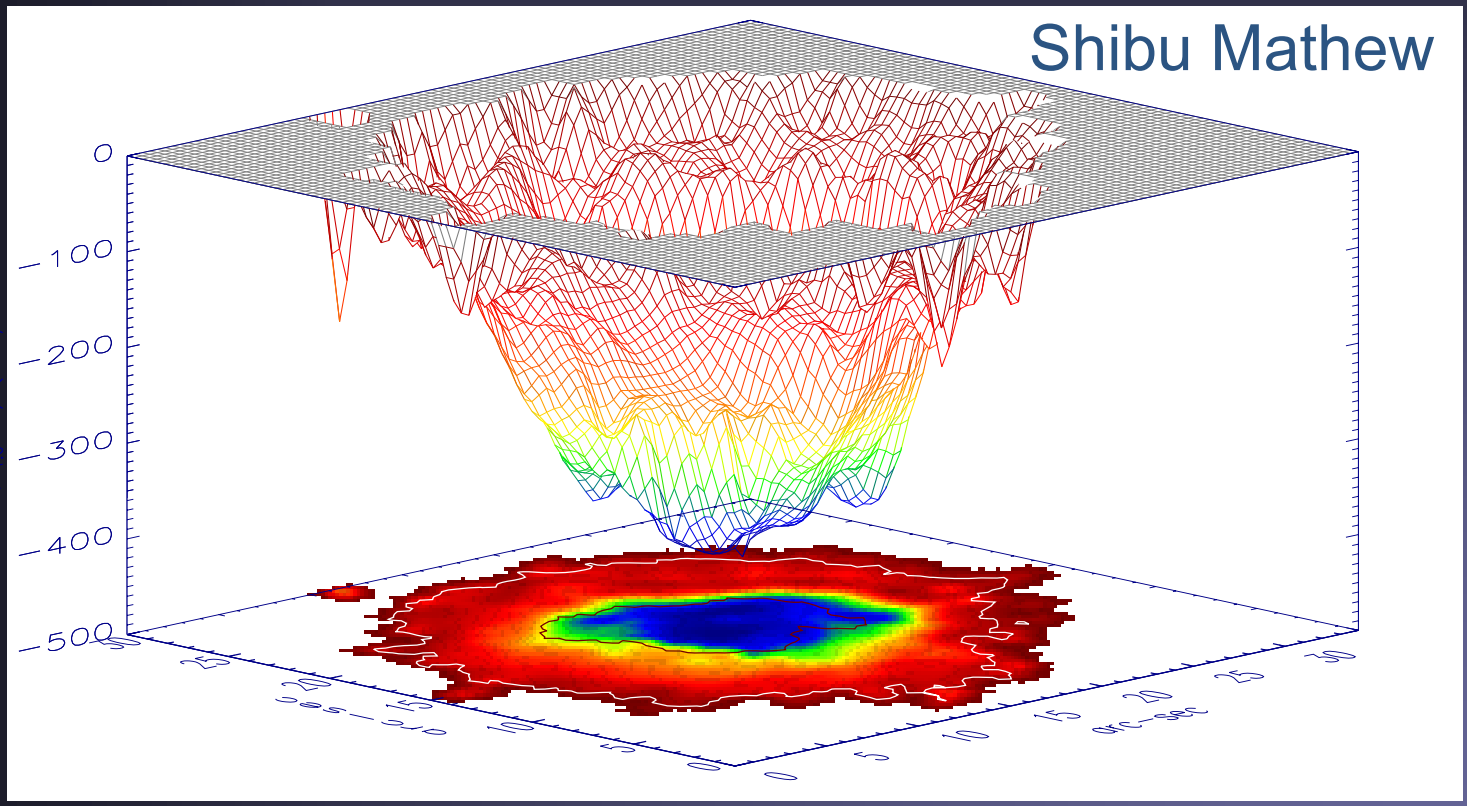

$B^2/8\pi + p = \text{const.}$ ➔ p lower in spot than outside ➔ density also lower ➔ opacity also lower ➔ we see deeper into spot

Magnetic elements

- Most of the magnetic flux on the solar surface occurs outside sunspots and pores (=smaller dark magnetic structures).
- These most common magnetic features, called magnetic elements, are small (diameters partly below 100 km), bright and concentrated in network and facular regions.
- Magnetic elements are usually described by thin magnetic flux tubes (i.e. bundles of nearly parallel field lines, expanding with height), like smaller, simpler versions of sunspots.

Surprisingly constant field strength

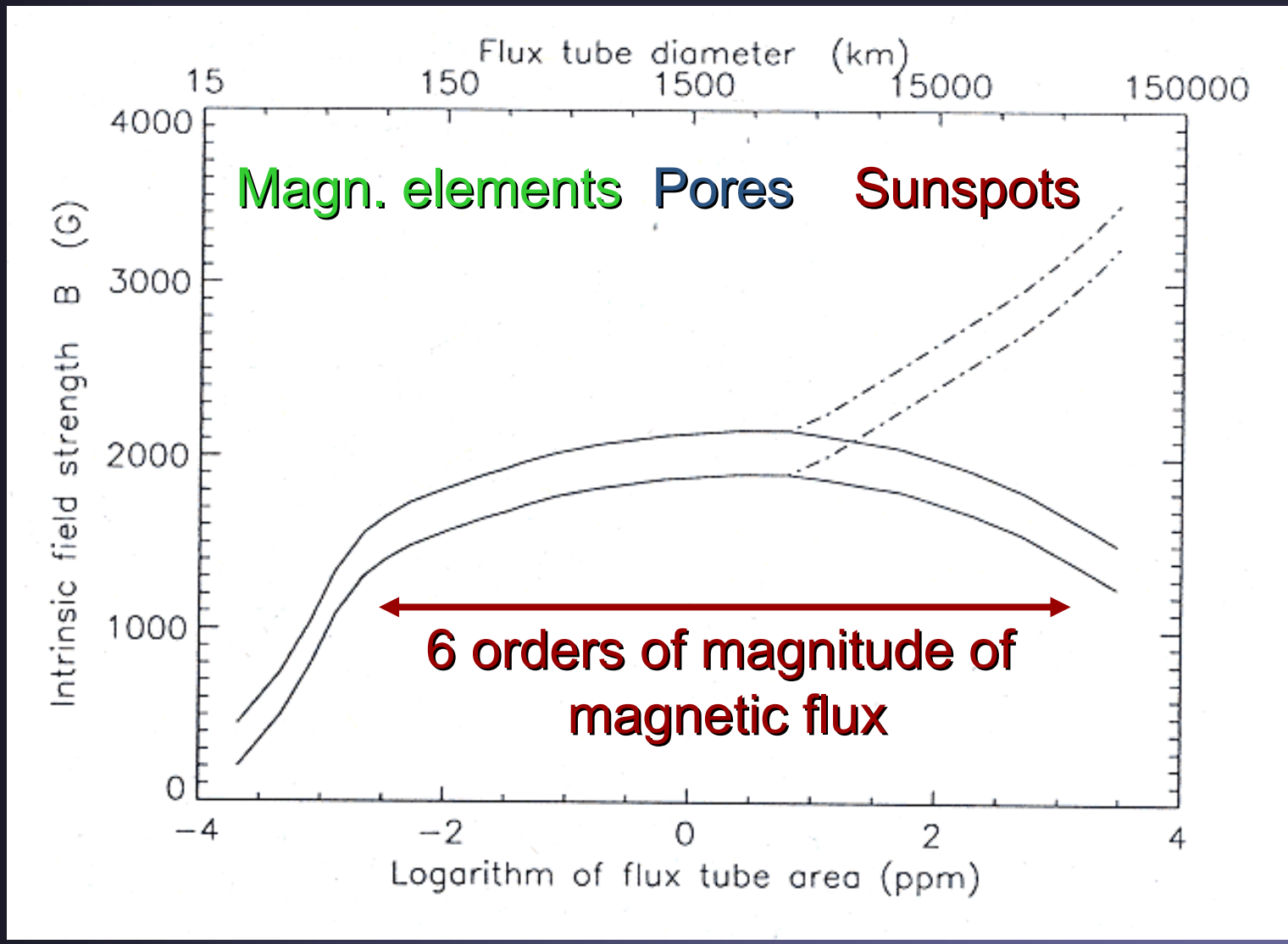

Temperature contrast vs. size

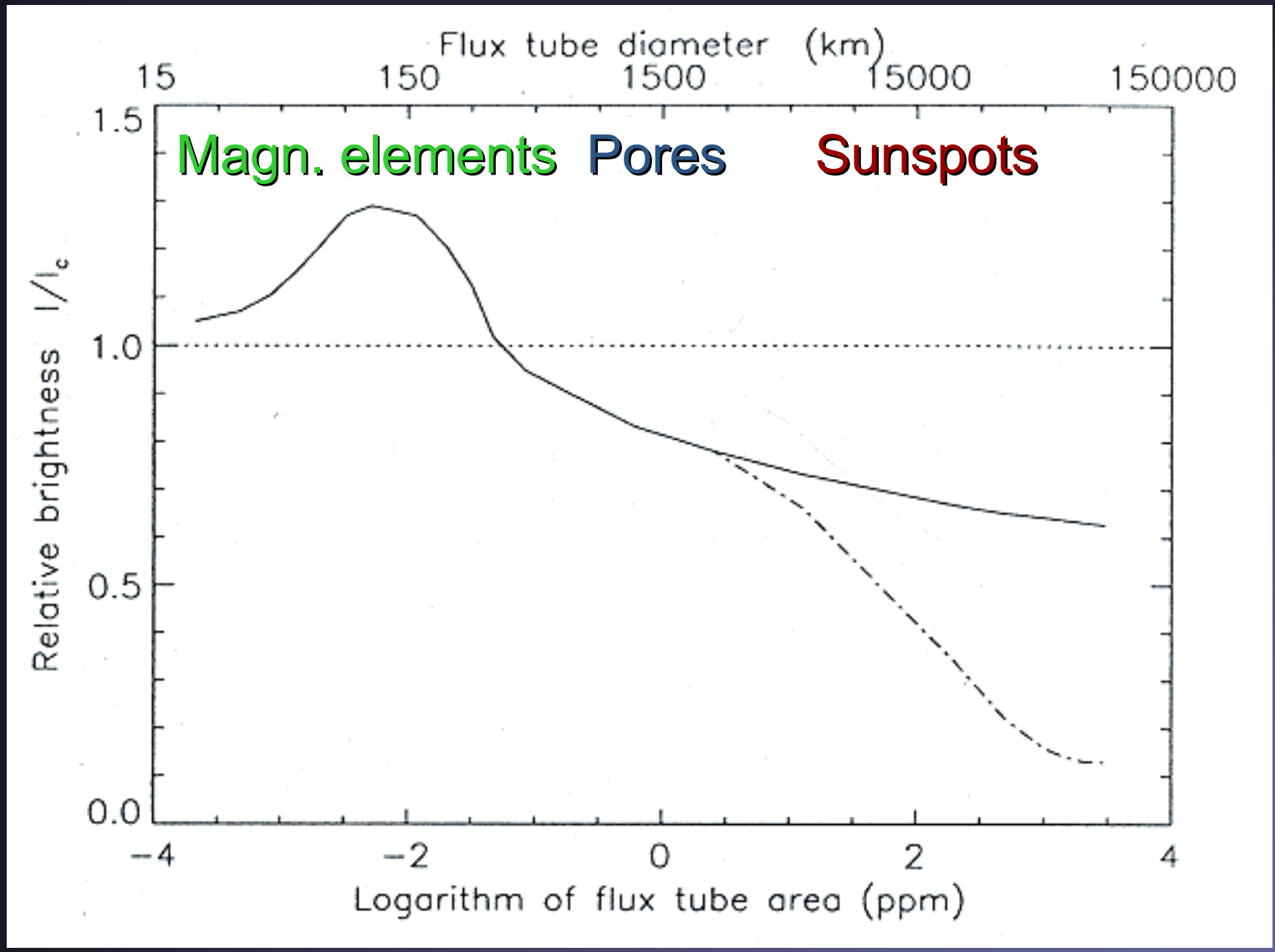

Temperature stratifications of quiet Sun, sunspot, magnetic element

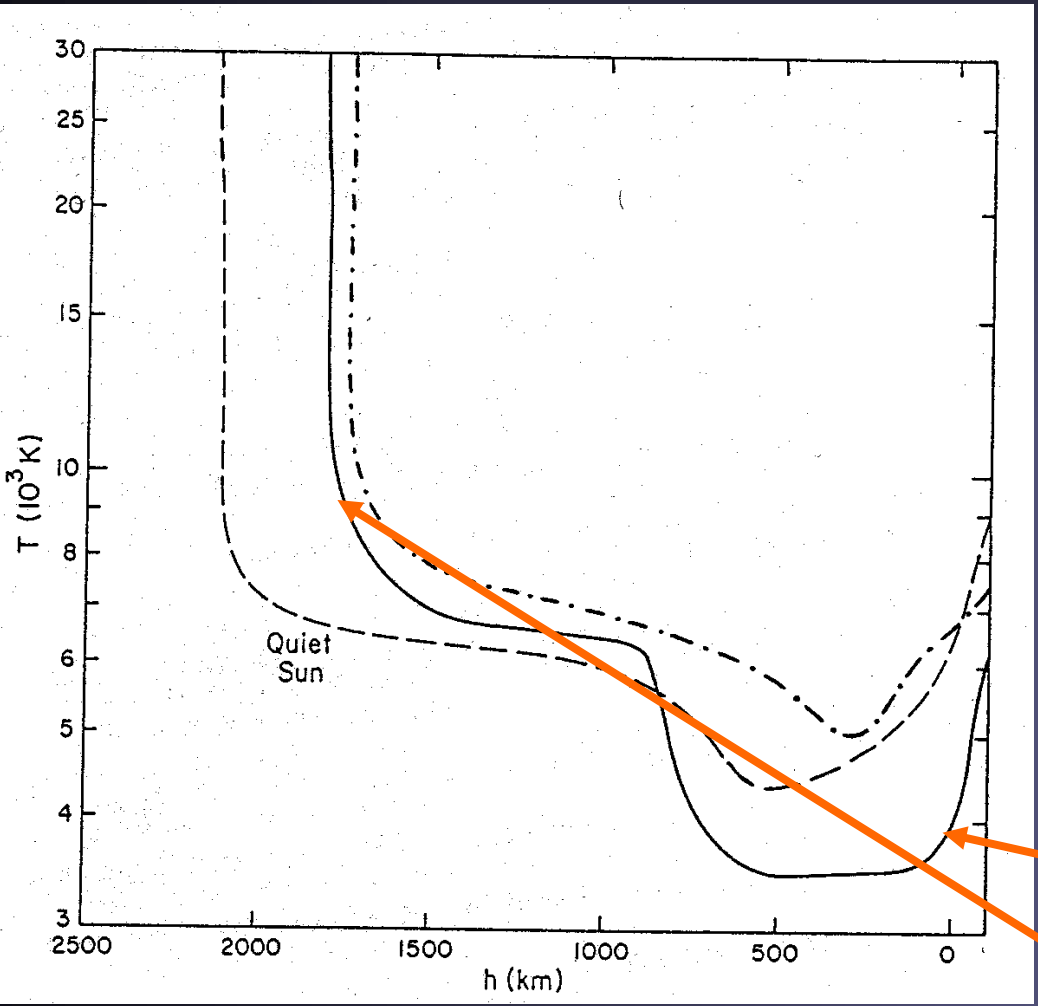

- Dashed: Quiet Sun atmosphere
- Solid: sunspot atmosphere
- Dot-dashed: active region plage, magnetic element
- Plage is hottest everywhere in atmosphere
- Sunspot cold (dark) in photosphere, but hot (bright) in chromosphere & transition region

Contrast of magnetic elements

Lower image: continuum contrast (i.e. brightness of magnetic elements relative to QS brightness) vs. mean B in a pixel.

Upper image: contrast in core of a line

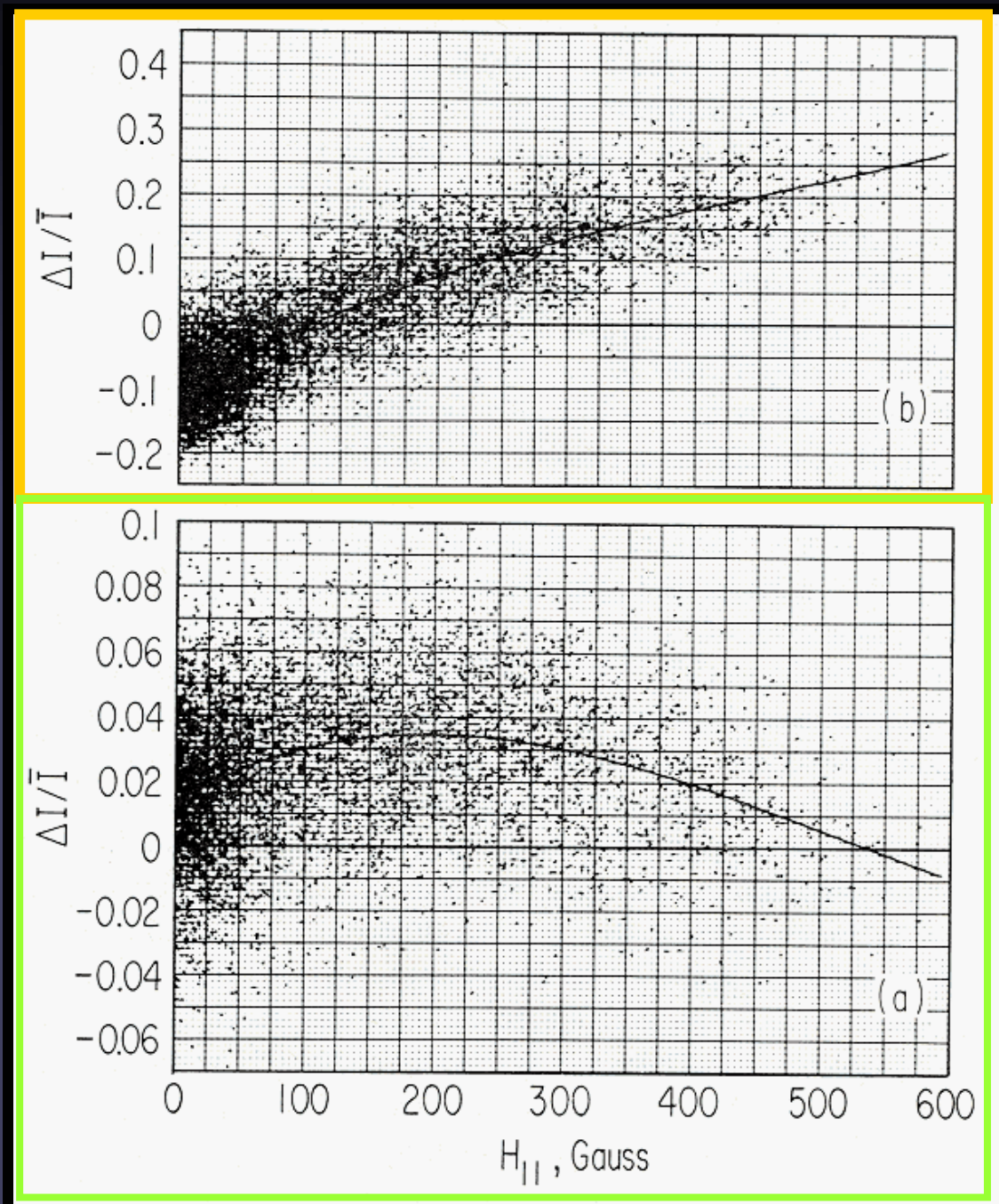

Why are magnetic elements bright?

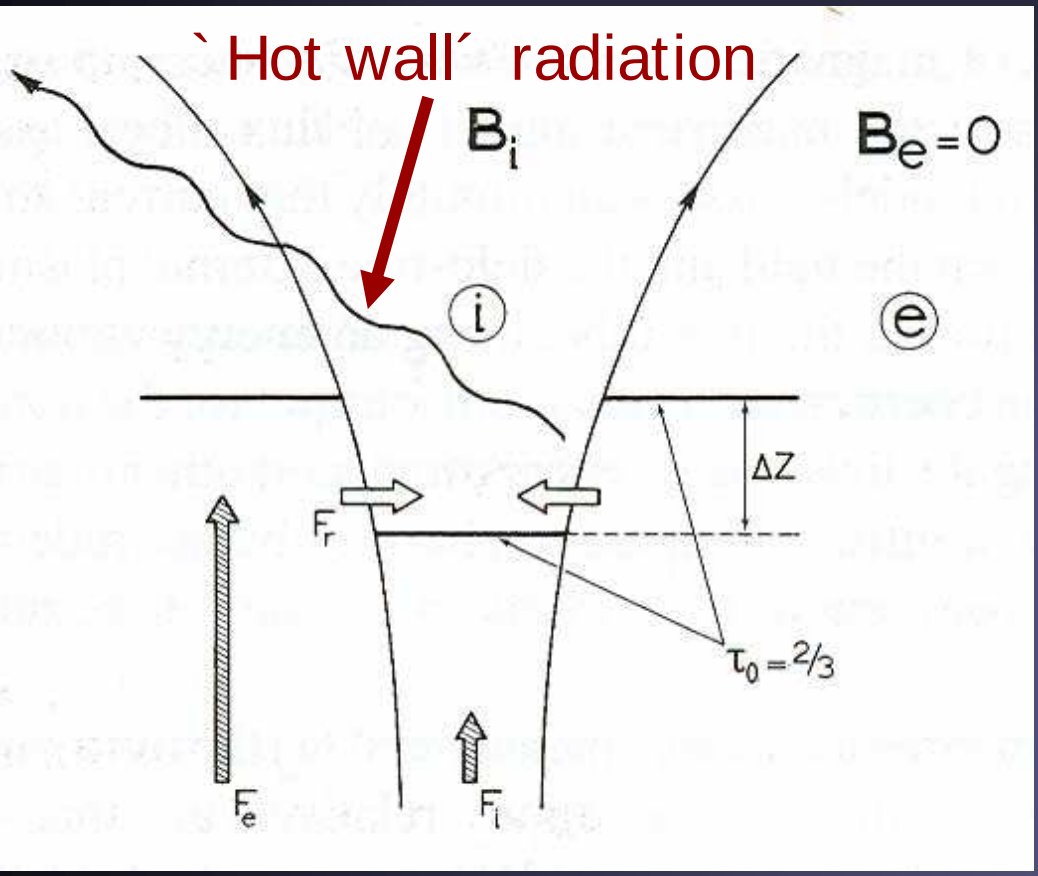

- Quenching of convection
- Partial evacuation
  - → enhanced transparency
  - → heating by `hot walls´
  - → *local flux excess*
- Inflow of radiation wins because the flux tubes are narrow (diameter ~ Wilson depression).
- High heat conductivity
  - → flux disturbance partly propagates into the deep convection zone
  - → Kelvin-Helmholtz time

Why this magnetic field structure?

- B-field structure of magn. elements driven largely by
  - horizontal pressure balance: $B^2/8\pi + p = \text{const}$
  - hydrostatic stratification (vertical pressure balance). For an isothermal atmosphere: $p = p_0 \exp(-z/H)$
- Since gas pressure drops exponentially with height, (for T=const), so must the field strength: $B = B_0 \exp(-z/2H)$
- Flux conservation: $\text{div}\, B = 0$, or: $\iint B(x, y, z)\, dx dy = \text{const}$
- B decreases exponentially with z ➔ area A of sunspot (=magnetic flux tube) increases exponentially: $A = A_0 \exp(z/H)$

Faculae lead to brightening of the whole Sun

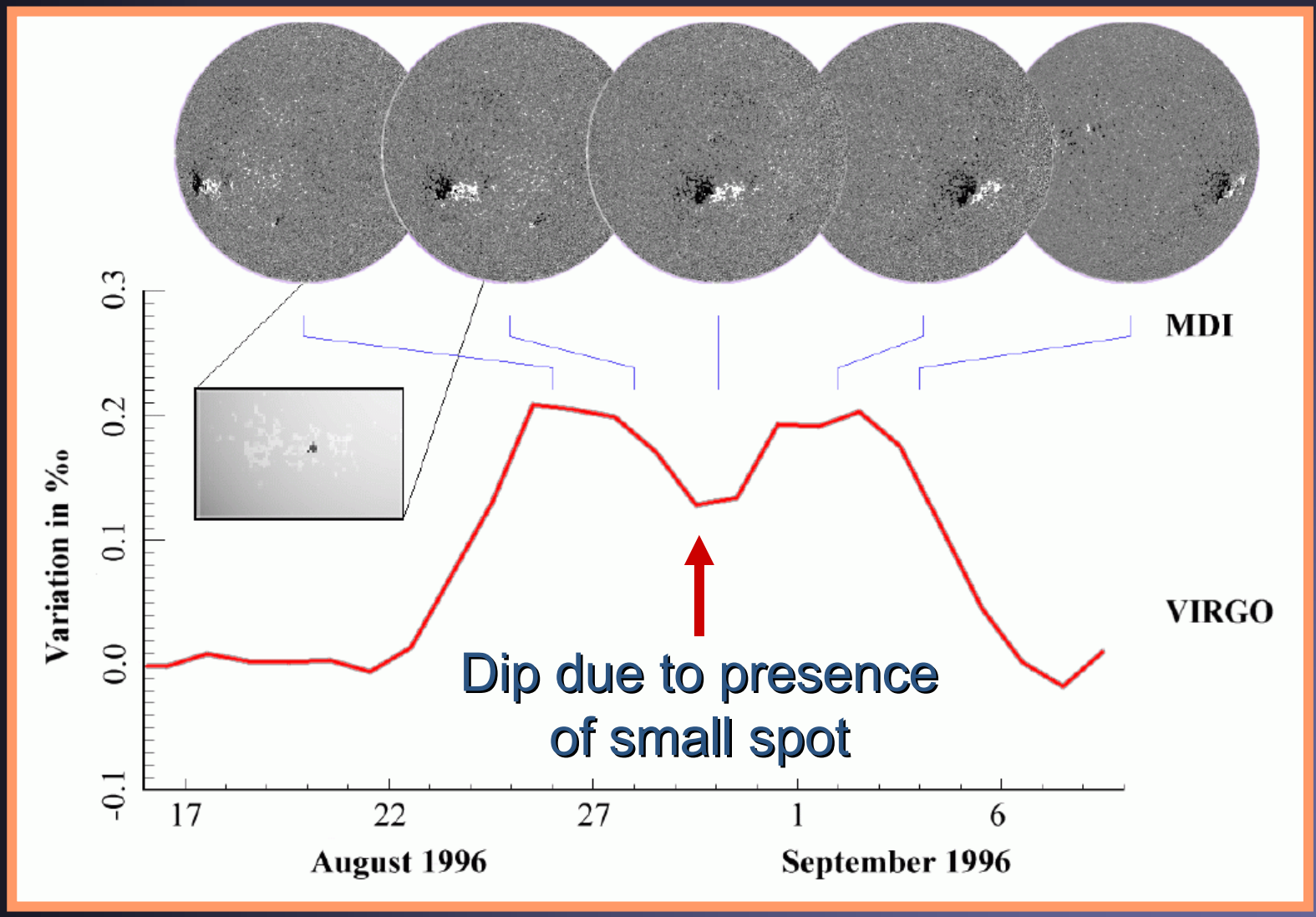

Why are faculae best seen near limb?

The Sun in White Light, with limb darkening removed

MDI on SOHO

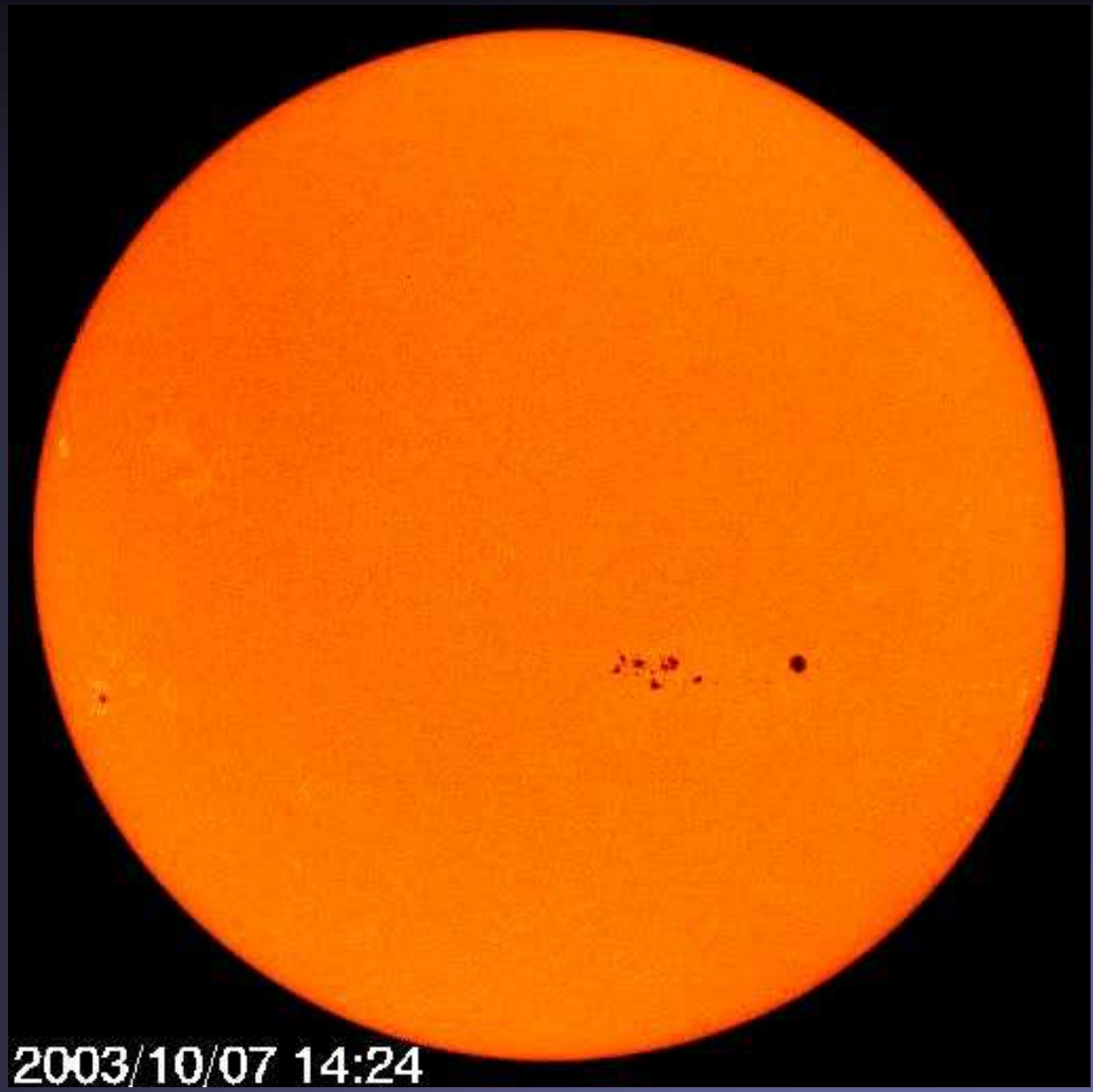

Flux-tube brightening near limb

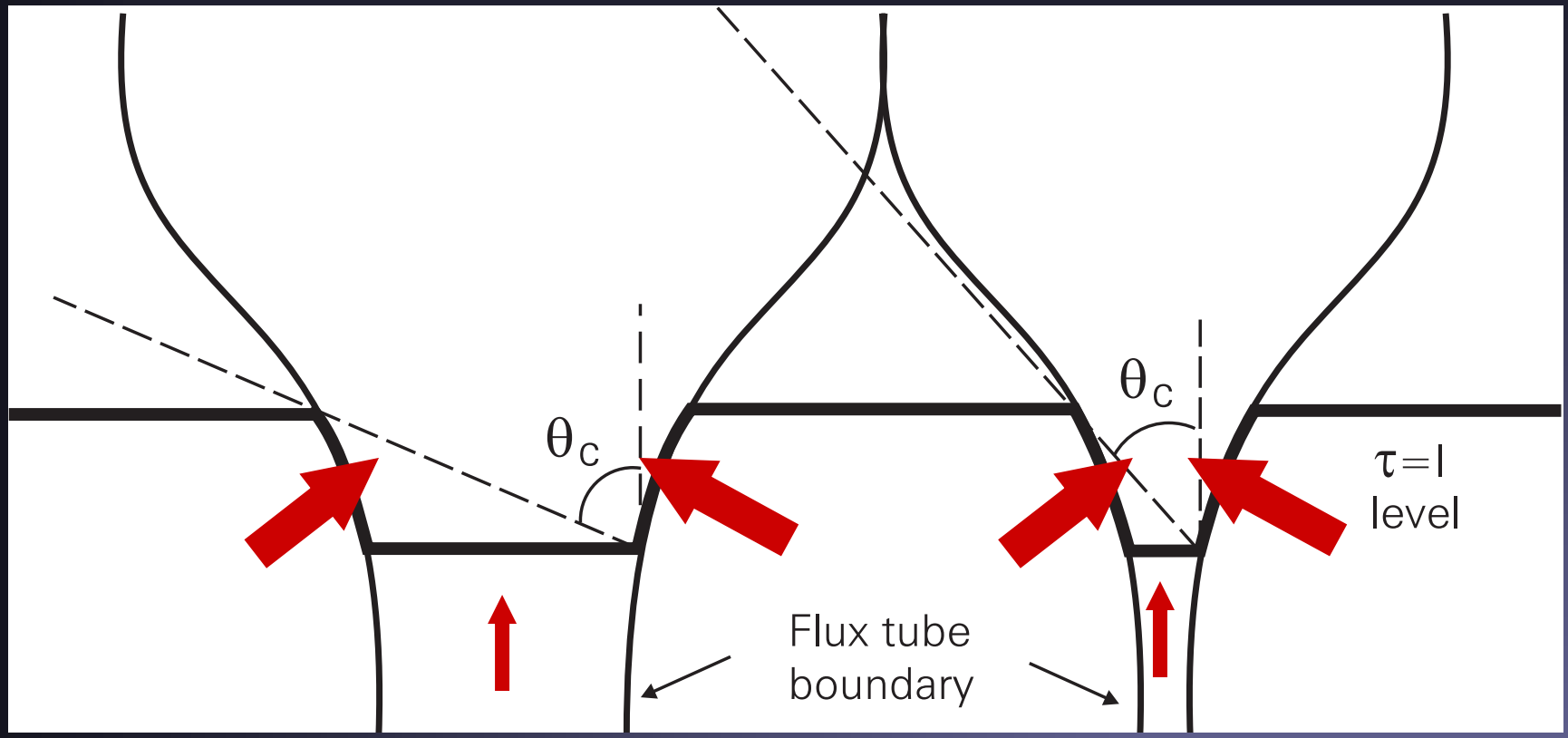

- The flux tubes expand with height (pressure balance
- Most energy radiates into them through walls, which are hot.
- They appear brightest when hot walls are well seen, i.e. near limb (closer to limb for larger tubes)

Facular brightening

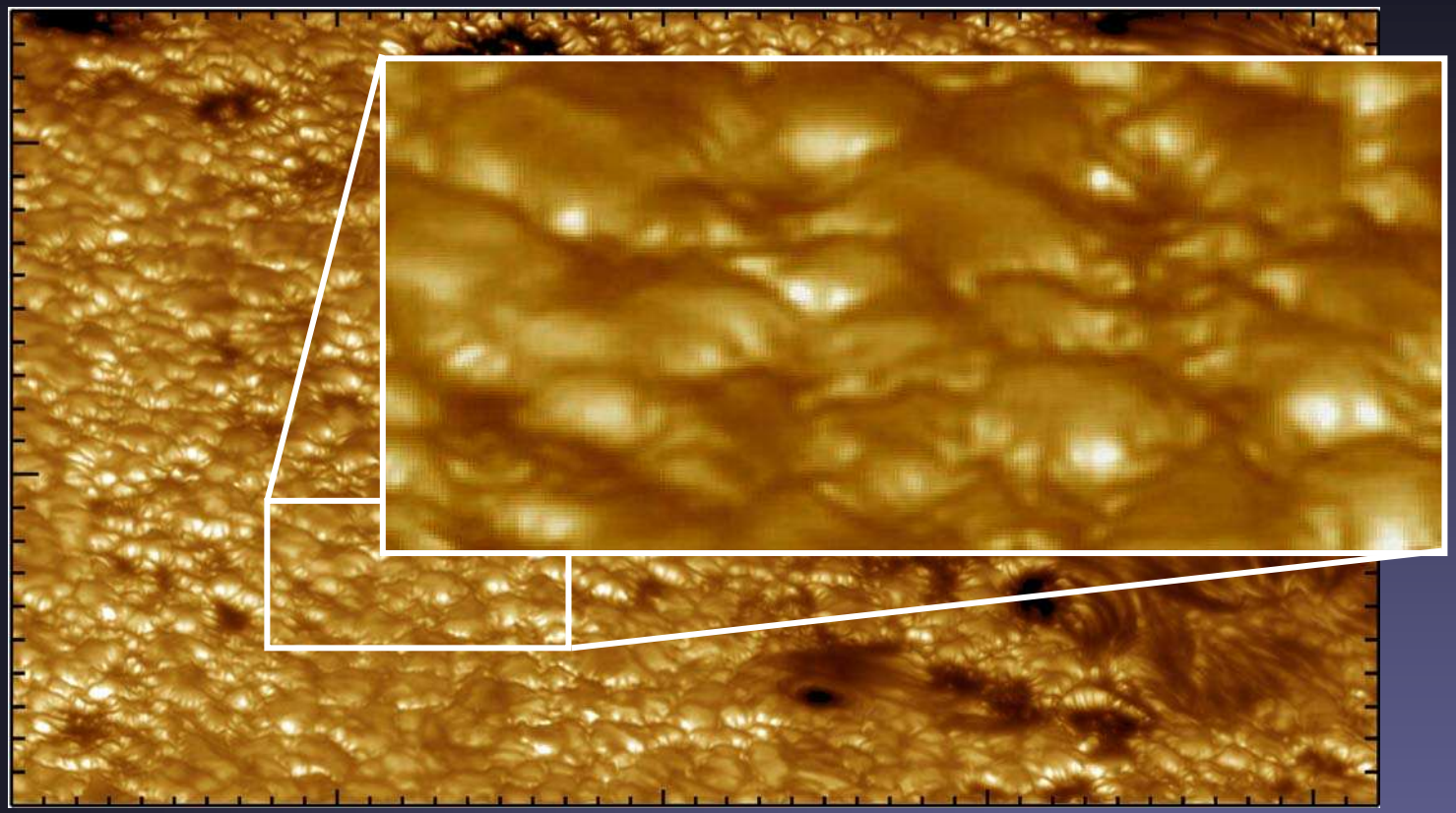

(continuum image: SST, La Palma θ=60° λ=488nm)

Recent observations reveal:
(Lites et al. 2004)

- 3D appearance of faculae
- extension up to 0.5”
- narrow dark lanes centerward of faculae

3-D radiation MHD simulations

- Similar to hydrodynamic simulations describing granulation, except that now the full MHD equations need to be solved ➔ Additional complication.
- Include realistic radiative transport of energy. Include solar surface to allow comparison with observations
- Suffer from same shortcomings as the HD simulations (too low Reynolds number) etc.

B_z
(Z=0)
>500G
>1000G
>1500G

6 Mm

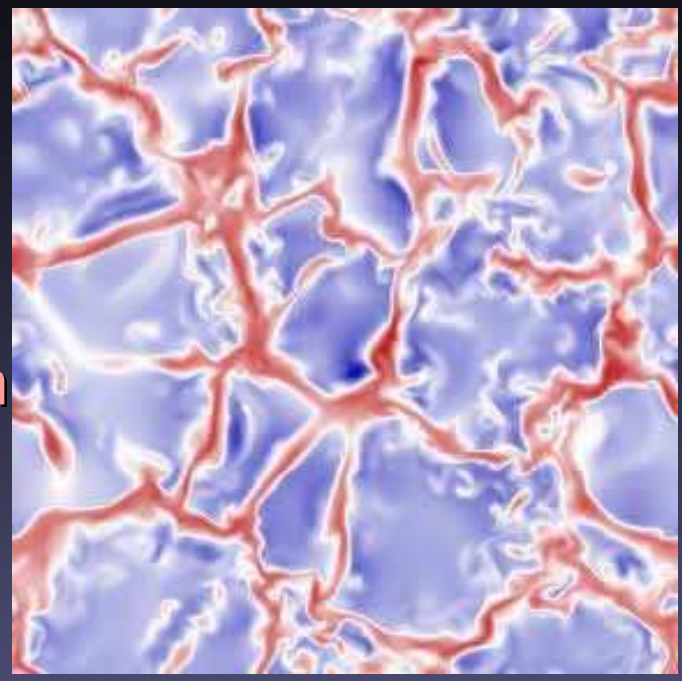

v_z
(Z=0)

3-D compressible radiation-MHD simulations

Plage: $B_Z(t=0) = 200$ G

Grid Size: 288 x 288 x 100

Vertical extent: 1.4 Mm

Horizontal extent: 6 Mm

Alexander Vögler et al.

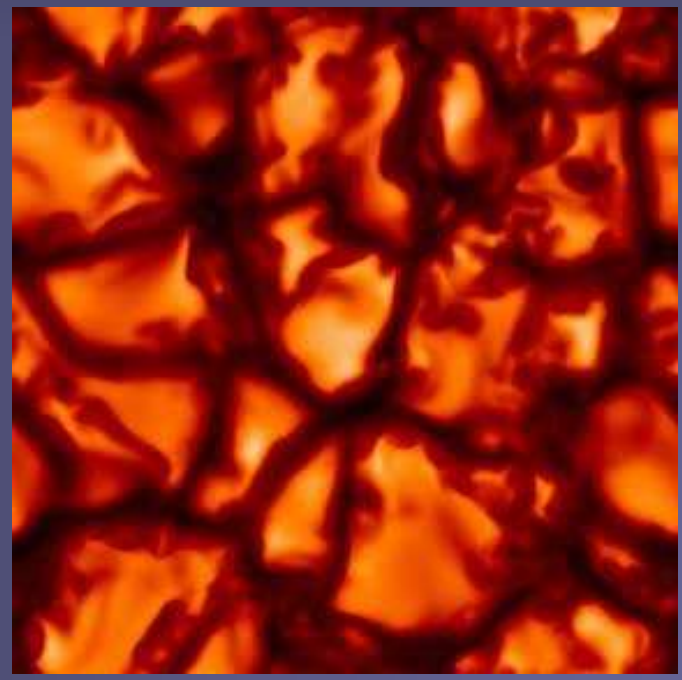

I_c
(Z=0)

B_z

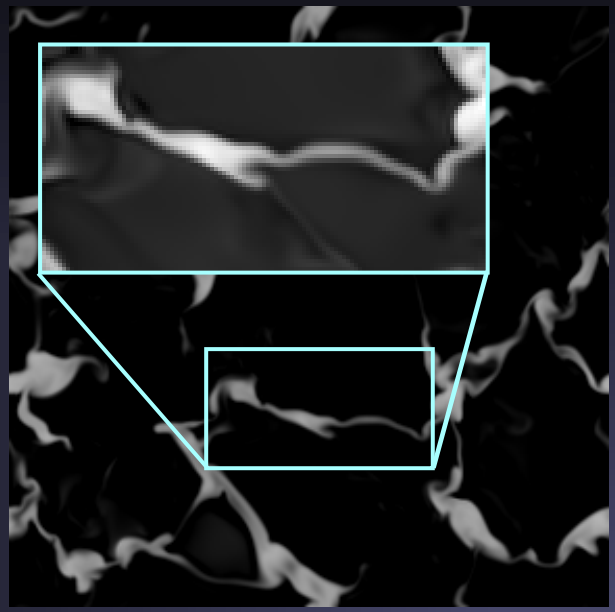

v_z

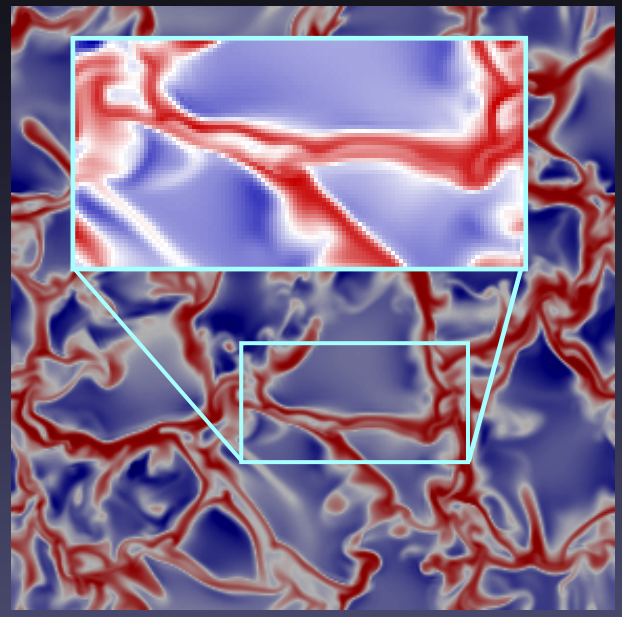

Details of thin magnetic

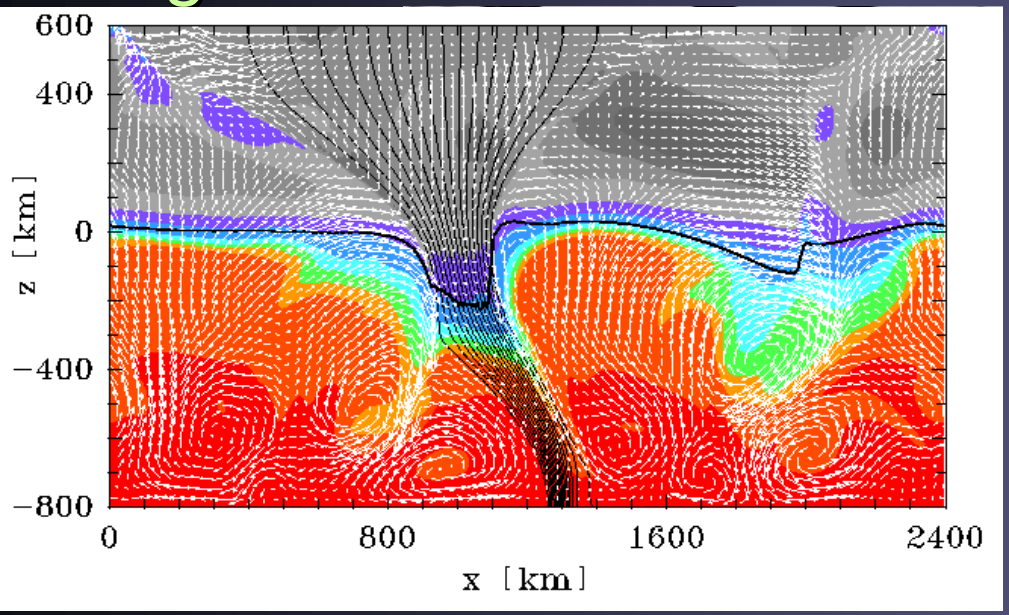

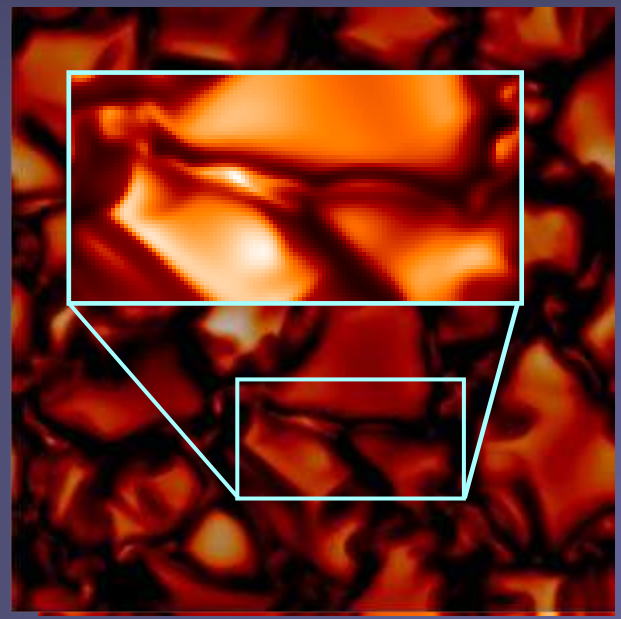

I_C

Horizontal cuts near surface level

Vögler et al. 2005

MHD simulations: from quiet Sun to strong plage

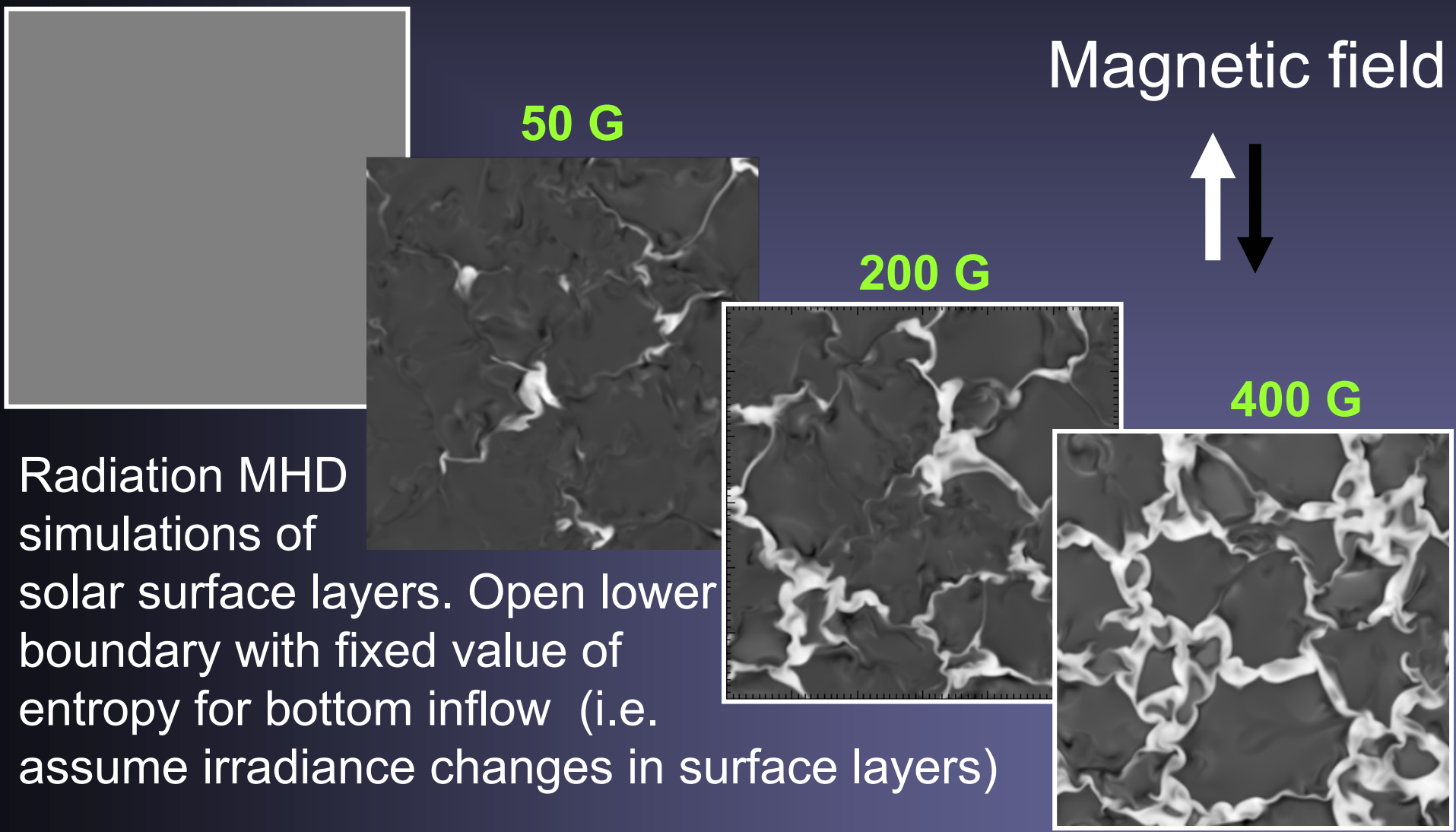

Radiation MHD simulations of solar surface layers. Open lower boundary with fixed value of entropy for bottom inflow (i.e. assume irradiance changes in surface layers)

MHD simulations: from quiet Sun to strong plage

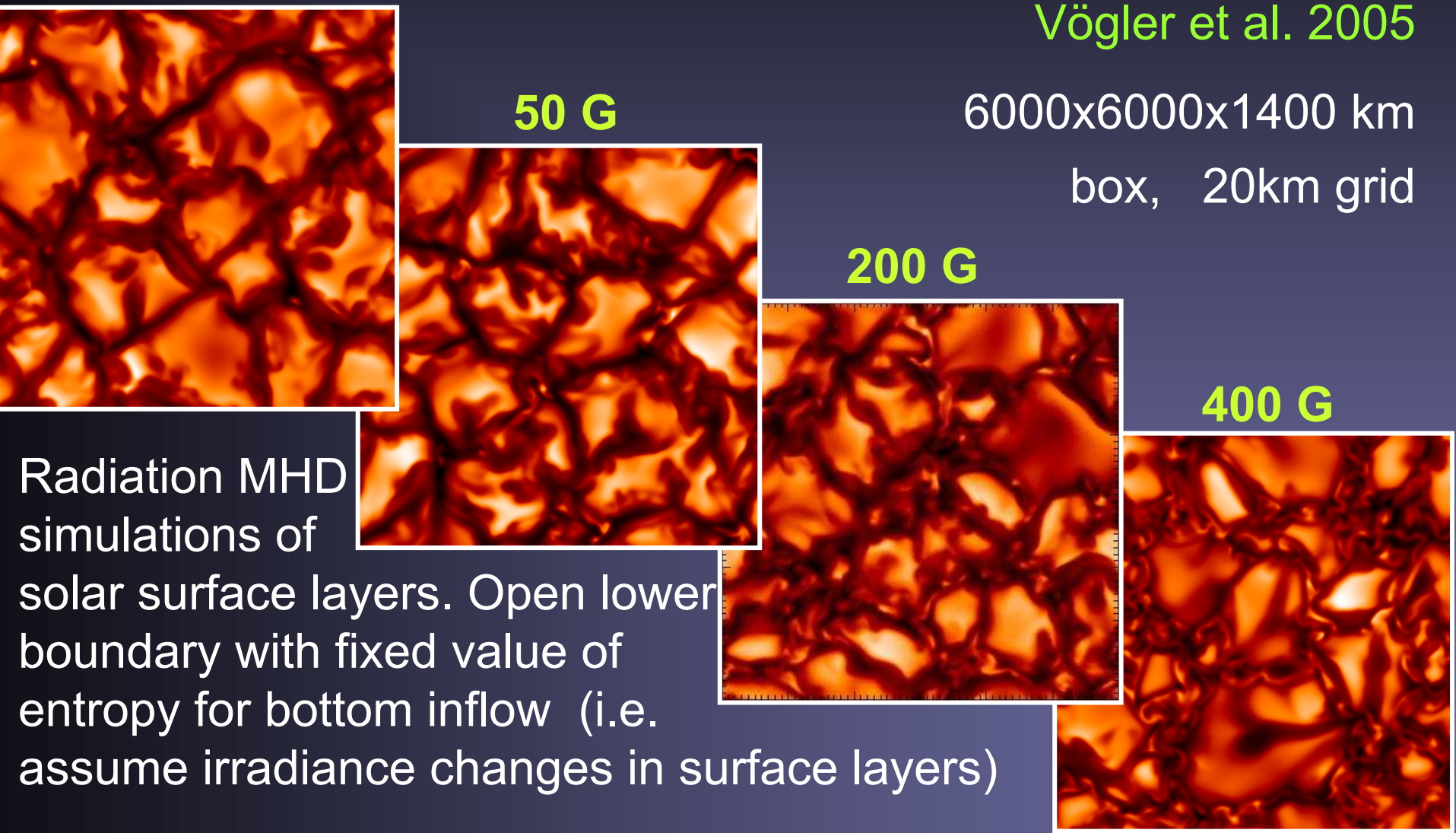

Vögler et al. 2005

6000x6000x1400 km box, 20km grid

Radiation MHD simulations of solar surface layers. Open lower boundary with fixed value of entropy for bottom inflow (i.e. assume irradiance changes in surface layers)

Vertical cut through sheet-like structure

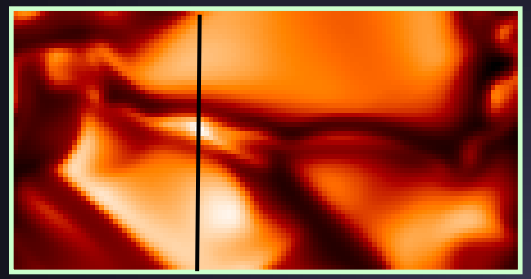

I

B_z

- partial evacuation leads to a depression of the τ=1 level
- lateral heating from hot walls (Spruit 1976)

➔ Brightness enhancement of small structures

Radiation flux vectors &

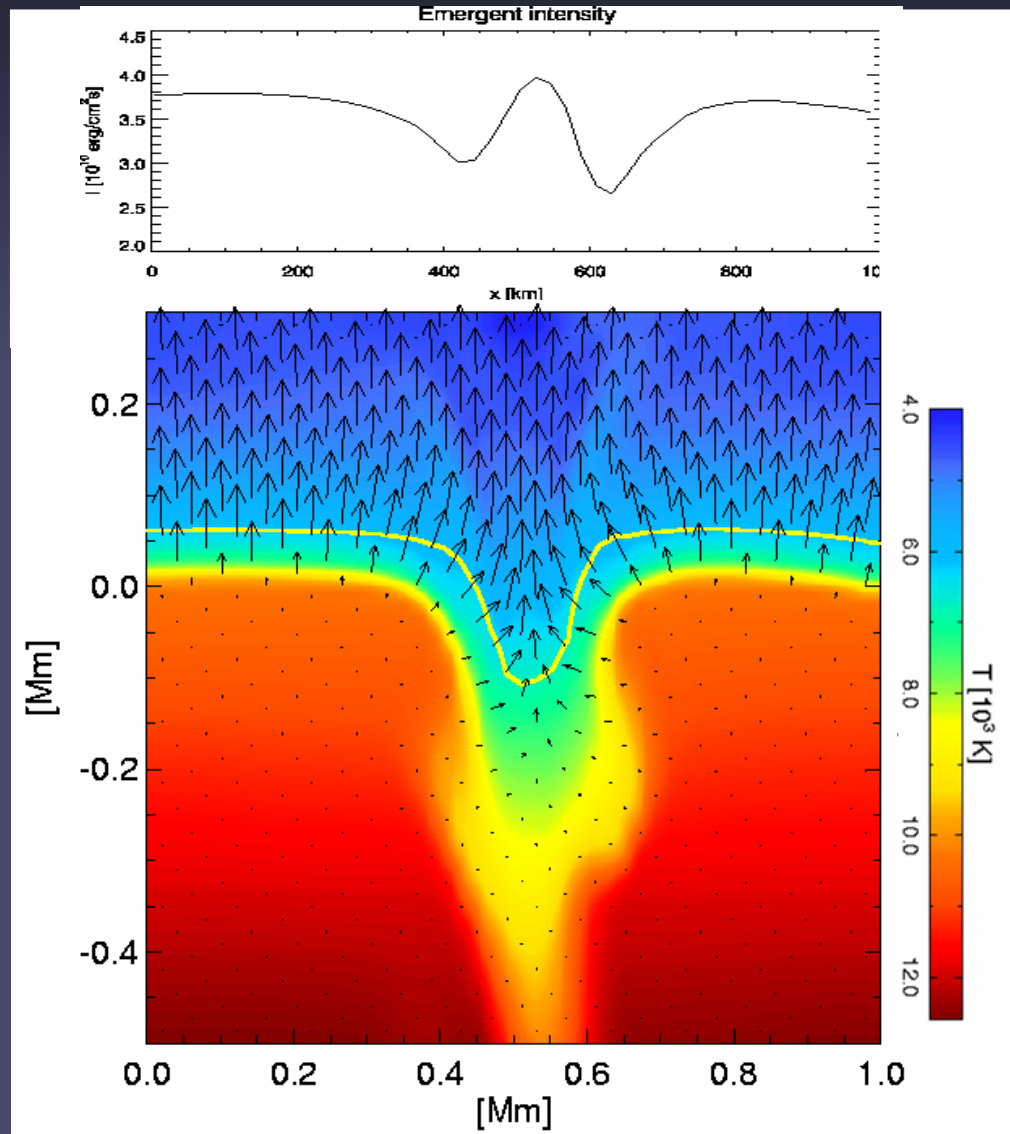

B_0=200 G: CLV of wavelength-integrated brightness

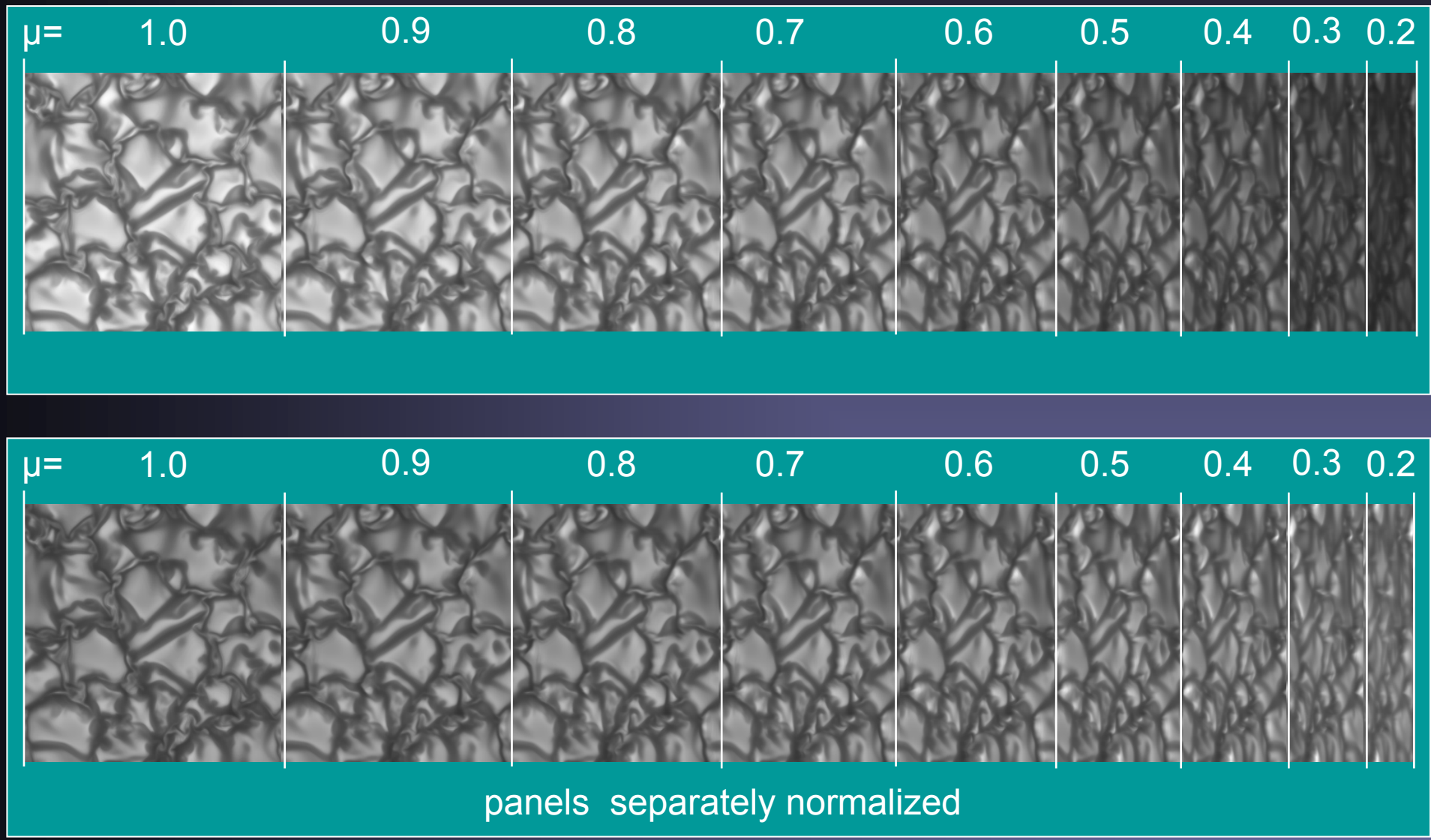

Facular brightening

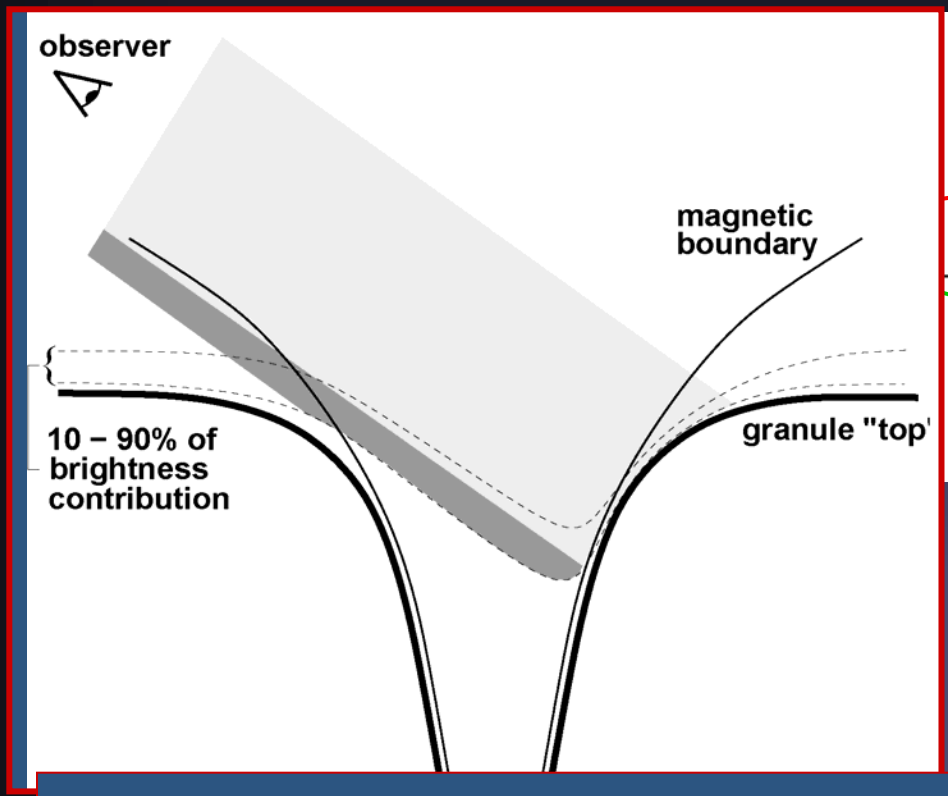

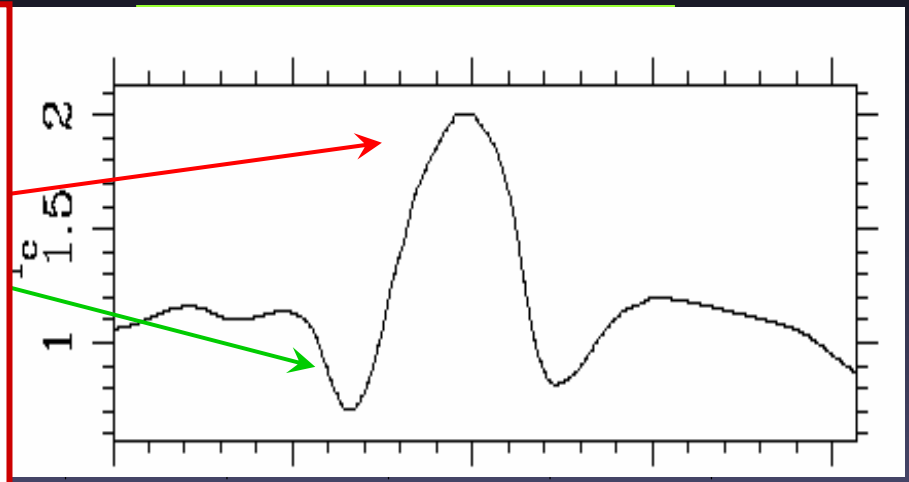

Facula: narrow layer of hot material on side and top of adjacent granule

Dark lane: - cool & tenuous material in adjacent flux concentration

- cool & dense material above neighbouring granule

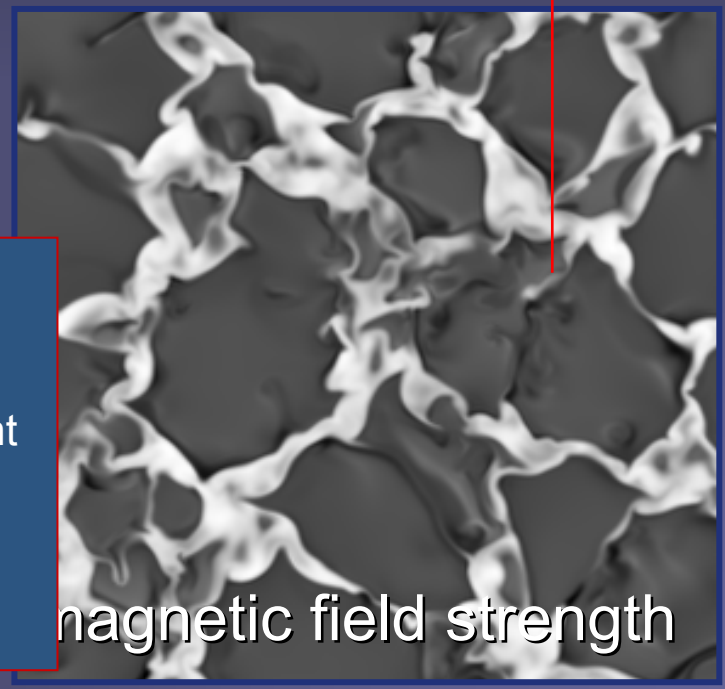

(Keller et al. 2004)

3-D simulations of mixed-polarity fields

Alexander Vögler, Robert Cameron, Manfred Schüssler

Mixed polarity simulations: diffusion & cancellation of opposite polarities (20 km resolution): $\langle B_{initial} \rangle = 200$G.

B_z

$B_z < 200$ G

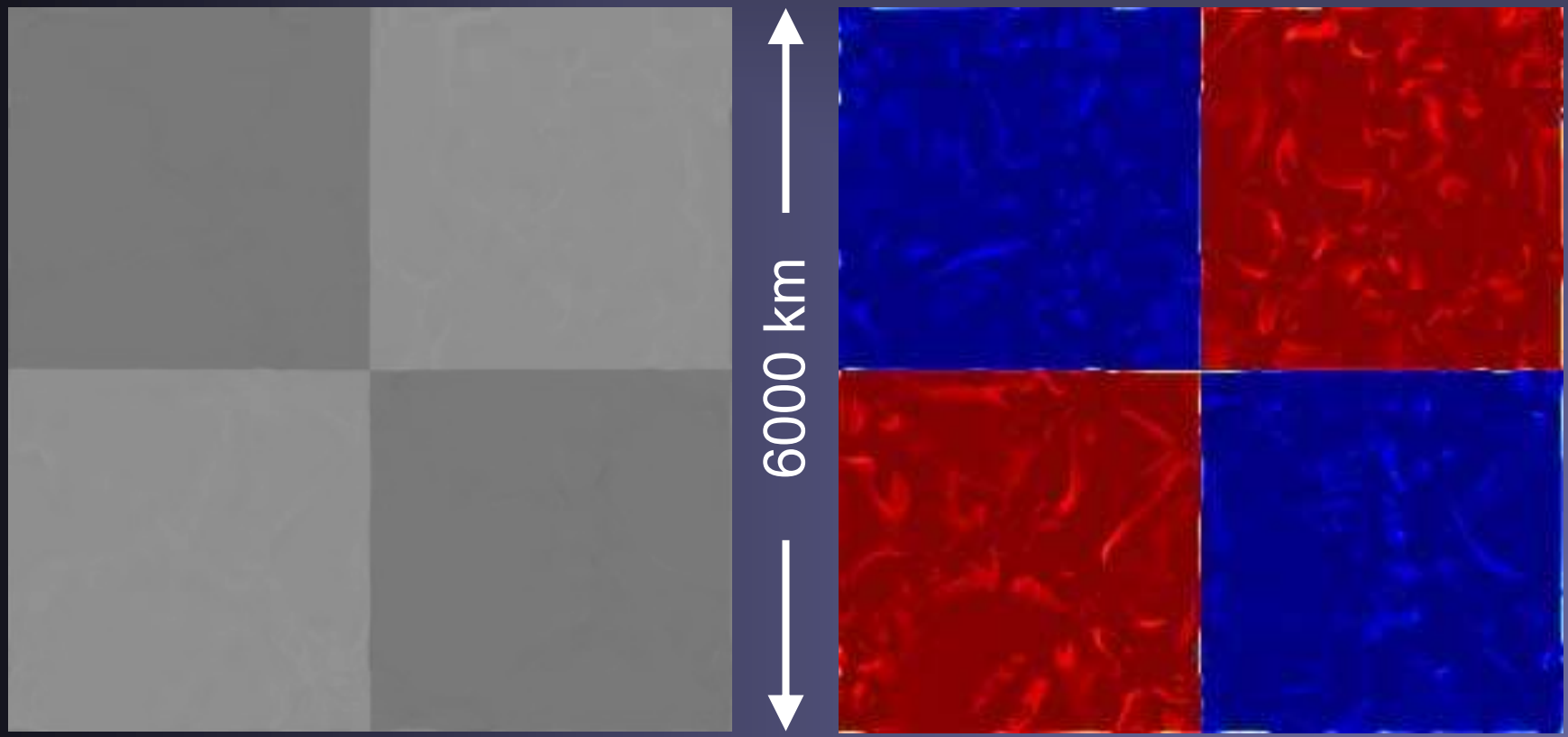

Simulations require computers...

Flux Tubes, Canopies, Loops and Funnels

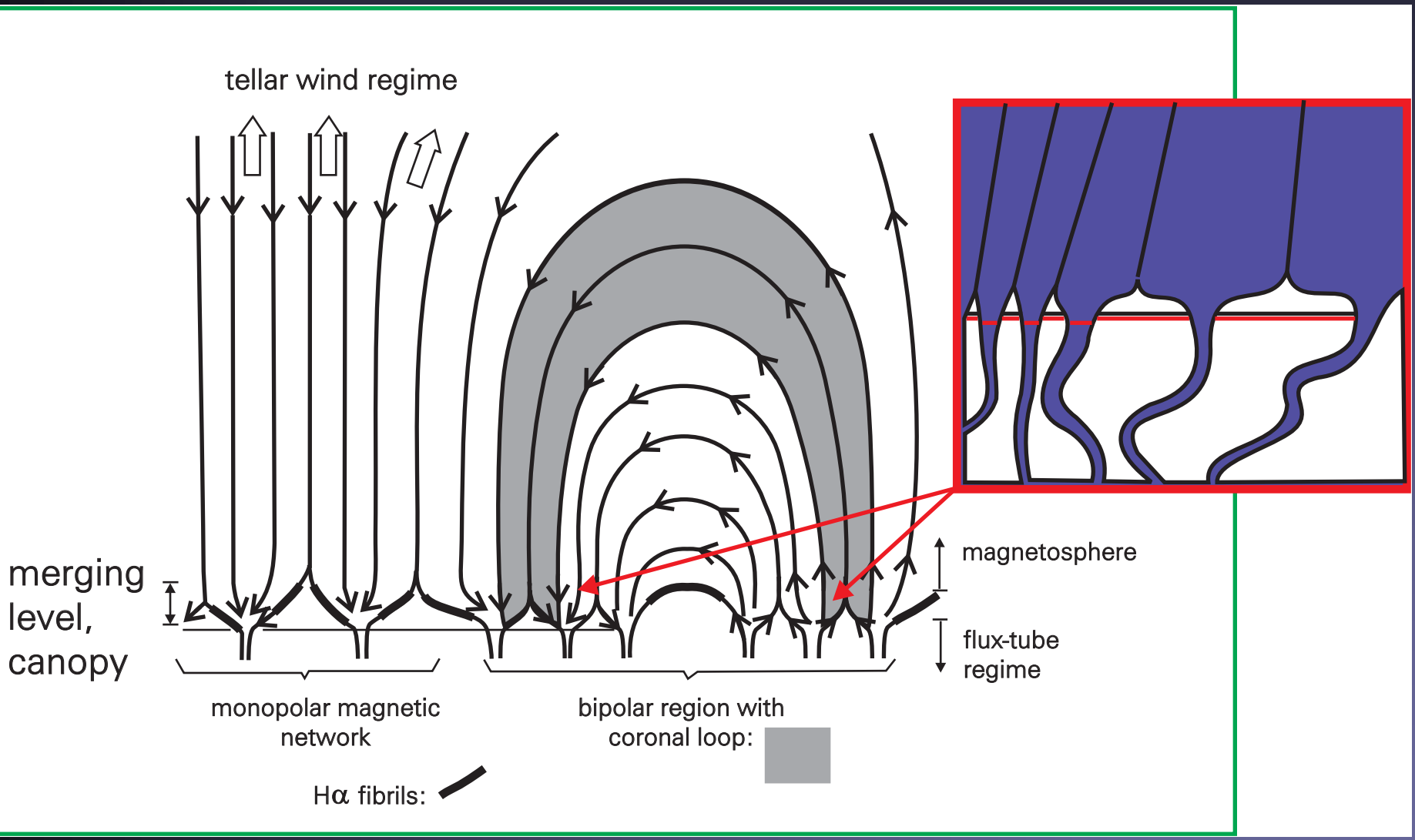

Coronal loops

- Coronal loops are closed field lines in the corona. However, closed flux must be *filled with plasma* before it can be called a *coronal loop*.
- Loop temps range from below 0.1MK to 10MK
- Often a given observations (in a given spectral band) samples radiation in a narrow range of temps. It sees only a small fraction of all loops.

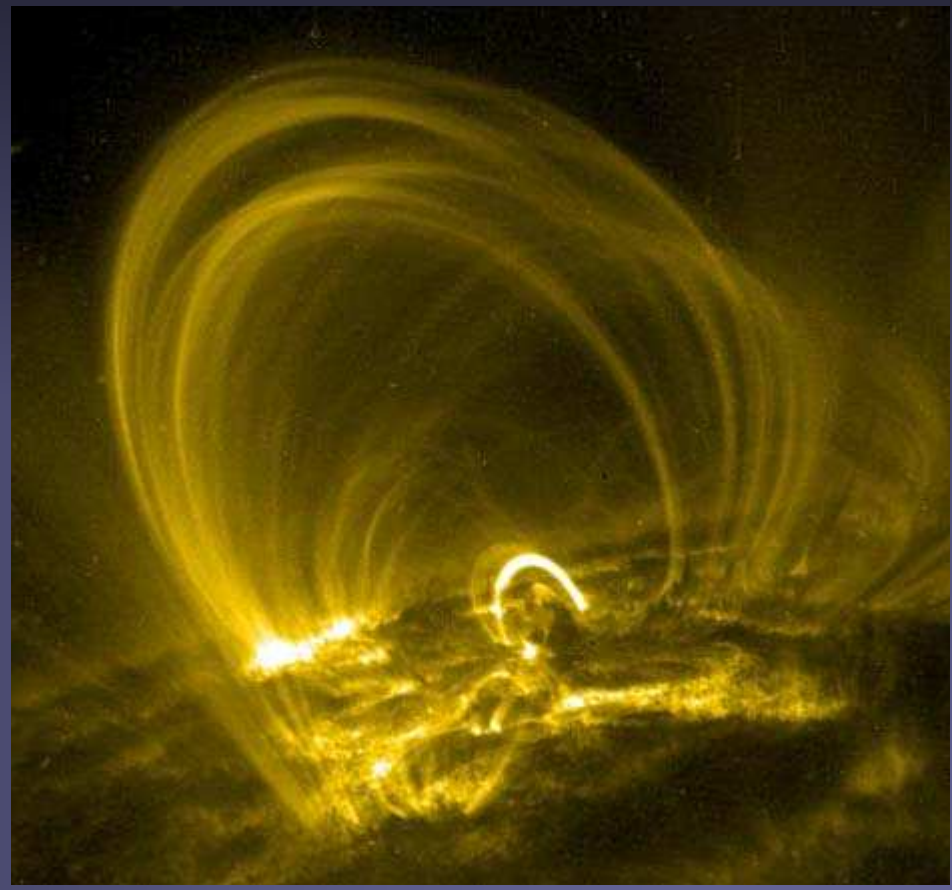

Loops at 0.9MK (TRACE Fe IX 171Å)

Coronal loops in 3-D

Yellow lines: First stereoscopic reconstruction of coronal loops observed by the two STEREO spacecraft looking at the Sun from different directions.

Red lines: magnetic field extrapolations starting from magnetogram on solar surface

Feng et al. 2007

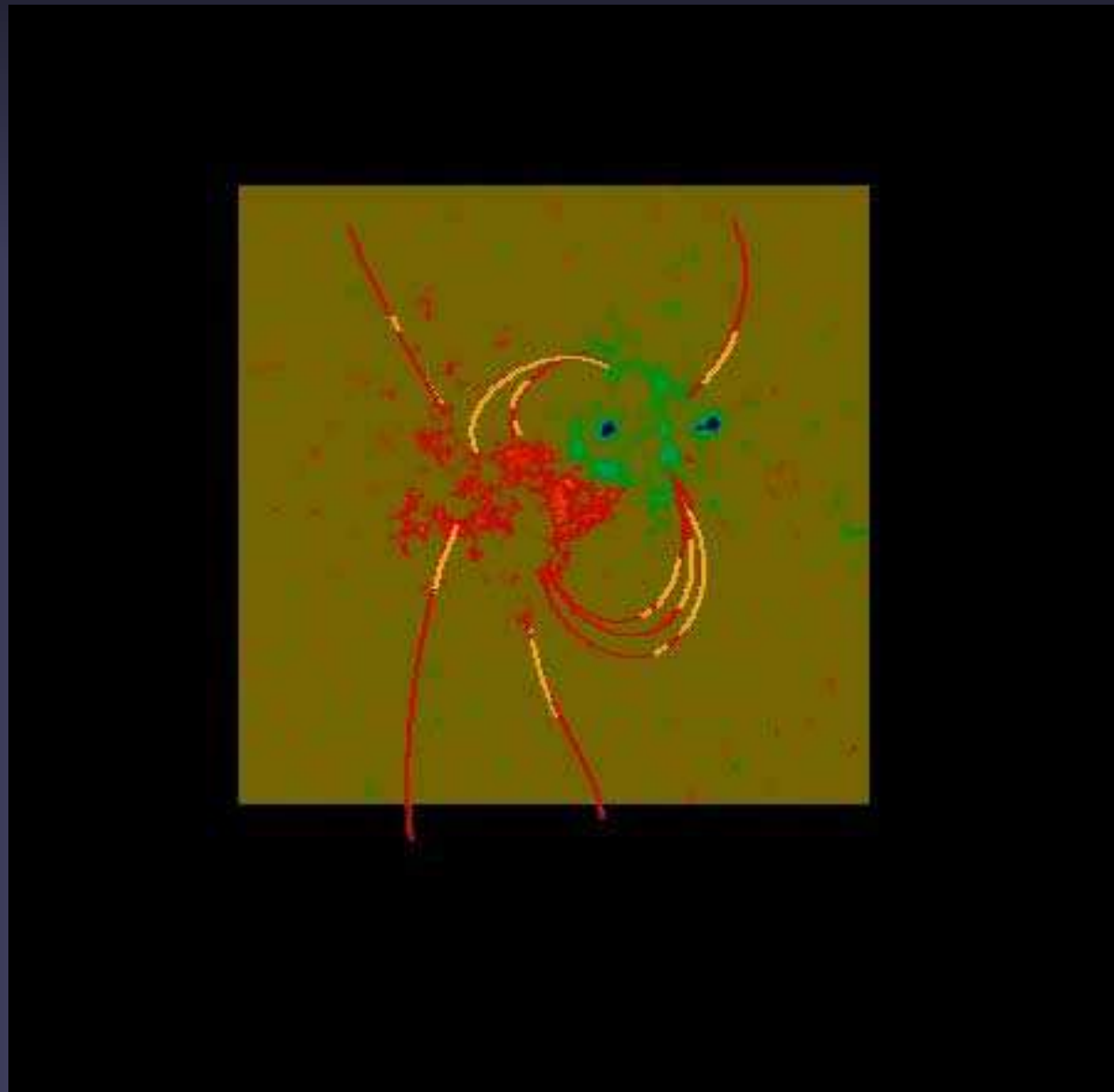

Structure of Cool Magnetic Loops

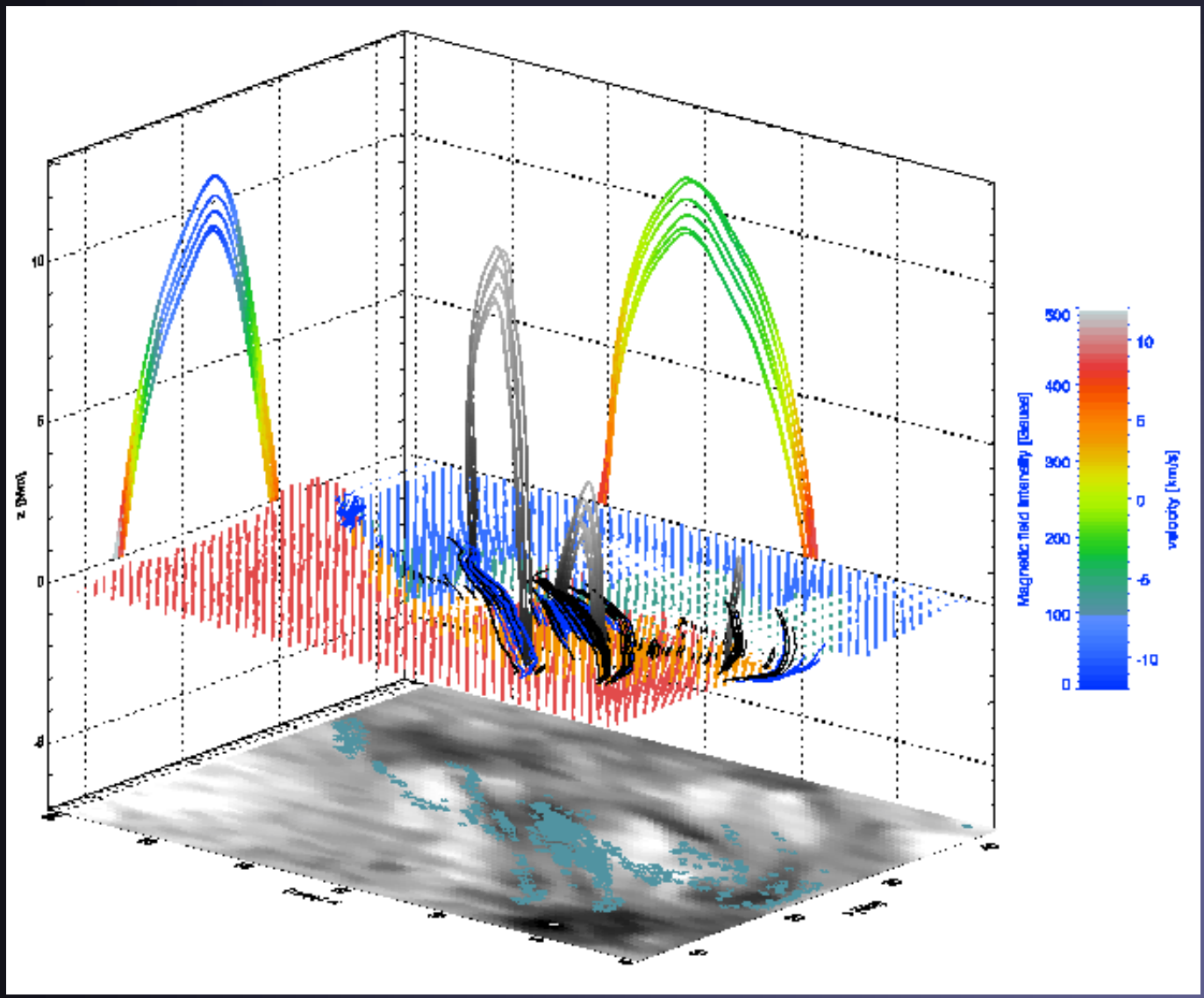

Magnetic loops deduced from measurements of He I 10830 Å

Stokes profiles in an emerging flux region.

Left projection: Field strength

Right projection: Vertical velocity

Andreas Lagg

Magnetic field extrapolations: Force free and potential fields

- General problem in solar physics: Magnetic field is measured mainly in the photosphere, but it makes music mainly in the corona.

→ Either improve coronal field measurements (currently difficult) or extrapolate from photospheric measurements into the corona.

- If $\beta << 1$ then we can neglect the influence of the gas on the field: the field is force-free. Considerable simplification of the computations
- If we further assume that there are no currents, the computations become even simpler (potential field).

Testing Magnetic Extrapolations

- Non-linear force-free fields reproduce the loops reconstructed from observations better than the linear force-free ones and far better than potential field extrapolations.
- Loops harbour strong currents while still emerging.

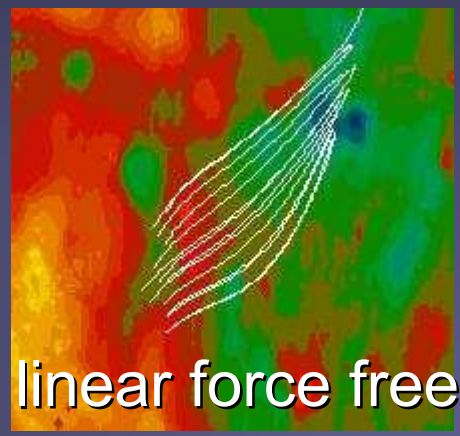

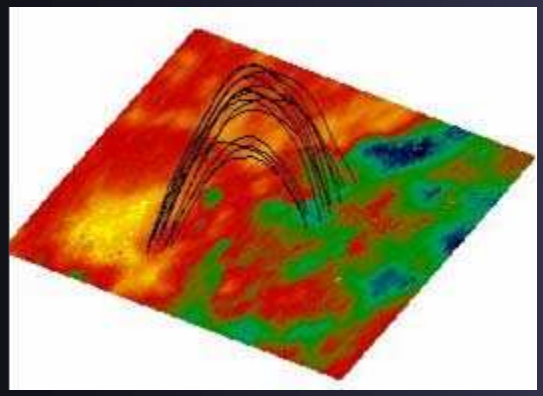

Wiegelmann et al. 2004

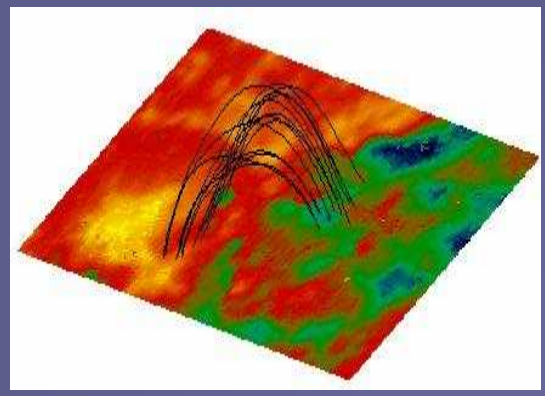

Prominences

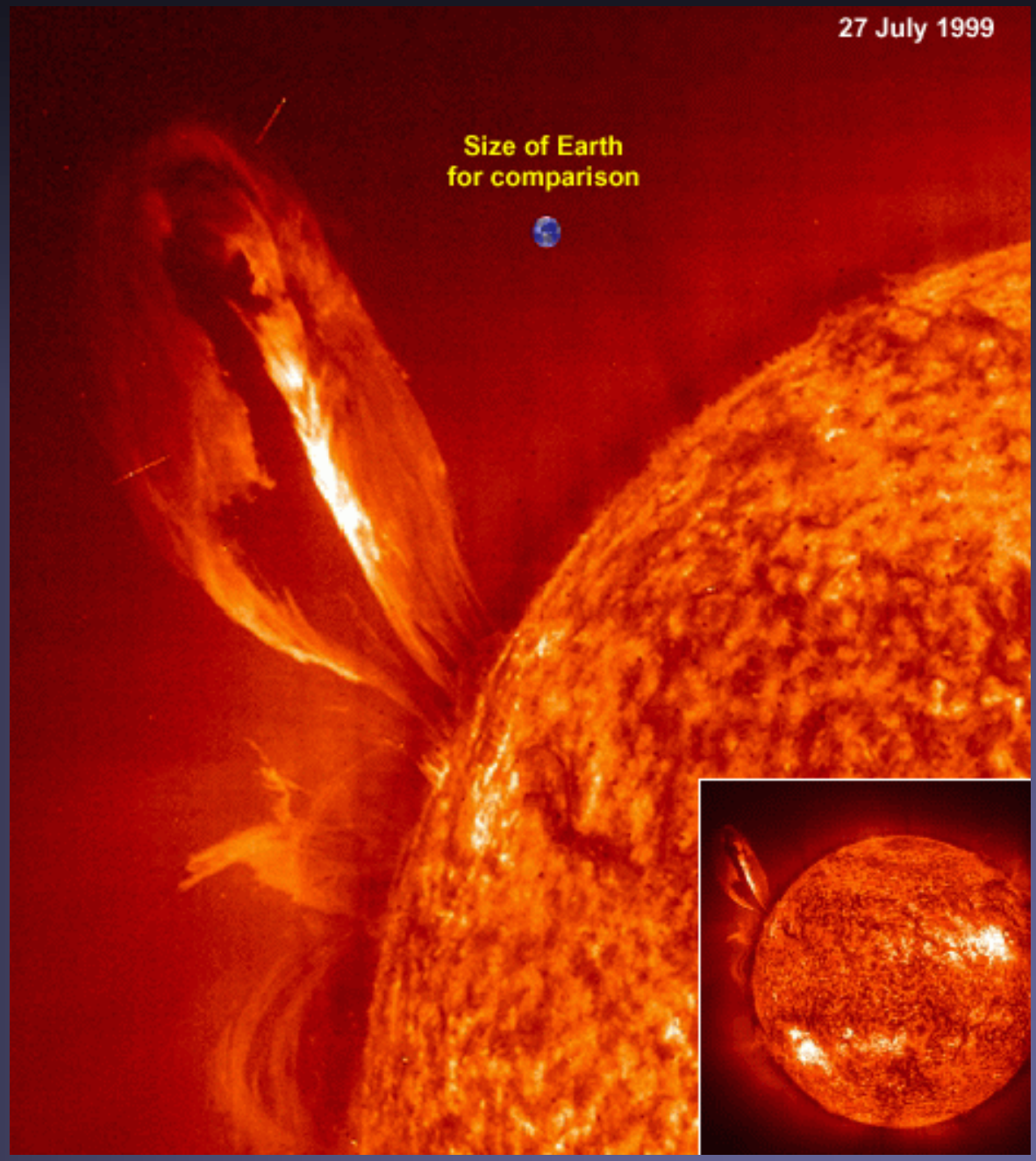

Prominence material supported by magnetic field

- Density of prominence material is orders of magnitude higher than of surrounding corona.
- Gas has to be supported against gravity.
- Magnetic field can provide this support, since ionized gas can only flow along field lines.

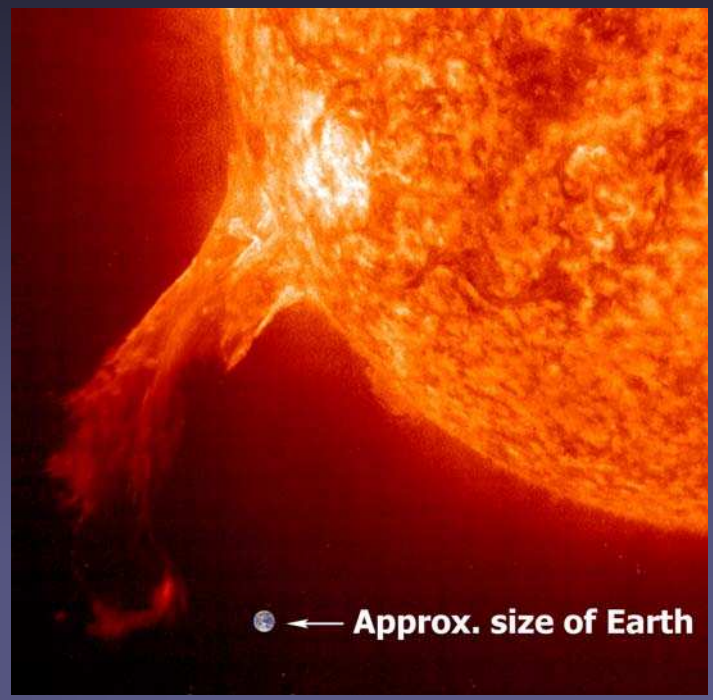

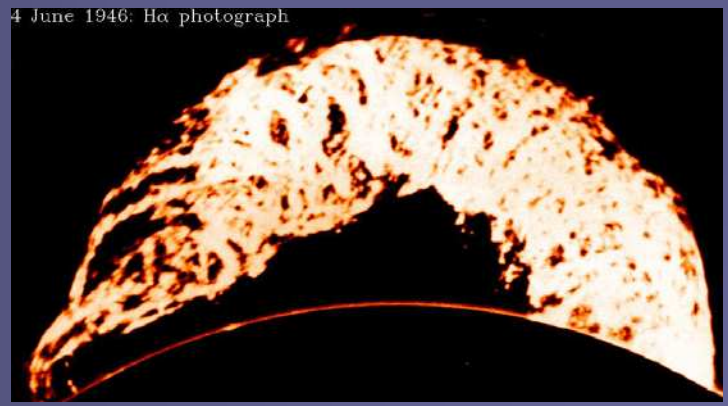

Prominence models

Kippenhahn-Schlüter (below), Kuperus-Raadu (below right) and flux tube (right; 3-D Kuperus-R.)

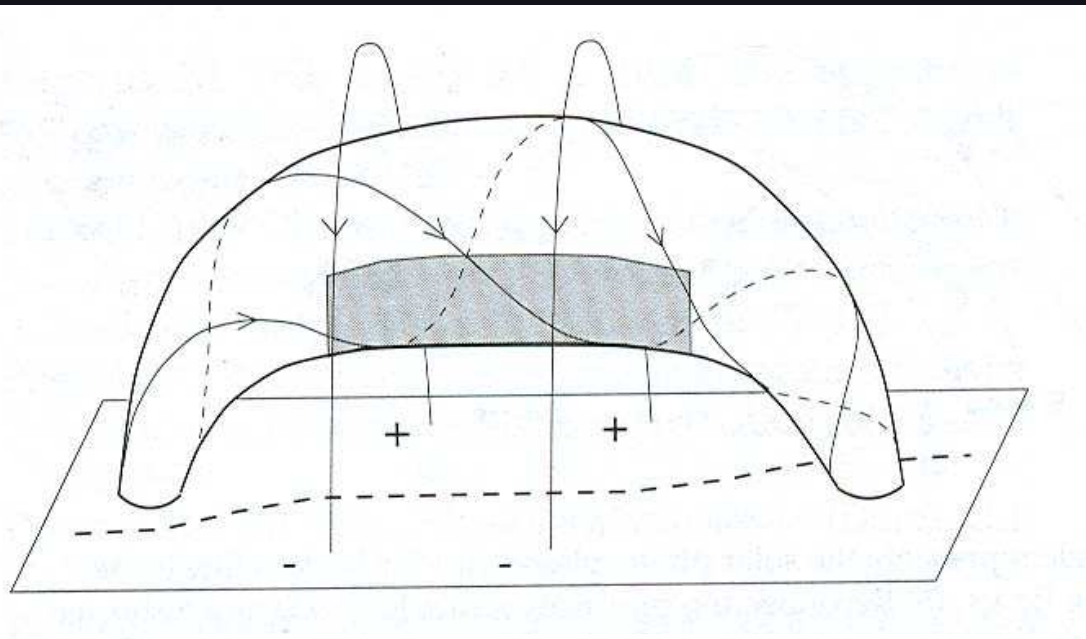

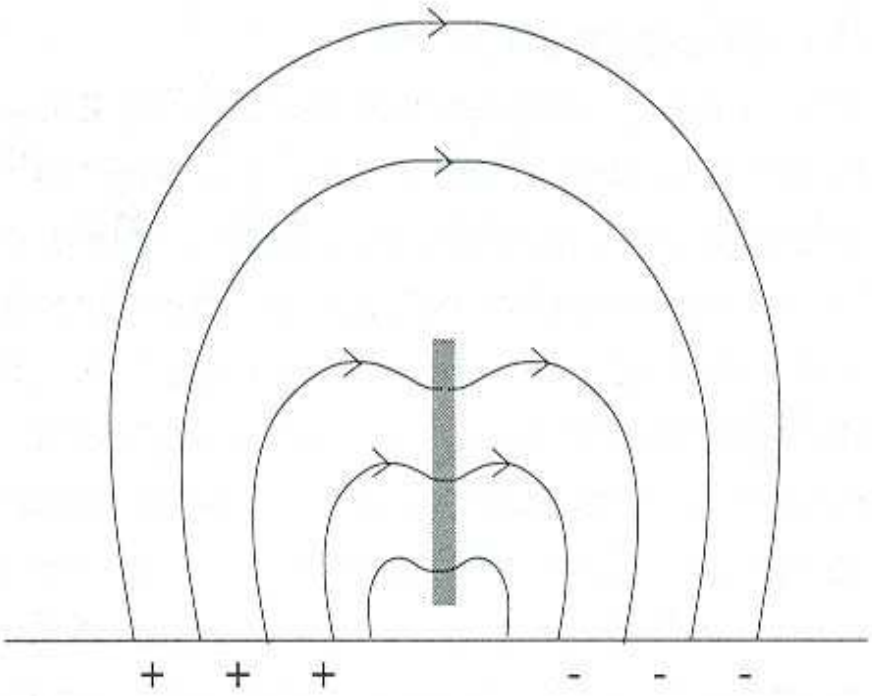

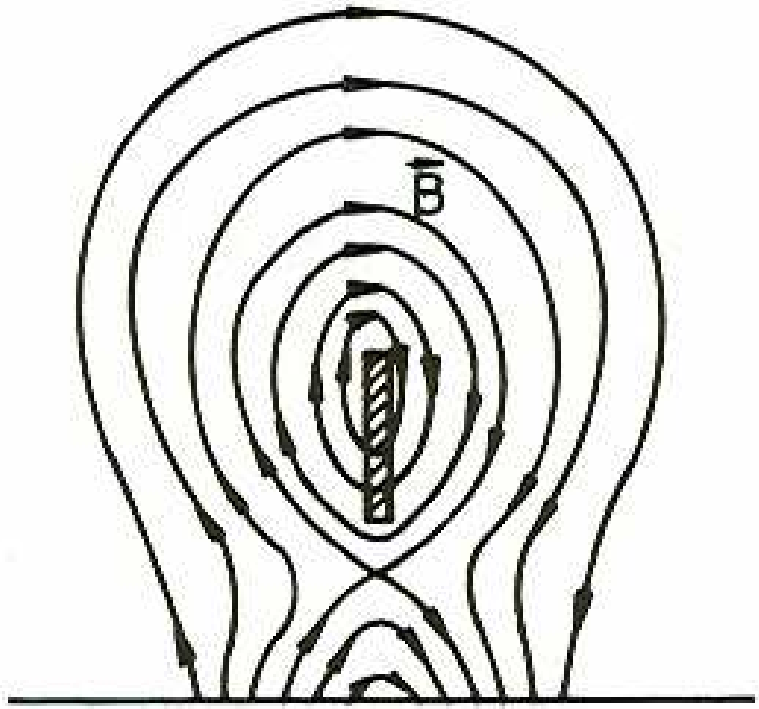

Large scale magnetic structure of the quiet Sun

- At large scales only dipolar component of magnetic field survives, since multipoles ➔ $B \sim r^{-n-1}$, where n=2 for dipole, n=3 for quadrupole, etc.
- Closer to sun ever higher order multipoles are important

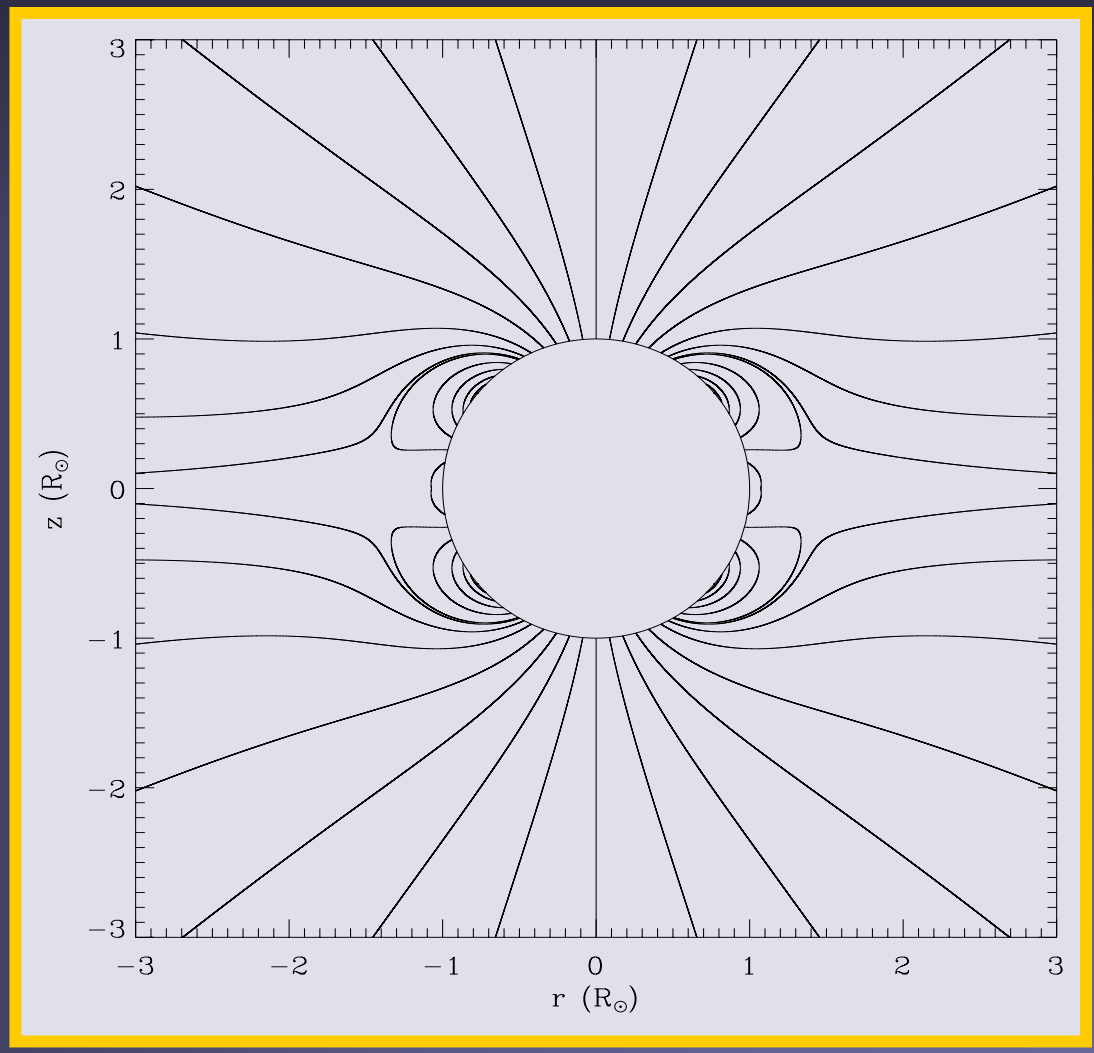

Solar current sheet at activity minimum

- At activity minimum solar magnetic field is like a dipole, whose field lines are stretched out by the solar wind.
- Field lines with opposite polarity lie close to each other near equator: euatorial current sheet.
- If dipole axis inclined to ecliptic: magnetic polarity at Earth changes over solar rotation.

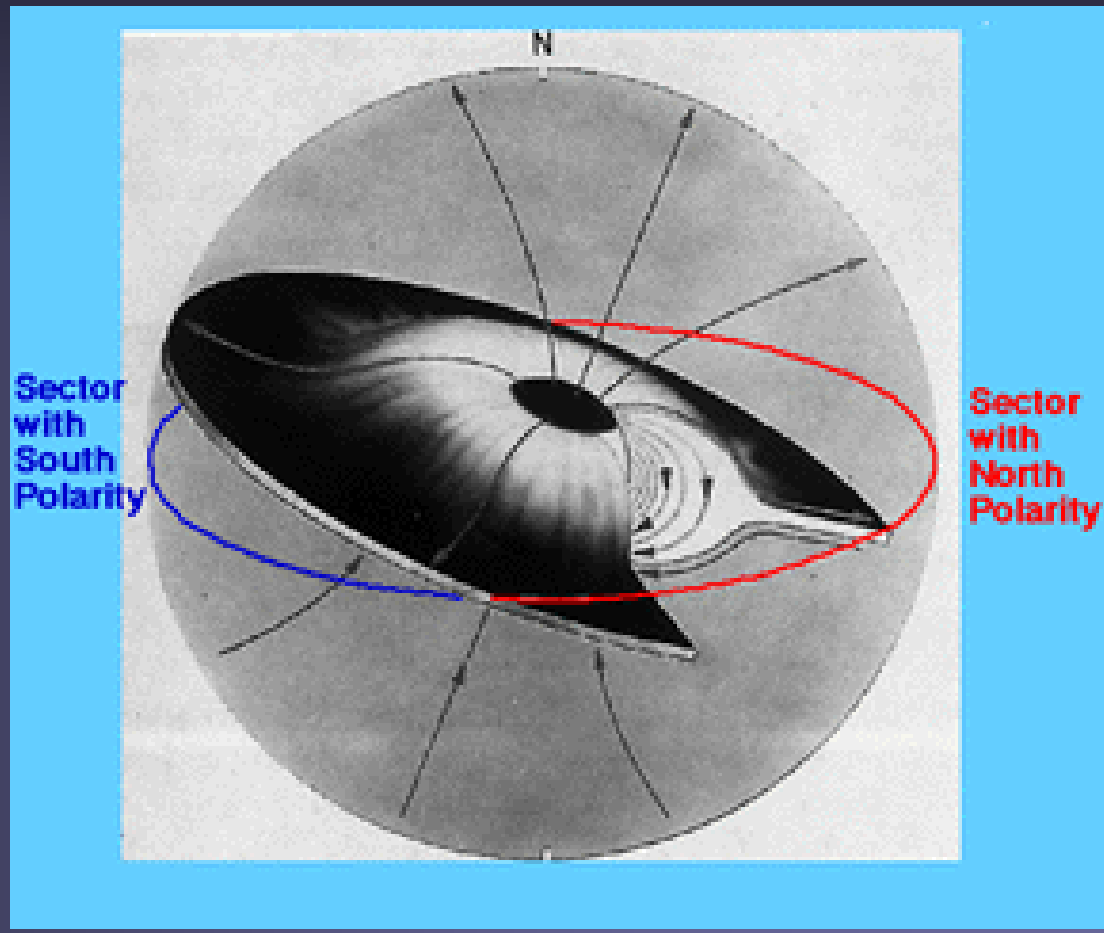

Heliospheric current sheet and Parker spiral

- Since solar wind expands radially beyond the Alfven radius (where the energy density in the wind exceeds that in the magnetic field) and the Sun rotates (i.e. the footpoints of the field), the structure of the field (carried out by the wind, but anchored on rotating surface) shows a spiral structure.

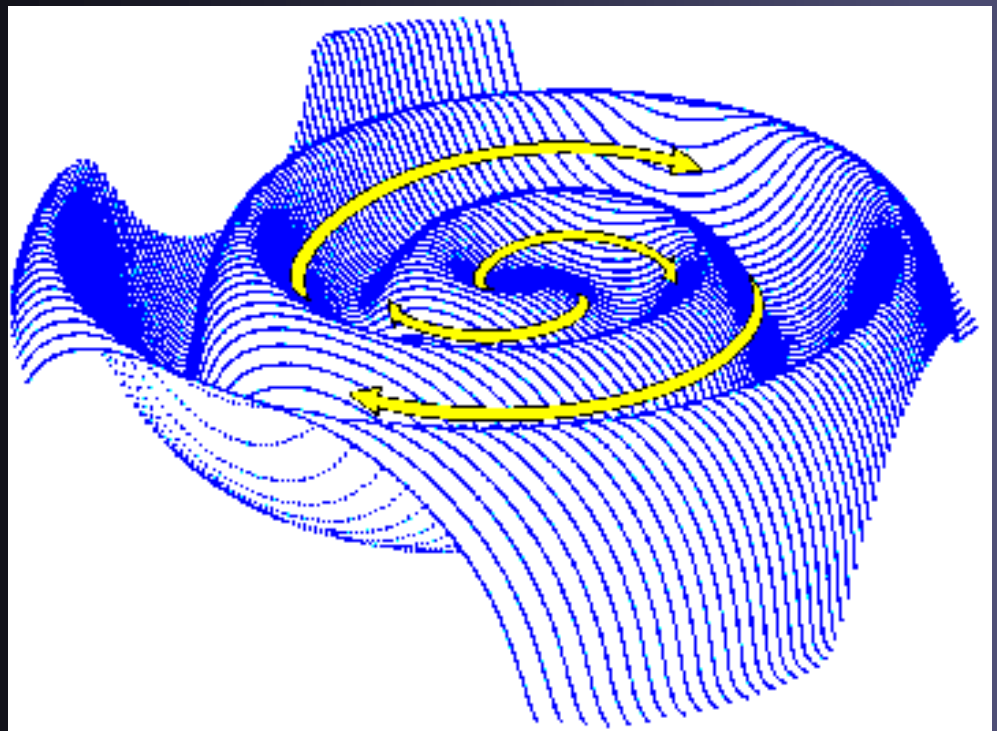

The Sun-Earth Connection

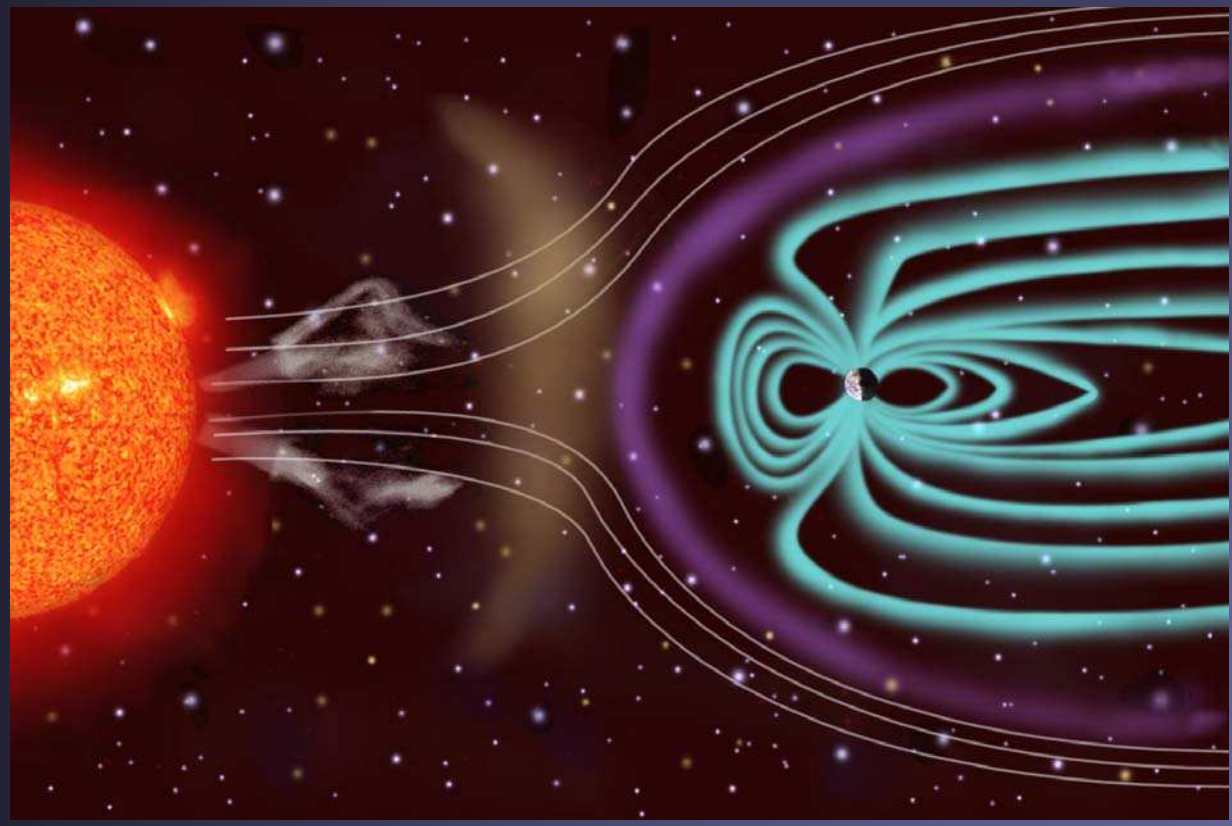

Solar influence on Earth

The variable activity of the Sun affects Earth in many ways:

short

- "Space weather": Disturbances in the Magnetosphere, Ionosphere, Upper atmosphere
- Satellite systems, Communication and Energy supply

long

- Global climate change
- Modulation of galactic cosmic rays hitting Earth

Space Weather

- Cause: variability of Sun & solar wind
- Solar components: solar energetic electro-magnetic (UV, X-rays, γ-rays) & particle radiation (eV to MeV)

- Affected natural systems: Earth's magnetosphere, ionosphere, thermosphere, stratosphere
- Technical systems in space & partly on Earth affected
- Potential health hazard: astronauts, airplane passengers & crew, inhabitants at high latitudes (ozone hole)

Causes of Space weather

- Variations of the solar electromagnetic radiation, in particular UV and X-radiation
- Solar wind
- Suprathermal particles (particle energies of eV)
- Energetic particles (keV to MeV)
- Cosmic rays (MeV to GeV)
- Meteorides, interplanetary dust, galactic Gamma-Ray-Bursts, etc.

From Sun

Other sources

The Sun and Space Weather: CMEs

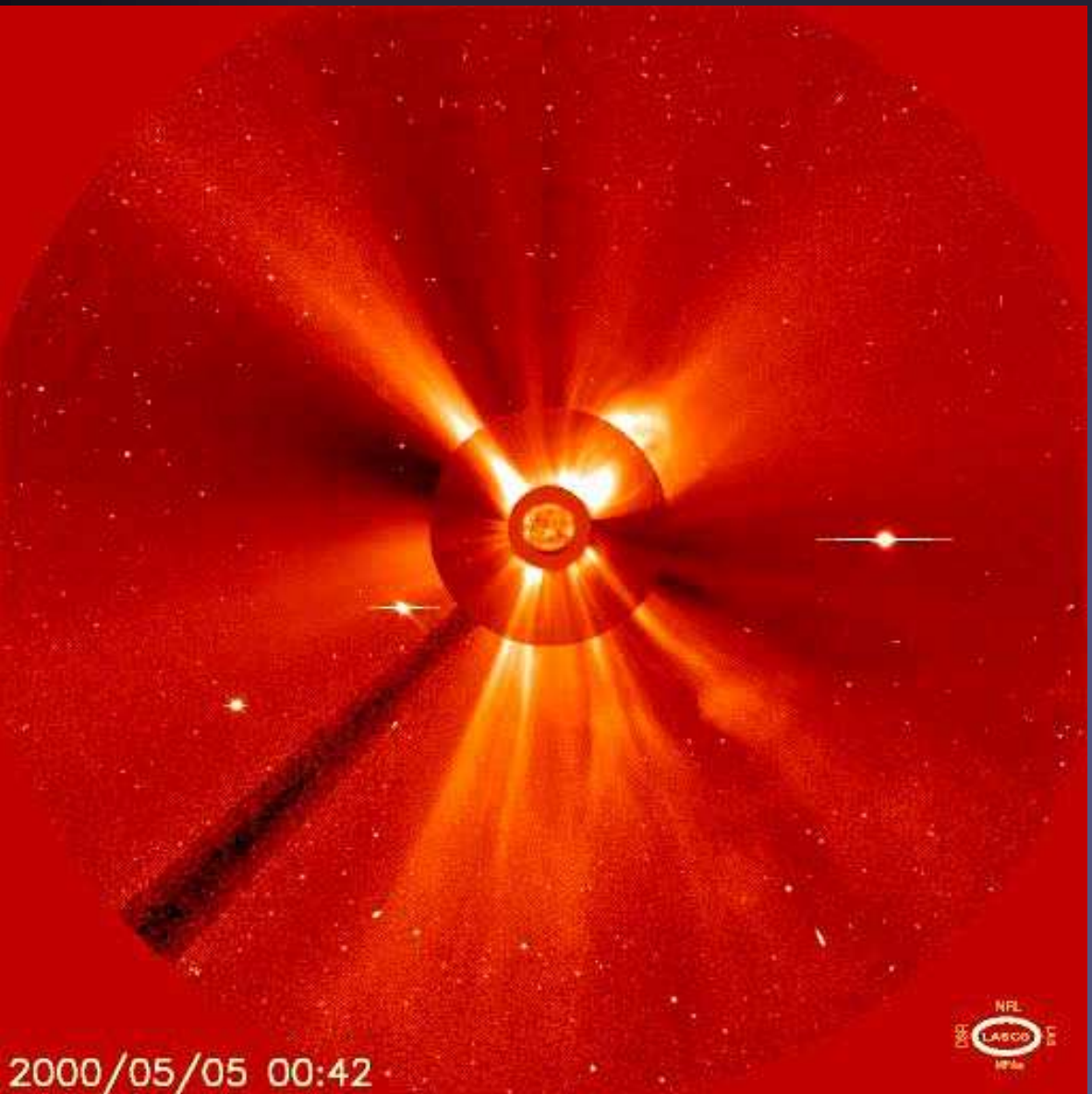

Composite of Sun and its extended corona (LASCO C2 + C3 EIT 304 Å)

Bright, overexposed dots are planets (Mercury, Venus, Jupiter, Saturn), fainter background objects are stars

R. Schwenn

Halo CMEs

Halo CMEs:

CMEs directed towards (or away from) Earth. The main cause of Space Weather.

Most difficult to detect! Most difficult to predict propagation speed.

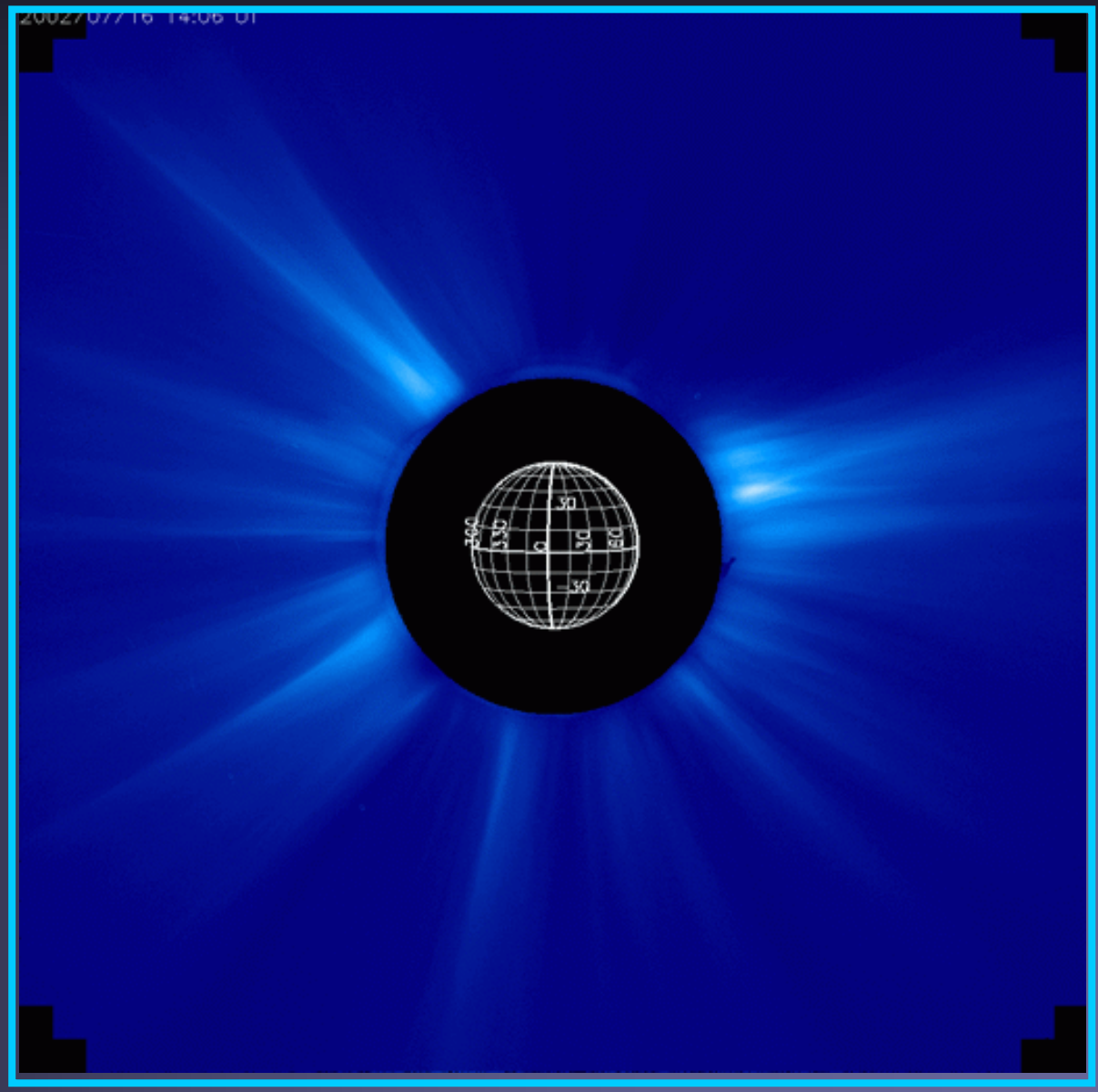

Effect of a CME directed to Earth

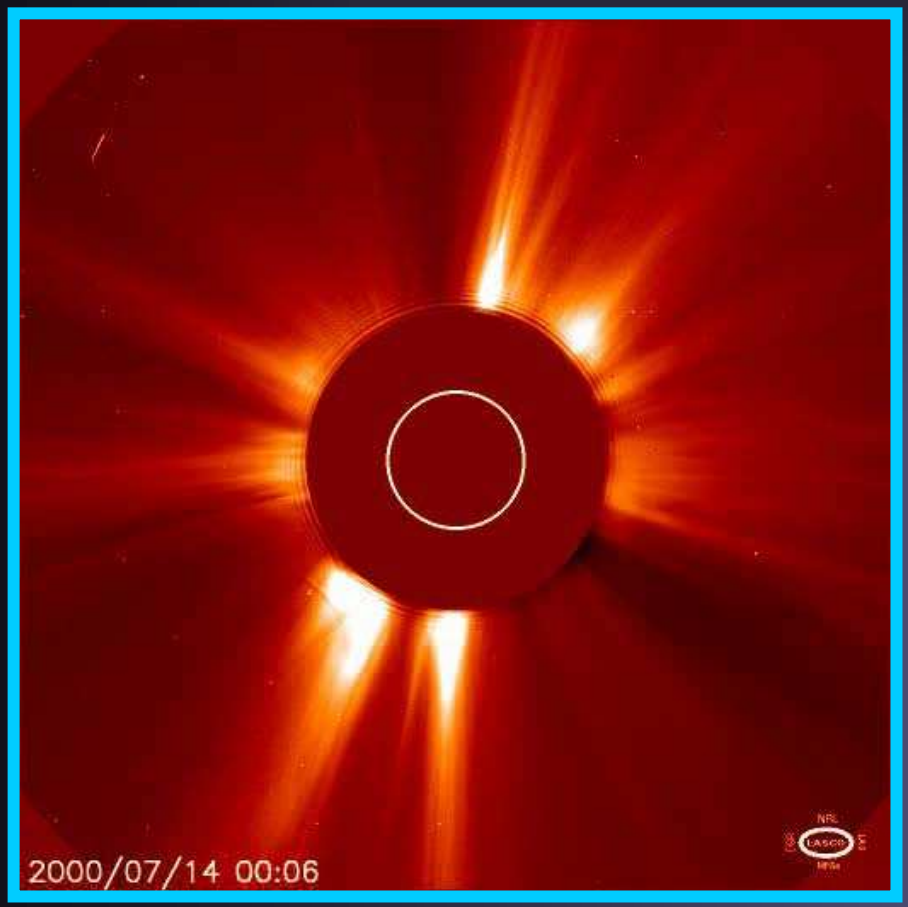

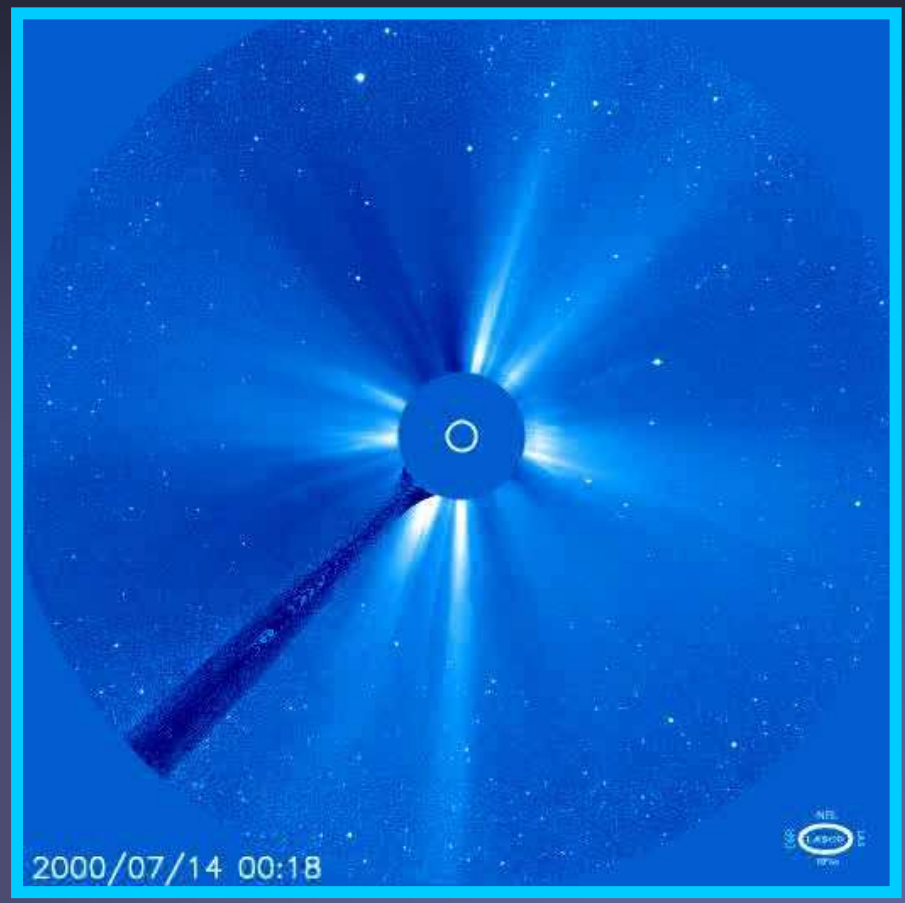

The largest solar particle events appear to result from shock associated coronal mass ejections (CMEs)

Interaction of Solar Wind with Magnetosphere of Earth

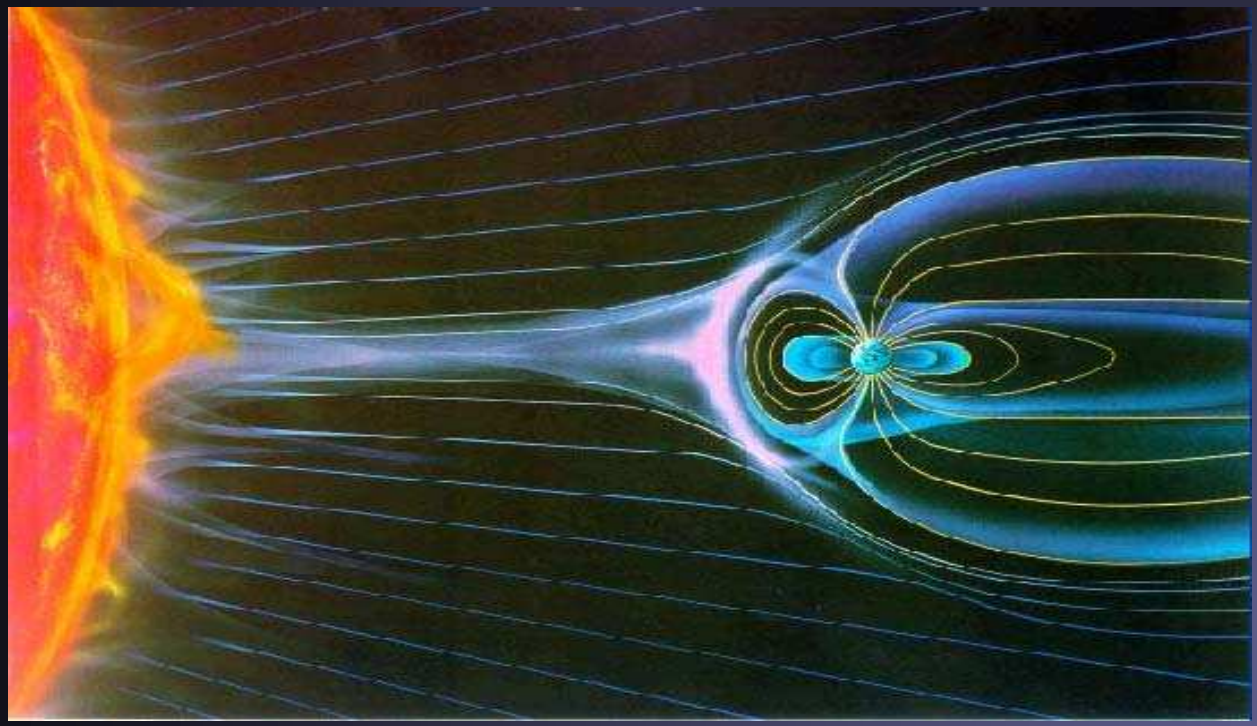

North

IMF - B_z Earth - B

South

Induced electric field: $\underline{E} = - \underline{V} \times \underline{B}$

Effective energy transfer into Magnetosphere in presence of southward component of IMF (e.g. through CMEs, CIRs, waves)

Geomagnetic Storm

Simulation of reaction of magnetosphere to passage of CME launched 6.1.97

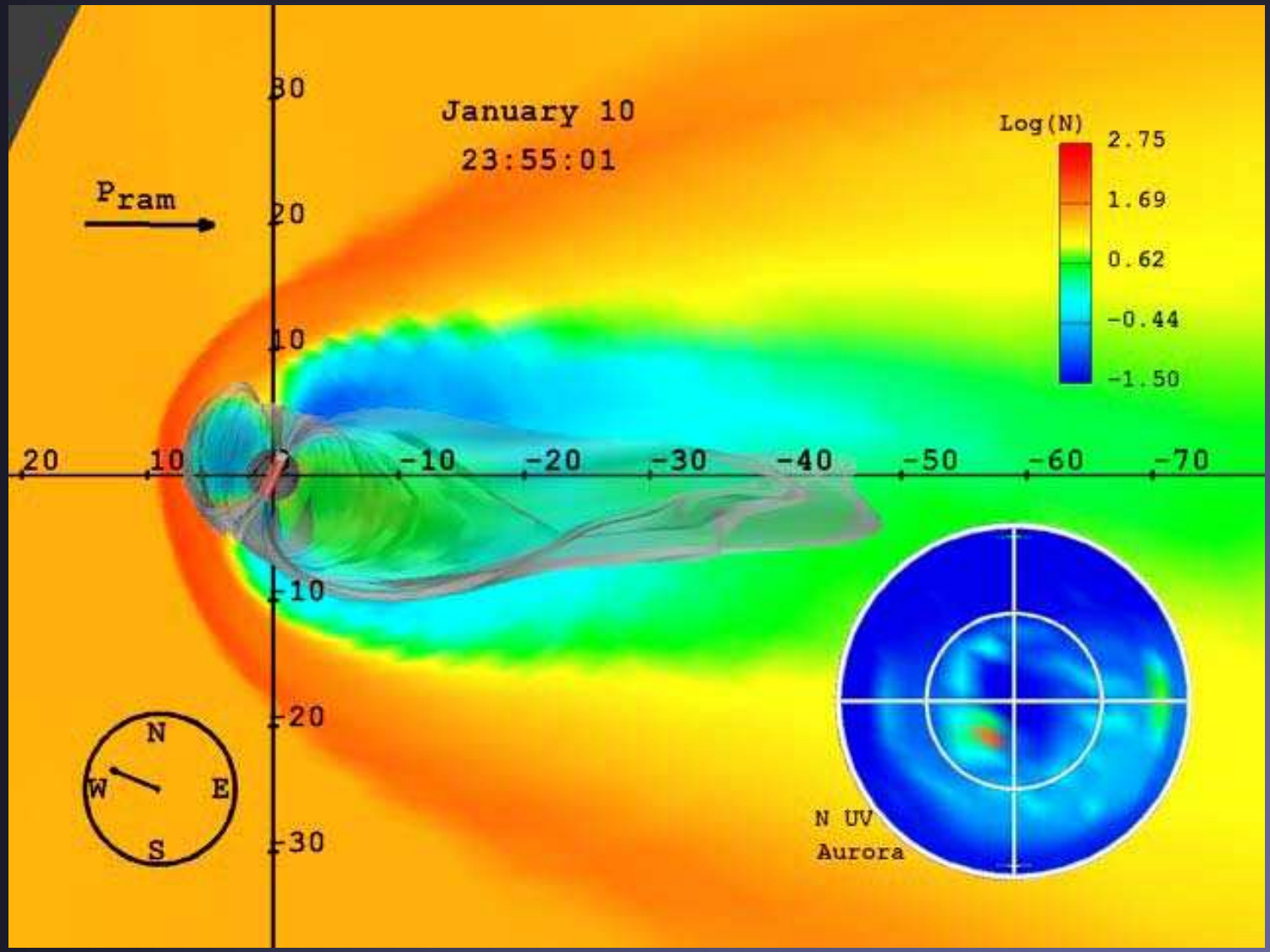

IMF B direction

Avge. solar wind speed: 410 km

Goodrich et al. 1998 GRL

Space Weather: the Aurora

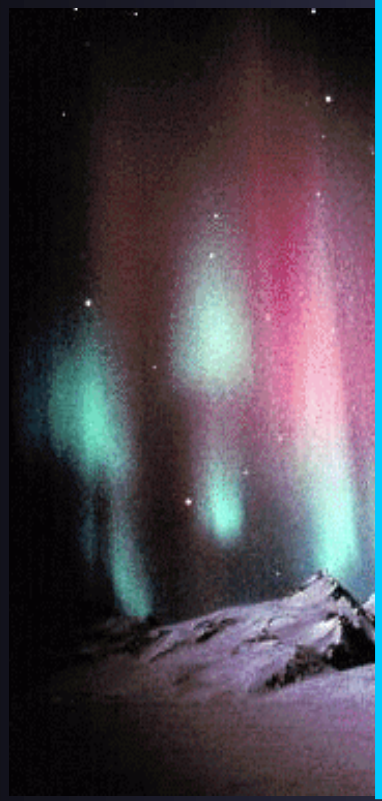

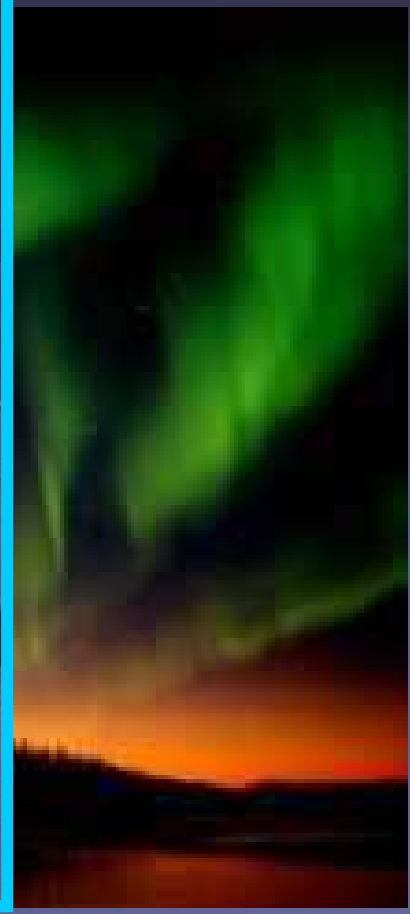

Influence of Solar Activity on Technical Systems

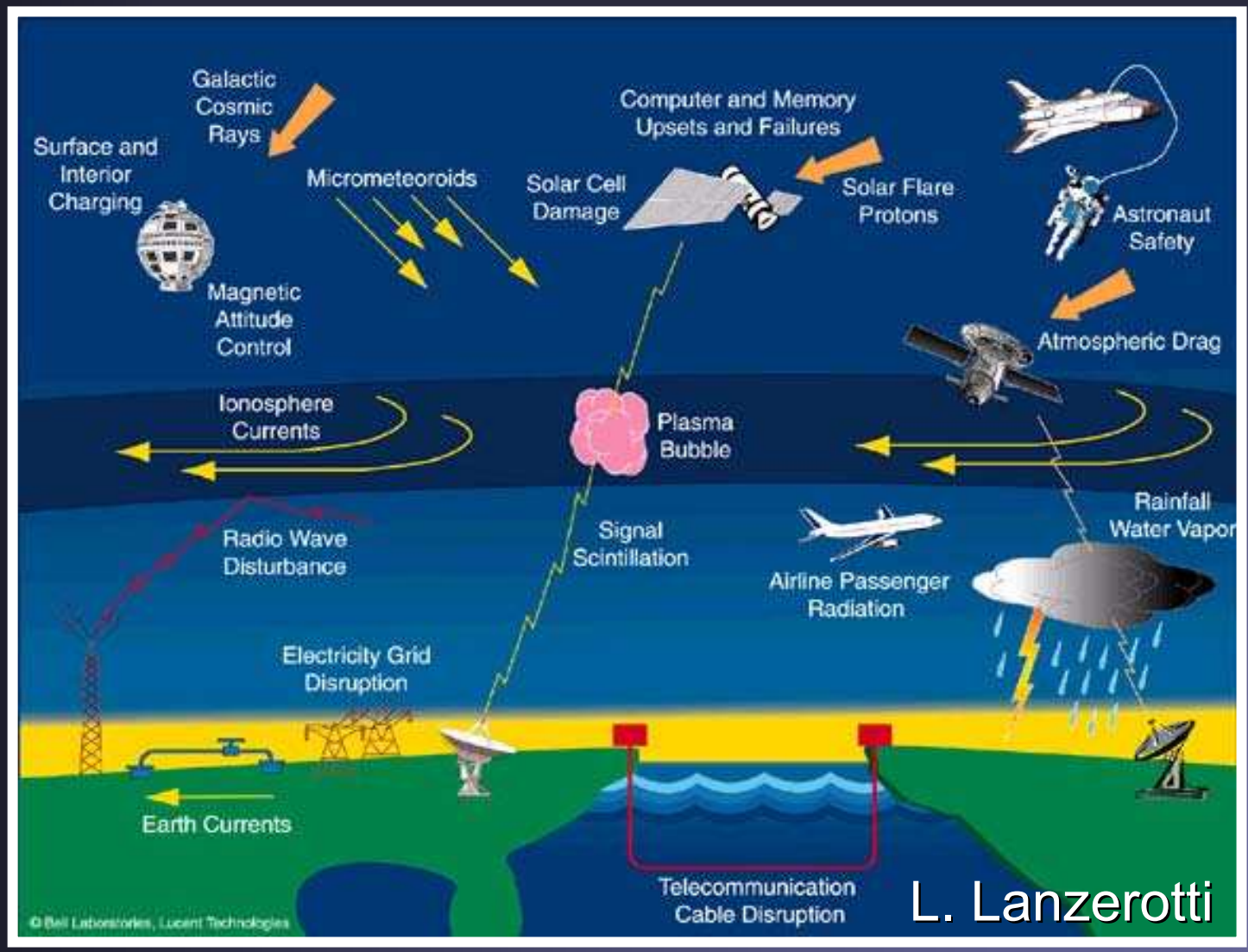

Ionospheric heating by UV radiation

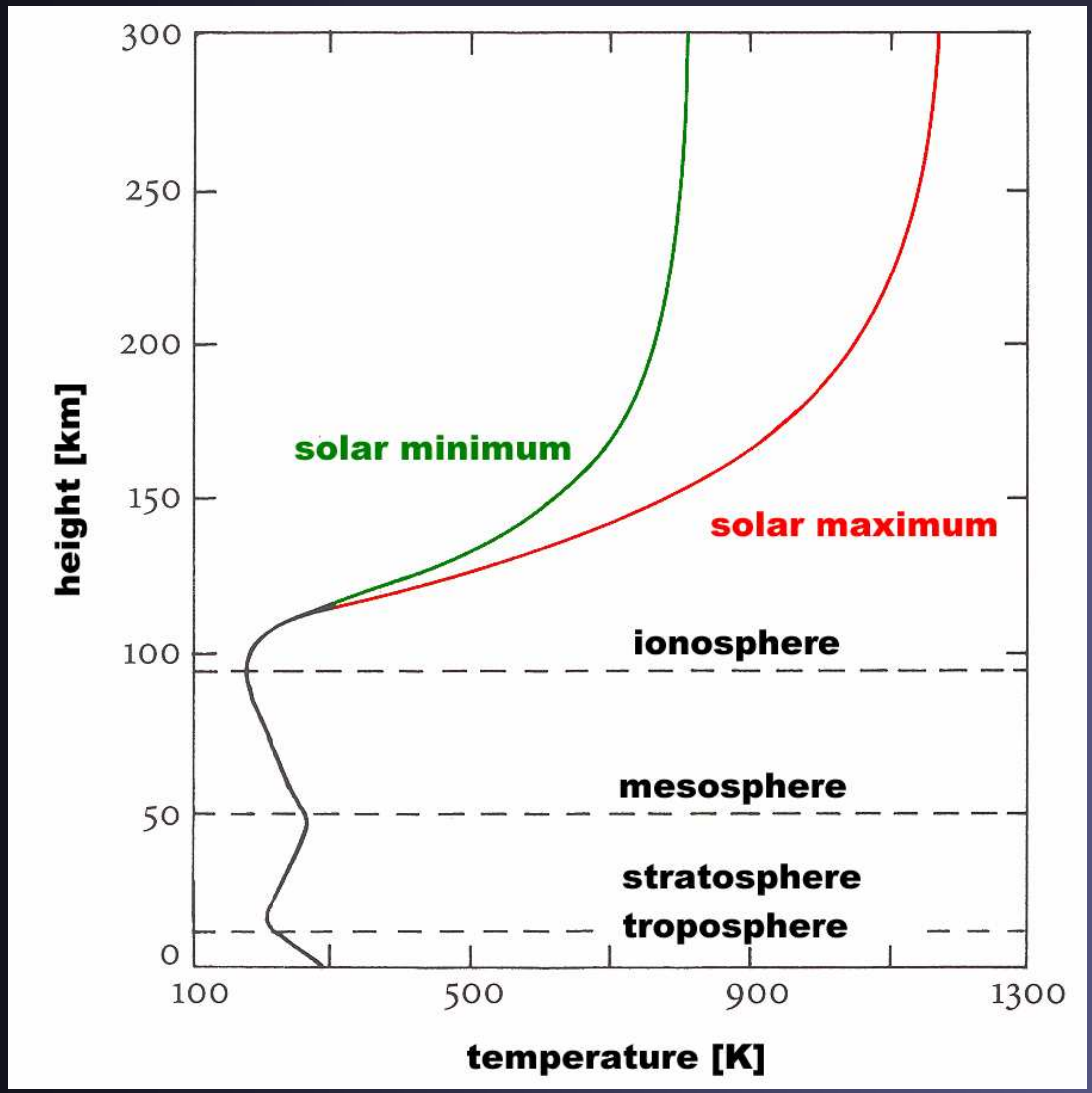

Most important solar radiation component is Lyα, whose strength changes by roughly a factor of 2 over a solar cycle.

Larger temperature means larger scale height: ionosphere expands

Increased Drag on Satellites

- Expanding atmosphere causes increased drag on low orbit satellites. They loose altitude & non-symmetrical satellites can start tumbling
  - Skylab re-entered several years earlier than planned
  - Hubble Space Telescope drops 10-15 km per year (Re-boosted by the Shuttle

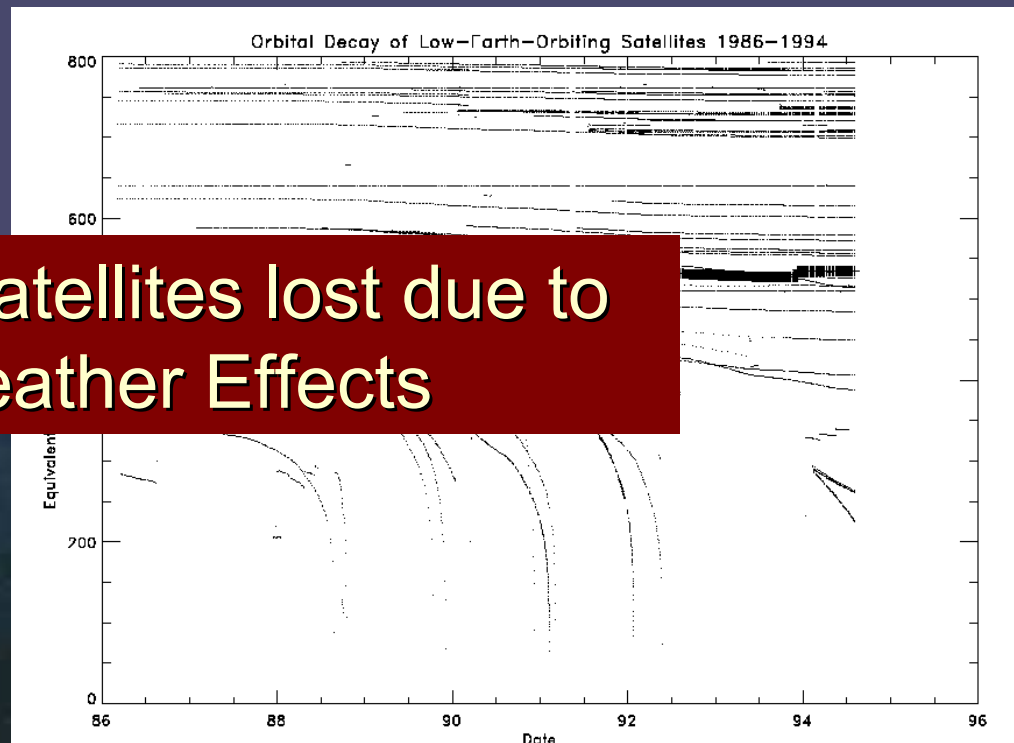

More than 12 satellites lost due to Space Weather Effects

Astronaut safety

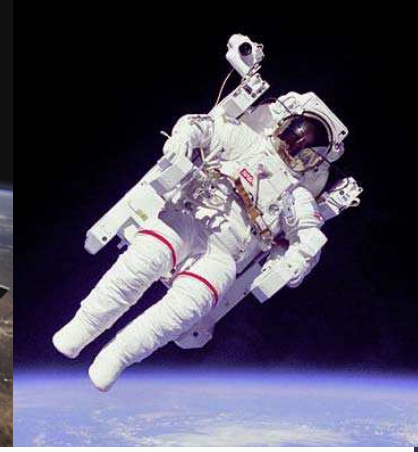

- Astronauts are particularly at risk
- The Earth's magnetosphere helps to protect the astronauts on, e.g. the ISS.
- Astronauts travelling to the moon etc. are very much at risk, however.

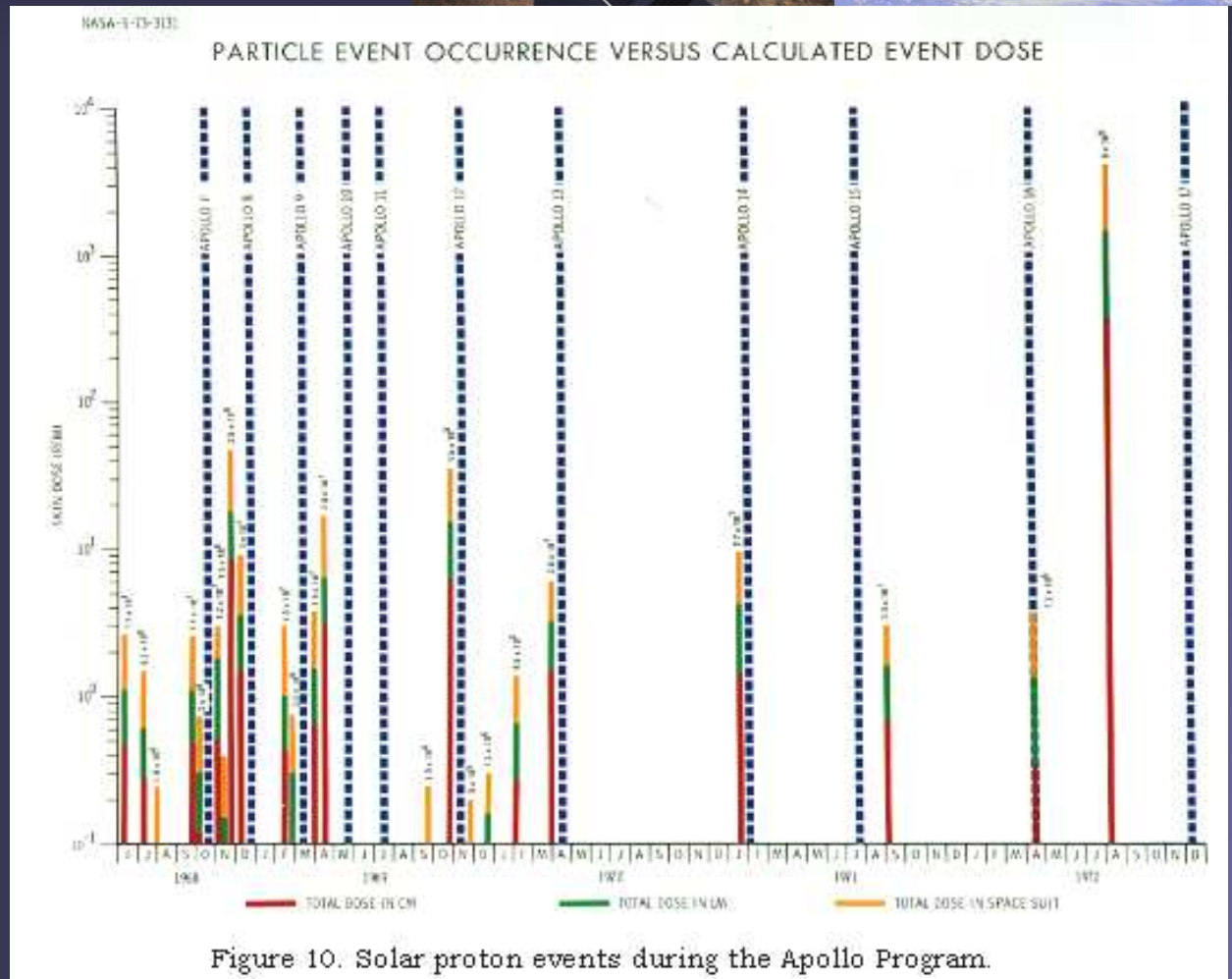

Figure 10. Solar proton events during the Apollo Program.

Bright Sun causes dark night

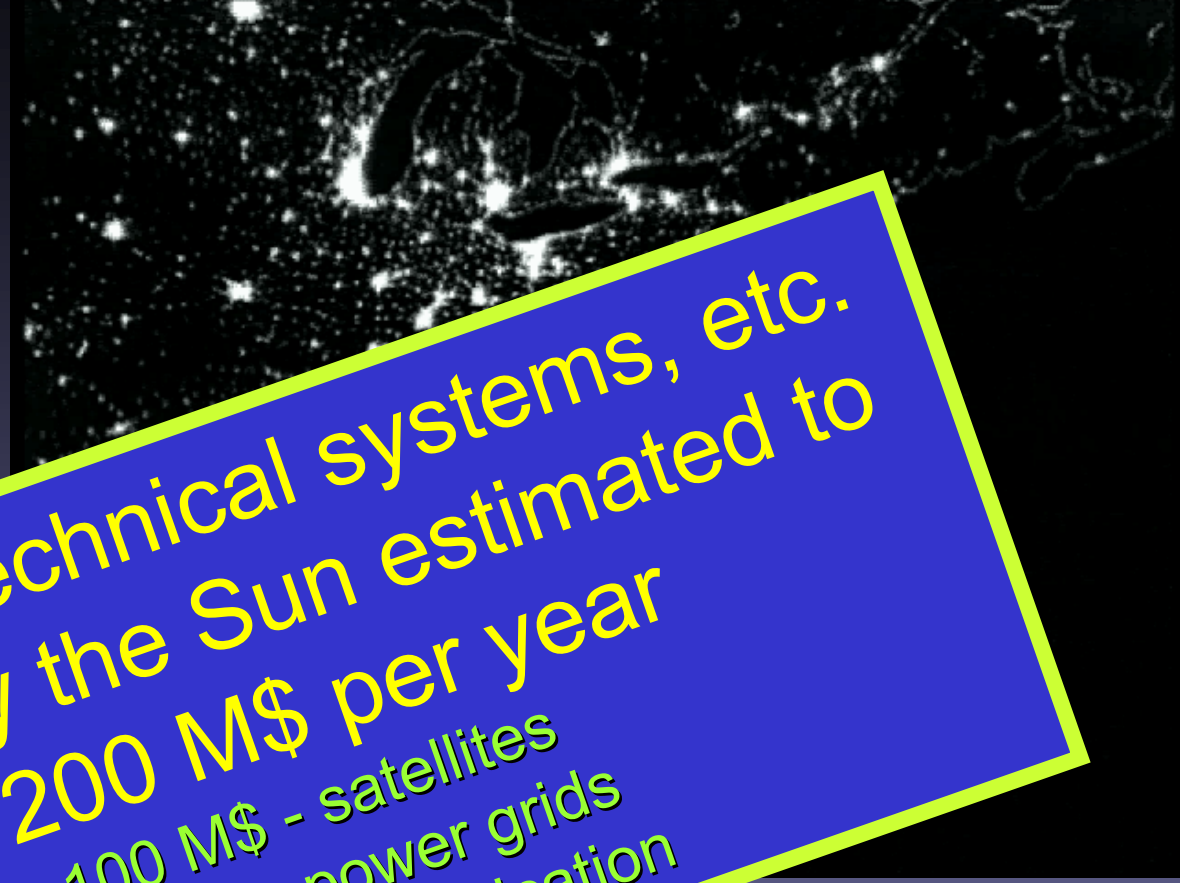

Blackout in C
and N
so
tra
last

Damage to technical systems, etc. produced by the Sun estimated to be > 200 M$ per year

100 M$ - satellites
100 M$ - power grids
10 M$ - communication

- S ations growing most rapidly
- Na largely satellite based: GPS, Galileo
- Sate oads increasingly sensitive
- Humans in Space: more and longer manned missions
- **Importance of Space Weather warnings will increase**

Does the Sun influence climate?

Answer depends on the considered time scale

- Time scales of billions of years: yes! The Sun's evolution makes it increasingly brighter (see sect. on solar interior)
- Time scales of 10^5-10^6 years: Ice ages are probably caused by changes in the Earth's orbital parameters (although changes in the Sun's radiative output may play a role).
- Time scales of centuries to millenia: there are increasing indications of a solar contribution to global climate change
- Shorter time scales: unclear

Climate evolution: the broader view

- The Earth today is cooler by 4-6 K than it was 10 Myears ago

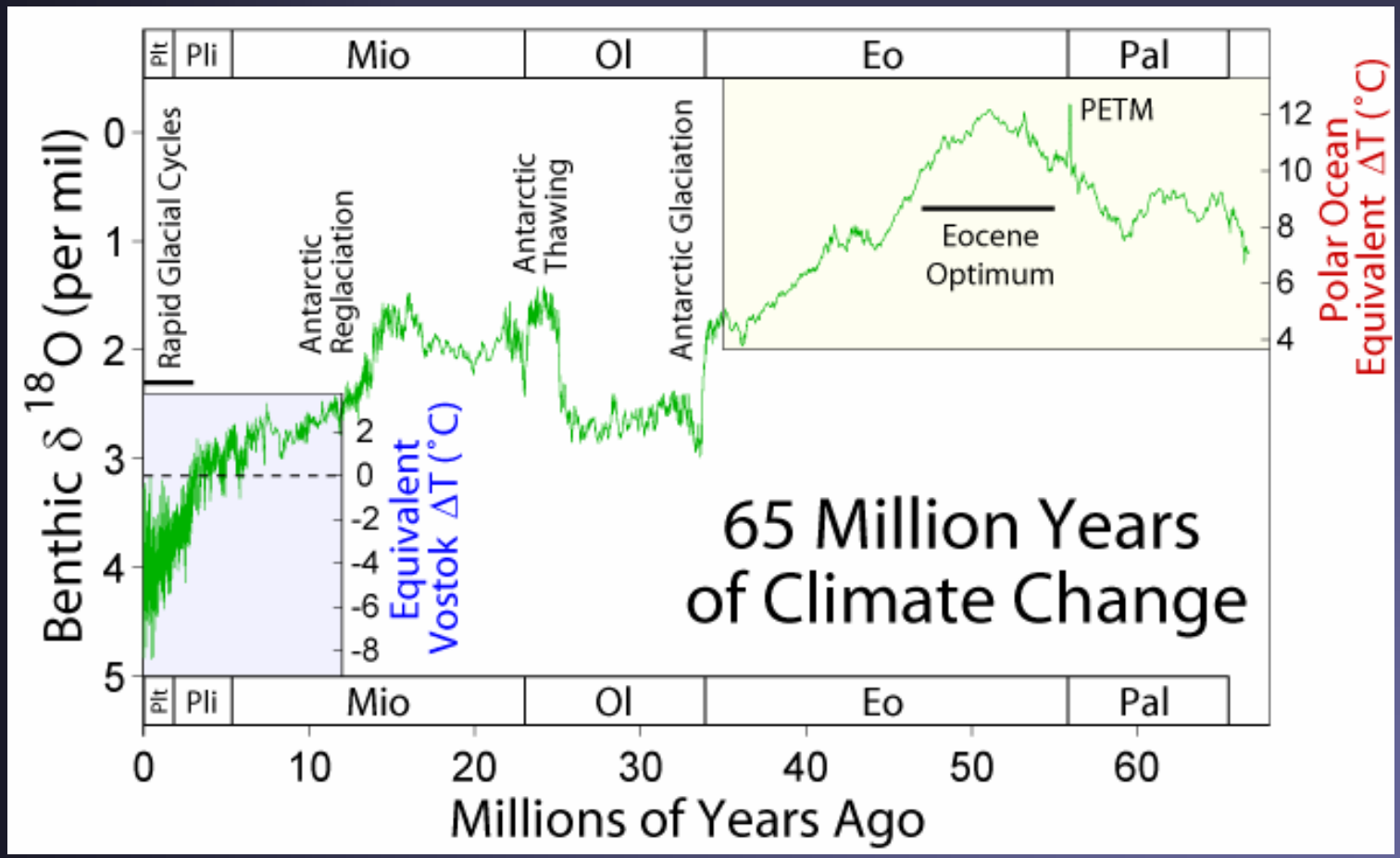

Ice ages and warm periods

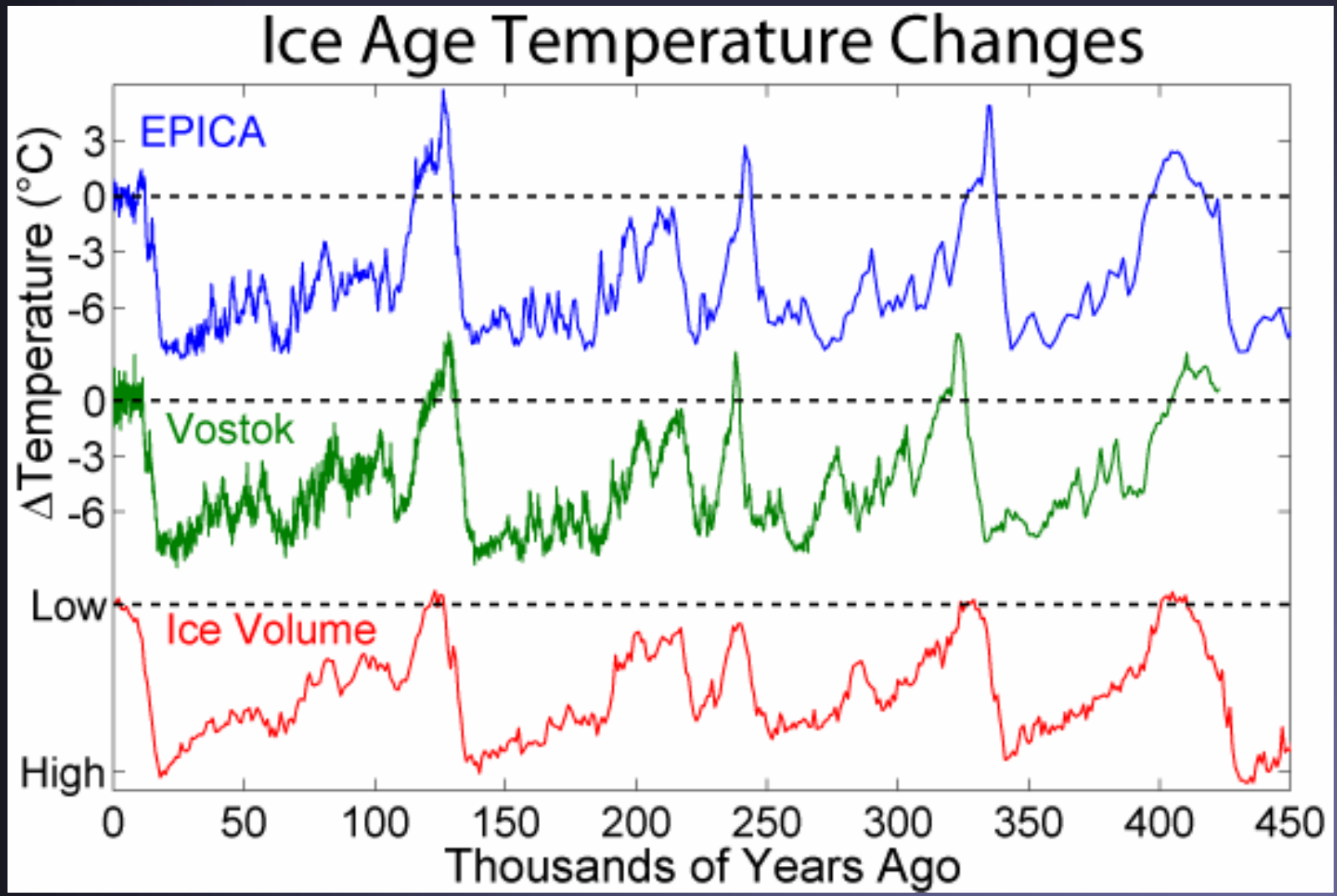

Accumulation of $\delta^{18}O$ in Greenland ice

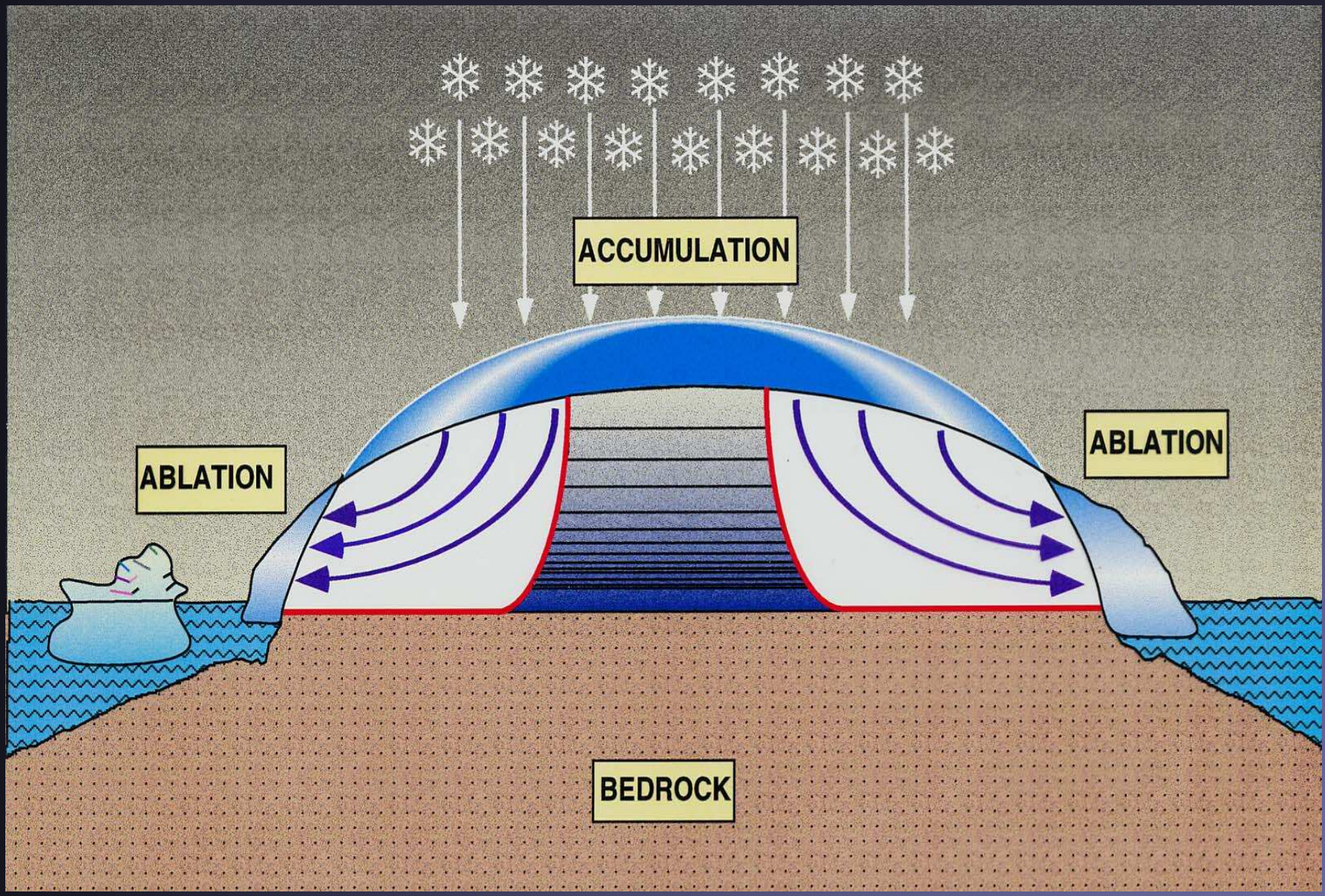

$\delta^{18}O$ signatures in Greenland ice

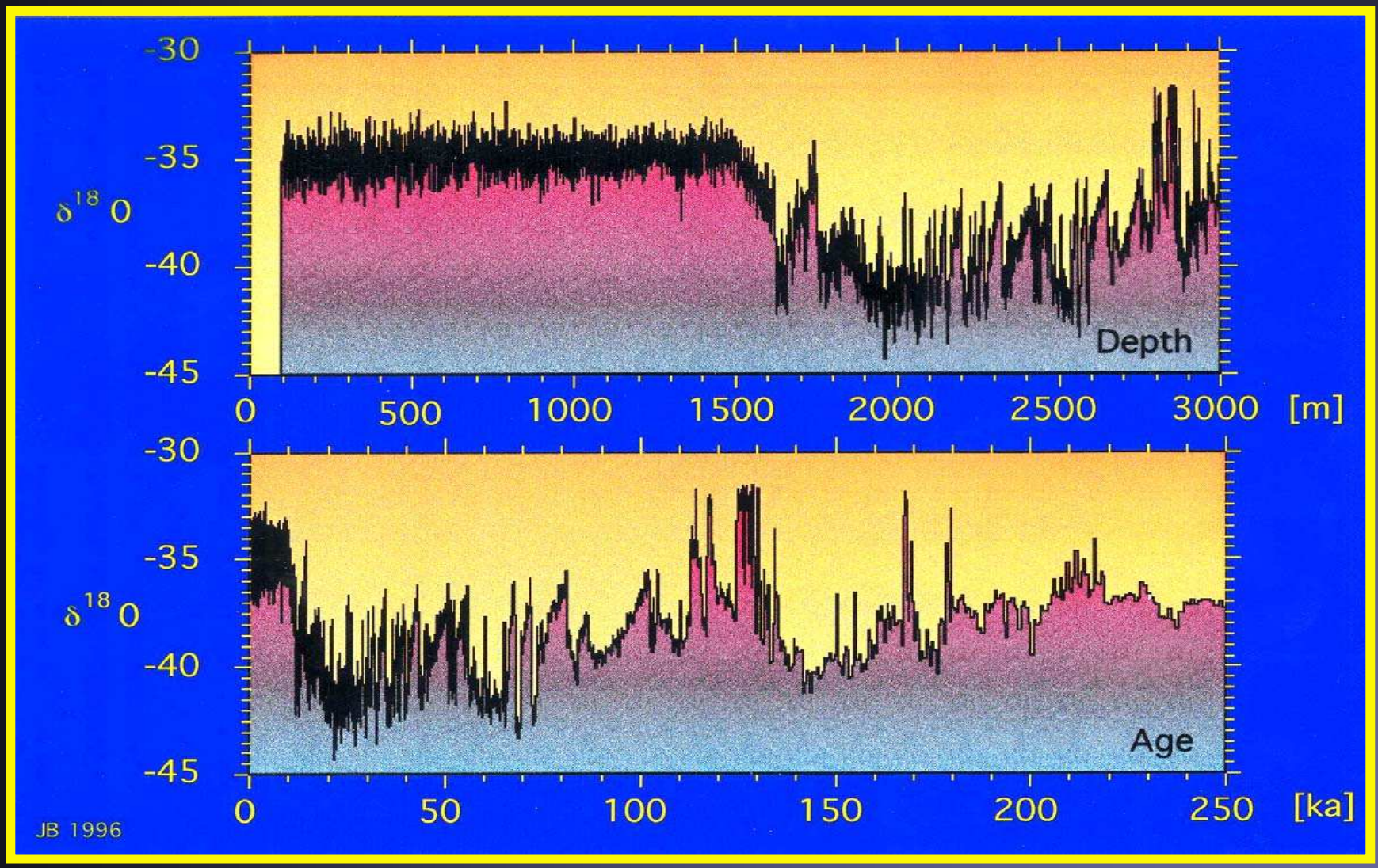

Ice ages and warm periods II

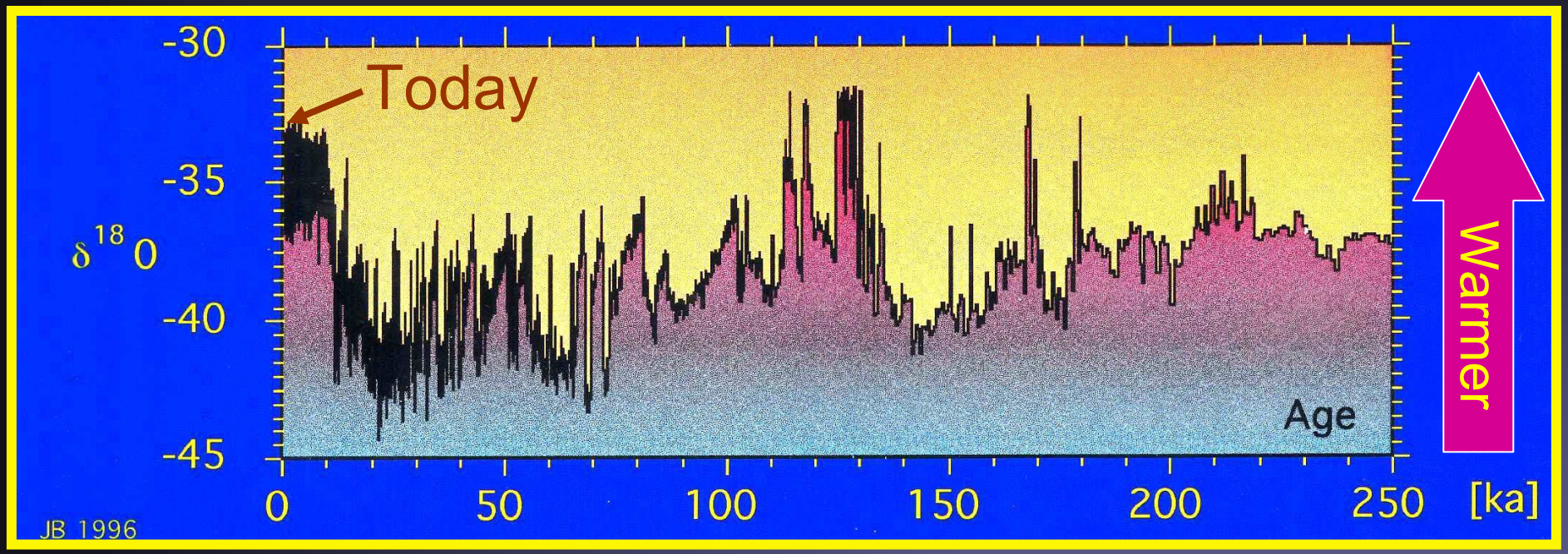

We live in a (rare) warm period (Holocene ≈ 12000 yrs) in times dominated by ice ages. Transitions are abrupt.

Milankovich-Theory: Changes in Earth's orbital parameters cause ice age cycles. Abrupt Transitions?

Cause of Ice ages

Milankovitch Theory

Ice ages are due to variations of the Earth's orbit.

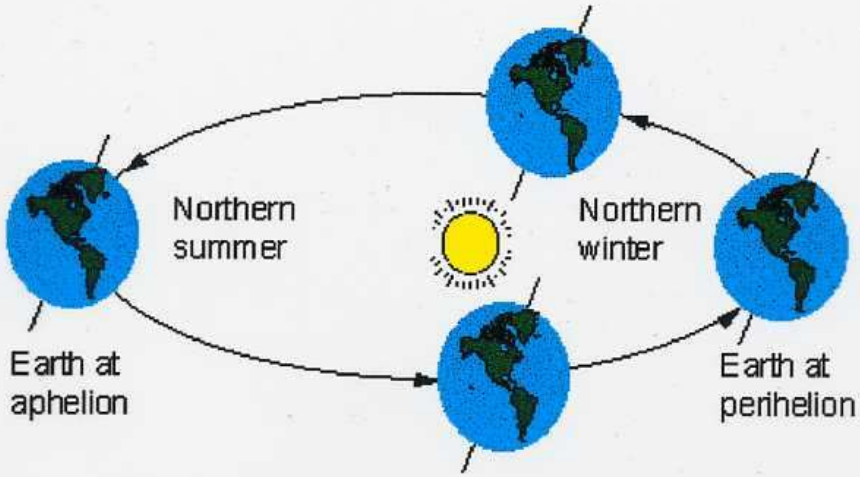

Precession of the equinoxes 19,0000-23,000 years

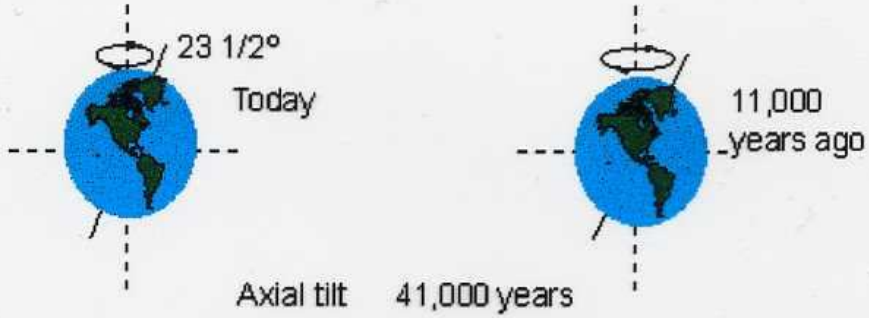

Ellipticity of the earth's orbit 90,000-100,000 years

Cause of Ice ages

Standard theory: Milankovic theory of orbital parameter changes of Earth, combined with non-symmetric distribution of continents.

Effect of the change of the eccentricity of the Earth's orbit on temperature on Earth: direct evidence

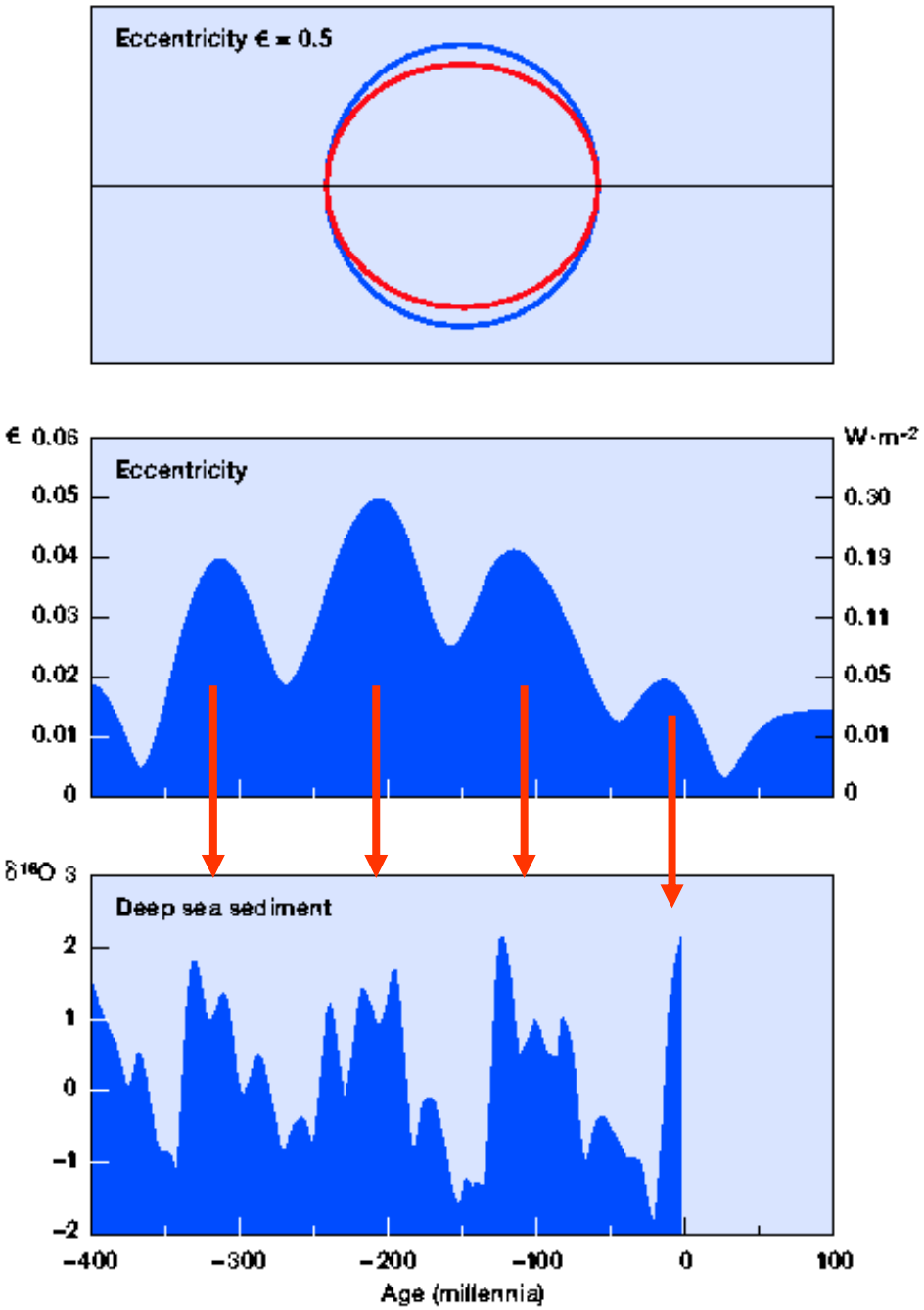

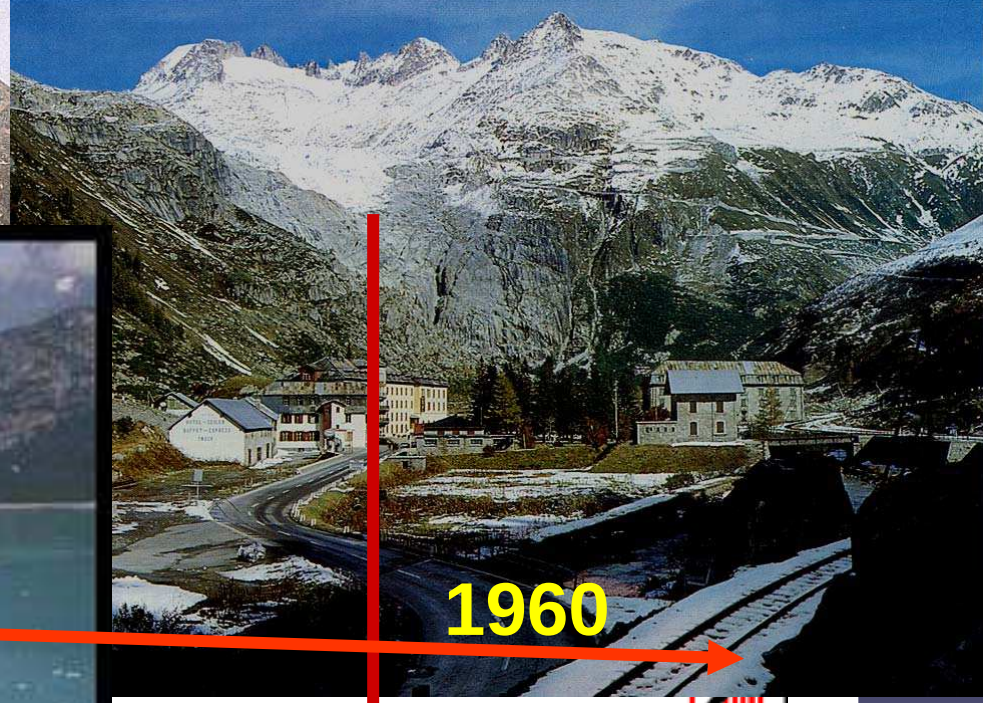
1960

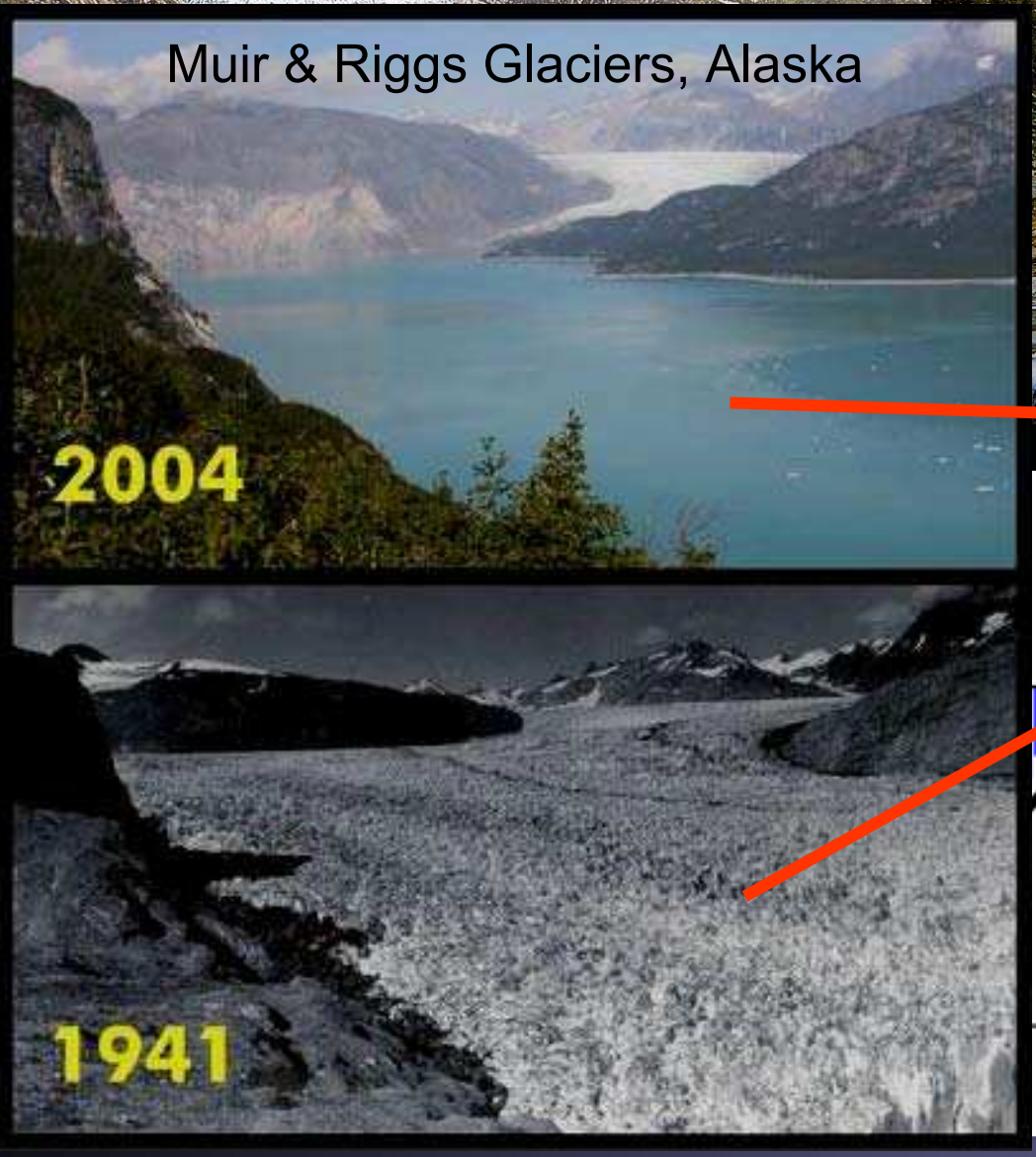
Muir & Riggs Glaciers, Alaska
2004
1941

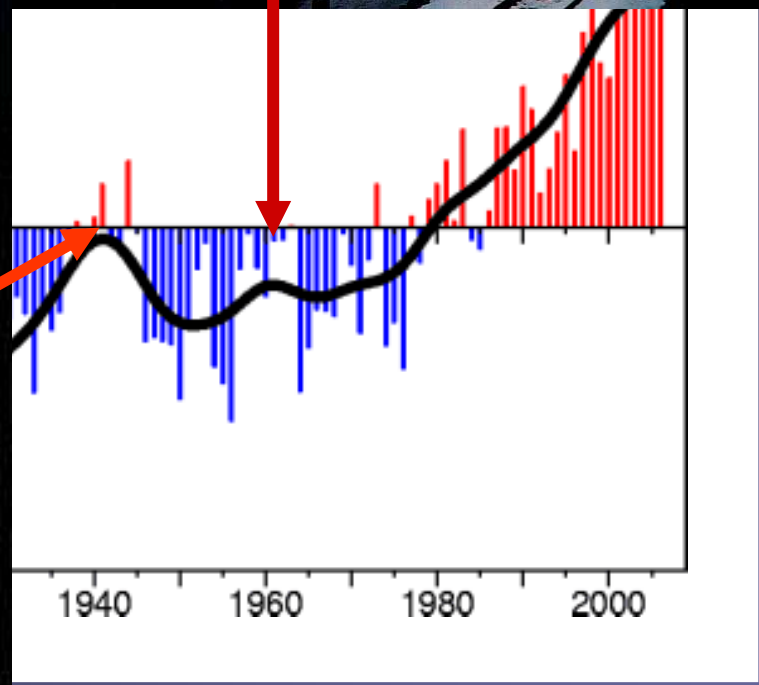
1940
1960
1980
2000

Is the Recent Temperature Rise Extraordinary?

Various temperature reconstructions suggest that the Earth is hotter now than in the last 2000 years

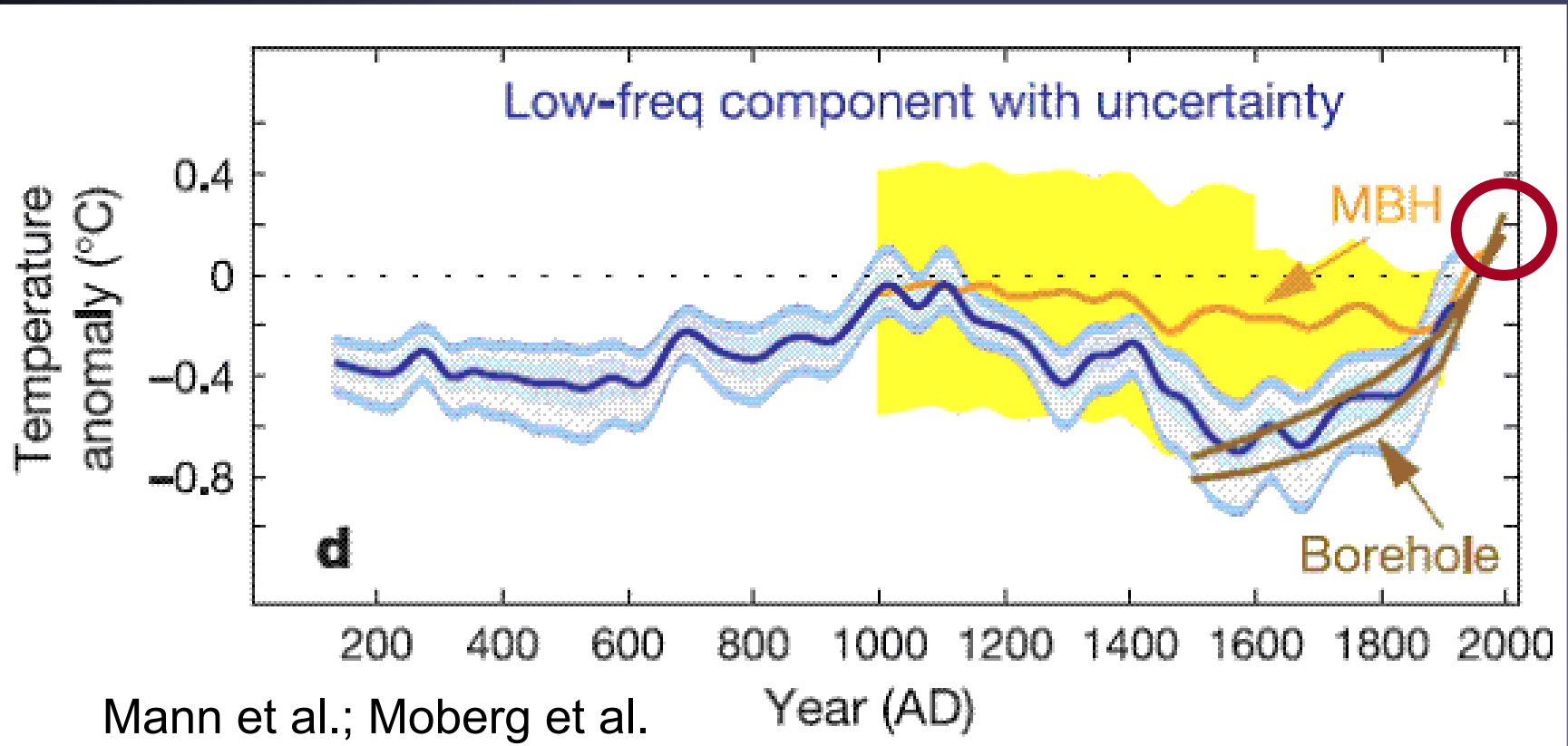

Mann et al.; Moberg et al.

Is Global Warming Man-made?

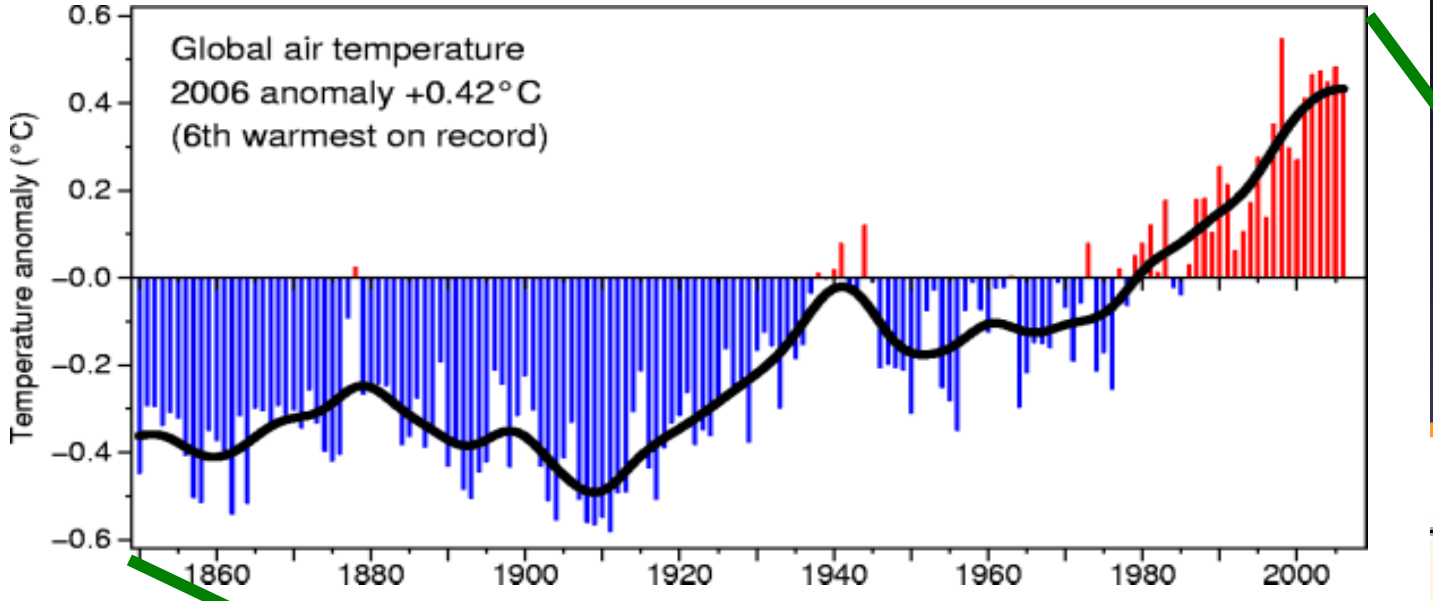

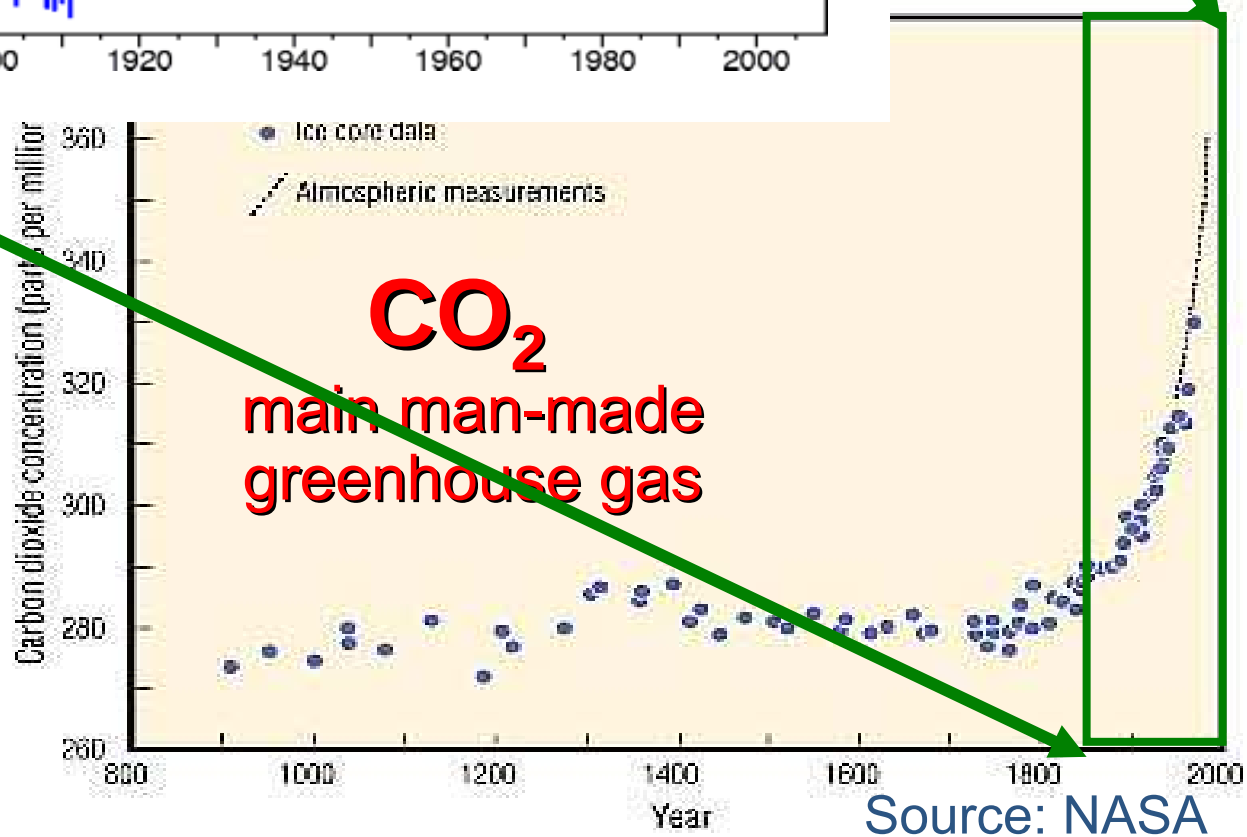

CO_2

main man-made greenhouse gas

Source: NASA

IPCC Predictions until 2100

Scenarios for emission of Greenhouse Gases → Predicted temperature over next 100 years

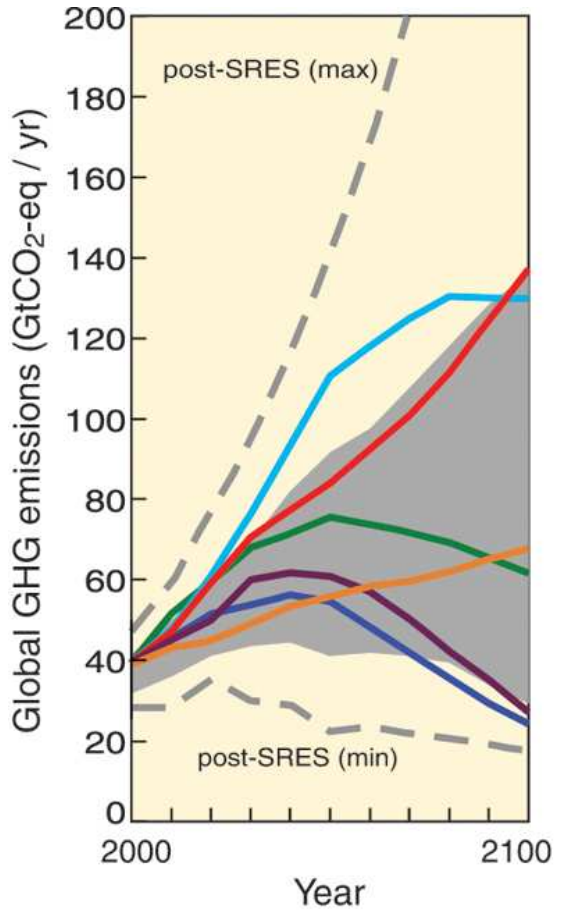

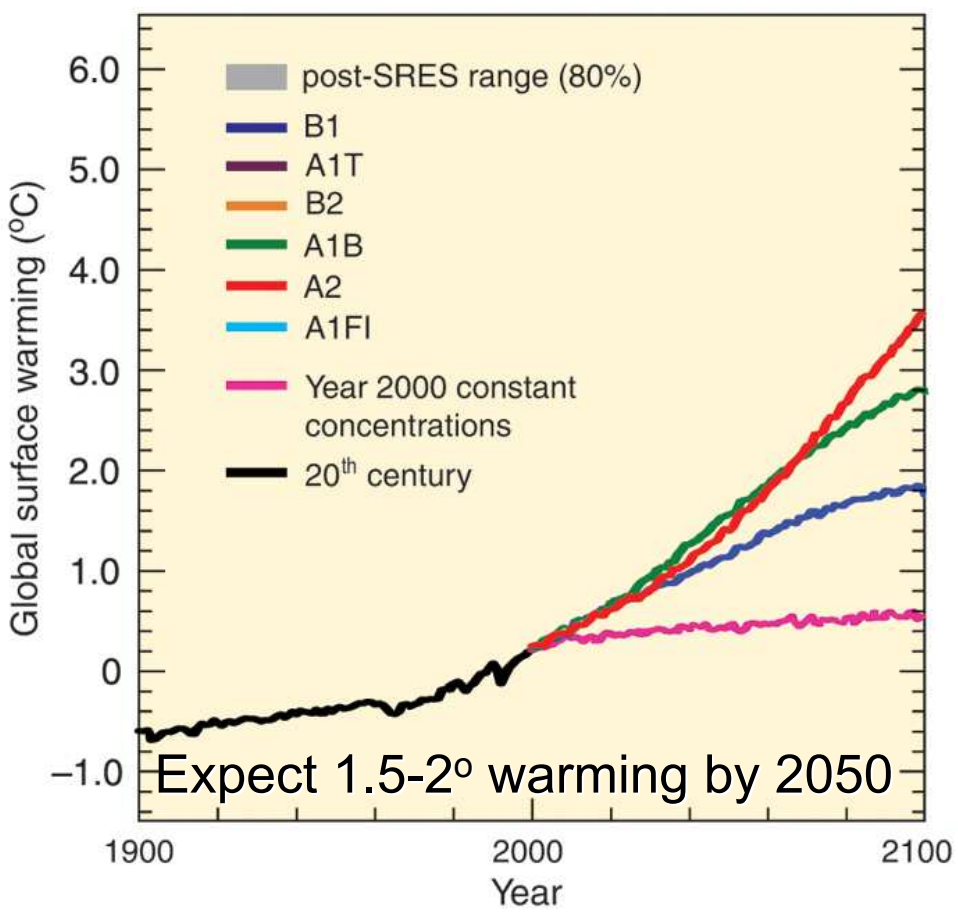

Warming is uneven over the globe

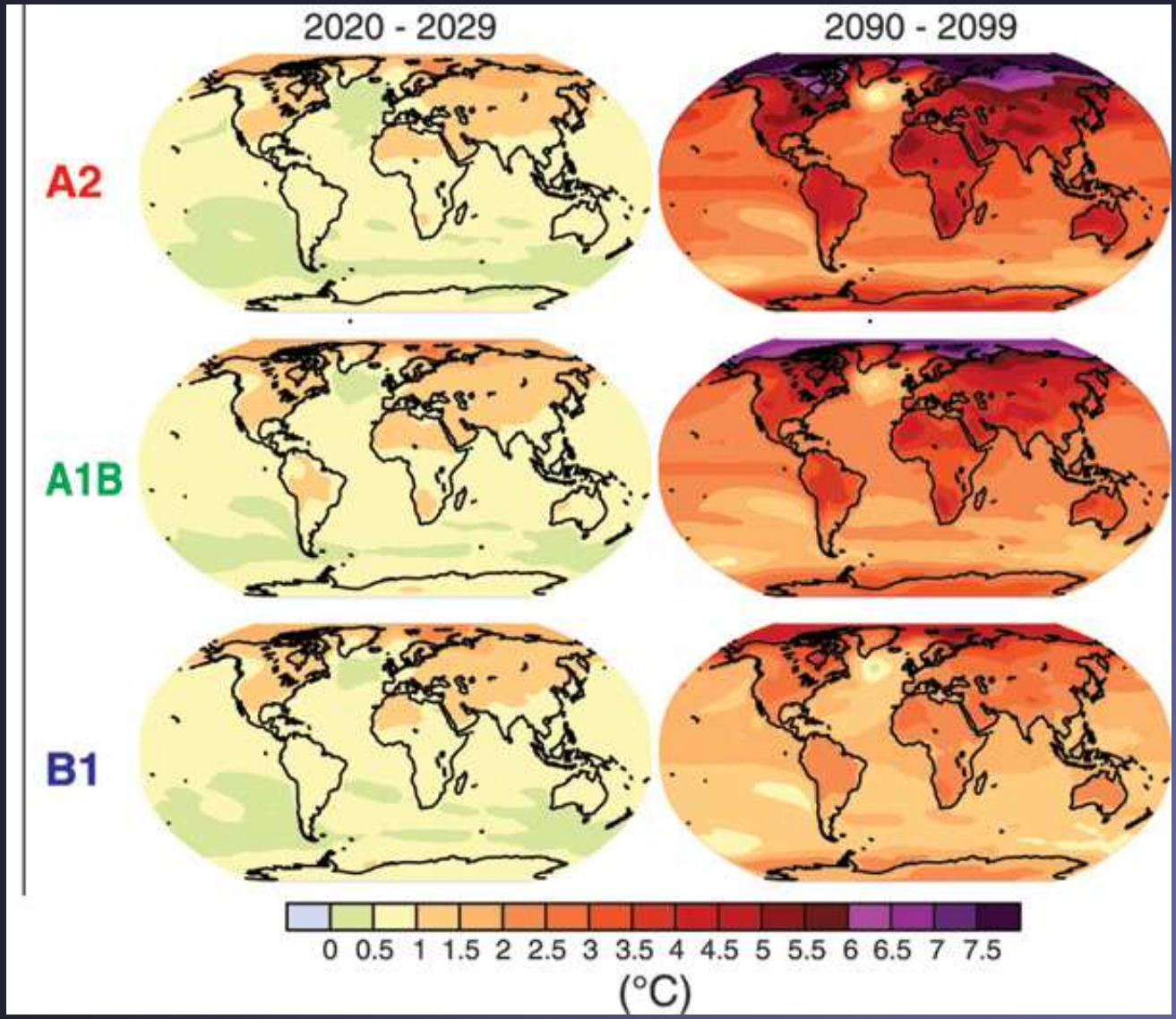

Some Consequences of Global Climate Change

Is everything understood?

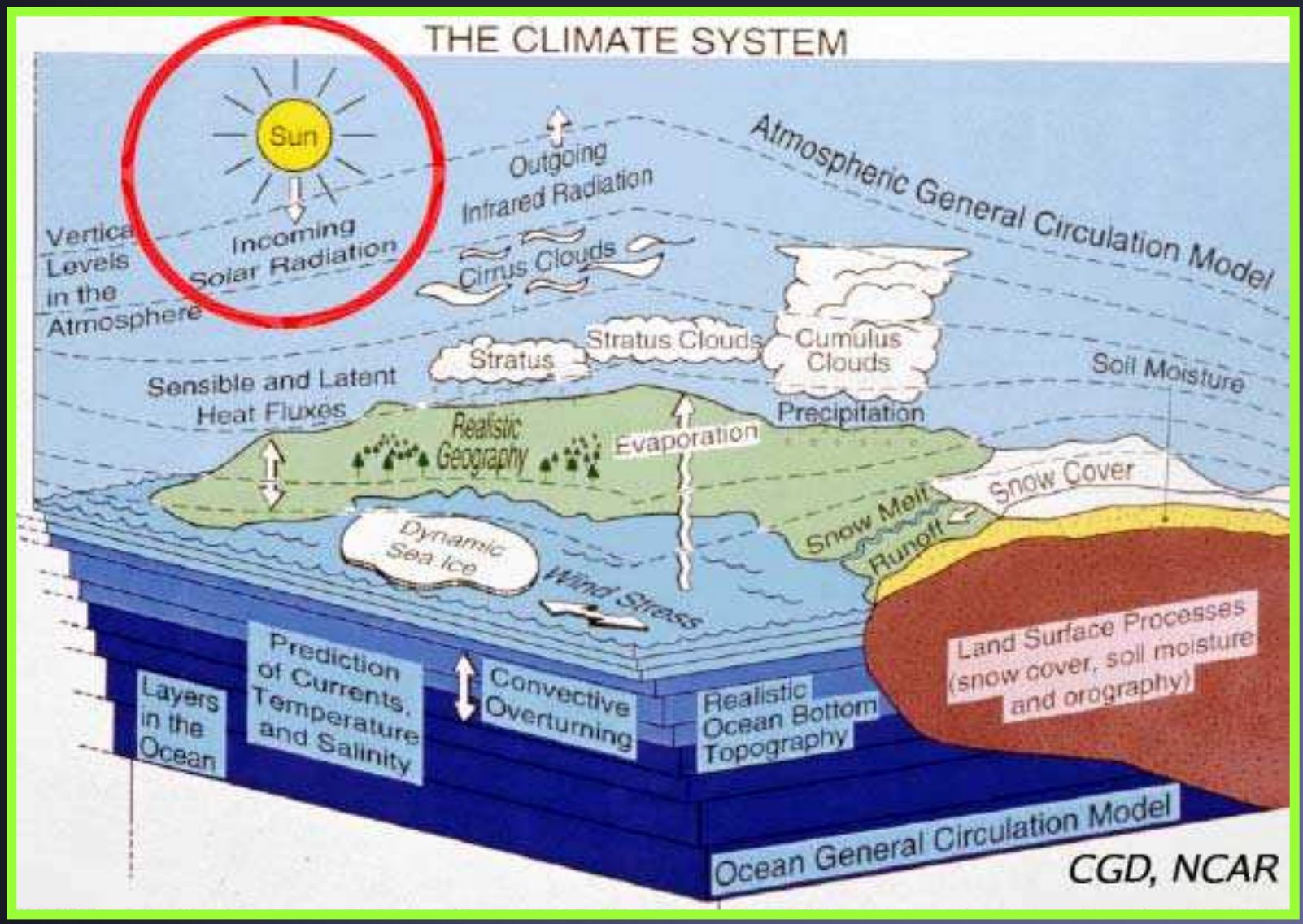

Could the Sun be to blame?

- The Sun delivers 1.36 kW / m^2. We get ≈ 1 kW / m^2 (at equator, at noon, if no clouds)
- In 20-30 min the Sun provides to Earth the yearly energy needs of Humanity

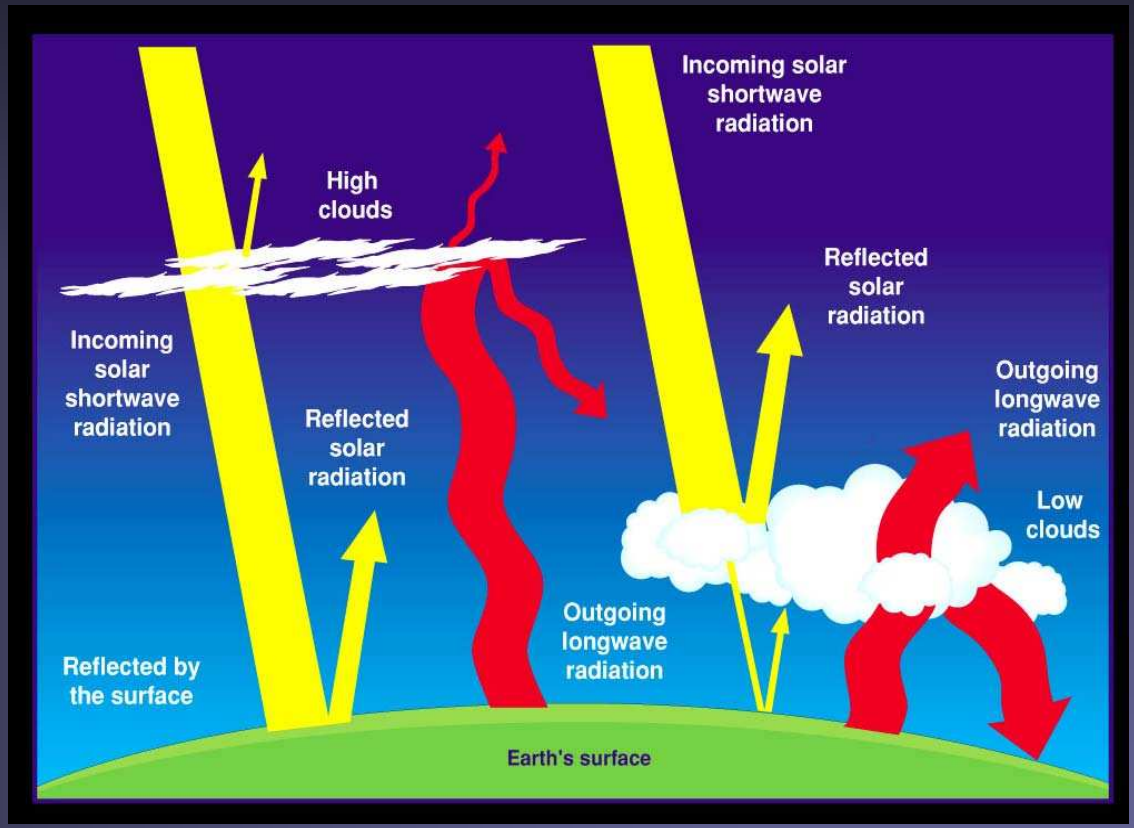

Without sunlight, no life (Our atmosphere would cool to below -200° C within weeks)

The life story of Greenland ice II

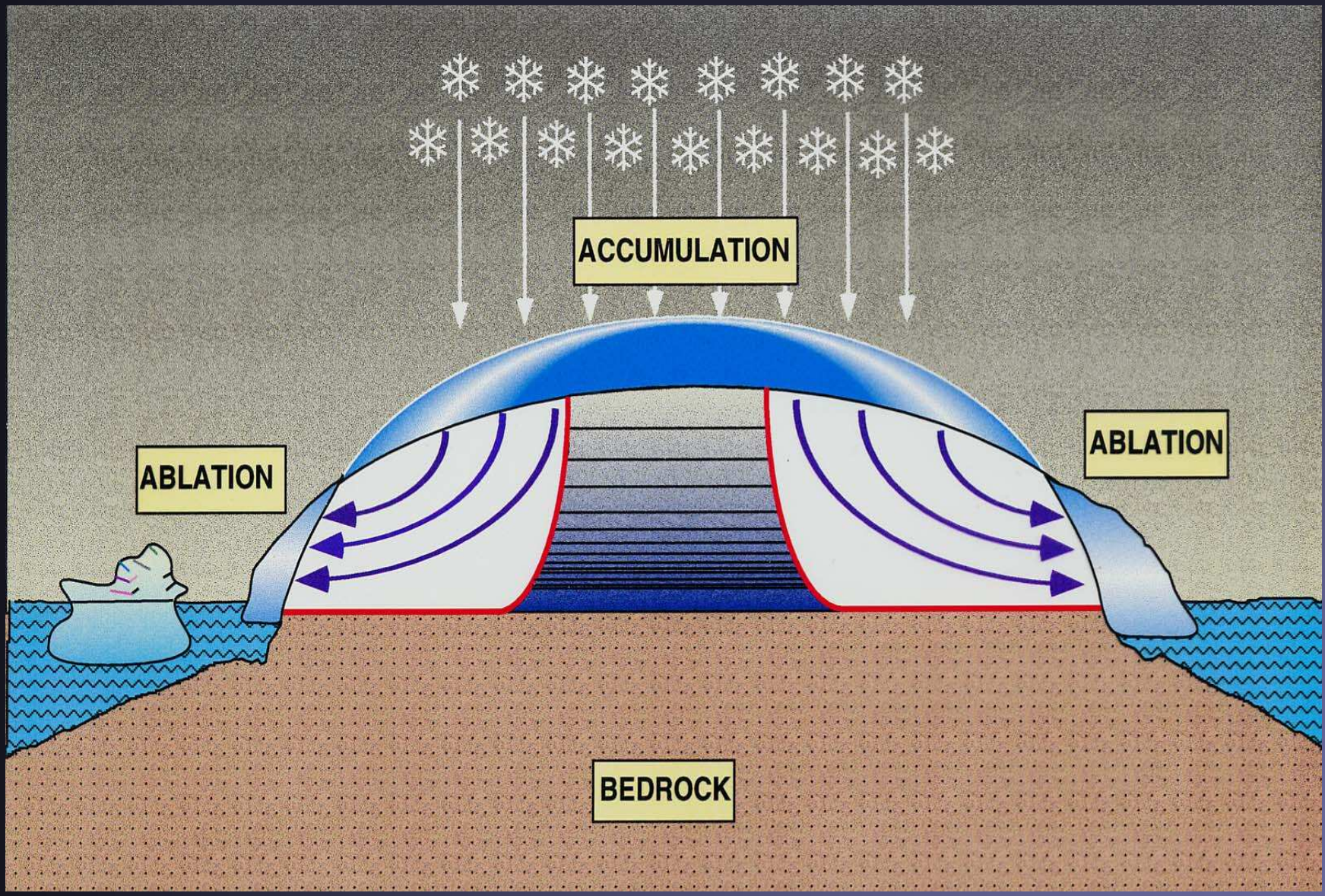


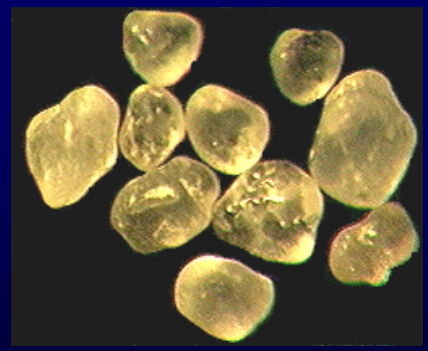

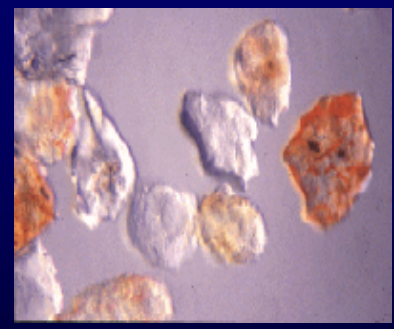

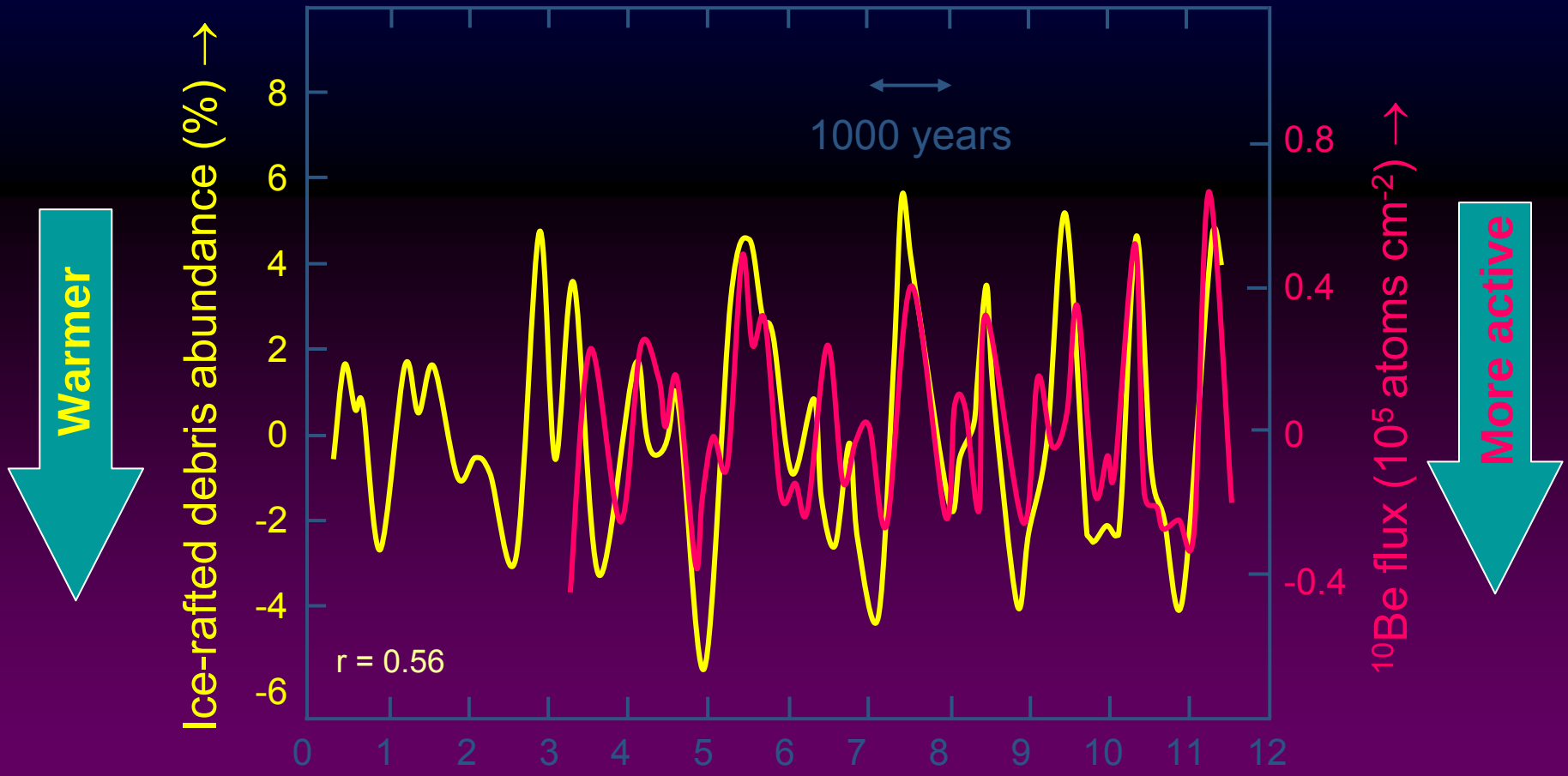

Fig.: M. Lockwood

(Bond et al., Science, 2001)

Sunspots and Climate over Last 1150 Years

- Sunspot numbers reconstructed over past 1150 years from ^{10}Be correlate with NH climate at 98% significance level.
- Mainly due to “hockey stick” shape, also seen in solar data!
- Analysis excludes last 25 years, when Sun did not behave like climate (Solanki & Krivova 2003)

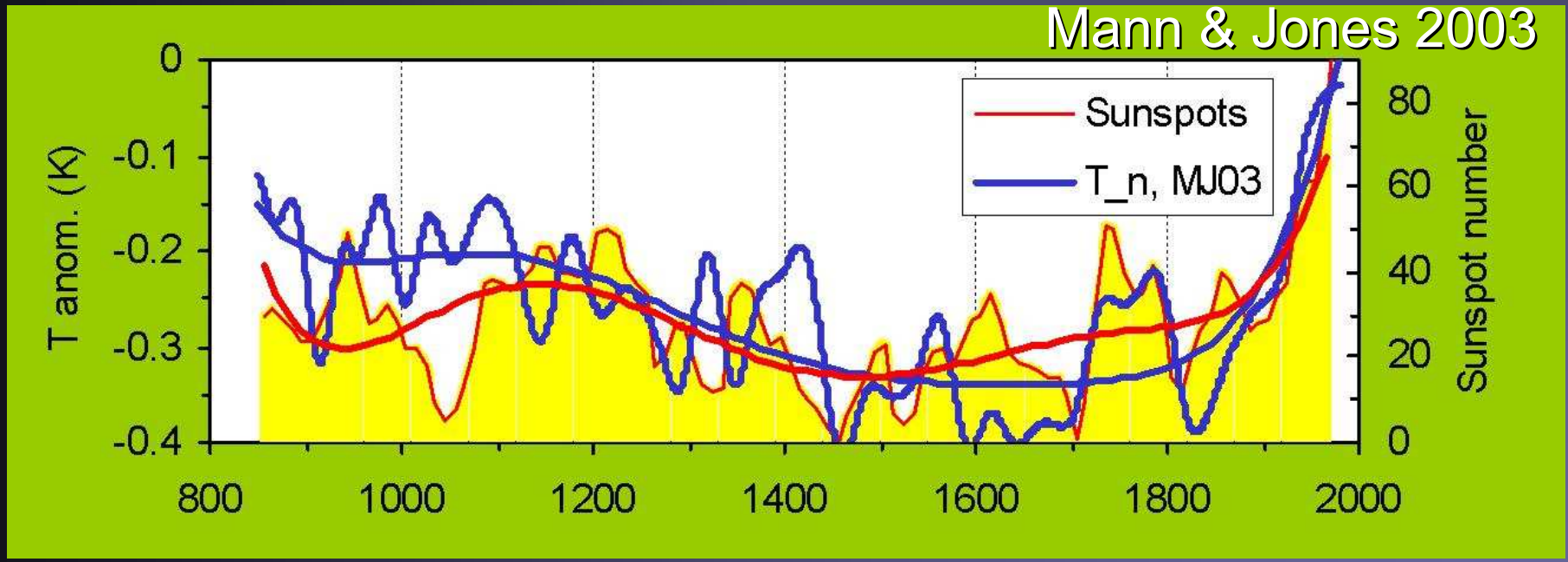

Usoskin, Schüssler, Solanki, Mursula 2004

Maunder Minimum & Little Ice Age

The Maunder Minimum corresponded to the Little Ice Age: Is there a connection?

The coldest decade in England since the 1690s;
1813/1814 – last Christmas Fair on the Thames

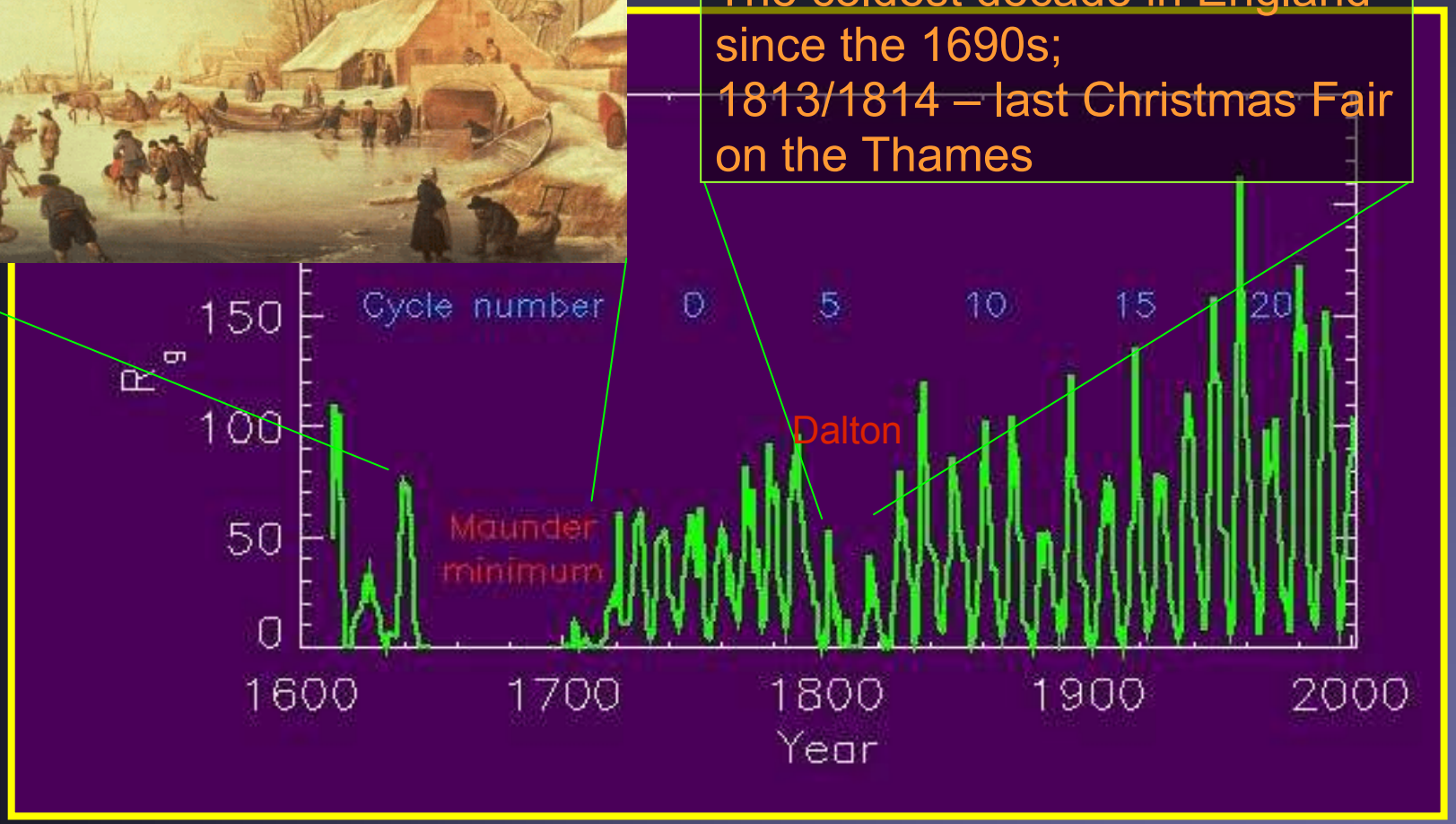

Paths by Which Sun Affects Climate

- Variations of total irradiance: change in total energy input to Earth's atmosphere [irradiance] = W/m^2 = flux at 1AU (above Earth's atmosphere)
- Variations of UV irradiance: influence on atmospheric chemistry (e.g. stratospheric ozone production and depletion)
- Modulation of cosmic rays: has been proposed to affect cloud cover.
- Energy carried by particles at 1 AU 0.002 W/m^2 (mainly protons and electrons) vs. 1365 W/m^2 from radiation

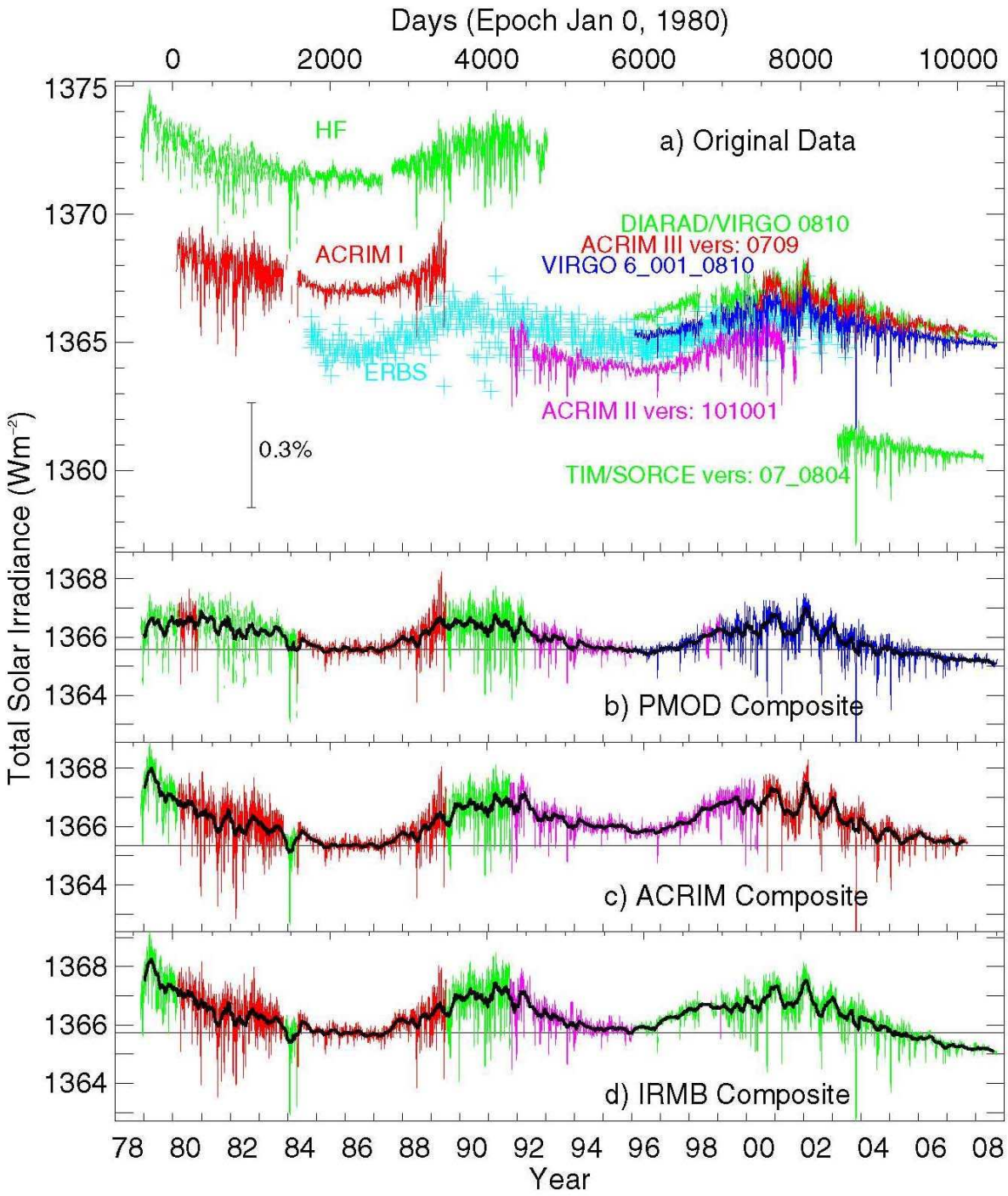

Measured Total Irradiance

8 different TSI radio-meters have been used, with offsets. Trend in composite depends on introduced corrections

PMOD homepage 2008

Measured total irradiance

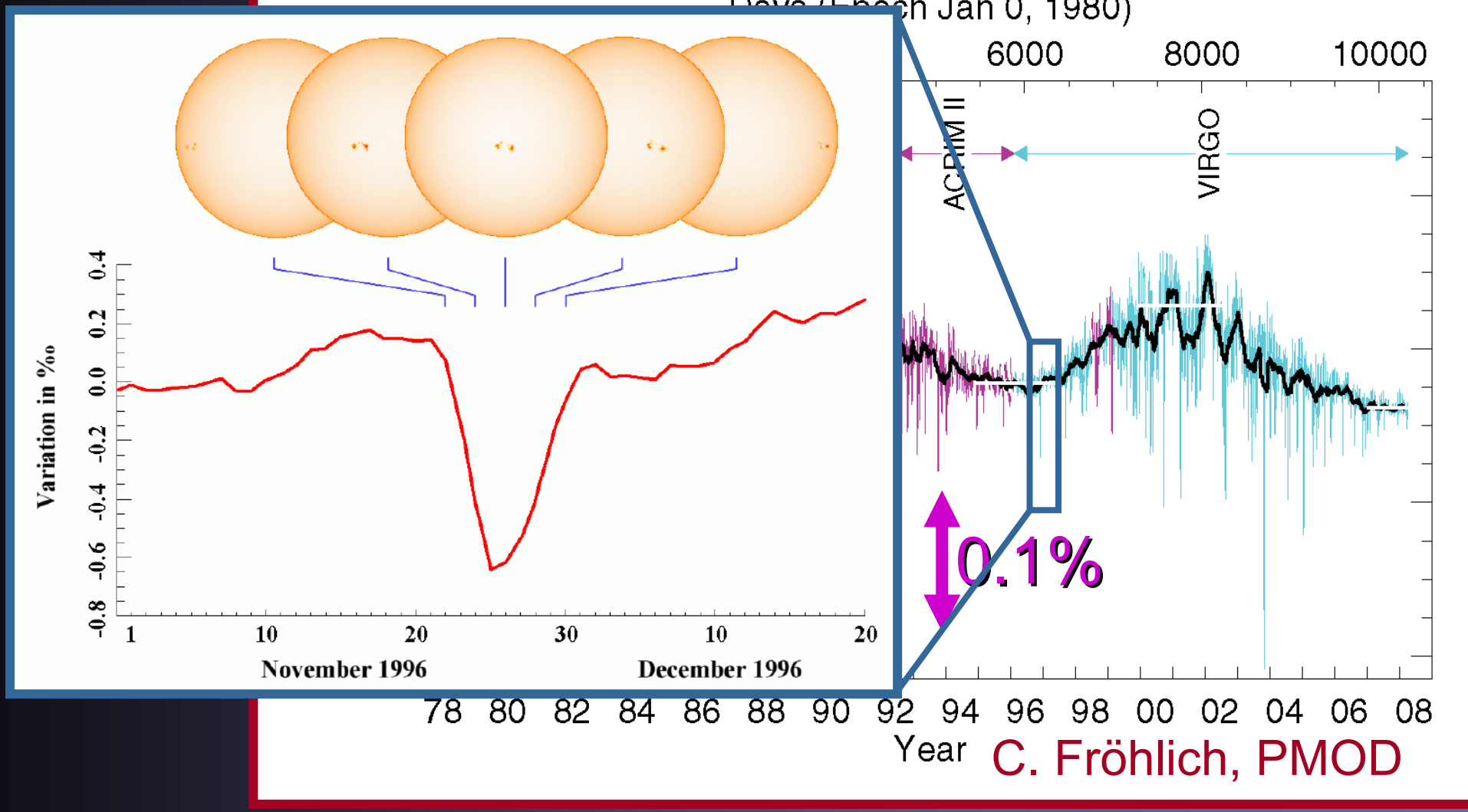

C. Fröhlich, PMOD

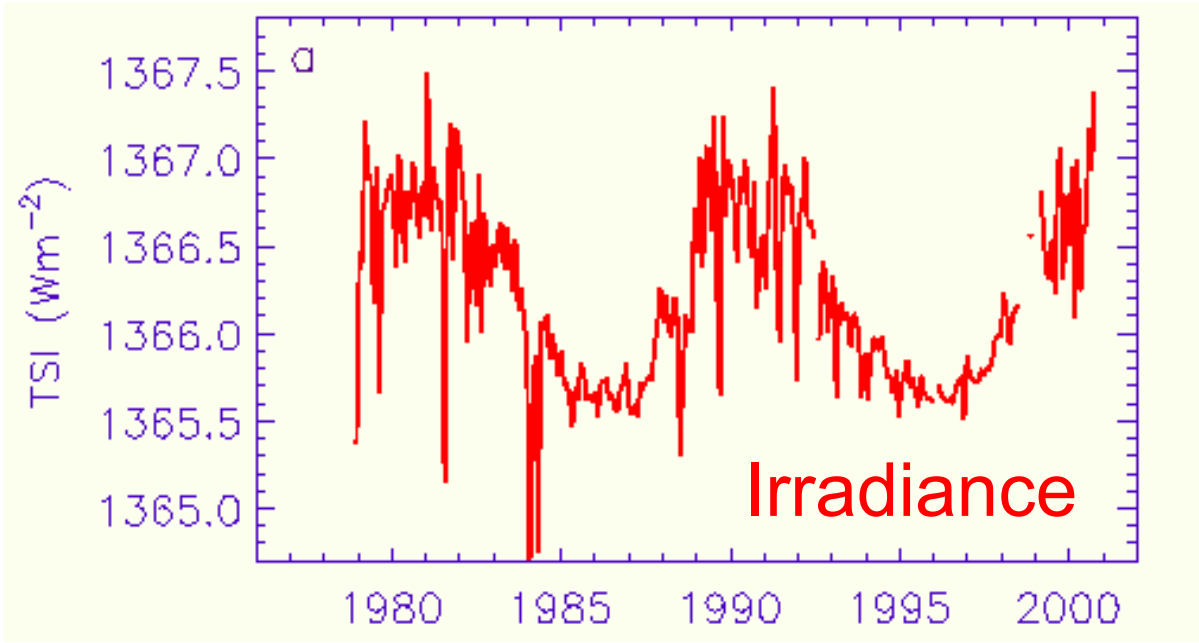
a
1367.5
1367.0
1366.5
1366.0
1365.5
1365.0
TSI (Wm^{-2})
Irradiance
1980
1985
1990
1995
2000

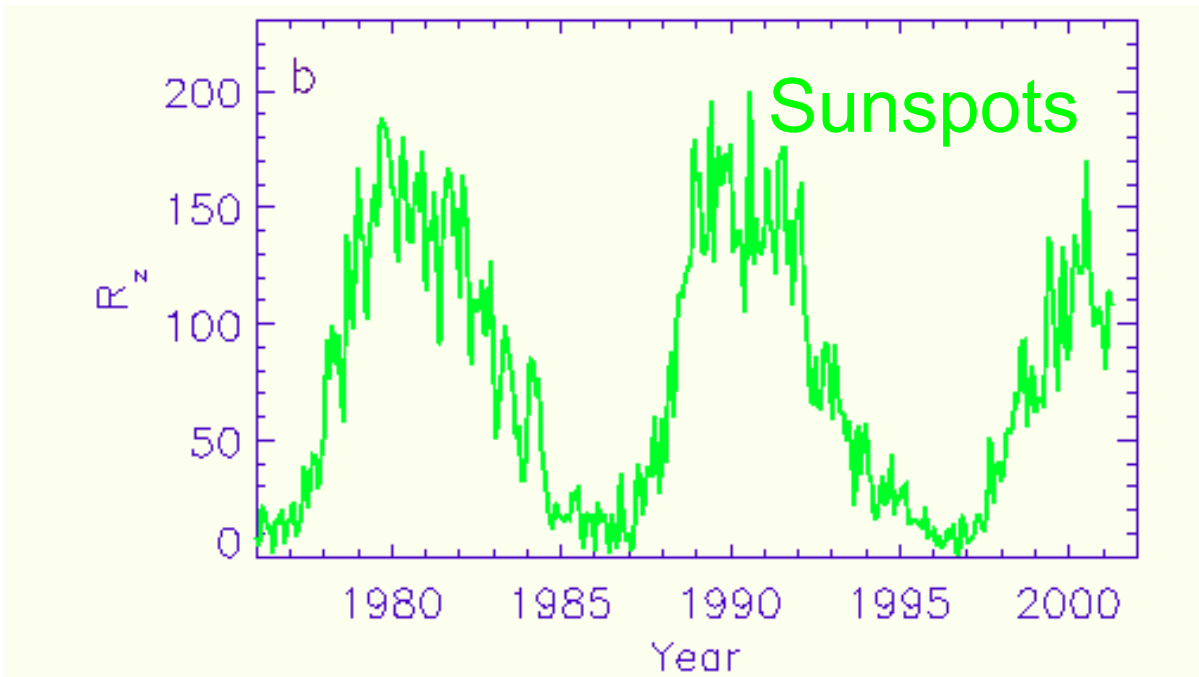
b
Sunspots
200
150
100
50
0
R$_z$
1980
1985
1990
1995
2000
Year

Faculae and Plage

Area increase of faculae from activity min to max is factor of 10-20 greater than of sunspots

Passage of a Facular Group

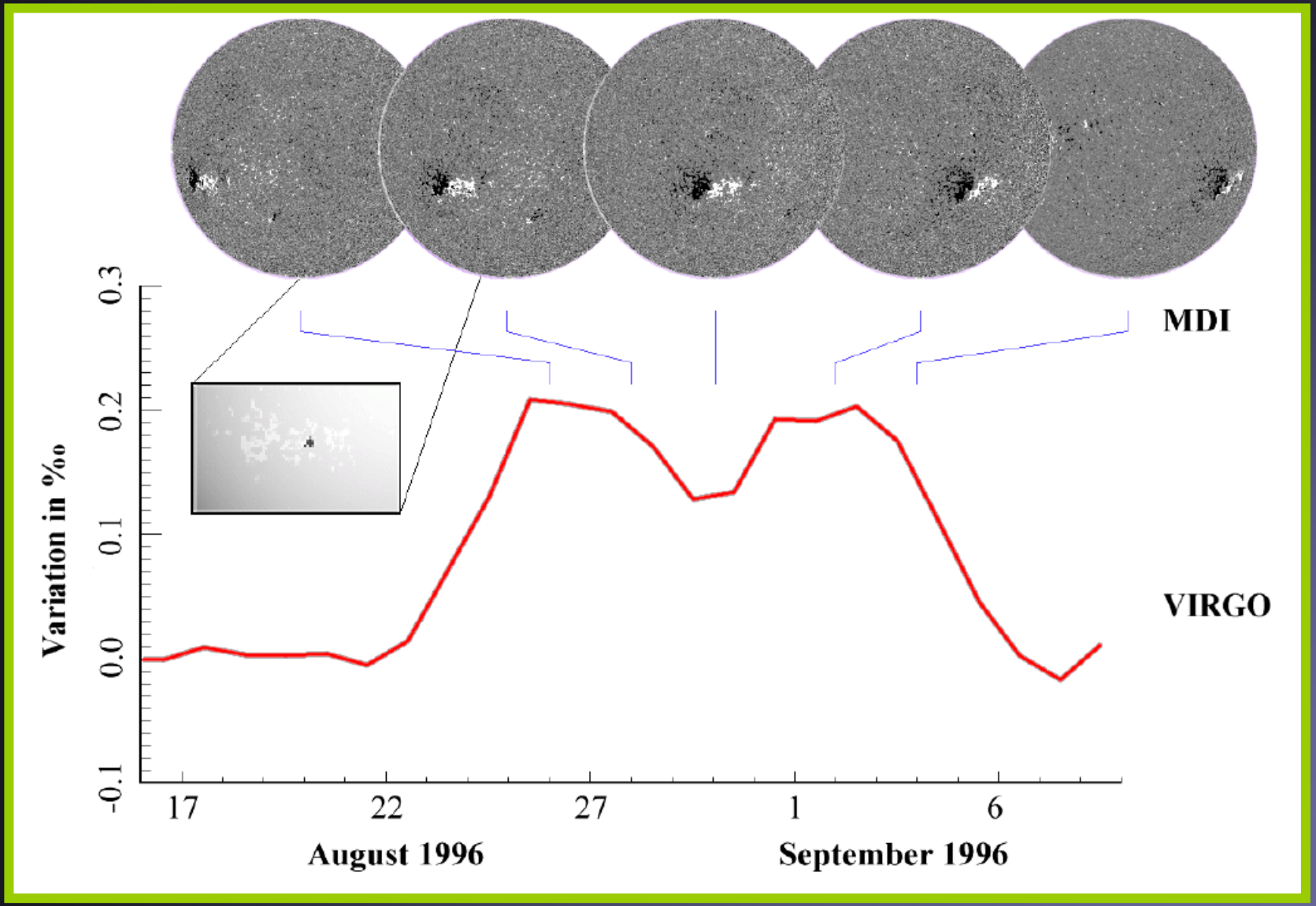

3- Component Model

- Assume that variation in irradiance is exclusively due to magnetic field at solar surface (for time scales day-decades)
- Total flux $F(\lambda,t)$ then depends on the intrinsic fluxes of each of the different types of magnetic features and the area fraction α that each covers
- Flux at 1AU = irradiance
- Magnetic features:
  - sunspots: subscript “s”
  - faculae: subscript “f”
- Background: field-free quiet Sun: subscript “q”

Total flux emitted by Sun

- Sum of filling factors = 1
- F_s , F_f and F_q are the fluxes that one would measure if that feature were to cover the whole Sun

$$
\begin{aligned}
F(\lambda, t) = & \ \alpha_s(t) F_s(\lambda) \\
& + \alpha_f(t) F_f(\lambda) \\
& + \left(1 - \alpha_s(t) - \alpha_f(t)\right) F_q(\lambda)
\end{aligned}
$$

3- Component Model

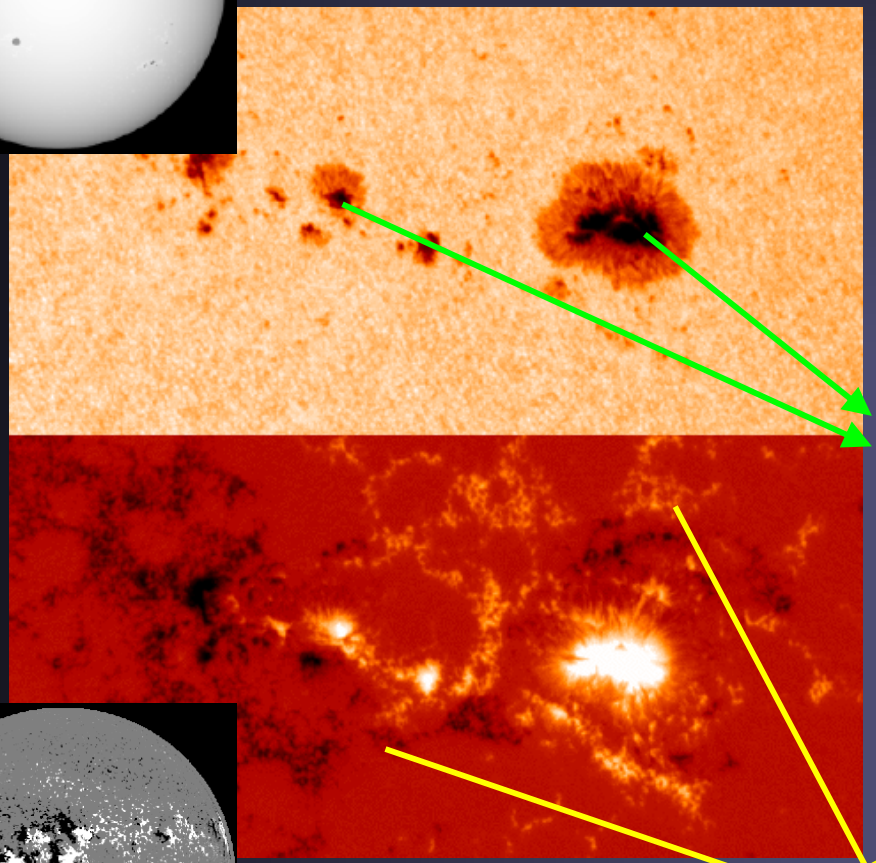

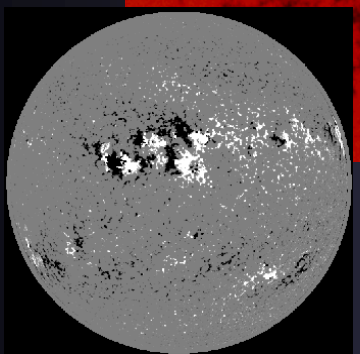

$F(\lambda)$ quiet Sun flux
(Fontenla et al. 1993)

$F(\lambda)$ sunspot flux; separate umbra/penumbra
(cool Kurucz models)

$\alpha_s(t)$ filling factor of sunspots
(MDI continuum)

$F(\lambda)$ facular flux
(modified model-F; Fontenla et al. 1993; Unruh et al. 2000)

$\alpha_f(t)$ filling factor of faculae
(MDI magnetograms)

B as source of irradiance changes

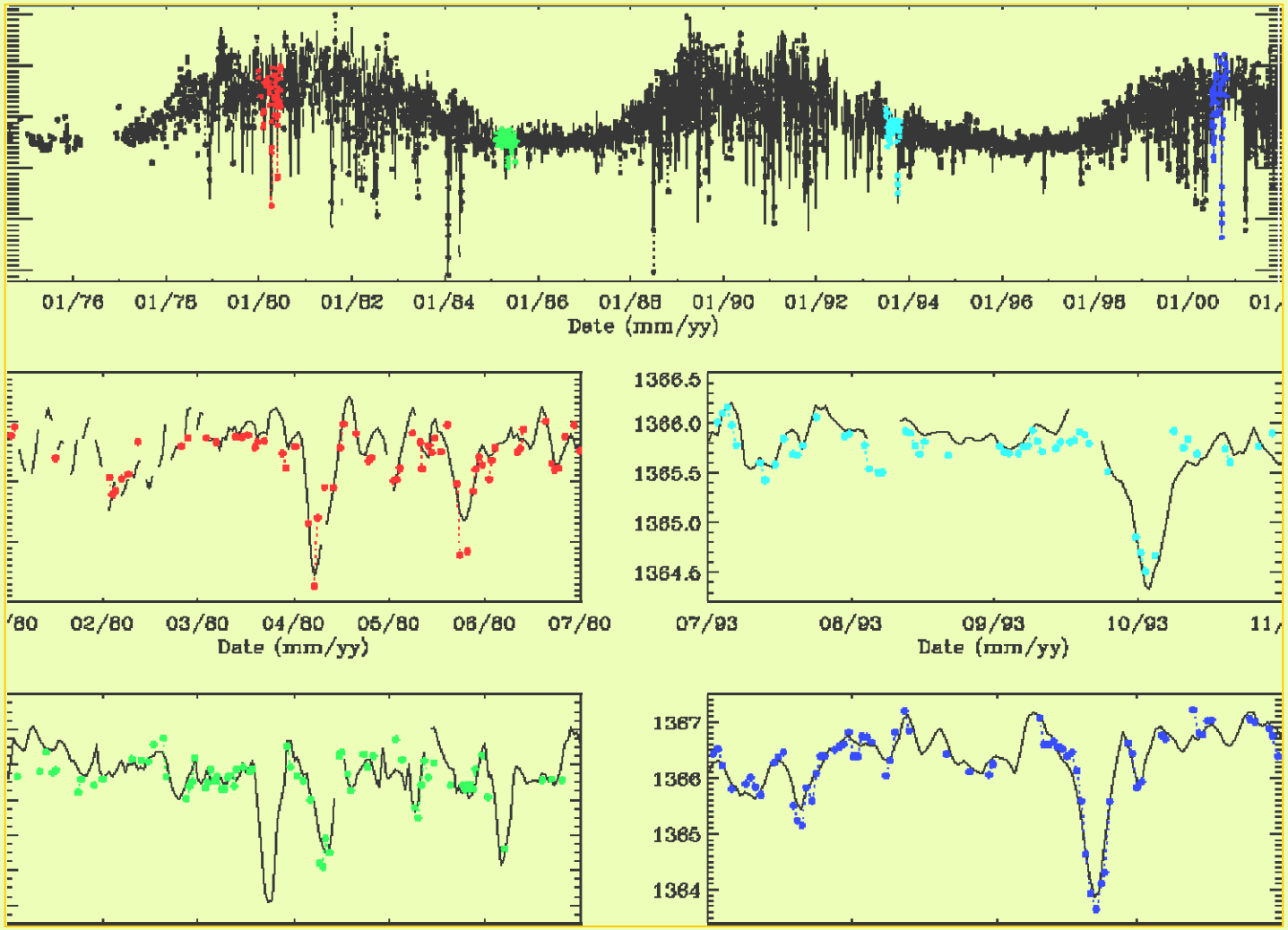

Wenzler, Solanki, Krivova 2005

Model vs. Observations

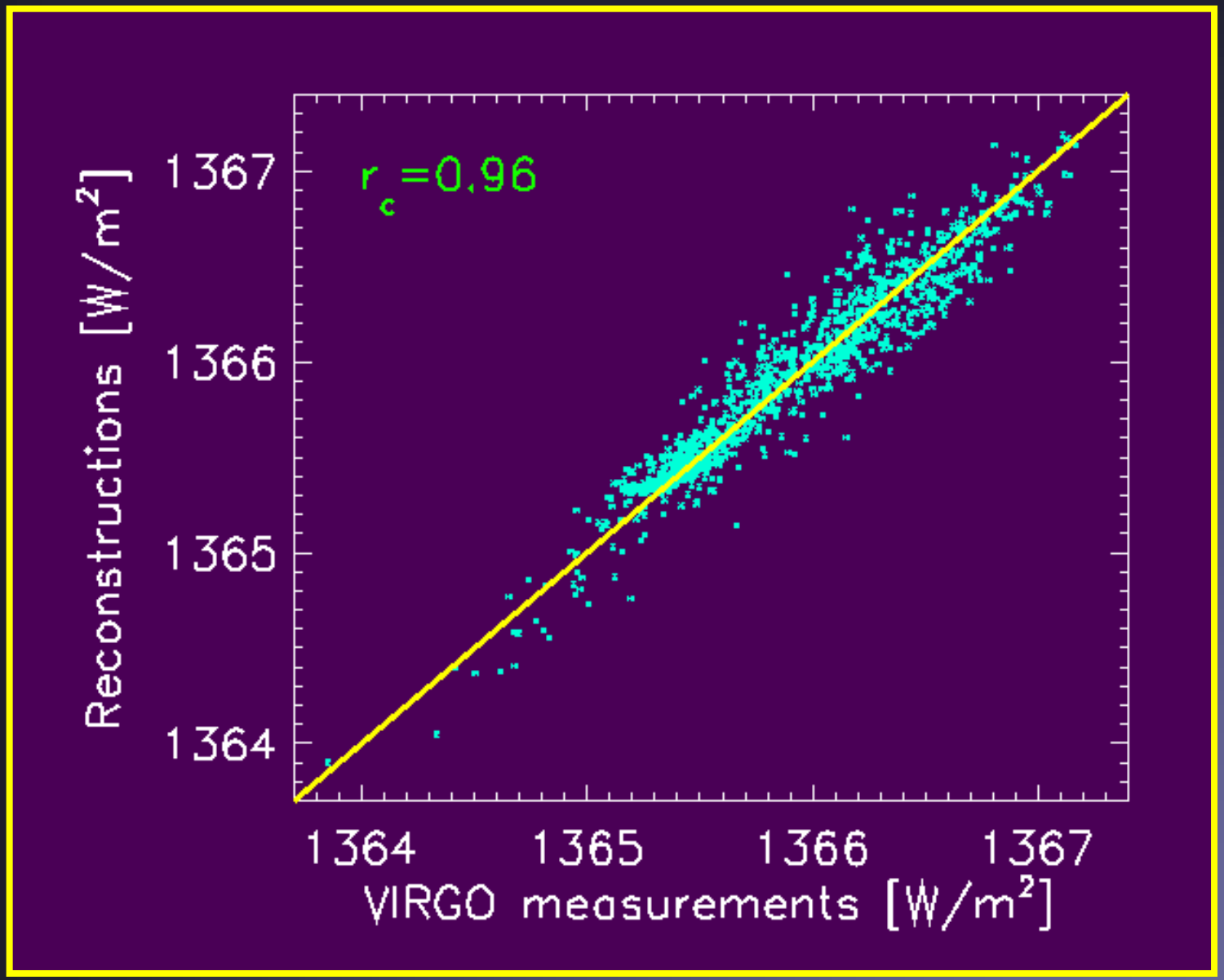

Spectral Irradiance

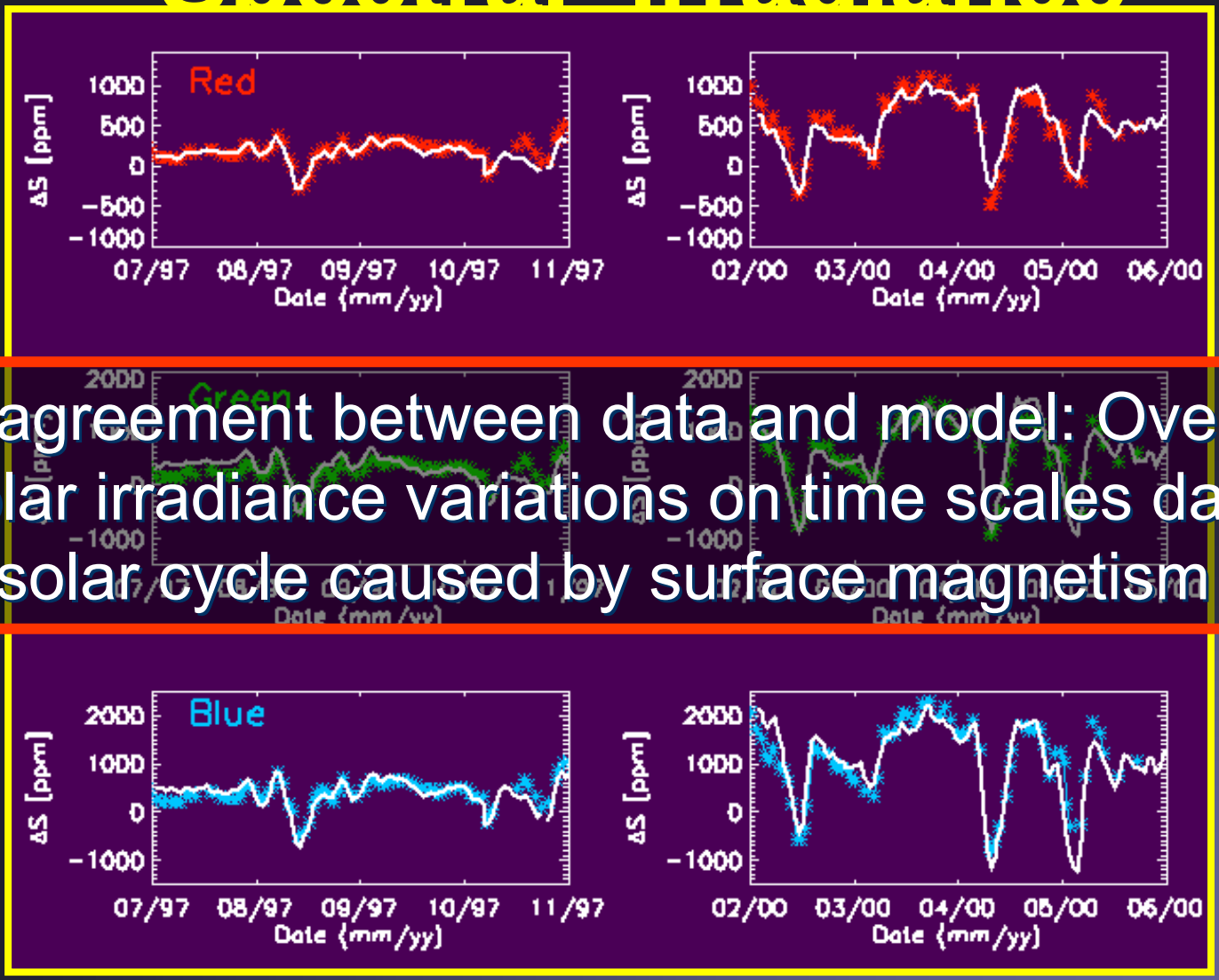

Good agreement between data and model: Over 90% of solar irradiance variations on time scales days – solar cycle caused by surface magnetism

Are there longer term variations of solar irradiance?

- No direct records of irradiance variations on longer time scales. Need to use models.
- Need to distinguish different periods
  - Since ~ 1800: good direct sunspot number measurements
  - Since 1611: telescopic sunspot number measurements
  - On longer time scales: first a proxy of the solar magnetic field must be reconstructed.

The aa geomagnetic index

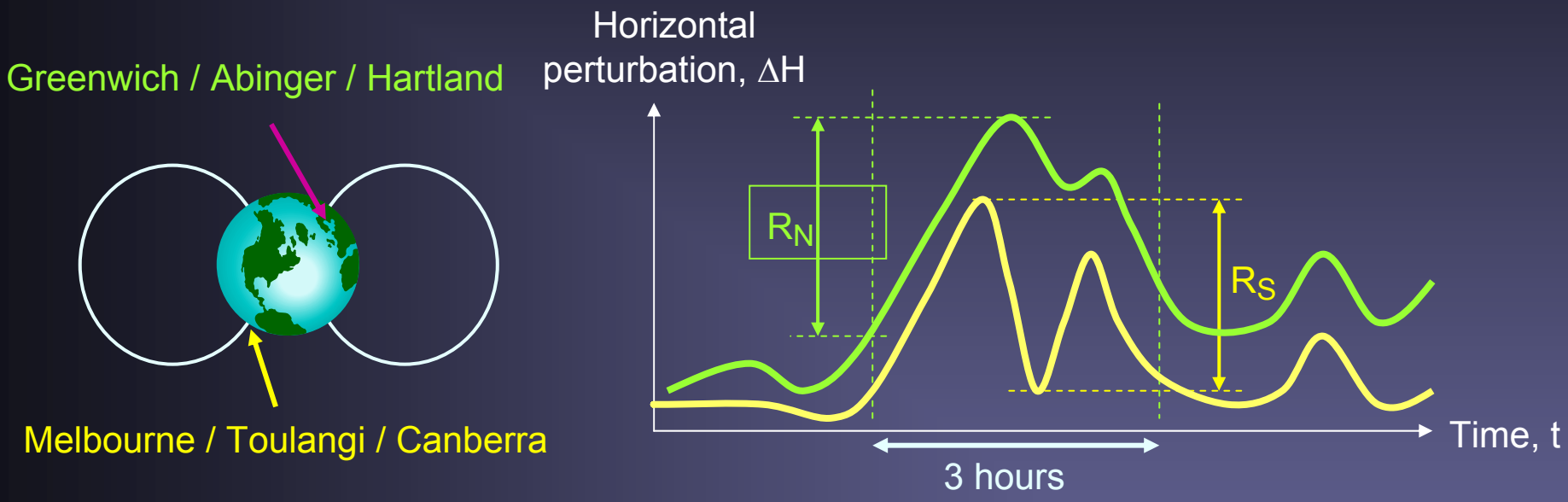

For each 3 hour interval the ranges of ΔH, R_N and R_S are scaled to give "K-values", K_N and K_S which are converted to aa_N and aa_S using an algorithm that allows for location of magnetometer

$$aa = (aa_N + aa_S)/2$$

Mayaud, 1976

Interplanetary Magnetic Field

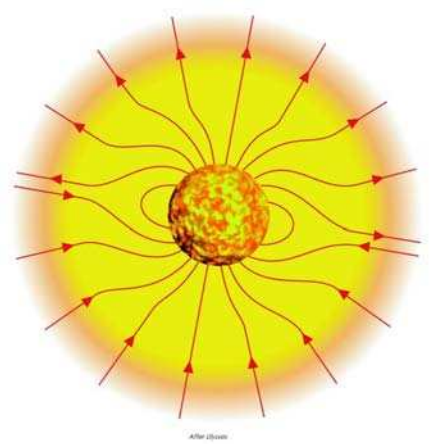

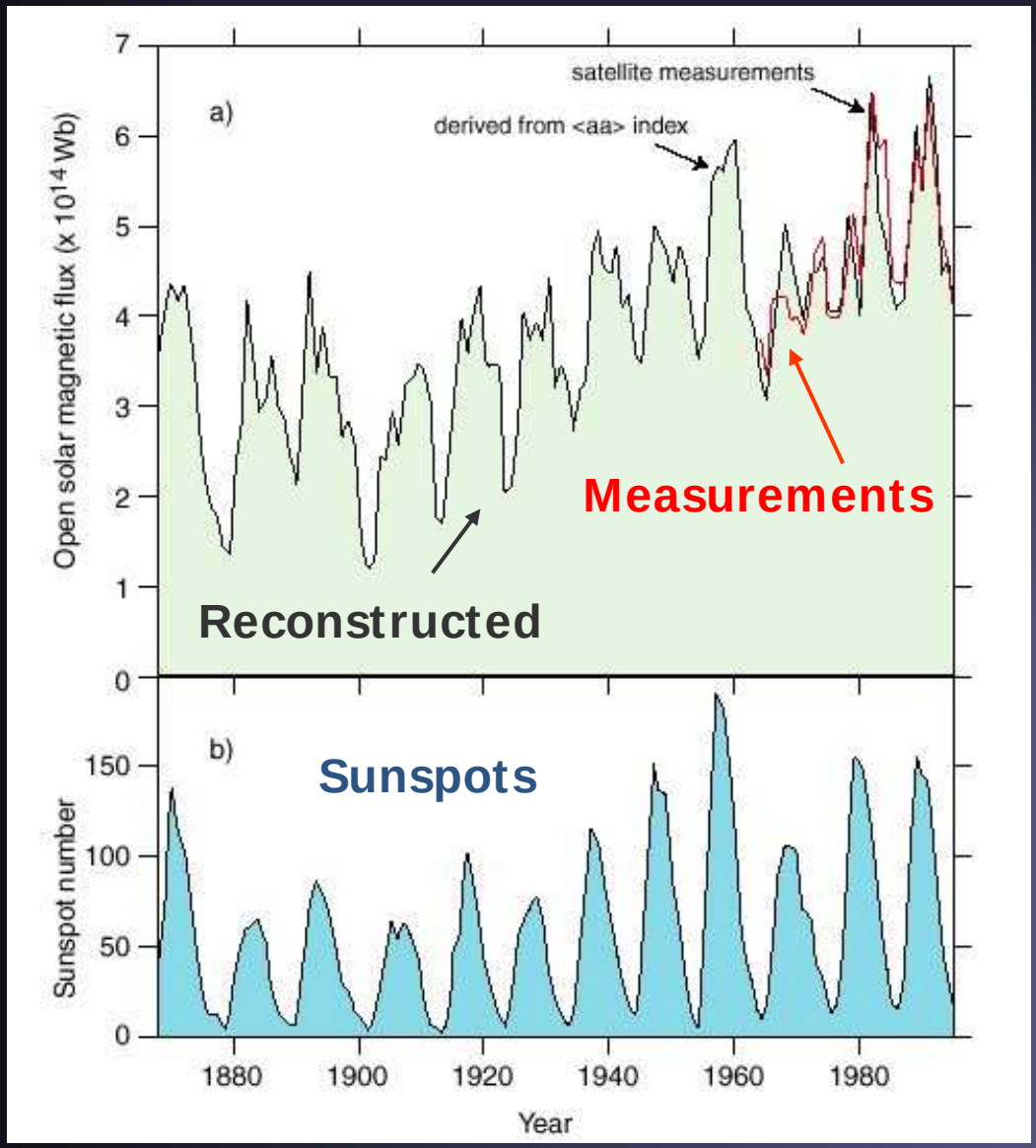

Lockwood et al. 1999 Nature

- Reconstructed from geomagnetic aa
- Open heliospheric flux doubled during the last century
- Solar origin of the secular trend?
- Does total magnetic flux show similar trend?

Active regions and ephemeral regions

$\dot{\Phi} \approx 3 \cdot 10^{23} \ldots 3 \cdot 10^{24}$ Mx/yr

$\dot{\Phi} \approx 2 \ldots 4 \cdot 10^{26}$ Mx/yr

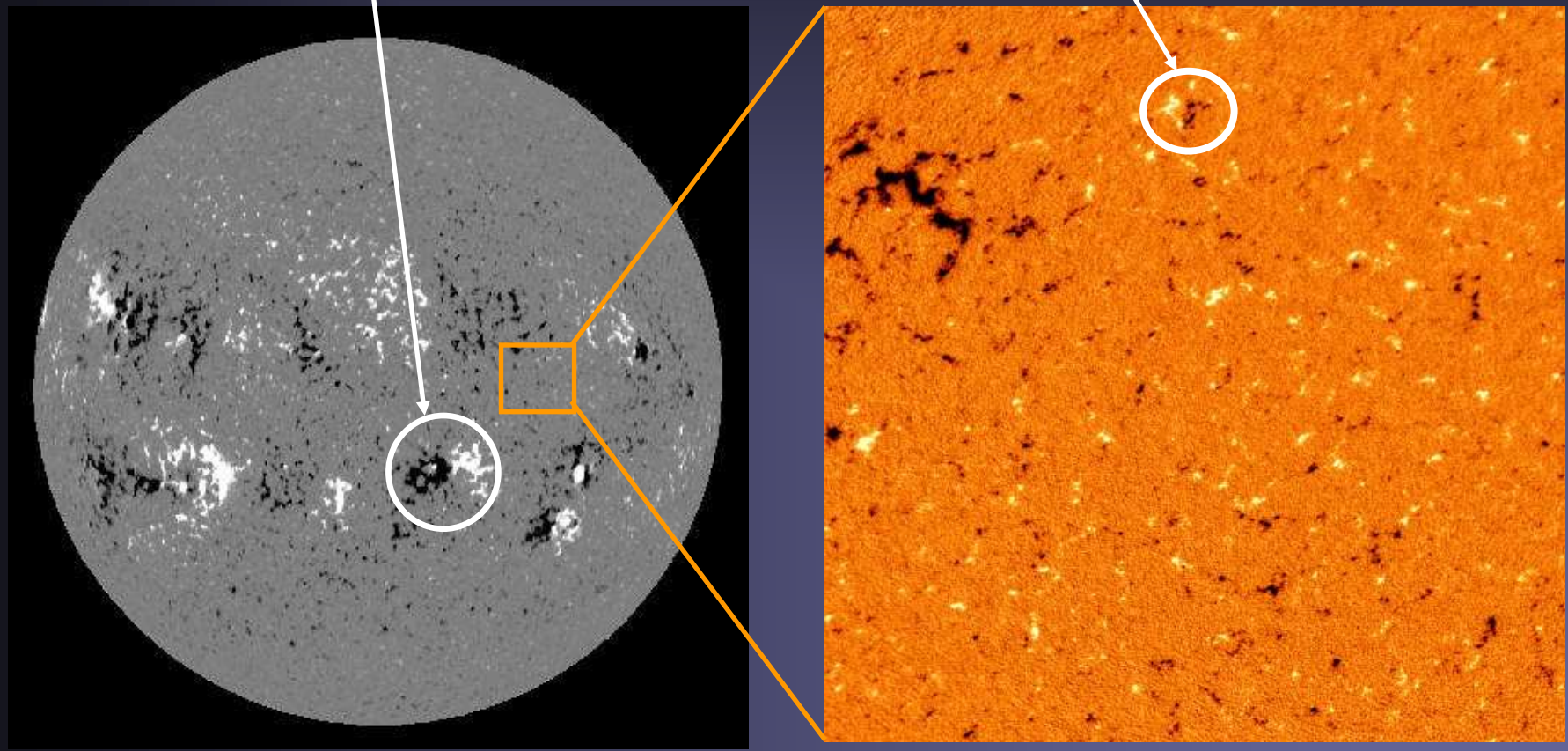

SOHO/MDI magnetograms

Solar cycle & ephemeral regions

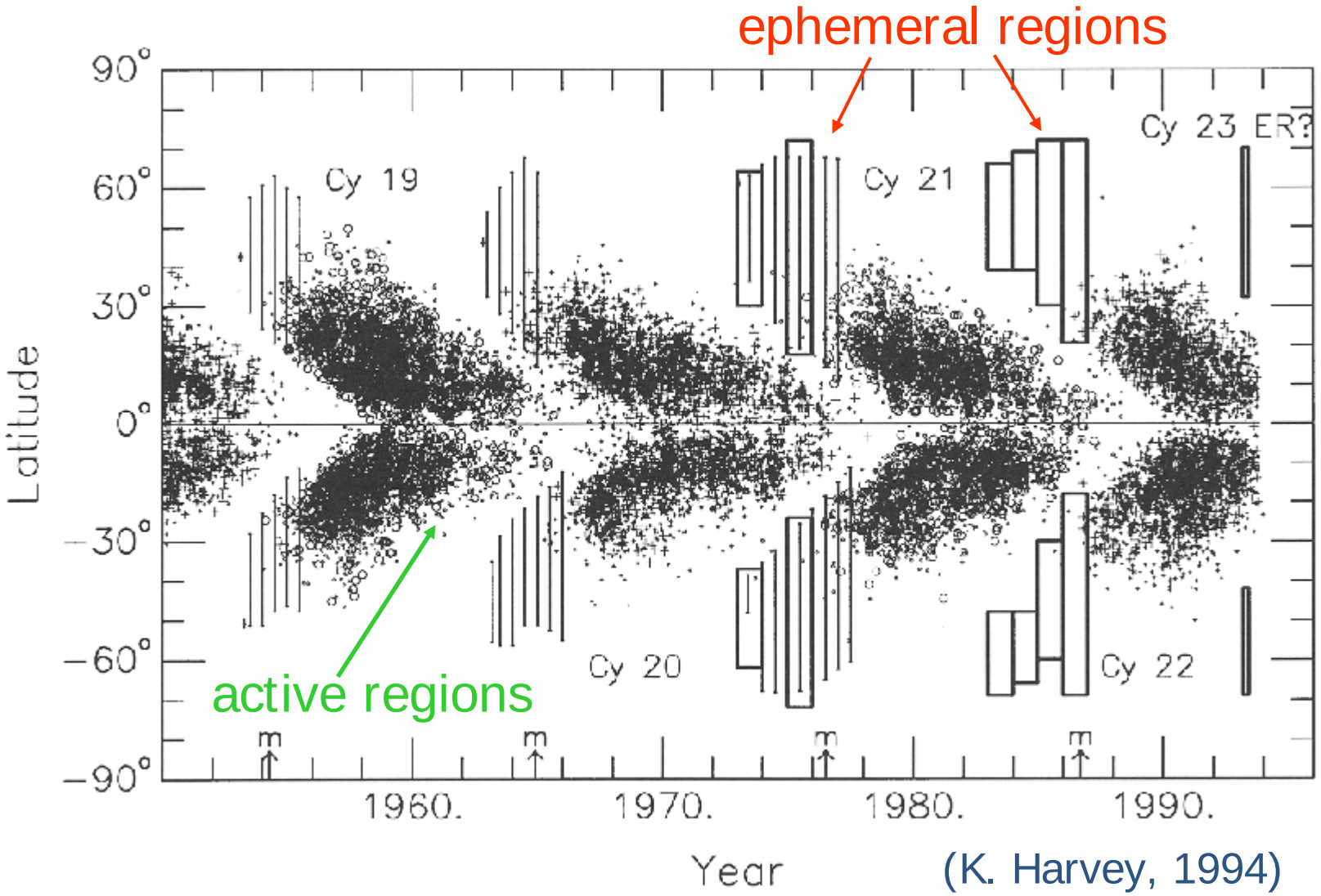

(K. Harvey, 1994)

Ephemeral Regions: Overlapping Cycles

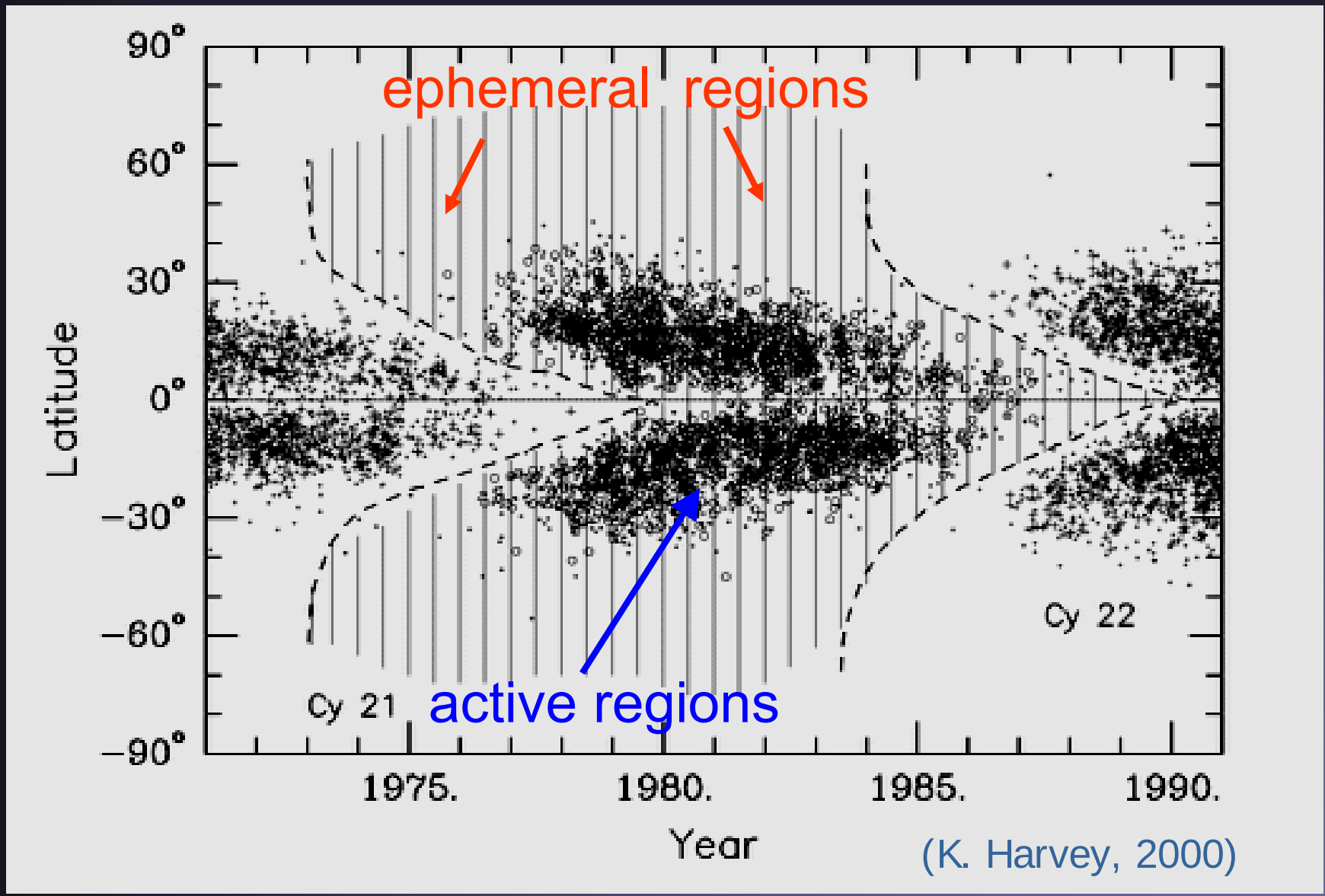

(K. Harvey, 2000)

A Coarse Model for the Secular Variation of the Sun´s Magnetic Flux

- Cyclic flux emergence in (large) *active regions* and (small) *ephemeral regions*

➔ take sunspot number *(R)* as a `proxy´

➔ extended cycle for ephemeral regions

- ER start earlier
- more extended, overlapping cycles

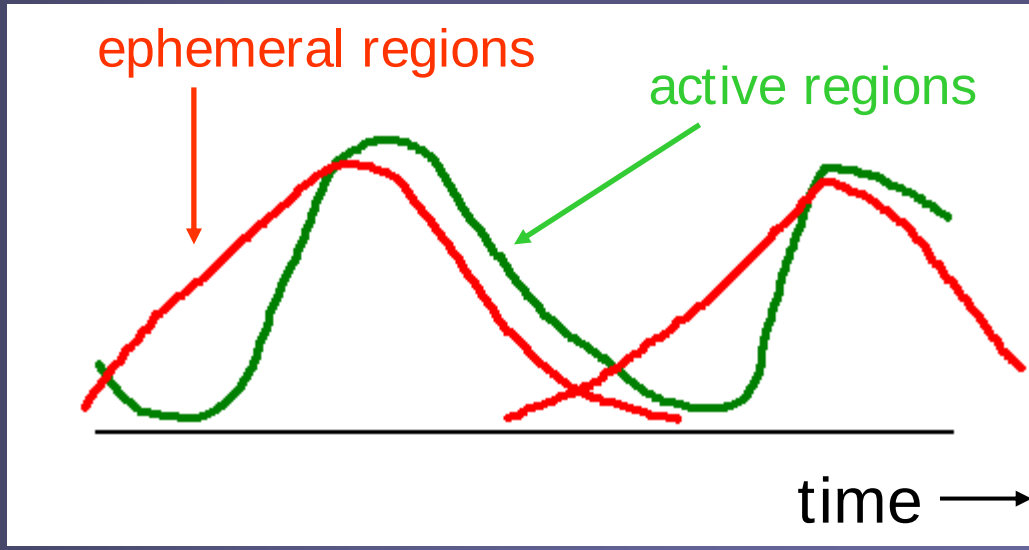

Solanki, Schüssler & Fligge 2000, 2002

Reconstruction of Open Flux back to 1700

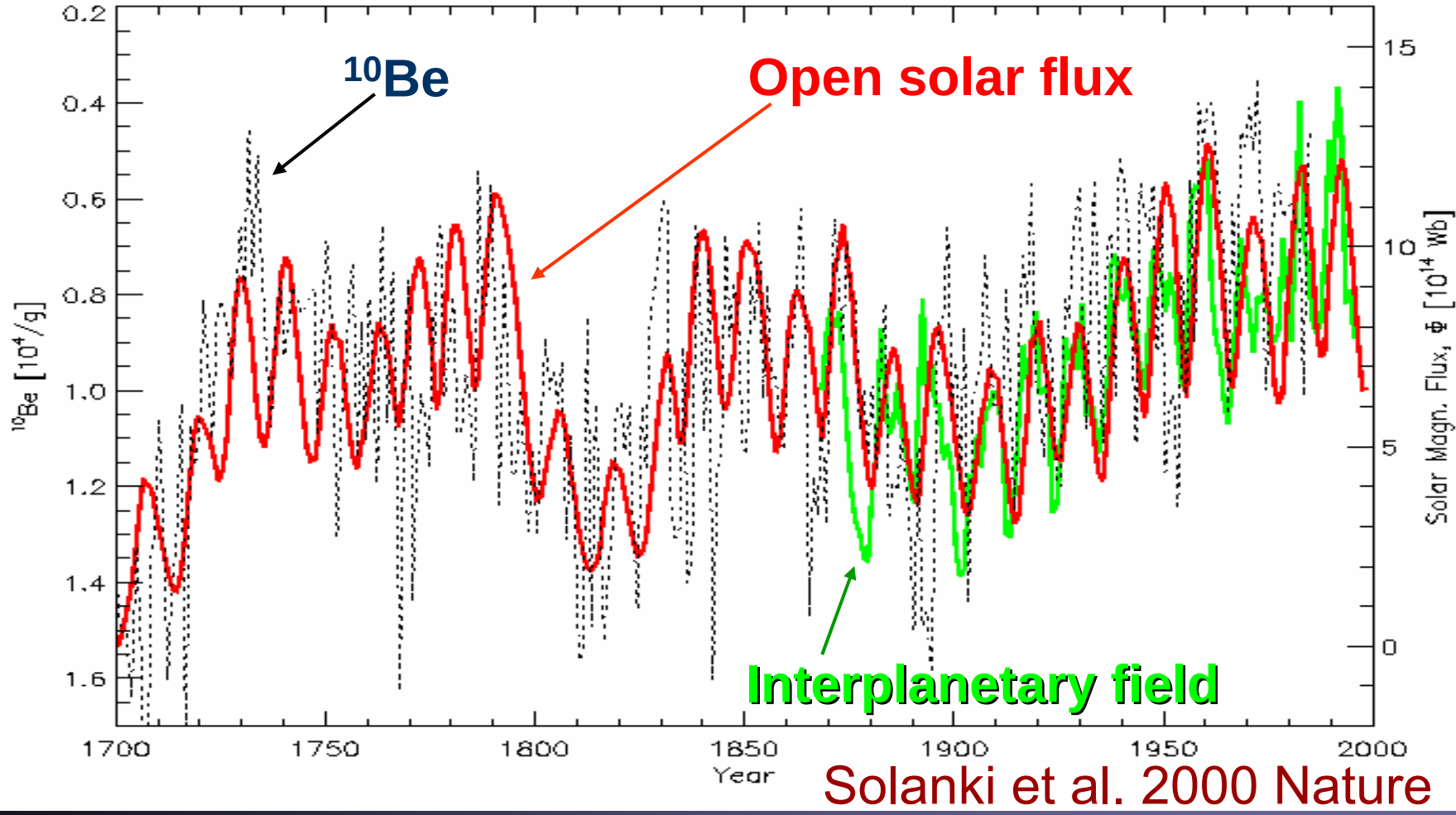

Model also predicts very similar trend for solar total magnetic flux ➔ solar irradiance should also show secular trend

Accumulation of ^{10}Be in Greenland ice

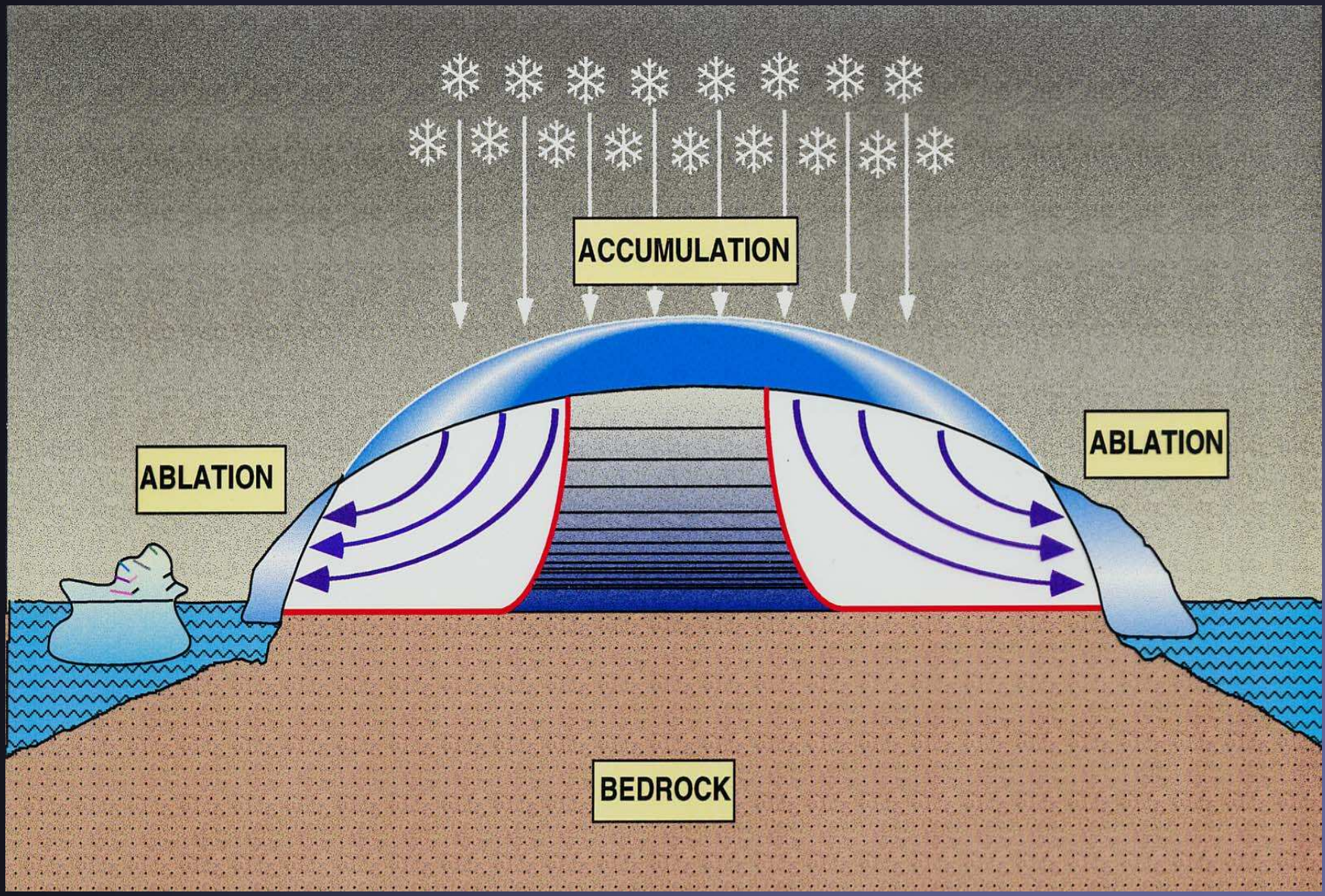

Modulation of cosmic rays

Cosmic rays = energetic particles from galactic sources. Solar magnetic field reduces number of particles reaching Earth. More active Sun ➔ less particles reach Earth

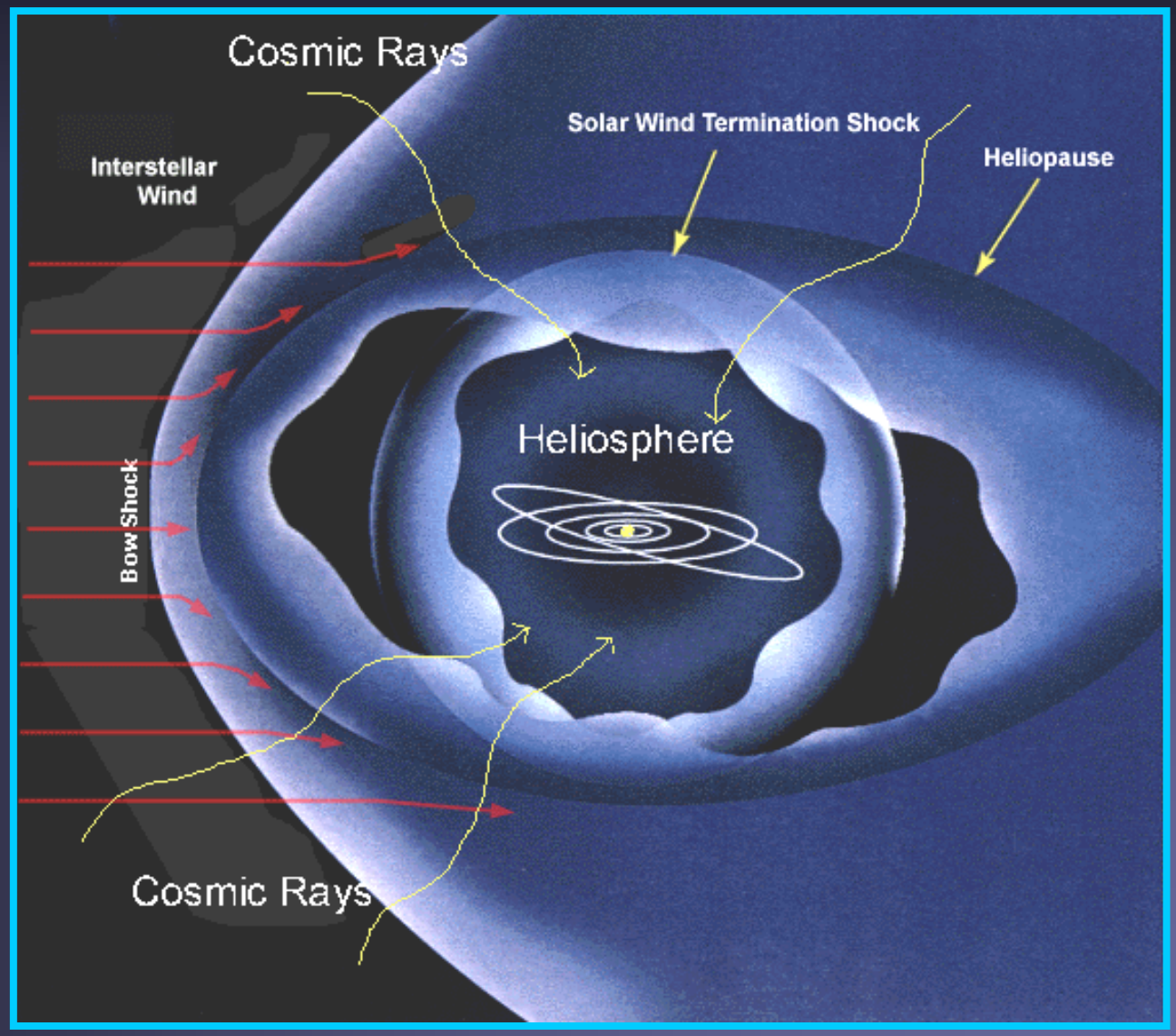

Effect of cosmic rays in atmosphere

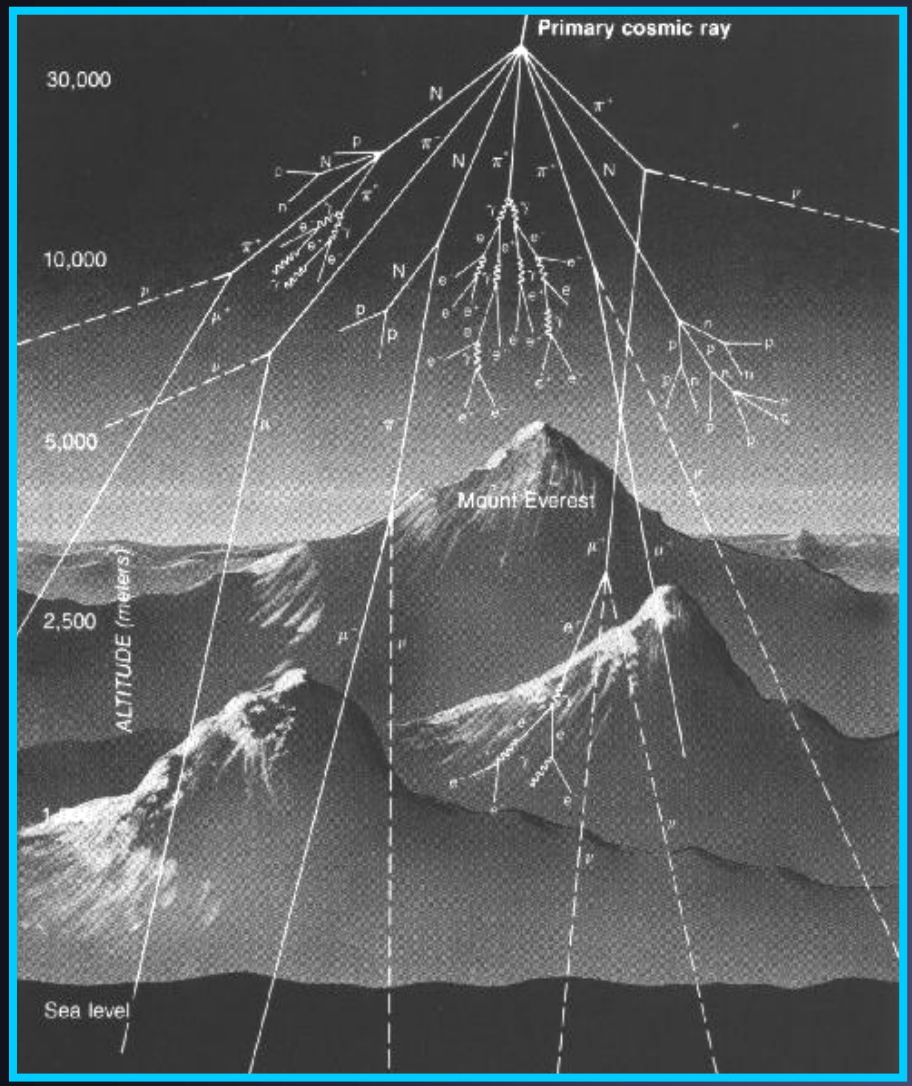

- Charged energetic CR particles interact with molecules in atmosphere

➔ particle showers: of interest to particle physicists

➔ Ionisation of many atoms

➔ Formation of neutrons, detected with neutron monitors

➔ Formation of cosmogenic isotopes: 10Be and 14C, etc.

Cosmic Rays, the Sun & Tree Rings

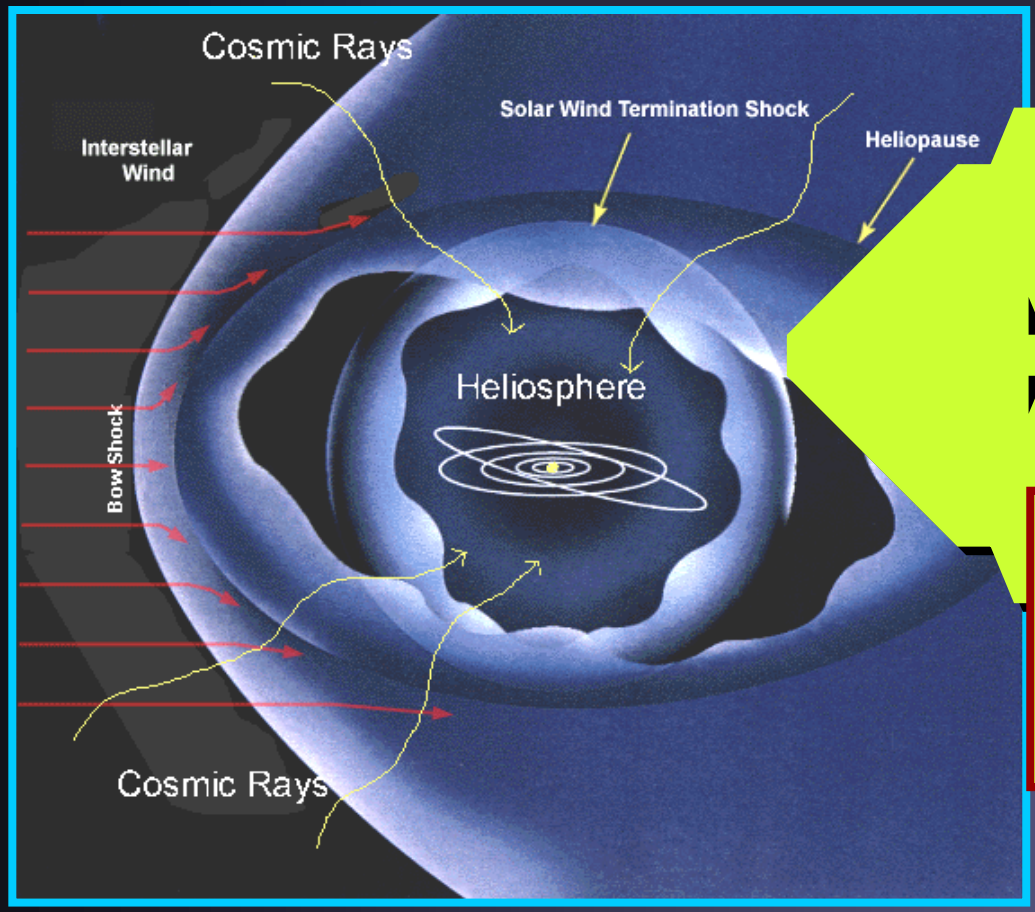

Flux of cosmic rays is changed by solar activity

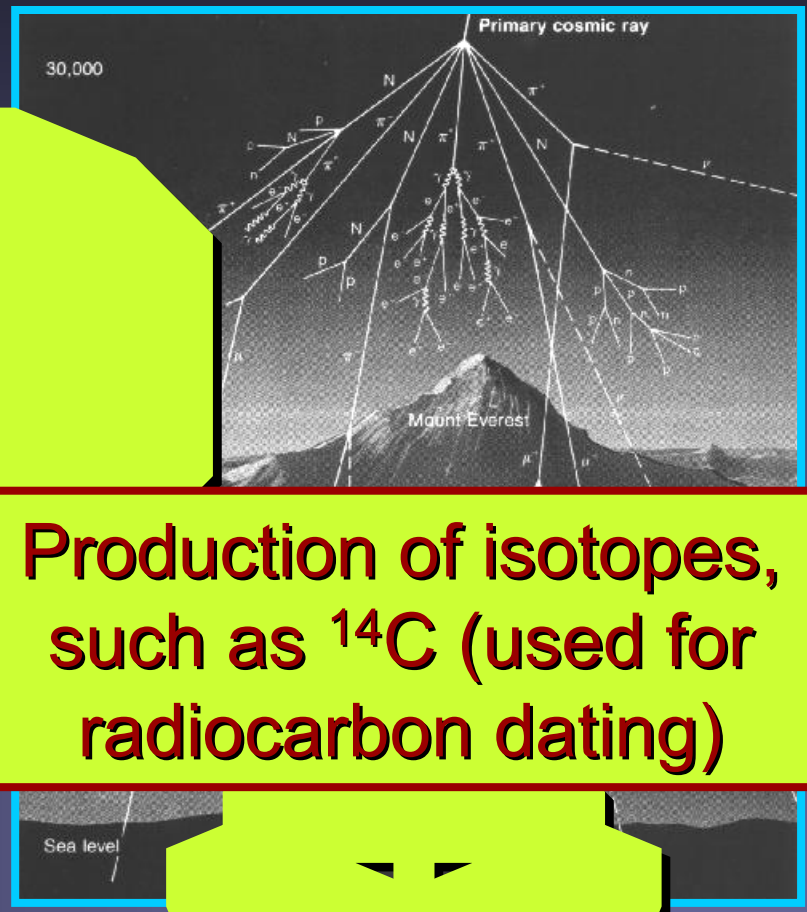

Production of isotopes, such as ^{14}C (used for radiocarbon dating)

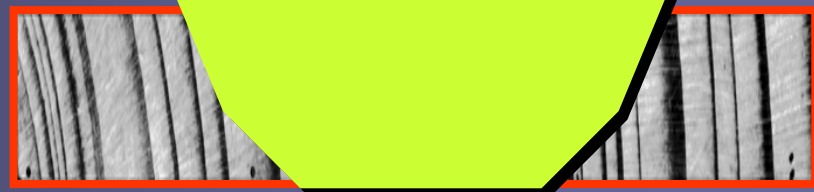

How did the Sun Behave since last Ice Age?

Number of Sunspots over last 11400 years reconstructed from ^{14}C in tree rings ➔ Sun is very active **today** compared to last **11000 years**

Solanki et al. 2004 Nature

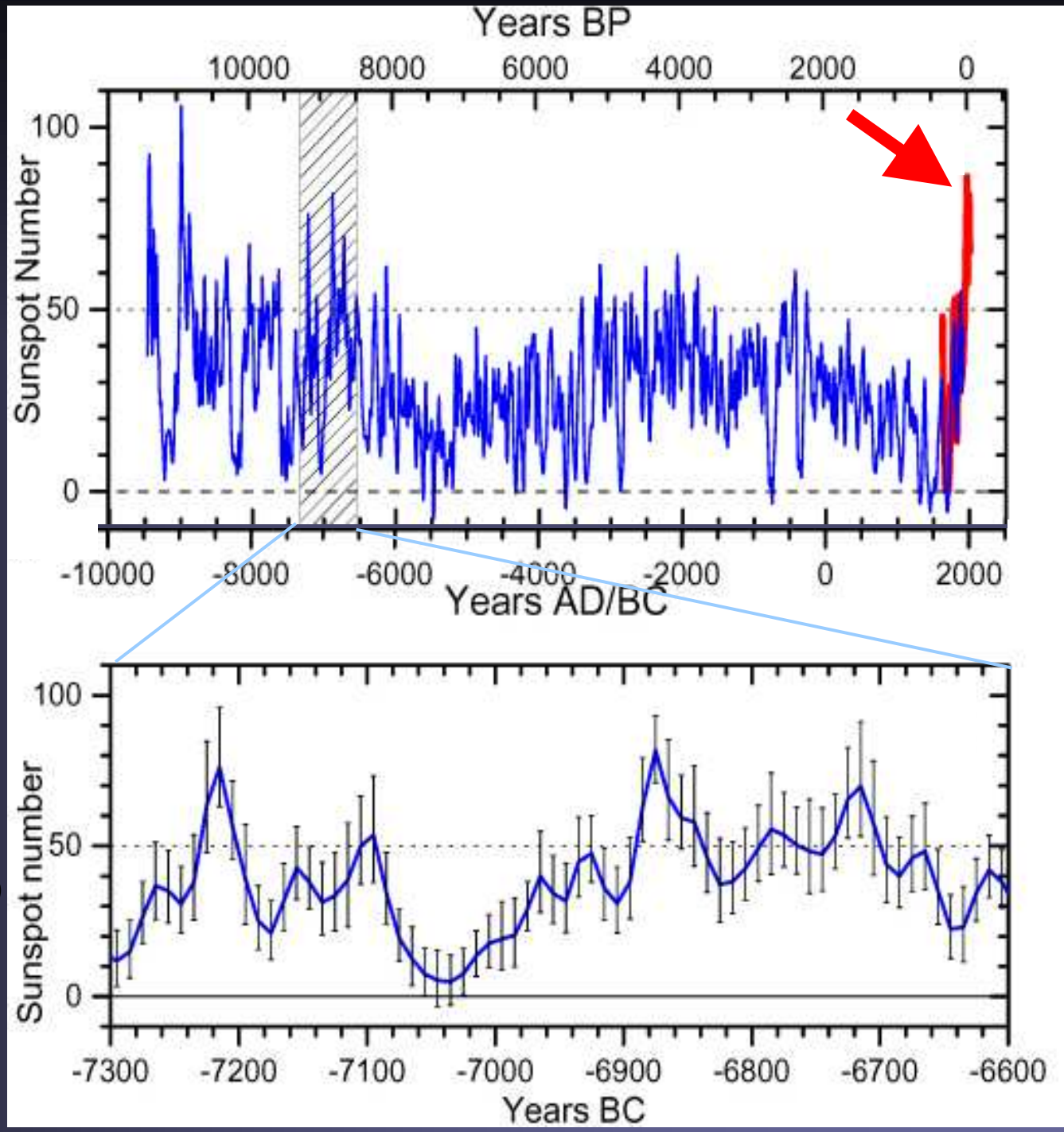

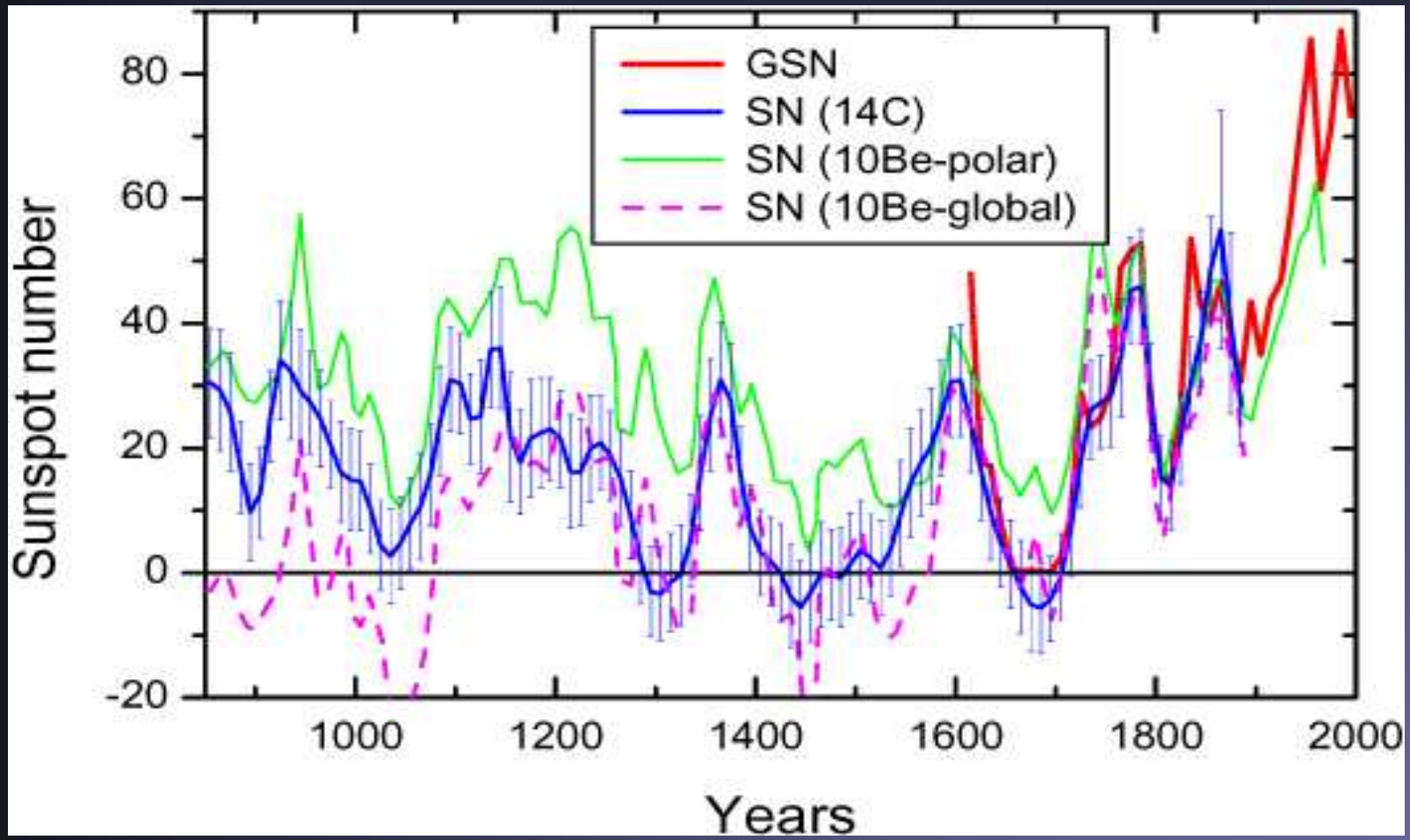
GSN
SN (14C)
SN (10Be-polar)
SN (10Be-global)
Sunspot number
80
60
40
20
0
-20
1000
1200
1400
1600
1800
2000
Years

Sunspot Number for Last 11400 Years

- ^{14}C from tree rings carries information on sunspots.
- Using physical models of all the steps connecting $\Delta^{14}C$ with sunspot number, it was possible to obtain sunspot number over 11400 years.

➔ Order of magnitude longer series than before

➔ Current episode of high solar activity is unique for the last 8000 years!

Solanki et al. 2004, Nature

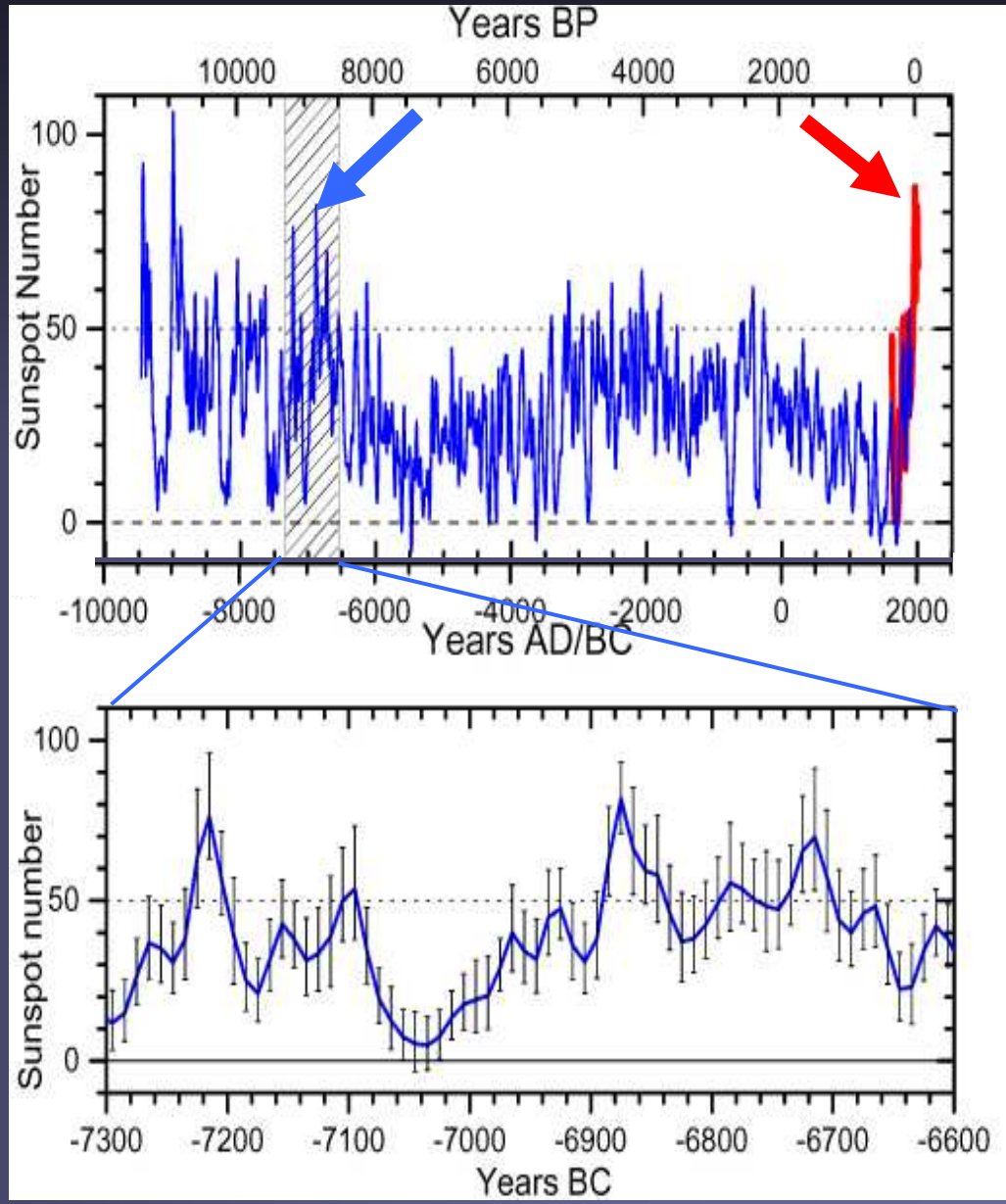

How long will the current episode of high activity last?

- Current high activity episode is one of the longest known
- Probability that it continues until 22nd century: below 1%

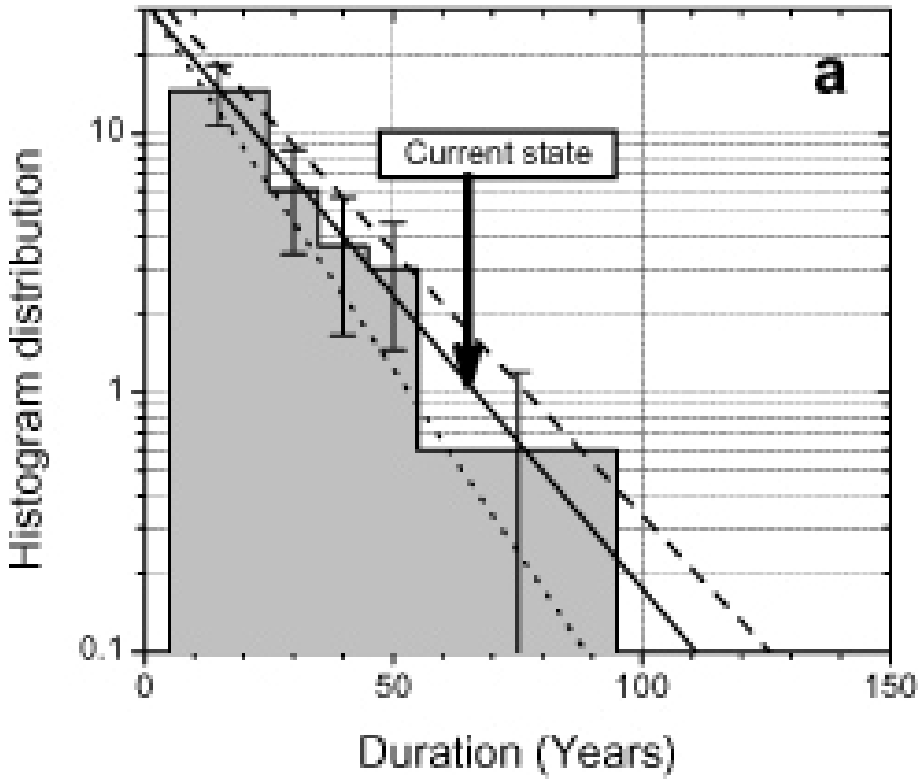

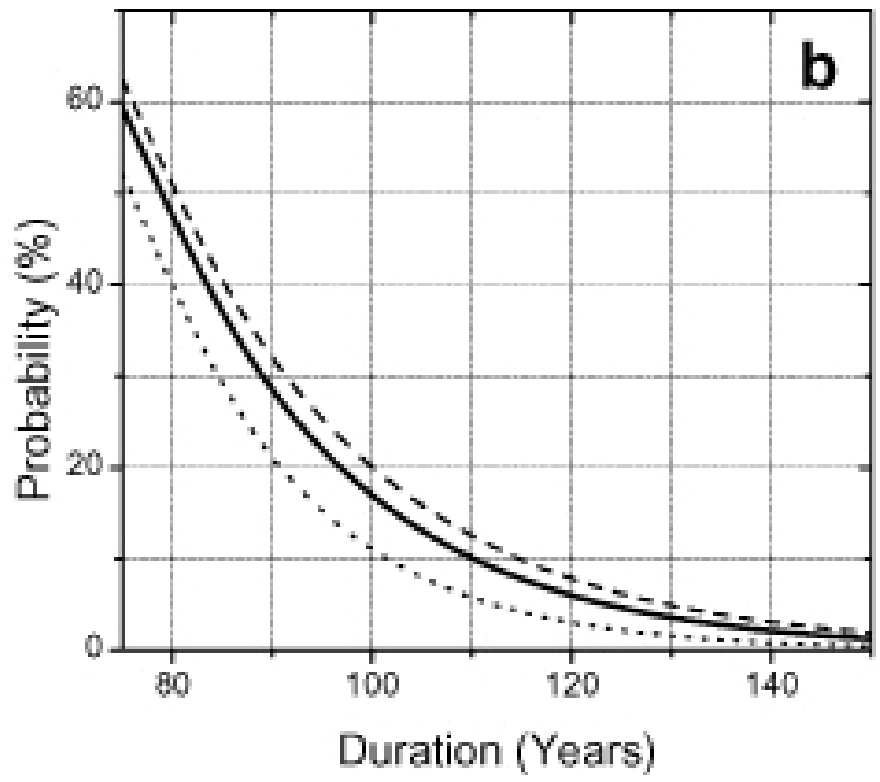

Solanki et al. 2004, Nature

Solar Irradiance and Climate